

METHODS IN MOLECULAR BIOLOGY™

Series Editor
John M. Walker
School of Life Sciences
University of Hertfordshire
Hatfield, Hertfordshire, AL10 9AB, UK

For further volumes:
<http://www.springer.com/series/7651>

Biological Aging

Methods and Protocols

Edited by

Trygve O. Tollefsbol

Department of Biology, University of Alabama at Birmingham, Birmingham, AL, USA

Editor

Trygve O. Tollefsbol
Department of Biology
University of Alabama at Birmingham
Birmingham, AL, USA

Additional material to this book can be downloaded from <http://extras.springer.com>

ISBN 978-1-4939-6313-3 ISBN 978-1-62703-556-9 (eBook)

DOI 10.1007/978-1-62703-556-9

Springer New York Heidelberg Dordrecht London

© Springer Science+Business Media New York 2007, 2013

Softcover reprint of the hardcover 2nd edition 2013

This work is subject to copyright. All rights are reserved by the Publisher, whether the whole or part of the material is concerned, specifically the rights of translation, reprinting, reuse of illustrations, recitation, broadcasting, reproduction on microfilms or in any other physical way, and transmission or information storage and retrieval, electronic adaptation, computer software, or by similar or dissimilar methodology now known or hereafter developed. Exempted from this legal reservation are brief excerpts in connection with reviews or scholarly analysis or material supplied specifically for the purpose of being entered and executed on a computer system, for exclusive use by the purchaser of the work. Duplication of this publication or parts thereof is permitted only under the provisions of the Copyright Law of the Publisher's location, in its current version, and permission for use must always be obtained from Springer. Permissions for use may be obtained through RightsLink at the Copyright Clearance Center. Violations are liable to prosecution under the respective Copyright Law.

The use of general descriptive names, registered names, trademarks, service marks, etc. in this publication does not imply, even in the absence of a specific statement, that such names are exempt from the relevant protective laws and regulations and therefore free for general use.

While the advice and information in this book are believed to be true and accurate at the date of publication, neither the authors nor the editors nor the publisher can accept any legal responsibility for any errors or omissions that may be made. The publisher makes no warranty, express or implied, with respect to the material contained herein.

Printed on acid-free paper

Humana Press is a brand of Springer

Springer is part of Springer Science+Business Media (www.springer.com)

Preface

The aim of this second edition of *Biological Aging: Methods and Protocols* is to provide an update of the most useful and promising methods currently available to study aging. Due in part to the encompassing nature of aging, many new tools for its analysis have emerged. *Biological Aging: Methods and Protocols* provides not only several of the established techniques but also some of the most recent and exciting breakthroughs in technology in this field that have served to advance the study of aging.

It would be unrealistic to attempt to amass all of the methods applied to biological aging in one book. The tools detailed in this book include established protocols such as aging cell culture as well as many more contemporary approaches such as nuclear transfer, microarray, and proteomics technologies. Collectively, these powerful protocols combined with the many other techniques that are presented are rapidly advancing the exciting and expanding field of biological aging.

Trygve O. Tollefsbol
Birmingham, AL, USA

Contents

<i>Preface</i>	<i>v</i>
<i>Contributors</i>	<i>ix</i>
1 Cell Senescence Culturing Methods	1
<i>Huaping Chen, Yuanyuan Li, and Trygve O. Tollefsbol</i>	
2 Digital Image Analysis of Cells Stained with the Senescence-Associated β-Galactosidase Assay	11
<i>Liran I. Shlush and Sara Selig</i>	
3 Analysis of Biomarkers of Caloric Restriction in Aging Cells	19
<i>Yuanyuan Li and Trygve O. Tollefsbol</i>	
4 Cell Sorting of Young and Senescent Cells.	31
<i>Graeme Hewitt, Thomas von Zglinicki, and João F. Passos</i>	
5 Studying the Replicative Life Span of Yeast Cells	49
<i>David A. Sinclair</i>	
6 Methods for Creating Mutations in <i>C. elegans</i> That Extend Lifespan	65
<i>Dayong Wang, Min Cao, Jessica Dinh, and Yuqing Dong</i>	
7 Aging Studies in <i>Drosophila Melanogaster</i>	77
<i>Yaning Sun, Jason Yolitz, Cecilia Wang, Edward Spangler, Ming Zhan, and Sige Zou</i>	
8 The Use of Calorie Restriction Mimetics to Study Aging	95
<i>Munehiro Kitada and Daisuke Koya</i>	
9 Using Somatic-Cell Nuclear Transfer to Study Aging	109
<i>Satoshi Kishigami, Ah Reum Lee, and Teruhiko Wakayama</i>	
10 Induction of Cellular Senescence by Oncogenic RAS	127
<i>Romi Gupta and Narendra Wajapeyee</i>	
11 Methods of Cellular Senescence Induction Using Oxidative Stress	135
<i>Zhe Wang, Dandan Wei, and Hengyi Xiao</i>	
12 Methods of Testing Pharmacological Drugs Effects on Aging and Life Span in Mice.	145
<i>Vladimir N. Anisimov, Irina G. Popovich, and Mark A. Zabezhinski</i>	
13 Mitochondria-Targeted Antiaging Gene Therapy with Adeno-associated Viral Vectors	161
<i>Dejia Li and Dongsheng Duan</i>	
14 Real-Time Bioluminescence Functional Imaging for Monitoring Tissue Formation and Regeneration	181
<i>Nadav Bleich Kimelman, Ilan Kallai, Dmitriy Sheyn, Wafa Tawackoli, Zulma Gazit, Gadi Pelled, and Dan Gazit</i>	
15 Exometabolomic Mapping of <i>Caenorhabditis elegans</i> : A Tool to Noninvasively Investigate Aging	195
<i>Robert J. Mishur, Jeffrey A. Butler, and Shane L. Rea</i>	

16	Detecting Polymorphisms in Human Longevity Studies: HLA Typing and SNP Genotyping by Amplicon Sequencing	215
	<i>Gilberto Vargas-Alarcón and Carmina Flores-Domínguez</i>	
17	Gel Electrophoresis-Based Proteomics of Senescent Tissues	229
	<i>Steven Carberry and Kay Ohlendieck</i>	
18	Single-Cell Semiconductor Sequencing	247
	<i>Andrea B. Kohn, Tatiana P. Moroz, Jeffrey P. Barnes, Mandy Netherton, and Leonid L. Moroz</i>	
19	Application of DNA Microarray Technology to Gerontological Studies	285
	<i>Kiyoshi Masuda, Yuki Kuwano, Kensei Nishida, and Kazuhito Rokutan</i>	
20	Epigenetic Biomarker to Determine Replicative Senescence of Cultured Cells	309
	<i>Carmen M. Koch and Wolfgang Wagner</i>	
21	Single-Neuron Transcriptome and Methylome Sequencing for Epigenomic Analysis of Aging	323
	<i>Leonid L. Moroz and Andrea B. Kohn</i>	
	<i>Index</i>	353

Contributors

- VLADIMIR N. ANISIMOV • *Department of Carcinogenesis and Oncogerontology, N.N. Petrov Research Institute of Oncology, St. Petersburg, Russia*
- JEFFREY P. BARNES • *Life Technologies, Foster City, CA, USA*
- JEFFREY A. BUTLER • *Barshop Institute for Longevity and Aging Studies, University of Texas Health Science Center at San Antonio, San Antonio, TX, USA*
- MIN CAO • *Department of Biological Sciences, Clemson University, Clemson, SC, USA*
- STEVEN CARBERRY • *Department of Biology, National University of Ireland Maynooth, Maynooth, Kildare, Ireland*
- HUAPING CHEN • *Department of Biology, University of Alabama at Birmingham, Birmingham, AL, USA*
- JESSICA DINH • *Department of Biological Sciences, Clemson University, Clemson, SC, USA*
- NADAV BLEICH KIMELMAN • *Skeletal Biotech Laboratory, The Hebrew University–Hadassah Faculty of Dental Medicine, Ein Kerem, Jerusalem, Israel*
- YUQING DONG • *Department of Biological Sciences, Clemson University, Clemson, SC, USA*
- DONGSHENG DUAN • *Department of Molecular Microbiology and Immunology, School of Medicine, The University of Missouri, Columbia, MO, USA*
- CARMINA FLORES-DOMÍNGUEZ • *Facultad de Ciencias de la Salud, Universidad Anahuac Mexico Norte Huixquilucan, Estado de Mexico, Mexico*
- DAN GAZIT • *Skeletal Biotech Laboratory, The Hebrew University–Hadassah Faculty of Dental Medicine, Ein Kerem, Jerusalem, Israel; Cedars-Sinai Medical Center, Department of Surgery, Regenerative Medicine Institute, Los Angeles, CA, USA*
- ZULMA GAZIT • *Skeletal Biotech Laboratory, The Hebrew University–Hadassah Faculty of Dental Medicine, Ein Kerem, Jerusalem, Israel; Cedars-Sinai Medical Center, Department of Surgery, Regenerative Medicine Institute, Los Angeles, CA, USA*
- ROMI GUPTA • *Department of Pathology, Yale University School of Medicine, New Haven, CT, USA*
- GRAEME HEWITT • *Ageing Research Laboratories, Centre for Integrated Systems Biology of Ageing and Nutrition, Institute for Ageing and Health, Newcastle University, Newcastle, UK*
- ILAN KALLAI • *Skeletal Biotech Laboratory, The Hebrew University–Hadassah Faculty of Dental Medicine, Ein Kerem, Jerusalem, Israel*
- SATOSHI KISHIGAMI • *Division of Biological Science, Graduate School of Biology-Oriented Science and Technology, KINKI University, Wakayama, Japan*
- MUNEHIRO KITADA • *Diabetology & Endocrinology, Kanazawa Medical University, Uchinada, Ishikawa, Japan*
- CARMEN M. KOCH • *Stem Cell Biology and Cellular Engineering, Helmholtz-Institute for Biomedical Engineering; RWTH Aachen University Medical School, Aachen, Germany*

- ANDREA B. KOHN • *The Whitney Laboratory for Marine Biosciences, University of Florida, Saint Augustine, FL, USA*
- DAISUKE KOYA • *Diabetology & Endocrinology, Kanazawa Medical University, Uchinada, Ishikawa, Japan*
- YUKI KUWANO • *Department of Stress Science, Institute of Health Biosciences, The University of Tokushima Graduate School, Tokushima, Japan*
- AH REUM LEE • *Division of Biological Science, Graduate School of Biology-Oriented Science and Technology, KINKI University, Wakayama, Japan*
- DEJIA LI • *Department of Occupational Environmental Health, School of Public Health, Wuhan University, Wuhan, People's Republic of China*
- YUANYUAN LI • *Department of Biology, University of Alabama at Birmingham, Birmingham, AL, USA*
- KIYOSHI MASUDA • *Department of Stress Science, Institute of Health Biosciences, The University of Tokushima Graduate School, Tokushima, Japan*
- ROBERT J. MISHUR • *Barshop Institute for Longevity and Aging Studies, University of Texas Health Science Center at San Antonio, San Antonio, TX, USA*
- LEONID L. MOROZ • *The Whitney Laboratory for Marine Biosciences, University of Florida, Saint Augustine, FL, USA*
- TATIANA P. MOROZ • *The Whitney Laboratory for Marine Biosciences, University of Florida, Saint Augustine, FL, USA*
- MANDY NETHERTON • *Life Technologies, Foster City, CA, USA*
- KENSEI NISHIDA • *Department of Stress Science, Institute of Health Biosciences, The University of Tokushima Graduate School, Tokushima, Japan*
- KAY OHLENDIECK • *Department of Biology, National University of Ireland Maynooth, Maynooth, Kildare, Ireland*
- JOÃO F. PASSOS • *Ageing Research Laboratories, Centre for Integrated Systems Biology of Ageing and Nutrition, Institute for Ageing and Health, Newcastle University, Newcastle, UK*
- GADI PELLED • *Skeletal Biotech Laboratory, The Hebrew University–Hadassah Faculty of Dental Medicine, Ein Kerem, Jerusalem, Israel; Cedars-Sinai Medical Center, Department of Surgery, Regenerative Medicine Institute, Los Angeles, CA, USA*
- IRINA G. POPOVICH • *Department of Carcinogenesis and Oncogerontology, N.N. Petrov Research Institute of Oncology, St. Petersburg, Russia*
- SHANE L. REA • *Barshop Institute for Longevity and Aging Studies, University of Texas Health Science Center at San Antonio, San Antonio, TX, USA*
- KAZUHITO ROKUTAN • *Department of Stress Science, Institute of Health Biosciences, The University of Tokushima Graduate School, Tokushima, Japan*
- SARA SELIG • *Laboratory of Molecular Medicine, Rappaport Faculty of Medicine and Research Institute, Technion and Rambam Health Care Center, Haifa, Israel*
- DMITRIY SHEYN • *Department of Surgery, Cedars Sinai Medical Center, Los Angeles, CA, USA; Cedars-Sinai Medical Center, Department of Surgery, Regenerative Medicine Institute, Los Angeles, CA, USA*
- LIRAN I. SHLUSH • *Campbell Family Cancer Research Institute, Ontario Cancer Institute, Princess Margaret Hospital, University Health Network, Toronto, Canada*

- DAVID A. SINCLAIR • *Paul F. Glenn Labs for the Molecular Biology of Aging, Harvard Medical School, Boston, MA, USA; Department of Genetics, Harvard Medical School, Boston, MA, USA*
- EDWARD SPANGLER • *Translational Gerontology Branch, National Institute on Aging, Baltimore, MD, USA*
- YANING SUN • *Translational Gerontology Branch, National Institute on Aging, Baltimore, MD, USA*
- WAFAT TAWACKOLI • *Department of Surgery, Cedars Sinai Medical Center, Los Angeles, CA, USA; Cedars-Sinai Regenerative Medicine Institute (CS-RMI), Cedars Sinai Medical Center, Los Angeles, CA, USA*
- TRYGVE O. TOLLEFSBOL • *Department of Biology, University of Alabama at Birmingham, Birmingham, AL, USA*
- GILBERTO VARGAS-ALARCON • *Department of Molecular Biology, Instituto Nacional de Cardiologia Ignacio Chavez, Mexico City, Mexico*
- THOMAS VON ZGLINICKI • *Ageing Research Laboratories, Centre for Integrated Systems Biology of Ageing and Nutrition, Institute for Ageing and Health, Newcastle University, Newcastle, UK*
- WOLFGANG WAGNER • *Stem Cell Biology and Cellular Engineering, Helmholtz-Institute for Biomedical Engineering; RWTH Aachen University Medical School, Aachen, Germany*
- NARENDRA WAJAPPEYEE • *Department of Pathology, Yale University School of Medicine, New Haven, CT, USA*
- TERUHIKO WAKAYAMA • *Center for Developmental Biology, RIKEN Kobe, Kobe, Japan*
- CECILIA WANG • *Laboratory of Experimental Gerontology, National Institute on Aging, Baltimore, MD, USA*
- DAYONG WANG • *Key Laboratory of Developmental Genes and Human Diseases in Ministry of Education, Medical School of Southeast University, Nanjing, People's Republic of China*
- ZHE WANG • *Department of Geriatrics, State Key Laboratory of Biotherapy and Cancer Center, West China Hospital, Sichuan University, Chengdu, People's Republic of China*
- DANDAN WEI • *Department of Geriatrics, State Key Laboratory of Biotherapy and Cancer Center, West China Hospital, Sichuan University, Chengdu, People's Republic of China*
- HENGYI XIAO • *Department of Geriatrics, State Key Laboratory of Biotherapy and Cancer Center, West China Hospital, Sichuan University, Chengdu, People's Republic of China*
- JASON YOLITZ • *Translational Gerontology Branch, National Institute on Aging, Baltimore, MD, USA*
- MARK A. ZABEZHINSKI • *Department of Carcinogenesis and Oncogerontology, N.N. Petrov Research Institute of Oncology, St. Petersburg, Russia*
- MING ZHAN • *Department of Systems Medicine and Bioengineering, Methodist Hospital Research Institute – Weill Cornell Medical College, Houston, TX, USA*
- SIGE ZOU • *Translational Gerontology Branch, National Institute on Aging, Baltimore, MD, USA*

Chapter 1

Cell Senescence Culturing Methods

Huaping Chen, Yuanyuan Li, and Trygve O. Tollefsbol

Abstract

Development of therapeutic approaches that slow or ablate the adverse physiological and pathological changes associated with aging has been considered as an important goal for gerontological research. As cellular senescence is characterized as the basis for aging in organisms, culturing and subculturing of normal human diploid fibroblasts to mimic the in vivo aging processes have been developed as major methods to investigate molecular events involved in aging. It has been established that normal human diploid fibroblasts can proliferate in culture for only finite periods of time. There are many ways to study aging in vitro. In this chapter, we will discuss some of the basic laboratory procedures for cell senescence culturing methods.

Key words Senescence, Aging, Biomarker, Fibroblasts, Cell culture

1 Introduction

Aging can be impacted by both environmental and inherent factors. The outcome of cellular aging is characterized by replicative senescence. Specifically, accumulation of damage in both nuclear and mitochondria DNA can lead to cellular senescence which may affect aging processes in organisms [1] (Fig. 1). It is generally accepted that human cells can only divide for a limited number of times. Gene mutations can accumulate during DNA replication, which ultimately lead to abnormal regulation of cell metabolism and physiology that contribute to the aging processes. Additionally, another well-known mechanism related to cell replicative senescence is the inability of normal somatic cells to fully maintain telomere DNA due to the lack of telomerase [2].

Cell senescence is a final, common pathway for actively dividing cells. It can be achieved through oncogenic- and replication-induced senescence [3, 4]. The cell culture model system has been widely used to study replicative cellular senescence. However, questions have been raised regarding whether such a procedure accurately represents aging in organisms. Cultivation requires that

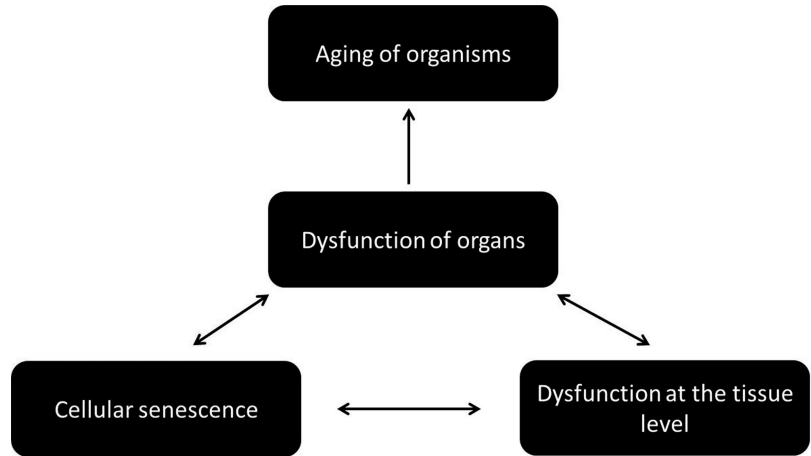


Fig. 1 Cellular senescence will lead to dysfunction of tissue and organs and eventually aging of organisms

cells continuously undergo proliferation which may stress cells unnaturally and does not occur in an organism [4]. Moreover, cells in culture and those in an intact organism differ drastically in metabolic needs, growth conditions, and many other factors. The conventional tenfold dilution of serum in culture media contains a lower concentration of protein than is normally found in extracellular tissue fluids [5]. In addition, it has been demonstrated that the needs of cultured cells differ from those of cells that are freshly isolated from intact tissue which require 13 amino acids for stable growth, whereas cells in an organism require 8–10 amino acids. Furthermore, many types of cells need to be maintained in conditioned medium or seeded at a high population density [6]. However, observations that the propagative life span of skin fibroblasts in cell culture declines as a function of donor age suggest a critical role of replication-mediated cellular senescence in aging [3, 7, 8]. Thus, the limited proliferative capacity of somatic cells appears to be an appropriate system to study human aging, as long as correct correlations are made between observed phenomena and physiology of the entire organism. The culture system exhibits the gradual, stepwise changes that permanently alter the organism, not so much in discrete phases as in a continuum of events that mirror the time from the fusion of the gametes to the demise of the organism. Another strategy is to approach the question from a therapeutic perspective by focusing on the prevention and treatment of the ailments known to increase with age. These studies have concentrated on specific age-related conditions with unfavorable consequences or the processes underlying many age-related dysfunctions [9, 10].

In this chapter, important concepts involved in aging cell culture as well as the detailed procedures involved with this process will be discussed. Specifically, in vitro signs of aging including morphological changes and aging biomarkers will be covered. Basic procedures involved in aging cell culture, such as subculturing, cell counting, cell freezing, and thawing will be also discussed. Common aging cell culture models such as fetal lung fibroblasts WI-38 and skin cells will be discussed. Major issues and experimental design considerations will also be evaluated.

1.1 In Vitro Signs of Aging

1.1.1 Morphological Changes During Cellular Aging

Characteristic morphological changes that accompany replicative senescence in cultured cells include increased cell size, nuclear size, nucleolar size, number of multinucleated cells, prominent Golgi apparatus, increased number of vacuoles in the endoplasmic reticulum and cytoplasm, increased numbers of cytoplasmic microfilaments, and large lysosomal bodies [11]. The increased cell and nuclear size and numbers of inclusion bodies observed in late-passage cells could be due to the increase of the intracellular content of RNA and proteins which might be caused by reduced protein degradation by proteasome-mediated pathways, decreased RNA turnover, the uncoupling of cell growth from cell division, and putative block of senescent cells in late G1. Aging cells also seem to exhibit an increased sensitivity to cell contact [11], perhaps as a result of changes in interactions with the extracellular matrix (ECM) or expression of secreted proteins [4], resulting in reduced harvesting and saturation densities [12].

1.1.2 Biomarkers of Aging

Cellular aging is characterized by altered cellular morphology as aforementioned above, expression changes of IGF-1, EGF, *c-fos*, increased activity for senescence-associated β -galactosidase (SA- β -GAL), increased formation of senescence-associated heterochromatin foci (SAHF) and promyelocytic leukemia protein nuclear bodies (PML NBs), permanent DNA damage, chromosomal instability, and an inflammatory secretome [13–15] (Fig. 2). They also display increased average cell cycle times, largely at the expense of longer G1 intervals. *IGF-1* is produced by many cell types and plays an important role in the regulation of cell proliferation. *IGF-1* mRNA production is reduced to an undetectable level in senescent cells, whereas *IGF-1* receptor mRNA production remains at a detectable level [16]. Epidermal growth factor (EGF) signaling has been postulated to impair downstream receptor binding in nonproliferating senescent human diploid fibroblasts [17]. A loss of *c-fos* in senescent WI-38 cells has also been reported, suggesting that the lack of proliferation in aging cells was due in part to selective repression of *c-fos* [18]. Staining for β -galactosidase has been widely used in many studies to determine the amount of senescence achieved in culture due to the specific staining of senescent cells in situ [19–21]. More recently, annexin A5 has been

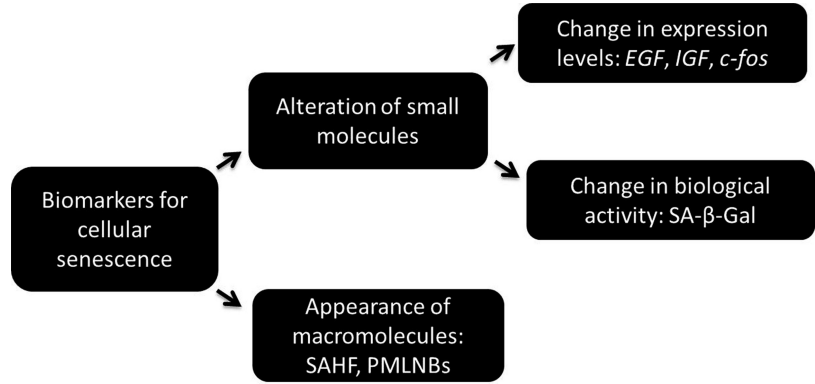


Fig. 2 Biomarkers for aging. Aging biomarkers include alteration of small molecules such as EGF, IGF, c-fos, and senescence-associated β -galactosidase (SA- β -GAL) and appearance of macromolecules such as senescence-associated heterochromatin foci (SAHF) and promyelocytic leukemia protein nuclear bodies (PMLNBs)

$$D = C + n + \left[\frac{B - A(2^n)}{A(2^{n+1}) - A(2^n)} \right]$$

Fig. 3 Equation to determine population doubling of aging cells in culture. Where A equals no. of cells plated, B equals no. of cells counted after growth period, C equals old population doubling, D equals new population doubling, and n equals the largest number that satisfies the equation $A(2^n) \leq B$

indicated to accumulate at the nuclear envelope during replicative senescence and drug-induced cellular senescence in primary human fibroblasts [22].

1.2 Quantification of Cellular Aging

Currently, a novel way to quantify cellular aging is through calculating population doublings that the cells undergo during the culturing process. Population doubling is defined as the number of times that the cell number is doubled. This is based on the observation that during cellular aging, the proliferative potential decreases. Generally, population doublings can be recorded by plating a specific number of cells and then counting those cells after a defined period of growth. If the population has doubled, for example, a plating of 1.0×10^6 cells is followed by a growth phase and a count of 2.0×10^6 ; one population doubling is added to the current age of the cells. However, because even counts as specified above are almost never achieved, a more precise method is needed for accuracy. Figure 3 outlines an equation in the aging research field that takes into account all the cells counted and results in a more exact population doubling.

1.3 Concepts in Culturing Aging Fibroblasts

For aging research, important terms have been introduced for convenience of study. These include cumulative population doublings (CPD), senescence, and senesced. CPD refers to the number of times that the cell number has been doubled. It has been used to measure the total number of cell divisions, and it can be affected by several biological factors including the maximum life span of the species, age of the donor, the site of the biopsy, and the culture conditions. If cultures fail to reach confluency in 1 week, the culture is termed as “senescence.” Cultures are considered to be “senescent” (at the end of their replicative life span) when they are unable to complete one population doubling during a 4-week period that includes three consecutive weeks of refeeding with fresh medium containing 10 % FBS. Generally, WI-38 cells with less than 30 population doublings are considered to be in early passage, and those at the end of their replicative life span are greater than 95 % life span completed. This translates to a population doubling of about 58–65, depending upon the subline that is being cultured.

2 Materials

The following materials, which must be sterile, are used to culture cells in vitro. Although antimicrobial agents can be added to culture media to prevent contamination, certain antibiotic-resistant microbial organisms existing in the environment can cause serious contamination. Thus, cell culturing should be performed under a laminar flow hood. For most aging cell types, an antibiotic/antimycotic solution of streptomycin, amphotericin B, and penicillin (Mediatech, Inc., <http://www.cellgro.com>) can be added to the medium at a final concentration of 1 % to adequately hinder the growth of bacteria, fungi, and yeast. Cells are cultured in a humidified 37 °C incubator with varied concentration of CO₂ depending on cell types. Medium, trypsin/EDTA solutions, and phosphate-buffered saline (PBS) should be warmed to 37 °C in a water bath before use. Different cell types may be cultured in different medium.

1. Monolayer cultures of cells.
2. Trypsin/EDTA solution (*see Note 1*).
3. Complete medium with serum.
4. Sterile Pasteur pipets.
5. 70 % (w/v) ethanol.
6. Sterile PBS without Ca²⁺ and Mg²⁺.
7. Tissue culture plastic ware (pipets, flasks, plates, cryovials, 15- and 50-mL conical tubes), all sterile.

3 Culturing Aging Fibroblasts

3.1 Procedures for Culturing Aging Fibroblasts

Human fetal lung fibroblasts, WI-38 cells, have been widely used as a cellular model to study molecular events associated with the aging process. The WI-38 cell line was originated from lung tissue of a therapeutically aborted fetus at 3 months gestational age. Additionally, fibroblasts explanted from the skin have also been widely used as a model to study the aging process.

The methods outlined as follows describe the trypsinization and subcultivation of monolayer cells, the freezing of monolayer cells, and the thawing and recovery of frozen cells. Notes have been added to discuss specific tips for aging cell culture.

3.1.1 Trypsinization and Subcultivation

Cells should be subcultured upon approximately 90 % confluence to avoid contact inhibition or transformation.

1. Remove media from primary culture with a sterile Pasteur pipet. Wash adherent cells with a small volume of sterile PBS to remove residual fetal bovine serum (FBS), which may inhibit trypsin.
2. Add sufficient 37 °C trypsin/EDTA solution (*see Note 1*) to cover the cell monolayer. Place in incubator for 1–2 min (*see Note 2*). Check cells with an inverted microscope to make sure cells are detached.
3. Add appropriate amount (2–6 mL) of warmed culture medium and disperse cells by gently pipetting up and down.
4. Add appropriate aliquots of the cell suspension to new culture vessels (*see Note 3*).
5. Incubate cultures, checking for adherence after 24 h.
6. Renew medium every 2–4 day.

3.1.2 Cell Counting

Cell counting is essential for aging cell culture research. Here we will describe the method of counting cells with a hemacytometer (Improved Neubauer).

1. Split cell cultures as in Subheading 3.1.1.
2. To check for viability, 0.75 mL of cells is mixed with 0.25 mL of trypan blue.
3. Nine microliters of this suspension is loaded onto the hemacytometer with coverslip and viewed under the microscope (100× magnification). Viable cells remain unstained.
4. After counting, calculate the number of cells per milliliter:
$$\text{cells/mL} = \text{average count per square of grid} \times \text{dilution factor} \times 10^4.$$

3.2 Freezing

Cells to be frozen should be in late-log-phase growth.

1. Dissociate monolayers with trypsin/EDTA (*see Note 1*) and resuspend cells in complete medium.
2. Count resuspended cells to determine viability and number.
3. Gently pellet cells for 5 min at approx $300\text{--}350 \times g$ (1,500 rpm in a swinging bucket or 45° fixed-angle rotor) and remove and discard supernatant above the pellet.
4. Resuspend cells in freezing medium (*see Note 4*) at a concentration of a 5×10^6 cells/mL. Aliquot cell suspension into labeled cryovials and freeze immediately.
5. Cells can be frozen at -80°C for short-term storage. (Optional: place cryovials into a styrofoam container or slow freezer such as the Nalgene[®] Cryo Freezing Container filled with isopropanol, which has a repeatable $-1^\circ\text{C}/\text{min}$ cooling rate to prevent the formation of damaging ice crystals.)
6. Transfer cells in cryovials to liquid nitrogen (-196°C) after 24 h for long-term storage.

3.2.1 Thawing and Recovery of Frozen Cells

1. Remove cryovial from liquid nitrogen and place in a 37°C water bath. Agitate gently until thawed.
2. Wipe vial with 70 % ethanol before putting under hood and opening.
3. Transfer cells to a sterile 15-mL conical tube containing medium prewarmed to 37°C . Centrifuge 5–10 min at $150\text{--}200 \times g$ (approx 1,000 rpm in a swinging bucket or 45° fixed-angle rotor). Discard supernatant containing residual dimethylsulfoxide (DMSO).
4. Resuspend pellet in 1-mL complete medium and transfer to culture plate/flask containing the appropriate amount of medium. Place in incubator. Check cells for adherence after 24 h.

3.2.2 Monitoring Aging Process Through Aging Biomarkers (β -Galactosidase Staining)

1. Monolayers at low cell density are placed in PBS containing 3 % formaldehyde for 5 min.
2. After three washes with PBS, stain cells overnight at 37°C in staining solution (150 mM NaCl, 2 mM MgCl_2 , 5 mM $\text{K}_3\text{Fe}(\text{CN})_6$, 5 mM $\text{K}_4\text{Fe}(\text{CN})_6$, 40 mM citric acid, and 12 mM sodium phosphate, pH 6) containing 1 mg/mL 5-bromo-4-chloro-3-indolyl β -D-galactoside.
3. Cells are then washed with PBS.
4. β -Galactosidase activity is monitored visually by scoring blue precipitate in the cytoplasm and photographed at $200\times$.

3.3 Aging Cell Culture: Major Issues and Experimental Design Considerations

In this section, some major issues related to aging cell culture are discussed, which include the in vitro cell culture model to study in vivo senescence and experimental design in aging-related cell culture studies.

3.3.1 Effect of Culture Conditions

Effects of culture conditions other than cell proliferation itself have also been investigated. One obvious difference in terms of the environment between *in vitro* and *in vivo* cell growth is exposure to direct light when cultured *in vitro*. Fluorescent light can cause DNA double strand breaks [23, 24]. Additionally, it has been shown that exposure to fluorescent light can damage photoactive components of cell culture medium [25]. Several other conditions have also been reported to induce a premature senescent phenotype, such as hydrogen peroxide [26], *tert*-butyl hydroperoxide [27], and ultraviolet [28] and gamma radiation [29]. Although the trypsinization procedure to remove adherent cells from culture dishes may also cause cellular stress, weekly trypsinizations have been shown to not affect the proliferative capacity of the mass culture [30].

3.3.2 Timeline

Aging studies that attempt to mimic cellular senescence are often time-consuming since it generally requires numerous population doublings for cells to acquire critically attenuated telomere lengths which triggers senescence. For studies in this regard, it is better to investigate one serially cultured sample at different ages than to examine a few different cultured samples at different time periods. It is important to freeze cells in liquid nitrogen at various ages while serially culturing aging cells. This can enable the investigator to restart the study at certain points if a problem arises with a culture. Many different cell lines used in aging research can be provided by the Coriell Institute (<http://ccr.coriell.org/nia/>).

4 Notes

1. Depending on the cell type, the concentration of trypsin may vary. Normally, 0.25 % (w/v) trypsin/0.2 % (w/v) EDTA solution is applied to most of the cell types to detach cells and chelate Ca^{2+} and Mg^{2+} ions that could hinder the action of trypsin.
2. Depending on the cell type, the incubation time varies from 1 to 5 min. The incubation time needs to be optimized according to experience (extended trypsin exposure damages cells).
3. Cells need to be seeded at proper density after splitting (e.g., WI-38 cells at early passage are seeded at $3 \times 10^3/\text{cm}^2$). This density will ensure that the cells are subconfluent, and therefore, possible effects of density on growth due to contact inhibition are minimal.
4. Freezing medium is composed of 90–95 % complete culture medium supplemented with 5–10 % DMSO or glycerol.

Acknowledgments

This work was supported in part by grant from the NIH (CA129415) and the American Institute for Cancer Research.

References

1. Chen H, Hardy TM, Tollefsbol TO (2011) Epigenomics of ovarian cancer and its chemoprevention. *Front Genet* 2:67
2. Chen H, Li Y, Tollefsbol TO (2009) Strategies targeting telomerase inhibition. *Mol Biotechnol* 41:194–199
3. Cristofalo VJ, Beck J, Allen RG (2003) Cell senescence: an evaluation of replicative senescence in culture as a model for cell aging in situ. *J Gerontol A Biol Sci Med Sci* 58:B776–B779, discussion 9–81
4. Cristofalo VJ, Lorenzini A, Allen RG et al (2004) Replicative senescence: a critical review. *Mech Ageing Dev* 125:827–848
5. Rubin H (1997) Cell aging in vivo and in vitro. *Mech Ageing Dev* 98:1–35
6. Rubin H (1966) A substance in conditioned medium which enhances the growth of small numbers of chick embryo cells. *Exp Cell Res* 41:138–148
7. Martin GM, Sprague CA, Epstein CJ (1970) Replicative life-span of cultivated human cells. Effects of donor's age, tissue, and genotype. *Lab Invest* 23:86–92
8. Schneider EL, Mitsui Y (1976) The relationship between in vitro cellular aging and in vivo human age. *Proc Natl Acad Sci* 73:3584–3588
9. Lai SR, Phipps SM, Liu L et al (2005) Epigenetic control of telomerase and modes of telomere maintenance in aging and abnormal systems. *Front Biosci* 10:1779–1796
10. Hadley EC, Lakatta EG, Morrison-Bogorad M et al (2005) The future of aging therapies. *Cell* 120:557–567
11. Cristofalo VJ, Pignolo RJ (1993) Replicative senescence of human fibroblast-like cells in culture. *Physiol Rev* 73:617–638
12. Cristofalo VJ (1988) Cellular biomarkers of aging. *Exp Gerontol* 23:297–307
13. Zhang R, Poustovoitov MV, Ye X et al (2005) Formation of MacroH2A-containing senescence-associated heterochromatin foci and senescence driven by ASF1a and HIRA. *Dev Cell* 8:19–30
14. Langley E, Pearson M, Faretta M et al (2002) Human SIR2 deacetylates p53 and antagonizes PML/p53-induced cellular senescence. *EMBO J* 21:2383–2396
15. Young AR, Narita M (2009) SASP reflects senescence. *EMBO Rep* 10:228–230
16. Ferber A, Chang C, Sell C et al (1993) Failure of senescent human fibroblasts to express the insulin-like growth factor-1 gene. *J Biol Chem* 268:17883–17888
17. Carlin C, Phillips PD, Brooks-Frederich K et al (1994) Cleavage of the epidermal growth factor receptor by a membrane-bound leupeptin-sensitive protease active in nonionic detergent lysates of senescent but not young human diploid fibroblasts. *J Cell Physiol* 160:427–434
18. Seshadri T, Campisi J (1990) Repression of c-fos transcription and an altered genetic program in senescent human fibroblasts. *Science* 247:205–209
19. Dimri GP, Lee X, Basile G et al (1995) A biomarker that identifies senescent human cells in culture and in aging skin in vivo. *Proc Natl Acad Sci* 92:9363–9367
20. Alexander K, Yang HS, Hinds PW (2004) Cellular senescence requires CDK5 repression of Rac1 activity. *Mol Cell Biol* 24:2808–2819
21. Stenderup K, Justesen J, Clausen C et al (2003) Aging is associated with decreased maximal life span and accelerated senescence of bone marrow stromal cells. *Bone* 33:919–926
22. Klement K, Melle C, Murzik U et al (2012) Accumulation of annexin A5 at the nuclear envelope is a biomarker of cellular aging. *Mech Ageing Dev* 133(7):508–522
23. Bradley MO, Sharkey NA (1977) Mutagenicity and toxicity of visible fluorescent light to cultured mammalian cells. *Nature* 266:724–726
24. Bradley MO, Hsu IC, Harris CC (1979) Relationship between sister chromatid exchange and mutagenicity, toxicity and DNA damage. *Nature* 282:318–320
25. Wang RJ (1976) Effect of room fluorescent light on the deterioration of tissue culture medium. *In Vitro* 12:19–22
26. Fripiat C, Chen QM, Remacle J et al (2000) Cell cycle regulation in H(2)O(2)-induced premature senescence of human diploid fibroblasts and regulatory control exerted by the papilloma virus E6 and E7 proteins. *Exp Gerontol* 35:733–745

27. Dumont P, Burton M, Chen QM et al (2000) Induction of replicative senescence biomarkers by sublethal oxidative stresses in normal human fibroblast. *Free Radic Biol Med* 28:361–373
28. Ma W, Wlaschek M, Hommel C et al (2002) Psoralen plus UVA (PUVA) induced premature senescence as a model for stress-induced premature senescence. *Exp Gerontol* 37:1197–1201
29. Seidita G, Polizzi D, Costanzo G et al (2000) Differential gene expression in p53-mediated G(1) arrest of human fibroblasts after gamma-irradiation or N-phosphonacetyl-L-aspartate treatment. *Carcinogenesis* 21:2203–2210
30. Hadley EC, Kress ED, Cristofalo VJ (1979) Trypsinization frequency and loss of proliferative capacity in WI-38 cells. *J Gerontol* 34:170–176

Chapter 2

Digital Image Analysis of Cells Stained with the Senescence-Associated β -Galactosidase Assay

Liran I. Shlush and Sara Selig

Abstract

Cellular senescence plays important roles in the aging process of complex organisms, in response to stress and in tumor suppression. Several markers can be used to identify senescent cells, of which the most widely used is the senescence-associated β -galactosidase (SABG) activity. Here we describe a procedure for digital image analysis of cells stained by the SABG staining technique at pH 6 or at pH 4. This analysis is highly reproducible and sensitive to subtle differences in staining intensities resulting from diverse cellular senescence pathways in culture.

Key words Senescence, β -Galactosidase, pH 6, pH 4, Digital analysis, BGAV

1 Introduction

Several markers of senescence have been described [1], among them senescence-associated β -galactosidase (SABG) activity. This marker has been the most extensively utilized biomarker for cellular senescence (CS) both in in vitro (reviewed in ref. 2) and in in situ [3–6] studies. The SABG method is a simple procedure, enables visualization of senescent cells in a heterogeneous population, and is specific for CS regardless of the initiating trigger [2]. The protein product of the lysosomal β -galactosidase 1 (GLB1) gene is the source of the SABG activity [7]. In senescent cells, both the mRNA and the protein levels of the GLB1 gene are significantly elevated, and the enzymatic activity increases concomitantly [7]. Consequently, the enhanced enzymatic activity in senescence can be detected not only at the optimal pH for activity, pH 4.5, but also at a suboptimal pH of 6.0. This finding constitutes the basis for the use of SBAG activity at pH 6.0 as a marker for cellular senescence [7].

Scoring of the SABG-stained cells has been based on experimentalist-dependent determination of a given cell staining as being positive and is not anchored in well-defined criteria. In addition, the blue staining in positive cells is impossible to quantify

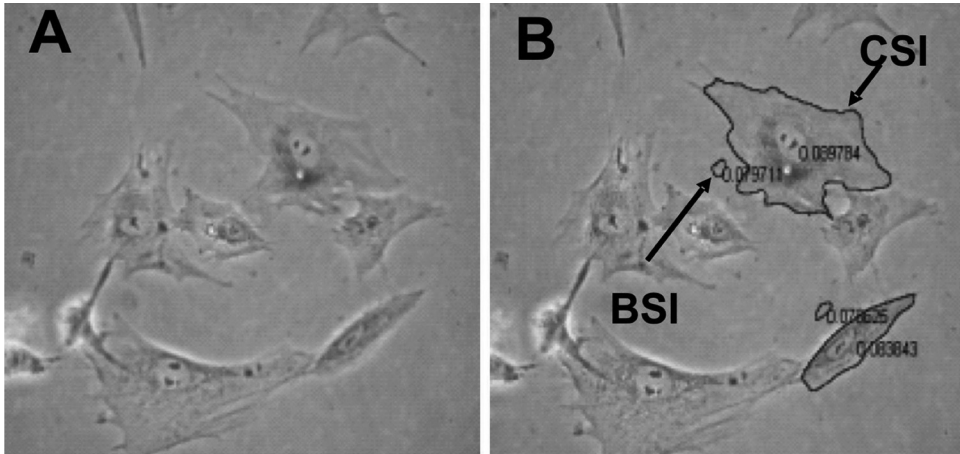


Fig. 1 Application of the digital image-processing tool to the standard SABG assay. **(a)** SABG staining at pH 6.0 of fibroblast cells at population doubling 34. **(b)** Image analysis of the field shown in Fig. 1a using the MATLAB tool described. The cell membrane borders and the background control area (*small circles*) are marked manually. The logarithmic ratio of the cytoplasmic staining intensity (CSI) divided by the background staining intensity (BSI) yields the BGAV. (Reproduced from Shlush et al. 2011 [9] with permission from BioMed Central)

objectively, such that cells with strong, moderate, or weak blue staining may all be recognized as equally positive. This renders the method insensitive to subtle effects of various stressors on CS and might contribute to the inconsistency in replicating SABG assay results in skin biopsies [8].

The limitation described above motivated us to develop a quantitative in situ SABG assay. We applied digital image processing to quantify the SABG staining, following the use of the previously described protocol of the in situ SABG assay [4]. This quantification method, based on color intensity analysis of photographed images of stained cells, generates values of cell staining intensity (CSI) measured in arbitrary intensity units. CSI values are the product of the ratio between the green plus blue values of each pixel in the manually marked cell cytoplasm and the total color (red, green, and blue) in the same cytoplasm, divided by the cell surface area. Standardization of each single CSI value is achieved by dividing the CSI value with the adjacent background staining intensity (BSI) value (Fig. 1a, b). In order to decrease the signal-to-noise ratio, we applied a logarithmic transformation to the ratio CSI/BSI and termed the value obtained β -galactosidase activity value (BGAV). The BGAVs are highly sensitive and reproducible [9]. In addition, we have also varied the pH of the assay to broaden the range of histochemically detectable activity and enable the detection of subtle changes in BGAVs, which are evident only when performing the SABG staining at the nonstandard pH 4.0 [9]. SABG staining can be applied also to OCT-frozen tissues [9, 10]; however, the quantitation of the resulting signals requires expertise in histological analysis of the relevant tissue.

2 Materials

2.1 SABG Staining Solution Components

1. MgCl_2 : 1 M solution in double distilled water (DDW). Weigh 9.5 g and dissolve in DDW to final volume of 100 ml. Store at room temperature (RT).
2. NaCl: 5 M solution in DDW. Weigh 29.2 g and dissolve in DDW to final volume of 100 ml. Store at RT.
3. $\text{K}_3\text{Fe}(\text{CN})_6$: 100 mM solution in DDW (*see Note 1*). Weigh 3.29 g and dissolve in DDW to final volume of 100 ml. Store at RT.
4. $\text{K}_4\text{Fe}(\text{CN})_6 \cdot 3 \text{H}_2\text{O}$: 100 mM solution in DDW (*see Note 1*). Weigh 4.22 g and dissolve in DDW to final volume of 100 ml. Store at RT.
5. Citric acid solution: 0.1 M solution in DDW. Weigh 1.92 g and dissolve in DDW to final volume of 100 ml. Store at RT.
6. Disodium phosphate (Na_2HPO_4) solution: 0.2 M solution in DDW. Weigh 2.83 g and dissolve in DDW to final volume of 100 ml. Store at RT.
7. X-gal (5-bromo-4-chloro-3-indolyl- β -D-galactoside) stock solution ($\times 20$): 20 mg/ml dissolved in dimethyl formamide (DMF) (*see Note 1*). Aliquot 1 ml portions and freeze at -20°C . We used X-gal from various sources and all worked well.

2.2 Preparation of the SABG Solution Mix

1. Components for the staining solution can be prepared in advance but should only be mixed together shortly before carrying out the staining.
2. Prepare a fresh mix of citric acid/phosphate buffer at the required pH. Staining at various pHs requires different ratios of the 0.1 M citric acid solution and the 0.2 M disodium phosphate solution:
For a citric acid/phosphate buffer at pH 4.0, mix 38.55 ml of 0.2 M Na_2HPO_4 with 61.45 ml of 0.1 M Citric acid.
For a citric acid/phosphate buffer at pH 6.0, mix 63.15 ml of 0.2 M Na_2HPO_4 with 36.85 ml of 0.1 M Citric acid.
Verify the pH with pH indicator (litmus) paper.
3. Thaw 1 ml of frozen 20 mg/ml X-gal and place on ice.
4. Mix the following components to prepare a 20 ml volume of staining solution:
12.4 ml of DDW, 40 μl of 1 M MgCl_2 (final concentration 2 mM), 600 μl of 5 M NaCl (final concentration 150 mM), 1 ml of 100 mM $\text{K}_3\text{Fe}(\text{CN})_6$ (final concentration 5 mM), 1 ml of 100 mM $\text{K}_4\text{Fe}(\text{CN})_6$ (final concentration 5 mM), 4 ml of the citric acid/phosphate solution (prepared at chosen pH), and 1 ml of 20 mg/ml X-gal (final concentration 1 mg/ml).

2.3 Cell Fixation Components

1. Cold phosphate-buffered saline (PBS). To prepare PBS dissolve 8 g of NaCl, 0.2 g of KCl, 1.44 g of Na₂HPO₄, and 0.24 g of KH₂PO₄ in 800 ml of H₂O. Adjust pH to 7.4 and add H₂O to a final volume of 1 L.
2. 25 % glutaraldehyde solution (Sigma G6257) (*see Note 1*).
3. Prepare fixation solution immediately before fixation by diluting 1:50 the 25 % glutaraldehyde solution with cold PBS to a final concentration of 0.5 % glutaraldehyde (*see Note 2*).

3 Methods

3.1 Preparing Cells for SABG Staining

1. Seed cells 48 h prior to staining at a density of $2-4 \times 10^4$ cells/well in a six well plate (*see Note 3*).

3.2 Staining Procedure

1. Remove media from cell culture.
2. Wash cells briefly with cold PBS.
3. Add 2 ml of 0.5 % glutaraldehyde to each well, and place on ice for 5 min.
4. Wash briefly twice with cold PBS.
5. Add 2 ml of freshly prepared SABG staining solution.
6. Incubate for 8 h at 37 °C. Do not incubate in a CO₂ incubator.
7. End staining procedure by washing 3×5 min with cold PBS.
8. Add 3 ml of PBS and store at 4 °C until images are collected (*see Notes 4 and 5*).

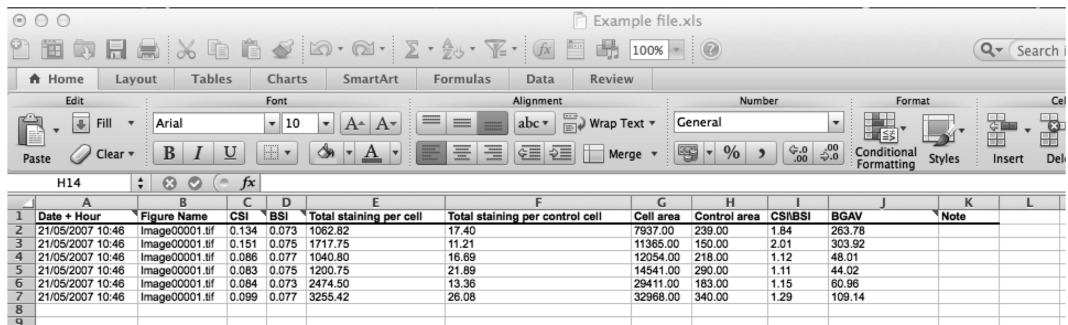
3.3 Microscopy and Image Acquisition

1. Color images of the SABG-stained cells should be captured with a color digital camera, mounted on an inverted light microscope, using a 10× objective. Any high-quality color digital camera is adequate. Optimal exposure should be set for each individual experiment and should be constant for all images taken for a specific experiment.
2. Images must be saved as TIFF files. Other formats are not acceptable for analysis.
3. A minimum of 250 cells should be analyzed for each experiment or time point in order to reach statistically valid BGAVs (*see Note 6*).

3.4 Digital Analysis of the Acquired Images

1. Use MATLAB package version 7.0 or above.
2. Download the MATLAB applications for cell marking (segmentGui.m) and for color analysis (postProcess3.m) from the following website:
<http://md.technion.ac.il/pictures/storage/45/47.zip>

3. The files: `postprocess3.m`, `segmentGui.asv`, `segmentGui.fig`, `segmentGui.m`, and `batchscript.m` must be placed in the same folder with the figures. Therefore, for each series of images analyzed, the above four files should be copied into the figures' directory.
4. Point MATLAB to the working folder (the folder with the images and applications of the software). Press on the three dots (...) on the MATLAB toolbar to open the browser for the folder window.
5. In the command window type `segmentGui` and then press "Enter".
6. Double click on the figure you want to analyze (*.tif).
7. Press the button "start segmentation."
8. Mark the button "whole cell segmentation."
9. Mark the cell borders (*see Note 7*) and press "Enter" when you finish marking each cell.
10. Mark a control region adjacent to the analyzed cell. The control region must be smaller than the smallest cell (in the figure) for the program to recognize it as a control region. Mark the control regions with three points, as near as possible to the cell itself (see example in Fig. 1) (*see Note 7*).
11. Press "stop segmentation" when you have finished analyzing all cells in a figure.
12. Press "save segmentation."
13. Close the `segmentGui` application (an error note will appear—ignore it).
14. For single-image analysis type in the MATLAB command window exactly the following:
`postProcess3 ("Image Name.tif")`
In the place of "Image Name" type the name of your specific image.
15. For multiple-image analysis type in the MATLAB command window the command "`batch_script`" and all the marked and saved figures will be analyzed (it may take a few minutes for analysis of 20 figures).
16. The output of `postProcess3.m` (for a single image) and of `batch_script` (for multiple images) will be both a figure file of the results and a text file (both will be created in the same directory of the processed images) that may be easily copied to EXCEL or to any other text editor.
17. After copying the data to an EXCEL file, the columns will appear in the same order as in the example file (Fig. 2).



	A	B	C	D	E	F	G	H	I	J	K	L
1	Date + Hour	Figure Name	CSI	BSI	Total staining per cell	Total staining per control cell	Cell area	Control area	CSI/BSI	BGAV	Note	
2	21/05/2007 10:46	Image00001.tif	0.134	0.073	1062.82	17.40	7937.00	239.00	1.84	263.78		
3	21/05/2007 10:46	Image00001.tif	0.151	0.075	1717.75	11.21	11365.00	150.00	2.01	303.92		
4	21/05/2007 10:46	Image00001.tif	0.086	0.077	1040.80	18.69	12054.00	218.00	1.12	48.01		
5	21/05/2007 10:46	Image00001.tif	0.083	0.075	1200.75	21.89	14541.00	290.00	1.11	44.02		
6	21/05/2007 10:46	Image00001.tif	0.084	0.073	2474.50	13.36	29411.00	183.00	1.15	60.96		
7	21/05/2007 10:46	Image00001.tif	0.099	0.077	3255.42	26.08	32968.00	340.00	1.29	109.14		
8												
9												

Fig. 2 An example of an EXCEL file containing the results produced by the MATLAB analysis of the SABG staining

3.5 Statistical Analysis

In most instances the BGAVs did not fit a normal distribution according to either Shapiro-Wilk W or Kolmogorov-Smirnov normality tests [9]. Therefore, rather than using a student's *t*-test, which assumes normal distribution, we use the Kolmogorov-Smirnov test for analysis of the BGAV values.

4 Notes

1. Handle with caution. This material is a biohazard.
2. Alternatively, fixation may be carried out using freshly prepared 3 or 4 % formaldehyde, at RT for 5 min, as described in other SABG staining protocols [11, 12].
3. This cell density ensures that cells will not reach confluence before staining is carried out and is adjusted for human primary fibroblasts. If rapidly growing cells are plated for staining, adjust the number of cells seeded in order to avoid confluent cultures at the day of staining. Avoid seeding cell clumps. These conditions will enable better scoring of SABG-positive cells.
4. We found that staining peaks 16 h after the SABG solution is replaced with PBS, and following 48 h the staining reaches a plateau and remains stable for as long as 2 months [9]. We therefore recommend acquisition of the images for analysis at least 48 h after removing the SABG solution and preferably during the first 2 weeks after the staining was performed.
5. When staining is carried out at pH 4, strong staining is evident in all cells after 8 h (see example in Fig. 3). Varying staining intensities are not apparent by visual inspection alone after staining at pH 4 and however are detected by digital analysis.
6. The number of images captured should be adjusted based on the density of the cells viewed per microscope field.

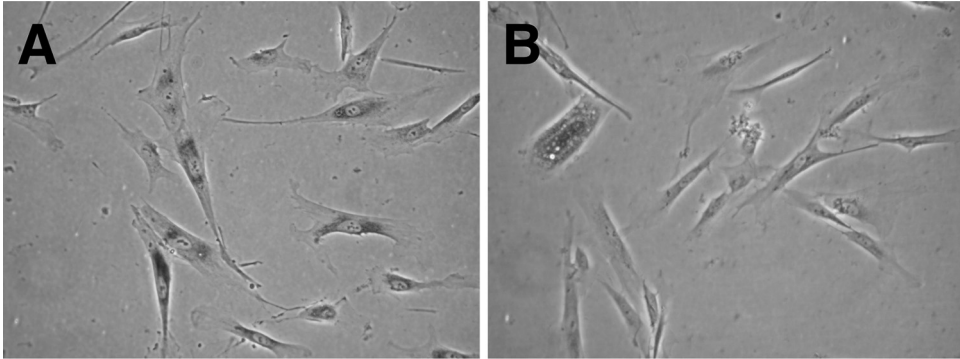


Fig. 3 SABG staining of primary fibroblasts (population doubling 38) at different pHs. **(a)** Staining at pH 4. **(b)** Staining at pH 6

7. A few tips for cell marking (segmentation):

- (a) The borders of adjacent cells must not overlap. If they do, analysis of the whole figure will fail. Therefore, mark cells that are far enough apart to avoid this problem.
- (b) Start marking at one point at the cytoplasmic border of the cell and continue by clicking with mouse left click along the border of the cytoplasm all around the cell until you reach the starting point. Once done press “Enter” and the line will close automatically.
- (c) When marking a cell – do not create any loops that will automatically be regarded as segments (cells) and will create an error.
- (d) You may mark one control area per figure to save time, although in most cases it will result in a much less accurate quantitation due to an unequal spread of background over the figure. Therefore, standardization to the figure background is best achieved by marking a background area adjacent to each analyzed cell.

Acknowledgments

This work was supported in part by The Legacy Heritage Biomedical Program of the Israel Science Foundation (grant No. 725/09—S.S.) and by a kind donation from the Slava Smolakowski Fund to Rambam Medical Center.

References

1. Campisi J, d’Adda di Fagagna F (2007) Cellular senescence: when bad things happen to good cells. *Nat Rev Mol Cell Biol* 8(9):729–740
2. Itahana K, Campisi J, Dimri GP (2007) Methods to detect biomarkers of cellular senescence: the senescence-associated beta-galactosidase assay. *Methods Mol Biol* 371:21–31
3. Braig M, Schmitt CA (2006) Oncogene-induced senescence: putting the brakes on tumor development. *Cancer Res* 66(6):2881–2884

4. Dimri GP, Lee X, Basile G, Acosta M, Scott G, Roskelley C, Medrano EE, Linskens M, Rubelj I, Pereira-Smith O et al (1995) A biomarker that identifies senescent human cells in culture and in aging skin in vivo. *Proc Natl Acad Sci USA* 92(20):9363–9367
5. Michaloglou C, Vredeveld LC, Soengas MS, Denoyelle C, Kuilman T, van der Horst CM, Majoor DM, Shay JW, Mooi WJ, Peeper DS (2005) BRAFE600-associated senescence-like cell cycle arrest of human naevi. *Nature* 436 (7051):720–724
6. Pendergrass WR, Lane MA, Bodkin NL, Hansen BC, Ingram DK, Roth GS, Yi L, Bin H, Wolf NS (1999) Cellular proliferation potential during aging and caloric restriction in rhesus monkeys (*Macaca mulatta*). *J Cell Physiol* 180 (1):123–130
7. Lee BY, Han JA, Im JS, Morrone A, Johung K, Goodwin EC, Kleijer WJ, DiMaio D, Hwang ES (2006) Senescence-associated beta-galactosidase is lysosomal beta-galactosidase. *Aging Cell* 5(2):187–195
8. Severino J, Allen RG, Balin S, Balin A, Cristofalo VJ (2000) Is beta-galactosidase staining a marker of senescence in vitro and in vivo? *Exp Cell Res* 257(1):162–171
9. Shlush LI, Itzkovitz S, Cohen A, Rutenberg A, Berkovitz R, Yehezkel S, Shahar H, Selig S, Skorecki K (2011) Quantitative digital in situ senescence-associated beta-galactosidase assay. *BMC cell biology* 12:16. doi:10.1186/1471-2121-12-16
10. Debacq-Chainiaux F, Erusalimsky JD, Campisi J, Toussaint O (2009) Protocols to detect senescence-associated beta-galactosidase (SA-beta-gal) activity, a biomarker of senescent cells in culture and in vivo. *Nat Protoc* 4 (12):1798–1806. doi:10.1038/nprot.2009.191
11. Kang HT, Lee KB, Kim SY, Choi HR, Park SC (2011) Autophagy impairment induces premature senescence in primary human fibroblasts. *PLoS One* 6(8):e23367. doi:10.1371/journal.pone.0023367
12. Zhang DY, Wang HJ, Tan YZ (2011) Wnt/beta-catenin signaling induces the aging of mesenchymal stem cells through the DNA damage response and the p53/p21 pathway. *PLoS One* 6(6):e21397. doi:10.1371/journal.pone.0021397

Analysis of Biomarkers of Caloric Restriction in Aging Cells

Yuanyuan Li and Trygve O. Tollefsbol

Abstract

Caloric restriction (CR) has been extensively documented for its profound role in effectively extending maximum lifespan in many different species. However, the accurate mechanisms, especially at the cellular level, for CR-induced aging delay are still under intense investigation. An emerging technique, recently explored in our laboratory, provides precisely controllable caloric intake in a cultured cellular system that allows real-time observation and quantitative analysis of the impact of CR on the molecular cellular level during the aging processes. This in vitro method allows investigation of the molecular mechanisms pertaining to how CR influences aging processes leading to life extension in human cellular systems. It will provide important clinical implications for future preventive approaches for aging and aging-related degeneration diseases in humans. Hence, we will discuss the detailed procedures of this novel technique as well as the analysis of relevant aging biomarkers and its broad application in the field.

Key words Caloric restriction, Aging, Cell senescence, β -Galactosidase assay

1 Introduction

Aging is an inevitable biological processes associated with degenerative changes at both the cellular and organic levels that result in multiple degenerative diseases and even death in senior populations. Advances in scientific understanding of basic aging mechanisms increase the likelihood of postponing aging processes and increasing the lifespan of humans. Among many well-investigated factors that effectively reverse the progression of aging, nutritional intervention has shown promising prospects due in part to its obvious merits such as safety and availability [1].

Energy control such as caloric restriction (CR), as a major nutritional manipulator, is by far the most effective environmental intervention that can extend maximum lifespan in many different species [2, 3]. Numerous studies have revealed the remarkable effects of CR on aging intervention and lifespan extension among

diverse species including yeast, worms, flies, fish, and even mammals such as mice [4–6]. In addition, studies in higher mammals such as nonhuman primates and humans revealed a profound influence of CR in delaying a wide range of aging-associated diseases such as cancer, diabetes, atherosclerosis, cardiovascular diseases, and neurodegenerative diseases [6–9]. However, besides the overwhelming effects of CR in experimental animal research, convincing outcomes between CR and aging delay/lifespan extension are limited in human studies primarily due to uncontrolled ethical limitations for long-term dietary control, especially lifelong CR studies, which can be much more easily controlled in animal studies. Potential mechanisms by which CR induces aging delay and prevents the onset of many aging-related degenerative diseases include the reduction of oxidative stress or regulation of metabolic pathways during aging progression [10–12]. However, the precise mechanisms of CR-induced longevity, especially in human systems, are not very well understood.

While acknowledging the maximal benefits of CR in experimental animals, it is of essential importance to apply this benefit to human health. A novel *in vitro* human cellular system explored in our laboratory could serve as a research bridge to investigate the effect of CR in human systems that may benefit future clinical applications [13, 14]. This *in vitro* system is designed to mimic CR-controlled longevity by reduction of glucose, the main caloric resource, in cell culture medium. This system allows more precise analysis of molecular mechanisms of CR and the effects of CR on human cellular lifespan, specifically at the cell molecular level. For example, a homogeneous cellular system provides an effective and consistent platform to monitor changes during aging progression which avoids fluctuant metabolic changes in organisms. Therefore, compared to aging research in experimental animals, this novel mammalian *in vitro* cellular system has numerous advantages and unique features that benefit sophisticated aging studies at the molecular level in human systems.

In this chapter, we will discuss detailed information on how to manipulate glucose concentrations and mimic CR effects in human cellular systems, population doubling (PD) calculations, aging biomarker observations during the aging processes, and data validation. This new technology detects molecular mechanisms of CR and CR-associated aging delay and lifespan extension in human cellular systems, which provides an excellent *in vitro* model to investigate aging and its important modulator, CR, especially for application to future human studies.

2 Materials

2.1 Cell Culture

2.1.1 Caloric Restriction (CR) in Cell Culture

1. Normal human fetal lung fibroblasts WI-38 (ATCC)
2. Dulbecco's modified Eagle medium (DMEM) with 4.5 g/L glucose (Invitrogen) for control cells
3. Glucose- and sodium pyruvate-free DMEM medium (Invitrogen) for CR cells
4. Glucose solution (Cellgro)
5. Fetal bovine serum (Atlanta Biologicals)
6. Penicillin/streptomycin (Mediatech)
7. Glucose Assay kit (BioVision)
8. 100 × 20 mm tissue culture disks (BD Falcon)

2.1.2 Population Doublings (PDs) Assessment

1. Microscopy (Nikon)
2. Neubauer hemocytometer

2.2 Aging Biomarkers Analysis

2.2.1 Senescence-Associated β -Galactosidase (SA- β -Gal) Activity Assay

1. Phosphate-buffered saline (PBS)
2. Senescence β -galactosidase staining kit (cell signaling)
3. 5-Bromo-4-chloro-3-indolyl beta-D-galactoside (X-Gal) (Sigma)

2.2.2 Age-Related Gene Analysis

1. RNA extraction and cDNA reverse transcription: RNeasy kit (Qiagen), 2-mercaptoethanol, SuperScript II kit (Invitrogen)
2. Protein extraction: RIPA lysis buffer (Upstate Biotechnology), protease inhibitors
3. Related primers and specific antibodies
4. SYBR Green qPCR Master Mix (Invitrogen)
5. Roche LC480 thermocycler (Roche)
6. Western-blot electrophoresis apparatus

2.2.3 Age-Related Oxidative Stress Analysis

1. Reactive oxygen species (ROS) detection assay (Abcam)
2. Superoxide dismutase (SOD) assay (Cell Biolabs)
3. Nitric oxide (NO) assay (Abcam)
4. Fluorescence spectroscopy

2.2.4 Age-Related DNA Damage Analysis

1. DNA purification kit (Promega)
2. DNA double-strand break assay (Cell Biolabs)

3. 8-Hydroxydeoxyguanosine (8-OHdG) DNA damage assay (Cell Biolabs)
4. Microplate reader

3 Methods

3.1 Cell Culture

3.1.1 Caloric Restriction (CR) in Cell Culture

The method described below is suitable for analysis of CR effects on cultured human cells. Normal diploid human fibroblasts such as fetal lung fibroblasts, skin fibroblasts, and vascular fibroblasts can be used for this study (*see Note 1*). We will use WI-38 human fetal lung fibroblasts as an example to describe this method [14]. Since glucose is the primary energy resource in culture medium, we have developed an in vitro system to mimic CR by reducing glucose concentration in cell growth medium. Control WI-38 cells grown in 100 mm culture plates are maintained in DMEM medium supplemented with regular glucose level at 4.5 g/L. To restrain glucose, cells are cultured in glucose- and pyruvate-free DMEM medium, and different CR levels can be obtained by adding various concentrations of glucose in the medium depending on the relevant study design. All culture media are supplemented with 10 % fetal bovine serum and 1 % penicillin/streptomycin in the presence of 5 % CO₂ at 37 °C. Culture media should be replaced once every other day. The actual glucose concentration in the glucose restriction medium will be assessed by the Glucose Assay kit.

3.1.2 PDs Assessment and Sample Collection During Aging Progression

1. WI-38 cells are typically within the range of 15–20 PDs (young cells) upon initiation of the experiment (*see Note 1*). Parallel culture control and CR cells should be set up in corresponding mediums and the experiments need be initiated synchronously.
2. PDs calculation: to quantify replication, cells are passaged weekly at a seeding density of 10⁵ cells per plate and counted using a hemocytometer until cells reach 90–95 % confluence. Cellular PDs are calculated based on the following formula: $\log[(\text{number of cells harvested})/(\text{number of cells seeded})]/\log 2$ (*see Note 2*) [15]. The first confluent cells are designated as PD 0 when the experiments are initiated. The duration of cellular lifespan can be equally divided in three stages including early (young), intermediate (middle age), and late passages (aging or senescence).
3. Harvest glucose restriction treated- and untreated-WI-38 cells and extract total RNA, DNA, and protein once a week during the cellular lifespan; carefully label and appropriately store samples at different PDs.

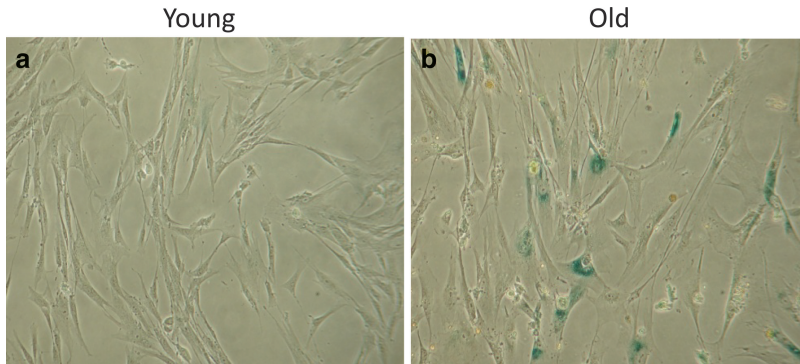


Fig. 1 Cellular senescence is determined by the senescence β -galactosidase (SA- β -gal) assay. Human WI-38 fibroblasts at a proliferating state (young, **a**) and senescence (old, **b**) are subjected to SA- β -gal staining and photographed. *Blue staining cells* are SA- β -gal positive or senescent cells. Magnification, $\times 100$

4. Determine cellular replicative senescence at the end of late passage in the cellular lifespan by morphological changes (*see Note 3*) and senescence-associated β -galactosidase (SA- β -Gal) activity assay. Experiments are considered to terminate when cells stop dividing and cellular senescence occurs.

3.2 Aging Biomarkers Analysis

3.2.1 Senescence-Associated β -Galactosidase (SA- β -Gal) Activity Assay

1. Treat the WI-38 normal human fetal lung fibroblasts with normal level of glucose and glucose restriction medium as described previously; measure SA- β -gal activity in control and CR cells weekly with PDs calculation [14].
2. Wash cells twice in phosphate-buffered saline (PBS) and then fix in 0.5 % glutaraldehyde for 10 min at room temperature.
3. Incubate cells at 37 °C with fresh senescence-associated β -gal (SA- β -gal) stain solution containing 1 mg/ml of 5-bromo-4-chloro-3-indolyl beta-D-galactoside (X-Gal) overnight according to the manufacturer's protocols (cell signaling).
4. Blue-dye precipitated cells are SA- β -gal-positive cells and are considered to have undergone cellular senescence (Fig. 1) (*see Note 4*). Positive-stained cells are counted by using a Nikon digital camera at 40-fold magnification. Counts should be performed at five random locations, and every field is counted three times for the determination of the mean percentage of positively stained cells.
5. Compare senescence rate (SA- β -gal-positive cells) in control and CR groups at different PDs during aging progression.

3.2.2 Age-Related Gene Analysis

1. Harvest the control and CR-treated WI-38 cells weekly at different PDs during the cellular lifespan and extract RNA,

Table 1
Selective age-related genes

Gene	Function in aging	Expression change during aging	References
<i>p16^{INK4a}</i>	Cell-cycle inhibitor; induce senescence growth arrest via activated p16–pRB pathway	Activation	[13, 14, 22]
<i>p21</i>	Cell-cycle inhibitor; induce senescence growth arrest via activated p21–p53 pathway	Activation	[22, 23]
<i>p53</i>	Tumor suppressor gene; induce senescence growth arrest via activated p21–p53 pathway	Activation	[22, 23]
<i>pRB</i>	Tumor suppressor gene; induce senescence growth arrest via activated p16–pRB pathway	Activation	[22, 24]
<i>hTERT</i>	Human telomerase reverse transcriptase; activate <i>hTERT</i> expression to elongate telomeres	Inactivation	[13, 14, 22]
<i>Ras</i>	Oncogene; cause oncogene-induced senescence	Activation	[22, 25]

reverse transcript cDNA and extract protein as described in Subheading 3.1.2, **step 3** followed by the routine protocols.

2. Analyze age-related gene expression such as *p16^{INK4a}* at RNA and protein levels by using the methods of real-time PCR and western blot followed by the routine protocols. Detection of specific age-related genes should be based on specific cell type as well as study design (Table 1) (*see Note 5*).
3. Monitor and compare age-related gene expression changes in control and CR-treated WI-38 cells at different PDs during the cellular lifespan.

**3.2.3 Age-Related
Oxidative Stress Analysis**

1. Harvest control and CR-treated WI-38 cells at different PDs during the cellular lifespan according to Subheading 3.1.2, **step 3**.
2. Analyze age-related oxidative stress parameters such as ROS, SOD, and NO according to the manufacturer’s protocols (*see Note 6*).
3. Compare alterations of these parameters in control and CR cells at different PDs during aging progression.

**3.2.4 Age-Related DNA
Damage Analysis**

1. Harvest the control and CR-treated WI-38 cells weekly at different PDs during the cellular lifespan and extract DNA according to Subheading 3.1.2, **step 3** followed by the routine protocols.

Table 2
Selective CR-related genes

Gene	Function in CR	Expression change	References
<i>SIRT1</i>	NAD-dependent histone deacetylase; activation of <i>SIRT1</i> is seen in different animal organs affected by CR	Increased expression	[14, 29]
<i>Foxo</i>	Forkhead transcription factors; controls various biological functions; involves CR-related longevity	Decreased expression	[29, 30]
<i>PGC-1α</i>	Regulates mitochondrial function and glucose homeostasis during CR	Increased expression	[29, 31]
<i>PPAR-γ</i>	Insulin sensitizer; increase insulin sensitivity during CR	Increased expression	[28, 32]
<i>Glucose-6-phosphate</i>	Involve energy metabolism such as glycolysis	Increased expression	[28]
<i>Hsp105</i>	Heat shock protein; stress-related gene	Decreased expression	[28]

2. Analyze age-related DNA damage parameters such as 8-OHdG by using commercially available kits (*see Note 7*).
3. Compare alterations of these parameters in control and CR cells at different PDs during aging progression.

3.2.5 Comparison of CR-Related Gene Profiles

1. Analyze CR-related gene expression such as *SIRT1* at the RNA and protein levels using real-time PCR and western blot followed by the routine protocols as described in Subheading 3.2.2 (*see Note 8* and Table 2).
2. Monitor and compare CR-related gene expression change in control and CR-treated WI-38 cells at different PDs during the cellular lifespan.

3.3 Data Interpretation

Our in vitro cellular system mimics CR by reducing glucose concentration in cell growth medium. Following consecutive treatment and monitoring, extended lifespan or increased PDs can be observed in CR-treated WI-38 cells. Delayed cell senescence rate can also be determined by SA- β -gal assay under CR treatment. In addition, CR treatment can prevent age-associated oxidative stress and DNA damage. Altered age- and CR-related gene expression profiles such as decreased expression of certain age-dependent genes and increased expression of CR-related genes can be observed in CR-treated cells. Therefore, by comparing these biomarkers, we can easily investigate the effects of CR on aging processes at the cellular and molecular levels in human systems (Fig. 2).

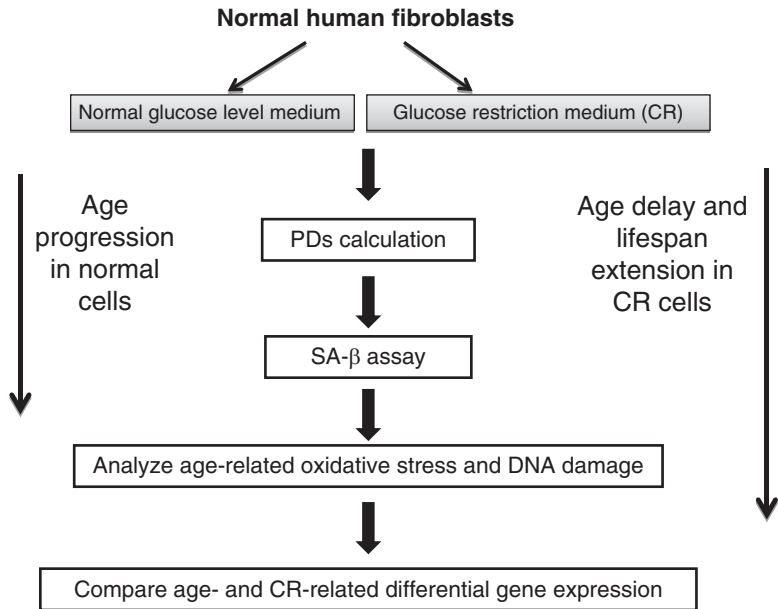


Fig. 2 Schematic representation of the procedure for aging biomarker analyses in the CR in vitro model

4 Notes

1. Normal human diploid fibroblasts such as fetal lung fibroblasts, skin fibroblasts, and vascular fibroblasts with a finite replicative lifespan in vitro are the most commonly used cell types to manifest aging [16, 17]. Other types of human normal cells including human lymphocytes and certain epithelial cells can also be applied in specifically designed aging studies [18]. To induce the CR effects in cell culture, glucose restriction treatment should be initiated at the young stage of cells to allow persistent stimulation and permanent changes that affect aging processes.
2. PDs calculation is the most critical procedure in this method. Counting using a hemocytometer may lead to potentially inaccurate PD calculations. Therefore, an automated cell counter is encouraged for use in this study.
3. Another important biomarker for aging is cellular morphology (Fig. 1). The steady loss of replicative potential is accompanied by a greater heterogeneity of cell sizes. Senescent cells tend to be much larger and irregular as compared to cells at their earlier PDs. An increase in nuclear size, nucleolar size, and in the number of cytoplasmic vacuoles can be observed in senescent cells by light microscopy.

4. The SA- β -gal assay is the most extensively utilized biomarker for aging that catalyzes the hydrolysis of β -galactosides into monosaccharides at pH 6.0 and develops blue staining only in senescent cells [19, 20]. SA- β -gal activity is routinely detected cytochemically, manually discriminating negative from positive cells by light microscopy. Flow cytometry-based SA- β -gal assay yields better differentiation to quantitatively calculate positive-stained fibroblasts as compared to the routine cytochemical-based method [21].
5. Senescent cells show striking changes in gene expression. These changes include activation of cell-cycle inhibitors, such as cyclin-dependent kinase inhibitors (CDKIs) *p21* and *p16* and repression of cellular proliferation-promoted genes such as *hTERT* (human telomerase reverse transcriptase), *c-FOS*, *cyclin A*, *cyclin B*, and *PCNA* (proliferating cell nuclear antigen) [14, 22–25]. A gene expression microarray assay will help to identify more differentiated expression genes between cells treated with normal level of glucose and glucose-restricted medium.
6. In contrast to cells cultured in normal level of glucose medium, cells in glucose-restricted (CR) medium tend to have longer lifespan which may be attributed to reduced oxidative stress. Therefore, the oxidative stress parameters such as ROS, SOD, and NO could serve as useful markers in this study [11]. Other oxidative stress markers can be applied in this study including protein oxidation/nitration markers such as protein carbonyl content (PCC) and lipid peroxidation marker such as 4-hydroxynonenal (4-HNE).
7. Stress-induced cellular senescence results in stress-related DNA damage, which can be detected by certain parameters such as 8-OHdG. Another obvious marker for senescent cells is the lack of DNA replication, which is typically detected by the incorporation of 5-bromodeoxyuridine or H^3 -thymidine. Some senescent cells can also be identified by the cytological markers of senescence-associated heterochromatin foci (SAHFs) and senescence-associated DNA-damage foci (SDFs) [22, 26, 27].
8. CR studies conducted in experimental animals have indicated that CR treatment induces overwhelming gene profile changes that may contribute to CR-induced aging delay and longevity. For example, upregulation of SIRT1, an NAD-dependent histone deacetylase, has been confirmed to correlate with CR-induced longevity [14, 29]. Other known CR-related genes can be detected to determine the efficacy of this in vitro CR system [28–32].

Acknowledgments

This work was supported by grants from the American Institute for Cancer Research (AICR), the National Cancer Institute (CA 129415), Susan G. Komen for the Cure, and the American Cancer Society Award (IRG-60-001-47). Y.L. was supported by a Postdoctoral Award (PDA) sponsored by AICR, a Junior Faculty Development Grant by American Cancer Society Award, and UAB Comprehensive Cancer Center (CA 13148-31).

References

- Mathers JC (2006) Nutritional modulation of ageing: genomic and epigenetic approaches. *Mech Ageing Dev* 127:584–589
- Weindruch R, Walford RL (1988) The retardation of aging and disease by dietary restriction. Charles C. Thomas, Springfield, IL, p 436
- Sinclair DA (2005) Toward a undefined theory of caloric restriction and longevity regulation. *Mech Ageing Dev* 126:987–1002
- Cooper T, Mockett R, Sohal B et al (2004) Effect of caloric restriction on life span of the housefly, *Musca domestica*. *FASEB J* 18:1591–1593
- Forster M, Morris P, Sohal R (2003) Genotype of age influence the effect of caloric intake on mortality in mice. *FASEB J* 17:690–692
- Colman R, Anderson R, Johnson S et al (2009) Caloric restriction delays disease onset and mortality in rhesus monkeys. *Science* 325:201–204
- Cruzen C, Colman RJ (2009) Effects of caloric restriction on cardiovascular aging in non-human primates and humans. *Clin Geriatr Med* 25:733–743
- Roth GS, Ingram DK, Lane MA (2001) Caloric restriction in primates and relevance to humans. *Ann N Y Acad Sci* 928:305–315
- Holloszy JO, Fontana L (2007) Caloric restriction in humans. *Exp Gerontol* 42:709–712
- Koubova J, Guarente L (2003) How does calorie restriction work? *Genes Dev* 17:313–321
- Sohal R, Weindruch R (1996) Oxidative stress, caloric restriction, and aging. *Science* 273:59–63
- Merry B (2002) Molecular mechanisms linking calorie restriction and longevity. *Int J Biochem Cell Biol* 34:1340–1354
- Li Y, Liu L, Tollefsbol TO (2010) Glucose restriction can extend normal cell lifespan and impair precancerous cell growth through epigenetic control of hTERT and p16 expression. *FASEB J* 24:1442–1453
- Li Y, Tollefsbol TO (2011) p16(INK4a) suppression by glucose restriction contributes to human cellular lifespan extension through SIRT1-mediated epigenetic and genetic mechanisms. *PLoS One* 6:e17421
- Greenwood S, Hill R, Sun J et al (2004) Population doubling: a simple and more accurate estimation of cell growth suppression in the in vitro assay for chromosomal aberrations that reduces irrelevant positive results. *Environ Mol Mutagen* 43:36–44
- Hayflick L (1979) The cell biology of aging. *J Invest Dermatol* 73:8–14
- Cristofalo VJ, Pignolo RJ (1993) Replicative senescence of human fibroblast-like cells in culture. *Physiol Rev* 73:617–638
- Bolognesi C, Abbondandolo A, Barale R (1997) Age-related increase of baseline frequencies of sister chromatid exchanges, chromosome aberrations, and micronuclei in human lymphocytes. *Cancer Epidemiol Biomarkers Prev* 6:249
- Dimri GP, Lee X, Basile G et al (1995) A novel biomarker identifies senescent human cells in culture and in aging skin in vivo. *Proc Natl Acad Sci USA* 92:9363–9367
- Lee BY, Han JA, Im JS et al (2006) Senescence-associated β -galactosidase is lysosomal β galactosidase. *Aging Cell* 5:187–195
- Noppe G, Dekker P, de Koning-Treurniet C (2009) Rapid flow cytometric method for measuring senescence associated beta-galactosidase activity in human fibroblasts. *Cytometry A* 75:910–916
- Campisi J, d'Adda di Fagagna F (2007) Cellular senescence: when bad things happen to good cells. *Nat Rev Mol Cell Biol* 8:729–740
- Jackson JG, Pereira-Smith OM (2006) p53 is preferentially recruited to the promoters of growth arrest genes p21 and GADD45 during replicative senescence of normal human fibroblasts. *Cancer Res* 66:8356–8360

24. Stein GH, Beeson M, Gordon L (1990) Failure to phosphorylate the retinoblastoma gene product in senescent human fibroblasts. *Science* 249:666–669
25. Mason DX, Jackson TJ, Lin AW (2004) Molecular signature of oncogenic ras-induced senescence. *Oncogene* 23:9238–9246
26. Narita M, Núñez S, Heard E et al (2003) Rb-mediated heterochromatin formation and silencing of E2F target genes during cellular senescence. *Cell* 113:703–716
27. d’Adda di Fagagna F, Reaper PM, Clay-Farrace L et al (2003) A DNA damage checkpoint response in telomere-initiated senescence. *Nature* 426:194–198
28. Lee CK, Klopp RG, Weindruch R et al (1999) Gene expression profile of aging and its retardation by caloric restriction. *Science* 285:1390–1393
29. Li Y, Daniel M, Tollefsbol TO (2011) Epigenetic regulation of caloric restriction in aging. *BMC Med* 25:98–110
30. Brunet A, Sweeney LB, Sturgill JF et al (2004) Stress-dependent regulation of FOXO transcription factors by the sirt1 deacetylase. *Science* 303:2011–2015
31. Schilling MM, Oeser JK, Boustead JN et al (2006) Gluconeogenesis: re-evaluating the FOXO1-PGC-1alpha connection. *Nature* 443:E10–E11
32. Sung B, Park S, Yu BP, Chung HY (2004) Modulation of PPAR in aging, inflammation, and calorie restriction. *J Gerontol A Biol Sci Med Sci* 59:997–1006

Chapter 4

Cell Sorting of Young and Senescent Cells

Graeme Hewitt, Thomas von Zglinicki, and João F. Passos

Abstract

Cellular senescence is the irreversible loss of proliferative potential and is accompanied by a number of phenotypic changes. First described by Hayflick and Moorhead in 1961, it has since become a popular model to study cellular aging. The replicative lifespan of human fibroblasts is heterogeneous even in clonal populations, with the fraction of senescent cells increasing with each population doubling (PD). Thus, the study of individual cells in mass culture is necessary in order to properly understand senescence and its associated phenotype. Cell sorting is a process that allows the physical separation of cells based on different characteristics which can be measured by flow cytometry. Here, we describe various methods by which senescent cells can be sorted from mixed cultures and discuss how different methods impact on the posterior analysis of sorted populations.

Key words Cell sorting, Cellular senescence, Flow cytometry

1 Introduction

Aging is characterized by random accumulation of unrepaired cellular and molecular damage. The stochastic nature of damage is thought to contribute to the extensive heterogeneity observed during the aging process [1].

Hayflick and Moorhead showed that embryo-derived fibroblasts can divide 50 ± 10 times before arresting irreversibly when cultured in vitro. The potential number of divisions that cells could undertake became known as the “Hayflick limit,” and the phenomenon was termed replicative senescence [2]. However, it was soon discovered that there was extensive heterogeneity in the division potential of individual cells and that the so-called Hayflick limit was not due to cells in a mass culture reaching senescence simultaneously, but rather to a progressive increase of the fraction of cells reaching senescence at each passage.

In their now classic experiment, Smith and Whitney showed heterogeneity in the doubling potential between cells from the

same clonal origin [3], suggesting that the replicative potential of individual cells is influenced by stochastic factors.

Other studies have shown that the fraction of proliferation-competent cells within a culture decreases progressively with the number of population doublings. These studies have used BrdU labeling [4], Ki67 [5], p21 [6] immunostaining, and a p53-reporter assay [7] to assess the proliferative capacity of cells. It was also shown that the percentage of cells stained positive for γ -H2A.X as a response to functionally uncapped telomeres increased gradually with population doubling level [8].

These data are consistent in showing that a proportion of cells drop out of the cell cycle at each PD and that this proportion increases with the age of the culture. The properties of these early “dropouts” are of great interest in the study of cellular aging and can be determined after physically separating these cells from mass culture.

Senescent cells, by definition, differ from proliferating cells in a wide variety of factors. These include gene expression [9], cell and nuclear size [10], shape and structure, mitochondrial mass, function and production of reactive oxygen species (ROS) [11], accumulation of age pigment (lipofuscin) [12], activity of β -galactosidase at near-neutral pH (senescence-associated β -galactosidase, SA- β -Gal) [13], secretion of proteins [14, 15], and chromatin remodeling [16]. Recently, increased expression of WNT16B [17] and decreased expression of LaminB1 [18] have been proposed as senescent biomarkers.

Not all of these markers are suitable for physical separation of cells using fluorescence-activated cell sorting (FACS). More importantly, no single marker is known to be completely specific to senescent cells, and a number of these markers differ gradually between proliferating and senescent cells. Recently, our group has proposed that a combination of Ki-67 or PCNA negativity and γ H2A.X positivity can be used to reliably assess the senescent state of cells both in vitro cultures and in mice tissue sections [6]. We first estimated fraction of senescent cells from observed growth curves using a mathematical model. Then, we tested several candidate senescent markers and compared them with the results from the model. Using this method we found that the combination of Ki67 negativity with high γ H2A.X foci density (>5 per nucleus) in fibroblasts provided the best fit to the mathematical model [6].

Here, we describe various methods by which senescent cells can be identified in mass culture and physically separated using FACS. Some of these methods use antibody staining of nuclear antigens that require the permeabilization and fixation of cells, which can severely limit the analytical choices available following sorting. These methods, however, will more often result in clearly separated populations of senescent and proliferating cells. In contrast, there are few markers that allow sorting of live senescent cells such as cell

size, lipofuscin content or fluorescent ROS-indicator dyes. These parameters generally vary gradually between the two populations, so specified cutoffs must be set. The limits of these cutoffs are not absolute and so the quantification of the frequency of senescent vs. non-senescent cells cannot be obtained, and sorting will result in an enrichment of senescent cells, but not in the production of a “pure” population.

2 Materials

2.1 Cell Culture

1. Dulbecco's modified Eagle's medium (DMEM) with 10 % fetal bovine serum, 1 % penicillin/streptomycin and 1 % glutamate.
2. $1\times$ phosphate-buffered saline [$1\times$ PBS].
3. Solution of trypsin–EDTA (5 g of trypsin, 2 g of EDTA per liter of distilled water).

2.2 Immunofluorescence Staining of Ki67 and γ H2A.X in Fixed Cells

1. Paraformaldehyde (2 %).
2. PBG-Triton: (0.2 % fish skin gelatin, 0.5 % bovine serum albumin [BSA] and 0.5 % Triton X-100 in phosphate-buffered saline [$1\times$ PBS]).
3. Rabbit polyclonal antibody anti-Ki67 (Abcam, cat. no. Ab15580).
4. Mouse monoclonal anti- γ H2A.X (Upstate Biotechnology, cat. no. 05-0636).
5. Anti-mouse fluorescein-conjugated secondary antibody Alexa Fluor 594 (Molecular Probes, cat. no. A-11005).
6. Anti-rabbit fluorescein-conjugated secondary antibody Alexa Fluor 488 (Molecular Probes, cat. no. A-21206).

2.3 BrdU Staining

1. Wash buffer: $1\times$ Ca^{2+} - and Mg^{2+} -free PBS with 0.5 % w/v bovine serum albumin BSA (Sigma).
2. Denaturing solution: 2 M HCl in $1\times$ Ca^{2+} - and Mg^{2+} -free PBS with 0.5 % w/v BSA (Sigma) [dissolve BSA in PBS prior to adding HCl to avoid permanent precipitation of the BSA].
3. Dilution buffer: $1\times$ Ca^{2+} - and Mg^{2+} -free PBS with 0.5 % v/v Tween-20 (Sigma), 0.5 % w/v BSA (Sigma).
4. FITC-labeled AntiBrdU monoclonal antibody (Pharmingen Cat#33284X) or FITC-labeled IgG control (Pharmingen Cat#35404X). Note: BrdU is a known carcinogen.
5. Propidium iodide (Note: Propidium iodide (PI) is known to be toxic and carcinogenic).
6. Ice-cold 70 % ethanol (BDH Lab Suppliers).
7. M sodium borate (Sigma), pH 8.

2.4 FACS Analysis and Sorting

1. FACS calibration beads of different sizes and/or fluorescence intensities (Sphero™ Rainbow Calibration Beads) (Pharmin-gen Cat No#556286) or (Partec 3 μ M calibration beads) (Partec Cat Code#05-4007).
2. 1 %Triton X-100, degassed PBS 1 \times .

2.5 Vital Stainings for ROS and MMP

1. Dihydrorhodamine 123 (DHR123) is available from Invitrogen either as powder (10 mg vial, Cat# D-632) or as ready-to-use 5 mM stock solution in DMSO (Cat# D-23806). A 10 mM stock solution of DHR123 is prepared by adding 2.89 ml DMSO to the 10 mg vial. As DHR123 is readily oxidized by air, the stock solution is immediately aliquoted under N₂ atmosphere in 100 μ l each and frozen at -20°C .
2. 5,5',6,6'-Tetrachloro-1,1',3,3'-tetraethylbenzimidazoly-carbocyanine iodide (JC-1) (Molecular Probes 5 mg, Cat# T-3168). To prepare a stock solution, dilute JC-1 at 2.5 mg/mL in dimethylsulfoxide (DMSO) by adding 2 mL of DMSO to the 5 mg vial. To avoid repeated freeze/thaw cycles, aliquot the stock immediately into portions, each sufficient for one day of experimental work, and store them at -20°C until required for use. Staining procedure must be carried under no direct intense light and incubation in the dark, since JC-1 is light sensitive.
3. Dihydroethidium (hydroethidine) is available in a 25 mg vial, as a stabilized 5 mM solution, or in 10 vials of 1 mg each from Invitrogen. As DHE is readily oxidized by air, it is advisable that 3 μ l aliquots are prepared under N₂ atmosphere and stored at -20°C . Staining procedure must be carried out under no direct, intense light and incubation in the dark, because DHE is light sensitive.
4. MitoSOX™ Red mitochondrial superoxide indicator is available from Invitrogen (50 mg vials Invitrogen Catalog # M36008). A stock solution 5 mM is prepared by adding 13 μ l DMSO to the 50 mg vial. As MitoSOX™ is readily oxidized by air, it is advisable that 3 μ l aliquots are prepared under N₂ atmosphere and store at -20°C .
5. RPMI 1640 phenol-free without additives (Sigma).
6. Dulbecco's modified Eagle's Medium (DMEM) without additives (Sigma).

3 Methods

3.1 Setting Up the Flow Cytometer

FACS machines vary considerably in complexity. There are highly sophisticated close-circuit multichannel high-speed sorting machines, which are operated by highly trained specialist personnel, dedicated exclusively to sorting. However, sorting can be done

sufficiently well on much simpler (and cheaper) machines typically characterized by a sorting chamber fitted to an existing flow cytometer (*see Note 1*). On these machines, sorting will be the exception rather than the rule. In these settings especially, a number of issues are worth keeping in mind before setting out to perform a cell sorting experiment:

1. Preparation and calibration of the flow cytometer: Sheath fluid needs to be of ultrapure quality and should be degassed before use, especially for sorters that rely on piezo crystal action. The system is calibrated using fluorescent beads to ensure optimum performance and reproducibility. Sorting efficiency and the quality of separation is tested using a mixture of two preparations of calibration beads of different sizes. Reanalysis of the sorted fractions should show more than 20-fold enrichment of the sorted fraction. Reanalysis of a defined volume can also be used to count the number of sorted particles obtained and thus to optimize the sorting conditions (*see Note 2*).
2. Sterility: Sterile sorting is possible even in simple flow cytometers. We sterilize the system by running 0.1 % hypochlorite solution both as sample and sheath fluid for 20–30 min and thoroughly swabbing external orifices with the same solution. Following bleaching sterile degassed $1 \times \text{Ca}^{2+}$ - and Mg^{2+} -free PBS is run through for 10 min in order to remove residual bleach which could have a cytotoxic effect. For the sorting experiments, sheath fluid is autoclaved and the container for sheath fluid is replaced by an autoclavable glass bottle. FACS tubes are pre-sterilized by 0.1 % bleach neutralized by washing with $1 \times \text{Ca}^{2+}$ - and Mg^{2+} -free PBS. Cells are sorted directly into flasks with DMEM medium containing 5 % penicillin/streptomycin in order to minimize the possibility of infection.
3. Sorting speed: Senescent fibroblasts are large and sensitive to shear stress. While some systems offer extremely high sorting speeds, we find that the quality and integrity of the recovered cells decreases at higher speeds. We use rates of about 300 cells/s as a safe upper margin to sort cells for analytical purposes. To obtain live senescent cells for further cultivation, we recommend sorting speeds of not more than 100 cells/s.

3.2 Sorting of Fixed Cells

3.2.1 Following Antibody Staining for Nuclear Antigens

Ki67 and PCNA are expressed in proliferating cells regardless of cell-cycle phase (G1, S, G2 and M phases) but are absent in nonproliferating cells (G0) and thus serve as potential “negative” markers of senescence. It has been shown that the fraction of Ki67-positive nuclei declines with each population doubling in human fibroblast and mesothelial cell cultures [5]. Increased expression of inhibitors of cyclin-dependent kinases p16 and p21 has been reported in senescent cells and can be used as “positive” marker for senescence (*see Note 3*). The formation of DNA damage foci,

more specifically, phosphorylation of Ser-139 of histone H2A.X (γ H2A.X formation) by ATM/ATR kinases, has been shown to increase gradually as cells grown in culture reach senescence [6], as well as in various tissues with age [19–21]. It is thought that these DNA damage foci are the result of telomere shortening, which contributes to telomere uncapping [8]. However, our group has recently demonstrated that acute stress (whether caused by oxidative stress or DNA-damaging agents) can contribute to DNA damage foci co-localizing with telomeres, irrespectively of telomere length [19]. While telomere-associated DNA damage is probably the best marker available for the detection of senescent cells, it cannot be accurately detected using conventional flow cytometry and will not be considered in this chapter.

Both DDR proteins and cyclin kinase inhibitors are not present exclusively in senescent cells. A DDR can be activated transiently and lead to a reversible cell-cycle arrest to allow for DNA damage to be repaired. For this reason the use of just one of these markers to assess senescence can lead to an overestimation of the senescent population. A combination of proliferation markers (such as Ki67 and PCNA) and DDR proteins might allow a more accurate separation of senescent cells [22]. Reliable antibodies for all of these markers are available from a number of major distributors.

Immunofluorescence
Staining of PCNA/Ki67
and γ H2A.X in Fixed Cells

1. Cell fixation: Cells are incubated in 1 mL of 2 % paraformaldehyde in PBS for 10 min at room temperature. Paraformaldehyde is removed and cells are washed three times for 5 min with $1 \times$ PBS.
2. Cell permeabilization: Cells are incubated for 45 min at room temperature with 1 mL PBG-Triton (*see Note 4*).
3. Permeabilization solution is removed and cells are resuspended in 400 μ L of Rabbit polyclonal antibody anti-Ki67 (first primary antibody) in a 1:250 dilution (diluted in PBG-Triton).
4. Cells are incubated for 1 h at room temperature with gentle agitation.
5. Cells are washed three times for 5 min each with PBG-Triton.
6. Following PBG-Triton removal, cells are resuspended in a solution containing an anti-rabbit fluorescein-conjugated secondary antibody Alexa Fluor 488 in a 1:4,000 dilution (diluted in PBG-Triton).
7. Cells are washed twice with PBG-Triton for 5 min.
8. 400 μ L of the mouse monoclonal anti- γ H2A.X (second primary antibody) in a 1:2,000 dilution (diluted in PBG-Triton) is added (*see Note 5*).
9. Cells are incubated for 45 min to 1 h at room temperature.
10. Cells are washed twice with PBG-Triton for 5 min.

11. Following PBG-Triton removal, cells are resuspended in a solution containing an anti-mouse fluorescein-conjugated secondary antibody Alexa Fluor 594 in a 1:4,000 dilution (diluted in PBG-Triton).
12. Cells are incubated for 45 min to 1 h at room temperature.
13. Following three washes with $1 \times$ PBS, cells are resuspended in $1 \times$ PBS at a density of about $10^6/\text{mL}$ and analyzed by FACS. The cell population is defined in a forward (FSC) vs. sideward scatter (SSC) dotplot. Apoptotic cells (recognized by lower FSC and higher SSC, *see* ref. 23) and debris (low in both FSC and SSC) are gated out. FL1 (or any other fluorescence channel if a different fluorophore is used) is set at logarithmic. Using isotype controls, the gain for FL1 is set to obtain unstained cells within the first decade. The sorting gate is set at the minimum between unstained and stained cells, and sorting is started at a rate of about 300 cells/s.

3.2.2 Sorting of Fixed Cells After BrdU Incorporation

The absence of DNA replication for prolonged time spans, as shown by the failure to incorporate nucleotide analogs like BrdU, is regarded as one of the best criteria of cellular senescence. On a cell population level, this marker appears to be more specific than, for instance, staining for senescence-associated β -galactosidase [24]. However, BrdU incorporation (or rather its absence) is less specific for positive selection of senescent cells, as this fraction might contain a significant number of cells that are only temporarily withdrawn from the cell cycle. For that reason, a combination of immunostaining for DDR proteins and BrdU incorporation can provide a better separation of senescent cells. The technique involves DNA denaturation at low pH and leads to significant DNA degradation (*see* **Note 6**).

1. Growing cells are treated for 48 h with $20 \mu\text{M}$ BrdU (*see* **Note 7**). Cell density is adjusted thus that the culture is still in exponential growth phase at the end of this period. Cells are harvested and counted.
2. Cells are centrifuged at $300 \times g$ for 5 min, washed in $1 \times \text{Ca}^{2+}$ - and Mg^{2+} -free PBS and recentrifuged for 5 min.
3. The supernatant is aspirated and the pellet is loosened by tapping the tube. Ice-cold 70 % ethanol is added dropwise while vortexing to a final concentration of $100 \mu\text{l}/10^6$ cells, and cells are fixed by incubation at room temperature for 20 min.
4. Cells are resuspended in 1 ml wash buffer and centrifuged at $300 \times g$ for 5 min. The supernatant is aspirated and the pellet is resuspended in fresh denaturing solution at a concentration of $150 \mu\text{l}/10^6$ cells.
5. Cells are denatured by incubation at room temperature for 20 min.

6. Cells are resuspended in 1 ml wash buffer and centrifuged at $300 \times g$ for 5 min.
7. The supernatant is discarded and the pellet is resuspended in 0.5 ml 0.1 M sodium borate, pH 8.5, and incubated at room temperature for 2 min to neutralize residual acid. 1 ml wash buffer is added and the cell sample volume is divided into tubes for test and control. These are centrifuged at $300 \times g$ for 5 min and the supernatant is aspirated.
8. FITC-labeled AntiBrdU monoclonal antibody (BD Pharmin-gen Cat#33284X) or FITC-labeled IgG control (BD Pharmin-gen Cat#35404X) is diluted in dilution buffer with 20 μ l of antibody per 30 μ l of buffer.
9. Cells are resuspended in diluted antibody at a concentration of $50 \mu\text{l}/10^6$ cells and incubated in the dark at room temperature for 30 min. 1 ml wash buffer is added and cells are centrifuged at $400 \times g$ for 5 min.
10. The supernatant is aspirated. At this step, cells can optionally be stained with propidium iodide (PI) to reveal the cell-cycle distribution at the end of the BrdU incubation period (*see Note 8*). Stained or unstained cells are diluted with 1 ml $1 \times \text{Ca}^{2+}$ - and Mg^{2+} -free PBS for analysis.
11. Cells are analyzed with 488 nm excitation. The cell population is defined in a forward versus sideward scatter dotplot. BrdU incorporation is measured in FL1, set at logarithmic. Using isotype controls, the gain for FL1 is set to obtain unstained cells within the first decade. The sorting gate is set at the minimum between unstained and stained cells. Alternatively, if cells are PI stained, a polygon gate can be used to define sorted cells in a FL1/FL3 dotplot. Sorting is performed at a rate of about 300 cells/s.

3.3 Sorting of Live Cells

Sorting of live cells is ideal insofar as it does pose no limits whatsoever for subsequent analysis. However, the choice of the sorting gate position and the resulting enrichment of senescent cells are to some extent arbitrary.

3.3.1 Size and Autofluorescence

An increased cell size has long been known as a characteristic of senescent cells [10]. Size, as measured by FSC, has been used to FACS-sort populations of cells with a senescent phenotype from a culture of immortalized fibroblasts [25]. The cellular content of lipofuscin, the undegradable, autofluorescent “age pigment,” increases with time not only in postmitotic cells but also in proliferating ones. This increase becomes faster as cells approach senescence, probably because of higher oxidative stress resulting in faster accumulation, slower “dissolution” onto daughter cells due to slower cycling [26] and a decrease in the activity of cellular degradation pathways [27].

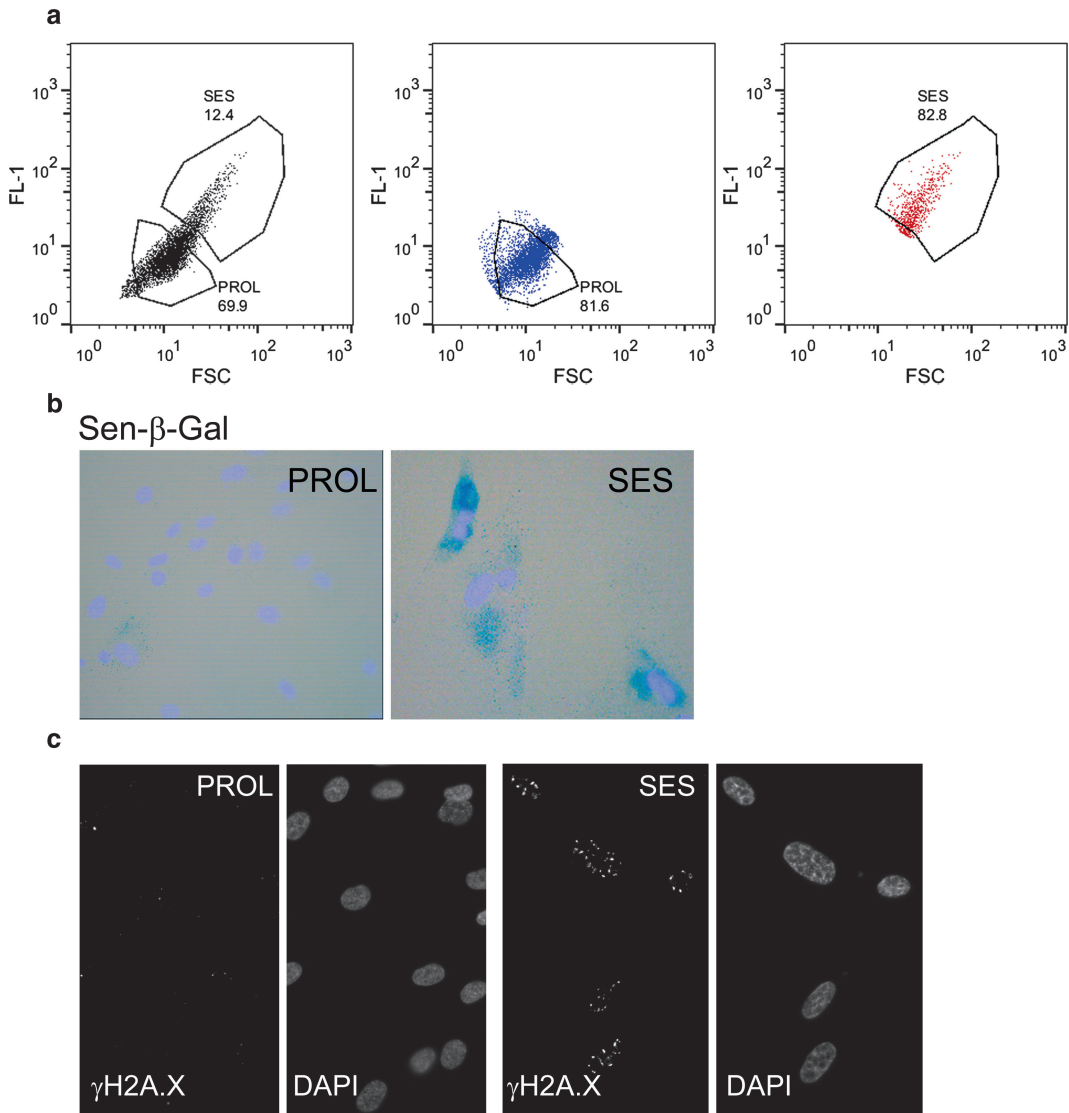


Fig. 1 Cell sorting of MRC-5 fibroblasts (PD 30), according to size (FSC) and lipofuscin content (FL-1). **(a) Left panel:** The gate for Senescent Sorted cells (SES) is defined so that it contains the cells with the highest values in FSC and FL1. Accordingly, the gate to sort proliferating cells (PROL, P5) contains the lowest quartile of all cells with respect to FSC and FL1. **Middle panel:** Reanalysis of MRC-5 sorted in the PROL gate. **Right panel:** Reanalysis of MRC-5 sorted in the SES gate. **(b)** Majority of SES cells are positive for Sen-β-Gal. **Light blue** (DAPI staining), darker cytoplasmic staining: Sen-β-Gal activity; **(c)** SES cells contain high frequency of γH2A.X foci

The combination of both cell size and autofluorescence (measured in FL-1) as sort parameters can allow good separation of senescent and proliferating cells in live cultures, as confirmed by using various markers of senescent cells including morphology and growth rates, Sen-β-gal, γ-H2A.X staining, telomere-associated DNA damage, and BrdU incorporation [11, 28, 29] (*see* Fig. 1).

1. Cells in the exponential growth phase are trypsinized and collected in DMEM plus 10 % FCS and immediately used for analysis and sorting in a FACS sorter (*see* **Note 9**).
2. Autofluorescence of unfixed cells is measured in FL1 (logarithmic). Cell size is monitored by FSC. FSC can be measured using either linear or logarithmic scale. Using linear scale for FSC, better resolution can be achieved (*see* ref. 28).
3. The population of live cells is defined in a FSC/SSC dotplot. Apoptotic cells and debris are gated out (*see* Subheading 3.2.1). Sorting gates are set in a FSC/FL1 dotplot. Using the upper and lower quartiles with respect to both FSC and FL1 to sort senescent and young proliferating cells, respectively, results in good resolution between the sorted populations (Fig. 1) and good enrichment of senescent cells [28] (*see* **Note 10**).
4. Cells are sorted at a rate of 100–300 cells/s and collected on ice. If cells must be concentrated, a low centrifugation speed ($200 \times g$) should be used (*see* **Note 11**).

3.3.2 Live Cell Stains for ROS and Mitochondrial Membrane Potential

Assessment of ROS levels in live cells using fluorescent ROS-indicator dyes has shown that in vitro senescence, like in vivo aging, is associated with high levels of endogenous reactive oxygen species [11]. The main source of ROS in cells is the mitochondrial electron transport chain and mitochondria have been implicated in cellular senescence. Changes in mitochondrial function have been reported during senescence [11, 30, 31], as well as damage to mtDNA [11]. While evidence is clear in establishing ROS as a major player in cellular senescence, there are still technical challenges to its detection in live cells. Many of the fluorescent dyes used for ROS detection are nonspecific and can be misused as a consequence the interpretation of results should be met with caution [32]. Although dichlorodihydrofluorescein diacetate (DCFH-DA) is commonly used for the fluorescent detection of ROS in cells, we have restrained from its use and will not include it in this chapter (*see* **Note 12**).

However, it has been shown that ROS-indicator dyes can be used to efficiently sort young and senescent cells [11]. FACS-sorted cells containing high MitoSOX intensity were shown to contain high levels of DNA damage, with the majority of DNA damage being located at telomeres [11]. Recently, we have shown that MitoSOX staining (a dye which detects mitochondrial superoxide anion) was as reliable a marker in detection of senescent cells as combination of Ki67/ γ H2A.X immunostaining [33].

DHR 123 Peroxide Staining (*See* **Note 13**)

1. Cells in exponential growth phase are trypsinized, collected in DMEM plus 10 % FCS, counted, washed once with PBS, and centrifuged for 5 min at $400 \times g$.
2. Supernatant is discarded.

3. Cell pellet is resuspended in 5 ml serum-free DMEM containing 15 μ l DHR123 stock solution (*see* Subheading 2) (final DHR123 concentration 30 μ M) (*see* **Note 14**).
4. Cells are incubated at 37 °C for 30 min in the dark.
5. After incubation, cells are centrifuged (400 \times *g*, 5 min) and supernatant discarded.
6. The pellet is resuspended in 3 ml of serum-free DMEM and is immediately used for analysis.
7. The population of live cells is defined in a FSC/SSC dotplot and apoptotic cells and debris are excluded. Median fluorescence is determined in FL1 (logarithmic), conveniently in a FSC/FL1 dotplot. Median autofluorescence of an unstained sample is also determined. Sorting gates are defined in FL1 (logarithmic), conveniently in a FSC/FL1 dotplot. Use the left and right quartiles with respect to FL1 to sort cells with highest (high FL1) and lowest (low FL1) peroxide levels (*see* **Note 15**).

JC-1 Staining (*See* **Note 16**)

1. Cells in the exponential growth phase are trypsinized and collected in DMEM plus 10 % FCS, counted, then washed in 1 \times PBS, and centrifuged at 400 \times *g* for 5 min.
2. Supernatant is discarded.
3. 1 \times 10⁵ cells are resuspended in 500 μ l of RPMI 1640 phenol-free without supplements (Sigma) and 1 μ l of JC-1 stock solution is added to give a final concentration of 1 μ g/ml (*see* **Note 14**).
4. The cells are incubated for 30 min at 37 °C.
5. The cells are harvested by centrifugation at 300 \times *g*, 4 °C for 5 min, washed with ice-cold PBS and resuspended in 200 μ l PBS at 4 °C.
6. The population of live cells is defined in a FSC/SSC dotplot and apoptotic cells and debris are excluded from sorting (*see* Subheading 3.2.1). FL1 and FL3 are set at logarithmic, and sorting gates are defined in a FL3/FL1 dotplot. The quartile of all cells with simultaneously the highest FL1 and lowest FL3 will be enriched for cells with low membrane potential, i.e. senescent cells. Accordingly, the quartile of cells with the lowest FL1 and highest FL3 constitutes the cells with the highest mitochondrial membrane potential.
7. To ensure that JC-1 staining is working, it is recommended that a control sample, in which mitochondria of all cells have been depolarized, be used. Treating cells with drugs able to collapse $\Delta\Psi$, such as the proton translocator carbonyl cyanide *p*-(trifluoromethoxy) phenylhydrazone (FCCP 20 μ M, 30 min), results in a dramatic change of the fluorescence distribution.

MitoSOX™ Mitochondrial
Superoxide Staining (See
Note 17)

1. Cells in the exponential growth phase are trypsinized and collected in DMEM plus 10 % FCS, counted, then washed in $1 \times$ PBS and centrifuged at $400 \times g$ for 5 min.
2. Supernatant is removed.
3. Cells are resuspended in 1 ml of serum-free DMEM containing 1 μ l of stock MitoSOX™ solution giving a final concentration of 5 μ M (see **Note 14**).
4. Cells are incubated, in the dark for 30 min at 37 °C.
5. Following incubation, cells are centrifuged at $400 \times g$ for 5 min.
6. Supernatant is removed.
7. Cells are resuspended in 3 ml of serum-free DMEM and immediately used for analysis.
8. The population of live cells is determined using a FSC/SSC scatter plot. Apoptotic cells and debris are excluded from analysis. Mean fluorescence is determined in FL3 (logarithmic) using a FSC/FL3 scatter plot. Median autofluorescence of an unstained control is also analyzed (see **Note 18**). Sorting gates are defined in FL3 (logarithmic), conveniently in a FSC/FL3 dotplot. Use the left and right quartiles with respect to FL3 to sort cells with highest (high FL3) and lowest (low FL3) superoxide levels.
9. The uptake of MitoSOX™ as a positively charged ion by mitochondria is dependent on membrane potential. Thus, an increase in fluorescence may be caused by increased superoxide production, an increased membrane potential, or a combination of both. Therefore, to aid the interpretation of results, further complimentary experiments should be carried out to assess membrane potential in parallel samples using JC1 or TMRM, for example [34].
10. Mitochondrial superoxide levels can vary with mitochondrial density; as such we recommend the use of Mitotracker green or NAO in a parallel sample to assess mitochondrial mass (see **Note 19**).

DHE Staining of Cellular
Superoxide (See **Note 20**)

1. Cells in the exponential growth phase are trypsinized and collected in DMEM plus 10 % FCS, counted, then washed in $1 \times$ PBS and centrifuged at $400 \times g$ for 5 min.
2. Supernatant is removed.
3. Cells are resuspended in 5 ml of serum-free DMEM containing 1 μ l of stock DHE solution giving a final concentration of 5 μ M (see **Note 14**).
4. Cells are incubated, in the dark for 30 min. at 37 °C.

5. Following incubation cells are and centrifuged at $400 \times g$ for 5 min.
6. Supernatant is removed.
7. Cells are resuspended in 3 ml of serum-free DMEM and immediately used for analysis.
8. The population of live cells is determined using a FSC/SSC scatter plot. Apoptotic cells and debris are excluded from analysis. Mean fluorescence is determined in FL3 (logarithmic) using a FSC/FL3 scatter plot. Median autofluorescence of an unstained control is also analyzed. Similarly to MitoSOX, sorting gates are defined in FL3 (logarithmic), conveniently in a FSC/FL3 dotplot. Use the left and right quartiles with respect to FL3 to sort cells with highest (high FL3) and lowest (low FL3) superoxide levels.

4 Notes

1. Magnetic affinity cell sorting (MACS) can also be used to sort cells. It is a method used for separation of cell populations based on surface markers. Cells are incubated with magnetic nanoparticles coated with antibodies raised against surface antigens and then sorted based on the presence or absence of magnetization. This method can only be used for sorting senescent cells based on expression of surface markers, so it is not applicable for most of the methods described in this chapter.
2. Before reanalysis, thorough cleaning of the flow cytometer is necessary to obtain reliable quantitative results. The cleaning function in most flow cytometers is not sufficient for this.
3. Most of the nuclear markers used in this section are at least somewhat sensitive to reversible growth arrest, e.g. by confluency or serum starvation. For instance, p21 is elevated in reversibly arrested G0 cells. On the other hand, evidence suggests that PCNA can occasionally be expressed in non-cycling G0 cells [35]. Background levels of DNA damage foci are slightly higher in S than in G1, possibly because of recognition of stalled replication forks [36], but might be suppressed in the absence of serum [37]. Cells should therefore reproducibly be sub-confluent at the time of sampling for sorting.
4. Permeabilization step, e.g. type of detergent and incubation time, should be optimized for different cell lines. Permeabilization has to be gentler for FACS compared to immunostaining as cells need to be kept intact while passing through the flow cytometer. Once optimized, cells should still appear as a well-defined population in FSC vs. SSC; at the same time, the permeabilization should allow efficient antibody penetration.

5. The antibody dilutions are given as an example only; concentrations must be optimized for each cell strain and antibody combination. Nevertheless, the indicated concentrations have been shown to work for several types of cancer cells, stem cells, and fibroblasts.
6. We isolated DNA from MRC-5 fibroblasts after processing for BrdU staining and analyzed it by pulsed field gel electrophoresis. Only heavily degraded DNA could be obtained, excluding all posterior analysis relying on high-molecular-weight DNA.
7. To obtain a more efficient selection of senescent cells, the BrdU incorporation time can be increased to up to 72 h. However, long-term BrdU treatment is cytotoxic and can also induce by itself a DNA damage response in some cell types [38]. Concentrations of BrdU should be optimized according to cell type used; the concentration provided has been optimized for MRC5 fibroblasts. Care must be taken not to expose cells to light while they are incorporating BrdU, as this amplifies DNA strand break generation.
8. For staining of DNA, incubate the cells in PI (Sigma) at 10 $\mu\text{g}/\text{ml}$ in PBS for 30 min in the dark at room temperature. Use 0.5 ml PI solution for 10^6 cells.
9. In growth-arrested cells, the rate of lipofuscin accumulation is increased because distribution of lipofuscin-containing lysosomes between daughter cells is the major if not the only way of diminishing lipofuscin levels. For that reason, exponentially growing cells should be used.
10. If the instrument is carefully calibrated from run to run, gate positions defined in a standard population of cells can be used for different experiments to measure quantitative shifts in the ratio between senescent and non-senescent cells (*see* ref. 28).
11. Sorting times including storage of cells in PBS can be lengthy (a few hours), and sorting itself constitutes a stress to the cells. At the end of this process, human fibroblasts become highly sensitive to shear stress, resulting in the loss of the majority of cells during centrifugation at higher G-force.
12. DCF is oxidized not only by various ROS and NOS decomposition products but also by cytochrome c and other peroxidases. It is prone to artefactual amplification of the fluorescence signal via redox cycling, thus leading to badly reproducible results, and it is a good substrate for various membrane transporters including the multidrug resistance protein MDR1 that is active in stem cells, thus compromising cellular retention.
13. Colorless dihydrorhodamine 123 is oxidized in live cells, e.g. by hydrogen peroxide in the presence of peroxidases, iron or cytochrome c, to form rhodamine 123. DHR also reacts with peroxynitrite. The fluorescent product of these reactions

accumulates in the mitochondria regardless of its origin. Rhodamine 123 fluoresces both in FL1 (green) and FL3 (red), but we find detection to be more sensitive in FL1.

14. When adding fluorescent dyes, make sure cells are fully resuspended as this can affect dye uptake.
15. The fluorescence of DHR123 in human fibroblasts remains fairly constant at room temperature and ambient light, for at least 1–2 h. If sorting takes longer than this, cells should be kept at 4 °C and away from light.
16. The JC-1 probe exists as a green-fluorescent monomer at low concentrations but forms aggregates at higher concentrations that exhibit a broad excitation spectrum and an emission maximum at 590 nm. JC-1 can be excited at 488 nm and detected in bivariate mode using the green channel for the monomer and the red channel for the aggregate. Mitochondrial uptake of JC-1 is dependent on membrane potential, with higher uptake (and higher probability of red fluorescence) at higher potential. Thus, the FL3/FL1 ratio is an indicator of mitochondrial membrane potential. Alternatively to using JC-1, a combination of TMRM and Mitotracker green can be used.
17. MitoSOX™ Red permeates live cells and is rapidly targeted to mitochondria (this mitochondrial uptake is driven by the presence of cationic triphenylphosphonium). This is a cationic derivative of dihydroethidium (DHE) and emits a red fluorescence (~590 nm) upon hydroxylation by superoxide anions. It is readily oxidized by superoxide but not other ROS. The oxidized product is highly fluorescent upon binding to nucleic acid.
18. MitoSOX™ staining intensity is generally quite low in certain cell types like human fibroblasts. For this reason a measure of autofluorescence for an unstained control must be taken as small changes in autofluorescence could significantly affect overall values of MitoSOX™ intensity.
19. For determination of mitochondrial mass by flow cytometry, one can use Mitotracker green (a green-fluorescent mitochondrial stain which localizes to mitochondria regardless of mitochondrial membrane potential) or nonyl acridine orange (NAO) which is well retained in the mitochondria independently of mitochondrial membrane potential and binds to mitochondrial cardiolipin. NAO strongly binds to plastic in the flow cytometer; thus, great care is needed not to contaminate the equipment, and unstained cells should be run as negative control after the final cleaning step.
20. Dihydroethidium (DHE), also known as hydroethidine, can be used to detect cellular superoxide levels. Cytosolic dihydroethidium exhibits blue fluorescence; once it is oxidized to 2-hydroxyethidium, it intercalates within DNA and stains the nucleus with a red fluorescence.

Acknowledgment

This work was supported by a BBSRC David Phillips Fellowship awarded to J.P.

References

1. Kirkwood TBL (2005) Understanding the Odd Science of Aging. *Cell* 120(4):437–447
2. Hayflick L, Moorhead PS (1961) The serial cultivation of human diploid cell strains. *Exp Cell Res* 25:585–621
3. Smith JR, Whitney RG (1980) Intracloal variation in proliferative potential of human diploid fibroblasts: stochastic mechanism for cellular aging. *Science* 207(4426):82–84
4. Kill IR et al (1994) The expression of proliferation-dependent antigens during the lifespan of normal and progeroid human fibroblasts in culture. *J Cell Sci* 107(2):571–579
5. Thomas E et al (1997) Different kinetics of senescence in human fibroblasts and peritoneal mesothelial cells. *Exp Cell Res* 236(1):355–358
6. Lawless C et al (2010) Quantitative assessment of markers for cell senescence. *Exp Gerontol* 45(10):772–778
7. Bond JA, Wyllie FS, Wynford-Thomas D (1994) Escape from senescence in human diploid fibroblasts induced directly by mutant p53. *Oncogene* 9(7):1885–1889
8. d'Adda di Fagagna F et al (2003) A DNA damage checkpoint response in telomere-initiated senescence. *Nature* 426(6963):194–198
9. Cristofalo VJ et al (1998) Age-dependent modifications of gene expression in human fibroblasts. *Crit Rev Eukaryot Gene Expr* 8(1):43–80
10. Cristofalo VJ, Kritchevsky D (1969) Cell size and nucleic acid content in the diploid human cell line WI-38 during aging. *Med Exp Int J Exp Med* 19(6):313–320
11. Passos JF et al (2007) Mitochondrial Dysfunction Accounts for the Stochastic Heterogeneity In Telomere-Dependent Senescence. *PLoS Biol* 5(5):e110
12. Terman A, Brunk UT (1998) Lipofuscin: Mechanisms of formation and increase with age. *APMIS* 106(2):265–276
13. Dimri GP et al (1995) A biomarker that identifies senescent human cells in culture and in aging skin in vivo. *Proc Natl Acad Sci USA* 92(20):9363–9367
14. Coppé JP et al (2008) Senescence-Associated Secretory Phenotypes Reveal Cell-Nonautonomous Functions of Oncogenic RAS and the p53 Tumor Suppressor. *PLoS Biol* 6(12):e301
15. Acosta JC et al (2008) Chemokine Signaling via the CXCR2 Receptor Reinforces Senescence. *Cell* 133(6):1006–1018
16. Narita M et al (2003) Rb-Mediated Heterochromatin Formation and Silencing of E2F Target Genes during Cellular Senescence. *Cell* 113(6):703–716
17. Binet R et al (2009) WNT16B Is a New Marker of Cellular Senescence That Regulates p53 Activity and the Phosphoinositide 3-Kinase/AKT Pathway. *Cancer Res* 69(24):9183–9191
18. Freund A et al (2012) Lamin B1 loss is a senescence-associated biomarker. *Mol Biol Cell* 23(11):2066–2075
19. Hewitt G et al (2012) Telomeres are favoured targets of a persistent DNA damage response in ageing and stress-induced senescence. *Nat Commun* 3:708
20. Herbig U et al (2006) Cellular Senescence in Aging Primates. *Science* 311(5765):1257–1257
21. Zglinicki TV et al (2005) Human cell senescence as a DNA damage response. *Mech Ageing Dev* 126(1):111–117
22. Lawless C et al (2010) Quantitative assessment of markers for cell senescence. *Exp Gerontol* 45(10):772–778
23. Sgonc R, Gruber J (1998) Apoptosis detection: An overview. *Exp Gerontol* 33(6):525–533
24. Wei W, Sedivy JM (1999) Differentiation between Senescence (M1) and Crisis (M2) in Human Fibroblast Cultures. *Exp Cell Res* 253(2):519–522
25. Gorbunova V, Seluanov A, Pereira-Smith OM (2003) Evidence that high telomerase activity may induce a senescent-like growth arrest in human fibroblasts. *J Biol Chem* 278(9):7692–7698
26. Sitte N et al (2001) Lipofuscin accumulation in proliferating fibroblasts in vitro: An indicator of oxidative stress. *Exp Gerontol* 36(3):475–486
27. Martinez-Vicente M, Sovak G, Cuervo AM (2005) *Protein degradation and aging*. *Exp Gerontol* 40(8,9):622–633
28. Martin-Ruiz C et al (2004) Stochastic Variation in Telomere Shortening Rate Causes

- Heterogeneity of Human Fibroblast Replicative Life Span. *J Biol Chem* 279(17): 17826–17833
29. Birket MJ et al (2008) The Relationship between the Aging- and Photo-Dependent T414G Mitochondrial DNA Mutation with Cellular Senescence and Reactive Oxygen Species Production in Cultured Skin Fibroblasts. *J Invest Dermatol* 129(6):1361–1366
 30. Hutter E et al (2004) Senescence-associated changes in respiration and oxidative phosphorylation in primary human fibroblasts. *Biochem J* 380(Pt 3):919–928
 31. Passos JF et al (2010) Feedback between p21 and reactive oxygen production is necessary for cell senescence. *Mol Syst Biol* 6:347
 32. Kalyanaraman B et al (2011) Measuring reactive oxygen and nitrogen species with fluorescent probes: challenges and limitations. *Free Radic Biol Med* 52(1):1–6
 33. Lawless C et al (2012) A Stochastic Step Model of Replicative Senescence Explains ROS Production Rate in Ageing Cell Populations. *PLoS One* 7(2):e32117
 34. Passos JF et al (2010) *Feedback between p21 and reactive oxygen production is necessary for cell senescence*. *Mol Syst Biol* 6:347
 35. Scholzen T, Gerdes J (2000) The Ki-67 protein: From the Known and the Unknown. *J Cell Physiol* 182:311–322
 36. D'Adda di Fagagna F et al (2003) *A DNA damage checkpoint response in telomere-initiated senescence*. *Nature* 426(6963):194–198
 37. Satyanarayana A et al (2004) Mitogen stimulation cooperates with telomere shortening to activate DNA damage responses and senescence signaling. *Mol Cell Biol* 24(12): 5459–5474
 38. Masterson JC, O'Dea S (2007) 5-Bromo-2-deoxyuridine activates DNA damage signalling responses and induces a senescence-like phenotype in p16-null lung cancer cells. *Anticancer Drugs* 18(9):1053–1068. doi:10.1097/CAD.0b013e32825209f6

Chapter 5

Studying the Replicative Life Span of Yeast Cells

David A. Sinclair

Abstract

The budding yeast *Saccharomyces cerevisiae* is a useful model for elucidating the pathways that control life span and the influence of environmental factors, such as calorie restriction (CR). For 75 years, CR has been studied for its ability to delay diseases of aging in mammals, from cancer to cardiovascular disease (McCay et al., *Nutr Rev* 33:241–243, 1975). In many other species, reducing calorie intake extends life span, including unicellular organisms (Jiang et al., *FASEB J* 14:2135–2137, 2000; Lin et al., *Science* 289:2126–2128, 2000), invertebrates (Rogina and Helfand, *Proc Natl Acad Sci U S A* 101:15998–16003, 2004), and rodents (Martín-Montalvo et al., *Oncogene* 30:505–520, 2011). Here we describe how to calorically restrict yeast cells, the methods used to determine the replicative life span (RLS) of budding yeast cells, how to selectively kill daughter cells using the mother enrichment program (MEP), how to measure recombination frequency at the rDNA locus, how to isolate large quantities of old cells, and how to analyze the circular forms of DNA known as extrachromosomal rDNA circles (ERCs), a cause of aging in *S. cerevisiae* (Petes, *Cell* 19:765–774, 1980; Sinclair and Guarente, *Cell* 91:1033–1042, 1997; Defossez et al., *Mol Cell* 3:447–455, 1999).

Key words Yeast aging, Life span, RLS, Bud scars, Mother cell enrichment program, ERC

1 Introduction

The quest to understand why we age and how to slow it has been a goal ever since humans evolved. In recent years, great strides have been made in elucidating genes that influence the pace of aging. Studying humans and even rodents is a daunting and costly task that is not amenable to genetic screening. Instead, many researchers have turned to simpler organisms with shorter life spans to identify conserved longevity genes and small molecules that might regulate it.

The simple dietary manipulation known as calorie restriction (CR) can extend life span of rodents and delay most age-related diseases. But what underlies this effect? In recent years, the budding yeast *Saccharomyces cerevisiae* has become one of the leading models for uncovering conserved causes of aging and understanding how CR works. Today, dozens of yeast longevity genes are known and we have a good understanding of how CR works in yeast, the best for any studied species [1, 2].

There are two ways to define yeast life span. One is the number of days a yeast culture remains viable in a hypometabolic stationary phase. This is known as the “chronological life span” [3]. Alternatively, one can determine life span for a single cell based on the number of times it divides, known as “replicative life span” or “RLS” [4].

Despite yeast being a simple eukaryote, accurately determining its replicative life span is not a simple task, even with the invention of the “mother enrichment program” or “MEP.” The MEP is an estradiol-inducible daughter killing system [5] that allows much higher purity of old cells. The MEP also allows RLS to be determined as a function of viability over time. But the system is not perfect: ~8 % of daughter cells in the MEP can still form microcolonies due to “leakiness” [5]. To precisely quantify mean and maximum RLS of a given strain, micromanipulation is still necessary. Only with time does one become skilled at this technique, and often beginners do not obtain reliable data the first time. Even using the MEP, very pure populations of old cells require a magnetically sorting procedure to separate the mothers from daughters in a culture.

2 Materials

2.1 Preparation of Yeast for Replicative Life Span Analysis

1. $2.2\times$ supplemented yeast extract/peptone (YEP) media: 22.2 g/L Bacto Yeast extract (Becton, Dickinson and Company), 44.4 g/L Bacto Peptone (Becton, Dickinson and Company) in water and filter sterilized with a 0.22 μm vacuum filter. Supplement the media by adding 40 mL/L 0.5 % adenine solution and 20 mL/L for the remaining 1 % amino acid solutions.
2. Use flat wooden toothpicks that have a rounded end opposite to the pointed tip. Diamond brand is suitable. Sterilize by autoclaving in a small beaker with aluminum foil on the top and toothpicks point down. Discard any toothpicks that have a sharp protruding splinter that could damage the agar.
3. 4 % agar: Bacto Agar (Becton, Dickinson and Company); 8 g of agar is added into 200 mL of water and autoclaved.
4. 18 M Ω Milli-Q grade water is used for all media preparations.
5. Petri plates: 100 \times 15 mm (Falcon).
6. Amino acid and adenine (Sigma-Aldrich) stock solutions (w/v): 0.5 % adenine, 1 % uridine, 1 % tryptophan, 1 % histidine, and 1 % leucine solutions are prepared with water and filter sterilized using a 0.22 μm vacuum filter. These supplement the auxotrophies that are particular to the W303AR strain of yeast. Different amino acids may be required for other strains.

7. $1.05 \times$ YEP: 10.5 g/L Bacto Yeast extract (Becton, Dickinson and Company), 21.1 g/L Bacto Peptone (Becton, Dickinson and Company) in water and autoclaved. Supplement after autoclaving as with the preparation of $2.2 \times$ YEP media, but use half the amount of solutions.
8. 40 % (w/v) glucose stock solution.
9. Dissection needle kit (Cora Styles Needles n Blocks, Cat. No. 1025, 105 Cypress Pt., Hendersonville, NC 28739, Phone# 828-629-9528). We use 10 or 25 μ M needles that are made by polishing flat the ends of optic fibers.
10. 17β -Estradiol (Sigma, St. Louis, MO), only if using the MEP.

2.2 Magnetic Sorting of Old Yeast

1. Phosphate-buffered saline (PBS): A $10 \times$ stock solution is prepared with 1.37 M NaCl, 27 mM KCl, 43 mM $\text{Na}_2\text{HPO}_4 \cdot 7\text{H}_2\text{O}$, 14 mM KH_2PO_4 , adjusted to pH 7.4 with HCl if required and then promptly autoclaved. A $1 \times$ working solution is made by diluting 1:10 with sterile water.
2. EZ-Link Sulfo-NHS-LC-Biotin, m.w. 556.59 (Thermo Scientific/Pierce).
3. Streptavidin-coated paramagnetic iron beads (Thermo Scientific/Pierce). Other labs have used Dynabeads streptavidin (Invitrogen/Life Technologies).
4. Calcofluor fluorescent brightener 28 (Sigma, St. Louis, MO).
5. 17β -Estradiol (Sigma, St. Louis, MO), only if using the MEP.

2.3 Isolation of ERCs

1. $1 \times$ TE buffer: 10 mM Tris-Cl, pH 8.0 and 1 mM EDTA, pH 8.0.
2. Sorbitol solution: 0.9 M sorbitol (Fisher), 0.1 M Tris-Cl, pH 8.0, 0.1 M EDTA are prepared with water and filter sterilized using a 0.22 μ m filter.
3. Zymolyase solution: Dissolve 0.3 mg/mL Zymolyase (20,000 U/g; ICN Immunobiologicals) in sorbitol solution and store at 4 °C.
4. 2-Mercaptoethanol.
5. 10 % (w/v) sodium dodecyl sulfate (SDS).
6. 5 M potassium acetate solution (do not adjust pH).

2.4 Analysis of ERCs

1. Random primed DNA labeling kit (Roche Diagnostics).
2. ProbeQuantTM Sephadex G-50 columns (Amersham Pharmacia).
3. dCTP³² (PerkinElmer).
4. Pre-hybridization buffer: 100 μ l boiled salmon sperm DNA (5 mg/mL stock ssDNA), 1 g dextran sulfate, 1 mL 10 %

SDS, 0.56 g NaCl in 10 mL water. Heat at 65 °C for 30 min to dissolve the salts into solution.

5. 10× TBE electrophoresis stock buffer: 0.89 M Tris base, 0.89 M boric acid, 20 mM EDTA, pH 8.0. A 1× working solution is made by diluting 1:10 with water.
6. 0.4 M NaOH solution.
7. 0.25 M HCl solution.
8. 20× SSC stock solution: 3 M NaCl, 0.3 M Na₃citrate·2H₂O. Adjust the pH to 7.0 with 1 M HCl. A 2× working solution is made by diluting 1:10 with water.
9. Nylon membrane (NEN).
10. Wash buffers: 2× SSC 0.1 % SDS (low stringency) at room temp, 1× SSC 0.1 % SDS (medium stringency) at 60 °C, 0.1× SSC 0.5 % SDS (high stringency) at 60 °C, 0.1× SSC (brief wash) at room temp.

2.5 Recombination Analysis

1. 1.05× YEP: prepared in the same manner as previously described.
2. 2.2× YEP: unlike 2.2× YEP that is prepared for life span assay plates, do not supplement this stock solution with adenine or histidine. The solution can also be autoclaved rather than filter sterilized. Otherwise, it is prepared in the same manner.
3. 3 % agar: Bacto Agar (Becton, Dickinson and Company); 6 g of agar is added into 200 mL of water and autoclaved.
4. Large Petri plates: 150 × 15 mm (VWR).
5. Glass beads for spreading can be obtained from Amazon.com from Carolina Biological Supply Company. They are sterilized by autoclaving.

3 Methods

3.1 Preparation of Yeast for Replicative Life Span (RLS) Analysis with and Without MEP

1. The day prior to starting the experiment, the yeast should be streaked onto agar plates containing media identical to that used for the life span assay. The yeast should be as fresh as possible. If taken directly from the freezer, allow at least 2 days of consecutive streaking for recovery. Use yeast only from a plate that has been struck within 24 h, i.e., as fresh and actively growing as possible. *See Note 1* for tips on handling the yeast and plates.
2. Using a sterile toothpick, transfer a tiny amount (barely visible to the eye) from the previous nights' streak onto a fresh plate that will be used for the life span analysis. The yeast should be a barely visible dot on the plate. Allow the transferred cells to grow for an additional 3–5 h at 30 °C.

3. After attaching the inverted plate onto the stage of the microscope, use the tip of the fiber-optic needle to drag a bunch of cells, i.e., however many will fit under the needle, approximately ≥ 1 cm away from the plated dot of cells. You may need to repeat this several times to move enough cells.
4. Find cells that are relatively small and healthy looking; i.e., round and exhibiting no aberrant morphology. Use the tip of the needle to array 40 cells, in sets of 5, planting a single column. Allow enough spacing between each cell so as to see no more than 3–5 cells within the field of view using a $10\times$ objective. Each group of 5 cells can be marked by stabbing the needle into the agar, i.e., use 1 stab, 2 stabs, 3, 4, and a right angle, any pattern that will help you to find and keep track of the column of cells on the plate. The same pattern can then be marked in a notebook with columns divided into groups of 5.
5. After arraying the cells, remove the prepared life span assay plate from the microscope stage and incubate at 30°C for 1–2 h, after first sealing the plate with Parafilm to prevent the loss of moisture. After returning the plate to the microscope, the yeast will have undergone about 1–2 divisions. If a cell died before the first division, we excluded it from the data set assuming the transfer was deleterious. Most wild-type strains divide at least five times before senescing.
6. With the needle, pull apart the cells and leave behind the smaller budded cell (Fig. 1). This starting “virgin” cell will henceforth be the mother cell during the assay. Discard the rest of the divided cells by moving them to the left, corresponding to about $1/3$ of a field of view away from the virgin mother cell. Not all cells will be ready for separation at the same time. Thus, you may need to come back after another 30 min to 1 h after the others were separated. Importantly, mother cells are dragged carefully in the opposite direction to the daughters every 2–5 divisions about $1/4$ of a field of view to avoid running out of nutrients. If using the MEP, first grow the mother cells on YPD medium with no estradiol. Move the founding virgin cells to agar with $1\ \mu\text{M}$ estradiol [5] (Fig. 2).
7. Incubate the sealed plate at 30°C for 1–2 h. After transferring the plate back to the microscope, pick off and, from now onwards, discard the smaller daughter buds from your starting virgin mother cell and record the number of divisions for each arrayed mother cell.
8. Repeat **step 7** throughout the day. The mother cells get enlarged after progressive divisions and eventually become much easier to tell apart from the daughter cells. Their rate of division will also slow down, with some old cells taking up to 4 h to divide. If a cell does not divide after 8 h we considered it

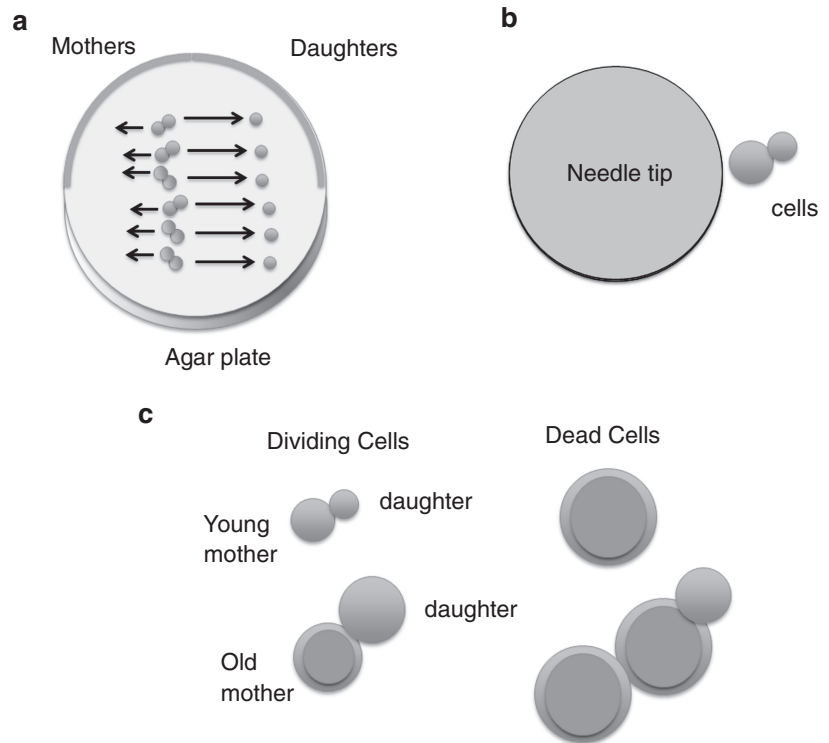


Fig. 1 The yeast replicative life span (RLS) assay. Individual yeast cells are planted in a single column on agar plates, using a 25 or 50 μm fiber-optic needle. If using the MEP, then the virgin cells are transferred from an island of YPD (yeast extract/Bacto Peptone/glucose) or the test medium to the same medium with 1 μM estradiol (*see* Fig. 2). Micromanipulation of yeast is typically performed using a 10 \times objective. After the placement of “virgin” mother cells in an array on the plate, daughter cells that bud off are removed using the needle and are swept away, at least one field of view, from the mother cells so as not to compete with them for nutrients. The amount of divisions each mother cell has undergone during each micromanipulation session is then recorded. (a) Move daughter cells at least one field of view away from the mothers, which can be moved in the opposite direction if daughter colonies grow too large. (b) Relative sizes of the 25 μm needle and young yeast cells. (c) Appearance of young mothers, old mothers, and dead cells. Cells at the end of life are always large, with a thick cell wall, and may have cells permanently attached. Their final morphology depends on the strain and the medium

dead because we did not see any cell produce a viable daughter after this time. Old cells may try to bud, and the attached bud may bud, but we do not consider these true offspring because the cells did not fully separate. Unless you are using the MEP, you can store plates in the cold room until the next day but it is preferable to let the cells divide as many times as possible during the day.

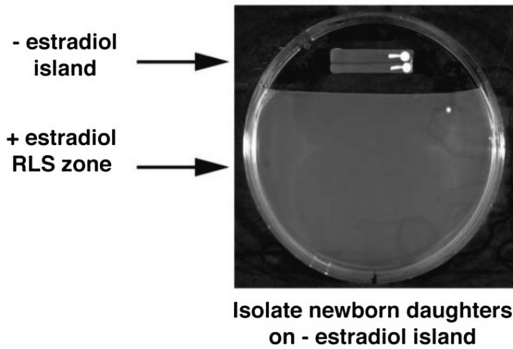


Fig. 2 Use of the mother enrichment program (MEP) in RLS assays (from ref. 5). After incubation on YPD (or the test medium) for at least two divisions, virgin cells are transferred to the estradiol-containing portion of the plate for life span analysis. Life spans are then performed, as described in Fig. 1. Image reproduced from ref. 5

9. When all of the cells have died (~10 days), you are now ready to graph their replicative life spans. Each row pertaining to each specific cell's division number is tallied, and the numbers are plotted as the % cells that are still alive during each round of division. For example, at the start of the assay, 100 % of the cells are alive after 0 divisions have occurred, whereas 0 % of the cells are alive at the amount of divisions that the last remaining mother cell has undergone.

3.2 Magnetic Sorting of Old Yeast Cells with and Without MEP

1. Inoculate 5 mL of $1 \times$ YPD with yeast and grow overnight at 30°C while shaking at 200 rpm.
2. Next morning, resuspend enough cells into 50 mL $1 \times$ YPD to reach an optical density at 600 nm (O.D. 600) of approx. 1.0 (2×10^7 haploid cells/mL) later that day. This usually entails diluting ~1 mL of overnight culture into 50 mL $1 \times$ YPD. The starting O.D. 600 should be about ~0.15–0.20.
3. When the O.D.600 reaches ~1.0, spin down cells with a clinical centrifuge at $1,000 \times g$ for 5 min. Wash cells once in 1 mL of sterile $1 \times$ PBS. Resuspend the cells in 1 mL $1 \times$ PBS and transfer into a microfuge tube.
4. The cells are now ready to be biotinylated. Remove the EZ-Link Biotin from the freezer and thaw at room temperature. It is VERY sensitive to moisture. When thawed, add 8 mg of sterile EZ-link biotin per 1×10^8 cells. Gently shake the cells for 15 min at room temperature.
5. Wash the cells 7 times using 1 mL $1 \times$ PBS to remove the excess biotin label.

6. Resuspend cells in 1 mL YPD. Determine the cell density using a hemacytometer. We use a Bright-Line hemacytometer (Hausser Scientific, Horsham, PA). Add 2×10^8 cells to 4 L of freshly made $1 \times$ YPD (autoclaved for 20 min). If using the MEP, 17β -estradiol is added to the culture after 2 h growth at 30° at a final concentration of $1 \mu\text{M}$. Shake at 30°C overnight or for up to 120 h if using the MEP. Viability can be assessed during this time if using the MEP, which serves as an indicator of RLS. Samples are taken and pelleted by centrifugation at $800 \times g$. All but 100 μL of the supernatant is removed, washed once with 1 mL of fresh YPD, and pelleted again. Cells are then resuspended in 500 μL YPD and plated on YPD. Colonies are counted after 3 days incubation at 30°C . Viability is calculated as CFUs/mL and expressed as percentage of viability compared to CFUs/mL at the 0 or 4 h time points [5] $1,000 \times g$ and thoroughly aspirate off as much medium as possible. Resuspend the cells in 20 mL cold $1 \times$ PBS and place on ice.
7. Wash the magnetic beads twice with $1 \times$ PBS. Add 250 μL of the washed magnetic bead slurry per 1×10^8 cells. Incubate on ice with occasional swirling for 2 h in order for the biotinylated cells to bind to the magnetic beads.
8. The sorting procedure is performed in a 4°C room. Add equal volumes of the resuspended magnetic bead-coated cells into 16×150 mm glass culture tubes and insert into a magnetic tube rack. We use a BioMag tube rack (Polysciences Inc., Warrington, PA) for the magnetic separation. Wait 15–20 min for the magnetic bead-coated older cells to move towards the side of the tube facing the magnet. Remove young cells that are still in the solution gently with a 10 mL pipette and save the solution. Add the same volume of cold $1 \times$ YPD into each tube so that the meniscus reaches the top of the magnet and wait 15–20 min again for magnetic separation to occur.
9. Repeat **step 6**, using cold $1 \times$ YPD each time and vortexing gently to resuspend the bead-coated cells. Repeat this step eight times. Check the yield using a hemacytometer. The recovery is typically 50 % of the starting amount of cells.
10. Count bud scars by first adding 20 μL of cells into 100 μL $1 \times$ PBS. Add a few grains of calcofluor fluorescence brightener and incubate for 5 min at room temperature. Add 1 mL $1 \times$ PBS and centrifuge at $1,000 \times g$ in a microfuge for 20 s. Wash cells once in 1 mL $1 \times$ PBS, spin down again, and resuspend in 100 μL of $1 \times$ PBS. With a single sorting most cells will have 4–9 bud scars.
11. Place approximately 10 μL of cells onto a glass slide and cover with a coverslip. Observe the stained bud scars using UV fluorescence microscopy. If your cell sorting has been

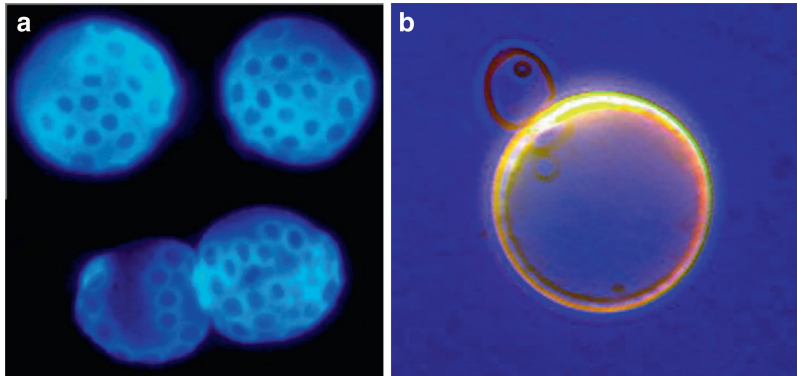


Fig. 3 Distinguishing old yeast cells from young. **(a)** Old yeast cells that have been sorted using magnetic sorting and stained with calcofluor dye. Each blue stained ring is a “bud scar,” a deposit of chitin that remains on the surface of the cell wall at each site of division (photo credit James Claus). **(b)** Young and old yeast cells stained with bromophenol blue, showing the larger size and thicker cell wall of the old mother cell

successful, your old population of cells should contain on average ~5–12 more bud scars per cell than the young population of cells (Fig. 3).

3.3 Isolation of ERCs

1. Resuspend cells in 500 μ l sorbitol solution. Add 25 μ l Zymolyase and 50 μ l of 0.28 M 2-mercaptoethanol (20 μ l 2-mercaptoethanol in 980 μ l water). Depending on the activity of the Zymolyase, incubate at 30 °C for 15–45 min. You can monitor the efficiency of spheroplasting (i.e., digestion of the cell wall) by adding ~2 μ l of 10 % SDS into a 10 μ l aliquot of cells. If 85–95 % cells appear lysed when viewed under a microscope, then they are ready for the next step (*see Note 2*).
2. Add 80 μ l of 10 % SDS, invert several times to mix and incubate for 20 min at 65 °C. The solution should become viscous.
3. Add 200 μ l of 5 M potassium acetate solution. Invert several times and leave on ice at least 30 min. A white precipitate should form.
4. Centrifuge for 3 min at 16,000–20,000 $\times g$ (or maximum speed) in a microcentrifuge for 10 min. Remove supernatant and add 1 mL 100 % ethanol. Mix well by inverting several times and centrifuge at 12,000 rpm (or maximum speed) for 10–20 min.
5. Resuspend the DNA pellet in 300 μ l TE. Add 1 μ l of 10 mg/mL of RNase and incubate for 30 min at 37 °C.
6. Precipitate the DNA by adding 1 mL of ice cold 100 % ethanol and centrifuging at 12,000 rpm (or maximum speed) in a microfuge for 10 min. After removing the ethanol, dry the pellet in a speed vac and resuspend in 50 μ l of TE. The resuspended DNA pellet can now be stored frozen at –80 °C.

3.4 Analysis of ERCs

1. The analysis of ERCs essentially involves performing a Southern blot and probing for ERCs with a radio-labeled rDNA fragment. Begin by casting a large 1 % agarose gel using $1\times$ TBE. Load samples, along with molecular weight markers and electrophorese overnight at 30 V.
2. Soak the gel for 30 min in 500 mL water containing 25 μ L of 10 mg/mL ethidium bromide solution and photograph with a ruler using UV light.
3. Wash the gel for 30 s with water and then soak the gel for 30 min in 0.25 M HCl, with gentle rocking.
4. Rinse the gel in water again and soak in 1 L of 0.4 M NaOH for 20 min, along with gentle rocking, to denature the DNA.
5. Set up a transfer apparatus, using 0.4 M NaOH as the transfer buffer. The transfer apparatus consists of a shallow glass tray that is filled two thirds of the way to the top with transfer buffer. A glass plate is then used to partially cover the top of the tray, leaving a 1–2 in. gap on either side. A rectangular piece of 3M Whatman paper is then cut, wetted in transfer buffer, and placed over the top of the glass plate, with the ends being sufficiently long enough to soak in the transfer buffer through the 1–2 in. gaps. This will act as a wick for the transfer. The wick should also be approximately an inch wider, on either side, than the nylon transfer membrane.
6. Drain the gel and place carefully on top of the wick, using a glass pipette to gently roll away any air bubbles that may be trapped under the gel.
7. Cut a piece of nylon transfer membrane, corresponding to the size of the gel. Wet the membrane in transfer buffer and lay on top of the gel, using the pipette to smooth away any air bubbles.
8. Cut three pieces of Whatman 3M paper corresponding to the same shape as the nylon membrane, only a few millimeters smaller at each edge. Soak the piece in transfer buffer and lay each of them on top of the membrane and gel, again using the glass pipette to carefully smooth away any air bubbles after each piece is laid.
9. Place a stack of paper towels, 3–4 in. high, on top the gel setup; lay a piece of glass plate over the stack and add a light weight on top to stabilize the plate. Use a bubble level to ensure the plate is perfectly level.
10. Wrap the outer part of the transfer apparatus, i.e., the exposed wick, with Saran wrap to prevent evaporation of the transfer buffer. The transfer apparatus is now left to transfer for 12 h.
11. Rinse the membrane with $2\times$ SSC to remove any agarose residue. The wet membrane is then irradiated with UV light (254 nm) at an intensity of 1,200 J/cm². This corresponds to a setting of 1,200 using a Stratagene UV crosslinker.

12. Add 10 mL pre-hybridization buffer into a 200 mL capacity cylindrical glass hybridization bottle (Boeckel Scientific). Place the transferred membrane into the bottle and incubate for 1 h at 65 °C while rolling.
13. The radio-labeled probe is prepared as per kit instructions. After the reaction is complete, bring the probe reaction volume up to 50 μ L with 1 \times TE. Prepare a Sephadex G-50 column by spinning for 1 min at 550 $\times g$, in order to compact the bead matrix. Pipette the 50 μ L probe reaction volume into the prepared Sephadex G-50 column and spin for 2 min at 550 $\times g$.
14. Boil the radio-labeled probe DNA for 5 min and carefully add into the bottle containing your membrane and pre-hybridization solution. Incubate overnight at 65 °C.
15. The membrane is washed with the wash buffers until counts are reduced to only severalfold over background. The exact washing times must be empirically determined by the user. The bound probe can now be analyzed using either a Phosphorimager cassette or X-ray film.

3.5 Recombination Analysis

1. Cells are first inoculated in the appropriate media, i.e., containing 2 % glucose for controls and either 0.1 or 0.5 % glucose for calorie-restricted cells, and preincubated overnight at 30 °C while shaking (*see Note 3*). The following day, cells are reinoculated into fresh media at an O.D. 600 of ~0.15–0.20 and allowed to grow until log phase has been reached (O.D. 600 of 0.8–1.0).
2. Prepare serial dilutions of cells in 1 \times PBS until a final concentration of 3–4 $\times 10^3$ cells/mL is reached. Pipette 500 μ L of this final dilution onto large plates and spread evenly using sterile glass beads along with a gentle shaking motion.
3. After the plates are dry, incubate at 30 °C until colonies are large enough to be easily counted by eye. This usually takes about 2 days of growth at 30 °C. Plates are then transferred into 4 °C for at least 2–3 days or until red pigmentation becomes evident, following a marker loss event.
4. Half-sector colonies are counted by eye on each plate. Colonies that are completely red are subtracted from the total colony number on each plate. A half-sector colony represents a marker loss event that has occurred during the first cell division. The wild-type W303AR strain, when grown in media containing 2 % glucose, has a recombination frequency of approximately 1×10^{-3} , whereas deleting *SIR2* elevates the frequency of recombination approximately tenfold, to approximately 1×10^{-2} .

4 Notes

1. Replicative life span analysis

- (a) Since the procedure takes approximately 10–14 days to complete, it is imperative that the agar plates do not overly dehydrate. Plates should always be carefully wrapped in Saran wrap or Parafilm when in the incubator or cold room. Plates should also be poured with more agar than usual to take into account dehydration and shrinkage of the agar. We usually pour the plates with the agar level reaching two thirds to three quarters of the way to the top of the plate.
- (b) The technique takes practice to manipulate cells and to differentiate the old mother from daughter cells, especially in the first two days when there is little size difference. The researcher should not let the yeast divide more than once when starting out. In this case, two researchers may work as a team to check on the cells every hour. The more experienced researcher can also help the novice distinguish mother from daughter.
- (c) If the agar eventually shrinks to a point at which it is difficult for the dissection needle to reach the surface, part of the plate's edge may be then carefully cut away using a hot scalpel to allow for more freedom of motion. However, it is best to reserve this until absolutely necessary since the larger opening will now permit faster dehydration to occur. Also, when cutting the plate, it should be tilted upwards to prevent any toxic fumes from the molten plastic from coming into contact with the cells.
- (d) Plates should be poured a day before using so that they are given ample time to evaporate away excess moisture; otherwise dissection becomes difficult. If you are testing the effect of a labile compound (e.g., resveratrol), however, you should make the compound freshly and use the plates within 24 h and complete the experiment as fast as possible, allowing cells to grow for 10–15 h per day. We took a microscope home so we could dissect late at night and first thing in the morning. Plates can be air-dried upside down in an incubator or a laminar low hood. If the plates change color (e.g., resveratrol plates turn brown), this is a sign that the compound has been compromised.

- (e) With the plates being continually opened and closed during this time period, it is important to avoid contamination. If a small fungal or bacterial growth occurs far from the plated yeast, it can be successfully removed by cutting away the contaminated section with a sterile scalpel blade. Another troublesome source of contamination may be the presence of fruit flies which given the chance, will walk all over the surface of the plate, usually ruining the experiment.
- (f) When a cell is picked up on the needle, the plates should be moved gently since a sudden jarring motion may cause a cell to drop off.
- (g) Old mother cells are especially fragile and must not be overly “bashed” with the tip of the dissection needle to dislodge recalcitrant daughter cells. At this point they have a higher tendency to “pop” under pressure. A good technique is to move the needle tip close to the daughters and allow them to move gently to the tip due to surface tension. Never lift a cell off the agar unless absolutely necessary and then only for 20 s or less, to avoid the cells drying out.
- (h) Obviously, mother cells should not be allowed to overgrow since it then becomes next to impossible to keep score, but they should also not be dissected too often since we have found that this tends to shorten their life span, possibly due to mechanical damage. Two to three divisions between each dissection session for W303 are about right.
- (i) Try to dissect the cells every day. Keeping the plates in the cold room for an entire day is acceptable, but longer periods, i.e., over an entire weekend, should be avoided because life span can be reduced. The rate at which the cells are dividing will determine how many times they can be dissected during the day.
- (j) Someone just beginning should limit themselves to no more than two columns of cells to dissect at once, i.e., one experiment and one control. Later on, as skill level and rapidity increases, 3–9 columns of cells may be attempted. We would discourage placing more than three columns of cells onto one plate, since this increases nutrient depletion and allows the plate to dehydrate faster since each individual plate is kept open longer during dissections.

- (k) For life span dissections, we have found it best not to autoclave the 2× YEP medium but to instead filter through a 0.22 μ m filter prior to use. We also supplement the medium with additional amino acids, corresponding to the auxotrophies that are unique to a strain. If a compound is added to the medium, be aware that it could be sensitive to light or oxygen. Such is the case for many polyphenols, e.g., resveratrol.
- (l) It is best that the cells be dragged across the surface of the agar with the needle, rather than being lifted off of the surface. This ensures that the cells are continuously in contact with the media.
- (m) The more dissections you can perform per day, especially during the first week, the better results you will obtain, i.e., longer overall life spans.
- (n) We use Petri plates that have been removed from the plastic wrapper and left out on the bench overnight, with the covers closed. This allows any potentially volatile plasticizers to evaporate from the plates.

2. Isolation of ERCs

- (a) When the yeast cell wall is digested, the spheroplasts will have a “ghostly” or clear outline when viewed under a light microscope. In contrast, yeast with intact cell walls will appear to be much more refractive.

3. Recombination analysis

- (a) Large plates for the recombination analysis should contain 2 % glucose, regardless of the starting glucose concentration during liquid culture; otherwise the red coloration will not develop.
- (b) It helps to store the plates for several days at 4 °C after colonies arise. Over time, the red coloration becomes more intense, allowing for easier detection of half-sectorized colonies.
- (c) The omission of histidine from the large plates allows for a more intense red coloration to develop, which allows for easier detection of sectorized colonies.

Acknowledgements

This work was supported by grants from the NIA/NIH, The Ellison Medical Foundation, and The Glenn Foundation for Medical Research.

References

1. Longo VD, Shadel GS, Kaeblerlein M, Kennedy B (2012) Replicative and chronological aging in *Saccharomyces cerevisiae*. *Cell Metab* 16:18–31
2. Medvedik O, Lamming DW, Kim KD, Sinclair DA (2007) MSN2 and MSN4 link calorie restriction and TOR to sirtuin-mediated lifespan extension in *Saccharomyces cerevisiae*. *PLoS Biol* 5:e261
3. Fabrizio P, Longo VD (2007) The chronological life span of *Saccharomyces cerevisiae*. *Methods Mol Biol* 371:89–95
4. Barton AA (1950) Some aspects of cell division in *Saccharomyces cerevisiae*. *J Gen Microbiol* 4:84–86
5. Lindstrom DL, Gottschling DE (2009) The mother enrichment program: a genetic system for facile replicative life span analysis in *Saccharomyces cerevisiae*. *Genetics* 183:413–422

Chapter 6

Methods for Creating Mutations in *C. elegans* That Extend Lifespan

Dayong Wang, Min Cao, Jessica Dinh, and Yuqing Dong

Abstract

The principle of commonly used methods to create mutations in the nematode *Caenorhabditis elegans* (*C. elegans*) is straightforward. In general, worms are exposed to a dose of mutagen resulting in DNA damages and mutations. Screening the progeny of the mutagenized animals for a certain phenotype is the regular forward genetic approach in *C. elegans*. A mutant selected from such a population is stabilized to recover a pure homozygous strain. In this chapter, we categorize the protocol into mutagenesis, phenotype screen, and outcross and provide time-tested procedures for their implementation to create long-lived worm mutants.

Key words *Caenorhabditis elegans*, Mutagenesis, Lifespan, Screen, Forward genetics, Mutation, Outcross

1 Introduction

Aging is an inevitable process which leads to progressive declines in multiple physiological functions of living organisms. The ultimate consequences of aging are degenerative diseases and death [1–3]. A thorough understanding of the underlying molecular mechanisms of the aging process will provide new measures to prevent age-related diseases. To this end, several simple model organisms have been employed in aging studies, such as budding yeast, *Drosophila melanogaster* (*D. melanogaster*), and *Caenorhabditis elegans* (*C. elegans*). These organisms all have short lifespans and are genetically tractable [4–6]. Of these models, *C. elegans* has been at the forefront of aging research for almost three decades since the first long-lived worm mutant was discovered [7]. In addition to the common advantages, such as a 2–3-week short lifespan, *C. elegans* also possesses the following attributes excellent for studying aging: (a) their transparent bodies make it relatively easy to observe the fate of cells and identify cellular abnormalities; (b) it is convenient to temporarily inactivate specific gene through RNAi by feeding

worms with bacteria which express corresponding double-stranded RNA [8]; and (c) many *C. elegans* genes have human homologs, and this feature holds promise that the principle of worm aging is conserved in human aging.

Recent studies of *C. elegans* aging have revealed a number of genes and genetic pathways important for longevity [6]. Almost all of these longevity genes are evolutionarily conserved in various organisms. Thus, it is concluded that the rate of aging and the onset of age-related diseases are genetically controlled. To elucidate the regulatory mechanisms of aging in worms, it is necessary to create long-lived genetic mutants for further genetic analyses. DNA mutagenesis followed by age-related screening is the most feasible and efficient strategy to obtain long-lived mutants in *C. elegans*. Several methods have been developed to generate mutations in *C. elegans* [9]. Here, we describe the routinely used chemical mutagenesis methods in combination with the approaches to analyze *C. elegans* lifespan to provide essential information required for creating long-lived *C. elegans* strains containing mutations.

2 Materials

1. Nematode growth medium (NGM): For 1 l of NGM, combine 3 g NaCl, 2.5 g bactopectone, and 17 g agar. Autoclave for 45 min, then add 1 ml of cholesterol (5 mg/ml in ethanol), 1 ml of 1 M MgSO₄, and 25 ml of 1 M KPO₄ buffer (stock: 102.2 g KH₂PO₄ and 57.06 g K₂HPO₄ in 1 l distilled H₂O, autoclaved, pH 6.0). When the medium cools to 55 °C, add 1 ml of 1 M CaCl₂.
2. Rich nematode growth medium (RNGM): As compared to the standard NGM, RNGM contains 3× bactopectone (7.5 g vs. 2.5 g). In addition, RNGM uses agarose (Invitrogen cat. no. 15510-027) to replace agar.
3. M9 buffer: 3 g KH₂PO₄, 6 g Na₂HPO₄, 5 g NaCl, 1 ml of 1 M MgSO₄, add H₂O to 1 l. Sterilize by autoclaving.
4. Alkaline hypochlorite: 0.5 M NaOH and 1 % sodium hypochlorite (household bleach contains 5 % sodium hypochlorite).

3 Methods

3.1 Chemical Mutagenesis

Chemical mutagens are broadly used to generate mutations in both prokaryotes and eukaryotes. Ethyl methanesulfonate (EMS), ethylnitrosourea (ENU), and ultraviolet-activated trimethylpsoralen (UV-TMP) have been proven to effectively induce mutations in *C. elegans* [10]. The common effect of EMS is to cause G/C→A/T transitions [11]. ENU is an alternative of EMS but produces a broader mutagenic spectrum including both transitions and

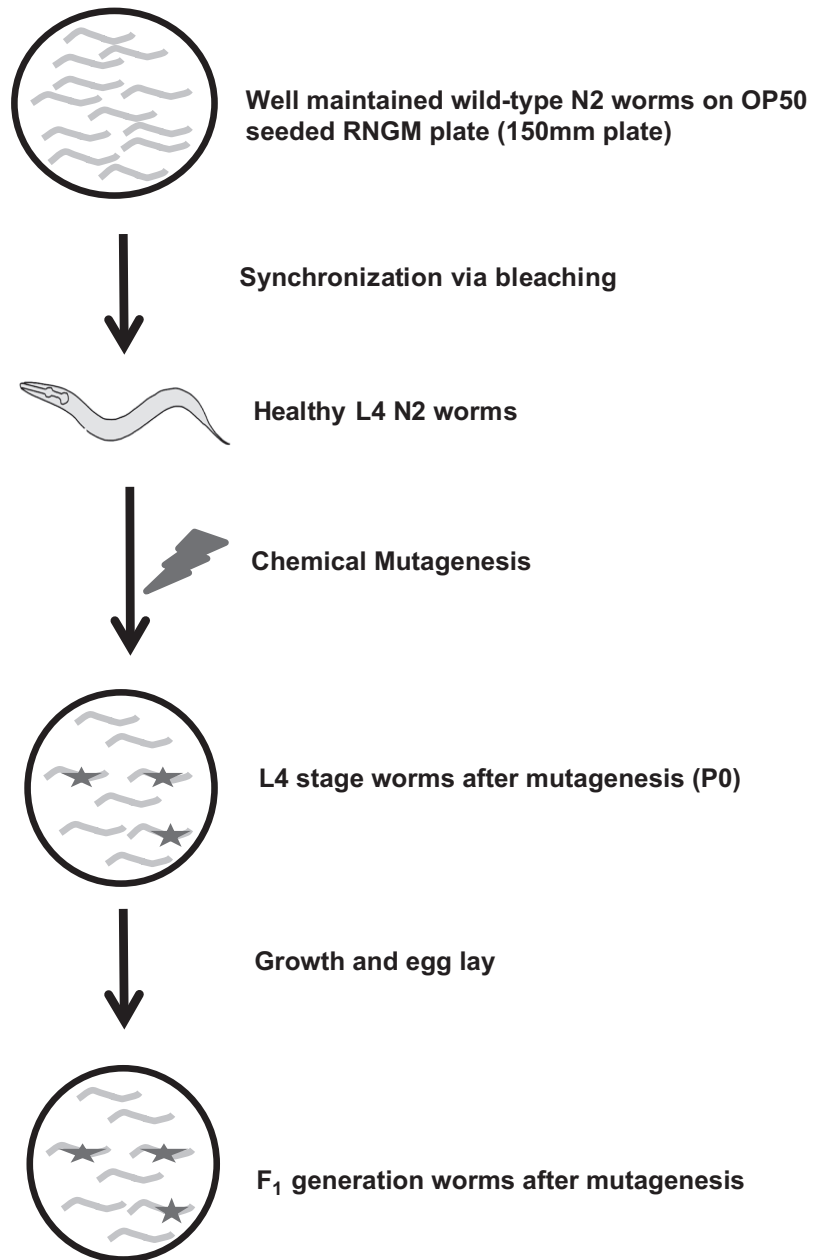


Fig. 1 A scheme of the mutagenesis protocol

transversions [10, 12, 13]. Both EMS and ENU have also been reported to cause small deletions and other chromosomal rearrangements [13, 14]. UV-TMP is now a major reagent used by the *C. elegans* Gene Knockout Consortium to generate deletions in worms [15]. Recent results from a genome-wide deep sequencing project revealed that UV-TMP can produce all manner of transitions and transversions in *C. elegans* [10]. A schematic representation of the mutagenesis protocol can be found in Fig. 1.

3.1.1 Synchronize Worms for Mutagenesis

1. Place ~30 L4 wild-type N2 hermaphrodites in each of the ten 150 mm RNGM plates seeded with *E. coli* OP50 (*see Note 1*).
2. Grow for 4 days at 20 °C to generate a large population of gravid adults (*see Note 2*).
3. Wash the gravid adults off of the plates with M9 buffer and transfer them to a 50 ml conical tube.
4. Pellet worms by centrifugation at $500 \times g$ for 1 min.
5. Carefully remove and discard the supernatant.
6. Resuspend worms in 30 ml of M9 buffer and repeat **steps 4 and 5** once (*see Note 3*).
7. Add 10 volumes of freshly prepared alkaline hypochlorite (*see Note 4*) and incubate for about 5 min with gentle rotation at room temperature.
8. Collect the released eggs by centrifugation at $500 \times g$ for 1 min at 4 °C and carefully remove the supernatant.
9. Add 10 volumes of ice-cold M9 buffer to wash the eggs and collect the eggs by centrifugation at $500 \times g$ for 1 min at 4 °C.
10. Wash three more times by repeating **step 9**.
11. Resuspend pellet in ~5 ml of M9 buffer. Leave the tube overnight at room temperature with gentle rotation on a lab rotator (*see Note 5*).
12. Distribute L1 worms equally to twenty 150 mm RNGM plates seeded with *E. coli* OP50 (*see Note 6*).
13. Grow for ~36 h at 20 °C, until most of worms are at L4 stage (*see Note 7*).
14. Wash the worms off of the plates with M9 buffer and collect them into one 50 ml conical tube.
15. Pellet worms by centrifugation at $500 \times g$ for 1 min.
16. Carefully remove and discard the supernatant.
17. Resuspend worms in 30 ml of M9 buffer and repeat **steps 15 and 16** once (*see Note 3*).

3.1.2 Mutagenesis (*See Note 8*)

EMS Mutagenesis

1. Prepare 6 ml of 100 mM EMS in M9 buffer in a 15 ml conical tube (*see Note 9*).
2. Resuspend washed L4 worms in 6 ml of M9 buffer and transfer the worm suspension into the 6 ml of EMS solution (final concentration of EMS is 50 mM).
3. Tighten the tube cap and seal it with parafilm.
4. Place the tube on the rotator at room temperature for 4 h.

5. Collect the mutagenized worms by centrifugation at $500 \times g$ for 1 min and carefully remove the supernatant (*see Note 10*).
6. Wash the worms five times with 10 volumes of M9 buffer. Collect the nematodes by centrifugation at $500 \times g$ for 1 min after each wash.
7. Plate the mutagenized worms equally to twenty 150 mm RNGM plates seeded with *E. coli* OP50 (*see Note 11*).
8. Grow for ~24 h at 20 °C, until most of worms become gravid adults (P0 generation) (*see Note 12*).

ENU Mutagenesis

1. Prepare 6 ml of 1 mM ENU in M9 buffer in a 15 ml conical tube (*see Note 13*).
2. Resuspend washed L4 worms in 6 ml of M9 buffer and transfer the worm suspension into the 6 ml of ENU solution (final concentration of ENU is 0.5 mM).
3. Tighten the tube cap and seal it with parafilm.
4. Place the tube on the rotator at room temperature for 4 h.
5. Collect the mutagenized worms by centrifugation at $500 \times g$ for 1 min and carefully remove the supernatant (*see Note 14*).
6. Wash the worms five times with 10 volumes of M9 buffer. Collect the nematodes by centrifugation at $500 \times g$ for 1 min after each wash.
7. Plate the mutagenized worms equally to twenty 150 mm RNGM plates seeded with *E. coli* OP50 (*see Note 15*).
8. Grow for ~24 h at 20 °C, until most of the worms become gravid adults (P0 generation) (*see Note 12*).

UV-TMP Mutagenesis

1. Prepare 2 mg/ml TMP stock solution in a 1.5 ml eppendorf tube (*see Note 16*).
2. Resuspend washed L4 worms in 12 ml M9 buffer and add 12 μ l TMP stock solution in it (final concentration of TMP is 2 μ g/ml) (*see Note 17*).
3. Tighten the tube cap and seal it with parafilm.
4. Place the tube on the rotator at room temperature in the dark for 1 h.
5. After soaking in TMP solution, spin at $500 \times g$ for 1 min to collect worms in the dark.
6. Wash the worms five times with 10 volumes of M9 buffer. Collect the nematodes in the dark by centrifugation at $500 \times g$ for 1 min after each wash.

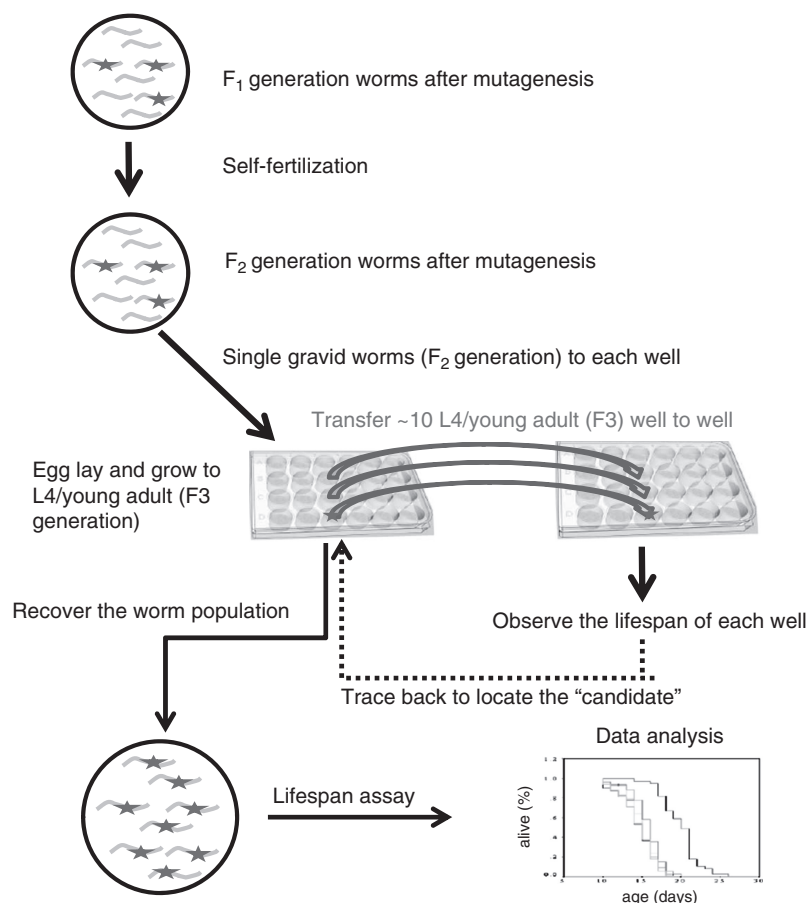


Fig. 2 A scheme of the lifespan assay protocol

7. Distribute the worms equally in the dark to each well of a sterile 12-well tissue culture plate and irradiate the suspension with 360 nm UV light for 90 s at 340 $\mu\text{W}/\text{cm}^2$ (see **Note 18**).
8. Pool the mutagenized worms and plate them equally to twenty 150 mm RNGM plates seeded with *E. coli* OP50.
9. Grow for ~24 h at 20 °C, until most worms are gravid adults (P0 generation).

3.2 Screen for the Long-Lived Mutants

Most lifespan assays are performed at 20 or 25 °C (see **Note 19**). A schematic representation of the lifespan assay protocol can be found in Fig. 2.

1. Wash the gravid adults (P0 generation) off of the plates with M9 buffer and transfer them to a 50 ml conical tube.
2. Follow **steps 4–11** in Subheading 3.1.1 to collect F₁ self-progeny.

3. Plate ~300 F₁ L1 worms on a 150 mm NGM plate which is seeded with *E. coli* OP50 (*see* **Note 20**).
4. Grow for ~3 days at 20 °C, until most worms are gravid adults.
5. Repeat **step 2** to harvest F₂ self-progeny.
6. Transfer F₂ L1 worms to a 150 mm NGM plate which is seeded with *E. coli* OP50. Grow for ~3 days at 20 °C, until most worms are gravid adults.
7. Place ~1,000 F₂ gravid adults individually onto 24-well NGM plates seeded with *E. coli* OP50 (stock plate), each well hosting one worm (*see* **Note 21**).
8. Give worms 2–4 h to lay eggs, then pick off the F₂ worms (*see* **Note 22**).
9. Allow eggs to hatch and grow up for ~3 days at 20 °C until worms become L4/young adults (F₃ progeny) (*see* **Note 23**).
10. Prepare fresh 24-well NGM–FUDR plates seeded with *E. coli* OP50 (*see* **Note 24**).
11. Transfer ~10 L4/young adult worms from each well of the stock plate to the freshly made 24-well NGM–FUDR plates (*see* **Notes 25 and 26**).
12. Monitor lifespan of worms by scoring mortality. Worms that fail to respond to gentle touching with a platinum wire within 5 s are scored as dead.
13. At the time when all of the control wild-type N2 worms were dead, the wells that still contain live worms are scored as “positive.”
14. Trace back to the stock plate and recover the “positive” worms (*see* **Note 27**).
15. Transfer 3–5 gravid adults from the “positive” population onto a 60 mm NGM plate seeded with *E. coli* OP50 and allow them to lay eggs at 20 °C.
16. After 2–4 h, pick off the parents (*see* **Note 22**).
17. Allow eggs to hatch and grow up for ~3 days at 20 °C, until worms become L4/young adults.
18. 14. Prepare three 35 mm NGM–FUDR plates seeded with *E. coli* OP50 (*see* **Note 28**).
19. 14. Transfer ~30 L4/young adult worms to each freshly made 35 mm NGM–FUDR plates (total ~90 worms).
20. Repeat **step 12** to conduct lifespan assay (*see* **Note 29**).
21. If the lifespan is significantly extended, the “positive” strain is determined to be a homozygous long-lived mutant (*see* **Note 30**).

3.3 Outcross (See Note 31)

1. Prepare adequate number of wild-type N2 males (*see* **Note 32**).
2. Place four of L4 mutant hermaphrodites and 5–8 N2 males in one NGM plate which is seeded with *E. coli* OP50.
3. After ~24 h at 20 °C, single each hermaphrodite into a new OP50-seeded NGM plate and allow each to lay eggs until sterile (*see* **Note 33**).
4. Transfer four F₁ hermaphrodites to a new NGM plate seeded with *E. coli* OP50 and allow them to self-fertilize at 20 °C.
5. At F₂ generation, single 12 gravid adults and transfer each onto a 35 mm NGM plate seeded with *E. coli* OP50 to lay eggs at 20 °C.
6. After 2–4 h, pick off the parents and allow eggs to hatch and develop for ~3 days at 20 °C (stock plate), until worms become L4/young adults (F₃ progeny) (*see* **Note 22**).
7. Follow **steps 10** and **11** in Subheading 3.2.
8. Monitor lifespan of worms by scoring mortality and analyze the data with SPSS software.
9. If the lifespan is significantly extended, trace back to the stock plate and recover the worms.
10. Follow **steps 15–20** in Subheading 3.2 to further confirm the longevity phenotype.
11. Apply the long-lived mutant for at least two more outcrosses (the more the better) by repeating **steps 1–10** (*see* **Note 34**).

4 Notes

1. Aseptically inoculate *E. coli* OP50 into sterile Luria Broth (10 g tryptone, 5 g yeast, 5 g NaCl, add H₂O to 1 l, pH 7.0) and grow the culture overnight without shaking at 37 °C. The overnight culture should be stored at 4 °C and can remain usable for several months [16].
2. Use a stereo microscope to check that most of the worms are gravid adults bloating with eggs.
3. These washes are to remove *E. coli* OP50.
4. The bleaching solution should be prepared fresh just before use.
5. Eggs will hatch and worms will be arrested at the L1 stage.
6. Determine the worm number to ensure a large number of worms (>10,000) used.
7. Worms at this stage have a white crescent at the developing vulva with a black dot in the middle.
8. EMS, ENU, and TMP are potent mutagens and carcinogens. When working with these chemicals, wear gloves and perform operations in a fume hood.

9. Add 64 μ l EMS (Sigma M0880) into 6 ml of M9 buffer. Cap the tube and invert several times until all oily looking spheres are dispersed.
10. To inactivate the EMS-containing solution, mix with an equal volume of “inactivation solution I” (0.1 M sodium hydroxide, 20 % w/v sodium thiosulfate) for 24 h.
11. Put any solid wastes that have been in contact with EMS into a large beaker filled with “inactivation solution I” and soak for 24 h before discarded.
12. Check the efficiency of a chemical mutagenesis [17]. A successful chemical mutagenesis is expected to yield ~1–2 % F₁ lethality and ~5–10 % F₁ sterility.
13. Stock solution of 50 mM ENU (Sigma N8509) is prepared in 100 % ethanol. Add 120 μ l EMS stock solutions into 6 ml of M9 buffer. Cap the tube and invert several times.
14. To inactivate the ENU-containing solution, mix with an equal volume of “inactivation solution II” (0.5 M sodium hydroxide, 20 % w/v sodium thiosulfate) for at least 1 h.
15. Put any solid wastes that have been in contact with ENU into a large beaker filled with “inactivation solution II” and soak for 1 h before discarded.
16. Stock solution of 2 mg/ml TMP (Sigma T6137) are prepared in DMSO. Briefly, 2 mg TMP is mixed with 1 ml DMSO in an eppendorf tube by vigorous vortex. The tube is wrapped in foil to screen out light.
17. The potency of TMP is particularly varied in different batches. Various TMP concentrations (2–30 μ g/ml) have been previously used [15].
18. Adjust the height of the two handheld UV lamps to generate the appropriate UV doses as measured with a UV dose meter.
19. To screen for the long-lived mutants that require an alternative temperature for survival and growth, an appropriate assay temperature can be determined accordingly.
20. The rest of F₁ L1 worms will develop into dauer without food. These worms can be stored on NGM plates at 11 or 16 °C for several months for further screening.
21. For a well of a 24-well plate, usually use 1.5 ml of NGM agar.
22. Simultaneously, use the well-maintained N2 worms to prepare eggs as controls.
23. Check the worms frequently until most worms are at L4 stage. Give them ~9 h thereafter to reach young adults.
24. Incorporate 50 μ g/ml FUDR (5-fluoro-2'-deoxyuridine) in the NGM to inhibit progeny production of wild-type *C. elegans*

in lifespan assays [18–21]. Considering that FUDR may influence the worms' lifespan, some scientists used temperature-sensitive sterile strains as an alternative way to avoid progeny interference [22–24].

25. To increase the power of screen, up to ~50 synchronized L4/young adults can be transferred in one well.
26. The ~10 synchronized L4/young adults from one well (stock plate) were transferred to a well (NGM–FUDR plate for life-span screen) marked with the location # of the stock plate.
27. Transfer the “positive” worms (as many as you can) from the stock plate to a 60 mm NGM plate seeded with OP50, then maintain the worm population for 1–2 generations at 20 °C.
28. OP50 is 10× concentrated from regular OP50 culture. Briefly, pellet bacteria cells from a 10 ml culture by centrifugation at $1,000 \times g$ at 4 °C, then remove 9 ml supernatant and resuspend the pellet in the remaining 1 ml supernatant.
29. The SPSS software (IBM, Version 20) is used to analyze the significance of the difference in lifespan between the candidate mutant and the control.
30. The F₂ animals were considered to have the genotype mutation/mutation. If self-progenies since F₃ generation continuously displayed the constant phenotype, the corresponding F₂ animal was determined to be the homozygous mutant.
31. Mutagen treatment will be likely to generate additional mutations besides the anticipated mutations. Therefore, it is desirable to remove as many as possible of these background mutations by repeated outcrossing against wild-type N2. All crosses should be done on NGM plates seeded with *E. coli* OP50.
32. Male animals can be induced by methanol treatment. Briefly, ~5–10 L4 hermaphrodites are transferred into 7 % methanol / M9 solution and incubated for 30 min, then drop back to NGM plate seeded with OP50. Grow the worms at 20 °C. A few males will be found in the F₁. Alternatively, male animals can be generated by heat shock. Approximately 5–10 L4 hermaphrodites are plated on NGM and shifted to 30 °C for ~6 h. Shift worms back to 20 °C and a few males should be found in the F₁. To maintain a male stock, put them with a few L4 hermaphrodites to ensure recovering more males in the next generation.
33. Successful outcross expects 50 % males in the progeny.
34. Mapping of newly isolated mutations in *C. elegans* refers to ref. 25.

Acknowledgements

We are indebted to A. Brown for editorial assistance. D.W. was supported by the National Natural Science Foundation of China (No. 81172698). Y.D. and M.C. are supported by Creative Inquiry fund of Clemson University and Yamada Research Grant. Y.D. was supported by grant from AFAR.

References

1. Luca D, d'Alessandro E, Bonacci S, Giraldi G (2011) Aging populations: the health and quality of life of the elderly. *Clin Ter* 162: e13–e18
2. Fontana L (2009) Modulating human aging and age-associated diseases. *Biochim Biophys Acta* 1790:1133–1138
3. Pizza V, Agresta A, D'Acunto CW, Festa M, Capasso A (2011) Neuroinflamm-aging and neurodegenerative diseases: an overview. *CNS Neurol Disord Drug Targets* 10:621–634
4. Helfand SL, Rogina B (2003) Genetics of aging in the fruit fly, *Drosophila melanogaster*. *Annu Rev Genet* 37:329–348
5. Kaerberlein M, Burtner CR, Kennedy BK (2007) Recent developments in yeast aging. *PLoS Genet* 3:e84
6. Kenyon CJ (2010) The genetics of ageing. *Nature* 464:504–512
7. Klass MR (1983) A method for the isolation of longevity mutants in the nematode *Caenorhabditis elegans* and initial results. *Mech Ageing Dev* 22:279–286
8. Grishok A (2005) RNAi mechanisms in *Caenorhabditis elegans*. *FEBS Lett* 579:5932–5939
9. Riddle DL, Blumenthal T, Meyer BJ et al (eds) (1997) Section II, induced mutations. *C. elegans* II, 2nd edn. Cold Spring Harbor Laboratory Press, Cold Spring Harbor, NY
10. Flibotte S, Edgley ML, Chaudhry I, Taylor J, Neil SE, Rogula A, Zapf R, Hirst M, Butterfield Y, Jones SJ et al (2010) Whole-genome profiling of mutagenesis in *Caenorhabditis elegans*. *Genetics* 185:431–441
11. Anderson P (1995) Mutagenesis. *Methods Cell Biol* 48:31–58
12. De Stasio E, Lephoto C, Azuma L, Holst C, Stanislaus D, Uttam J (1997) Characterization of revertants of unc-93(e1500) in *Caenorhabditis elegans* induced by N-ethyl-N-nitrosourea. *Genetics* 147:597–608
13. De Stasio EA, Dorman S (2001) Optimization of ENU mutagenesis of *Caenorhabditis elegans*. *Mutat Res* 495:81–88
14. Jansen G, Hazendonk E, Thijssen KL, Plasterk RH (1997) Reverse genetics by chemical mutagenesis in *Caenorhabditis elegans*. *Nat Genet* 17:119–121
15. Barstead RJ, Moerman DG (2006) *C. elegans* deletion mutant screening. *Methods Mol Biol* 351:51–58
16. Byerly L, Cassada RC, Russell RL (1976) The life cycle of the nematode *Caenorhabditis elegans*. I. Wild-type growth and reproduction. *Dev Biol* 51:23–33
17. Lesa GM (2006) Isolation of *Caenorhabditis elegans* gene knockouts by PCR screening of chemically mutagenized libraries. *Nat Protoc* 1:2231–2240
18. Hosono R (1978) Sterilization and growth inhibition of *Caenorhabditis elegans* by 5-fluorodeoxyuridine. *Exp Gerontol* 13:369–374
19. Mitchell DH, Stiles JW, Santelli J, Sanadi DR (1979) Synchronous growth and aging of *Caenorhabditis elegans* in the presence of fluoro-deoxyuridine. *J Gerontol* 34:28–36
20. Gandhi S, Santelli J, Mitchell DH, Stiles JW, Sanadi DR (1980) A simple method for maintaining large, aging populations of *Caenorhabditis elegans*. *Mech Ageing Dev* 12:137–150
21. Hosono R, Mitsui Y, Sato Y, Aizawa S, Miwa J (1982) Life span of the wild and mutant nematode *Caenorhabditis elegans*. Effects of sex, sterilization, and temperature. *Exp Gerontol* 17:163–172
22. Aitlhadj L, Sturzenbaum SR (2010) The use of FUDR can cause prolonged longevity in mutant nematodes. *Mech Ageing Dev* 131:364–365
23. Dillin A, Hsu AL, Arantes-Oliveira N, Lehrer-Graiwer J, Hsin H, Fraser AG, Kamath RS, Ahringer J, Kenyon C (2002) Rates of behavior and aging specified by mitochondrial function during development. *Science* 298:2398–2401
24. Hansen M, Hsu AL, Dillin A, Kenyon C (2005) New genes tied to endocrine, metabolic, and dietary regulation of lifespan from a *Caenorhabditis elegans* genomic RNAi screen. *PLoS Genet* 1:119–128
25. Lambie EJ (2011) Mapping mutations in *C. elegans*. *Methods Cell Biol* 106:3–22

Chapter 7

Aging Studies in *Drosophila Melanogaster*

Yaning Sun, Jason Yolitz, Cecilia Wang, Edward Spangler,
Ming Zhan, and Sige Zou

Abstract

Drosophila is a genetically tractable system ideal for investigating the mechanisms of aging and developing interventions for promoting healthy aging. Here we describe methods commonly used in *Drosophila* aging research. These include basic approaches for preparation of diets and measurements of lifespan, food intake, and reproductive output. We also describe some commonly used assays to measure changes in physiological and behavioral functions of *Drosophila* in aging, such as stress resistance and locomotor activity.

Key words Aging, *Drosophila melanogaster*, Lifespan, Reproduction, Locomotor activity, Mitochondrial function, Oxidative stress, Starvation

1 Introduction

Drosophila melanogaster is a widely used model organism that has distinct advantages in aging research, including short lifespan (mean lifespan, 2–3 months), low maintenance requirements, rich genetic resource, and ease to perform genetic manipulation [1]. More importantly, the *Drosophila* genome is fully sequenced with more than 50 % of fly genes having homologs in humans [2, 3]. Moreover, more than 75 % of known human disease genes, covering a broad range of disorders, have fly homologs [4]. These features make *Drosophila* an ideal model organism for studying the mechanisms of aging and for developing effective aging interventions, which are relevant to aging research in humans.

Lifespan measurement is the basic method used to determine the effects of genetic and nongenetic factors involved in aging [5]. A number of issues need to be carefully considered to avoid artifacts or confounds that may cause misinterpretation of the results when conducting lifespan studies. First, genetic background and control

Jason Yolitz and Cecilia Wang have contributed equally to this project.

lines must be taken into consideration in order to minimize inbreeding depression and heterosis effects on lifespan [6, 7]. A number of genetic approaches have been developed to generate mutations and manipulate gene expression for aging research in *Drosophila*, which include insertion mutagenesis by P-element, gene expression alterations by the Gal4–UAS system, inducible gene expression by the GeneSwitch Gal4 (GSG)–UAS system, and gene knockdown by RNA interference (RNAi) [8, 9]. These approaches are instrumental in investigating molecular mechanisms of aging, such as identifying single genes that are involved in modulating lifespan. For examples, *methuselah* (*mtb*) is the first gene that has been found to increase *Drosophila* lifespan when mutated by a P-element insertion [10]. In genetic studies, however, genetic backgrounds may mask or exaggerate any differences in lifespan between mutant and control animals. To reduce the undesirable effects of genetic backgrounds, experimental lines should be backcrossed for more than five generations to an appropriate wild-type control line. Commonly used control lines include *Canton S*, *Oregon R*, and *Dahomey*, *y w*, and *w¹¹¹⁸*. When possible, one should use the GSG–UAS system, which allows for conditionally altering gene expression in a temporal- and/or tissue-specific manner by the compound RU486 added to the food [8]. By using this approach, control and mutant flies have the same genetic background and differ only in the food that they are fed. More importantly, the GSG–UAS system can be used to induce changes in gene expression in adult flies, which allows for bypassing any interference or possible lethality effect caused by a mutation during developmental stages.

Second, aging is modulated by both genetic and environmental factors. Diet is a major environmental factor that has a huge impact on lifespan in *Drosophila* and many other species [11]. Two commonly used diets in *Drosophila* lifespan studies are based on cornmeal and sugar–autolyzed yeast (SY) diets. Diet composition is a critical determinant of lifespan [11]. This notion has been confirmed by numerous dietary restriction studies. Dietary restriction (DR) by diluting all or specific nutrients in the diet has been shown to extend lifespan in many species, ranging from yeast, worms, flies, rodents, to primates [12]. The importance of diet composition has been further demonstrated in recent nutritional geometric studies, which employ diets with various amounts of sugar and autolyzed yeast to show that the carbohydrate-to-protein (C:P) ratio is more critical than single nutrients in determining lifespan in flies [13, 14]. For example, Lee et al. reported that *Drosophila* has an optimal mean lifespan on the SY diet with the C:P ratio at 16:1 [13]. Autolyzed yeast is the only protein source in SY diets.

Third, measurement of food intake should be carried out along with lifespan measurements considering the impact of nutrient intake on lifespan. The purpose of measuring food intake is to

determine whether any genetic manipulation or aging intervention affects lifespan by directly influencing aging processes or indirectly through affecting food intake. Two major methods have been widely used to measure food intake in *Drosophila*. One is the indirect method, which estimates food uptake by measuring the uptake of a dye or radioactive tracer added in the food [15–17]. The second method is to directly measure the amount of liquid food consumed by flies using a capillary feeder (CAFE) [18].

Only after carefully considering the confounding factors in lifespan measurements can one start to investigate the mechanisms of aging and develop effective aging interventions. A number of physiological, biochemical, and behavioral assays are routinely conducted in these studies. One commonly conducted physiological assay is to measure flies' resistance to various stressors, such as oxidative stress, starvation, heat or cold shock, and desiccation. Lifespan and stress response are often closely associated, and long-lived populations tend to be more stress resistant [19, 20]. The free radical theory of aging proposes that cumulative damage to biological macromolecules by reactive oxygen species (ROS) leads to irreversible cell damage and an overall functional decline with age [21]. Oxidative stress resistance is typically measured by feeding flies paraquat (*N,N'*-dimethyl-4,4'-bipyridinium dichloride), which produces various ROS upon ingestion and consequently induces oxidative damage [22]. Starvation resistance measurement is the evaluation of the ability of flies to deal with an energy shortage, an event that often occurs in real-life environments. Due to the central role of energy for organisms, improving starvation resistance could be one of the mechanisms that play a role in lifespan extension. The starvation assay is typically performed by measuring the survival of adult flies on water only [23]. However, longevity is not necessarily tightly correlated with resistance to oxidative stress and starvation resistance. The free radical hypothesis of aging has been challenged by numerous studies showing that animals with higher levels of oxidative damage do not necessarily have shorter lifespan than controls [24]. Moreover, long-lived animals including flies show no difference and even sometimes display a decrease in resistance to oxidative stress and starvation [25–28].

The second lifespan-related physiological assay is to measure lifetime reproductive output. The “cost of reproduction” concept in aging argues for a negative correlation between reproductive output and survival due to a “trade-off” in life history traits [29–32]. In *Drosophila*, long-lived flies tend to decrease early reproduction [33], while selection for late-life reproduction often identifies lines with increased lifespan [34, 35]. In addition, sterile flies tend to live longer than their fertile controls [36, 37], and long-lived mutants have reduced fecundity or fertility [31]. Methods to assess reproductive output include measuring lifetime

egg production in once-mated females or progeny number from the mating of females and males.

The third and perhaps most important lifespan-related assay is to assess healthspan. Although the precise definition of healthspan is still controversial, one healthspan parameter is locomotor activity, which can be used to assess changes in an animal's mobility, circadian rhythm, sleep patterns, and even cognitive function in aging [38]. The connection between locomotor activity and aging has been well established. For example, aging is associated with a gradual decline in locomotor activities in almost all species tested so far [38–40]. Two methods for assessment of locomotor behaviors are commonly employed in *Drosophila* aging studies. One is the rapid iterative negative geotaxis (RING) assay (Fig. 2), which tests the climbing ability of adult flies [41, 42]. “Negative geotaxis” refers to an innate escape response elicited by mechanical stimulation, in which flies ascend the wall of a container after being tapped to the bottom of the container. The climbing speed has been demonstrated to decline with age in *Drosophila*. The other method used to measure locomotor activity takes advantage of the *Drosophila* activity monitoring (DAM) system [43]. Typically flies are kept individually in sealed activity tubes placed in the DAM system, and the fly activity is measured by the frequency of an “activity event”, which is recorded each time a fly breaks an infrared light beam across the middle of the activity tube. The activity event data can be used to analyze a wide range of behaviors, such as circadian rhythm, sleep patterns, hypoactivity, and hyperactivity [44–46]. Similar to humans, *Drosophila* experience a decline in sleep time with aging [47]. With appropriate modifications, the DAM system is also suitable for monitoring stimulation responses to a variety of stimuli, such as noise, vibration, rotation, heat, and chemicals [43, 45, 46]. Besides the two relatively simple systems described above, sophisticated video tracking systems have been developed to analyze various behaviors, such as movement pattern and courting for *Drosophila* and other fly species. These assessments can be performed under various culture conditions, including individual or groups of flies in capillary tubes, standard fly vials with food, or other types of apparatus [48, 49]. These advanced systems have been used to measure healthspan parameters by recording lifetime behavioral changes, locomotor activity, and even gene expression using green fluorescent protein-marked flies [50, 51].

In this review, we will describe some of the basic approaches for aging studies in *Drosophila* (Fig. 1). We will cover methods to prepare foods and flies for lifespan measurement and protocols to assess stress resistance, reproductive output, and locomotor activity. Comprehensive mitochondrial assays can be found in a recent review [52]. The protocols described here are fundamental to the investigation of the mechanisms by which any genetic factor, dietary intervention, and other nongenetic factors influence healthspan and lifespan.

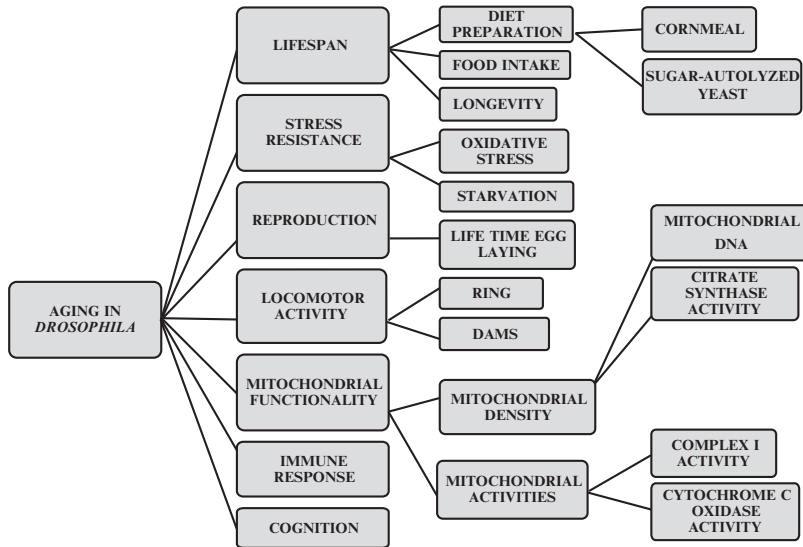


Fig. 1 Flow chart of basic assays to assess lifespan, age-related changes in physiological and behavioral function in *Drosophila*

2 Materials

2.1 Diet Preparation

Yellow cornmeal (*see Note 1*).

Agar.

Active dry yeast (Baker's yeast).

Dextrose (D-Glucose).

Sugar (Sucrose).

Autolyzed yeast (enzymatic yeast hydrolysate).

Methyl 4-hydroxybenzoate (tegosept; to make a 10 % stock solution, add 86.4 g tegosept to 800 mL 70 % ethanol).

Acid mix (Add distilled water to 836 mL propionic acid to bring the final volume to 1 L. Add distilled water to 83 mL phosphoric acid to bring the final volume to 1 L. Mix the two diluted acid solutions to make a 2 L acid mix.)

2.2 Strains and Culture Conditions

Fly strains are maintained on the cornmeal diet. For lifespan assays, flies are maintained at 25 °C, 60–65 % humidity, and a 12-h light/12-h dark cycle in a climate-controlled incubator.

2.3 Food Intake

FD&C blue #1 dye.

Spectrophotometer.

Custom-made fly chamber (Fig. 2).

Calibrated 10 μ L capillary.

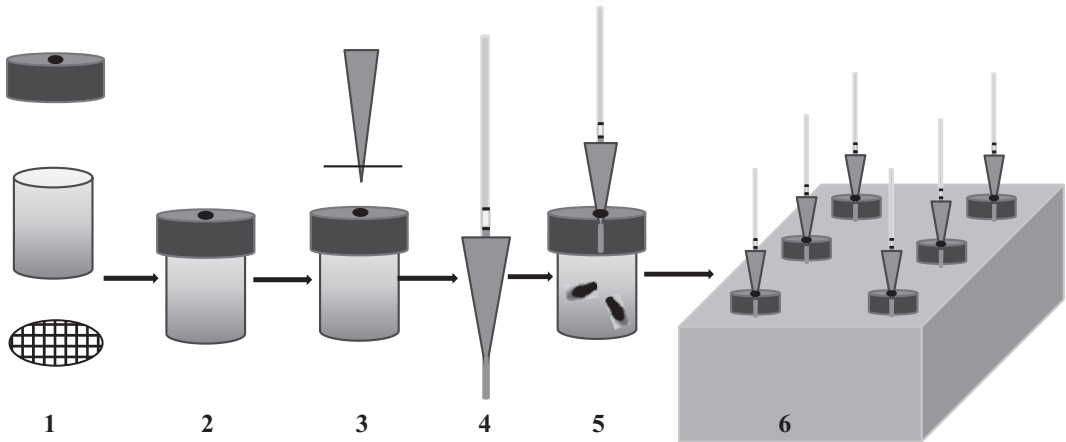


Fig. 2 The setup for the capillary feeder (CAFE) assay. (1) Parts for a fly chamber, (2) the fly chamber, (3) cut pipette tip, (4) an assembled feeding capillary, (5) an assembled fly feeding chamber with flies, and (6) a foam rack holding feeding chambers

2.4 Stress Assays

Filter paper discs.

Paraquat (methyl viologen dichloride or 1,1'-dimethyl-4,4'-bipyridinium dichloride).

Sucrose.

2.5 Locomotor Activity

RING apparatus.

Digital camera.

Drosophila activity monitor system.

3 Methods

3.1 Cornmeal Food

Among the many available recipes for cornmeal food, the two most commonly used recipes are based on those developed by the Lewis laboratory and the Lakovaara laboratory, respectively [53, 54]. Detailed recipes can be found in the Bloomington *Drosophila* Stock Center website (<http://flystocks.bio.indiana.edu>) (Bloomington, IN, USA). The following procedure is based on the Lewis recipe, which is more commonly used in aging studies. The Lewis recipe contains 17 L distilled water, 93 g agar, 1,716 g cornmeal, 310 g Baker's yeast, 517 g sugar, 1,033 g dextrose, and 200 mL acid mix, which results in approximately 18 L cornmeal food (*see Note 1*).

1. Dissolve 93 g agar in 13 L boiling water.
2. Add 1,716 g cornmeal and 310 g active dry yeast slowly to the boiling agar while mixing continuously to avoid clumps. Simmer for an hour while mixing continuously.

3. Dissolve 517 g sucrose and 1,033 g dextrose in 4 L hot water and add to the agar–cornmeal–yeast slurry. Reduce heat and mix until homogenous.
4. Cool the food to 60–65 °C before adding 200 mL acid mix and mix well.
5. Pour or dispense the food into vials or bottles. Cover vials or bottles in the tray with cheese cloth and dry overnight before plugging.

3.2 Sugar–Autolyzed Yeast (SY) Diet

The SY diets with desired amounts of sugar and autolyzed yeast are made by mixing appropriate volumes of the two base solutions, 20 % (w/v) sugar and 20 % (w/v) autolyzed yeast, both containing 1.5 % (w/v) agar [55] (*see Note 1*).

1. Add 200 g sugar and 15 g agar to 800 mL distilled water, and add 200 g autolyzed yeast and 15 g agar to 800 mL distilled water in autoclavable containers.
2. Place food containers in a boiling water bath for an hour. Also boil an extra 500 mL water to be used in **step 4**.
3. Remove the sugar solution and autolyzed yeast solution from the water bath and cool them down to 60–65 °C before adding 20 mL tegosept to each solution. For aging intervention studies, pharmacological and nutraceutical agents can be added to the sugar solution at this step.
4. Add ~200 mL water to each solution to bring the final volume to 1 L.
5. Mix proper amounts of sugar solution, autolyzed yeast solution, and water to achieve desired sugar and autolyzed yeast contents before pouring into vials or bottles to make SY diets. For example, add equal amounts of sugar solution and autolyzed yeast solution together to make an SY diet with 10 % sugar, 10 % autolyzed yeast, and 1.5 % agar, which we refer to as the SY1:1 diet.

3.3 Lifespan Measurement

Fly cultures are performed at 25 °C, 60–65 % humidity, and a 12-h light/12-h dark cycle in a climate-controlled incubator. Proper control strains should be selected in each experiment (*see Note 2*). The following procedure is based on the protocol using once-mated flies [55, 56].

1. To prepare flies for lifespan experiments, put approximately 50 females and an approximately equal number of males in each 6 oz bottle with cornmeal food (*see Note 2*). Allow the parental flies to mate and lay eggs for 4–5 days before clearing them out.
2. Check emerged flies after 10–14 days. Clear any flies that are enclosed on the first day and then collect adult flies within 24-h eclosion daily for the next 3 days.

3. Transfer emerged flies of mixed sexes daily to 6 oz bottles with cornmeal food or an SY diet, such as SY1:1, and let the flies mate for 24 h. Each bottle should have no more than 200 flies. Record the birth date.
4. After mating, males and females are separated under light anesthesia by humidified CO₂. Place 20 males or females in each vial with cornmeal food or the SY diet used in **step 3**. Set up at least five vials as replicates for each lifespan assay (*see Note 2*).
5. After another 24 h, flies are transferred to fresh vials with cornmeal food or desired SY diets.
6. Transfer flies into fresh vials every 2–3 days (or three times a week) and record the number of dead flies at each transfer.
7. Analyze data with suitable software to calculate mean lifespan and standard error. Plot survival curves by the Kaplan–Meier method and determine statistical differences between groups for mean lifespan by the Mantel–Cox log rank test (*see Note 2*).
8. Age-dependent mortality rates can be calculated according to the Gompertz model using the equation $m(t) = \alpha \times \exp(b \times t)$, where $m(t)$ is the mortality rate at time t , α is the age-independent mortality rate or the initial mortality rate, and b is the age-dependent mortality rate.
9. Maximum lifespan analysis is conducted on the longest-lived 10 % of flies in each treatment. $p < 0.05$ is considered statistically significant.

3.4 Food Intake

3.4.1 Food Tracer Method

The method using FD&C blue #1 dye as the food tracer is described here, and food intake is quantified as uptake of the blue dye [17].

1. Prepare the blue diet by mixing FD&C blue #1 dye to cooled cornmeal or SY food to a final concentration of 0.5 % and pouring 5 mL food to each vial.
2. Transfer five flies of 7–14 days old to each vial containing the blue diet. Age-matched control flies are transferred to non-dyed food. Allow flies to feed for 30 min. Set up 5–6 vials as replicates for each treatment.
3. While waiting, dissolve 0.5 g dyed food in 15 mL distilled water. Prepare serial twofold dilutions of the stock solution by 8- to 128-folds. After centrifuging at $12,000 \times g$ for 2 min, measure the absorbance of dilutions at 625 nm to generate a standard curve of the absorbance.
4. Transfer both experimental and control flies in each vial into a 1.5 mL microcentrifuge tube and then snap freeze in liquid nitrogen (*see Note 3*).

5. Separate fly heads from the bodies by briefly vortexing the tube (*see Note 3*).
6. Collect and homogenize fly bodies in 200 μ L distilled water with a plastic pestle and then add 800 μ L distilled water. Centrifuge at $12,000 \times g$ for 2 min.
7. Transfer 0.9 mL supernatant to a new tube and bring to a final volume of 1.5 mL with distilled water, and centrifuge again for 2 min.
8. Immediately measure the sample absorbance at 625 nm using a spectrophotometer (*see Note 3*). The absorbance from control flies is used to correct for background absorbance of flies.
9. Calculate food intake by using the net absorbance and the standard curve generated in **step 3**.

3.4.2 CAFE Method

The CAFE method described here is based on the protocol published by Ja et al. with some modifications [18, 57] (*see Note 3*).

1. To make a fly chamber (Fig. 2), cut a 15 mL plastic tube (1.5 cm diameter) to 2 cm height from the end with cap, seal the open end with a nylon mesh, and poke a hole of ~2 mm diameter in the cap to hold a 200 μ L pipette tip.
2. Cut off 1–2 mm from the tip of a 200 μ L pipette tip with a sharp blade. Make sure the capillary can go through but not drop through it.
3. Add 1 mL water in each hole of a foam rack for 15 mL tubes, which typically have 5×5 holes and are used to house fly chambers.
4. Transfer one or two flies under light CO₂ to each chamber and use a 200 μ L pipette tip to temporarily block the hole in the cap to prevent flies from escaping. Allow flies to recover from CO₂ anesthesia for at least 15 min.
5. Draw 2–3 mm mineral oil first to each calibrated 10 μ L capillary to minimize food evaporation; then draw 20–30 mm liquid SY food without agar to ensure that the food does not drip out when placed vertically in the fly chamber. Wipe off any food outside the capillary with tissue paper. Mark the food level on the capillary with a marker pen as the starting volume.
6. Put the filled capillary through a cut 200 μ L pipette tip with 2–3 mm of the capillary over the pipette tip, and replace the empty tip on the chamber cap.
7. Load the CAFE chambers containing flies and filled capillaries onto the foam rack with water. Each rack should hold 8–12 chambers. Put the rack in an incubator at 25 °C and 70 % humidity. Set up 8–16 chambers as replicates for each treatment.

8. Two capillaries with food are set up in separate chambers without flies and placed in the foam rack to correct for evaporation.
9. After 24-h feeding, mark the food level on both feeding capillary and evaporation controls. Food intake is recorded as the length between the two marks on the feeding capillary subtracted from the average length between the two marks on evaporation controls.
10. Convert the length to the volume of food based on calibration of the capillary. Each 5 mm length typically equals to 1 μL of liquid food when using the 10 μL capillary.
11. Repeat **steps 5–10** with new capillaries to measure food intake for 3 consecutive days.
12. Food intake is calculated by averaging daily food consumption per fly over 3 days.

3.5 Stress Assays

3.5.1 Oxidative Stress Resistance

Oxidative stress resistance is based on flies' resistance to paraquat feeding [10, 58].

1. Flies are prepared and aged for 7–14 days as described in Subheading 3.3.
2. Prepare paraquat vials by adding 600 μL 20 mM paraquat in 5 % sucrose solution into vials, each with 2–3 pieces of 22 mm filter discs (*see Note 4*).
3. Transfer 20 flies into each paraquat vial. 6–10 vials are set up as replicates for each treatment.
4. Record the number of dead flies once every 12 h.
5. Transfer flies to fresh vials with the paraquat solution every 48 h.

3.5.2 Starvation Assay

Follow steps in Subheading 3.5.1 by substituting the paraquat solution with 600 μL autoclaved water on filter discs.

3.6 Reproductive Output

This protocol is used to measure the lifetime egg production of once-mated females [59] (*see Note 5*).

1. Fly preparation follows **steps 1–4** in Subheading 3.3.
2. Place five once-mated females in each vial on cornmeal or a desired SY diet. Set up 6–8 vials as replicates for each treatment.
3. Transfer flies daily to fresh food until all flies are dead.
4. Count the number of dead flies and eggs laid in old vials after each transfer (*see Note 5*).
5. To calculate age-specific reproductive output, divide the total number of eggs produced daily by the number of surviving flies.

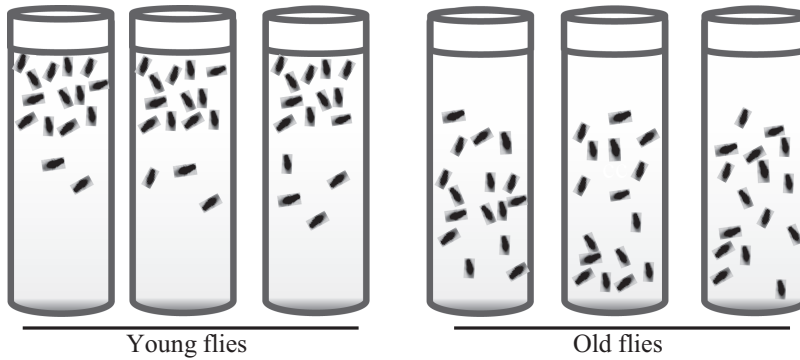


Fig. 3 The rapid iterative negative geotaxis (RING) assay for measuring locomotor activities of young and old flies. Young flies generally climb faster than old flies after tapped to the bottom of the vials

6. To calculate the lifetime reproductive output, divide the total amount of eggs produced by the total number of females used for the experiment.

3.7 Locomotor Activity

3.7.1 Rapid Iterative Negative Geotaxis (RING) Assay

The procedure is based on the RING device and protocol described by Nicols et al. [42] (Fig. 3).

1. Prepare flies following **steps 1–5** in Subheading 3.3.
2. Transfer 20 flies without anesthesia to each new polystyrene vial and assemble vials into the RING apparatus.
3. Allow flies to acclimate to the environment for 15–20 min.
4. Place a digital camera ~1 m away in front of the apparatus and focus the camera onto the apparatus, and set a timer to 3 s.
5. Sharply tap the apparatus down on the bench three times to knock all flies down to the bottom of the vial.
6. Start a 3-s countdown timer immediately after the third tap.
7. Take a picture after 3 s.
8. Repeat **steps 5–7** after a 1-min rest for 5–6 times.
9. Upload images onto a computer and calculate the height that each fly climbs in each vial.
10. Calculate the mean height that flies climb in each group and perform statistical analysis.

3.7.2 *Drosophila* Activity Monitoring (DAM) System

The procedures are based on a previously described protocol [43].

1. Before the experiments, set the incubator to desired light cycle and temperature. A typical experiment is run at 25 °C and a 12 h light/12 h dark cycle for 3–5 days (*see Note 6*).
2. Pour desired liquid SY food in a beaker to a depth of approximately 2–2.5 cm.
3. Position activity tubes vertically in the beaker.

4. Once food solidifies, remove tubes by rotating the ends or by moving them side to side against the food until they are free.
5. Wipe out any residual food outside the walls of tubes with tissue paper. Cover the food end of each tube with a cap that has a hole in the middle (*see Note 6*).
6. Anesthetize flies under light CO₂ and transfer one fly to each activity tube (*see Note 6*).
7. Cap the open end of the tube with a tiny piece of cotton ball.
8. Place tubes into individually numbered and evenly spaced holders in the activity monitor so that the center of each tube is in the holder. Each holder has its own infrared red sensor for recording the activity of the fly in each activity tube.
9. Wrap a rubber band around every 3–4 tubes to hold them in place, and put the activity monitor in the environmentally controlled incubator.
10. Connect the activity monitor to a computer with the DAM system software.
11. Set the activity reading to any desired interval with the DAM system software.
12. Start run when all conditions are set. Do not open the incubator while locomotor activity is being measured (*see Note 6*).
13. Once the recording is stopped, export the data from the DAM system to a computer for analyzing locomotor activity, circadian rhythm, and sleep patterns [43, 45, 46].

4 Notes

1. Adjust the total volume of the food to be prepared based on whether the cooking is done with an electric stove, steamer, or electric kettle. Adjust the amount of agar or use a mixture of yellow and white cornmeal at an optimal ratio, such as 1:1, to achieve desirable and consistent texture of the cornmeal food [54]. Additional cornmeal recipes can be found on the Bloomington Stock Center website (www.flystock.bio.indiana.edu). The sugar and autolyzed yeast portions of the SY diets are cooked separately to minimize the Maillard browning reaction between sugar and protein, which damages protein and potentially affects the survival of flies. Tegosept and other pharmacological and nutraceutical reagents should be added after the food is cooled down to 60–65 °C to minimize heat-induced loss of activities. To minimize tegosept crystallization in the solution, the tegosept stock solution is kept in a tightly capped bottle at –20 °C or is prepared fresh every time one makes fly food. The SY diets used

in aging studies are recommended to have 1.5 % agar, which provides appropriate texture for flies, based on studies by the Partridge lab [55]. For dietary restriction studies, 8 % cornmeal can be added to the SY diets, which may minimize the confounding effect of water consumption on lifespan [60]. It should be noted that flies fed diluted food may compensate the low calorie content in the food by increasing the volume of food intake [18]. Dispense 5–10 mL of food per vial and 50 mL per 6 oz bottle. To minimize cross-contamination, use zippered pillowcases to cover freshly made food. Cooked food can last up to a few weeks if stored at 4 °C. Supplements that are temperature sensitive even at 60–65 °C can be pipetted as a solution onto the food surface after the food is dispensed to vials and cooled down to the room temperature. A food dye can be used to show the uniformity of supplements soaked into the food.

2. Age of parental flies should be less than 1 week and the density of eggs laid in each bottle should be kept between 100 and 200 to minimize the developmental influence on adult lifespan. When sorting out flies for lifespan measurements, do not anesthetize flies for more than 15 min under CO₂ as this may result in brain damage or reduced lifespan. To further reduce the toxicity of CO₂, humidify CO₂ by running it through a bubbler in dH₂O on its way to the fly pad. A minimum of five vials of flies (~100 flies) per group should be used for each lifespan experiment to minimize the impact of sample size and obtain enough statistical power [61]. Lifespan assays can be performed using once-mated or continuously mated flies in vials, bottles, or cages, as long as fly density and environmental conditions, such as temperature, humidity, and light/dark cycle, are well controlled. In statistical analysis, the log rank test may yield very low *P* values for small and probably biologically insignificant differences when the number of animals is large. To obtain more robust and biologically meaningful results, use Student's *t*-test or ANOVA to compare mean or median lifespan using mean or median lifespan from each vial rather than lifespan of individual flies.
3. The feeding period in the food tracer method is limited to approximately 30 min to ensure that the ingested dye is mostly, if not all, retained in the fly. The food tracer method can be used for measuring food intake on the solid food. However, flies have to be sacrificed in each measurement. This prevents longitudinal monitoring of food intake, such as days or lifetime of flies, which is valuable for aging studies. The CAFE assay is suitable for such long-term studies, but only applies to liquid diet. Minimize the presence of air bubbles to ensure the flow of the liquid in the capillary. Addition of water to the holes in the rack for holding fly chambers helps to maintain the humidity in the fly chamber

and reduce evaporation of liquid food in the capillary. It should be noted that it is still controversial whether feeding the liquid food in the CAFE setup reflects the natural feeding environment of flies [17]. Lifespan of flies fed the liquid food is generally shorter than those fed moist and solid agar food [13, 62].

4. For oxidative stress, adjust paraquat concentrations based on the sensitivity of control lines to oxidative stress in each experiment so that approximately 50 % of control flies still survive in day 2 on paraquat treatment. Most commonly used concentrations are 15–30 mM in 5 % sucrose solution. The filter discs may fall out of the vials when the flies are transferred to fresh vials. Use strips of filter paper cut to a proper size so that the wet filter paper can be tightly pressed around the bottom inside the perimeter of the vials to prevent fallout [63].
5. Reproductive output can also be measured with mixed males and females by counting either egg production or the number of eclosed flies. In reproductive output experiments with once-mated females, flies can be transferred to fresh vials every 2–3 days instead of every day. However, to do so, one should be careful not to count any emerged larvae. Count the egg shells that the larvae leave behind on the food for egg counting. Similar to the lifespan assay, the reproduction assay can be performed using once-mated or continuously mated flies in vials or bottles.
6. For measuring locomotor activity with the DAM system, make sure the activity tubes remain moist but without any water droplet before transferring flies [43]. The presence of the hole in the cap minimizes the movement of the food in the activity tube to maintain roughly similar amount of open space among tubes. Flies should not be touching the food when they are transferred to the activity tube to avoid getting stuck. The center of each tube should be aligned with one another and in the center of the holder in the activity monitor. To achieve appropriate alignment, gently push one side of the activity tubes against the wall or a flat surface to align their centers after wrapping the tubes with the rubber bands. Perform the recording for at least 3–4 consecutive days to reduce variations in locomotor activity.

Acknowledgements

We would like to thank three anonymous reviewers for their constructive comments on the manuscript. This work was supported by the Intramural Research Program at the National Institute on Aging, NIH, to S.Z.

References

1. Partridge L, Tower J (2008) Yeast, a feast: the fruit fly *Drosophila* as a model organism for research into aging. In: Guarente L, Partridge L, Wallace DC (eds) Molecular biology of aging. Cold Spring Harbor Laboratory Press, Cold Spring Harbor, NY, pp 267–308
2. Adams MD, Celniker SE, Holt RA et al (2000) The genome sequence of *Drosophila melanogaster*. Science 287:2185–2195
3. Myers EW, Sutton GG, Delcher AL et al (2000) A whole-genome assembly of *Drosophila*. Science 287:2196–2204
4. Reiter LT, Potocki L, Chien S et al (2001) A systematic analysis of human disease-associated gene sequences in *Drosophila melanogaster*. Genome Res 11:1114–1125
5. Finch CE, Ruvkun G (2001) The genetics of aging. Annu Rev Genomics Hum Genet 2:435–462
6. Swindell WR, Bouzat JL (2006) Inbreeding depression and male survivorship in *Drosophila*: implications for senescence theory. Genetics 172:317–327
7. Fry JD, Heinssohn SL, Mackay TF (1998) Heterosis for viability, fecundity, and male fertility in *Drosophila melanogaster*: comparison of mutational and standing variation. Genetics 148:1171–1188
8. McGuire SE, Mao Z, Davis RL (2004) Spatio-temporal gene expression targeting with the TARGET and gene-switch systems in *Drosophila*. Sci STKE 2004:pl6
9. Tower J (2000) Transgenic methods for increasing *Drosophila* life span. Mech Ageing Dev 118:1–14
10. Lin YJ, Seroude L, Benzer S (1998) Extended life-span and stress resistance in the *Drosophila* mutant methuselah. Science 282:943–946
11. Piper MD, Partridge L, Raubenheimer D et al (2011) Dietary restriction and aging: a unifying perspective. Cell Metab 14:154–160
12. Fontana L, Partridge L, Longo VD (2010) Extending healthy life span – from yeast to humans. Science 328:321–326
13. Lee KP, Simpson SJ, Clissold FJ et al (2008) Lifespan and reproduction in *Drosophila*: new insights from nutritional geometry. Proc Natl Acad Sci U S A 105:2498–2503
14. Skorupa DA, Dervisefendic A, Zwiener J et al (2008) Dietary composition specifies consumption, obesity, and lifespan in *Drosophila melanogaster*. Aging Cell 7:478–490
15. Carvalho GB, Kapahi P, Benzer S (2005) Compensatory ingestion upon dietary restriction in *Drosophila melanogaster*. Nat Methods 2:813–815
16. Edgecomb RS, Harth CE, Schneiderman AM (1994) Regulation of feeding-behavior in adult *Drosophila melanogaster* varies with feeding regime and nutritional state. J Exp Biol 197:215–235
17. Wong R, Piper MD, Wertheim B et al (2009) Quantification of food intake in *Drosophila*. PLoS One 4:e6063
18. Ja WW, Carvalho GB, Mak EM et al (2007) Prandiology of *Drosophila* and the CAFE assay. Proc Natl Acad Sci U S A 104:8253–8256
19. Haigis MC, Yankner BA (2010) The aging stress response. Mol Cell 40:333–344
20. Kirkwood TBL, Austad SN (2000) Why do we age? Nature 408:233–238
21. Harman D (1956) Aging: a theory based on free radical and radiation chemistry. J Gerontol 11:298–300
22. Arking R, Buck S, Berrios A et al (1991) Elevated paraquat resistance can be used as a bioassay for longevity in a genetically based long-lived strain of *Drosophila*. Dev Genet 12:362–370
23. Huey RB, Suess J, Hamilton H et al (2004) Starvation resistance in *Drosophila melanogaster*: testing for a possible ‘cannibalism’ bias. Funct Ecol 18:952–954
24. Salmon AB, Richardson A, Perez VI (2010) Update on the oxidative stress theory of aging: does oxidative stress play a role in aging or healthy aging? Free Radic Biol Med 48:642–655
25. Force AG, Staples T, Soliman S et al (1995) Comparative biochemical and stress analysis of genetically selected *Drosophila* strains with different longevity. Dev Genet 17:340–351
26. Hoffmann AA, Harshman LG (1999) Desiccation and starvation resistance in *Drosophila*: patterns of variation at the species, population and intrapopulation levels. Heredity (Edinburgh) 83(Pt 6):637–643
27. Kapahi P, Zid BM, Harper T et al (2004) Regulation of lifespan in *Drosophila* by modulation of genes in the TOR signaling pathway (May 25, pg 885, 2004). Curr Biol 14:1789
28. Finkel T, Holbrook NJ (2000) Oxidants, oxidative stress and the biology of ageing. Nature 408:239–247

29. Flatt T, Promislow DE (2007) Physiology. Still pondering an age-old question. *Science* 318:1255–1256
30. De Loof A (2011) Longevity and aging in insects: is reproduction costly; cheap; beneficial or irrelevant? A critical evaluation of the “trade-off” concept. *J Insect Physiol* 57:1–11
31. Flatt T (2011) Survival costs of reproduction in *Drosophila*. *Exp Gerontol* 46:369–375
32. Tatar M (2010) Reproductive aging in invertebrate genetic models. *Ann N Y Acad Sci* 1204:149–155
33. Zwaan B, Bijlsma R, Hoekstra RE (1995) Direct selection on life-span in *Drosophila melanogaster*. *Evolution* 49:649–659
34. Hutchinson EW, Shaw AJ, Rose MR (1991) Quantitative genetics of postponed aging in *Drosophila melanogaster*. 2. Analysis of selected lines. *Genetics* 127:729–737
35. Partridge L, Prowse N, Pignatelli P (1999) Another set of responses and correlated responses to selection on age at reproduction in *Drosophila melanogaster*. *Proc R Soc Lond B Biol Sci* 266:255–261
36. Barnes AI, Wigby S, Boone JM et al (2008) Feeding, fecundity and lifespan in female *Drosophila melanogaster*. *Proc Biol Sci* 275:1675–1683
37. Sgro CM, Partridge L (1999) A delayed wave of death from reproduction in *Drosophila*. *Science* 286:2521–2524
38. Iliadi KG, Boulianne GL (2010) Age-related behavioral changes in *Drosophila*. *Ann N Y Acad Sci* 1197:9–18
39. Shively CA, Willard SL, Register TC et al (2011) Aging and physical mobility in group-housed Old World monkeys. *Age (Dordrecht)* 69(9 Suppl):219S–220S
40. Francois M, Morice AH, Blouin J et al (2011) Age-related decline in sensory processing for locomotion and interception. *Neuroscience* 172:366–378
41. Gargano JW, Martin I, Bhandari P et al (2005) Rapid iterative negative geotaxis (RING): a new method for assessing age-related locomotor decline in *Drosophila*. *Exp Gerontol* 40:386–395
42. Nichols CD, Becnel J, Pandey UB (2012) Methods to assay *Drosophila* behavior. *J Vis Exp* 61: e3795
43. Pfeifferberger C, Lear BC, Keegan KP et al (2010) Locomotor activity level monitoring using the *Drosophila* activity monitoring (DAM) system. *Cold Spring Harb Protoc* 2010:pdb prot5518
44. Allada R, Chung BY (2010) Circadian organization of behavior and physiology in *Drosophila*. *Annu Rev Physiol* 72:605–624
45. Pfeifferberger C, Lear BC, Keegan KP et al (2010) Processing sleep data created with the *Drosophila* activity monitoring (DAM) system. *Cold Spring Harb Protoc* 2010:pdb prot5520
46. Pfeifferberger C, Lear BC, Keegan KP et al (2010) Processing circadian data collected from the *Drosophila* activity monitoring (DAM) system. *Cold Spring Harb Protoc* 2010:pdb prot5519
47. Koh K, Evans JM, Hendricks JC et al (2006) A *Drosophila* model for age-associated changes in sleep:wake cycles. *Proc Natl Acad Sci U S A* 103:13843–13847
48. Branson K, Robie AA, Bender J et al (2009) High-throughput ethomics in large groups of *Drosophila*. *Nat Methods* 6:451–457
49. Grover D, Yang J, Ford D et al (2009) Simultaneous tracking of movement and gene expression in multiple *Drosophila melanogaster* flies using GFP and DsRED fluorescent reporter transgenes. *BMC Res Notes* 2:58
50. Zou S, Liedo P, Altamirano-Robles L et al (2011) Recording lifetime behavior and movement in an invertebrate model. *PLoS One* 6:e18151
51. Ardekani R, Huang YM, Sancheti P et al (2012) Using GFP video to track 3D movement and conditional gene expression in free-moving flies. *PLoS One* 7:e40506
52. Frazier AE, Thorburn DR (2012) Biochemical analyses of the electron transport chain complexes by spectrophotometry. *Methods Mol Biol* 837:49–62
53. Lakovaara S (1969) Malt as a culture medium for *Drosophila* species. *Dros Inform Ser* 44:128
54. Lewis EB (1960) A new standard food medium. *Dros Inform Ser* 34:117–118
55. Bass TM, Grandison RC, Wong R et al (2007) Optimization of dietary restriction protocols in *Drosophila*. *J Gerontol A Biol Sci Med Sci* 62:1071–1081
56. Sun X, Seeberger J, Alberico T et al (2010) Acai palm fruit (*Euterpe oleracea* Mart.) pulp improves survival of flies on a high fat diet. *Exp Gerontol* 45:243–251
57. Sun X, Komatsu T, Lim J et al (2012) Nutrient-dependent requirement for SOD1 in lifespan extension by protein restriction in

- Drosophila melanogaster*. Aging Cell 11:783–793
58. Arking R, Buck S, Berrios A et al (1991) Elevated paraquat resistance can be used as a bioassay for longevity in a genetically based long-lived strain of *Drosophila*. Dev Genet 12:362–370
 59. Boyd O, Weng P, Sun X et al (2011) Nectarine promotes longevity in *Drosophila melanogaster*. Free Radic Biol Med 50:1669–1678
 60. Ja WW, Carvalho GB, Zid BM et al (2009) Water- and nutrient-dependent effects of dietary restriction on *Drosophila* lifespan. Proc Natl Acad Sci U S A 106:18633–18637
 61. Pletcher SD, Khazaeli AA, Curtsinger JW (2000) Why do life spans differ? Partitioning mean longevity differences in terms of age-specific mortality parameters. J Gerontol A Biol Sci Med Sci 55:B381–B389
 62. Mair W, Piper MDW, Partridge L (2005) Calories do not explain extension of life span by dietary restriction in *Drosophila*. PLoS Biol 3:1305–1311
 63. Bayne AC, Mockett RJ, Orr WC et al (2005) Enhanced catabolism of mitochondrial superoxide/hydrogen peroxide and aging in transgenic *Drosophila*. Biochem J 391:277–284

The Use of Calorie Restriction Mimetics to Study Aging

Munehiro Kitada and Daisuke Koya

Abstract

Calorie restriction (CR) has a variety of effects on extending lifespan and delaying the onset of age-related diseases, and it is accepted as the only established experimental antiaging intervention. Several pharmacological agents that can replicate the beneficial effects of CR, called calorie restriction mimetics (CRMs), have been identified. The nutrient-sensing pathways including those involving sirtuins (especially SIRT1) and mammalian target of rapamycin (mTOR) may regulate the physiology of CR, and candidate CRMs that modulate these specific pathways have been identified and investigated using animal models. In this chapter, we focus on candidate CRMs including sirtuin-activating compounds (STACs) and mTOR inhibitors, their slowing of aging, and methods for evaluation of lifespan and metabolic disorders.

Key words Calorie restriction, Calorie restriction mimetics (CRMs), SIRT1, Resveratrol, Sirtuin-activating compounds (STACs), mTOR, Rapamycin

1 Introduction

Calorie restriction and antiaging effect. Aging is a universal process that affects all organs and age-related disruptions in cellular homeostasis result in organ dysfunction. Calorie restriction (CR) promotes longevity and slows aging. In 1935, McCay et al. first reported that rats subjected to 40 % CR had up to 50 % longer median and maximum lifespans than rats fed a standard diet [1]. After this discovery, numerous studies revealed that CR retards aging or extends lifespan in yeast, worms, flies, and rodents. Colman et al. also reported that 30 % CR delayed the onset of numerous age-associated pathologies, including diabetes, cancer, cardiovascular disease, and brain atrophy, and decreased mortality in rhesus monkeys [2]. In addition, Fontana et al. showed that CR for an average of 6 years improved metabolism in humans, as indicated by the levels of serum insulin, cholesterol, C-reactive protein (CRP), and tumor necrosis factor (TNF)- α as well as by carotid intima-media thickness [3]. This group also observed that long-term CR ameliorated the decline in left ventricular diastolic function and decreased the levels of serum tumor

growth factor (TGF)- β 1, TNF- α , and high-sensitivity CRP [4]. Thus, CR has a variety of beneficial effects on lifespan extension and delays the onset of age-related disorders. CR is defined as the restriction of food intake without malnutrition in organisms normally fed ad libitum and it is accepted as the only established antiaging experimental paradigm [5]. Although some reports have shown that the restriction of specific nutrients such as protein and methionine can increase the lifespan [6, 7], the lifespan extension due to reduced food intake is mainly due to reduced calorie intake [5].

Calorie restriction mimetics (CRMs): Pharmacological agents that can replicate the beneficial effects of CR are called calorie restriction mimetics (CRMs). Ingram et al. defined the characteristic activities of CRMs as follows: A CRM (1) mimics the metabolic, hormonal, and physiological effects of CR; (2) activates the stress response pathways observed in CR and enhances stress protection; (3) produces CR-like effects on longevity, reduces age-related disease, and maintains more youthful function; and (4) does not significantly reduce food intake in the short term (although a long-term reduction in food intake is expected) [8]. The nutrient-sensing pathways that include sirtuins, especially SIRT1, the mammalian target of rapamycin (mTOR), and AMP-activated protein kinase (AMPK) appear critical for cellular homeostasis and for coping with starvation. These pathways also represent important regulators of cell growth and proliferation, mitochondrial function, autophagy, and survival. In addition, these signaling pathways are regulated by cross talk with one another. Therefore, the nutrient-sensing pathways may regulate the physiological processes involved in CR. Candidate CRMs that modulate these pathways, which include sirtuin-activating compounds (STACs), AMPK activators, and mTOR inhibitors, have been identified and investigated using animal models. Other candidate CRMs, such as 2-deoxyglucose which inhibits glycolysis, have also been explored [9]. In this chapter, we will focus on STACs and mTOR inhibitors, which have been well studied in recent aging research, and examine how the effects of CRMs on lifespan extension or retardation of age-related metabolic disorders, including obesity-induced abnormalities in animal models, are typically assessed.

Sirtuin-activating compounds (STACs): One molecule through which CR exerts beneficial effects on lifespan extension or delays age-related diseases is silent information regulator 2 (Sir2), a NAD⁺-dependent deacetylase that was initially identified in studies of aging in yeast [10]. Homologues of Sir2 in higher eukaryotes are known as sirtuins. SIRT1, the sirtuin that is most closely related to Sir2, is one of seven mammalian sirtuins and has been well studied [11]. SIRT1 can act as antiaging molecules in the context of CR and environmental stress [12]. Numerous reports in animal models have clearly shown that SIRT1 regulates multiple biological

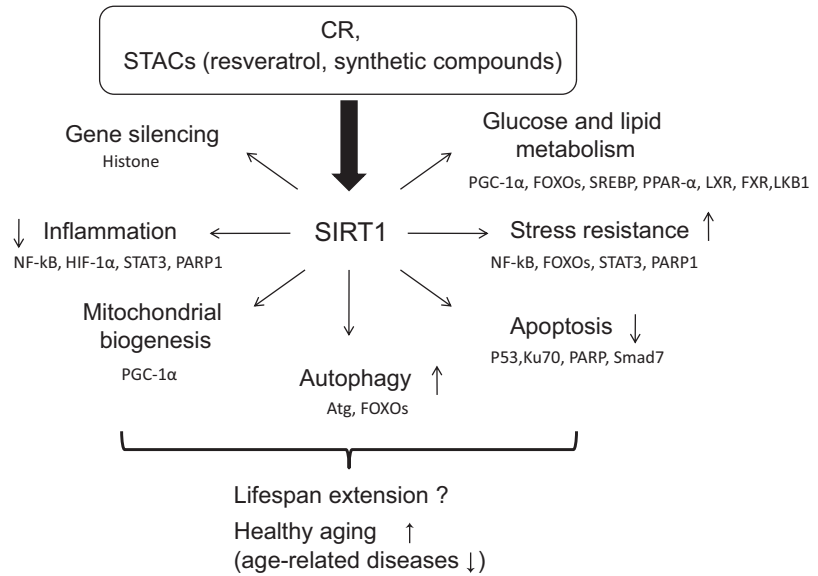


Fig. 1 The biology of SIRT1: SIRT1 regulates multiple biological processes including gene silencing, glucose and lipid metabolism, stress resistance, mitochondrial biogenesis, cell survival, apoptosis, autophagy, and inflammation, through deacetylation of its target proteins

processes, including gene silencing, glucose and lipid metabolism, stress resistance, mitochondrial biogenesis, cell survival, apoptosis, autophagy, and inflammation (Fig. 1). These effects are exerted through the deacetylation of more than a dozen proteins, including transcription factors and transcriptional coregulatory proteins [13] (Fig. 1). The significance of SIRT1 on the effects of CR has been demonstrated in genetically altered mice. Bordne et al. reported that *Sirt1* transgenic mice exhibited a CR-like phenotype, exhibiting reduced levels of blood cholesterol, adipokines, insulin, and fasting glucose and greater glucose tolerance than control mice [14]. However, in another study, *Sirt1* deficiency in mice failed to extend lifespan under CR [12]. In addition, according to the one controlled intervention trial that evaluated the effect of CR on age-related variables in non-obese young adults, a 25 % reduction in calorie intake for 6 months led to the overexpression of SIRT1 and peroxisome proliferator-activated receptor (PPAR)- γ coactivator-1 α (PGC-1 α) in the skeletal muscle, accompanied by an increase in mitochondrial function and a decrease in visceral fat mass, insulin resistance, body temperature, metabolic rate, and levels of oxidative stress [15]. However, CR can extend lifespan in the absence of Sir2, not only in yeast but also in *C. elegans* and *Drosophila* [16–19]. Therefore, it is controversial and currently unclear whether SIRT1 itself is crucial for CR-related lifespan extension; however, SIRT1 activation can retard the progress of age-related diseases and

prolongation of so-called healthy aging, which are known beneficial effects of CR, by regulating multiple biological processes as described above. Thus, sirtuins, especially SIRT1, are potential targets of CRMs that improve metabolism rather than those that affect longevity. The regulation of SIRT1 activity is closely related to that of AMPK. AMPK activation by increasing NAD⁺ production [20] and, conversely, SIRT1 activation leads to an increase in AMPK activation through the deacetylation of liver kinase B1 (LKB1), a molecule upstream of AMPK [21]. Several SIRT1 activators such as resveratrol have been either identified or synthesized and evaluated for their antiaging effects [22].

Resveratrol: Screening compounds for their abilities to activate sirtuins led to the discovery of 18 small molecules, including resveratrol (3,5,4'-trihydroxystilbene) [23], a natural polyphenolic compound found in grapes and red wine. Resveratrol enhances the longevity of some short-lived organisms, including yeast, worms, and flies, in a Sir2-dependent manner [24] and also extends the lifespan of fish [25]. In rodent models, resveratrol has the beneficial effects on longevity and metabolism in high-fat diet-induced obese mice [26, 27], and these effects are associated with AMPK/SIRT1 activation; however, resveratrol has no effect on lifespan extension in standard diet-fed mice. In humans, Timmers et al. reported that administering oral resveratrol (150 mg/day) to obese male patients for 30 days had CR-like effects, improving obesity-related metabolic abnormalities by activating the AMPK/SIRT1 pathway in the skeletal muscle [28]. Thus, the beneficial effects of resveratrol against metabolic abnormalities in age-related disorders, including high-fat-induced obesity, are exerted through AMPK and/or SIRT1 activation.

Synthetic sirtuin activators: Synthetic compounds (such as SRT1720, SRT1460, and SRT2183) that are structurally distinct from resveratrol but have potent SIRT1-activating activities in vitro have been synthesized by Sirtris Pharmaceuticals. Among these compounds, SRT1720 has been well studied and exerts many beneficial effects in animal models through its SIRT1-dependent effects on lifespan extension or the amelioration of high-fat diet-induced metabolic impairments. Although resveratrol activates AMPK either directly or indirectly, SRT1720 may not activate AMPK.

mTOR inhibitor (rapamycin): mTOR, a serine/threonine protein kinase, has been implicated in the regulation of cell growth, endoplasmic reticulum stress, metabolism, stress resistance, translation, and autophagy through the sensing of nutrient/energy levels and growth factors such as insulin and cytokines in cells [29]. CR leads to a reduction in TOR signaling [30], and the genetic downregulation of TOR is sufficient to increase lifespan in yeast, worms, and flies [31–34]. Therefore, TOR inhibitors have been proposed as

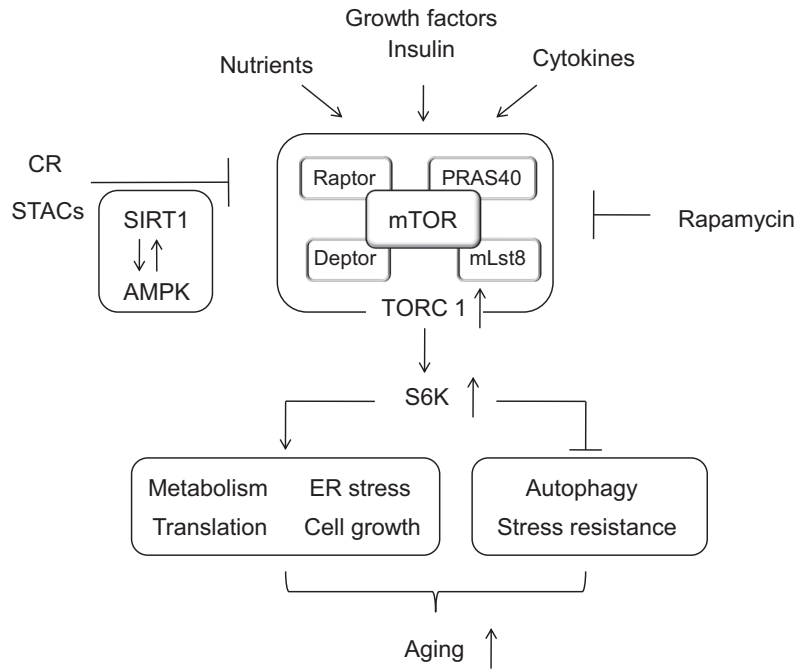


Fig. 2 The TOR network in aging: The TOR pathway is activated by nutrients and growth factors such as insulin and cytokines. Rapamycin is an mTOR inhibitor and CR activates SIRT1 and AMPK, leading to the inhibition of mTOR

candidate CRMs for lifespan extension. Rapamycin is known as not only an immunosuppressive or antitumor agent but also as an inhibitor of mTOR. The beneficial effects of mTOR inhibition on longevity and slow aging in animal models have been shown using rapamycin. Harrison et al. demonstrate that the mTOR inhibitor rapamycin can extend the lifespan of mice by approximately 15 % in females and 10 % in males [35]. The mTOR protein is found in two protein complexes. mTOR complex 1 (TORC 1) contains TOR and the associated proteins Raptor (regulatory-associated protein of TOR), mLst8, PRAS40, and Deptor in mammals [36], while mTORC2 consists of TOR and Rictor (rapamycin-insensitive companion of mTOR), mLst8, and mSIN 1 (mammalian stress-activated protein kinase interacting protein 1). Although chronic rapamycin treatment inhibits both mTORC1 and mTORC2, the effects of rapamycin on longevity are thought to be mediated by its blockade of TORC1 activity. However, the inhibition of mTORC2 by rapamycin causes insulin resistance and impairs glucose homeostasis through adverse effects on hepatic gluconeogenesis [37]. Moreover, mTOR may also be negatively regulated by other nutrient-sensing pathways such as the SIRT1 and AMPK pathways [38] (Fig. 2).

Measurements of aging (lifespan and metabolism): CR can extend the lifespan and delay the onset of age-related disorders including metabolic impairments. Therefore, the effects of CRMs on aging study are typically evaluated by lifespan estimations and measuring changes in metabolic disorders. Usually, long experimental periods and large sample sizes are necessary for lifespan estimations. In this chapter, we discuss the protocol used in the previous report as one example [35]. Insulin resistance and high levels of insulin in the blood are involved in aging, and CR increases insulin sensitivity. Loss-of-function mutations in the insulin signaling system result in lifespan extension in several species, such as *C. elegans* [39], *D. melanogaster* [40, 41], and mice [42]. Therefore, the estimation of insulin sensitivity is necessary. The glucose clamp technique is known as the gold standard method for estimating insulin sensitivity in vivo; however, it is difficult to perform for all animals. Therefore, insulin sensitivity is often assessed by measuring plasma or serum insulin concentrations, blood glucose levels, IPGTT (intraperitoneal glucose tolerance test), and IPITT (intraperitoneal insulin tolerance test) at the end of experiments. Because low insulin-like growth factor-1 (IGF-1) is implicated in CR-induced longevity, plasma or serum IGF-1 concentration is often measured [5]. In addition, SIRT1 induces mitochondrial biogenesis, leading to improvements in glucose and lipid metabolism. Therefore, mitochondrial biogenesis and function should be evaluated by measuring mitochondrial DNA contents and citrate synthase activity (representing mitochondrial function) and by morphological observation under an electron microscope [26]. Moreover, SIRT1 activation can be estimated by the deacetylation levels of target proteins such as PGC-1 α [26]. The inhibitory effects of rapamycin on mTOR are evaluated by measuring the activity of the S6 ribosome, a molecule downstream of mTORC1 [35].

2 Materials

2.1 CRMs

1. *Trans*-resveratrol (Sigma-Aldrich, St. Louis, MO).
2. Rapamycin (LC Labs, Woburn, MA) (*see* **Note 1**).

2.2 Measurement of Blood Glucose, Insulin, Lipids, and IGF-1

1. The ultrasensitive mouse insulin assay kit (Morinaga Institute of Biological Science, Yokohama, Japan) [43].
2. The L-type TG H kit, Cholesterol E-test kit, and NEFA C-test kit (Wako Chemicals, Osaka, Japan) [43].
3. Serum IGF-I levels were quantified using double-antibody EIA and single-antibody direct ELISA kits (Diagnostic Systems Laboratories, Webster, TX, USA) [26].

2.3 Mitochondrial DNA Contents [27]

1. mtDNA-specific PCR (16S rRNA), forward 5'-CCGCAAG-GAAAGTGAAAGAC-3', and reverse 5'-TCGTTTGGTTTCG GGGTTTC-3' and nuclear-specific PCR (hexokinase 2 gene, intron 9), forward 5'-GCCAGCTCTCCTGATTTTAGTGT-3', and reverse 5'-GGGAACACAAAAGACCTCTTCTGG-3'
2. QuantiTect STBR Green PCR Kit (Qiagen, Hilden, Germany).

2.4 Citrate Synthase Activity [26]

1. Lysis buffer: 10 mM sodium phosphate, pH 7.2 with 1 % NP-40, 1 % sodium deoxycholate, 0.1 % SDS, 150 mM NaCl 2 mM EDTA, phosphatase inhibitor cocktail 1 (Sigma-Aldrich, St. Louis, MO), 1 mM vanadate, 20 mM NaF, and one tablet of complete protease inhibitor (Roche, Basel, Switzerland)/15 ml.
2. Assay buffer: 0.1 mM DNTB (Sigma-Aldrich, St. Louis, MO), 0.3 mM acetyl CoA (Roche, Basel, Switzerland), and 0.5 mM oxaloacetate (Sigma-Aldrich, St. Louis, MO) in 50 mM Tris-HCl, pH 8.0.

2.5 Immuno-precipitation (SIRT1 Activity) [26] and Immunoblotting (AMPK [26] and Activated S6 Ribosomal Protein [35])

1. Lysis buffer: 10 mM sodium phosphate, pH 7.2 with 1 % NP-40, 1 % sodium deoxycholate, 0.1 % SDS, 150 mM NaCl 2 mM EDTA, phosphatase inhibitor cocktail 1 (Sigma-Aldrich, St. Louis, MO), 1 mM vanadate, 20 mM NaF, and one tablet of complete protease inhibitor (Roche, Basel, Switzerland)/15 ml.
2. Protein A/G Sepharose (Sigma-Aldrich, St. Louis, MO).
3. Anti-PGC1 α antibody (H300) (Santa Cruz Biotechnology, Santa Cruz, CA) and anti-acetyl-lysine antibody (Cell Signaling Technology, Beverly, MA).
4. Anti-phospho-AMPK α (Thr172) and anti-AMPK α (23A3), anti-S6 ribosomal protein (5G10), and anti-phospho-S6 ribosomal protein (Ser235/236) antibodies (Cell Signaling Technology, Beverly, MA).
5. Horseradish peroxidase-coupled secondary antibody (Amersham Biosciences).

3 Methods

3.1 Administration of CRMs to Mice

Oral intake is the major delivery route used for resveratrol (0.04–0.4 % resveratrol mixed in chow (22–400 mg/kg BW/day)) [26, 27], SRT1720 (2 g/kg mixed in chow (100 mg/kg BW/day)) [44] or administered to mice on a high-fat (60 %) [26, 27, 44] or standard [45] diet, and rapamycin (14 mg/kg in chow (2.24 mg /kg BW/day)) administered to mice on standard diet [35, 46]. The duration of the treatment is dependent on the purpose of the experiment. For lifespan estimations, long-term

treatment will be necessary, while 8 weeks to 6 months is usually sufficient to assess metabolic changes.

In detail (methods from the report written by Baur et al. [26]):

1. Male C57BL/6NIA mice at 11 months of age are purchased and are maintained on a standard purified mouse diet (AIN-93G) for 1 month prior to the start of the experiment.
2. Mice are fed the standard AIN-93G diet or AIN-93G plus 0.04 % resveratrol ad libitum for an additional 6 weeks, while high-calorie diets are prepared.
3. Mice on AIN-93G are either continued on the standard diet or switched to high-calorie AIN-93G (modified by adding hydrogenated coconut oil to provide 60 % of calories from fat), and the group receiving AIN-93G plus 0.04 % resveratrol is switched to the high-calorie diet plus 0.04 % resveratrol.

3.2 Evaluation of Lifespan [35]

1. Mice are examined at least daily for signs of ill health and are euthanized for humane reasons if they are so severely moribund that they are considered unlikely to survive for more than an additional 48 h.
2. A mouse is considered severely moribund if it exhibits more than one of the following clinical signs: (a) inability to eat or to drink; (b) severe lethargy, as indicated by a lack of response to external stimulation (e.g., reluctance to move when gently prodded with a forceps); (c) severe balance or gait disturbance; (d) rapid weight loss over a period of 1 week or more; or (e) a severely ulcerated or bleeding tumor.
3. The age at which a moribund mouse is euthanized is taken as the best available estimate of its natural lifespan. The number of dead mice is also noted at each daily inspection. Bodies are fixed for later necropsy.

3.3 Evaluation of Metabolism

3.3.1 Measurement of Glucose, Insulin, and IGF-1 Levels

For glucose and insulin measurements, blood samples were taken by tail venipuncture. For insulin measurements, whole blood is spun at 14,000 rpm in a benchtop centrifuge for 7 min to pellet the blood cells. The plasma is transferred to a fresh tube and placed on dry ice, after which it is stored at -80°C . Insulin levels are measured using the appropriate assay kits. Glucose levels are measured using a glucose meter. The IGF-1 levels in the plasma are measured using the appropriate assay kits.

3.3.2 Glucose Tolerance Tests

1. The mice are fasted overnight for 14 h followed by intraperitoneal glucose injection (1 g/kg body BW).
2. Blood glucose and insulin levels are measured in tail blood collected at 0, 15, 30, 60, and 120 min after the injection.

3.3.3 *Insulin Tolerance Tests*

1. Mice are administered an injection of human regular insulin (Novolin R; Novo Nordisk, Clayton, NC) at 0.75 U/kg BW intraperitoneally after a 6-h fast.
2. Blood glucose is measured at 0, 15, 30, and 60 min.

3.3.4 *Lipid Profiles*

The total cholesterol, triglyceride, and free fatty acid levels are measured using the assay kits.

3.4 *Mitochondrial Biogenesis (in the Liver or Muscle)*

3.4.1 *Mitochondrial DNA Contents [27]*

1. Selected tissues are homogenized and digested with Proteinase K overnight in a lysis buffer for DNA extraction via conventional phenol-chloroform method or in a lysis buffer containing 10 % Chelex 100 resin for the direct analysis of liberated nucleic acids.
2. Quantitative PCR is performed in duplicate on 30- to 50-fold diluted DNA or lysates, using 10 μ M each primer (mtDNA-specific PCR (16S rRNA)) and nuclear-specific PCR (hexokinase 2 gene, intron 9) and QuantiTect STBR Green PCR Kit in a LightCycler 480 (Roche Diagnostics, Mannheim, Germany) with a program of 20 min at 95 °C, followed by 50–55 cycles of 15 s at 95 °C, 20 s at 58 °C, and 20 s at 72 °C.
3. The production of a single amplification is verified by an integrated post-run melting curve analysis.
4. Exponential amplification efficiency is verified during each PCR run using a standard dilution series made from pooled samples.
5. Results are calculated from the difference in threshold cycle (ΔC_T) values for mtDNA and nuclear-specific amplification.
6. Data are expressed as mitochondrial genomes per diploid nuclei.

3.4.2 *Electron Microscopic Observation of Mitochondria [26]*

1. Portions of harvested tissues, such as the liver and muscle, are cut into small tissue blocks (1 mm³) and fixed in 2 % glutaraldehyde in 0.1 M potassium phosphate sodium buffer at 4 °C.
2. After postfixation with 2 % osmium tetroxide, tissues are dehydrated in a series of graded ethanol solutions. Ethanol is then substituted for propylene oxide, and the samples are embedded in epoxy resin.
3. Ultrathin sections are double stained with uranyl acetate and lead citrate.
4. Sections are examined with a JEM1200EX electron microscope (JEOL, Tokyo) at 80 keV.
5. Mitochondrial area and number are estimated in several micrographs which were taken for the cells of animals. The mitochondrial area is measured using the ImageJ software, and the number of mitochondria per cell is counted manually by an observer who is blinded to the identity of the sample.

3.4.3 Citrate Synthase Activity [26]

1. A 200-mg sample of frozen tissue is placed in 3 ml lysis buffer and pulsed twice for 15 s each at $12,500 \times g$ in a tissue homogenizer.
2. The homogenate is cleared by centrifugation at $12,500 \times g$ for 15 min.
3. A 100- μ g aliquot of protein is used for each assay.
4. The increase in absorbance at 412 nm is measured every 30 s over 15 min at 23 °C in the assay buffer in the presence of the substrate oxaloacetate. The blank contained all reagents except for the tissue homogenate.
5. The maximal enzymatic activity (V_{\max}) is determined as the maximal slope in the linear range.
6. Each sample is assayed in triplicate and the results are expressed as the fold change relative to the control (set at 100 %).

3.5 Measurement of SIRT1 Activation [26]

SIRT1 activation is analyzed by assessing the deacetylation of target proteins; this deacetylation is detected by immunoblotting using an antibody specific for acetylated lysine after immunoprecipitation using an antibody against the target protein, e.g., PGC-1 α (*see Note 2*).

1. Total protein extracts are dissected and snap frozen in liquid nitrogen, stored at -80°C , ground into powder under liquid nitrogen, dissolved in 10 volumes of ice-cold buffer, and cleared by centrifugation at $12,500 \times g$ for 10 min at 4°C .
2. PGC-1 α is immunoprecipitated with a rabbit anti-PGC-1 α antibody or rabbit IgG as a control and protein A/G Sepharose beads followed by incubation at 4°C for 4 h.
3. The immunoprecipitates are washed extensively, resolved by SDS-PAGE, and transferred to nitrocellulose membranes.
4. The membranes are blocked and then incubated with anti-acetyl-lysine antibody overnight.
5. The membranes are washed and then incubated with horseradish peroxidase-coupled secondary antibody.
6. After washing, the blots are visualized using an enhanced chemiluminescence detection system.

3.6 AMPK Activation [26] or the Effectiveness of Rapamycin (S6 Ribosomal Protein Activation [35])

1. Tissues from animals are dissected and snap frozen in liquid nitrogen, stored at -80°C , ground into powder under liquid nitrogen, and dissolved in 10 volumes of ice-cold buffer.
2. After sonication and centrifugation at $12,500 \times g$ for 10 min at 4°C , lysates are quantified, and 30–40 μ g of soluble protein from each extract are loaded on a 4–12 % gradient polyacrylamide gel for electrophoresis.

3. The proteins are then transferred to nitrocellulose membranes, blocked, and incubated with the primary antibodies against phospho-AMPK, AMPK, S6 ribosomal protein (5G10), or phospho-S6 ribosomal protein, followed by a secondary antibody for detection with a chemiluminescence detection system.

4 Notes

1. Rapamycin that was microencapsulated by Southwest Research Institute (San Antonio, TX) using a spinning disk atomization coating process with the enteric coating material Eudragit S100 (Röhm Pharma, Germany) [35]. The encapsulated rapamycin is released in the small intestine rather than the stomach.
2. Anti-acetylated target protein antibodies such as anti-acetylated NF- κ B (p65) antibody or anti-acetylated p53 antibody can be purchased from Cell Signaling Technology or Abcam (MA, USA).

Acknowledgements

This work was supported by a Grant from Novo Nordisk Pharma, a Grant-in-Aid for Scientific Research (C) (24591218), and a Grant for Promoted Research from Kanazawa Medical University (S2012-4) to M. Kitada and by Grants for Collaborative Research (C2012-1) and Specially Promoted Research from Kanazawa Medical University (SR2012-06) and the Fourth Annual Research Award Grant of Japanese Society of Anti-Aging Medicine to D. Koya.

References

1. McCay CM, Crowell MF, Maynard LA (1989) The effect of retarded growth upon the length of life span and upon the ultimate body size. 1935. *Nutrition* 5:155–171, discussion 172
2. Colman RJ, Anderson RM et al (2009) Caloric restriction delays disease onset and mortality in rhesus monkeys. *Science* 325:201–204
3. Fontana L, Meyer TE, Klein S et al (2004) Long-term caloric restriction is highly effective in reducing the risk for atherosclerosis in humans. *Proc Natl Acad Sci U S A* 101:6659–6663
4. Meyer TE, Kovacs SJ, Ehsani AA et al (2006) Long-term caloric restriction ameliorates the decline in diastolic function in humans. *J Am Coll Cardiol* 47:398–402
5. Masoro EJ (2005) Overview of caloric restriction and ageing. *Mech Ageing Dev* 126:913–922
6. Masoro EJ, Iwasaki K, Gleiser CA et al (1989) Dietary modulation of the progression of nephropathy in aging rats: an evaluation of the importance of protein. *Am J Clin Nutr* 49:1217–1227
7. Zimmerman JA, Malloy V, Krajcik R et al (2003) Nutritional control of aging. *Exp Gerontol* 38:47–52
8. Ingram DK, Zhu M, Mamczarz J et al (2006) Calorie restriction mimetics: an emerging research field. *Aging Cell* 5:97–108
9. Ingram DK, Roth GS (2011) Glycolytic inhibition as a strategy for developing calorie restriction mimetics. *Exp Gerontol* 46:148–154
10. Imai S, Armstrong CM, Kaeblerlein M et al (2000) Transcriptional silencing and longevity

- protein Sir2 is an NAD-dependent histone deacetylase. *Nature* 403:795–800
11. Guarente L (2011) Franklin H. Epstein lecture: sirtuins, aging, and medicine. *N Engl J Med* 364:2235–2244
 12. Boily G, Seifert EL, Bevilacqua L et al (2008) SirT1 regulates energy metabolism and response to caloric restriction in mice. *PLoS One* 3:e1759
 13. Michan S, Sinclair D (2007) Sirtuins in mammals: insights into their biological function. *Biochem J* 404:1–13
 14. Bordone L, Cohen D, Robinson A et al (2007) SIRT1 transgenic mice show phenotypes resembling caloric restriction. *Aging Cell* 6:759–767
 15. Civitarese AE, Carling S, Heilbronn LK et al (2007) Calorie restriction increases muscle mitochondrial biogenesis in healthy humans. *PLoS Med* 4:e76
 16. Jiang JC, Wawryn J, Shantha Kumara HM et al (2002) Distinct roles of processes modulated by histone deacetylases Rpd3p, Hda1p, and Sir2p in life extension by caloric restriction in yeast. *Exp Gerontol* 37:1023–1030
 17. Kaerberlein M, Kirkland KT, Fields S et al (2004) Sir2-independent life span extension by caloric restriction in yeast. *PLoS Biol* 2: E296
 18. Smith DL Jr, McClure JM, Matecic M et al (2007) Calorie restriction extends the chronological lifespan of *Saccharomyces cerevisiae* independently of the sirtuins. *Aging Cell* 6:649–662
 19. Burnett C, Valentini S, Cabreiro F et al (2011) Absence of effects of Sir2 overexpression on lifespan in *C. elegans* and *Drosophila*. *Nature* 477:482–485
 20. Canto C, Gerhart-Hines Z, Feige JN et al (2009) AMPK regulates energy expenditure by modulating NAD⁺ metabolism and SIRT1 activity. *Nature* 458:1056–1060
 21. Price NL, Gomes AP, Ling AJ et al (2012) SIRT1 is required for AMPK activation and the beneficial effects of resveratrol on mitochondrial function. *Cell Metab* 15:675–690
 22. Baur JA, Ungvari Z, Minor RK et al (2012) Are sirtuins viable targets for improving healthspan and lifespan? *Nat Rev Drug Discov* 11:443–461
 23. Howitz KT, Bitterman KJ, Cohen HY et al (2003) Small molecule activators of sirtuins extend *Saccharomyces cerevisiae* lifespan. *Nature* 425:191–196
 24. Wood JG, Rogina B, Lavu S et al (2004) Sirtuin activators mimic caloric restriction and delay ageing in metazoans. *Nature* 430:686–689
 25. Valenzano DR, Terzibasi E, Genade T et al (2006) Resveratrol prolongs lifespan and retards the onset of age-related markers in a short-lived vertebrate. *Curr Biol* 16:296–300
 26. Baur JA, Pearson KJ, Price NL et al (2006) Resveratrol improves health and survival of mice on a high-calorie diet. *Nature* 444:337–342
 27. Lagouge M, Argmann C, Gerhart-Hines Z et al (2006) Resveratrol improves mitochondrial function and protects against metabolic disease by activating SIRT1 and PGC-1 α . *Cell* 127:1109–1122
 28. Timmers S, Konings E, Bilet L et al (2011) Calorie restriction-like effects of 30 days of resveratrol supplementation on energy metabolism and metabolic profile in obese humans. *Cell Metab* 14:612–622
 29. Zoncu R, Efeyan A, Sabatini DM (2011) mTOR: from growth signal integration to cancer, diabetes and ageing. *Nat Rev Mol Cell Biol* 12:21–35
 30. Yilmaz OH, Katajisto P, Lamming DW et al (2012) mTORC1 in the Paneth cell niche couples intestinal stem-cell function to calorie intake. *Nature* 486:490–495
 31. Stanfel MN, Shamieh LS, Kaerberlein M et al (2009) The TOR pathway comes of age. *Biochim Biophys Acta* 1790:1067–1074
 32. Kaerberlein M, Powers RW III, Steffen KK et al (2005) Regulation of yeast replicative life span by TOR and Sch9 in response to nutrients. *Science* 310:1193–1196
 33. Jia K, Chen D, Riddle DL (2004) The TOR pathway interacts with the insulin signaling pathway to regulate *C. elegans* larval development, metabolism and life span. *Development* 131:3897–3906
 34. Kapahi P, Zid BM, Harper T et al (2004) Regulation of lifespan in *Drosophila* by modulation of genes in the TOR signaling pathway. *Curr Biol* 14:885–890
 35. Harrison DE, Strong R, Sharp ZD et al (2009) Rapamycin fed late in life extends lifespan in genetically heterogeneous mice. *Nature* 460:392–395
 36. Kapahi P, Chen D, Rogers AN et al (2010) With TOR, less is more: a key role for the conserved nutrient-sensing TOR pathway in aging. *Cell Metab* 11:453–465
 37. Lamming DW, Ye L, Katajisto P et al (2012) Rapamycin-induced insulin resistance is mediated by mTORC2 loss and uncoupled from longevity. *Science* 335:1638–1643

38. Blagosklonny MV (2010) Calorie restriction: decelerating mTOR-driven aging from cells to organisms (including humans). *Cell Cycle* 9:683–688
39. Kenyon C, Chang J, Gensch E et al (1993) A *C. elegans* mutant that lives twice as long as wild type. *Nature* 366:461–464
40. Clancy DJ, Gems D, Harshman LG et al (2001) Extension of life-span by loss of CHICO, a *Drosophila* insulin receptor substrate protein. *Science* 292:104–106
41. Tatar M, Kopelman A, Epstein D et al (2001) A mutant *Drosophila* insulin receptor homolog that extends life-span and impairs neuroendocrine function. *Science* 292:107–110
42. Bluher M, Kahn BB, Kahn CR (2003) Extended longevity in mice lacking the insulin receptor in adipose tissue. *Science* 299:572–574
43. Kitada M, Kume S, Imaizumi N et al (2011) Resveratrol improves oxidative stress and protects against diabetic nephropathy through normalization of Mn-SOD dysfunction in AMPK/SIRT1-independent pathway. *Diabetes* 60:634–643
44. Minor RK, Baur JA, Gomes AP et al (2011) SRT1720 improves survival and healthspan of obese mice. *Sci Rep* 1:70
45. Pearson KJ, Baur JA, Lewis KN et al (2008) Resveratrol delays age-related deterioration and mimics transcriptional aspects of dietary restriction without extending life span. *Cell Metab* 8:157–168
46. Wilkinson JE, Burmeister L, Brooks SV et al (2012) Rapamycin slows aging in mice. *Aging Cell* 11:675–82

Using Somatic-Cell Nuclear Transfer to Study Aging

Satoshi Kishigami, Ah Reum Lee, and Teruhiko Wakayama

Abstract

In mammals, a diploid genome following fertilization of haploid cells, an egg, and a spermatozoon is unique and irreproducible. This implies that the generated unique diploid genome is doomed with the individual's inevitable demise. Since it was first reported in 1997 that Dolly the sheep had been cloned, many mammalian species have been cloned successfully using somatic-cell nuclear transfer (SCNT). The success of SCNT in mammals enables us not only to reproduce offspring without germ cells, that is, to “passage” a unique diploid genome, but also to address valuable biological questions on development, nuclear reprogramming, and epigenetic memory. Successful cloning can also support epigenetic reprogramming where the aging clock is reset or reversed. Recent work using iPS cell technology has explored the practicality and led to the recapitulation of premature aging with iPSCs from progeroid laminopathies. As a result, reprogramming tools are also expected to contribute to studying biological age. However, the efficiency of animal cloning is still low in most cases and the mechanism of reprogramming in cloned embryos is still largely unclear. Here, based on recent advances, we describe an improved, more efficient mouse cloning protocol using histone deacetylase inhibitors (HDACis) and latrunculin A, which increases the success rates of producing cloned mice or establishing ES cells fivefold. This improved method of cloning will provide a strong tool to address many issues including biological aging more easily and with lower cost.

Key words Somatic-cell nuclear transfer, Oocyte, Nuclear reprogramming, Aging, Reproduction, Mouse

1 Introduction

In nature, a diploid genome of an individual mammal is generated only through fertilization between an egg and a spermatozoon which are produced via meiosis. Therefore, each diploid genome is unique and distinctive between individuals. The unique diploid genome sets of individuals are normally doomed due to either individual longevity or finite cellular lifespan, termed the “Hayflick limit” [1]. However, it was first reported in 1997 that a sheep had been cloned [2], which enabled us to reproduce the unique diploid genome without passing through germ line. Following the success of cloning mice and cow, more than ten additional mammalian

species have been cloned successfully using somatic-cell nuclear transfer (SCNT).

SCNT is a powerful and often unique tool to address valuable biological questions that define nuclear equivalence between zygotes and differentiated cells. The success of SCNT has demonstrated that nuclei from highly differentiated cells can be reprogrammed and that the genetic information of donor nuclei is not lost during development and differentiation [3]. This finding confirmed the concept that nuclear totipotency should be intrinsically retained for any cell types and that epigenetic, rather than genetic, mechanisms are responsible for keeping cells in their state of differentiation. Another important issue is whether animals cloned from an adult would display the biological age of the founder (the donor of nucleus). Actually the length of Dolly's telomere was reported to be apparently shorter than the founder's [4]. In contrast, in some cloned animals telomere length was not only restored but extended beyond that of the founder [5, 6].

An interesting question has been raised whether somatic nuclear transfer (SCNT) can restore the cellular senescence and transcends the natural limit. If this is true, a diploid genome could theoretically have eternal lifespan both as cells and individuals [7]. In mouse experiments, at least several rounds of serial cloning were possible. However, the cloning success rate decreased with increasing generations. Finally, only one cloned mouse was produced in the sixth generation from more than 1,000 nuclear transfers [8]. The telomere lengths and the possibility of premature aging in the recloned mice were found having no abnormalities in either. Similar results have been reported in cattle [9], which failed to produce a third generation. The recloning of cats [10] and pigs [11, 12] has also been studied, but those reached only the second and third generations, respectively. Thus, currently successive recloning is limited without an identifiable reason. This kind of analysis may provide a model system to approach new biological aspect of "aging" during "passage" of the diploid without germ cells. Further, this advantage of SCNT, which reproduce individuals without germ cells, also allows us to propagate infertile mice such as senescent mice [13], hermaphrodite [14], or even frozen body [15]. Interestingly, cloning success rate decreases with the age, suggesting that "reprogrammability" of somatic cells may be dependent on the age of donor individuals.

Regardless, SCNT appears to be able to reset the aging clock for perpetuating a species. Again, the success of SCNT itself requires that an adult cell still retain all the information necessary to generate an entire organism. This success also indicates the nuclei of an adult somatic cell can be rejuvenated and totipotency restored in the oocyte cytoplasm. Recently, reprogramming technologies appear to be strong tools for studying aging [16, 17]. For example, iPS technologies demonstrated the recapitulation of premature aging

with iPSC from Hutchinson-Gilford progeria syndrome [18, 19]. SCNT is also expected to further the study of aging as a whole individual rather than at the cellular level.

While cloning efficiencies can range from 0 to 20 %, efficiency rates of only 1–2 % are typical for mice [20]. These inefficiencies have been limiting practical applications of SCNT. Moreover, many abnormalities in mice cloned from somatic cells have been reported, including abnormal gene expression in embryos [21–23], abnormal placentas [24, 25], obesity [26, 27], and early death of clones from Sertoli cells [28]. These two issues have been main concerns in SCNT technologies to overcome. Regardless, the success of SCNT gives promise to numerous applications such as species preservation, livestock propagation, and cell therapy for medical treatment by nuclear transfer embryonic stem cells (ntESCs) [14, 29]. Furthermore, recently, the low efficiency of cloning mice has been significantly improved by finding a new protocol of SCNT using histone deacetylase inhibitors [30]. This finding led to cloning even “unclonable strain” [31, 32].

SCNT has been the unique tool to address biological questions including aging. After improvement by HDACi, it should be expected that SCNT can contribute more to addressing these questions as well as its applications since sometimes the low efficiency itself has made it impossible to address these questions. In this chapter, we describe an improved, more efficient mouse cloning protocol using histone deacetylase inhibitors (HDACis) and latrunculin A.

2 Materials

2.1 Stock Solution

2.1.1 Reagents

1. Pregnant mare serum gonadotropin (PMSG): PMSG (Sigma-Aldrich, St. Louis, MO, USA; G4527) is dissolved in normal saline at 50 IU/mL and stored in aliquots at -20°C .
2. Human chorionic gonadotropin (hCG): hCG (Sigma-Aldrich; C8554) is dissolved in normal saline at 50 IU/mL and stored in aliquots at -20°C .
3. 0.5 mg/mL CB stock solution ($\times 100$): add 2 mL dimethyl sulfoxide (DMSO, Sigma-Aldrich; D2650) to a vial with 1 mg cytochalasin B (Sigma-Aldrich; C6762). Divide into small tubes (10–20 μL) and store at -20°C . Highly toxic.
4. 100 mM SrCl_2 stock solution ($\times 10$): $\text{SrCl}_2 \cdot 6\text{H}_2\text{O}$ (Sigma-Aldrich; S0390) is dissolved in distilled water (DW) at 100 mM and stored in aliquots at room temperature.
5. 40 mM EGTA stock solution ($\times 100$): ethylene glycol-bis (β -aminoethyl ether)- N,N,N',N' -tetraacetic acid tetrasodium salt (EGTA, Sigma-Aldrich; E8145) is dissolved in DW at 40 mM and stored in aliquots at 4°C .

6. 10 μ M TSA stock solution (HDACi, $\times 200$): add 3.311 mL DMSO to a vial with 1 mg trichostatin A (TSA, Sigma-Aldrich; T8552) and then take 2 μ L of this stock and dilute with 198 μ L of DMSO (10 μ M). Divide into small tubes (5–10 μ L) and store at -30°C .
7. 1 mM SCR stock solution (HDACi, $\times 200$): add 3.064 mL DMSO to a vial with 1 mg scriptaid (SCR, Sigma-Aldrich; S7817) and then take 5 μ L of this stock and dilute with 95 μ L of DMSO (50 μ M). Divide into small tubes (5–10 μ L) and store at -30°C ($200\times$ SCR stock solution).
8. 1 mM LATA stock solution ($\times 200$): add 237.2 μ L DMSO to a vial with 100 μ g latrunculin A (LATA, Sigma-Aldrich; L5163). Divide into small tubes (10–20 μ L) and store at -30°C .
9. Anesthetic stock solution: mix 5 g of 2,2,2-tribromoethyl alcohol (Sigma-Aldrich; T48402) with 5 mL 2-methyl-2-butanol (Sigma-Aldrich; 240486) in a 50°C water bath until fully dissolved. Add 1.25 mL of this mixture to 50 mL normal saline solution and store at 4°C .
10. 50 mM PMSF stock solution: phenylmethanesulfonyl fluoride (PMSF, Sigma-Aldrich; P7626) is dissolved in ethanol at 50 mM and stored in aliquots at 4°C ($100\times$ stock solution).

2.1.2 Oocyte Culture Media

1. HEPES-buffered Chatot, Ziomek, and Bavister (HEPES-CZB) medium [33] is used for gamete handling and SCNT under air.
2. Synthetic oviductal medium enriched with potassium (KSOM, Millipore, Temecula, CA, USA; MR-020P-5D) is used for oocyte and cloned embryo culture.

2.1.3 Fibroblast Cell Culture Media

Tail tip or embryonic fibroblast (EF) cells are cultured in EF medium: Dulbecco's Modified Eagle's Medium (DMEM, Sigma-Aldrich; D6429) supplemented with 10 % fetal bovine serum (FBS, Gibco; 26140-079) and 1 % penicillin–streptomycin solution (Sigma-Aldrich; P7539).

2.1.4 Nuclear Isolation Media (NIM)

NIM is used for frozen donor cells: 123.0 mM KCl, 2.6 mM NaCl, 7.8 mM NaH_2PO_4 , 1.4 mM KH_2PO_4 , 3 mM EDTA disodium salt, and 0.5 mM PMSF. The pH is adjusted to 7.2 by addition of a small quantity of 1 M KOH.

2.2 Equipment and Tools

1. Inverted microscope with Hoffman optics from Olympus (Tokyo, Japan; model IX71).
2. Micromanipulator set from Narishige (Tokyo, Japan; model MMO-202ND, <http://www.narishige.co.jp/>).
3. Pipette puller (P-97) and glass pipette (B100-75-10) from Sutter Instrument Co. (Novato, CA, USA; <http://www.sutter.com>).

4. Microforge from Narishige (Tokyo, Japan; model MF-900).
5. Warm plate from Tokai Hit (Shizuoka, Japan, model MATS-U55R30; <http://www.tokaihit.com/english/top/index.html>).
6. Piezo impact drive system from Prime Tech Ltd. (Ibaraki, Japan; model PMM-150FU or PMM4G; <http://www.prime-tech-jp.com/en/01products/index.html>).
7. Humidified incubator; 37 °C, 5 % CO₂.
8. Tissue culture hood.
9. Centrifuge.

2.3 Preparations of Microtools and Media

2.3.1 Preparation of Holding, Enucleation, and Injection Micropipettes

1. Micropipettes can be made in-house or ordered from several companies (e.g., Prime Tech Ltd., <http://www.primetech-jp.com/en/01products/psk.html>). First, we use a Sutter pipette puller (P-97) to divide the glass pipette into two parts. Each part could be used to make pipettes. For the holding pipette, the outside diameter (OD) should be smaller than that of the oocyte (e.g., OD 70–80 μ m, inner diameter (ID) 10 μ m). The ID of the enucleation pipette is 8–10 μ m. The ID of the injection pipette depends on nuclear donor cell type: 6–7 μ m for cumulus cells and 7–8 μ m for fibroblasts or ES cells. If you are purchasing pipettes, ask the supplying company to bend all pipettes close to the tip (about 300 μ m back) at 20–25° using a microforge.
2. For optimizing the power of the piezo unit, a small amount of mercury (about a 3–5 mm long column) needs to be inserted into the enucleation and injection pipette using a 1 mL syringe and a 30-gauge needle. Fill the syringe part way with mercury, insert the needle into the back of the pipette and inject a mercury droplet into the needle (*see Note 1*). Pipettes can be stored in a 10 cm dish at room temperature.

2.3.2 Preparation of Media and Dishes with Media

1. Enucleation media: add 2 μ L of CB stock solution to 198 μ L of HEPES-CZB medium. The final concentration of CB is 5 μ g/mL. The manipulation dish includes three types of media, HEPES-CZB, enucleation medium, and polyvinylpyrrolidone (PVP; 360 kDa; Irvine Scientific, Santa Ana, CA, USA; 99311). Each droplet should be 10–15 μ L in volume on the lid of a 10 cm dish, as shown in Fig. 1, and covered with mineral oil. To distinguish the different media easily, draw separation lines on the dish.
2. Oocyte and embryo culture media: place 20 \times 10 μ L droplets of KSOM on a 6 cm cell culture dish and cover this with sterile mineral oil (Sigma-Aldrich; M8410). Because this dish is used for oocyte culture from collection to artificial activation, it must be prepared at first and warmed in a 37 °C incubator with 5 % CO₂.

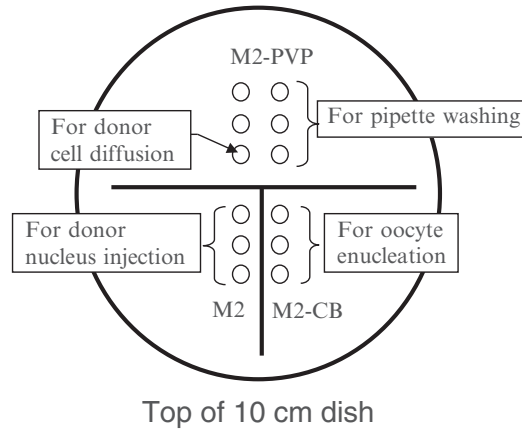


Fig. 1 Manipulation chamber: *above the line* is the M2-PVP medium for pipette washing, donor cell diffusion, and picking up nucleus. *Right under the line* is the M2-CB medium for oocyte enucleation. *Left under the line* is the M2 medium for donor nuclei injection into enucleated oocytes

- Oocyte activation media: Add 10 μL of SrCl_2 stock solution (final 5 mM), 10 μL of EGTA stock solution (final 2 mM), 1 μL of LATA stock solution (final 5 $\mu\text{g}/\text{mL}$) (*see Note 2*), and 1 μL of one of the HDACi stock solution to 186 μL of KSOM. Reconstructed oocyte activation dish: place three rows of oocyte activation medium droplets, two rows of reprogramming enhancement medium, and two rows of KSOM on a 6 cm dish. Each droplet should be 10–15 μL in volume. Then cover this dish with mineral oil and draw separation lines on the dish.

2.4 Setting Up the Micromanipulator

- Attach the holding pipette to one side of the micromanipulator. On the other side, attach the enucleation pipette to the pipette holder of the piezo unit. Fix the piezo unit on the micromanipulator. The top of the pipette holder must be screwed in tightly, or you cannot cut the zona pellucida of the oocyte by piezo pulses smoothly. Expel any air and oil and a few drops of mercury from the enucleation pipette for washing in PVP medium. Wash both the inside and outside of the pipette using PVP medium until no oil remains. The piezo unit must be applied with high power and high speed for at least 30 s continuously to be effective.

2.5 Mouse and Strains

- Donor cells: usually hybrid mouse strains such as B6D2F1 (C57BL/6 \times DBA/2), B6C3F1 (C57BL/6 \times C3H/He), or B6129F1 (C57BL/6 \times 129 \times 1/Sv) can be used as donors. Inbred strains such as C57BL/6 or C3H/He can be

used but they have a lower embryonic development rate than hybrid strains.

2. Oocytes: B6D2F1 mice (about 2–3 months old) are used as a source of oocytes. B6D2F1 oocytes are very translucent and the metaphase spindle is easy to find.
3. Recipients and vasectomized male mice: the ICR (CD-1) strain is used for the production of pseudopregnant surrogate mothers, for lactating foster mothers and for vasectomized males.

3 Methods

3.1 Oocyte Collection

1. Hormone priming for superovulation: female mice (8–10 weeks) are superovulated by an injection of 5 IU of PMSG into the abdominal cavity 3 days before an experiment and then injected with hCG (5 IU) 48 h later (1 day before an experiment). We usually do this from 5 to 6 p.m.
2. Collection of oocytes: collect oocyte–cumulus cell complexes (COCs) from the oviductal ampullae at 14–15 h after hCG injection (usually we collect oocytes at 9 a.m.) and transfer them into a 50 μ L droplet of HEPES-CZB containing 0.1 % hyaluronidase (Sigma-Aldrich; H4272) for 5 min. Select good oocytes, wash them twice and then move them to an oocyte culture dish prepared as above. The number of oocytes in a drop depends on each person's skill or the type of experiment. We recommend that all oocytes in one drop must be manipulated within 15 min. Therefore, place ~20 embryos per drop, according to your skill level.

3.2 Donor Cell Preparation

3.2.1 Cumulus Cells

Cumulus cells are the easiest to prepare as nuclear donors because they can be collected after oocyte selection and transferred to a PVP droplet in the manipulation chamber without washing; also, there is no need to remove hyaluronidase from the medium.

3.2.2 Sertoli Cells

Sertoli cells are the best choice. Sertoli cells collected from neonatal mouse testes (immature Sertoli cells) are suitable nuclear donors for SCNT and usually give better results than cumulus cells [34, 35]. On the other hand, those from the adult testis are too large to be injected. Thus, the age of donors will affect the success rate. We recommend the use of newborn males at less than 6 days of age.

3.2.3 Tail Tip Fibroblasts

Tail tip cells must be prepared at least 2 weeks before SCNT [24]. Cut the whole or a part of tail into sections at least 2 cm long and wash them in 70 % ethanol carefully. Remove the skin in a sterile tissue culture hood and cut the tail into many small pieces on a 6 cm plastic

dish. Culture the fragments in 10 mL DMEM in a 5 % CO₂, 37 °C incubator until they are used. There is no need to passage the cells.

3.2.4 ES or ntES Cells

Thawed ES cells should be cultured at least 2 days before doing NT. If you use cultured ES cells, they also need to be passaged for 2 days in 6-well dishes before an experiment. Each individual ES cell line, even if from the same genetic background, will lend itself to this procedure to a different degree, yielding varying results for embryonic development [29, 36–38]. The number of passages of ES cell lines is also important and will have to be determined empirically for each line. Note that these are pluripotent cells, not differentiated somatic cells, so they are not appropriate for genomic reprogramming experiments.

3.2.5 Special Cells (Frozen Brain and Blood Cells)

Frozen mouse brain tissue must be broken into small pieces (1–2 mm³) on dry ice. Homogenize the material under 500 µL of NIM in a 1.5 mL tube using a pestle, then filter it using a cell strainer (BD Falcon, BD Biosciences, San Jose, CA, USA; 352235) and collect the supernatant. This will contain many naked nuclei. For collecting blood cells, take 1–2 µL of blood cells from the frozen-thawed mouse tail and add this to 500 µL of NIM.

3.3 Collection of Donor Cells

3.3.1 Cultured Cells

For collecting cultured cells such as fibroblasts or ES cells, remove the culture medium from the dish or flask and wash them in Dulbecco's phosphate-buffered saline (D-PBS(–), Wako Pure Chemical Industries, Osaka, Japan; 045-29795). Remove the PBS, add trypsin-EDTA (Gibco; 25200-056), and then incubate 5–20 min in a 37 °C incubator with 5 % CO₂. Add EF medium and triturate the cells to produce a single cell suspension. Spin down the cells in a centrifuge at $300 \times g$ for 5 min and wash them with D-PBS(–) by centrifugation at least three times. Because trypsin is very toxic at the time of nuclear injection, the donor cells must be washed thoroughly. Make a very concentrated cell suspension in EF medium. The final volume should be less than 10 µL. Pick up 1–3 µL of this suspension and put the cells in a PVP medium droplet in the micromanipulation chamber. Completely mix the donor cells with PVP medium, or they will aggregate and be hard to manipulate.

3.3.2 Non-cultured Fresh Cells

For non-cultured cells such as Sertoli cells, wash them at least three times in phosphate-buffered saline (PBS) to remove any enzyme by centrifugation ($176 \times g$ for 5 min). Cumulus cells can be used directly without any washing.

3.3.3 Frozen Cells

Frozen cells suspended in NIM can be collected by centrifugation. Introduce a few microliters of suspension into NIM in the manipulation chamber instead of the PVP medium.

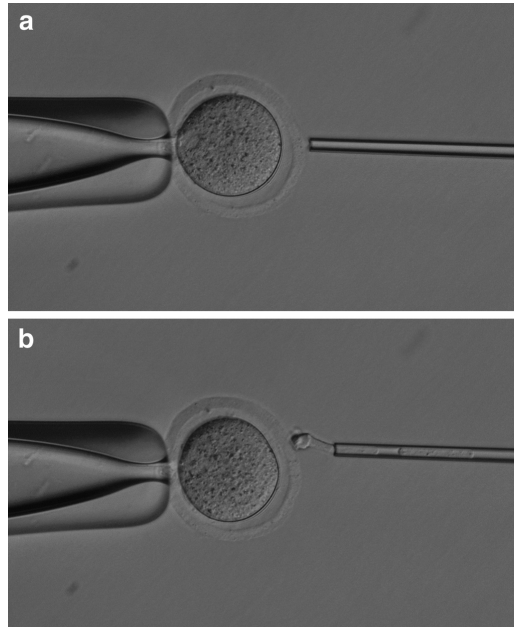


Fig. 2 Oocyte enucleation. **(a)** Rotate and find the metaphase II spindle and place it to 8–10 o'clock position. Then hold this oocyte on the holding pipette, and remove the spindle by suction without breaking the plasma membrane and gently pull away the pipette from oocytes. **(b)** Push out the spindle in order to check the enucleation, which is harder than the cytoplasm

3.4 Enucleation

1. Place one group of oocytes in a droplet of enucleation medium into the micromanipulation chamber. Wait for 5–10 min before starting enucleation, because CB can make the oolemma more flexible and reduce lysis of oocytes.
2. Finding the metaphase II (MII) spindle of the oocyte is the key point in this step (*see Note 3*). It can be recognized using Nomarski differential interference or Hoffman modulation contrast optics. Although you can use 4',6-diamidino-2-phenylindole or Hoechst DNA dyes to stain the nuclei, they are harmful to the oocyte and hamper embryonic development. Rotate the oocyte to place the spindle at between 8 and 10 o'clock and then attach the oocyte firmly to the holding pipette (Fig. 2).
3. Cut through the zona pellucida using a few piezo pulses (*see Note 4*). Add a slight negative pressure inside the pipette as this increases the power of the pulse. To avoid damaging the oocyte, ensure there is a large space between the zona pellucida and the oolemma; this should be approximately as wide as the thickness of the zona pellucida.

4. Insert the enucleation pipette into the oocyte without using piezo pulses, to avoid breaking the oolemma. The MII spindle looks like a small sphere under Nomarski or Hoffman optics and is harder than the cytoplasm, so you can feel its consistency through the micromanipulator. Remove the MII spindle by aspiration with a minimal volume of cytoplasm. Aspirating too much cytoplasm might hamper embryonic development. The oocyte membrane and spindle must be pinched off slowly, drawing the needle out carefully until the oolemma seals (Fig. 2).
5. When you have finished with one group of oocytes, wash them twice in KSOM to remove the CB completely and return them to the incubator in KSOM for at least 30 min before starting donor cell injection. If the CB is not completely washed out, many oocytes will lyse after injection. Your intense concentration is required in the next step (injection of somatic or ES cells), so once all the enucleation of oocytes has been finished, you should take a short rest before starting injection.

3.5 Donor Nucleus Injection

1. Transfer a group of enucleated oocytes [10–20] into HEPES-CZB medium. The number of oocytes per droplet depends on each individual's skill level. The important point is that each group should be finished within 15 min (*see Note 5*). Add a few microliters of donor cell suspension to a PVP droplet (*see Note 6*). Remove the donor nuclei from the cells by gently aspirating them in and out of the injection pipette (Fig. 3a) until each nucleus is clearly separate from any visible cytoplasmic material (Fig. 3b). We usually take up 5–10 nuclei at the same time into the injection pipette.
2. Move the injection pipette to the HEPES-CZB droplet containing the enucleated oocytes. Stabilize an enucleated oocyte using a holding pipette. Cut the zona pellucida with a few piezo pulses (power level 2–3 and speed 5–6). Reduce the power level of the piezo unit (power level 1–2 and speed 1) because the oolemma is weaker than the zona pellucida and the survival rate of oocytes after injection will be better with this reduced power.
3. Push one nucleus near the tip of the pipette and advance the pipette at the same time until it almost reaches the opposite side of the oocyte's cortex. Apply only one reduced piezo pulse to puncture the oolemma at the pipette tip. This is indicated by a rapid relaxation of the oocyte membrane. You must not apply any piezo pulses until the pipette reaches the opposite side. If the piezo power is applied with the tip of the pipette in the middle of the oocyte, the oocyte will die after injection. Release the donor nucleus into the ooplasm immediately with a minimal amount of PVP medium (*see Note 7*). Gently withdraw the injection pipette from the oocyte.

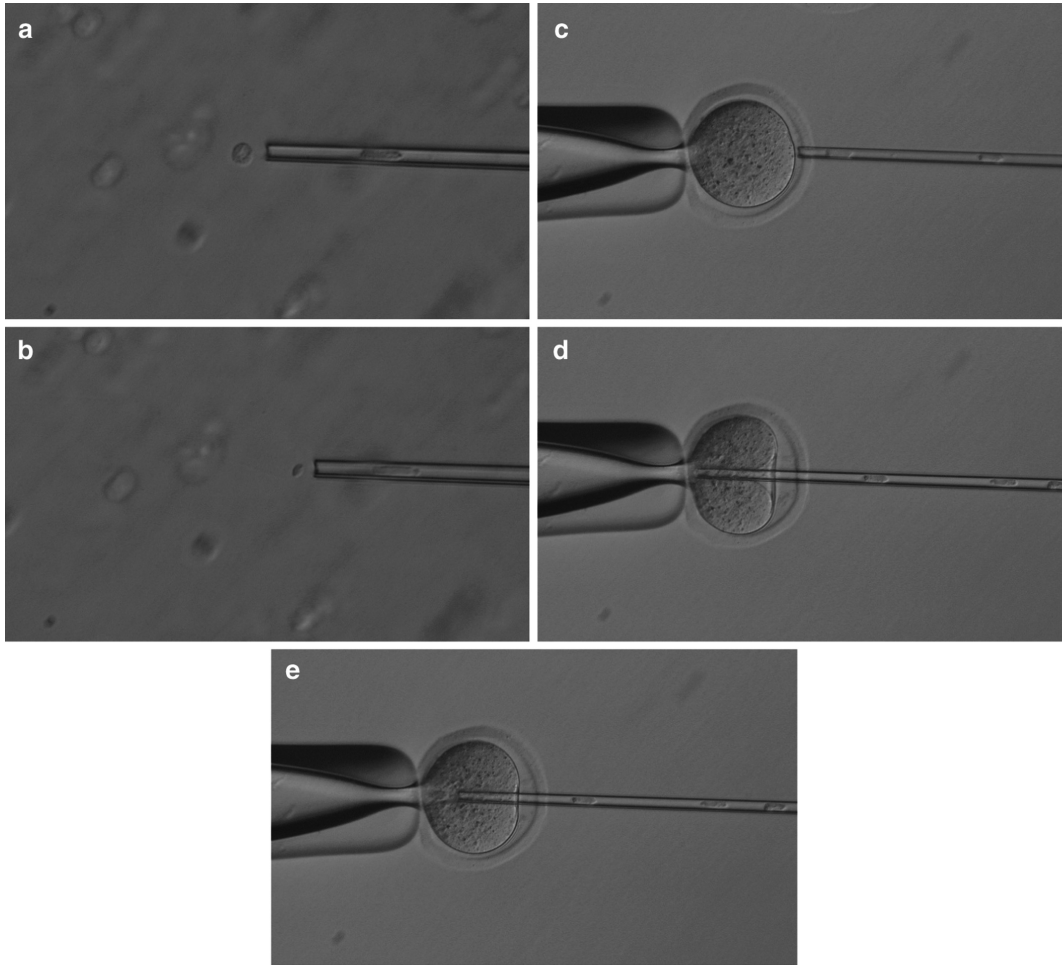


Fig. 3 Donor nucleus collection and injection. **(a, b)** Donor nuclei are gently aspirated in and out of the injection pipette until their nuclei are largely devoid of visible cytoplasmic material. **(b)** Push out the spindle in order to check the enucleation, which is harder than the cytoplasm. **(c)** Hold the enucleated oocyte and cut the zona pellucida using piezo pulses. **(d)** Insert the injection pipette into the enucleated oocyte. **(e)** Apply the single piezo pulse to break the membrane, and immediately inject the donor nucleus

4. When all the nuclei have been injected into oocytes, you should wash the injection pipette in a PVP dish by expelling some mercury and applying power from the piezo unit. This washing step is essential to prevent the pipette from getting sticky.
5. When one group of oocytes has been used for NT, keep them in this drop for 10–15 min then transfer them into KSOM. Culture these oocytes for at least 30 min in the 5 % CO₂ incubator before activation (*see Note 8*).

3.6 Oocyte Activation and Embryo Culture

1. Activation medium should be prepared at least 30 min before use. This dish must be placed in a CO₂ incubator for equilibration. Transfer oocytes into the activation medium including HDACi

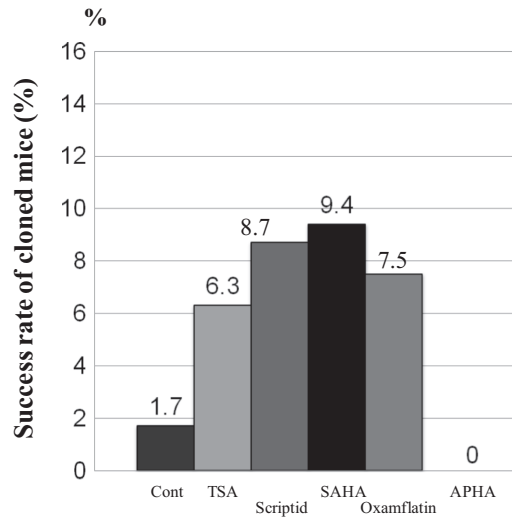


Fig. 4 Effects of histone deacetylase inhibitor (HDACi) treatment on mouse cloning. Full term development of cloned mice using different HDACi. The success rate was significantly increased when cloned embryos were cultured with TSA, Scriptaid, Oxamflatin, and SAHA

such as TSA, SCR or others (*see Note 9*) and wash them twice, then culture them for 10 h in a 5 % CO₂ incubator at 37 °C.

2. After 10 h activation, all embryos must be washed twice in KSOM droplets (*see Note 10*). Examine the rate of oocyte activation (*see Note 11*). If NT and activation are done properly, those oocytes should each possess two or three pseudo-pronuclei. Move the cloned embryos to a new KSOM dish for long-term culture to blastocyst stage. In some cases, some batches of mineral oil are toxic. Therefore, it is advisable to test all new batches of oil by culturing embryos in drops of KSOM, overlaid with the new oil. Always set up a control group of embryos cultured under oil of known quality. Cloned embryos can be used either for production of cloned mice or establishment of ntES cells (Figs. 4 and 5).

3.7 Production of Cloned Mice

3.7.1 Embryo Transfer and Caesarian Section

1. Prepare foster mothers by mating estrous ICR female mice with normal males on the same day or 1–2 days before the experiment: these will be used for receipt of NT pups derived by Caesarian section at E19.5. Foster mothers are needed for NT pups because NT litters are too small to stimulate lactation in the surrogate mothers.
2. Prepare pseudopregnant mothers by mating estrous ICR female mice with vasectomized males on the same day as the experiment.
3. Cloned embryos can be transferred at different stages. Embryos at the two-cell (24 h after NT) or four- to eight-cell

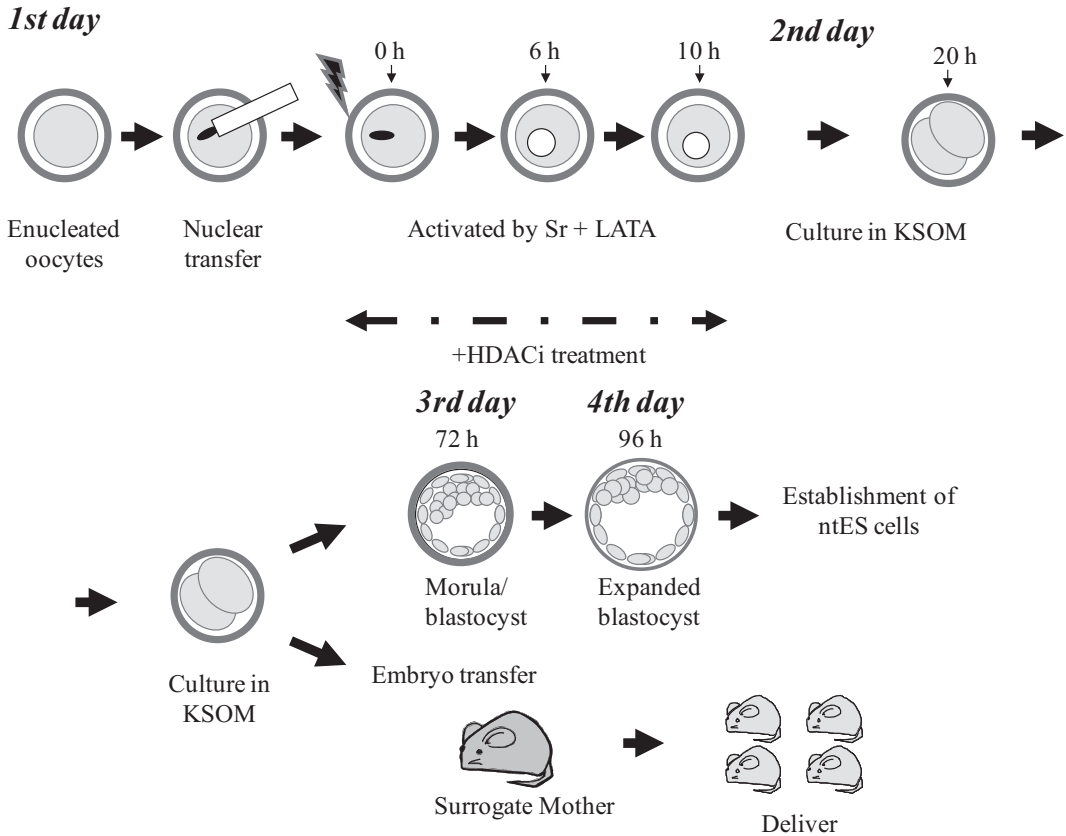


Fig. 5 An experimental scheme of somatic-cell nuclear transfer with HDACi and LATA. According to the standard procedure of mouse cloning, donor nuclei from somatic cells are injected into enucleated oocytes. These reconstructed oocytes are activated in activation media. After 10 h activation, the activation medium is changed to KSOM medium. These cloned embryos are cultured in KSOM until subjected to embryo transfer into the surrogate mother (second day), examination of blastocyst formation (third or fourth day), or establishment for ntES cells (third or fourth day)

(48 h after NT) can be transferred into the oviducts of the recipients at 0.5 days post copulation (dpc). On the other hand, morulae/blastocysts (72 h after NT) or blastocysts (96 h after NT) can be transferred into the uterus of pseudopregnant mice at 2.5 dpc.

4. Cloned mouse fetus frequently shows abnormality such as placentomegaly, so a Caesarian section is required to recover the cloned mouse fetuses securely (*see Note 12*). Euthanize the surrogate mother at 18.5 or 19.5 dpc (usually at 19.5 dpc). Remove the uterus from the abdomen and dissect out the cloned pups with their placentas. Wipe away the amniotic fluid from the skin, mouth, and nostrils carefully and stimulate the pups to breathe by rubbing their backs or pinching them gently with blunt forceps. Warm the pups on a 37 °C hotplate

and then transfer the cloned pups to the cage of a naturally delivered foster mother. The foster mother should be moved from the cage first. Take some soiled bedding from the cage and nestle the cloned pups in the bedding material so that they take on the odor of the bedding. Remove some pups from the foster mother's litter and then mix in the cloned pups. Finally, return the mother to the cage and leave the animal room quietly.

4 Notes

1. Mercury needs to be introduced when preparing the enucleation and injection pipette (*see* Subheading 3.1). This operation must be done in a working fume hood and you need to wear appropriate protective gloves because mercury volatilizes and is toxic if inhaled or absorbed through the skin.
2. EGTA is added for chelating Ca^{2+} in media for efficient Sr^{2+} incorporation into the oocytes [39]. You can use other media for oocyte activation but have to adjust EGTA concentration depending on the Ca^{2+} concentration in that media. Also, you can use CB instead of LATA. In that case, the reconstructed oocytes are activated by activation media with CB. For 10 h of TSA treatment, after 6 h activation, activated oocytes are cultured in KSOM medium including TSA for another 4 h and transferred into KSOM without TSA.
3. Sometimes you cannot detect the MII spindle at the enucleation step. We always maintain the oocytes at 25 °C to do this. However, this temperature can allow the spindle microtubules to disperse and become unclear, so you will need to warm the manipulation chamber to 37 °C and the spindle will become visible again. Oocyte transparency also depends on the mouse strain: we find that B6D2F1 mice are better oocyte donors than some others.
4. When you first use the piezo unit, you should examine whether you can cut the zona pellucida smoothly. If you cannot do so, check the connection between the pipette and the pipette holder. The top of the pipette holder must be screwed in tightly. Expel all oil inside the pipette, as this might have reduced the piezo unit's power transmission. There should be a slight negative pressure inside the pipette to enhance piezo power.
5. During micromanipulation, you might find that the pipette gets sticky. The condition of the pipette is very important: it will affect not only the oocyte survival rate but also embryo development after NT. Wash the pipette in PVP medium completely. PVP will cover both the inside and outside of the

pipette to keep the surface slick. Without this step, the pipette soils rapidly and needs to be changed.

6. When donor cells are transferred to the PVP droplet, mix them with the PVP medium using sharp tweezers for at least 30 s. If the donor cells are not mixed thoroughly with the PVP medium, they will aggregate and it will be difficult to isolate single cells. ES cells are especially sensitive and fragile and it is better to make a new ES cell suspension every 30 min.
7. Sometimes it is difficult to release the donor nucleus from the pipette. If so, the pipette is probably too dirty. It must be washed frequently using PVP medium by expelling some mercury and applying power from the piezo unit. Otherwise, the pipette should be changed.
8. There are many factors that can induce oocyte lysis after injection, such as the pipette having too large an ID, excessively high room temperature, or the pipette insertion being too shallow. A large pipette causes the piezo power to be too strong and this can increase the rate of oocyte lysis. The process of NT should be performed at room temperature (25–26 °C). Do not use a warm plate for the microinjection process. The injection pipette must be inserted very deep into the oocyte before applying the piezo pulse. In addition, you need practice. If you are a novice, all the oocytes will lyse immediately after injection. One month after starting practice, about half of your oocytes might survive. One year later, about 80 % of oocytes will survive, if you continue to practice diligently. Reconstructed oocytes should be placed in HEPES-CZB medium for at least 10 min. If they are transferred to KSOM immediately after injection, nearly 15 % of them will undergo lysis from the damage of injection.
9. You can use SAHA and oxamflatin as other HDACi [40]. Also, when ES cells are used as the source of donor nuclei, HDACi supplementation does not work well. If G2/M cell cycle phase ES cells are used as a source of donor nuclei, CB must be omitted from the medium.
10. We cannot avoid the death of cloned embryos during activation. During strontium treatment, up to 10 % of the oocytes will die and the medium will become contaminated. Do not worry, because this is normal and the surviving oocytes are usually undamaged. Therefore, check the activation medium with fresh intact oocytes as necessary.
11. When the activation has finished, you should check the rate of pseudo-pronuclear formation in the cloned embryos. If you cannot confirm this formation, it means you have failed this time. There are several reasons why oocytes do not form pseudo-pronuclei. Usually it is because of a failure to break

the donor cell membrane or failure of oocyte activation. The injection pipette must be smaller than the donor cell. If the donor cell has a tough cell membrane (e.g., tail tip fibroblasts), apply piezo power to break the donor cell membrane at the time of cell pickup.

12. All cloned mice to date have been born with abnormal and hypertrophic placentas and they often die just after birth from respiratory failure. At present there is no way to avoid this lethal phenotype.

Acknowledgments

We gratefully acknowledge discussions with Drs. J. Kimura and T. Castranio.

References

1. Hayflick L, Moorhead PS (1961) The serial cultivation of human diploid cell strains. *Exp Cell Res* 25:585–621, Epub 1961/12/01
2. Wilmut I, Schnieke AE, McWhir J, Kind AJ, Campbell KH (1997) Viable offspring derived from fetal and adult mammalian cells. *Nature* 385(6619):810–813, Epub 1997/02/27
3. Meissner A, Jaenisch R (2006) Mammalian nuclear transfer. *Dev Dyn Am Assoc Anat* 235(9):2460–2469, Epub 2006/08/02
4. Shiels PG, Kind AJ, Campbell KH, Waddington D, Wilmut I, Colman A et al (1999) Analysis of telomere lengths in cloned sheep. *Nature* 399(6734):316–317, Epub 1999/06/09
5. Lanza RP, Cibelli JB, Blackwell C, Cristofalo VJ, Francis MK, Baerlocher GM et al (2000) Extension of cell life-span and telomere length in animals cloned from senescent somatic cells. *Science* 288(5466):665–669, Epub 2000/04/28
6. Kubota C, Yamakuchi H, Todoroki J, Mizoshita K, Tabara N, Barber M et al (2000) Six cloned calves produced from adult fibroblast cells after long-term culture. *Proc Natl Acad Sci U S A* 97(3):990–995, Epub 2000/02/03
7. Kishigami S, Wakayama S, Hosoi Y, Iritani A, Wakayama T (2008) Somatic cell nuclear transfer: infinite reproduction of a unique diploid genome. *Exp Cell Res* 314(9):1945–1950, Epub 2008/03/19
8. Wakayama T, Shinkai Y, Tamashiro KL, Niida H, Blanchard DC, Blanchard RJ et al (2000) Cloning of mice to six generations. *Nature* 407(6802):318–319, Epub 2000/10/03
9. Kubota C, Tian XC, Yang X (2004) Serial bull cloning by somatic cell nuclear transfer. *Nat Biotechnol* 22(6):693–694, Epub 2004/05/25
10. Yin XJ, Lee HS, Yu XF, Kim LH, Shin HD, Cho SJ et al (2008) Production of second-generation cloned cats by somatic cell nuclear transfer. *Theriogenology* 69(8):1001–1006, Epub 2008/03/25
11. Cho SK, Kim JH, Park JY, Choi YJ, Bang JI, Hwang KC et al (2007) Serial cloning of pigs by somatic cell nuclear transfer: restoration of phenotypic normality during serial cloning. *Dev Dyn Am Assoc Anat* 236(12):3369–3382, Epub 2007/09/13
12. Kurome M, Hisatomi H, Matsumoto S, Tomii R, Ueno S, Hiruma K et al (2008) Production efficiency and telomere length of the cloned pigs following serial somatic cell nuclear transfer. *J Reprod Dev* 54(4):254–258, Epub 2008/05/21
13. Mizutani E, Ono T, Li C, Maki-Suetsugu R, Wakayama T (2008) Propagation of senescent mice using nuclear transfer embryonic stem cell lines. *Genesis* 46(9):478–483, Epub 2008/09/11
14. Wakayama S, Kishigami S, Van Thuan N, Ohta H, Hikichi T, Mizutani E et al (2005) Propagation of an infertile hermaphrodite mouse lacking germ cells by using nuclear transfer and embryonic stem cell technology. *Proc Natl Acad Sci U S A* 102(1):29–33, Epub 2004/12/25

15. Wakayama S, Ohta H, Hikichi T, Mizutani E, Iwaki T, Kanagawa O et al (2008) Production of healthy cloned mice from bodies frozen at -20°C for 16 years. *Proc Natl Acad Sci U S A* 105(45):17318–17322, Epub 2008/11/05
16. Rando TA, Chang HY (2012) Aging, rejuvenation, and epigenetic reprogramming: resetting the aging clock. *Cell* 148(1–2):46–57, Epub 2012/01/24
17. Freije JM, Lopez-Otin C (2012) Reprogramming aging and progeria. *Curr Opin Cell Biol* 24(6):757–764, Epub 2012/09/11
18. Liu GH, Barkho BZ, Ruiz S, Diep D, Qu J, Yang SL et al (2011) Recapitulation of premature ageing with iPSCs from Hutchinson-Gilford progeria syndrome. *Nature* 472(7342):221–225, Epub 2011/02/25
19. Zhang J, Lian Q, Zhu G, Zhou F, Sui L, Tan C et al (2011) A human iPSC model of Hutchinson Gilford Progeria reveals vascular smooth muscle and mesenchymal stem cell defects. *Cell Stem Cell* 8(1):31–45, Epub 2010/12/28
20. Wakayama T, Perry AC, Zuccotti M, Johnson KR, Yanagimachi R (1998) Full-term development of mice from enucleated oocytes injected with cumulus cell nuclei. *Nature* 394(6691):369–374, Epub 1998/08/05
21. Boiani M, Eckardt S, Scholer HR, McLaughlin KJ (2002) Oct4 distribution and level in mouse clones: consequences for pluripotency. *Genes Dev* 16(10):1209–1219, Epub 2002/05/23
22. Kishigami S, Hikichi T, Van Thuan N, Ohta H, Wakayama S, Bui HT et al (2006) Normal specification of the extraembryonic lineage after somatic nuclear transfer. *FEBS Lett* 580(7):1801–1806, Epub 2006/03/04
23. Bortvin A, Eggan K, Skaletsky H, Akutsu H, Berry DL, Yanagimachi R et al (2003) Incomplete reactivation of Oct4-related genes in mouse embryos cloned from somatic nuclei. *Development* 130(8):1673–1680, Epub 2003/03/07
24. Wakayama T, Yanagimachi R (1999) Cloning of male mice from adult tail-tip cells. *Nat Genet* 22(2):127–128, Epub 1999/06/16
25. Tanaka S, Oda M, Toyoshima Y, Wakayama T, Tanaka M, Yoshida N et al (2001) Placentomegaly in cloned mouse concepti caused by expansion of the spongiotrophoblast layer. *Biol Reprod* 65(6):1813–1821, Epub 2001/11/22
26. Tamashiro KL, Wakayama T, Akutsu H, Yamazaki Y, Lachey JL, Wortman MD et al (2002) Cloned mice have an obese phenotype not transmitted to their offspring. *Nat Med* 8(3):262–267, Epub 2002/03/05
27. Tamashiro KL, Wakayama T, Blanchard RJ, Blanchard DC, Yanagimachi R (2000) Postnatal growth and behavioral development of mice cloned from adult cumulus cells. *Biol Reprod* 63(1):328–334, Epub 2000/06/22
28. Ogonuki N, Inoue K, Yamamoto Y, Noguchi Y, Tanemura K, Suzuki O et al (2002) Early death of mice cloned from somatic cells. *Nat Genet* 30(3):253–254, Epub 2002/02/12
29. Wakayama T, Tabar V, Rodriguez I, Perry AC, Studer L, Mombaerts P (2001) Differentiation of embryonic stem cell lines generated from adult somatic cells by nuclear transfer. *Science* 292(5517):740–743, Epub 2001/04/28
30. Kishigami S, Mizutani E, Ohta H, Hikichi T, Thuan NV, Wakayama S et al (2006) Significant improvement of mouse cloning technique by treatment with trichostatin A after somatic nuclear transfer. *Biochem Biophys Res Commun* 340(1):183–189, Epub 2005/12/17
31. Kishigami S, Bui HT, Wakayama S, Tokunaga K, Van Thuan N, Hikichi T et al (2007) Successful mouse cloning of an outbred strain by trichostatin A treatment after somatic nuclear transfer. *J Reprod Dev* 53(1):165–170, Epub 2006/11/02
32. Thuan NV, Kishigami S, Wakayama T (2010) How to improve the success rate of mouse cloning technology. *J Reprod Dev* 56(1):20–30, Epub 2010/03/06
33. Chatot CL, Ziomek CA, Bavister BD, Lewis JL, Torres I (1989) An improved culture medium supports development of random-bred 1-cell mouse embryos in vitro. *J Reprod Fertil* 86(2):679–688, Epub 1989/07/01
34. Inoue K, Ogonuki N, Mochida K, Yamamoto Y, Takano K, Kohda T et al (2003) Effects of donor cell type and genotype on the efficiency of mouse somatic cell cloning. *Biol Reprod* 69(4):1394–1400, Epub 2003/06/13
35. Ogura A, Inoue K, Ogonuki N, Noguchi A, Takano K, Nagano R et al (2000) Production of male cloned mice from fresh, cultured, and cryopreserved immature Sertoli cells. *Biol Reprod* 62(6):1579–1584, Epub 2000/05/20
36. Wakayama T, Rodriguez I, Perry AC, Yanagimachi R, Mombaerts P (1999) Mice cloned from embryonic stem cells. *Proc Natl Acad Sci U S A* 96(26):14984–14989, Epub 1999/12/28
37. Wakayama S, Ohta H, Kishigami S, Thuan NV, Hikichi T, Mizutani E et al (2005) Establishment of male and female nuclear transfer embryonic stem cell lines from different mouse strains and tissues. *Biol Reprod* 72(4):932–936, Epub 2004/12/17

38. Wakayama S, Mizutani E, Kishigami S, Thuan NV, Ohta H, Hikichi T et al (2005) Mice cloned by nuclear transfer from somatic and ntES cells derived from the same individuals. *J Reprod Dev* 51(6):765–772, Epub 2005/10/18
39. Kishigami S, Wakayama T (2007) Efficient strontium-induced activation of mouse oocytes in standard culture media by chelating calcium. *J Reprod Dev* 53(6):1207–1215, Epub 2007/10/17
40. Ono T, Li C, Mizutani E, Terashita Y, Yamagata K, Wakayama T (2010) Inhibition of class IIb histone deacetylase significantly improves cloning efficiency in mice. *Biol Reprod* 83(6):929–937, Epub 2010/08/06

Induction of Cellular Senescence by Oncogenic RAS

Romi Gupta and Narendra Wajapeyee

Abstract

Cellular senescence is a state of permanent cell cycle arrest, which has been shown to prevent neoplastic transformation. Oncogenes are pro-proliferative genes that promote survival and proliferation of cancer cells. Paradoxically, introduction of an activated oncogene leads to activation of a state similar to cellular senescence, which is referred to as oncogene-induced senescence. Studies have shown that oncogene-induced senescence function as a barrier to neoplastic transformation. Here, we describe a protocol for inducing cellular senescence by oncogenic RAS in primary human fibroblast. The approach that we describe here is of general utility and can be applied to study senescence induction by other defined genetic elements, for example, other activated oncogenes.

Key words Cellular senescence, Oncogene-induced senescence, RAS, p16, SA β -gal assay, p53

1 Introduction

Human cells can undergo only defined number of cell division after which they cease to grow in culture. This phenomenon was first observed by Hayflick and Moorhead and was described as replicative senescence [1]. Further studies have indicated that human cells undergo replicative cellular senescence due to progressive shortening of telomeres [2]. Telomere shortening induces DNA damage response (DDR) pathway, which induces irreversible cell cycle arrest leading to a state of replicative senescence [3].

Oncogenes are known to promote cell survival, cellular proliferation, and survival of cancer cells. However, paradoxically, introduction of an activated oncogene into a primary human or mouse cell leads to a state similar to replicative senescence [4].

Several studies have used oncogenic RAS as a prototype to study the phenomenon of oncogene-induced senescence and have identified the regulators and mechanisms of oncogene-induced senescence [5–7]. RAS is probably most commonly found oncogenic activation in human cancers and at least 30 % of the cancers harbor mutations in one of the three RAS proto-oncogenesis.

For a detailed overview of RAS oncogenes and cellular senescence, we refer the reader to two excellent reviews by Karnoub and Weinberg [8] and Nardella et al. [9].

Here in this chapter, we provide a detailed protocol for inducing senescence using activated oncogenic RAS in primary human fibroblast. The protocol provided here can be used to study senescence inducing ability of other oncogenes or genes that are suspected to function by inducing cellular senescence.

2 Materials

2.1 Generation of Retroviral Particles, Determination of MOI, and Transduction with Retrovirus Particles

1. 293T cells.
2. Gag-pol plasmid (Addgene).
3. pCI-VSVG plasmid (Addgene).
4. Transfection reagent, such as Effectene (Qiagen).
5. 0.45 μ m syringe filters (Millipore).
6. DMEM high glucose (1 \times), liquid, with L-glutamine and sodium pyruvate (Sigma-Aldrich).
7. 10 % FBS/Pen-Strep (Life Technologies).
8. Polybrene (Sigma-Aldrich).
9. Puromycin (Clontech).
10. Crystal violet staining solution: 40 % methanol, 10 % acetic acid, 50 % ddH₂O, and 0.01 % crystal violet.
11. IMR-90 fibroblasts (ATCC).
12. pBABE puro retroviral vector (Addgene).
13. pBABE puro/HRAS v12 retroviral vector (Addgene).
14. Centricon columns (Millipore).

2.2 Monitoring Oncogene-Induced Senescence

1. PKH26 red fluorescent cell linker kit (Sigma-Aldrich).
2. Sodium citrate (Sigma-Aldrich).
3. Na₂HPO₄ (Sigma-Aldrich).
4. NaCl (Sigma-Aldrich).
5. MgCl₂ (Sigma-Aldrich).
6. Potassium ferricyanide (Sigma-Aldrich).
7. X-gal (Sigma-Aldrich).
8. 37 % formaldehyde solution (Sigma-Aldrich).
9. p16 antibody (Cell Signaling).
10. p53 antibody (Santa Cruz Biotech).
11. p21 antibody (Santa Cruz Biotech).
12. PVDF membrane (PerkinElmer).

13. Immunoblot apparatus (Biorad).
14. Transfer apparatus (Biorad).
15. Anti-mouse IgG HRP-linked for ECL (GE Healthcare Biosciences).
16. ECL kit (Pierce).
17. DAPI (Sigma).

3 Methods

Carry out all procedures at room temperature unless otherwise specified.

3.1 Generation of HRAS v12 and Empty Vector Retroviral Particles

1. Plate 3×10^6 293T cells in 100 mm tissue culture dishes. Plate one additional dish, which will be transfected with an empty retroviral vector alone.
2. After 36 h, transfect cells with 10 μ g oncogenic RAS plasmid or empty vector plasmid along with 1 μ g Gag-pol plasmid DNA and 1 μ g pCI-VSVG plasmid DNA using Effectene transfection reagent as per the supplier's instructions.
3. After 48 h post-transfection, collect the culture supernatants, which contain retroviral particles.
4. Filter the culture supernatants using 0.45 μ m syringe filters.
5. Concentrate the virus tenfold using Centricon columns (cutoff 4 kDa) (*see Note 1*).

3.2 Determining the Multiplicity of Infection (MOI) for Retroviruses

1. Plate 1×10^5 293T cells in each well of a 6-well plate, using one plate for each pool.
2. Let the 293T cells grow for 36 h. After which, perform serial dilutions of each retrovirus. First, label six microfuge tubes as " 10^{-1} ," " 10^{-2} ," " 10^{-3} ," " 10^{-4} ," " 10^{-5} ," and " 10^{-6} ." Add 1 ml of the DMEM media with 10 % FBS/1XPen-Strep into each tube. Add 110 μ l of retroviral supernatant in the first tube, resulting in a 1/10 dilution (10^{-1}). Mix it well and then remove 100 μ l of the 10^{-1} dilution and add it to the second tube to create a 10^{-2} dilution. Repeat the same to generate 10^{-3} , 10^{-4} , 10^{-5} , and 10^{-6} dilutions.
3. Label the wells of the 6-well plates as " 10^{-1} ," " 10^{-2} ," " 10^{-3} ," " 10^{-4} ," " 10^{-5} ," and " 10^{-6} ." Aspirate the media from all the wells and add 1 ml of serially diluted retroviral supernatant with Polybrene (10 μ g/ml) to the appropriate well.
4. After 24 h, remove the media and add 2 ml of fresh DMEM media with 10 % FBS/Pen-Strep.
5. After 24 h of changing the media, add puromycin (1.0 μ g/ml) to select for cells carrying the retroviral HRAS v12.

6. Change the media with puromycin every 3 days.
7. After 2 weeks, stain the colonies that survive puromycin selection using crystal violet staining solution.
8. Calculate the MOI of the retroviral supernatants as follows:

$$\text{MOI} [\text{particle-forming units (pfu)/ml}] = \text{number of colonies} \times \text{dilution factor} \times 10.$$

For example, if you observe five colonies in the 10^{-4} dilution plate, the calculation will be: $5 \times 10^4 \times 10 = 5 \times 10^5$ pfu/ml (*see Note 2*).

3.3 Transduction of IMR-90 Cells with Activated HRAS v12 or Empty Vector Retrovirus

1. Plate 1.2×10^6 IMR-90 fibroblasts in two individual 100 mm tissue culture dishes (*see Note 3*).
2. After 24 h, transduce the IMR-90 fibroblasts with HRAS v12 or empty vector retrovirus in a total volume of 5 ml of DMEM media with 10 % FBS/Pen-Strep and Polybrene (10 $\mu\text{g/ml}$) to achieve infection at an MOI of 20 (*see Note 4*).
3. After 24 h, change the media and add 10 ml of DMEM media with 10 % FBS/Pen-Strep.
4. After 24 h of changing the media, add puromycin (1.0 $\mu\text{g/ml}$) to enrich the cells that carry integrated HRAS v12 or empty vector retrovirus. Change the media after 3 days with fresh puromycin. It usually takes 6 days to completely select cells carrying retrovirus by puromycin.

3.4 Monitoring the Induction of Cellular Senescence

Oncogene-induced senescence can be measured using different assays. Here, we present three such assays. Together these assays allow for the identification of cells that have undergone senescence. Additional assays can also be used to supplement these results, for example, BrdU incorporation assay and DAPI staining to identify the senescence-associated heterochromatin foci (SAHF).

3.4.1 Measurement of Proliferation Using PKH26-Based Cell Membrane Labeling

Induction of oncogene-induced senescence leads to reduced proliferation. Therefore, measuring proliferation may indicate induction of cellular senescence. However, it is important to note that reduced proliferation alone cannot be used to confirm senescence induction. Proliferation should be monitored along with other two assays (SA β -gal assay and p16 immunoblot). Below we describe the protocol for measuring proliferation using PKH26-based cell membrane labeling.

1. Label the empty vector or HRAS v12-transduced IMR-90 cells using PKH26 red fluorescent cell linker kit for general cell membrane labeling (Sigma-Aldrich) as per the manufacturers instruction. It is recommended that equal number of cells should be counted before labeling so that the observed differences are not due to different cells to PKH26 ratio.

2. Monitoring the labeled cells at days 3, 5, and 7 by flow cytometry analysis (*see* **Note 5**).

3.4.2 Senescence-Associated β -Galactosidase (SA β -gal) Assay

The methodology to detect SA β -gal has been extensively described earlier [10] as well as in this edition. We provide a short protocol here, which will allow readers to perform SA β -gal assay. Additionally, a chapter elsewhere in this volume will provide a detailed description of SA β -gal assay for monitoring senescence induction.

1. Wash cells twice with $1 \times$ PBS (pH 7.3) for 5 min with gentle rocking.
2. Add fixing solution (3.7 % paraformaldehyde) to cover cells and fix them for 5 min.
3. Wash cells three times with $1 \times$ PBS, 5 min per wash with gentle rocking.
4. Add staining solution to cover the cells and stain the cells from 12 to 18 h at 37 °C and protect the cells from light during the staining process.
5. Wash the cells three times with $1 \times$ PBS for 5 min with gentle rocking.

3.4.3 Monitoring the Increase in p16, p53, and p21 Expression by Immunoblot Analysis

1. Lyse the IMR-90 cells after 7 days of transduction with either empty vector or oncogenic HRAS v12.
2. Run the lysates on a 12 % SDS-PAGE.
3. Perform immunoblot analysis using anti-p16 antibody (Cell Signaling), anti-p53 antibody (Santa Cruz Biotech), or anti-p21 (Santa Cruz Biotech) antibody and monitor the expression of p16, p53, and p21 in empty vector or oncogenic HRAS v12-infected cells using ECL-based detection method (*see* **Note 6**).

3.4.4 Monitoring the Cells for Senescence-Induced Heterochromatin Foci (SAHF)

Previous studies have shown that cells that undergo oncogene-induced senescence also show a remarkably high increase in heterochromatinization. This phenomenon can be easily visualized by simple cell biology techniques and referred to as senescence-induced heterochromatin foci (SAHF). Below we provide a protocol to monitor the SAHF.

1. Plate 5×10^4 cells in a 6-well plate.
2. Transduce the cells at 20 MOI with either HRAS v12 retrovirus or an empty vector.
3. Fix the cells with 4 % paraformaldehyde for 10 min at room temperature after 7 days post-transduction.
4. Stain the cells with DAPI (0.1 mg/ml) for 5 min.
5. Wash three times with $1 \times$ PBS.
6. Visualize using fluorescent microscope for SAHF.

4 Notes

1. It is important to note that freeze thawing will lead to reduced titer. Therefore, we recommend to avoid multiple freeze thawing. One way to do this is to make small 1 ml aliquots for virus supernatant.
2. Aim for an MOI of at least $\sim 2 \times 10^5$ pfu/ml.
3. Although we recommend to use IMR-90 cells, other primary cells or other fibroblast can also be used. For example, BJ fibroblast, WI-38 fibroblast, primary human lung epithelial cells, and primary human melanocytes can also be used depending upon the research question. Based on the level of p16 expression, it is observed that both IMR-90 and WI-38 fibroblasts undergo robust senescence upon introduction of activated RAS such as HRAS v12. Furthermore, in addition to HRAS v12, other oncogenic RAS such as NRAS and KRAS can also be used. However, in our experience, these other RAS genes are less efficient in inducing senescence due to their weaker ability to activate MAP kinase pathway compared to HRAS v12.
4. The purpose of transducing the cells at 20 MOI is to ensure that all the cells are transduced with HRAS v12 retrovirus.
5. It is important to analyze both empty vector-infected IMR-90 cells and HRAS v12-infected cells to ensure that the reduction in growth is due to activation of cellular senescence and not due to cells reaching confluency.
6. Detection of p16 levels might require use of high sensitivity ECL kit like Femto kit from Pierce.

Acknowledgement

Narendra Wajapeyee is a Kimmel Scholar for Translational Cancer Research and is supported by grants from American Association for Cancer Research, Leukemia Research Foundation, and Elsa U. Pardee Foundation.

References

1. Hayflick L (1995) The limited in vitro lifetime of human diploid cell strains. *Exp Cell Res* 37:614–636
2. Finkel T, Serrano M, Blasco MA (2007) The common biology of cancer and ageing. *Nature* 448:767–774
3. d'Adda di Fagagna F et al (2003) A DNA damage checkpoint response in telomere-initiated senescence. *Nature* 426:194–198
4. Serrano M, Lin AW, McCurrach ME, Beach D, Lowe SW (1997) Oncogenic ras provokes premature cell senescence associated with accumulation of p53 and p16INK4a. *Cell* 88:593–602
5. Narita M et al (2006) A novel role for high-mobility group proteins in cellular senescence and heterochromatin formation. *Cell* 126:503–514

6. Narita M et al (2003) Rb-mediated heterochromatin formation and silencing of E2F target genes during cellular senescence. *Cell* 113:703–716
7. Young AR et al (2009) Autophagy mediates the mitotic senescence transition. *Genes Dev* 23:798–803
8. Karnoub AE, Weinberg RA (2008) RAS oncogenes: split personalities. *Nat Rev Cancer* 9:517–531
9. Nardella C, Clohessy JG, Alimonti A, Pandolfi PP (2011) Pro-senescence therapy for cancer treatment. *Nat Rev Cancer* 11:503–511
10. Itahana K, Campisi J, Dimri GP (2007) Methods to detect biomarkers of cellular senescence: the senescence-associated beta-galactosidase assay. *Methods Mol Biol* 371:21–31

Methods of Cellular Senescence Induction Using Oxidative Stress

Zhe Wang, Dandan Wei, and Hengyi Xiao

Abstract

Normal somatic cells do not divide indefinitely and have their finite replicative lifespan. This property leads to an eventual arrest of cell division termed cell senescence. Human diploid fibroblasts offer a typical model for studying cell senescence in vitro. Various approaches to evoke oxidative stresses, such as the exposures of cells to ultraviolet light, ethanol, tert-butyl hydroperoxide (t-BHP), and peroxide hydrogen (H_2O_2), have been used to study the onset of cellular senescence. The early onset of cellular senescence induced by these stresses is termed stress-induced premature senescence (SIPS). In this manuscript, we will mainly summarize the basic knowledge and experimental approaches important for the induction of SIPS by H_2O_2 , since H_2O_2 is the most commonly used inducer of SIPS in vitro and an endogenous source of cellular oxidative stress. Several assays methods generally used for testifying cell senescence are introduced.

Key words Senescence, Oxidative stress, H_2O_2 , Fibroblasts, SA- β -gal, Cell cycle arrest, SAHF, Comet assay, DNA damage, Telomere length analysis

1 Introduction

Cellular senescence is defined as a permanent cell cycle arrest that is resistant to growth factors and other signals that induce cell proliferation [1]. This phenomenon was firstly reported by Hayflick et al., who observed that human diploid fibroblasts (HDFs) exhibit finite proliferative potential in vitro [2]. Now, it is accepted that many types of somatic proliferative cells preserve the ability to undergo cellular senescence, while senescence contributes to aging process and age-related disease in vivo via the mechanisms not yet fully understood [3]. The cells that can become senescent in vitro include human keratinocyte, melanocyte, and endothelial cells. [4–6].

Based on the ways of induction and the mechanisms involved, cellular senescence is mainly classified into three types. The first, also the most thoroughly investigated type of cell senescence, is replicative senescence (RS), which features as telomere attrition and

the activation of p53/p21 pathway at least in early stage [7, 8]. The second type of cell senescence is termed as stress-induced premature senescence (SIPS), which is induced by various stressors, such as oxidative stress and ultraviolet rays [4, 9, 10]. The third type of cell senescence is oncogene-induced senescence (OIS), which is triggered by overactivation of certain oncogenes, in particular the *ras* gene [11–13]. Generally, SIPS and OIS have no significant telomere attrition but prominently in the activation of p16/p38 pathway [14, 15]. In some literatures, the term oxidant-induced premature senescence is also used in reference to premature senescence induced by oxidative stress [10].

Several essential phenotypes have been utilized to identify senescent cells. They include (1) cell cycle arrest at G1 phase, usually detected as the lack of DNA replication; (2) flat and enlarged cell morphology; (3) exceptional activation of lysosome, indicating by positive staining for senescence-associated β -galactosidase activity (SA- β -gal) [16–19]; (4) protruded heterogenization of chromatin (senescence-associated heterochromatin *foci*, SAHF) [20, 21]; (5) telomere shorting, but as mentioned above, it is not a reliable sign for SIPS and OIS [9, 22]; and (6) elevated expressions of several cell cycle inhibitory genes, such as p16, p53, and p21 [6–8, 23].

Senescence of HDFs is the most classical experimental model for cellular aging. The studies based on RS have contributed a lot for understanding of telomere-related aging mechanism, while SIPS is often used for the study of oxidative stress. Up to now, various inducers which can cause intense oxidative stresses in cells have been utilized for the induction of SIPS in cell culture system. They include H₂O₂ [9, 24], ultraviolet light [25], tert-butyl hydroperoxide [26], and ethanol [26]. H₂O₂ has been the most commonly used inducer of SIPS, partially because it is classically thought of as a natural inducer of oxidative stress [27–30]. Therefore, we focus on summarizing the detailed protocols for induction and detection of cellular senescence using H₂O₂ in this chapter. Some alternative methods used for SIPS induction are briefly mentioned in **Note 5** also.

2 Materials

2.1 Cell Culture

1. Cell incubator setting up at 37 °C, with 5 % CO₂ and 100 % humidity.
2. Human diploid fibroblasts WI-38 (ATCC, USA).
3. Dulbecco's modified Eagle's medium (DMEM) (GIBCO) supplemented with 10 % heat-inactivated fetal bovine serum, 100 μ g/ml penicillin, and 100 μ g/ml streptomycin (GIBCO).

4. H_2O_2 (30 % (W/W) solution from Sigma). Freshly diluted before the experiments.
5. Dulbecco's phosphate-buffered saline (PBS) (without Ca^{2+} and Mg^{2+} , Sigma).
6. Trypsin–EDTA in PBS (10× Trypsin–EDTA solution from Invitrogen).

2.2 SA- β -Gal Assay

1. Light microscope.
2. PBS.
3. 0.1 mol/l citric acid solution.
4. 0.2 mol/l sodium phosphate solution.
5. Citric acid/sodium phosphate buffer, pH 5.0 or 6.0.
6. 200 mg/ml X-gal solution (5-bromo-4-chloro-3-indolyl-beta-D-galactopyranoside, Sigma).
7. 5 mol/l sodium chloride (NaCl).
8. 100 mmol/l potassium ferrocyanide solution.
9. 100 mmol/l potassium ferricyanide solution.
10. 1 mol/l magnesium chloride solution (MgCl_2).
11. 4 % paraformaldehyde fixative solution.
12. Fresh prepared SA- β -gal staining solution: 1 mg/ml X-gal, 40 mmol/l citric acid/sodium phosphate, pH 6.0, 5 mmol/l potassium ferrocyanide, 5 mmol/l potassium ferricyanide, 150 mmol/l NaCl, and 2 mmol/l MgCl_2 .

2.3 Cell Morphology, Proliferation Assay, and Cell Cycle Analysis

1. Inverted phase contrast microscope with digital image detector.
2. Hemocytometer.
3. 70 % ice-cold ethanol.
4. 100 $\mu\text{g}/\text{ml}$ RNase A (Sigma).
5. 1 $\mu\text{g}/\text{ml}$ propidium iodide (Sigma).
6. 0.1 % Triton-X100.
7. FACScan (fluorescence-activated cell sorting, Becton–Dickinson, San Jose, CA).

2.4 Single-Cell Gel Electrophoresis Assay (Comet Assay)

1. 0.5 % normal melting agarose (Sigma).
2. 0.7 % low melting agarose (Sigma).
3. Dimethyl sulfoxide (DMSO, Sigma).
4. 5 mol/l sodium chloride (NaCl).
5. 0.4 mol/l Tris–HCl, pH 7.5.
6. 10 % Triton-X100 in distilled water.
7. 1 mol/l sodium hydroxide (NaOH).

8. 0.5 mol/l disodium ethylenediaminetetraacetate dihydrate (Na₂EDTA, Sigma).
9. Alkaline lysis buffer: 10 % DMSO, 1 % Triton-X100, 2.5 mol/l NaCl, 10 mmol/l Tris-HCl, 100 mmol/l Na₂EDTA, and pH 10.
10. Alkaline buffer solution with NaOH (10 mmol/l) and Na₂EDTA (200 mmol/l) at pH 13.2.
11. 2 µg/ml ethidium bromide.
12. Fluorescence microscope.
13. Horizontal gel electrophoresis chamber

2.5 Telomere Length Analysis

1. Genomic DNA extracted from cells, using EasyPure genomic DNA kit (Trans Inc, Beijing).
2. Restriction endonuclease HinfI and RsaI (Roche).
3. 0.8 % agarose gel.
4. Nylon membrane (Hybond N, Amersham).
5. ³²P-labeled telomeric oligonucleotide probe (TTAGGG)₄.
6. Denaturing solution: 1.5 mol/l NaCl and 0.5 mol/l NaOH.
7. Neutralization solution: 0.5 mol/l Tris-HCl (pH 7.0) and 1.5 mol/l NaCl.
8. Solution containing 0.75 mol/l NaCl, 30 mmol/l sodium citrate, and 1 % SDS.
9. 20× SSC: 3 mol/l NaCl, 0.3 mol/l sodium citrate.
10. X-ray film.

2.6 The Formation of Senescence-Associated Heterochromatin Foci

1. 100 µg/ml 4',6-diamidino-2-phenylindole (DAPI).
2. PBS.
3. Methanol.
4. Fluorescence microscope.

2.7 RT-qPCR

1. Trizol (Gibco, USA).
2. Chloroform, isopropyl alcohol, 75 % ethanol (in DEPC-treated water), and RNase-free water.
3. Centrifuge and rotor capable of reaching up to 12,000 × g (e.g., Eppendorf 5415R).
4. First-Strand cDNA Synthesis SuperMix (Invitrogen, USA).
5. Primers: p16, ATCATCAGTCACCGAAGGTC (sense) and CTCAAGAGA AGCCAGTAACC (antisense); p21, CCGAAGTCA GTTCCTTGTGGAG (sense) and TTAGGGCTTCCTCTTGGAGAAG (antisense); p53, GGACAG CCACGT CTGTGACTTG (sense) and CCAGTGGTTTCTTCTTTGGCTG (antisense); and GAPDH, AACCATGAGAAGTATGACAACAGC (sense) and CATGTGGGG CCATGAGGTCCACCAC (antisense).

6. Real-time fluorescence quantitative PCR reagent (e.g., TransStart Top Green qPCR SuperMix, TransGen Biotech, Beijing).
7. Bio-Rad iCycler iQ5 PCR Thermal Cycler (Bio-Rad, USA).

3 Method

Protocols described in this chapter are optimized for human diploid fibroblasts. If different cells are to be used, dose-response experiments should be carried out to obtain the sublethal amounts of H_2O_2 . As a guide titrations in the range of 50–800 $\mu\text{mol/l}$ should be carried out [28]. The protocols mentioned below are summarized from our experience and some published reports.

Cells are seeded and treated with H_2O_2 and incubated at 37 °C until the collection time points as described in Subheading 3.1. At the end of incubation, cells are collected and used for the assays as described in Subheadings 3.2–3.6 [9].

3.1 H_2O_2 Treatment

1. 10^5 cells are inoculated into each of 35 mm cell culture dish or each well in 6-well plate (*see Note 1*).
2. In the next day, sublethal amounts of H_2O_2 (100–200 $\mu\text{mol/l}$) are added for 2 h at 37 °C. Prolonged H_2O_2 treatment is performed by adding 10 $\mu\text{mol/l}$ H_2O_2 with medium change every 3 days. Parallel cultured control cells grow in the media without H_2O_2 (*see Note 2*).
3. H_2O_2 is washed with PBS for terminating the treatment. Cells are kept on the incubation in normal medium for more than 3 days.
4. Cells are microscopic observed, photographed, or used for assays. The treated and untreated cells are always compared.
5. *See Notes 3 and 4.*

3.2 SA- β -Gal Assay

1. Wash cells adhering in well twice in PBS.
2. Fix with 4 % paraformaldehyde for 5 min at room temperature. Prolonged fixation will inactivate the enzyme.
3. Wash three times in PBS, each for 3 min.
4. Add freshly prepared staining solution (pH 6.0, 2 ml/well of 6-well plate).
5. Incubate at 37 °C in a humidified chamber overnight. Do not use CO_2 incubator.
6. Examine the blue staining using a light microscope. Positive staining could be evaluated next day. The blue-stained cells are counted in several randomly selected fields under microscope, and the result is expressed as a percentage of positive cells. To avoid false positive resulted from cell confluence, this assay should be performed in sub-confluent cultures displaying comparable cell density [31].

7. Despite of above routinely conducted detection method for SA- β -gal activity, a flow cytometric SA- β -gal activity assay method appears in recent years. In this new assay system, C₁₂FDG (5-dodecanoylamino fluorescein di- β -D-galactopyranoside) acts as a SA- β gal substrate, and it becomes fluorescent and membrane impermeable. Briefly, C₁₂FDG is added to the medium and incubated with cells for 1 h at 37 °C, 5 % CO₂. After incubation, the cells are trypsinized, washed with PBS, resuspended in 200 μ l PBS, and analyzed immediately using a FACS Calibur flow cytometer [32, 33].

3.3 Cell Morphology, Proliferation Assay, and Cell Cycle Analysis

1. For morphology observation, cells are examined by microscope at 10 \times , 40 \times , and 100 \times magnification every day. Flat and enlarged cells will be observed from the third day after treatment. The cells should be plated at a low density to enable them fully enlarge.
2. For proliferation assay, 1×10^4 of cells are inoculated in six-well plates in three replicates for each time point. At 24 h intervals for maximal 16 days, cells are harvested after trypsinization, and the numbers of cells were counted under microscope, using a hemocytometer. Data are presented as the mean \pm standard deviation from three replicates, and the statistical significance is calculated by Student's *t*-test.
3. For cell cycle analysis, cultured cells are harvested after trypsinization, washed twice with PBS, and fixed with 70 % ice-cold ethanol at 4 °C overnight. Following the treatment with 100 μ g/ml RNaseA at 37 °C for 30 min, cellular DNA is stained with 1 μ g/ml propidium iodide/0.1 % Triton-X100 for 30 min, and DNA contents are measured by FACScan. Cell cycle distribution is analyzed with Cell Fit software (Becton–Dickinson, San Jose, CA).

3.4 Single-Cell Gel Electrophoresis Assay (Comet Assay)

This method is also called comet assay. It is used to detect DNA strand breaks which usually happen during the process of SIPS [34]. As senescent cells have lowered DNA repair capacity and accumulated DNA breaks, in this assay, they generally show a nucleus with a long tail, which is not present in healthy nonsenescent cells.

1. Glass slides are prepared by loading with 85 μ l of 0.5 % normal melting agarose.
2. Freshly harvested cells are mixed with 75 μ l of 0.7 % low melting agarose at room temperature and applied to the prepared slides.
3. Treat slides with alkaline lysis buffer for 1 h.
4. Place slides in a horizontal gel electrophoresis chamber containing alkaline buffer solution (pH 13.2).
5. After a 20-min DNA “unwinding” period, perform electrophoresis at 25 V and 300 mA for 20 min.

6. Following neutralization in 0.4 mol/l Tris-HCl (pH 7.5) for 20 min, stain cellular DNAs inside the slides with ethidium bromide.
7. Examine slides with a fluorescence microscope. Take images and measure the tail length of each nucleus (diameter of the nucleus plus migrated DNA). Dozens of randomly selected cells need be examined for each sample. H₂O₂-treated cells generally have low DNA repair capacity comparing to untreated control cells, indicating an accumulation of DNA breaks.

3.5 Telomere Length Analysis

Telomeres act as cumulative sensors for oxidative stress since the accumulation of single-strand DNA breaks can accelerate the shortening of telomeres. Besides, the induction of premature senescence by hyperoxia is thought to result from accelerated telomere shortening [35]. Although other methods can be used for measuring telomere length, we introduce a classic protocol here based on Southern blot analysis.

1. Digest genomic DNA (15 µg) with HinfI (10 U) and RsaI (10 U).
2. Digested DNA fragments are subjected to electrophoresis in a 0.8 % agarose gel, transferred on Hybond N membrane, and UV cross-linked.
3. Conduct the protocol for Southern blot hybridization. Hybridization is carried out for 12–15 h at 42 °C in a solution containing γ -³²P-labeled telomeric oligonucleotide probe (TTAGGG)₄.
4. After washing out free probe, autoradiograph images are obtained from the blots by exposing to X-ray film for 12–24 h at room temperature.
5. To calculate the TRF (terminal restriction fragment), the images are scanned with a densitometer, and the data are analyzed as described [7].
6. The mean TRF length is defined as $\sum (OD_i)/\sum (OD_i/L_i)$, where OD_i is the densitometer output and L_i the length of the DNA at position i.
7. The amount of telomeric DNA is calculated by integrating the volume of each smear in Image Quant software (Molecular Dynamics, Sunnyvale, CA).
8. See Note 5.

3.6 Assay for SAHF Formation

In nucleus of senescent cells, chromatin undergoes dramatic remodeling through the formation of domains of facultative heterochromatin called SAHF, showing as compacted punctate DAPI-stained *foci* of DNA in senescent cell nuclei. SAHF is now gradually

accepted as contributor for irreversible cell cycle exit in many senescent cells [21]. A representative protocol is as follows:

1. Wash the cells once with PBS and fixed with methanol for 5 min.
2. Incubate with DAPI (1 $\mu\text{g}/\text{ml}$) for 5 min in dark.
3. DAPI-treated cells are gently washed three times with PBS. Each for 5 min.
4. Refeed with medium containing no DAPI.
5. DAPI-treated cells are examined by fluorescence microscopy. Compacted punctate DAPI-stained *foci* of DNA can be found in many senescent cell nuclei.

3.7 RT-qPCR

1. Total RNA is extracted with Trizol reagent.
2. Use total RNA as the template for the reverse transcription.
3. It is important to include no RT control to reveal the presence of contaminating gDNA.
4. Primers are described in Subheading 2.7 [23]. Glyceraldehyde-3-phosphate dehydrogenase (GAPDH) is used as reference gene in this assay.
5. Perform reactions in duplicate (triplicate if C_t s are >35). If the data from these differ by $>0.5 C_t$, the reactions should be repeated. If the reproducibility is consistently low, the assay should be re-optimized. It is more important to run biological duplicates, as these will identify the true variability within the data [36].
6. Data analysis via iQTM5 Optical System Software, monitoring by GAPDH as internal reference. The expressions of p16, p53, and p21 genes are shown as relative fold change.

4 Notes

1. It is important that nonconfluent cultures to be used because nonsenescent cells maintained at confluent can cause false-positive staining in SA- β -gal assay.
2. As reported in ref. 37, it is difficult to achieve a 100 % cell cycle arrest and the induction of senescence by a single H_2O_2 treatment, because a fraction of treated cells can recover from oxidative stress and reenter cell cycle. Therefore, it may be necessary to treat the cells with H_2O_2 for a second time.
3. It is necessary to include positive and negative controls for any assay.

4. There are alternative methods used for SIPS induction. For instance, HDFs treated with repeated sub-cytotoxic dose of ultraviolet light at 250 mJ/cm² [25], repeated 30 μ M t-BHP [26], and repeated 4 % ethanol (v/v) [26], all go to SIPS, respectively. The melanocytes exposed to sublethal doses of UV [4] fate the same.
5. With prolonged H₂O₂ treatment, significant telomere shortening will occur in human fibroblasts cells. However, in the case of acute treatment by sublethal doses of H₂O₂, telomere shortening does not usually occur.

Acknowledgment

This work was supported by the grant from National Natural Science Foundation of China (Grant Number 81273224), and from West China Hospital of Sichuan University for (Huaxi Grant 137080022). We thank all team members in our lab for the wonderful cooperation.

References

1. Stein GH, Drullinger LF, Robetorye RS, Pereira-Smith OM, Smith JR (1991) Senescent cells fail to express cdc2, cycA, and cycB in response to mitogen stimulation. *Proc Natl Acad Sci U S A* 88:11012–11016
2. Hayflick L, Moorhead PS (1961) The serial cultivation of human diploid cell strains. *Exp Cell Res* 25:585–621
3. Vijg J, Campisi J (2008) Puzzles, promises and a cure for aging. *Nature* 454 (7208):1065–1071, Review
4. Toussaint O, Medrano EE, von Zglinicki T (2000) Cellular and molecular mechanisms of stress-induced premature senescence (SIPS) of human diploid fibroblasts and melanocytes. *Exp Gerontol* 35:927–945
5. Kurz DJ, Decary S, Hong Y, Trivier E, Akhmedov A, Erusalimsky JD (2004) Chronic oxidative stress compromises telomere integrity and accelerates the onset of senescence in human endothelial cells. *J Cell Sci* 117 (Pt 11):2417–2426
6. Lewis DA, Yi Q, Travers JB, Spandau DF (2008) UVB-induced senescence in human keratinocytes requires a functional insulin-like growth factor-1 receptor and p53. *Mol Biol Cell* 19(4):1346–1353
7. Harley CB, Futcher AB, Greider CW (1990) Telomeres shorten during aging of human fibroblast. *Nature* 345:458–460
8. Shawi M, Autexier C (2008) Telomerase, senescence and ageing. *Mech Ageing Dev* 129:3–10, Review
9. Duan J, Duan J, Zhang Z, Tong T (2005) Irreversible cellular senescence induced by prolonged exposure to H₂O₂ involves DNA-damage-and-repair genes and telomere shortening. *Int J Biochem Cell Biol* 37(7):1407–1420
10. Chen QM (2000) Replicative senescence and oxidant-induced premature senescence - beyond the control of cell cycle checkpoints. *Ann N Y Acad Sci* 908:111–125
11. Mallette FA, Gaumont-Leclerc MF, Ferbeyre G (2007) The DNA damage signaling pathway is a critical mediator of oncogene-induced senescence. *Genes Dev* 21:43–48
12. Lowe SW, Cepero E, Evan G (2004) Intrinsic tumour suppression. *Nature* 432:307–315
13. Ferbeyre G, de Stanchina E, Lin AW, Querido E, McCurrach ME, Hannon GJ, Lowe SW (2002) Oncogenic ras and p53 cooperate to induce cellular senescence. *Mol Cell Biol* 22:3497–3508
14. Davis T, Kipling D (2009) Assessing the role of stress signalling via p38 MAP kinase in the premature senescence of ataxia telangiectasia and werner syndrome fibroblasts. *Biogerontology* 10(3):253–266
15. Frippiat C, Dewelle J, Remacle J, Toussaint O (2002) Signal transduction in H₂O₂-induced senescence-like phenotype in human diploid

- fibroblasts. *Free Radic Biol Med* 33 (10):1334–1346
16. Kurz DJ, Decary S, Hong Y, Erusalimsky JD (2000) Senescence-associated (beta)-galactosidase reflects an increase in lysosomal mass during replicative aging of human endothelial cells. *J Cell Sci* 113(Pt 20):3613–3622
17. Dimri GP, Lee X, Basile G et al (1995) A biomarker that identifies senescent human cells in culture and in aging skin in vivo. *Proc Natl Acad Sci U S A* 92:9363–9367
18. Itahana K, Campisi J, Dimri GP (2007) Methods to detect biomarkers of cellular senescence: the senescence associated beta-galactosidase assay. *Methods Mol Biol* 371:21–31
19. Shlush LI, Itzkovitz S, Cohen A, Rutenberg A, Berkovitz R, Yehezkel S, Shahar H, Selig S, Skorecki K (2011) Quantitative digital in situ senescence-associated β -galactosidase assay. *BMC Cell Biol* 12:16
20. Kosar M, Bartkova J, Hubackova S, Hodny Z, Lukas J, Bartek J (2011) Senescence-associated heterochromatin foci are dispensable for cellular senescence, occur in a cell type- and insult-dependent manner and follow expression of p16(ink4a). *Cell Cycle* 10(3):457–468
21. Zhang R, Chen W, Adams PD (2007) Molecular dissection of formation of senescence-associated heterochromatin *foci*. *Mol Cell Biol* 6:2343–2358
22. von Zglinicki T, Saretzki G, Docke W (1995) Mild hyperoxia shortens telomeres and inhibits proliferation of fibroblasts: a model for senescence? *Exp Cell Res* 220:186–193
23. Wang XY, Wang YG, Wang YF (2011) Ginsenoside Rb1, Rg1 and three extracts of traditional Chinese medicine attenuate ultraviolet B-induced G1 growth arrest in HaCaT cells and dermal fibroblasts involve down-regulating the expression of p16, p21 and p53. *Photodermatol Photoimmunol Photomed* 27(4):203–212
24. Calini R, Chevanne M, Mocali A (1998) Premature Induction of aging in sublethally H₂O₂-treated young MRC5 fibroblasts correlates with increased glutathione peroxidase levels and resistance to DNA breakage. *Mech Ageing Dev* 105(1–2):137–150
25. Debacq-Chainiaux F, Borlon C, Pascal T, Royer V, Eliaers F, Ninane N, Carrard G, Friquet B, de Longueville F, Boffe S, Remacle J, Toussaint O (2005) Repeated exposure of human skin fibroblasts to UVB at subcytotoxic level triggers premature senescence through the TGF- β 1 signaling pathway. *J Cell Sci* 118(Pt 4):743–758
26. Dumont P, Chainiaux F, Eliaers F, Petropoulou C, Remacle J, Koch-Brandt C, Gonos ES, Toussaint O (2002) Overexpression of apolipoprotein J in human fibroblasts protects against cytotoxicity and premature senescence induced by ethanol and tert-butylhydroperoxide. *Cell Stress Chaperones* 7 (1):23–35
27. Toussaint O, Dumont P, Dierick JF, Pascal T, Fripiat C, Chainiaux F, Sluse F, Eliaers F, Remacle J (2000) Stress-induced premature senescence. Essence of life, evolution, stress, and aging. *Ann N Y Acad Sci* 908:85–98
28. Chen JH, Ozanne SE, Hales CN (2007) Methods of cellular senescence induction using oxidative stress. *Methods Mol Biol* 371:179–190
29. Burdon RH (1995) Superoxide and hydrogen peroxide in relation to mammalian cell proliferation. *Free Radic Biol Med* 18:775–794
30. Chen Q, Ames B (1994) Senescence-like growth arrest induced by hydrogen peroxide in human diploid fibroblast F65 cells. *Proc Natl Acad Sci U S A* 91:4130–4134
31. Severino J, Allen RG, Balin S, Balin A (2000) Is beta-galactosidase staining a marker of senescence in vitro and in vivo? *Exp Cell Res* 257:162–171
32. Okamoto Y, Monjushiro H, Fukumoto T, Watarai H (2006) Measurement of hydrolysis kinetics of galactose-substituted fluorescein by beta-galactosidase at the toluene-water interface by spinning microtube fluorometry. *Anal Bioanal Chem* 385(8):1430–1438
33. Noppe G, Dekker P, de Koning-Treurniet C, Blom J, van Heemst D, Dirks RW, Tanke HJ, Westendorp RG, Maier AB (2009) Rapid flow cytometric method for measuring senescence associated β -galactosidase activity in human fibroblasts. *Cytometry A* 75(11):910–916
34. Singh NP, McCoy MT, Tice RR (1988) A Simple technique for quantitation of low levels of DNA damage in individual cells. *Exp Cell Res* 175:184–191
35. Naka K, Tachibana A, Ikeda K, Motoyama N (2004) Stress-induced premature senescence in hTERT-expressing ataxia telangiectasia fibroblasts. *J Biol Chem* 279:2030–2037
36. Nolan T, Hands RE, Bustin SA (2006) Quantification of mRNA using real-time RT-PCR. *Nat Protoc* 1:1559–1582
37. Chen JH, Stoeber K, Kingsbury S, Ozanne SE (2004) Loss of proliferative capacity and induction of senescence in oxidatively stressed human fibroblasts. *J Biol Chem* 279:49439–49446

Chapter 12

Methods of Testing Pharmacological Drugs Effects on Aging and Life Span in Mice

Vladimir N. Anisimov, Irina G. Popovich, and Mark A. Zabezhinski

Abstract

The methodology of testing antiaging drugs in laboratory mice is presented. It is based on more than 40-year-long authors' experience in the field and includes the selection of mouse strain, sex, age at start of treatment, housing conditions, design of the long-term study, some noninvasive methods of assessment of biomarkers of aging, life-span parameters, pathology examination, and statistical treatment of the results.

Key words Antiaging drugs, Testing, Biomarkers of aging, Mice

1 Introduction

There is the growing scientific and public interest to the development of new antiaging drugs. Accordingly, there is the need to create standard guidelines for testing such drugs and for evaluation of life extension potential as well as other late effects (like carcinogenic and cancer preventive effects of chemicals) [1–3]. One of the approaches was used by International Programme for Chemical Safety [4]. Some principles of a program for testing biological interventions to promote healthy aging were discussed at U.S. National Institute on Aging [5, 6]. In present work, we described the methodology of testing of compounds with potential geroprotective activity based on more than 40-year-long experience in the field at the Laboratory of Carcinogenesis and Aging, N.N. Petrov Research Institute of Oncology (St. Petersburg, Russia). We used the complex approach to the testing including a study on carcinogenic risk, carcinogenic safety, and antiaging potential with evaluation of biomarkers of aging, life-span parameters, as well as characteristics of tumor and nontumor pathology [3].

Guidelines for testing should include such significant points as animal models, regime of testing, and biomarkers/endpoints. Mammals are most appropriate animal models, because their

biology is sufficiently homologous to that in humans. Mice are the most appropriate models in terms of husbandry, costs, and length of life. One of the most significant problems is the choice of mouse strain. To have a strain with genetic diversities and spectre of pathologies close to human population, application of four-way crossed mice is proposed by some authors [5, 6]. Another way to solve this problem is to use different strains in one study. This approach was used in our studies where we combined outbred (SHR or NMRI) mice, inbred CBA or 129/Sv mice, as well as senescent accelerated SAMP-1 mice and transgenic HER-2/neu mice [3, 7–14].

Testing regimen should be nontoxic, simple, not stressful, and appropriate for human application. During the study, a number of biomarkers of aging could be included into the battery of tests. Some of them could be monitored during life of mice (Table 1). Another biomarkers could be practically studied by sacrificing of groups mice at various age (6–15 per group)—cross-sections protocol (Table 2). However, some methods are very costly and require higher number of animals in groups [8]. At last, some characteristics of aging could be estimated only *postmortem* after death of each and/or all animals involved into the study (Table 3). It is worthy to note that there are age-associated changes in factors responsible for the rate of penetration of drugs into the body, their distribution, and the rate of their elimination from the organism, including xenobiotic metabolism and inactivation enzymes activity, and they might have an essential effect on the pharmacokinetics and the pharmacodynamics of drugs [4, 8].

For most of our studies, besides of survival parameters, we registered body weight, body temperature, food and water consumption, physical activity and muscular strength, learning capacity, and estimated estrous function. To evaluate late effects of drugs, we have also conducted pathomorphological examination, including tumor diagnostics. For general evaluation of the effect of drugs on aging, life span, carcinogenesis, and nontumor pathology, adequate mathematical and statistical models were used. Due to widely recognized gender peculiarities in some age-related phenotypes and age-associated diseases, using animals of both sexes is most appreciated [11, 15].

2 Material

2.1 Animals

1. Strain choice. For strain selection, we recommend using two or more strains in one study, combining outbred and inbred strains. Additionally, for special mechanistic studies, genetically modified mice could be used [16–18].

Table 1
Parameters which could be monitored during life span in mice

Function, parameters	Changing with age
<i>Phenotypic characteristics</i>	
Body weight	Increases until the age of 16–20 months, decline afterwards
Body temperature	Decreases
Hair graying	Increases
Boldness	Increases
Vibrisses lost	Increases
<i>Behavior</i>	
Locomotor activity	Decreases
Muscular strength	Decreases
Physical fatigability	Decreases
Cognitive capacity	Decreases
Learning capacity	Decreases
Gait abnormality	Increases
<i>Reproductive function</i>	
Estrus function: length of the estrus cycle (days)	Increases
Fraction of mice with regular estrus cycles (%)	Decreases
Fraction of mice with irregular estrus cycles (%)	Increases
Fertility: pregnancy and delivery rate	Decreases
Number of offspring per litter	Decreases
<i>Pathology</i>	
Osteoporosis	Increases
Cataract	Increases
Skin ulceration	Increases
Lordosis/kyphosis	Increases

2. The strain(s) must be well characterized in terms of their genetics, survival, and pathologies. The most important aspect is a long-term experience in the use of selected strain in a laboratory where a study will be done.
3. Mice of both sexes could be used.

2.2 Housing Requirements

1. The animals should be kept in standard conditions of temperature and humidity. Animal facility systems and general requirements are well described [19, 20].
2. Female mice should be kept as possible in equal number per cage (5, 7, or 10) for both in the control and experimental groups. Males should be kept single at a cage due to territorial fights.
3. Illumination should be standard as 12 h light/12 h darkness.
4. Animals should receive tap water and food (standard pellet) ad libitum.

Table 2
Characteristics of aging which could be evaluated in cross-section studies in serum or tissues of mice

Function	Parameter, test	Changing with aging
Oxidative stress	Reactive oxygen species (ROS) generation: <ul style="list-style-type: none"> • Luminol-dependent chemiluminescence • Electron paramagnetic signal Lipid peroxidation (LPO): <ul style="list-style-type: none"> • Diene conjugates • Schiff bases • Malonic dialdehyde (MDA) DNA damage: <ul style="list-style-type: none"> • Carbonyl residues • 8-hydroxy-2'-deoxyguanosine (8-OH-dG) • NO synthase 	Increases
Antioxidative defense system activity	Total antioxidative activity (TAA): <ul style="list-style-type: none"> • Riboflavin chemiluminescence • Cu,Zn superoxide dismutase • Catalase • Glutathione peroxidase • Vitamin E 	Decreases
Protein glycosylation	Advanced glycosylation end products (AGEs)	Increases
DNA damage	DNA adducts formation DNA hypomethylation: 5-methylcytosine (5mC)	Increases
Genomic instability	Mutations	Increases
	Chromosome aberrations	Increases
	Gene expression with microarray technology	
Tissue proliferation	Mitotic index	Tissue dependent
	<i>Ki67</i>	
	Apoptosis: <i>p53</i>	Increases
	Focal hyperplasia Cell-to-cell communication	Decreases
Cellular senescence	Number of senescent cells in tissues Senescence-associated heterochromatic foci (SAHF) senescence-associated- β -galactosidase (SA- β -gal) activity, γ -H2AX histone	Increases
DNA repair efficacy	O ⁶ -alkyltransferase activity Excision repair efficacy	Depends on a tissue
Tolerance to glucose	The level of glucose in the blood after glucose loading ^a	Decreases
Susceptibility to insulin	The level of glucose in the blood after insulin injection ^a	Decreases

(continued)

Table 2
(continued)

Function	Parameter, test	Changing with aging
Hormonal status ^a	Melatonin level and circadian rhythm	Decreases
	Growth hormone, IGF-1, leptin,	Decreases
	Corticosterone, DHEA, estradiol-17 β , testosterone	Decreases
	Prolactin	Increases
	Triiodothyronine (T3); thyroxine (T4)	Decreases
Fat metabolism ^a	Serum level of cholesterol, α -cholesterol, β -lipoproteins, triglycerides, FFA	Increases
Immune function	T cell subsets; cytokines	Decreases
	Reaction of blast transformation with ConA or PHA	Decreases

^aTests performed in mice after the overnight starvation**Table 3**
Characteristics of aging which could be estimated *postmortem*

Characteristics	Parameters
Life span	Mean ($M \pm m$), median, maximum Mean life span of last 10 % survivors, days
Population aging rate	Aging rate (α), days ⁻³
Mortality rate	MRDT (mortality rate doubling time), days Initial mortality rate (β), days ⁻⁵
Tumorigenesis	Incidence of benign and malignant tumors Latent period of tumors Tumor localization and pathomorphology
Nontumor pathology	Sarcopenia Hepatitis Nephropathy Arteriosclerosis Cardiopathy Pneumonia Colitis Infection

2.3 Equipment and Reagents

1. Electronic balance (for estimation of body weight and food consumption).
2. Bottles with marked volume (for water consumption).
3. Plastic chamber 30 cm \times 21 cm \times 9 cm (for physical activity).
4. Electronic thermometer (for body temperature) is used.

3 Methods

3.1 Age at Start of Treatment

Long-term studies should be started at the age of 2–3 months, just after maturity of the females. For additional mechanistic studies, experiments could be also started later. In the NIA, ITP treatments were started at the age of 4, 9, 10, 12, or 20 months [6, 21].

3.2 Randomization in Groups

Just before the start of an experiment, animals should be randomly divided into control and experimental groups.

1. The number of animals should be sufficient for further statistical analysis. Fifty animals in each test group are generally accepted as a minimum adequate number and as a reasonable compromise between cost and avoidance of false-negative or false-positive results [1]. A moderate increase in group size will produce only small decrease in the likelihood of obtaining false results [22], whereas the increase in workload is considerable. Control group could be twice the size of any experimental groups.
2. All mice should be individually marked.
3. Control mice could be left intact and/or could be treated by the solvent using the same doses and regimen as in experimental groups.
4. Supplementary number of mice should be included in both control and each experimental groups in a case of additional study on age-related dynamics of biochemical, metabolic, and hormonal parameters. Groups of 10–15 animals each could be sacrificed at the age of 3, 12, and 18–21 months after overnight starvation.

3.3 Route, Dosage, and Regimen of Treatment

1. The best route of administration of a compound is with drinking water or supplementation to food. Some compounds, low soluble or nonsoluble in water, might be dissolved in a small amount of ethanol and then dissolved in water for proper concentrations.

For exact dosage of low-soluble compounds gastric intubation could be used.

2. It is acceptable for parenteral route, if tested compounds are administered by subcutaneous injections (0.1 mL) of buffered solution in flank of the body. Intraperitoneal or intravenous injections are more stressful and risky for infection.
3. Testing two or more drug doses is recommended, including the dose proposed for usage in humans. Doses should be not higher than a maximum tolerated dose (MTD) [3].
4. In a case of administration of a drug with drinking water or food, a treatment 5 or 7 day a week could be recommended.

Gastric intubations are performed 3–5 times a week; parenteral injections are usually performed once a week.

5. The best regimen is long-term continuous exposure until natural death of the animals. However, in some cases, intermittent exposure could be used [7].

3.4 General Observation

During the study, the animals should be under daily observation, with regular registration of the amount of drinking water and consumed food, body weight and temperature, estimation of physical strength and activity, and estrous function, and such signs of aging as boldness, loss of vibrisses, hair color changes, graying, skin ulceration or tumor appearance, kyphosis, and reduced locomotor activity should be registered at individual charts.

Once a week, all mice should be palpated to detect mammary or soft tissues tumors. They could be measured with calipers in the two perpendicular diameters. Progressively growing masses of >3 mm in mean diameter should be regarded as tumors. The time of appearance of these tumors detected by palpation, localization, and size needs to be registered on special charts (Fig. 1).

The animals should be observed until their natural deaths and sacrificed only when moribund. The date of each death should be registered, and survival time should be estimated.

3.5 Food Consumption

This parameter should be monitored once a month during the all period of observation until a natural death of last animals in a group.

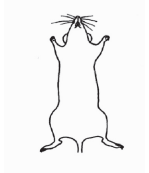
Study #	Year
Species	
Strain	
Sex: male __ female __	
Number	
Date of birth	
Date of death	
Life span ____ days	
Histological number:	
Pathomorphological description:	
Macroscopic description:	
	

Fig. 1 A chart for registration of pathology in rodents

Ten grams of a standard lab chow per mouse should be placed to cleaned food container in a cage, and the amount of nonconsumed food (in a food container and on the bottom of cage) should be weighted 24 h later; calculations of gram per mouse per day values should be performed. Caloric restriction (CR) is the known intervention that has been shown considerably to increase the life span to reduce the incidence and retard the onset of age-related diseases, including cancer, to increase resistance to stress and toxicity, and to maintain function and vitality in laboratory animals at more youthful levels [23, 24]. In laboratory rodents, CR commonly involves a lifetime reduction in dietary caloric intake of the order of 30–50 % from ad libitum levels. The alternative feeding (food supply into a cage each other day) could be used for the CR. The same amount of food as the group with the least food intake during the previous time period (pair-fed controls) could be useful in testing of CR mimetics [25].

3.6 Water Consumption

Water consumption should be also monitored monthly. A bottle with a drinking tap water should contain 10 mL water per mouse and a volume of water drunk consumed in 24 h should be expressed in milliliters per mouse per day.

3.7 Body Weight

Individual body weight of mice should be measured monthly. Weekly weighting is more time and work consuming and in reality gives no additional information. We recommend measuring body weight at the same time of a day.

3.8 Body Temperature

Once every 3 months, simultaneously with weighing, rectal body temperature should be measured with electronic thermometer.

The mice will be fixed in usual position sitting on grill with a tail turned up. The electrode of thermometer should be immersed in glycerol and introduced into rectum in a distance about 1.0 cm. Initially, rectal body temperature could decrease due to stress and angiospasm. Thus, it is necessary to wait until the mouse will be quiet and body temperature stabilized.

3.9 Estrous Function

1. Once every 3 months, vaginal smears, taken daily for 3 weeks from the animals, should be cytologically examined to estimate the phases of their estrous functions.
2. The thin cotton-ended sticks should be moistened with sterile water, and smears should be taken and displayed at the preliminary marked glass for histological slides.
3. Cytological evaluation of the estrous phases should be performed in 1–2 h after collection. It is possible to investigate nonstained vaginal smears using a drop of a condenser of a microscope under 80–100× magnification. The record of daily vaginal smears examination for each individually marked

animal should be correctly performed, and proestrus, estrus, metaestrus, and diestrus phases should be registered [26].

4. The following parameters of estrous function should be evaluated:
 - (a) A length of each estrous cycle from the first estrous phase registered to each next first estrus day and then a mean length of the cycle in a group.
 - (b) A ratio of phases of estrous cycle.
 - (c) A rate of estrous cycles of various length (%). Usually we subdivide it as <5, 5–7, and >7 days.
 - (d) Fraction of mice with regular cycles (%).
 - (e) Fraction of mice with irregular cycles (%).

3.10 Method of Estimating Physical Activity of Mice in the “Open-Field” Test

There are a number of modifications of “open-field” test [27, 28]. At present, both horizontal (locomotion) and vertical activities (rearing) could be monitored by infrared beams, and this information is relayed to a computer with software that automatically records the location and activity of the animal. Behavioral output includes the numbers of horizontal beam-breaks or the distance traveled and the number of vertical beam-breaks or rears. In addition, activities in the center and peripheral zones of the open field as well as activity maps can be generated. The test could be performed in a simple modification:

1. The mice should be tested each 3 months, e.g., at the age of 6, 9, 12, and 18 months in the daytime from 10 a.m. to 5 p.m., thus alleviating the circadian rhythm effects on physical activity.
2. Animals of each group should be placed one by one in a plastic chamber measuring 30 cm × 21 cm × 9 cm, at the bottom of which squares (5 cm × 5 cm) were drawn: five squares in length and four squares in breadth.
3. Each mouse should be observed moving in the cage, and its locomotion parameters were estimated: (a) the number of crossed squares in the field (a square was considered crossed if the animal stepped over its border at least with two paws), (b) the number of vertical sets (when the animal rose to its hind paws), and (c) the duration of grooming reaction of muzzle, body, and genitalia. As a way to exclude the possibility of smell-associated orientation reaction, the chamber floor should be wiped with a wet cloth after each animal.

3.11 Method of Studying Muscular Strength and Physical Fatigability

1. The mice should be tested at the age of 6, 9, 12, and 18 months in the daytime from 10 a.m. to 5 p.m.
2. After weighing, the mice are suspended on a string stretched to an altitude of 80 cm, so that they would hang by the string, clutching at it with their front paws.

3. The time until the moment of their fatigue and fall is registered in seconds.
4. In 20 min, the mice are suspended again and the time for which they managed to hold on is measured.
5. A discrepancy between these two indices is regarded as a parameter of physical restoration. It could be additionally estimated in relation to body weight.

3.12 Methods of Studying Learning Capacity (Maze Tests)

1. The mice should be tested at the age of 6, 9, 12, and 18 months in the daytime from 10 a.m. to 5 p.m.
2. Animals of each group should be placed one by one in a plastic or wooden chamber consisted one round platform 20 cm in diameter and eight radial roads (50 cm length and 8 cm wide) with food box at the end of each.
3. Each mouse should be placed at the center of round platform for 10 min and estimate (a) the total time of visiting of all eight food boxes and (b) number of mistakes (repetitive visited of each road). As a way to exclude the possibility of smell-associated orientation reaction, the chamber floor should be wiped with a wet cloth after each animal.

There are several modifications of a maze test, aimed to study various aspects of learning and memory in rodents [29].

3.13 Pathomorphological Examination

1. All the animals that died or were sacrificed when moribund should be autopsied. At autopsy, their skin and all internal organs should be examined.
2. Revealed neoplasia should be classified according to the recommendations of the International Agency of Research on Cancer (IARC) as “fatal” (i.e., those that directly caused the death of the animal) or “incidental” (for the cases in which the animal died of a different cause) [30].
3. Main internal organs, all tumors, as well as other lesions should be excised and fixed in 10 % neutral formalin. After routine histological processing, the tissues should be embedded in paraffin.
4. Thin, 5–7 μm histological sections should be stained with hematoxylin–eosin (and, if necessary, with additional methods, including histochemical and immunohistochemical) and microscopically examined; regarding the experimental group which the mice belonged, this should be a blind process.
5. Tumors should be classified in accordance with IARC recommendations [31]. Nontumor pathology should be classified according to the standard classifications [32].

3.14 Statistics

1. Experimental results should be statistically processed by the methods of variation statistics [30, 33]. The significance of the discrepancies should be defined according to Student's *t*-criterion, Fischer's exact method, a chi-square analysis, and a nonparametric criterion of Wilcoxon–Mann–Whitney.
2. For discrepancies in neoplasm incidence to be estimated, an IARC method of combined contingency tables calculated individually for the fatal and incidental tumors [30] as well as a prevalence analysis [34] should be applied. Because mice did not display carcinomas in all mammary glands, the mean number of palpable mammary carcinomas per mouse could be calculated as the cumulative number of incident tumors/number of tumor-bearing mice.
3. For survival and risk analysis, Cox's method [35] is the most useful. To test two groups survival equality, Taron's life table test [36] could be used. All reported values for survival tests should be two-sided.

3.15 Mathematical Models and Estimations

1. The mathematical model could be used to describe survival under the treatment [37]. The model is the traditional Gompertz model with survival function,

$$S(x) = \exp \left\{ -\frac{\beta}{\alpha} [\exp(\alpha x) - 1] \right\}$$

where parameters α and β are associated with the aging rate and the initial mortality rate, respectively. Parameter α is often characterized by the value of mortality rate doubling time (MRDT), calculated as $\ln(2)/\alpha$.

2. Parameters for the model should be estimated from empirical data by use of the maximum likelihood method implemented in the Gauss statistical system [38].
3. Confidence intervals for the aging rate parameter estimates should be calculated by profiling the log-likelihood function [35].

4 Notes

1. Critical review of available data on the effect of life extension drugs [3, 8, 21] has shown that from the point of view of the current guidelines, a lot of studies are invalid. Tested drugs were often given to a small number of animals (10–20); the treatments started at the old age of animals, where a lot of more weak animals would die and more robust would survive; the observation stopped at the age of 50 % mortality or at some other voluntary time, but not at the natural death of last survivor;

the autopsy and correct pathomorphological examination sometimes were not performed or were incomplete; the body weight gain and food consumption were not monitored, etc.

2. The special problem is the selection of mouse strain. For testing pharmacological drugs, genetic and other characteristics should be analyzed. For example, C57BL/6j mice are most common animal model in life-span extension studies [39]. However, due to genetically dependent deficiency in melatonin production by pineal gland in C57BL/6j mice [40], this strain could not be an adequate model. Some serious arguments support the use of hybrid or outbred mice [16, 41].
3. Spontaneous and induced genetic modifications, homozygous null mutations, and knockout and transgenic mammalian animals were also introduced into experimental gerontology [16–18]. It is worth of note that although the effects of some genetic manipulations are not expressed except at specific times in the animal's life, because these genetic manipulations are in effect during embryonic development as well as throughout adult life, there are significant limitations in the interpretations of the data obtained. Some of them were discussed elsewhere [8, 42, 43]. On the one hand, the elimination of an activity or a pathway can lead to erroneous conclusion about the function of a gene because resulting compensation can markedly alter the physiology of the animal. On the other hand, overexpression of a transgene may readily yield no effect on life span or on any other aging parameter of the animal for that matter. Jazwinski [42] has noted that overexpression of a transgene will likely create interactions with other genes and with the environment, both external and internal. Nevertheless, we have used mutant and transgenic mice for study of effect of some drugs on longevity [3, 7–14].
4. There are a number of examples of gender differences in the response to antiaging drugs [3, 11, 15, 21]. However, when resources are limited, a choice of sex of mice is very important. We prefer to use female mice, which are not so aggressive as males. Another advantage of females is a possibility of a monitoring of estrous function and wider spectrum of tumors including than that in males.
5. In general, a fairly wide range of husbandry conditions yields similar life-span results. Different frequency of cage changes (1, 2, or 3 weeks), and different cage ventilation rates have not shown any differences in health status [44]. Fairly dirty, unsanitary conditions had no significant effect on the life span [45]. It seems also that animals raised in specific pathogen-free (SPF) conditions do not show a significant improvement in survival curves. While some reports did show an improved life

span from germ-free husbandry [46, 47], it was, however, shown that germ-free animals had a lower caloric intake with that being the likely cause of life-span extension [48].

6. The food quality and control are important issue [20, 49]. To know the content in lipids, kind of animal proteins, fibers, and relevant oligoelements may be important, because of the great relevance of food quality used in animal facility, particularly when substances which may interfere with the nutritional status have to be studied. In our experiments, we routinely used the granular diet produced by agricultural company “Volosovo” (Leningrad Region, Russia) and, since 2005, of “Laborator-korm” (Moscow, Russia). Both these diets contain natural ingredients—wheat, corn, powdered milk, soya, and fish meal—and were balanced in a relative amount of proteins, fat, vitamins, and microelements [3]. In general, these diets are similar to NIH-31 rat and mouse ration [6].
7. An experiment must be initiated at the age after which growth has ceased (2–4 months), so that any life extension due to growth retardation is not a potential artifact. In some reports, a treatment has been started at 9, 10, 12, 18, or 20 months [3, 6, 8, 21]. We believe that use of such design as basic is not a correct for evaluation of premature aging preventive potential of the compound tested.
8. For correct choice of the route of drug administration, the data on solubility and stability of a compound in the water or in food are very important. If compound given with drinking water is sensible to illumination, bottles of dark glass should be used.
9. Concerning regimen of treatment, intermittent exposure could be only recommended, if in previous mechanistic studies it was shown that intermittent exposure is the most safe and effective [3, 7, 8, 50].
10. Estimation of water and food consumption, as well as of body weight and temperature should be performed at the same time of the day. During analysis of estrous function, it is necessary to continue to take vaginal smears until the end of the last estrous cycle.
11. For final analysis, it is significant to compare the effects of different doses of drug tested, to extrapolate experimental data to humans [8, 50–52].
12. The ultimate goal of research in this field is the choice of geroprotectors for studies in humans. To achieve these goals, the international standards for preclinical and clinical studies of antiaging drugs, as well as for evaluation of results of such studies, should be developed [3, 8, 52]. In the coming years, the perspective direction could be the development of new biomarkers, based mostly on biochemical and genetic methods,

for short-term screening of such drugs [53, 54]. At present, cooperative studies on antiaging drugs conducted in various laboratories, using different approaches in a single long-term experiment (“economic experiment”), could be promising [3]. It should be mentioned that for the best extrapolation to humans, besides of mice, other animals’ species should be used.

Acknowledgments

This chapter was supported in part by grants # 14.740.11.0115 from the Russian Federation Ministry of Education and Science, # 11-04-00317 from the Russian Foundation for Basic Research, and grant # NSh-6383.2012.4 from the President of Russian Federation.

References

1. Montesano R, Bartsch H, Vainio H, Wilbourn J, Yamasaki H (eds) (1986) Long-term and short-term assays for carcinogens: a critical appraisal. IARC Sci Publ 83, IARC, Lyon
2. Vainio H, Magee P, McGregor D, McMichael AJ (eds) (1992) Mechanisms of carcinogenesis in risk identification. IARC Sci Publ 116, IARC, Lyon
3. Anisimov VN, Zabezhinski MA, Popovich IG, Pliss GB, Bespalov VG, Alexandrov VA, Stukov AN, Anikin IV, Alimova IN, Egormin PA, Panchenko AV, Piskunova TS, Semenchenko AV, Tyndyk ML, Yurova MN (2012) Rodent models for the preclinical evaluation of drugs suitable for pharmacological intervention in aging. *Expert Opin Drug Discov* 7(1):85–95
4. Anisimov VN, Birnbaum L, Butenko G, Cooper R, Fabris N et al (1993) Principles for evaluating chemical effects on the aged population (Environmental Health Criteria 144). WHO, Geneva
5. Warner HR, Ingram D, Miller RA, Nadon NL, Richardson AG (2000) Program for testing biological interventions to promote healthy aging. *Mech Ageing Dev* 115:199–208
6. Nadon NI, Strong R, Miller RA, Nelson J, Javors M, Shrp ZD, Peraba JM, Harrison DE (2008) Design of aging intervention studies: the NIA interventions testing program. *Age* 30:187–199
7. Anisimov VN, Alimova IN, Baturin DA, Popovich IG, Zabezhinski MA, Manton KG, Yashin AI (2003) The effect of melatonin treatment regimen on mammary adenocarcinoma development in HER-2/neu transgenic mice. *Int J Cancer* 103:300–305
8. Anisimov VN (2008) Molecular and physiological mechanisms of aging, vol 1, 2, 2nd edn. Nauka, St. Petersburg
9. Anisimov VN, Arbeev KG, Popovich IG, Zabezhinski MA, Rosenfeld SV, Piskunova TS, Arbeeva LS, Semenchenko AV, Yashin AI (2004) Body weight is not always a good predictor of longevity in mice. *Exp Gerontol* 39:305–319
10. Anisimov VN, Zavarzina NY, Zabezhinski MA, Popovich IG, Zimina OA, Shtylick AV, Michalski AI, Yashin AI (2001) Melatonin increases both life span and tumor incidence in female CBA. *J Gerontol Biol Sci* 56A(7):B1–B13
11. Anisimov VN, Piskunova TS, Popovich IG, Zabezhinski MA, Tyndyk ML, Egormin PA, Yurova MN, Semenchenko AV, Kovalenko IG, Poroshina TE, Berstein LM (2010) Gender differences in metformin effect on aging, life span and spontaneous tumorigenesis in 129/Sv mice. *Aging (Albany, NY)* 2:945–958
12. Anisimov VN, Alimova IN, Baturin DA, Popovich IG, Zabezhinski MA, Rosenfeld SV, Manton KG, Semenchenko AV, Yashin AI (2003) Dose-dependent effect of melatonin on life span and spontaneous tumor incidence in female SHR mice. *Exp Gerontol* 38:449–461
13. Anisimov VN, Zabezhinski MA, Popovich IG, Piskunova TS, Yurova MN, Semenchenko AV, Tyndyk ML, Yurova MN, Rosenfeld SV, Blagosklonny MV (2011) Rapamycin increases lifespan and inhibits spontaneous tumorigenesis in inbred female mice. *Cell Cycle* 10:4230–4236
14. Anisimov VN, Popovich IG, Zabezhinski MA, Rosenfeld SV (2004) Spontaneous mutagenesis, carcinogenesis and aging in SAM mice:

- effect of melatonin, epitalon and neuronol. In: Takeda T (ed) *Proceedings of the 19th SAM Meeting*, Kyoto, 17–18 July 2004, pp 101–102
15. Harrison DE, Strong R, Sharp ZD, Nelson JF, Astle CM, Flurkey K, Nadon NL, Wilkinson JE, Frenkel K, Carter CS, Pahor M, Javors MA, Fernandez E, Miller RA (2009) Rapamycin fed late in life extends lifespan in genetically heterogeneous mice. *Nature* 460:392–395
 16. Anisimov VN (1987) *Carcinogenesis and aging*, vol 1. CRC, Boca Raton
 17. Ingram DK, Jucker M (1999) Developing mouse models of aging: a consideration of strain differences in age-related behavioral and neural parameters. *Neurobiol Aging* 20:137–145
 18. Anisimov VN (2003) Aging and cancer in transgenic and mutant mice. *Front Biosci* 8: S883–S902
 19. Pooley SM (1974) Housing requirements – general considerations. In: Melby EC, Altman NH (eds) *Handbook of laboratory animal science*, vol I. CRC, Cleveland, pp 21–60
 20. Van Zutphen LF, Baumans V, Beynen AC (eds) (2001) *Principles of laboratory animal science*. Elsevier, New York
 21. Spindler SR (2012) Review of the literature and suggestion for the design of rodent survival studies for the identification of compounds that increase health and life span. *Age* 34:111–120
 22. Page NP (1977) Chronic toxicity and carcinogenicity guidelines. *J Environ Pathol Toxicol* 1:161–182
 23. Weindruch R, Walford R (1988) The retardation of aging and disease by dietary restriction. C.C.Thomas, Springfield, IL
 24. Masoro EJ (2009) Caloric restriction-induced life extension of rats and mice: a critique of proposed mechanisms. *Biochim Biophys Acta* 1790:1040–1048
 25. Anisimov VN, Ukraintseva SV, Anikin IV, Popovich IG, Zabezhinski MA, Berstein LM, Arutjunyan AV, Ingram DK, Lane MA, Roth GS (2005) Effects of phentermine and phenformin on biomarkers of aging in rats. *Gerontology* 51:19–28
 26. Nelson JF, Felici LS, Randall PK, Sims C, Finch CE (1982) A longitudinal study of estrous cyclicity in aging C57BL/6J mice: I. Cycle frequency, length and vaginal cytology. *Biol Reprod* 27:327–339
 27. Gould TD (2009) Mood and anxiety related phenotypes in mice. *Neuromethods* 42. doi:10.1007/978-1-60761-303-9_1, Humana Press, a part of Springer Science +Business Media, LLC
 28. Porsolt RD, Bertin A (1977) Behavioral despair in mice: a primary screening test for antidepressants. *Arch Int Pharmacodyn* 229:327–336
 29. Deacon RMJ, Rawlins JNP (2006) T-maze alternation in the rodent. *Nat Protoc* 1:7–12
 30. Gart JJ, Krewski D, Lee PN, Tarone S, Wahrendorf J (1986) *Statistical methods in cancer research*, vol III—the design and analysis of long-term animal experiments. IARC Sci Publ 79, IARC, Lyon
 31. Turusov VS, Mohr U (eds) (1994). *Pathology of tumours in laboratory animals*, vol I. Tumours of the mouse, 2nd edn. IARC Sci Publ 111. IARC, Lyon
 32. Percy DH, Barthold SW (2007) *Pathology of laboratory rodents and rabbits*, 3rd edn. Blackwell, Ames, IA
 33. Goubler EV (1978) *Computing methods of pathology analysis and recognition*. Meditsina, Leningrad
 34. McKnight B, Crowley J (1984) Tests for differences in tumor incidence based on animal carcinogenesis experiments. *J Am Stat Assoc* 80:639–648
 35. Cox DR, Oakes D (1996) *Analysis of survival data*. Chapman & Hall, London
 36. Taron RE (1975) Tests for trend in life table analysis. *Biometrika* 62:679–682
 37. Marchuk GI, Anisimov VN, Romanyukha AA, Yashin AI (2007) Gerontology in silico: establishment of new discipline. Mathematical models, data analysis and calculation experiments. Binom, Moscow
 38. Gauss system and graphic manual (1994). Aptech Systems, Maple Valley
 39. Sprott RL, Ramirez I (1997) Current inbred and hybrid rat and mouse models. *ILAR J* 38:104–108
 40. Goto M, Oshima I, Tomita T, Ebihara S (1989) Melatonin content of the pineal gland in different mouse strains. *J Pineal Res* 7:195–204
 41. Miller RA, Chrips C, Jackson AU, Galecki AT, Burke DT (2002) Coordinated genetic control of neoplastic and nonneoplastic diseases in mice. *J Gerontol Biol Sci* 57A:B3–B8
 42. Jazwinski SM (1999) Longevity, genes, and aging: a view provided by a genetic model system. *Exp Geront* 34:1–6
 43. Morgan WW, Richardson A, Sharp ZD, Walter CA (1999) Application of exogenously regulatable promoter systems to transgenic models for the study of aging. *J Gerontol Biol Sci* 54: B30–B40

44. Reeb-Whitaker CK, Paigen B, Beamer WG, Bronson RT, Churchill GA, Schweitzer IB, Myer DD (2001) The impact of reduced frequency of cage changes on the health of mice housed in ventilated cages. *Lab Anim* 35:58–73
45. Chino F, Makinodan T, Lever WE, Peterson WJ (1971) The immune systems of mice reared in clean and in dirty conventional laboratory farms. I. Life expectancy and pathology of mice with long life spans. *J Gerontol* 26:497–507
46. Gordon HA, Bruckner-Kardoss E, Wostmann BS (1966) Aging in germ-free mice: life tables and lesions observed at natural death. *J Gerontol* 21:380–387
47. Pollard M (1970) Senescence in germfree rats. *Gerontologia* 17:333–338
48. Snyder DL, Pollard M, Wostmann BS, Luckert P (1990) Life span, morphology, and pathology of diet-restricted germ-free and conventional Lobund-Wistar rats. *J Gerontol* 45: B52–B58
49. Baranova LN, Romanov KP, Yamshanov VA (1986) Study of the level of benzo(a)pyrene and N-nitrosamines in the food of laboratory animals. *Vopr Onkol* 5:54–57
50. Anisimov VN, Popovich IG, Zabezhinski MA (2007) Methods of evaluating the effect of pharmacological drugs on aging and life span in mice. *Methods Mol Biol* 371:227–236
51. Khabriev RU (ed) (2005) Manual on experimental (preclinical) study of new pharmacological compounds, 2nd edn. Meditsina, Moscow
52. Anisimov VN (2006) Premature ageing prevention: limitations and perspectives of pharmacological interventions. *Current Drug Res* 7:1485–1504
53. Anisimov SV (2007) Application of DNA microarray technology to gerontological studies. *Methods Mol Biol* 371:249–266
54. Arkadieva AV, Mamonov AA, Popovich IG, Anisimov VN, Mikhelson VM, Spivak IM (2011) Metformin slows down ageing processes at the cellular level in SHR mice. *Tsitologiya* 53:166–174

Mitochondria-Targeted Antiaging Gene Therapy with Adeno-associated Viral Vectors

Dejia Li and Dongsheng Duan

Abstract

Transgenic expression of catalase in mitochondria using a transgenic strategy extends life span and prevents aging-related pathology in mice. However, transgenic overexpression is not suitable for a clinical application. Adeno-associated virus (AAV) is the most promising gene delivery vehicle. Here we outline strategies on the generation of an AAV vector expressing the mitochondria-targeted catalase gene (AV.RSV.MCAT). We also describe methods for evaluating physiological impact of AV.RSV.MCAT on muscle contractility and running performance in mice.

Key words AAV, Adeno-associated virus, Free radical, Mitochondria, Targeted expression, Antioxidant gene therapy, Muscle, Aging, Catalase, Treadmill

1 Introduction

Reactive oxygen species (ROS) has long been implicated in aging and various neuromuscular diseases [1, 2]. The mitochondria are the primary source and major target of cellular ROS [3, 4]. Mitochondrial oxidative stress contributes significantly to human aging and disease [5]. For this reason, strategies that target ROS scavengers to mitochondria may hold tremendous potential for extending life expectancy and life quality.

Catalase is a highly conserved housekeeping antioxidant enzyme. It dehydrates two molecules of H_2O_2 to two molecules of H_2O and one molecular of O_2 . In most mammalian cells, catalase is located in the matrix of peroxisomes. Interestingly, forced expression of catalase in the mitochondria results in much more potent protection against oxidative stress in cultured cells [6–8]. The effect of mitochondria-targeted catalase (MCAT) on aging was uncovered recently by Rabinovitch and colleagues [9–12]. While transgenic overexpression of peroxisomal catalase did not prolong mouse life expectancy, transgenic mice carrying the MCAT gene showed significantly increased median and maximal life span.

Furthermore, aging-related pathologies were greatly mitigated. These exciting results reveal a possibility of treating aging-related diseases and potentially extending life span in human patients.

Gene therapy is originally developed to cure inherited genetic diseases by introducing a normal gene [13]. Gene delivery strategies that are initially designed for treating disease may also be utilized to improve cellular function in healthy subjects [14]. Of available gene transfer vehicles, adeno-associated virus (AAV) stands out as an extremely safe and effective vector for local or whole-body gene transfer [15]. Wild-type AAV is not associated with any known human diseases, while recombinant AAV may persist in human body for at least 10 years without causing significant safety concern [16]. We have recently demonstrated that intravascular injection of AAV-9 not only resulted in robust body-wide transduction in rodents, saturated gene transfer can also be achieved in large mammals such as dogs [17, 18]. AAV vectors thus provide an excellent platform for the translation of exciting transgenic study results to humans in the future.

Investigators have generated several catalase overexpressing viral vectors including AAV catalase virus [19, 20]. Preclinical studies of AAV catalase virus suggest that this vector is safe in muscle and also ameliorates optic neuritis in the eye [19, 21, 22]. However, based on transgenic study [9], we predict that the existing AAV catalase vector cannot prolong life span because catalase is expressed in the cytosol and peroxisomes but not mitochondria. To develop a therapeutic antiaging viral vector, we engineered a novel AAV-9 virus harboring the mitochondria-targeted catalase gene (AV.RSV.MCAT). Preliminary studies suggest that AV.RSV.MCAT is well tolerated in normal mice and systemic AV.RSV.MCAT injection does not elicit noticeable toxicity. These studies also confirmed ectopic catalase expression in the mitochondria. Most importantly, treadmill running performance is significantly enhanced in mice that received AV.RSV.MCAT treatment at the neonatal period [23].

In this protocol, we outline the procedures used in the generation and characterization of the AV.RSV.MCAT vector.

2 Materials

2.1 Generation of the AV.RSV.MCAT Vector

2.1.1 Generation of the cis-MCAT Plasmid

1. Vent DNA polymerase (New England Biolabs). This is a high-fidelity thermophilic DNA polymerase. It has a low polymerase chain reaction (PCR)-related mutation rate. Store at -20°C .
2. T4 DNA ligase (New England Biolabs). This enzyme catalyzes the formation of a phosphodiester bond between juxtaposed 5' phosphate and 3' hydroxyl termini in duplex DNA. This enzyme will join blunt-end and cohesive-end DNA fragments. Store at -20°C (*see Note 1*).

3. SCS110 Competent Cells (Stratagene, La Jolla, CA, USA). The expression cassette (including AAV-inverted repeats and the MCAT gene) can be methylated when propagated in bacterial cells. SCS110 is an *endA*⁻ derivative of the JM110 strain. The SCS110 strain is ideal for preparing plasmid or phagemid DNA free of Dam or Dcm methylation so that the DNA can be restriction digested by methylation-sensitive restriction enzymes. Store at -80 °C (*see Note 2*).
4. The *cis* plasmid carrying the vector genome (ITR-promoter-target gene-pA-ITR) (ITR stands for inverted terminal repeat).
5. The mitochondrial-tagged human catalase cDNA (MCAT) plasmid (poCAT) can be obtained from Dr. Rabinovitch at University of Washington, Seattle, WA.
6. Reagents and equipment for standard agarose gel electrophoresis.
7. 14 ml polypropylene round-bottomed tubes (Becton Dickinson Labware, Franklin Lakes, NJ, USA).
8. S.O.C. medium (Gibco-BRL). Store at room temperature.
9. Amp selection LB agar plates (100 µg/mL, ampicillin). Store at 4 °C.
10. Plasmid Miniprep Kit.
11. Standard materials for large-scale plasmid preparation with CsCl₂/ethidium bromide equilibrium centrifugation.

2.1.2 Recombinant AAV-9 AV.RSV.MCAT Production

1. Adenoviral helper plasmid (pHelper provides adenoviral helper function (Stratagene, La Jolla, CA)).
2. pRep2/Cap9 helper plasmid. This plasmid encodes AAV replication proteins and AAV-9 capsid. It can be obtained from Dr. James Wilson at the University of Pennsylvania, Philadelphia, PA.
3. 2.5 M CaCl₂. Sterilize by filtration and store at -20 °C.
4. 2× HBS buffer: 0.3 M NaCl, 1.5 mM Na₂HPO₄, and 40 mM HEPES, pH 7.05 ± 0.05. Sterilize by filtration and store at -20 °C. As pH affects transduction efficiency, it is highly suggested to double check pH before each usage.
5. DNase I (Sigma, 11 mg protein/vial, total 33 K [kunitz] units).
6. pcis-MCAT plasmid. This plasmid contains the ubiquitous Rous sarcoma virus (RSV) promoter, the mitochondrial-tagged human catalase cDNA, and the simian virus 40 (SV40) polyadenylation sequence.
7. 0.25 % Trypsin (Gibco-BRL). Store at 4 °C.
8. 10 % Sodium deoxycholate. Store at room temperature.

9. Misonic Cell Disruptor S3000 (Misonix, NY).
10. Cell lifter (Corning Incorporated, Corning, NY, USA).
11. HEPES AAV dialysis buffer: 20 mM HEPES, and 150 mM NaCl, pH 7.8. Sterilize by filtration and store at 4 °C.
12. Dialysis tubing: 12,000 MW cutoffs (Gibco-BRL). Store at 4 °C.
13. AAV digestion buffer: 0.4 M NaOH and 20 mM EDTA. Freshly made before use.
14. Slot blot hybridization solution (5× SSC, 5× Denhardt's solution, 1 % sodium dodecyl sulfate (SDS), and 50 % formamide, add 100 µg/mL denatured salmon sperm DNA just before use).
15. Dry ice bath, dry ice, and 95 % ethanol.
16. HEK293 cells: (ATCC #CRL-1573). This is a hypotriploid human fetal kidney cell line transformed by sheared human adenovirus type 5 DNA. These cells are split 1:6 every 3 days and should not be allowed to overgrow. We recommend routinely testing the cell culture for mycoplasma contamination. Cells infected with mycoplasma generally grow much slower and do not attach to tissue culture plates well.
17. Culture medium for HEK293 cells: DMEM/10 %FBS/1 %PS. DMEM (Dulbecco's modified Eagle's medium), high glucose with L-glutamine (Gibco-BRL, Grand Island, NY, #11965-092). Store at 4 °C; Fetal bovine serum (FBS) with a high plating efficiency (Gibco-BRL, #26140079). Store at -20 °C; 100 × penicillin G (10,000 Unit/mL) and streptomycin (10 mg/mL) (PS) (Gibco-BRL, #15140-122). Store at -20 °C.

2.2 In Vivo Evaluation of MCAT Expression

2.2.1 Local Muscle Injection

1. 2–3-day-old BL6 mice (C57BL/6ScSn-Dmdmdx/J; The Jackson Laboratory).
2. Masks and gloves.
3. Biohazardous containers.
4. Cotton swabs.
5. Individual ventilation cages.
6. Needle holders (Accurate Surgical & Scientific Instruments Corp., Westbury, NY, USA).
7. 33G gas-tight Hamilton syringe and needle (Hamilton Company Reno, NV, USA).
8. Light source at an oblique angle such as a fiber optic lamp with movable arms.
9. AAV-9 in HEPES solution at 3×10^{11} viral particles per animal. 1×10^{10} viral particles/µL.

2.2.2 Systemic Facial Vein Injection

1. 1–2-day-old BL6 mice (C57BL/6ScSn-Dmdmdx/J; The Jackson Laboratory).
2. Tattoo dye.
3. 33-Gauge gas-tight Hamilton syringe (Hamilton, Reno, NV).
4. Dissecting microscope.
5. Light source at an oblique angle such as a fiber optic lamp with movable arms.
6. AAV-9 in HEPES solution at 1×10^{12} viral particles per animal. 1×10^{10} viral particles/ μ L.

2.2.3 Analysis of MCAT Activity

1. 0.05 M phosphate buffer (PB), pH 7.8. Store at 4 °C.
2. 30 mM H₂O₂ in 0.05 M phosphate buffer, pH 7.8. Make the 30 mM H₂O₂ freshly for each activity assay and the 30 mM H₂O₂ can be kept at 4 °C or room temperature during experiment.
3. UV–Vis Spectrometer.
4. Bio-Rad protein assay kit (Bio-Rad laboratories, Hercules, CA).
5. Catalase (Sigma, St Louis, MO). This serves as a positive control for catalase activity assay. Aliquots of different concentration can be stored at –20 °C.

2.2.4 Quantifying MCAT Expression by Western Blot

Preparation of Whole Muscle Lysate for Western Blot

1. Homogenization buffer: pH 7.8, 0.05 M PB containing 1 % protease inhibitor cocktail (Roche, Indianapolis, IN). Use 10 mL homogenization buffer per 1 mg wet muscle weight. Store at 4 °C. During experiment the PB can be stored at 4 °C or room temperature.
2. Desktop centrifuge (Eppendorf centrifuge, model 5417C).
3. Bio-Rad protein assay kit (Bio-Rad laboratories, Hercules, CA).
4. Motor for muscle tissue grinding.
5. Liquid nitrogen.

Muscle Mitochondria Isolation

1. Homogenization buffer:
IBm1 – 67 mM sucrose; 50 mM Tris–HCl, pH 7.4; 50 mM KCl; 10 mM EDTA; and 5 % BSA. Adjust pH with 10 N HCl.
IBm2 – 250 mM sucrose; 3 mM EGTA/Tris; and 10 mM Tris–HCl, pH 7.4. Adjust pH with 10 N HCl.
2. PBS buffer (containing 10 mM EDTA and 0.2 % trypsin).
3. Teflon tissue tearor (model 985370-395, BioSpec Products, Inc.).
4. 10 % BSA in PBS buffer.
5. Bio-Rad protein assay kit (Bio-Rad laboratories, Hercules, CA).
6. Eppendorf centrifuge, model 5417C; Eppendorf–Netheler–Hinz GmbH, Hamburg, Germany.

7. Centrifuge, Sorvall Evolution RC. Rotor, SS34.
8. Tissue tearor (model 985370-395, BioSpec Products, Inc. Bartlesville, OK).

Muscle Western Blot

1. ECL Western blotting detection reagents (Amersham Biosciences, Pittsburgh, PA).
2. PVDF immobilon-P transfer membrane (EMD Millipore Corporation, Billerica, MA).
3. TBST: 1× TBS (10 mM Tris-HCl, pH 8.0; 150 mM NaCl) with 0.1 % (v/v) Tween.
4. Coomassie staining solution: 0.25 % (w/v) Coomassie blue R250, 45 % methanol, and 10 % (v/v) glacial acetic acid in water.
5. Destaining solution: 45 % (v/v) methanol and 10 % (v/v) glacial acetic acid.
6. Stripping buffer: 75 mM Tris-HCl at pH 6.8, 100 mM DTT, and 2 % SDS (w/v).
7. Blocking buffer: 5 % dry milk powder and 0.1 % Tween-20 in TBST.
8. Equipment and buffer solutions for protein SDS-PAGE electrophoresis.
9. Anti-catalase antibody (Cat# 219010 Calbiochem, San Diego, CA, USA).
10. Rabbit polyclonal to prohibitin antibody (ab28172-100 Abcam, Cambridge, MA, USA).
11. Running gel (12.5 %).
12. Stacking gel (4.5 %).
13. Tris-SDS running buffer: 1.5 M Tris, pH 8.8; 8 mM disodium EDTA; and 0.4 % SDS.
14. Tris-SDS stacking buffer: 0.5 M Tris-HCl, pH 6.8; 8 mM disodium EDTA; and 0.4 % SDS.
15. 10 % APS (ammonium persulfate, Bio-Rad Cat # 161-0700). 100 mg APS in 1 mL of distilled water (remains stable for 24 h at room temperature and 1 week at 4 °C).
16. SDS running buffer (4 l of 5× concentrations): 200 mM Tris, pH 8.8; 9 mM disodium EDTA; and 1.9 M glycine, 0.5 % SDS.
17. SDS sample dissociation buffer: 2 % SDS; 62.5 mM Tris, pH 6.8; 10 % glycerol; 3 % β-mercaptoethanol, and a few drops of a 5 % bromophenol blue.
18. Goat anti-rabbit IgG (H&L) horseradish peroxidase-conjugated affinity-purified antibody (Chemicon International, Cat # AP132P).

**2.2.5 Checking Catalase
Localization by Double
Immunostaining**

1. DakoCytomation pen (DakoCytomation, Glostrup, Denmark).
2. KPBS: 356 μM KH_2PO_4 , 1.64 mM K_2HPO_4 , 160 mM NaCl.
3. Gelatin (Sigma).
4. Blocking solution for immunofluorescence (IF) staining: KPBS + 1 % goat serum.
5. DPX mounting media (BDH, VWR International Ltd, Leicestershire, UK).
6. KPBSG (KPBS + 0.2 % gelatin).
7. 2-Methylbutane (Sigma).
8. Tissue-Tek OCT (Sakura Finetek Inc., USA).
9. Iodoacetic acid (Sigma, final concentration 10 mM).
10. Alexa 488-labeled goat anti-rabbit antibody (Molecular Probes, Eugene, OR; diluted 1:200).
11. Alexa 594-conjugated goat anti-mouse antibody (Molecular Probes, Eugene, OR; diluted 1:200).
12. M.O.M kit (Vector Laboratories, Inc.).
13. Rabbit antihuman catalase antibody, IgG (Cat# 219010 Calbiochem, San Diego, CA, USA) (<http://www.calbiochem.com>).
14. Cytochrome C (CytC) antibody, purified mouse anti-cytochrome monoclonal antibody, Clone: 6H2.B4, and IgG1. BD Pharmingen, San Jose, CA, USA (<http://www.bdbiosciences.com>).
15. Confocal microscope with automatic image analysis system.

**2.3 Evaluation of the
Effect of Mitochondrial
Catalase Expression**

**2.3.1 In Vitro EDL Muscle
Function Assay**

1. Anesthetic cocktail: 25 mg/mL ketamine, 2.5 mg/mL xylazine, and 0.5 mg/mL acepromazine dissolved in 0.9 % NaCl. Keep the cocktail away from light and store at 4 °C.
2. Heating lamp (Tensor Lighting Company, Boston, MA, USA).
3. Regular dissecting forceps and scissors (World Precision Instruments, Sarasota, FL, USA).
4. Microdissecting scissors and forceps (straight and 45° angled) (Fine Science Tools, Foster City, CA, USA).
5. Bread silk suture #4-0 (SofSilk USSC Sutures, Norwalk, CT, USA).
6. Stereo dissecting microscope (Nikon, Melville, NY, USA).
7. Ringer's buffer: 1.2 mM NaH_2PO_4 , 1 mM MgSO_4 , 4.83 mM KCl, 137 mM NaCl, 24 mM NaHCO_3 , 2 mM CaCl_2 , and 10 mM glucose, pH 7.4. Store at 4 °C.
8. Circulating water bath (Fisher Scientific, Waltham, MA, USA).
9. Oxygen tank containing 95 % O_2 and 5 % CO_2 (Airgas National, Charlotte, NC, USA).

10. Digital caliper (Fisher Scientific).
11. Microbalance (Fisher Scientific).
12. In vitro muscle function assay system (Aurora Scientific, Aurora, ON, Canada). The system consists of a 300B or 305B dual mode transducer that measures/controls the muscle force and length, a 701A stimulator, a 604B signal interface, and an 805A in vitro test apparatus equipped with a vertically mounted tissue organ bath.
13. A custom-made 2 in. long stainless steel hook and a custom-made 2.5 in. long stainless steel hook.
14. Dynamic muscle control (DMC) software (Aurora Scientific). The software controls the force–length transducer and the stimulator. It allows real-time acquisition of the force and length data.
15. Dynamic muscle control data analysis (DMA) software (Aurora Scientific). The software analyzes the contractile data acquired by the DMC software.

2.3.2 In Vivo Evaluation of Running Distance by Treadmill

1. Exer 3/6 treadmill system (Columbus Instruments). The system includes a treadmill with an electrical stimulus and a control unit. The control unit regulates the treadmill speed and the intensity of the electrical shock. The system allows simultaneous analysis up to six animals in separate compartments.
2. Fan.

3 Methods

3.1 Generating AV.RSV.MCAT Vectors

3.1.1 Generating Catalase *cis* Plasmids with the OTC Leading Sequence

1. Cut out the catalase gene and OTC leading sequence from the original plasmid and insert it into the backbone of AAV *cis* plasmid; catalase expression is regulated by the RSV promoter and the SV40 polyA. Use standard molecular cloning methods to generate this construct.
2. Transformation of competent cells, transform 2 μ L of the ligation mixture into the competent cells. Plate transformation reactions on ampicillin LB agar plates.
3. Diagnostic digestion of the plasmid with restriction enzymes that recognize unique sites in the plasmid (*see* **Note 3**).
4. Large-scale preparation of the pcis.RSV.MCAT construct (*see* **Note 4**).

3.1.2 Recombinant AAV-9 AV.RSV.MCAT Production

1. Split 293 cells at 1:3 to 150 mm culture plates. Seed a total of 15 plates for one production. Change to fresh culture medium about 1–2 h before transfection (*see* **Note 5**).
2. When cells are ~70–80 % confluent, prepare to do the plasmid transfections (*see* **Note 6**).

3. Warm up $2 \times$ HBS and 2.5 M CaCl_2 at 37°C water bath for at least 30 min (*see Note 7*).
4. Change medium on plates with fresh DMEM/10 %FBS/1 %PS about 1–2 h before transfection (*see Note 8*).
5. Preparing DNA–calcium phosphate precipitate. Co-transfect three plasmids to make AAV-9 vector. These include the *cis* plasmid, pRep2/ Cap9, and pHelper. For each vector preparation (15×150 mm plates), use 187.5 μg of the *cis* plasmid, 187.5 μg pRep2/ Cap9, and 562.5 μg pHelper (at a ratio of 1:1:3). Mix all plasmids thoroughly in 15.2 mL H_2O . Add 1.68 mL of 2.5 M CaCl_2 to a final concentration of 250 mM. Generate DNA–calcium phosphate precipitate by slowly dropping the DNA/ CaCl_2 mixture to 16.8 mL of $2 \times$ HBS. In general, it takes 15–30 min room temperature incubation to form a high-quality precipitate (*see Note 9*).
6. Gently add the DNA–calcium phosphate precipitate to 293 cells drop by drop to the culture plates. Then mix the solution in the medium by gentle shaking and put back in the incubator (*see Note 10*).
7. 62–65 h after transfection, collect cells with a cell lifter. Spin down the cells in a benchtop centrifuge ($2,000 \times g$, 20 min at 4°C); add 9 mL 10 mM Tris–HCl (pH 8.0). Freeze/thaw cell lysate 8–10 times using dry ice/ethanol and a 38°C water bath. Add 10 mM Tris–HCl (pH 8.0) to increase volume to ~ 18 mL, and sonicate cell lysate at the power output of 5.5 for 10 min on ice (*see Note 11*).
8. Digest cell lysate with DNase I at 37°C for 45 min (we normally use half vial of Sigma DNase I for each 15 plates viral preparation). Sonicate cell lysate again at the power output of 5.5 for 7 min (on ice). Digest lysate with one-tenth volume of 0.05 % trypsin and 10 % sodium deoxycholate for 30 min in 37°C water bath. Clear cell lysate by spinning at $3,200 \times g$ for 30 min at 4°C . Carefully transfer supernatant to a new tube.
9. Adjust the volume to 29 mL with 10 mM Tris–HCl (pH 8.0) and add 18.2 g CsCl_2 (this is equal to 0.613 g/mL). The final volume should be about 32.5 mL. Incubate for 30 min at 37°C . Shake well (invert tube several times) to dissolve all CsCl_2 . Then keep at room temperature for 1–1.5 h. Spin at $3,200 \times g$ for 30 min at 4°C . Carefully load the supernatant into six 5 mL Beckman ultracentrifugation tubes in an SW55Ti rotor. Spin at $200,000 \times g$ for 40 h at 4°C (*see Note 12*).
10. Collect fractions from the bottom of the tube with a 20-G needle. Identify the viral containing fractions by slot blot (*see below*) (*see Note 13*).

11. Combine fractions with the highest viral titer and centrifuge again at $200,000 \times g$ for 40 h at 4 °C. Collect fractions as described in **step 6** and identify highest viral fraction by slot blot (see below). The expected yield from fifteen 150 mm plates preparation is $\sim 1 \times 10^{13}$ vg particles (*see Note 14*).
12. The viral stock may be stored at 4 °C for 1 month before dialysis.
13. Dialyze the viral stock in HEPES buffer (4 °C for 2×24 h).
14. Store the dialyzed viral at 4 °C and use it in 1 week.
15. Slot blot viral titer determination. Use duplicated sets of viral stock aliquots (1, 5, and 10 μ L) and plasmid copy number controls (10^7 , 10^8 , 10^9 , 10^{10} , 10^{11} molecules/ μ L) in slot blot. Denature samples in 50 μ L AAV digestion buffer at 100 °C for 10 min. Then immediately chill samples on ice and bring up volume to 400 μ L with digestion buffer. Load samples onto Hybond-N plus membrane with a Bio-Dot SF manifold microfiltration apparatus. After blotting, cross-link DNA to the membrane with UV irradiation. Pre-hybridize the membrane, then hybridize the membrane with a 32 P-labeled transgene-specific probe in the slot blot hybridization solution. Determine the viral particle titer by comparing the intensity of the viral stock band to that of the plasmid standards.

3.2 Evaluating Catalase Expression

3.2.1 Local Muscle Injection

1. For all animal experiments, get approval from the Institute Animal Care and Use Committee and follow NIH guidelines. Two muscles have been used to evaluate AAV transduction efficiency including the tibialis anterior (TA) muscle and the extensor digitorum longus (EDL) muscle.
2. Fix the 2–3-day-old neonatal mice with tap.
3. Extend the limb with the TA muscle facing forward.
4. Insert a 33-G Hamilton needle into the middle belly of the TA muscle. Slowly inject 30 μ L AAV vectors into the muscle while slowly backing out the injection needle.
5. Place mice on heating pad during recovery and monitor hourly for 5 h.

3.2.2 Systemic Facial Vein Injection

1. Turn on the electronic heat pad 10 min before the experiment.
2. Adjust the light source position so that it illuminates your microscope field. A moderate light intensity is best to visualize the vein.
3. Mix tattoo dye with virus solution (6 μ L/mL virus), and fill your syringe with virus. The volume should not exceed 100 μ L.

4. Position the animal in view of the microscope with your non-injecting hand, and place your index finger on the side of the mouse muzzle and your middle finger just caudal to the ear bud.
5. Identify the temporal vein. It should be visible through the skin just anterior to the ear bud and inferior to small peripheral vasculature.
6. Insert the needle into the facial vein, slowly inject 100 μ L virus into the vein, and slowly back out the injection needle (*see Note 15*).
7. Place mice on heating pad during recovery and monitor hourly for 5 h.

3.2.3 Determining Catalase Activity

1. Turn on spectrophotometer and open catalase assay program.
2. Turn on UV light 30 min before the experiment.
3. Calculate the sample volume for 200 μ g protein according to the protein concentration.
4. Add 200 μ g of sample to 2 mL of PB and mix well (first take the same volume of PB out). Split sample to two 1 mL aliquot.
5. Prepare 30 mM H_2O_2 freshly (add 34 μ L of 30 % H_2O_2 to 10 mL PB).
6. Put 1.5 mL of PB in quartz cuvette, and click "Blank."
7. Read sample.
 - (a) Add 0.5 mL of PB to 1 mL of the sample aliquot; the readings (at 0 and 30 s) will be A_i PB and A_f PB (*see Note 16*).
 - (b) Dump reaction solution and put the remaining 1 mL of sample to quartz cuvette. Then add 0.5 mL of freshly prepared 30 mM H_2O_2 to this sample in quartz cuvette (mix immediately using pipette, count 3, then "Read" the sample). The reading (at 0 and 30 s) will be A_i H_2O_2 and A_f H_2O_2 .
8. Calculate the catalase activity (K/g) with formula $K/g = [3 \ln (A_i/A_f)]/VP_t$.

3.2.4 Quantifying Catalase Expression by Western Blot

Preparation Whole Muscle
Lysate for Western Blot

1. Kill the mouse by cervical dislocation.
2. Harvest TA muscle and rinse it briefly in PB to remove the blood (if no blood there, ignore this step).
3. Put the muscle into mortar; add little liquid nitrogen to freeze the muscle. Grind it into very fine powder quickly, then add 0.3 mL PB, and grind again. Transfer the homogenate to a 1.5 mL EP tube on ice (0.2 mL PB is used for completely

transfer) (total 0.3 mL PB for EDL muscle), followed by a sonication at power of 6.0 for 5 min.

4. Centrifuge at $6,149 \times g$ for 5 min at cold room.
5. Collect supernatant (*see* **Note 17**).

Muscle Mitochondria Isolation

1. Isolate the gastrocnemius muscle.
2. Weigh 300 mg gastrocnemius muscle and rinse the muscle in 5 mL ice-cold PBS containing 10 mM EDTA (*see* **Note 18**).
3. Mince the muscle into small pieces using scissors. The minced muscles were suspended in 5 mL of ice-cold PBS supplemented with 10 mM EDTA and 0.2 % trypsin for 30 min, and then the minced muscle were put into a 15 mL tube (*see* **Note 19**).
4. Centrifuge the muscle at $200 \times g$ (1,372 rpm) for 5 min.
5. The pellet was suspended in IBm1. The ratio between tissue and isolation buffer is 1:10 (w:v, mg/ μ L).
6. Homogenize the muscle pellet using a tissue tearor (model 985370-395, BioSpec Products, INC. Bartlesville, OK) operated at 1,600 rpm in an Oak Ridge tube on ice, 2×15 s with a 30 s interval (*see* **Note 20**).
7. Centrifuge at $700 \times g$ for 10 min at 4 °C.
8. Transfer the supernatant to another centrifuge tube and centrifuged at $8,000 \times g$ for 10 min at 4 °C (*see* **Note 21**).
9. Resuspend pellet in 5 mL of ice-cold IBm2 and centrifuge at $8,000 \times g$ for 10 min at 4 °C (*see* **Note 22**).
10. Resuspend the pellet in 0.5 mL, 50 mM, pH 7.4 PB for Western blot [19]. Determine the protein concentration by a protein assay kit (Bio-Rad). The protein concentration would be 6–10 μ g/ μ L; store aliquot sample at –80 °C.

Catalase Western Blot

1. Thaw the protein samples on ice, and add sample dissociation (loading) buffer into protein samples at ratio of 1:1.
2. Seal the sample tubes and heat at 95 °C for 5 min.
3. Load samples and run the gel at 100 V for 1–1.5 h.
4. Rinse gel by water, then set up transferring “sandwich.”
5. Transfer the proteins to the PVDF membrane with Bio-Rad model: 100 V for 1 h at 4 °C.
6. Rinse the membrane by water and put it into 20 mL blocking solution (5 % milk) for 1 h.
7. Wash the membrane by 20 mL of 0.1 % TBST, and shake 10 min for three times.
8. Add primary antibody (usually at 1:1,000), and shake at room temperature for 2 h or 4 °C overnight.

9. Wash the membrane by TBST three times, 5 min each wash.
10. Add secondary antibody (usually at 1:2,000), and shake at room temperature for 1 h.
11. Wash the membrane by TBST three times, 5 min each wash.
12. Incubate the membrane in equal volumes of detection reagent 1 and 2 for 1 min.
13. Drain off detection reagent and wrap blots with Saran wrap.
14. Expose and develop film as required (*see* **Note 23**).

3.2.5 Checking Catalase Localization by Double Immunostaining

1. Snap freeze freshly isolated muscle sample in liquid nitrogen-cooled 2-methylbutane in Tissue-Tek OCT. Cut 8 μ m muscle cryosections.
2. Air-dry the slide.
3. Fix with 4 % paraformaldehyde for 10 min at room temperature.
4. Wash slides with KPBS 5 min for three times.
5. Block slides with KPBS + 1 % goat serum for 30 min at room temperature.
6. Incubate with KPBSG (KPBS + 0.2 % gelatin) for 5 min.
7. Incubate with primary antibody (1:500 rabbit anti-catalase antibody and 1:400, mouse monoclonal antibody against cytochrome C) in KPBSG + 1 % goat serum for 2 h at room temperature or 4 °C overnight.
8. Pour off the primary antibody and wash the slides with KPBSG + 1 % goat serum 5 min for three times.
9. Incubate with the secondary antibody (Alexa 594-conjugated goat anti-mouse antibody, 1:200; Alexa 488-conjugated goat anti-rabbit antibodies, 1:200) with a dilution 1:200 in KPBSG + 1 % goat serum for 1 h at RT.
10. Pour off the secondary antibody and rinse with KPBSG + 1 % goat serum 5 min for three times.
11. Coverslip with prolong gold antifading reagent (Invitrogen).

3.3 Evaluation of Effect of Mitochondrial Catalase Expression

3.3.1 In Vitro EDL Muscle Function Assay

1. Anesthetize the mouse with intraperitoneal injection of 3 μ L/g body weight of the anesthetic cocktail.
2. Fill the organ bath with the Ringer's buffer. Turn on the circulating water bath to 30 °C and start to equilibrate the Ringer's buffer with 95 % O₂ and 5 % CO₂ (*see* **Notes 24** and **25**).
3. Adjust the hook to the suitable position.
4. Turn on the dual mode level system and the simulator. Load the DMC program, and set the parameters at the dynamic muscle control and data acquisition panel as following: test duration, 3 s; update frequency, 500 Hz; sampling frequency,

1,000 Hz; input style, rise/fall; first stimulation, 1 s; last stimulation, 2 s; stimulation delay, 6 ms; and pulse width, 200 ms. Set the stimulator parameters as following: trigger mode, follow; pulse phase, biphasic; current multiplier, 100×; and current adjust, 8.5.

5. Record mouse and experimental information (body weight, date of birth, gender, strain, ear tag number, project title).
6. Prepare the dissection tools such as clips and scissors. Prepare the cotton rinsed in the Ringer's buffer.
7. Position the mouse face up on the dissection board and carefully peel off the skin to expose the hind limb muscles. Constantly superfuse the exposed muscles with the Ringer's buffer.
8. Dissect the remaining skin towards the metatarsal bones to expose the distal tendon of the TA muscle. Gently peel off the fascia on the surface of the TA muscle. Cut off the extensor ligament that covers the distal TA tendon. Lift up the distal TA tendon with a pair of 45° microdissection forces and separate it from the distal EDL tendon. Cut off the TA tendon and slowly peel off the TA muscle towards the knee to expose the EDL muscle. Cut out the TA muscle from its proximal attachment near the knee (*see Note 26*).
9. Identify the EDL tendon and clear it from the surrounding connective tissue and fat. Tie a double square knot with a bread silk suture around the distal EDL tendon. Cut the distal tendon inferior to the suture knot. Gently pull off the EDL muscle from the distal end. Separate the EDL muscle from connective tissue and vessels beneath the muscle with a pair of microdissection scissors. Tie a double square knot around the proximal EDL tendon, and tie another double square knot using the same suture to secure the proximal EDL tendon to the distal end of the steel hook. Cut the proximal EDL tendon superior to the suture knot, and remove the intact EDL muscle. Attach the proximal end of the steel hook to the level arm of the transducer. Vertically position the EDL muscle between two platinum electrodes before securing the distal EDL tendon to a fixed clamp (*see Note 27*).
10. Submerge the EDL muscle in the Ringer's buffer and adjust the muscle length to generate a 1 g resting tension. Allow the muscle to equilibrate for 10 min.
11. Adjust the muscle length to generate a resting tension of 1 g. Stimulate the muscle at 4 Hz (twitch stimulation). Record muscle force. Rest for ~1 min. Repeat twitch stimulation at resting tension of 1 g for two times (*see Note 28*).

12. Rest muscle for 1 min. Adjust the muscle length to generate a resting tension of 1 g, and stimulate muscle at 150 Hz for three times with 1 min interval.
13. Rest muscle for 5 min. Adjust the muscle length to generate a resting tension of 1 g, and stimulate muscle with a single pulse at 4 Hz. Record the force as the absolute twitch force (*see Note 29*).
14. Rest muscle for 5 min. Adjust the muscle length to generate a resting tension of 1 g, and stimulate muscle at 50, 80, 120, and 150 Hz. Rest 1 min between stimulations. Record the forces as the absolute tetanic forces under each stimulation frequency.
15. Rest muscle for 10 min. Adjust the muscle length to generate a resting tension of 1 g, and apply 10 cycles of eccentric contraction. For each cycle, stimulate muscle at 150 Hz for 700 ms. During the last 200 ms of stimulation, stretch the muscle for 10 % Lo (0.5 Lo/s). After each stimulus, restore the muscle length to Lo at a speed of 0.5 Lo/s. Allow a 2 min rest between each cycle of eccentric contraction. Record the tetanic force of the first 500 ms stimulation for each cycle. The tetanic force of the first cycle is arbitrarily designated as 100 % (*see Note 30*).
16. Detach the EDL muscle from the steel hook and force transducer. Cut the proximal and distal EDL tendons at the muscle tendon junction. Blot the muscle with Kimwipes twice and record the muscle weight (*see Note 31*).
17. Calculate the EDL muscle cross-sectional area using the equation of cross-sectional area = (muscle mass, in gram)/[1.06 g/cm³ × (optimal fiber length, in cm)]. 1.06 g/cm³ is the muscle density. The optimal fiber length is calculated as 0.44 × Lo. 0.44 represents the ratio of the fiber length to the Lo of the EDL muscle.
18. Load the DMA program and open the file containing the force data. Analyze the data using the software. Export the data to an Excel file. The force value obtained from the DMA program represents the absolute force. Calculate the specific muscle force by dividing the absolute force with the cross-sectional area. Calculate the force drop after eccentric contraction with the formula of Force drop % = $(F_1 - F_n)/F_1$. F_1 is the tetanic force obtained during the first cycle. F_n is the tetanic force obtained during the n th cycle.

3.3.2 In Vivo Evaluation of Running Distance by Treadmill

1. Record mouse/experimental information (body weight, date of birth, gender, strain, ear tag number, project title).
2. Check to make sure there is no visible injury in the limbs and toes. Record room temperature. Set up the electric shocker at the intensity of 7 and the repetition rate of 9. Adjust the inclination of the treadmill platform with the Jiffy-Jack.

Turn on the fan to the low setting and have the air blow in the same direction as the mouse is running.

3. Acclimate the mouse to the treadmill for 3 days. On day 1, place the mouse on an unmoving flat treadmill for 2 min, an unmoving 15° downhill treadmill for 5 min, a 15° downhill treadmill at the speed of 5 m/min for 15 min, and a 15° downhill treadmill at the speed of 10 m/min for 5 min (*see Note 32*).
4. On day 2, place the mouse on an unmoving 15° downhill treadmill for 2 min, a 15° downhill treadmill at the speed of 5 m/min for 5 min, and a 15° downhill treadmill at the speed of 10 m/min for 10 min.
5. On day 3, perform the same type of training as on day 2 except extend the last step from 10 to 15 min.
6. On day 4, subject the mouse to a single bout of 15° downhill running starting at the speed of 10 m/min. Twenty minutes later, increase the treadmill speed 1 m/min every 2 min until the mouse is exhausted. Continuously nudge the mouse to keep it stay on the track. Exhaustion is defined as the point at which the mouse spends more than 10 s on the shocker without attempting to resume running when nudged (*see Note 33*).
7. Record the running time at each speed and calculate the running distance.

4 Notes

1. To shorten the reaction time, ligations may be done at room temperature (20–25 °C). For cohesive (sticky) ends, use 1 µL of T4 DNA ligase in a 20 µL reaction for 30 min. For blunt ends, use 1 µL of T4 DNA ligase in a 20 µL reaction for 2 h.
2. Cells may be concentrated by centrifuging at $800 \times g$ for 10 min. Pipette 200 µL SOC medium from the bottom of the tube, and then spread the mixture with a sterile spreader. Tilt and tap the spreader to remove the last drop of cells.
3. We usually used two enzymes, one enzyme recognizes the unique site in the backbone and the other enzyme recognizes the unique site in the MCAT gene.
4. Prior to the large-scale preparation of the pcis.RSV.MCAT plasmid, we suggest to transfect the plasmid into 293 cells and confirm catalase expression by immunocytochemistry or Western blot.
5. To maintain cells propagated, it is important to establish a liquid nitrogen stock at ≤ 50 % confluence. 293 cells grown at

high confluence may lose the cell propagation ability and thus reduce the yield of AAV production.

6. To achieve high titers, it is important that 293 cells are healthy and plated at optimal density. Cells should be passaged at 70–80 % confluence. 293 cells grown at high confluence often yield low viral titer.
7. This step is required; DNA–phosphate precipitate will form under specific temperature.
8. Care should be taken to avoid blowing up the cells. When exchanging solutions, gently pipette down the side of the dish and not directly onto the cells to prevent disruption of the cell monolayer.
9. A high-quality precipitate is essential to high viral yield. We recommend routinely monitoring calcium phosphate precipitate on a coverslip using a phase contrast microscope. If there is no apparently precipitate, prepare the mixture again.
10. Do not allow the transfection mixture to sit too long before it is added to the cells. Prolonged incubation may reduce transfection efficiency.
11. 48 h after transfection, check the cells every 12 h. If there are a lot of dead cells suspended in the medium, harvest the cells immediately. Do not let cells grow more than 72 h after transfection.
12. In this protocol, we described a CsCl_2 ultracentrifugation-based protocol for AAV-9 purification. However, column purification (HPLC or FPLC) methods have been developed for many different AAV serotypes. It is expected that a column purification method will become available in the near future for AAV-9 [24].
13. We usually collect 12 tubes of virus and 11 drops of virus in every tube. According to our experiences, tubes 5, 6, 7, and 8 usually contain higher concentration of virus.
14. To accelerate this process, one may use higher spin speed. However, centrifugation time should be adjusted accordingly.
15. The tattoo dye can show us if the needle is inserted in the vein. If the virus solution is leaking around the vein, stop injection immediately and try the facial vein on the contralateral side.
16. Since there is no H_2O_2 , the reading should be the same for Ai PB and Af PB. Occasionally, difference is detected due to instability of the machine/background noise. The line should be very stable at the horizontal line during the assay.
17. We usually measure the catalase activity immediately after harvest. Alternatively, protein pellet can be stored at -80°C and the catalase activity measured later.

18. It is better to use EDTA instead of EGTA. EGTA also chelates Mg^{2+} . Mg^{2+} can influence mitochondrial function as well as the kinetics of CytC release.
19. Precool the glassware on ice for 10 min before starting the procedure. Each step must be performed at 4 °C to minimize activation of phospholipases and proteases.
20. Wear protective gloves while you are using the homogenizer to avoid injury if the potter breaks down.
21. The white foamy material near the top of the tube consists of lipids. Remove the foamy material by wiping the inside of the tube with a sheet of Kimwipes.
22. When the supernatant is poured off, the loose upper part of the mitochondrial pellet may be detached as well. Pipette out the supernatant carefully when the mitochondrial pellet tends to pour off.
23. There are usually two bands for catalase Western blot: one band is endogenous catalase, and the other band stands for transgenic catalase.
24. We strongly suggest using the freshly prepared Ringer's buffer. Discard the buffer if it is more than 2 weeks old. Some investigators have included 6–25 mM tubocurarine chloride in their Ringer's buffer. However, we found this is not necessary.
25. The contractility and fatigability of isolated mouse muscles are affected by temperature. We found that 30 °C yielded consistent force output without inducing apparent fatigue. The Ringer's buffer should be equilibrated with 95 % O_2 and 5 % CO_2 for at least 20 min before each use. During force measurement, one should adjust oxygen valve to allow for a steady flow of gas without generating large bubbles.
26. Take extreme care to avoid cutting the blood vessels during dissection. The rupture of the vessels at the proximal end of the TA muscle may cause bleeding, which will cover the muscle tissue. When it is bleeding, remove the blood with a thin piece of Ringer's buffer-soaked cotton.
27. To clearly expose the proximal EDL tendon, one may need to cut open the distal biceps femoral muscle. While taking the EDL muscle out, there will be bleeding from the vessels beneath the muscle. This can be stopped with a thin piece of Ringer's buffer-soaked cotton. When mounting the EDL muscle, make sure it is positioned right in the middle of two electrodes.
28. We usually obtain the optimal muscle length at a resting tension of 1 g.
29. Prior to the twitch and tetanic force measurement, we usually stimulate the muscle for 0.5 s at 150 Hz three times to warm up the muscle. Rest the muscle for 1 min and adjust the muscle

length to the optimal muscle length between each warm-up stimulus. This treatment stabilizes muscle and allows consistent muscle force output during subsequence measurements.

30. After two rounds of stimulation, the resting tension will be around 0.7 g. If the resting force reduces to less than 0.2 g, adjust the muscle length again to obtain a resting tension of 0.5 g.
31. When measuring the muscle weight, make sure to remove the tendons and sutures. We recommend cut right at the position of the muscle tendon junction.
32. 26. To test skeletal muscle function, we recommend using 15° downhill treadmill running. Downhill treadmill running induces damaging eccentric contraction. Hence, it can more accurately reflect skeletal muscle-specific effect.
33. Caution should be taken when using the time spent on the electric shocker as an indicator for exhaustion. Individual animal may display different running styles. Mice that do not run willingly or do not show a consistent running style should be excluded from the study.

Acknowledgments

The studies are supported by grants from the National Institutes of Health AR-49419 and the Muscular Dystrophy Association. We thank Dr. James Wilson (University of Pennsylvania, Philadelphia, PA) for providing the AAV-9 packaging plasmid.

References

1. Jackson MJ, O'Farrell S (1993) Free radicals and muscle damage. *Br Med Bull* 49:630–641
2. Tidball JG, Wehling-Henricks M (2007) The role of free radicals in the pathophysiology of muscular dystrophy. *J Appl Physiol* 102:1677–1686
3. Wei YH, Lee HC (2002) Oxidative stress, mitochondrial DNA mutation, and impairment of antioxidant enzymes in aging. *Exp Biol Med* (Maywood) 227:671–682
4. Barja G, Herrero A (2000) Oxidative damage to mitochondrial DNA is inversely related to maximum life span in the heart and brain of mammals. *FASEB J* 14:312–318
5. Lee HC, Wei YH (2012) Mitochondria and aging. *Adv Exp Med Biol* 942:311–327
6. Bai J, Rodriguez AM, Melendez JA, Cederbaum AI (1999) Overexpression of catalase in cytosolic or mitochondrial compartment protects HepG2 cells against oxidative injury. *J Biol Chem* 274:26217–26224
7. Arita Y, Harkness SH, Kazzaz JA, Koo HC, Joseph A, Melendez JA, Davis JM, Chander A, Li Y (2006) Mitochondrial localization of catalase provides optimal protection from H₂O₂-induced cell death in lung epithelial cells. *Am J Physiol Lung Cell Mol Physiol* 290:L978–L986
8. Kohler JJ, Cucoranu I, Fields E, Green E, He S, Hoying A, Russ R, Abuin A, Johnson D, Hosseini SH, Raper CM, Lewis W (2009) Transgenic mitochondrial superoxide dismutase and mitochondrially targeted catalase prevent antiretroviral-induced oxidative stress and cardiomyopathy. *Lab Invest* 89:782–790
9. Schriener SE, Linford NJ, Martin GM, Treuting P, Ogburn CE, Emond M, Coskun PE, Ladiges W, Wolf N, Van Remmen H, Wallace DC, Rabinovitch PS (2005) Extension of murine life span by overexpression of catalase targeted to mitochondria. *Science* 308:1909–1911

10. Treuting PM, Linford NJ, Knoblaugh SE, Emond MJ, Morton JF, Martin GM, Rabinovitch PS, Ladiges WC (2008) Reduction of age-associated pathology in old mice by overexpression of catalase in mitochondria. *J Gerontol A Biol Sci Med Sci* 63:813–822
11. Dai DF, Santana LF, Vermulst M, Tomazela DM, Emond MJ, MacCoss MJ, Gollahon K, Martin GM, Loeb LA, Ladiges WC, Rabinovitch PS (2009) Overexpression of catalase targeted to mitochondria attenuates murine cardiac aging. *Circulation* 119:2789–2797
12. Mao P, Manczak M, Calkins MJ, Truong Q, Reddy TP, Reddy AP, Shirendeb U, Lo HH, Rabinovitch PS, Reddy PH (2012) Mitochondria-targeted catalase reduces abnormal APP processing, amyloid beta production and BACE1 in a mouse model of Alzheimer's disease: implications for neuroprotection and lifespan extension. *Hum Mol Genet* 21:2973–2990
13. Kay MA (2011) State-of-the-art gene-based therapies: the road ahead. *Nat Rev Genet* 12:316–328
14. Baoutina A, Alexander IE, Rasko JE, Emslie KR (2007) Potential use of gene transfer in athletic performance enhancement. *Mol Ther* 15:1751–1766
15. Mingozzi F, High KA (2011) Therapeutic in vivo gene transfer for genetic disease using AAV: progress and challenges. *Nat Rev Genet* 12:341–355
16. Buchlis G, Podsakoff GM, Radu A, Hawk SM, Flake AW, Mingozzi F, High KA (2012) Factor IX expression in skeletal muscle of a severe hemophilia B patient 10 years after AAV-mediated gene transfer. *Blood* 119:3038–3041
17. Yue Y, Ghosh A, Long C, Bostick B, Smith BF, Kornegay JN, Duan D (2008) A single intravenous injection of adenoassociated virus serotype-9 leads to whole body skeletal muscle transduction in dogs. *Mol Ther* 16:1944–1952
18. Bostick B, Ghosh A, Yue Y, Long C, Duan D (2007) Systemic AAV-9 transduction in mice is influenced by animal age but not by the route of administration. *Gene Ther* 14:1605–1609
19. Liu M, Yue Y, Li D, Duan D (2007) Catalase overexpression does not impair extensor digitorum longus muscle function in normal mice. *Muscle Nerve* 36:833–841
20. Rex TS, Tsui I, Hahn P, Maguire AM, Duan D, Bennett J, Dunaief JL (2004) Adenovirus-mediated delivery of catalase to retinal pigment epithelial cells protects neighboring photoreceptors from photo-oxidative stress. *Hum Gene Ther* 15:960–967
21. Qi X, Hauswirth WW, Guy J (2007) Dual gene therapy with extracellular superoxide dismutase and catalase attenuates experimental optic neuritis. *Mol Vis* 13:1–11
22. Guy J, Qi X, Hauswirth WW (1998) Adeno-associated viral-mediated catalase expression suppresses optic neuritis in experimental allergic encephalomyelitis. *Proc Natl Acad Sci U S A* 95:13847–13852
23. Li D, Lai Y, Yue Y, Rabinovitch PS, Hakim C, Duan D (2009) Ectopic catalase expression in mitochondria by adeno-associated virus enhances exercise performance in mice. *PLoS One* 4:e6673
24. McClure C, Cole KL, Wulff P, Klugmann M, Murray AJ (2011) Production and titration of recombinant adeno-associated viral vectors. *J Vis Exp* 27:e3348

Chapter 14

Real-Time Bioluminescence Functional Imaging for Monitoring Tissue Formation and Regeneration

Nadav Bleich Kimelman, Ilan Kallai, Dmitriy Sheyn, Wafa Tawackoli, Zulma Gazit, Gadi Pelled, and Dan Gazit

Abstract

Real-time bioluminescence functional imaging holds great promise for regenerative medicine because it improves the researcher's ability to analyze and understand the healing process. Using transgenic mice coupled with gene-modified cells, one can employ this method to monitor host and graft activity in various models of tissue regeneration. We implemented real-time bioluminescence functional imaging to analyze bone formation by following a unique protocol in which the *luciferase* reporter gene, driven by an *osteocalcin* promoter, is used to visualize host and graft activity during bone formation. Real-time bioluminescence functional imaging can be used to assess the "host reaction" in transgenic mice models; it can also be used to assess "graft activity" in other animals in which genetically labeled stem cells have been implanted or direct gene delivery has been applied. The suggested imaging protocol requires 25 min per sample. However, special attention must be given to the layout of the experimental design, which determines the specific activity that will be analyzed.

Key words Imaging analysis, Bioluminescence imaging, Tissue engineering, Bone regeneration, Osteocalcin

1 Introduction

Regenerative medicine involves the development of biological replacements for use in restoring function in damaged tissues or organs, which occur due to aging, among other causes [1]. Previously, we demonstrated success in the use of both direct gene delivery [2] and genetically engineered mesenchymal stem cells (MSCs, multipotent adult stem cells) for regeneration of skeletal tissue including bone [3, 4]. Other investigators have used unmodified cells or protein therapy to achieve the same goal of bone regeneration [5, 6]. In the past, to evaluate new therapies for tissue regeneration, invasive methods, such as histological, immunohistochemical, and biochemical analyses, among others, were the only tools available for the researcher. Since novel molecular imaging

Table 1
Advantages of BLI

	Advantage	Compared with
Cost of operation and required reagents	Low	MRI, PET, SPECT,CT
Tissue penetration	High in rodents	Fluorescence imaging
Potential cell/tissue damage	Low	PET, SPECT (require radiotracers), CT (radiation)
Background signal	None	PET, SPECT, CT
Signal quantification and analysis	Straightforward	MRI, PET, SPECT, CT

MRI magnetic resonance imaging, *PET* positron emission tomography, *SPECT* single-photon emission computed tomography, *CT* computed tomography

systems have been developed, new, noninvasive methods can be used to monitor tissue repair in real time, over prolonged periods of time, and in the same subjects. Others and we have used bioluminescence-imaging (BLI) systems to monitor implanted cell survival for prolonged periods of time. Table 1 presents the main advantages of BLI compared with other noninvasive imaging systems.

This procedure required the *luciferase* gene to be activated by a constitutive promoter such as ubiquitin [7, 8]. However, to monitor tissue regeneration or formation in a noninvasive manner—an ability that holds great promise for regenerative medicine because it affords the researcher the opportunity to explore the function of implanted cells or inserted genes as well as the host reaction—one must use tissue-specific promoters that conditionally activate the *luciferase* gene. Those promoters allow for in vivo differentiation of implanted cells or host cells that is reported by the *luciferase* gene expression. Moreover, the ability to perform quantitative analysis, and thus to compare different treatments, improves our ability to analyze and understand the healing process and to gain novel insights into the bone formation process [2, 3, 8–12].

This protocol requires the use of transgenic mice and either gene-modified cells or a gene-delivery vector that harbors the same transgene as the transgenic mice. Special attention should be given to the choice of gene and animal model. One should choose a promoter for a major gene that is characteristic of the desired healing process (such as *vascular endothelial growth factor* for vascular regeneration or *collagen type 2* for cartilage formation). The promoter should drive a reporter gene that permits noninvasive real-time monitoring (such as *luciferase*). In this protocol *osteocalcin*-driven *luciferase* reporter system was used to monitor bone formation. This system is based on the use of the *luciferase* reporter gene, driven by an *osteocalcin*

promoter (*Oc-Luc*), to monitor osteogenic activity in vivo. Other types of luciferase, such as Renilla or Metridia, may also be suitable for this protocol. Osteocalcin (Oc) is a bone tissue-specific protein expressed by osteoblasts, odontoblasts, and hypertrophic chondrocytes at the onset of tissue mineralization, and it accumulates in the bone extracellular matrix [12]. It has a predicted expression pattern that is coupled with bone formation [2, 3, 8]; thus, it can be a valuable tool for monitoring bone formation. This system is a specific application of our protocol—the technical aspects can apply to any functional *promoter*-driven *luciferase* system with appropriate modifications according to the specific system used. When the target of the analysis is the host reaction to either the introduction of bone-forming cells or delivery of a bone-inducing gene, Oc-Luc transgenic mice are used as recipients of either cells [3] or genes [2]. When the focus is the activity of implanted cells (a graft), labeled cells are used in various recipients. Throughout this protocol, the term “host activity” relates to host-mediated bone formation or osteogenic activity. The term “graft activity” relates to graft-mediated bone formation. After the selection of an appropriate experimental system, the BLI system is used to monitor *Oc-Luc* activity noninvasively and longitudinally [12]. With adequate modifications one can apply a similar approach to many other models of tissue regeneration. This method was previously used to monitor host and graft osteogenic activity both in vivo and in vitro [2, 3, 8–12]. Real-time bioluminescence functional imaging can serve as a unique powerful tool for analyzing and monitoring tissue formation and manipulation. We have developed unique protocols that enable the user to analyze both host and graft activity. Using those generic protocols, analysis of data generated from additional functional imaging systems will be possible.

2 Materials

2.1 Experimental Design

To perform proper quantitative analysis of the reported activity, whether it is bone formation or other, one must first choose a robust experimental design that focuses on the desired phenomena. We suggest two experimental setups for analyzing the following:

1. *Host activity following osteogenic induction:* In this model bone-inducing cells—usually genetically modified MSCs that express an osteogenic gene—are implanted in either an ectopic or orthotopic location in an Oc-Luc transgenic mouse. *Luciferase* activity is then recorded during bone formation [3, 10, 11]. Alternatively, a bone-inducing gene is delivered in vivo to an Oc-Luc transgenic mouse. Again, *luciferase* activity is recorded during bone formation, and it represents the osteogenic reaction of the host to the delivered gene [2]. This model can also be performed using other bone inducers such as recombinant proteins.

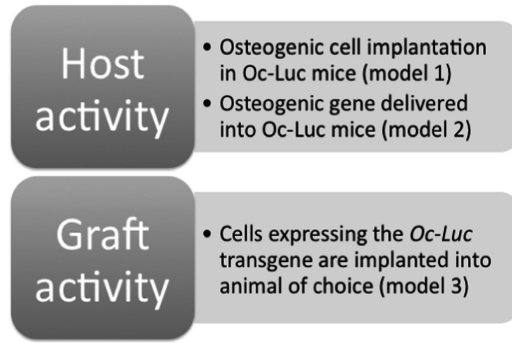


Fig. 1 Summarizes the main models used with this protocol

2. *Graft activity*: Here the implanted cells are transduced with the *Oc-Luc* transgene, which is used to report osteogenic differentiation by *luciferase* expression. The cells are osteogenically induced, and their differentiation is monitored in vitro and in vivo, thus providing a representation of graft activity [8].

2.2 Animal Models and Cells

1. pGL.3 *luciferase* (Promega, Madison, WI, USA) was used to generate Oc-Luc transgenic mice and to analyze host activity following direct gene delivery [3, 12]. pGL.4 *luciferase*-2 (Promega, Madison, WI, USA), which is codon optimized, was used to generate the osteocalcin-luciferase vector for transduction of implanted cells.
2. For analyzing host activity:
 - (a) Oc-Luc transgenic mice are needed for an analysis of host activity using real-time bioluminescence functional imaging (Fig. 1). If a different model is used, one should have the appropriate transgenic mice. The details regarding the development of the Oc-Luc mice strain are detailed elsewhere [12].
 - (b) After the transgenic mice have been obtained, one should use either cell implantation or gene delivery to induce bone formation. When bone formation is the final target of the analysis, *bone morphogenetic protein* (BMP)—expressing cells or plasmids—can be used, as well as any other strategy. One can use fracture models or no intervention at all to evaluate the natural osteogenic activity of the host, as previously demonstrated [9, 12].
3. For analyzing graft activity:
 - (a) For an analysis of graft activity, one should obtain cells that stably express the *Oc-Luc* transgene.
 - (b) If another model is used, one should obtain cells that stably express the same transgene as the aforementioned mice.

Such cells (*Oc-Luc*-expressing MSCs) were obtained by using a lentiviral vector, which provides stable transduction. The cells were further induced osteogenically and then implanted in a rat bone defect [8].

4. To obtain statistically meaningful results, one should perform power analysis to determine the number of samples for each experimental group. In our model, power calculations indicated that an “*n*” of six animals is required in order to archive 80 % power at a 0.05 significance level when BLI is used to monitor osteocalcin expression over time [8].
5. In each experiment, do not forget to include a negative control. For each area of focus, the experiment should contain the following models (specific to bone formation. Alterations in this design may be required for other applications):
 - (a) *Host activity following cell implantation*: cells or animals that have not been stimulated for osteogenic induction.
 - (b) *Host activity following gene delivery*: an empty plasmid or a nonosteogenic plasmid.
 - (c) *Graft activity*: cells that express the *Oc-Luc* transgene but are not osteogenically induced.

Cautions: Research protocols involving the use of animal subjects should be reviewed by the investigator’s institutional animal care and use committee (IACUC) to avoid any unnecessary discomfort or pain to the animal subject and to determine whether alternatives exist to animal research. All animal experiments should be performed in accordance with relevant guidelines and regulations of protocols approved by the investigator’s institutional animal research review committee. Personnel should be trained in animal handling.

2.3 Reagents

1. Hair removal cream (Veet® Hair Removal Gel Cream for Sensitive Skin, Reckitt Benckiser Group plc, Slough, UK). If furless mice are used, no hair removal cream is needed. Shaving is not optimal but can also serve as an option. Care should be taken because of the effect of fur residue on signal intensity. Whenever possible, using a hair removal cream is recommended.
2. Dry and wet gauze. For wet gauze use PBS.
3. D-Luciferin, potassium salt (Cat# E1605, Promega Corporation, Madison, WI, USA). The use of endotoxin-free D-luciferin can be considered if any immunological reaction is identified. We have not encountered any such reaction in our experiments. The use of luciferin as a substrate for the luciferase enzyme depends on your animal model and experimental design. Luciferin can be administrated systemically or locally.
 - (a) For systemic administration, dilute luciferin to 15.75 mg/ml in PBS. Luciferin can be systemically applied in an intravenous

[i.v.], s.c., or intraperitoneal [i.p.] manner, with little difference in the data generated [13], although the biodistribution of luciferin significantly varies depending on its administration route [14]. In general, the i.p. method is preferred because of its ease of use compared with the i.v. method. However, if the model used target locations in the i.p. area, s.c. administration may be preferred [13].

- (b) For local administration, dilute luciferin to 50 mg/ml in PBS. Because biodistribution of luciferin changes according to its method of administration, it is very important to adhere to one administration method throughout the entire experiment
 - (c) Diluted stock solutions should be sterilized through a 0.2- μ m filter.
 - (d) Protect the luciferin solution from light, and store luciferin aliquots in -80°C according to the manufacturer's instructions.
4. Becton Dickinson polypropylene tuberculin syringes (Cat# Z192082-100EA, Sigma-Aldrich, St. Louis, MO, USA). Other brands of syringes can be used.
 5. Anesthesia: ketamine-xylazine mixture (75 mg/kg ketamine and 10 mg/kg xylazine injected intraperitoneally). Other types of anesthesia, such as isoflurane gas, which is now available in some of the BLI systems, can be used. Please note that different anesthesia types can influence the imaging data (*see* Subheading 4).

2.4 Equipment

1. This protocol was designed for use with preclinical IVIS molecular imaging systems (Caliper Life Sciences, Hopkinton, MA, USA), based on a cooled (-90°C) camera with a large CCD chip area for high-sensitivity light detection (Fig. 2).
2. Image acquisition and analysis is handled by Living Image® 3.2 software (Caliper Life Sciences). The procedure steps are described in general terms; other similar equipment and software can be used instead of the ones listed.

3 Methods

3.1 Preparation of the Animal for Imaging

1. To avoid light scattering and masking, animal fur overlying the region of interest (ROI) should be completely removed before image acquisition (unless you are using furless mice such as the NOD/SCID strain).
2. According to the experimental design, fur overlying an additional reference region should be removed as well.



Fig. 2 Layout of the imaging system. **(a)** The IVIS molecular imaging systems (Caliper Life Sciences, Hopkinton, MA, USA). **(b)** A representative image of a mouse implanted with *luciferase*-expressing MSCs subcutaneously. Note the anesthesia mask in which the mouse nose is located, the area from which hair was removed, and the overlaid pseudocolor image

3. Cut the fur using a hair clipper and apply a thick layer of hair removal cream.
4. Wait ~1 min before you remove the cream with dry gauze.
5. Use wet gauze to remove any leftover cream.
6. Make sure all fur is removed from the ROI before proceeding.

3.2 Injection of Luciferin

This step depends on the experimental design and animal model used.

1. Systemic administration—Inject the luciferin solution (15.75 mg/ml) intraperitoneally. Inject 8 μ l solution/g body weight (e.g., 3.15 mg luciferin in 200 μ l PBS for a 25-g mouse).
2. Local administration—Inject the luciferin solution (50 mg/ml) subcutaneously or intramuscularly, close to the region of

bone formation. A 50- μ l injection (2.5 mg luciferin) should be sufficient.

3. Wait 2–3 min and anesthetize the animal according to your approved IACUC protocol.

Note: When administering luciferin locally (**step 2**), the animal should be anesthetized prior to the luciferin injection. (Switch the order of **steps 2** and **3**.)

3.3 Image Acquisition

1. Place the anesthetized animal in the imaging chamber. Based on our experience, as well as the experience of others [15], the position of the animal can affect the imaging results. We strongly recommend keeping a standard position for all animals in the study.
2. Set the field of view (FOV) by adjusting the position of the stage and lens to fit all required ROIs in the frame.
3. Set the imaging device for the luminescence imaging mode (the excitation filter will be blocked and the emission filter opened).
4. Manually set the exposure time, binning, and F/stop, or select automatic settings (recommended).
5. Approximately 10 min after the luciferin injection (Subheading 3.2, **step 2**), the signal will be at its peak. Acquire the image at the peak signal time.
6. If luciferin is administrated locally, acquire the image ~2 min following luciferin injection.

3.4 Image Analysis

1. Using the image analysis software, determine the target ROI for signal measurement.
2. Use a background ROI with the exact same dimensions placed either in a dark area of the image or on the animal's skin.
3. Save the photon flux data of the signal and background.
4. Subtract the background reading from the target reading.
5. When using Oc-Luc transgenic mice for evaluating host activity, the ROI signal should be relative to the animal's native *Oc-Luc* expression. That is determined by measuring the signal at the base of the tail (for each measurement) and dividing the background and target readings by the tail reading. We recommend using mice of similar age and sex to minimize data variation. Please note that while the background reading should be close to zero and it represents the “blank” reading of the system, the transgenic mice tail reading is higher and represents the intensity of the transgene expression in a specific specimen.

4 Notes

1. Use only in rodent models due to the fact that the bioluminescence signal decreases as it passes through animal tissues—approximately a tenfold decrease for each centimeter of tissue depth [16]. While this has little effect in rodents as long as the animal position is standardized, it prevents the use of this technology in larger animals. Even if one tried to use this method to image superficial locations in large animals, the high cost of the luciferin substrate required would render this application unattractive.
2. If large animal models are targeted, one can use the same methodology with an alternative reporter gene, such as the *human sodium iodide symporter (hNIS)* gene. This reporter gene can be used to trace cells using a SPECT or CT system and has proved successful in preclinical pig animal models [17].
3. The bioluminescence signal is dependent on a reaction involving ATP, magnesium, and luciferin [16]. Lack of any of these substances—as well as a lack of oxygen or adequate pH—might alter the recorded signal.
4. The BLI system is surface weighted. Thus, changes in the position of the imaged animal, implant geometry, or tissue optical properties may also affect quantification [15, 16].
5. The kinetics of light emission in BLI systems should be determined for each experimental model, especially because of the fact that the rate of luciferin biodistribution depends on many parameters (type, size and location of the graft, route of substrate injection and more). It is therefore strongly recommended that the investigator perform an in situ validation of the imaging results [16] by performing either an immunohistochemical analysis or a luciferase biochemical assay and standardize the experimental design and the imaging protocol by performing a pilot experiment in which the optimal protocol will be set.
6. When host activity is analyzed using this system, a common artifact is the endogenous *osteocalcin* promoter activity noted in transgenic Oc-Luc mice. This activity can mask signals from specific sites such as the mandible or tail.
7. It is essential to use animals of the same sex and age because reporter expression varies [9, 12].
8. When other genes serve as the imaging target, one should take those limitations into account and verify that the chosen imaging technique and gene of interest are capable of generating meaningful data.

9. Measurements can be performed at various intervals, from every few hours [9] up to every few weeks [8], depending on the experimental design.
10. For the bone formation analysis, we recommend imaging every few days for at least 2 weeks.
11. If one wants to repeat a measurement, a 30-min interval is recommended, as this is the usual time needed for signal elimination [14].
12. When using the *Oc-Luc* system for imaging of host activity, one should avoid locations with high endogenous activity (such as the mandible, tail, and pelvis).
13. When graft activity is targeted, the only limitation is cell number. This should be determined experimentally in a pilot assay (Fig. 3).
14. Hair removal cream can cause burns on the animal's skin. In this case, apply the cream for less time.
15. Make sure all leftover cream is removed following use.
16. Make sure to inject luciferin at 37 °C.
17. At all times keep luciferin protected from light.
18. If no luciferase signal is recorded following systemic luciferin injection, recheck your injection technique and consider changing it.
19. If no luciferase signal is recorded following local luciferin injection, consider applying a greater amount of luciferin.
20. Make sure that the imaging chamber is dark before imaging.
21. If a “blurred” image is recorded, make sure that the animal is properly anesthetized.
22. A luciferin kinetic study (a sequence of images starting 5 min after the luciferin injection) should be performed for each animal model to determine the peak signal time.
23. Be sure to record the signal at the same time post luciferin injection for all of the animals in the experiment.
24. Use the same anesthesia method throughout the experiment. In some models, the type of anesthesia can influence the luminescence peak and peak time [15]. Optionally, you can compare several anesthesia types.
25. Make sure the same settings (time following luciferase injection, exposure time, binning, and F/stop) are strictly kept. Failing to do so will result in high variance of data.
26. When using *Oc-Luc*—expressing cells implantation, make sure the cells stably express the *Oc-Luc* transgene during cell differentiation. This should be determined in vitro or in vivo before the imaging is performed.

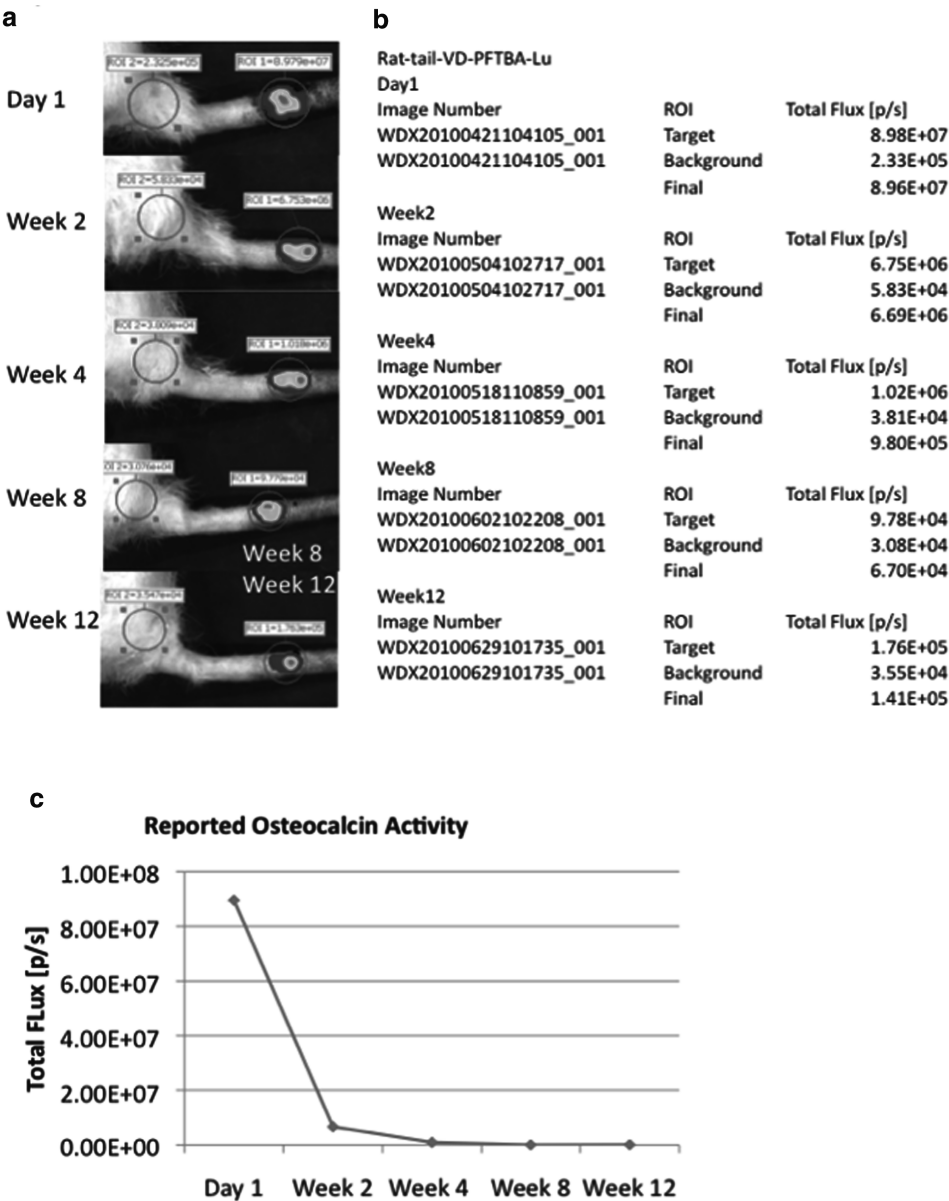


Fig. 3 Representative data set for graft activity analysis [8]. This figure demonstrates the different stages of data collection and presentation. **(a)** Representative real-time bioluminescence functional imaging images taken during the experiment, from day 1 to week 12 following cell implantation. Note the background and target ROIs (1 and 2) marked on the rat picture, including the total flux reading. Also note that the color scale (blue—less intense, red—most intense) is different between time points as the scale changes. **(b)** Quantitative data set obtained in the same rat. Note that for each time point, target and background readings are recorded and the final value is calculated. **(c)** A graph representing the collected data in **a** and **b** (Color figure online)

27. Make sure the cells survive following implantation in the host environment. Verification of cell survival can be done in a pilot or parallel experiment by implanting cells that express the *luciferase* gene constitutively into the relevant model and monitoring their survival [8].
28. Make sure the luciferin injection does not harm the implanted cells. This is very important when cells are implanted in a “closed” area (knee, intervertebral disc).
29. In case that luminescence is highly variable between time points, make sure the background ROI has the same dimensions as the target ROI.
30. When Oc-Luc mice are used, make sure that they express the transgene adequately. Be sure to use the bioluminescence signal from the tail base as a normalizing factor. If another transgenic system is used, be sure to record endogenous activity and to develop a proper normalizing protocol. Failing to do so may result in highly variable luminescence between time points.
31. Plan your experiment while taking into account that certain areas are highly active in the Oc-Luc mice (tail base, mandible). Consider performing a pilot study to confirm that the target signal is not masked. This also applies to other *promoter*-driven *luciferase* systems with proper modifications according to the location of the endogenous signal.

Acknowledgments

We acknowledge funding from the Telemedicine and Advanced Technology Research Center (TATRC), the US Army Medical Research and Materiel Command (Grant No. 0821700), the National Institutes of Health (Grant No. R01AR056694), and the California Institute for Regenerative Medicine (CIRM RT1-01027). We also acknowledge funding from the Ministry of Science and Technology, State of Israel, which supports a “Levi Eshkol fellowship” to I.K.

References

1. Paesold G, Nerlich AG, Boos N (2007) Biological treatment strategies for disc degeneration: potentials and shortcomings. *Eur Spine J* 16:447–468
2. Sheyn D, Kimelman-Bleich N, Pelled G, Zilberman Y, Gazit D, Gazit Z (2008) Ultrasound-based nonviral gene delivery induces bone formation in vivo. *Gene Ther* 15:257–266
3. Kimelman-Bleich N, Pelled G, Sheyn D, Kallai I, Zilberman Y, Mizrahi O, Tal Y, Tawackoli W, Gazit Z, Gazit D (2009) The use of a synthetic oxygen carrier-enriched hydrogel to enhance mesenchymal stem cell-based bone formation in vivo. *Biomaterials* 30:4639–4648
4. Kimelman N, Pelled G, Gazit Z, Gazit D (2006) Applications of gene therapy and adult stem cells in bone bioengineering. *Reg Med* 1:549–561

5. Kimelman N, Pelled G, Helm GA, Huard J, Schwarz EM, Gazit D (2007) Review: gene- and stem cell-based therapeutics for bone regeneration and repair. *Tissue Eng* 13:1135–1150
6. Sheyn D, Mizrahi O, Benjamin S, Gazit Z, Pelled G, Gazit D (2010) Genetically modified cells in regenerative medicine and tissue engineering. *Adv Drug Deliv Rev* 62:683–698
7. Li Z, Suzuki Y, Huang M, Cao F, Xie X, Connolly AJ, Yang PC, Wu JC (2008) Comparison of reporter gene and iron particle labeling for tracking fate of human embryonic stem cells and differentiated endothelial cells in living subjects. *Stem Cells* 26:864–873
8. Sheyn D, Kallai I, Tawackoli W, Cohn Yakubovich D, Oh A, Su S, Da X, Lavi A, Kimelman-Bleich N, Zilberman Y, Li N, Bae H, Gazit Z, Pelled G, Gazit D (2011) Gene-modified adult stem cells regenerate vertebral bone defect in a rat model. *Mol Pharm* 8(5):1592–1601
9. Gafni Y, Ptitsyn AA, Zilberman Y, Pelled G, Gimble JM, Gazit D (2009) Circadian rhythm of osteocalcin in the maxillomandibular complex. *J Dent Res* 88:45–50
10. Aslan H, Ravid-Amir O, Clancy BM, Rezvan-khah S, Pittman D, Pelled G, Turgeman G, Zilberman Y, Gazit Z, Hoffmann A, Gross G, Domany E, Gazit D (2006) Advanced molecular profiling in vivo detects novel function of dickkopf-3 in the regulation of bone formation. *J Bone Miner Res* 21:1935–1945
11. Hasharoni A, Zilberman Y, Turgeman G, Helm GA, Liebergall M, Gazit D (2005) Murine spinal fusion induced by engineered mesenchymal stem cells that conditionally express bone morphogenetic protein-2. *J Neurosurg Spine* 3:47–52
12. Iris B, Zilberman Y, Zeira E, Galun E, Honigman A, Turgeman G, Clemens T, Gazit Z, Gazit D (2003) Molecular imaging of the skeleton: quantitative real-time bioluminescence monitoring gene expression in bone repair and development. *J Bone Miner Res* 18:570–578
13. Inoue Y, Kiryu S, Izawa K, Watanabe M, Tojo A, Ohtomo K (2009) Comparison of subcutaneous and intraperitoneal injection of D-luciferin for in vivo bioluminescence imaging. *Eur J Nucl Med Mol Imaging* 36:771–779
14. Berger F, Paulmurugan R, Bhaumik S, Gambhir SS (2008) Uptake kinetics and biodistribution of ^{14}C -D-luciferin—a radiolabeled substrate for the firefly luciferase catalyzed bioluminescence reaction: impact on bioluminescence based reporter gene imaging. *Eur J Nucl Med Mol Imaging* 35:2275–2285
15. Cui K, Xu X, Zhao H, Wong ST (2008) A quantitative study of factors affecting in vivo bioluminescence imaging. *Luminescence* 23:292–295
16. Sadikot RT, Blackwell TS (2005) Bioluminescence imaging. *Proc Am Thorac Soc* 2:537–540, 511–512
17. Dwyer RM, Schatz SM, Bergert ER, Myers RM, Harvey ME, Classic KL, Blanco MC, Frisk CS, Marler RJ, Davis BJ, O'Connor MK, Russell SJ, Morris JC (2005) A preclinical large animal model of adenovirus-mediated expression of the sodium-iodide symporter for radioiodide imaging and therapy of locally recurrent prostate cancer. *Mol Ther* 12:835–841

Exometabolomic Mapping of *Caenorhabditis elegans*: A Tool to Noninvasively Investigate Aging

Robert J. Mishur, Jeffrey A. Butler, and Shane L. Rea

Abstract

Metabolomic analyses can provide valuable information about the internal metabolism of an organism; however, these studies can become quickly complicated by the large number of metabolites that are often detected. Overcoming this limitation requires high-resolution analytical separation techniques, coupled with high-power deconvolution software. Additionally, much care must be taken in metabolomic sample preparation to quench active enzymes and avoid artifactual changes in the metabolome. Here we present a relatively simple and straightforward technique, exometabolome mapping, which bypasses each of these concerns, is noninvasive, and provides a concise summary of the key metabolic processes operative in an organism. We illustrate our method using the nematode *C. elegans*, an organism which has been widely exploited in aging studies; however, with only minimal modification, our technique is extendible to other sample types, and indeed we have successfully used it both to perform yeast footprinting and to study the excreted metabolic end products of human kidney cancer cell lines.

Key words Metabolomics, Metabonomics, Aging, Exometabolome mapping, *Caenorhabditis elegans*

1 Introduction

Metabolomics is an “omics” science which seeks to examine the metabolome—the ensemble of metabolic reactants, intermediates, and products of a cell, tissue, or organism. In a hierarchical sense, metabolomics falls at the very bottom of genomics (DNA), transcriptomics (RNA), and proteomics (proteins). Understanding which metabolic pathways are operative in a system, and how these pathways are interwoven into networks, is changing how we view disease and aging.

Caenorhabditis elegans is a well-studied model organism which has been exploited over the past several decades to make advances in multiple fields, including aging, genetics, and neurobiology [1–4]. When grown in liquid culture, *C. elegans* excretes metabolites directly into its surrounding medium. This ensemble of excreted metabolites—the exometabolome—is distinct from

defecatory waste products and can be easily collected and mined. Since *C. elegans* defecates continually every 45 s [5], the intestine is cleared prior to the end of our washing procedure, ensuring that only excreted metabolites are collected. Because the exometabolome of *C. elegans* consists of only a few hundred types of metabolites (compared with potentially thousands of internal ones), and because the exometabolome is essentially free of other interfering compounds, including metabolic enzymes, to a first approximation the key operational elements of intermediary metabolism can be reconstructed.

The abundance of aging studies which have been accomplished using *C. elegans* stems from its short lifespan (15 days at 25 °C, [6]), the ease with which genetic manipulations can be carried out, and its high reproductive rate. Moreover, the great abundance of genetic mutants, RNAi clones, and environmental interventions that significantly alter worm lifespan [7–11] have made *C. elegans* one of the premier model organisms used to investigate aging processes. Ongoing studies in our laboratory have revealed that several long-lived genetic variants of *C. elegans* share a unique type of metabolism. These findings raise the possibility that metabolic configuration, per se, may contribute to lifespan extension in this organism. In this regard, we have previously reported that the exometabolome of long-lived mitochondrial (Mit) mutants of *C. elegans* can be distinguished from that of wild-type animals using HPLC [12]. Here we present detailed methods for the collection, derivatization, and analysis of the exometabolome from *C. elegans* using gas chromatography–mass spectrometry (GC-MS). Raw GC-MS dataset files for wild-type worms and long-lived *eat-2(ad465)* mutants are provided as training tools. The *eat-2(ad465)* mutant strain has impaired pharyngeal pumping, resulting in slowed eating, and is used to study calorie restriction, an established intervention to increase lifespan, in *C. elegans* [13].

2 Materials

All solutions should be prepared using the highest-purity water available. We recommend using double-distilled water. Unless otherwise noted, all solutions can be stored at room temperature. All solvents should be LC/MS grade or better.

2.1 Bacterial Food Stock

1. *E. coli* bacteria (OP50): Purchased from the Caenorhabditis Genetics Center, Minneapolis, MN (<http://www.cbs.umn.edu/CGC/>).
2. Luria Bertani (LB) broth: Dissolve 10 g bacto-tryptone, 5 g yeast extract, and 5 g sodium chloride in 800 mL water, and then add water to bring to a total volume of 1 L. Aliquot into

- 2 × 1 L glass autoclavable bottles (500 mL/bottle) and autoclave for 30 min using liquid cycle settings (*see Note 1*).
3. Once LB has cooled to room temperature, transfer 500 mL to a 2-L Erlenmeyer flask.
4. Inoculate LB with a single colony of *E. coli* (OP50), and incubate overnight at 37 °C on a platform shaker set at 200 rpm (*see Note 2*).
5. Following incubation, use a spectrometer to measure the absorbance of the bacterial stock (1:10 dilution in LB) at 595 nm. If the optical density (OD₅₉₅) of the diluted stock is less than 0.3, the culture should be concentrated by centrifugation (4,250 × *g*, 10 min, 4 °C) and resuspended in a lesser volume of LB.
6. Dilute OP50 to a final OD₅₉₅ of 2.5 (undiluted), aliquot into 50-mL conical tubes, and store aliquots at 4 °C.

2.2 BNGM Agar Plates

For our experiments we culture animals on BNGM agar plates. These differ from traditionally used nematode growth medium (NGM) plates in that they contain a greater amount of bacteriological peptone, which allows for growth of a thicker lawn of bacteria.

1. Bacteriological peptone (Sigma-Aldrich).
2. Sodium chloride.
3. Agar.
4. Polystyrene petri dishes, 100 mm × 15 mm (Fisher).
5. Calcium chloride, 1 M: Dissolve 147.02 g calcium chloride monohydrate in 800 mL water, and then add water to bring to a total volume of 1 L. Aliquot into 500-mL glass autoclavable bottles (200 mL/bottle), and autoclave for 30 min using liquid cycle settings (*see Note 1*).
6. Cholesterol, 5 mg/mL: In a 500-mL beaker, dissolve 1.0 g cholesterol in 200 mL 95 % ethanol with gentle heating. Filter sterilize the solution using a polystyrene filter system with a 0.22-μm polyethersulfone membrane (Corning).
7. Magnesium sulfate, 1 M: Dissolve 120.4 g anhydrous magnesium sulfate in 800 mL water, and then add water to bring to a total volume of 1 L. Aliquot into 500-mL glass autoclavable bottles (200 mL/bottle), and autoclave for 30 min using liquid cycle settings (*see Note 1*).
8. Potassium phosphate, 1 M: Dissolve 98.0 g anhydrous potassium phosphate (monobasic) and 48.0 g anhydrous potassium phosphate (dibasic) in 800 mL water. Check the pH with pH paper or a pH meter, it should be near 6. Add water to bring to a total volume of 1 L, and aliquot into 500-mL glass autoclavable bottles (200 mL/bottle). Autoclave for 30 min using liquid cycle settings (*see Note 1*).

9. In a 4-L polypropylene beaker (Nalgene), mix 20 g peptone, 6 g sodium chloride, 40 g agar, and 2 L water. Using a magnetic stir bar, stir to partly dissolve. Autoclave contents, with stir bar, for 1.75 h using liquid cycle settings.
10. Following autoclave cycle, allow heated solution to partially cool by stirring at room temperature for 30 min. Then add 2 mL 1 M calcium chloride, 2 mL 5 mg/mL cholesterol, 2 mL 1 M magnesium sulfate, and 50 mL 1 M potassium phosphate.
11. Using an automatic liquid dispenser (Wheaton Omnispense), or manually, dispense 10 mL of solution into each 10-cm dish, until all solution is used (*see Note 3*). Cover dishes and allow to dry at room temperature for 2 days.
12. Dilute OP50 (OD₅₉₅ 2.5) 1:750 using LB; you will need 0.5 mL of this solution per plate.
13. Using an automatic pipet with a sterile tip, spot 500 μ L of OP50 dilution per plate, six at a time. Once plates have been spotted, spread the bacteria evenly across the plates using a sterile 60-mm cell spreader (Fisher). Before starting, and after each set of six plates, sterilize the spreader by submerging in 95 % ethanol. Then remove the spreader and pass it through a flame to burn off the alcohol.
14. Allow the bacteria to dry on the plates for 1 day. Plates that are to be used within 1 week can be stored at room temperature. Plates that will not be immediately used can be stored at 4 °C for 1–2 months.

2.3 S-Basal Buffer

1. In a 1-L beaker, mix 4.4 g anhydrous potassium phosphate (dibasic), 3.4 g anhydrous potassium phosphate (monobasic), and 5.85 g sodium chloride.
2. Add water to the beaker to fill to approximately 800 mL and stir until all salts are dissolved. The pH should be between 6 and 7.
3. Add water to bring to a final volume of 1 L.
4. Aliquot into 500-mL autoclavable glass bottles (300–400 mL per bottle).
5. Loosely cap bottles and autoclave for 30 min (liquid cycle). Let cool to room temperature prior to removing from the autoclave. Store cooled S-Basal at room temperature. At least one bottle should be stored at 4 °C, for use in sucrose flotation.

2.4 Sucrose Flotation and Exometabolome Collection

1. S-Basal (25 and 4 °C).
2. Polypropylene conical tubes, 15 and 50 mL (*see Note 4*).
3. Pasteur pipets.

4. Sucrose, 50 % w/v: In a 50-mL graduated polypropylene tube, weigh 25 g sucrose. Fill with water to the 40-mL line, and then vortex or sonicate until sucrose is completely dissolved. Fill to the 50-mL line with water, and then sterilize the solution by passing it through a 25-mm Nalgene syringe filter with a 0.2- μ m cellulose acetate membrane (Thermo). Store the sterilized solution at 4 °C.
5. Gelatin, 0.5 % w/v: Dissolve 50 mg gelatin in 10 mL water.
6. Glass petri dishes (custom-made from Kimax) (3-cm inner diameter), sterilized.
7. Polymer filter membranes, 0.2- μ m nylon-66 membrane (Life Science Products, Cat. No. 6502-413X; *see* **Note 5**).

2.5 Protein Quantification Components

1. Sodium dodecyl sulfate (SDS), 1.25 % w/v: Dissolve 2.5 g SDS in 200 mL water.
2. Pierce BCA protein assay kit (Thermo; *see* **Note 6**).

2.6 Standards

1. 3,4-Dimethoxybenzoic acid (Sigma-Aldrich). In a 15-mL conical polypropylene tube (Becton Dickinson), mix 18.2 mg 3,4-dimethoxybenzoic acid with 9 mL water and adjust the pH to 10 with 1 M NaOH, and then bring the final volume to 10 mL with water (10 mM final concentration). Protect the solution from light by wrapping the tube with aluminum foil and store at room temperature.
2. Sodium phenylpyruvate monohydrate (Alfa Aesar): Dissolve 10.2 mg sodium phenylpyruvate monohydrate in 10 mL water (5 mM). Partition into 1 mL aliquots and store in 2-mL conical polypropylene tubes (Eppendorf, Cat. No. 022363352; *see* **Note 5**). Further partition 1 mL of solution into 100 μ L aliquots and store all aliquots at –80 °C. Each time a 100 μ L aliquot is used, it should be disposed of afterwards. One milliliter aliquots can be thawed once and partitioned into 100 μ L aliquots as needed.
3. L-Norvaline (Alfa Aesar): Dissolve 5.9 mg L-norvaline in 10 mL water (5 mM). Partition into 1 mL aliquots and store in 2-mL conical polypropylene tubes (Eppendorf, Cat. No. 022363352; *see* **Note 5**). Further partition 1 mL of solution into 100 μ L aliquots and store all aliquots at –80 °C. Each time a 100 μ L aliquot is used, it should be disposed of afterwards. One milliliter aliquots can be thawed once and partitioned into 100 μ L aliquots as needed.
4. 3-Methylvaleric acid (Sigma-Aldrich): In a 15-mL conical polypropylene tube (Becton Dickinson), mix 12.5 μ L 3-methylvaleric acid with 10 mL water (10 mM). Store at 4 °C.
5. Amino Acid Standard H (Thermo): 2.5 mM each (in 0.1 N HCl) ammonia, L-alanine, L-arginine, L-aspartic acid, L-glutamic acid, glycine, L-histidine, L-isoleucine, L-leucine, L-lysine

HCl, L-methionine, L-phenylalanine, L-proline, L-serine, L-threonine, L-tyrosine, L-valine; 1.25 mM L-cystine.

6. Group A standards: 100 μ L each (10 mM stocks, prepared in water at 25 °C unless otherwise noted) 3-methyl-2-oxopentanoic acid, L-malate, fumaric acid (made neutral with NaOH), lactate, DL-2-hydroxybutyrate, hypoxanthine (hot water), 400 μ L S-Basal. Separate into 100 μ L aliquots and store at -80°C .
7. Group B standards: 100 μ L each (10 mM stocks, prepared in water at 25 °C unless otherwise noted) 4-methyl-2-oxovalerate, succinate, pyruvate, xanthine (hot water), ethanolamine, 3-hydroxy-3-methylbutyrate, 400 μ L S-Basal. Separate into 100 μ L aliquots and store at -80°C .
8. Group C standards: 100 μ L each (10 mM stocks, prepared in water at 25 °C unless otherwise noted) 3-methyl-2-oxobutanoic acid, citrate, α -ketoglutarate, 2-oxobutyrate, citramalate, urea, 400 μ L S-Basal. Separate into 100 μ L aliquots and store at -80°C .
9. Volatiles standards: In 50 mL S-Basal, dissolve each of the following (1 mM each)—4.8 mg sodium propionate, 4.2 μ L methacrylic acid, 4.6 μ L butyric acid, 4.5 μ L isobutyric acid, 6.3 mg sodium 3-hydroxybutyrate, 5.4 mg lithium acetoacetate, 5.0 mg tiglic acid, 5.0 mg 3-methylcrotonic acid, 6.3 μ L hexanoic acid, 5.5 μ L valeric acid, 5.5 μ L isovaleric acid, 4.4 mg acetoin, 5.5 μ L 2-methylbutyric acid. Store at 4 °C.

2.7 Derivatization Reagents

1. Acetonitrile.
2. Diethyl ether (*see* **Note 7**).
3. Hydrochloric acid (1 M).
4. GC-MS autosampler vials (specific for MS instrument).
5. Conical glass inserts (Supelco, Cat. No. 24703).
6. Nitrogen gas (or other inert gas) cylinder with regulator.
7. Rubber tubing (should fit gas regulator).
8. Pasteur pipets.
9. Methoxylamine hydrochloride (Sigma-Aldrich). This should be prepared fresh prior to derivatizing each batch of samples by dissolving 20 mg in 1 mL of anhydrous pyridine (*see* **Note 8**). This volume will be sufficient to derivatize up to 25 samples. Store unused methoxylamine hydrochloride (dry powder) in a desiccator. Unused methoxylamine hydrochloride/pyridine solution should be properly disposed.
10. *N*-Methyl-*N*-(*tert*-butyldimethylsilyl)trifluoroacetamide + 1 % *tert*-butyldimethylchlorosilane (MTBSTFA + TBDMS, Thermo Scientific). This should be purchased as 1 mL aliquots in glass ampules. Discard opened ampules after use. Store unopened ampules at 4 °C.

2.8 Software

The following software will be used to analyze GC-MS spectral data. All programs listed here are free to download and use and are available at the URLs listed below. In the following section, we have chosen to present a highly supervised method for analysis, to aid the novice researcher with limited experience in manipulating the multidimensional data produced by GC-MS; however, it should be noted that alternate software programs are available which will largely automate this process (*MetaboliteDetector* [14], *MetaboAnalyst* [15]).

1. *Automated Mass Spectral Deconvolution and Identification System* (AMDIS)—<http://chemdata.nist.gov/mass-spc/amdis/downloads/>
2. *MSSearch*—<http://chemdata.nist.gov/mass-spc/ms-search/downloads/>
3. *MET-IDEA*—<http://bioinfo.noble.org/download/>
4. *LIB2NIST*—http://chemdata.nist.gov/mass-spc/ms-search/Library_conversion_tool.html
5. *Python* (optional)—<http://www.python.org/>

3 Methods

3.1 Exometabolome Collection

1. Synchronous populations of animals should be grown on 10-cm BNGM agar plates spotted with OP50 bacteria (*see Note 9*). Animals should be plated at a density of 10,000/10-cm plate (11,000 worms can be used for mutant strains of smaller adult size), to allow them to reach gravid adulthood without starving. We use 120,000 animals (approximately 0.3 g) for each analysis (60,000 minimum; *see Note 10*). The number of animals needed will depend on the sensitivity of the mass spectrometer used for the analysis. Plates should be stored in a 20 °C incubator until animals reach gravid adulthood.
2. Using S-Basal (10 mL per plate), wash animals off of BNGM agar plates. Wash plates five at a time, and combine the washes in a 50-mL conical polypropylene tube. Allow animals to settle by gravity, and then remove and discard the supernatant. Combine animals into a single 50-mL tube, and then wash five more times with 50 mL S-Basal. It will take approximately 5–6 min for the animals to settle with each wash. This method is preferable to centrifugation, since it selectively removes eggs and L1 larvae from the animal pool.
3. *This should be done concurrently with step 2:* Gelatin passivate two 15-mL conical polypropylene tubes (one should be pre-weighed) by adding 0.5 mL gelatin to each tube, bringing the total volume to 10 mL with distilled water, and capping and

inverting to coat the inside of the tube. This solution should also be used to passivate the inside of two glass Pasteur pipets. This procedure helps to prevent animals from sticking to the inside of glass and plasticware. Thoroughly wash tubes and pipets by rinsing five times with double distilled water.

4. *This should be done concurrently with step 2:* To the pre-weighed tube, aliquot 10 mL cold (4 °C) S-Basal. To the other tube, aliquot 7 mL 50 % sucrose. Keep both tubes on ice until ready to use.
5. Following the final wash, reduce the total volume in the tube to 3 mL. This is best done by aspirating the supernatant down to the 5-mL gradation line and then removing 2 mL with an automatic pipet.
6. Pour the cold sucrose into the 50-mL tube, and then transfer back into the gelatin-passivated tube. Immediately centrifuge at $2,400 \times g$ for 3 min at 4 °C. *The centrifuge should be prechilled prior to this step (see Note 11).* Use the cold S-Basal as a balance.
7. Using a gelatin-passivated Pasteur pipet, transfer the floating animals to the second passivated tube, containing cold S-Basal (*see Note 11*).
8. Pellet animals at 1,200 rpm (2 min, $280 \times g$) at 4 °C. *The centrifuge should be prechilled prior to this step (see Note 11).*
9. Remove and discard supernatant. Wash the pellet two more times by filling the tube with room temperature S-Basal and centrifuging.
10. Carefully remove the supernatant down to the worm pellet, and weigh the tube to determine the mass of the loosely packed animals.
11. Add S-Basal to bring the total volume to 1.4 mL (loosely packed worms have a density near 1 g/mL) and transfer to a 3-cm glass dish using the second gelatin-passivated Pasteur pipet. Place the dish (uncovered) in a loosely sealed container with moist paper towels to minimize sample loss through evaporation. Then place the entire assembly on an orbital shaker set at 100 rpm and agitate at room temperature for 18 h. This step is necessary to prevent the animals from going anoxic during the collection period. If available, the shaker can be placed in an incubator set at 20 °C for the 18-h period.
12. At the end of the incubation period, transfer the animals and supernatant to a 1.5-mL polypropylene microcentrifuge tube using a gelatin-passivated Pasteur pipet (*see step 3*). Centrifuge for 3 min at $2,000 \times g$, and filter the supernatant through a 0.2 μ m nylon syringe filter. Aliquot into 100 μ L portions into 1.5-mL polypropylene tubes (Eppendorf, Cat. No. 022363352; *see Note 5*), and store the worm pellet and the aliquotted supernatant at -80 °C.

3.2 Protein Extraction and Quantification

To control for variations in the number of animals per experiment, as well as for the fact that different genetic mutants will have different adult sizes, the intensity of metabolite GC peaks will be normalized to the total protein content of the animals contributing to the sample.

1. Thaw frozen worm pellets at room temperature. Add S-Basal to adjust the total volume of each tube to 1.0 mL and transfer to 15-mL conical polypropylene tubes.
2. Add 1.25 % SDS to bring the total volume in each tube to 5 mL. This will result in a final SDS concentration of 1.0 % w/v.
3. Puncture the lids of the polypropylene tubes with a hot needle. Place tubes in boiling water for 5 min. Allow tubes to cool briefly (30–60 s) and then mix by briefly vortexing (2 s). Return to boiling water for an additional 5 min, and then remove and allow to briefly cool before proceeding.
4. Place samples in a centrifuge, and centrifuge for 5 min at $2,400 \times g$, and then remove the supernatant, *carefully avoiding the loose cuticle pellet (see Note 12)*.
5. Quantify the total protein in each sample using a commercially available protein assay kit. The manufacturer's instructions on the assay kit should be followed. If samples are not to be used immediately for protein quantification, they can be stored at $-80\text{ }^{\circ}\text{C}$ (*see Note 13*).

3.3 Derivatization Procedure for Standard (Nonvolatile) Metabolites

Internal standards should be added to samples and samples dried overnight, *the night prior to derivatization and analysis by GC-MS*.

1. Thaw previously frozen aliquots (100 μL) of exometabolome samples to be analyzed on ice. In 1.5-mL polypropylene tubes (Eppendorf, Cat. No. 022363352; *see Note 5*), prepare each of the following. Blank, 100 μL S-Basal; full standards, 100 μL S-Basal, 10 μL group A standards, 10 μL group B standards, 10 μL group C standards, and 5 μL amino acid standards.
2. To each sample to be derivatized (including blank and standards samples), add 575 μL acetonitrile (*see Note 14*) and 10 μL each of 3,4-dimethoxybenzoate, phenylpyruvate, and norvaline.
3. Dry samples overnight in a vacuum centrifuge (no heat).
4. *The following morning*, add 40 μL methoxylamine HCl to each dried sample and top tubes with dry nitrogen gas. This is done by inserting a glass Pasteur pipet into a piece of rubber tubing connected to the gas tank regulator and using the tip of the pipet to blow nitrogen or inert gas into samples tubes for 5–10 s. Vortex samples briefly (2–5 s) and incubate for 90 min at $30\text{ }^{\circ}\text{C}$. Samples should be mixed by vortexing at least once during this period.

5. Add 60 μL MTBSTFA + TBDMS to each sample and top with dry nitrogen. Incubate for 1 h at 80 °C (*see Note 15*).
6. Pellet any insoluble material (mostly salt) by centrifugation, and transfer 50 μL to a glass insert inside a glass autosampler vial. Top with dry nitrogen and seal.

3.4 Derivatization Procedure for Volatile Metabolites

This procedure is for derivatization of the compartment of the exometabolome which contains highly volatile metabolites (e.g., short-chain fatty acids) that would be lost during the drying step of the standard derivatization procedure. All steps in this procedure should be performed *the same day as samples are to be analyzed by GC-MS*.

1. Thaw previously frozen aliquots (100 μL) of exometabolome samples on ice. In 1.5-mL polypropylene tubes (Eppendorf, Cat. No. 022363352; *see Note 5*), prepare each of the following. Blank, 100 μL S-Basal; full standards, 100 μL S-Basal and 10 μL volatiles standards.
2. To each sample, add 20 μL 1 M HCl; the pH should be between 1 and 2.
3. Extract metabolites by adding 300 μL diethyl ether to each sample and vortexing for 30 min at room temperature.
4. Centrifuge samples at $800 \times g$ for 5 min to separate phases. Remove and save the upper organic layer.
5. Using a gentle stream of nitrogen, concentrate the organic phase to approximately 50 μL .
6. Add 40 μL methoxylamine HCl to each sample and top tubes with dry nitrogen gas. Vortex samples and incubate for 90 min at 30 °C. Samples should be mixed by vortexing at least once during this period.
7. Add 30 μL MTBSTFA + TBDMS to each sample and top with dry nitrogen. Incubate for 30 min at 80 °C (*see Note 15*).
8. Transfer 50 μL of each sample to glass inserts inside glass autosampler vials. Top with dry nitrogen and seal. Keep samples cool until analysis.

3.5 GC-MS and Analysis of Mass Spectral Data

We highly recommend that novice GC-MS users send their samples to a mass spectrometry facility for analysis. Many institutions will have an on-site facility equipped for GC-MS; however, if samples must be shipped off-site for analysis, we have found that overnight shipping on dry ice results in insubstantial loss of sample integrity.

We analyze our samples using a Thermo Fisher TRACE DSQ single quadrupole mass spectrometer. The following parameters will allow a competent technician to reproduce the analysis. GC: column, ZB-5MS (Phenomenex; Torrance CA), 30 m \times 0.25 mm, 0.25- μm film thickness; carrier gas, helium; linear velocity, 1 mL/min (constant flow); injection, split, 10-mL/min split flow; injector

temperature, 220 °C; column temperature program (standard metabolites), initial temperature of 70 °C held for 1 min followed by an increase to 310 °C at 5 °C/min; column temperature program (volatile metabolites), initial temperature of 50 °C held for 1 min, followed by an increase to 80 °C at 10 °C/min. Hold for 3 min at 80 °C and then increase to 275 °C at a rate of 30 °C/min. MS conditions: ionization, electron impact (70 eV); detection, positive ion; full scan analyses, m/z 50— m/z 700 at 2 scans/s.

Analysis of GC-MS data consists of (1) peak deconvolution, (2) peak integration, (3) preprocessing the dataset (e.g., removing artifactual peaks and low-abundance features), (4) metabolite identification, and (5) data visualization and clustering. Here we will present a basic flow-through for processing raw GC-MS data. Due to the limited space available, we will only cover the basic functions needed to process the data; however, many of the software programs that are employed have functionalities beyond what is described here. We have provided a comprehensive software tutorial as a supplementary online file to address some of these functions. This tutorial is presented in a format that would be understandable by a new graduate student entering a lab and who has no prior experience in MS. Before proceeding, make sure all of the software programs listed in Subheading 2.8 are installed on your computer. Detailed installation instructions for these programs can be found in the supplementary tutorial file. The following section assumes a basic familiarity with GC-MS terminology; those researchers with no prior experience with GC-MS are advised to skip this section and go straight to the online tutorial.

1. The format of the raw GC-MS data files will depend on the instrument manufacturer. For example, data acquired on Thermo instruments will be in the format “.RAW.” These will need to be converted into a universal format before continuing. For our purposes, we will require data to be in the “.CDF” format. The proprietary software that comes with your instrument should be able to convert its MS data into this format. If you do not have access to this software, you can request that the MS facility provide you with data in “.CDF” format.
2. The software program *AMDIS* will be used to identify peaks and to deconvolute peaks that partially co-elute. Using this program, open one of your data files, or, alternatively, use one of the example files provided with the tutorial.
3. Select the “Settings” tab under the “Analyze” menu—note that this will be inaccessible unless a file is open. A complete discussion of the settings which can be optimized is given in the supplementary software tutorial. Make sure that the correct instrument type is selected under the “Instrument” tab. When you are finished, click save and then press the button that says “Run.”

Table 1
Example of a partial ion retention time list

287.1	27.85	100066	False	False
250.1	27.92	100144	True	True
299.15	27.95	100067	False	False
198.16	28.69	100070	False	False
345.19	28.83	100072	False	False
303.14	29.13	100074	False	False
171.1	29.28	100075	False	False
272.11	30.85	100077	False	False
357.09	30.93	100174	False	False
332.42	31	100170	False	False
218.05	31.1	100078	False	False
292.12	31.1	100079	False	False
239.02	31.28	100080	True	True
288.17	31.44	100081	False	False
271.17	31.91	100165	False	False

4. *AMDIS* will attempt to identify unique peaks in the GC trace. Once one of these peaks is selected, the center panel will display the *total ion count* peak, as well as several representative masses which best describe the shape of that peak. Write down the retention time of each peak, and the mass which best describes it. Try to avoid using masses 73, 75, and 147—these are due to rearrangement of the derivatizing group and are common to many peaks.
5. In order to integrate the peaks in your GC trace, you will need to create an ion retention time (IRT) list. Using standard spreadsheet software, such as *Microsoft Excel*, create a new spreadsheet. The first two columns should contain the masses (column 1) and retention times (column 2) of each of the peaks you identified using *AMDIS*. The third column will contain a unique ID which you assign to each peak. The last two columns will indicate whether a particular metabolite is to be used as a calibration standard for mass (column 4) or retention time (column 5). Identify your three internal standards and enter values of “TRUE” in both of these columns. For all other metabolites enter “FALSE” in both columns (*see Note 16*). An example of what this file should look like is given in Table 1. Save the file as a tab-delimited text file with the extension “.ION” and exit *Excel*. Close *AMDIS*; you do not need to

save the “.FIN” and “.ELU” files that this program will automatically create.

6. Following identification and deconvolution in *AMDIS*, you will open your data in *MET-IDEA*. All of your data (including runs for your blank and standards) should be in the same folder as the IRT list which you just created.
7. Once opening *MET-IDEA*, you can adjust the settings by selecting “Parameter Setup” under the “Tools” menu (see the supplementary tutorial file for a description of these settings). After adjusting the settings, select “Start” under the “MET-IDEA” menu.
8. Browse to find your IRT list (you will need to change the file extension type to make this file visible). Select the boxes for “Show intermediate results,” “Calibrate Retention Time,” and “Calibrate Mass Data,” and then press “OK.”
9. After prompting you to save your calibration data, the program will integrate the peaks in your IRT list for each of the spectra in the folder, and read out an integrated peak area in arbitrary units. Check the integration limits on each of these peaks and adjust them accordingly (see **Note 17**). The amount of time this takes will depend on how well you optimized your parameters. A description of common integration errors is found in the software tutorial.
10. After you have checked your peaks, transpose your data, then select “OK,” and save your results. *Met-IDEA* will save these as an “.OUT” file, which can be opened as a delimited text file in *Excel*. This will contain a list of peaks with their integrated values for each dataset.
11. Before visualizing your data, you will need to do some preprocessing on the “.OUT” file. First, you should identify an appropriate noise cutoff for your data. A good way to do this is to integrate several areas of data which do not contain any well-defined peaks. Select integration limits appropriate to the average peak width on your instrument (typically around 0.1 min). For our instrument, we have determined that an integrated intensity of less than 10,000 is likely noise. Any peak which has an integrated intensity less than your experimentally determined threshold in all samples can be considered noise, and these rows removed from the data file. Also, any peaks which are due to artifacts (including phosphate) should be removed at this point.
12. Normalize your data by dividing every peak in a sample by the intensity of 3,4-dimethoxybenzoate and by the total amount of protein (experimentally determined, in mg) for that sample and then multiplying by 100,000,000 to return the data to its original scale. This can be done either in *Excel* or by running

a script using the programming language *Python*, as described in the online tutorial file. After doing this, remove the lines corresponding to your exogenously added internal standards. You may also remove the data columns for your blank and standards samples.

13. Reformat the first column to remove the retention time and mass for each component. Where possible, replace the ID numbers with appropriate names. Identities of compounds can be determined through library matching with *MSSearch* or *AMDIS* if an appropriate mass spectral library is available. Most available MS libraries are in “.MSP” format; if using *AMDIS* for library matching, you will need to use the program *LIB2NIST* to convert your library to the correct format for this software. The MS library used in our laboratory is included in the online supplemental files. Identities can also be confirmed by running standards. More information on MS libraries and the types of fragmentation patterns produced by *t*-BDMS derivatized compounds can be found in the supplementary tutorial file.
14. We use the online program *GenePattern* for visualization and clustering of data. This software is free to use after registration. To use this program, your data must be reformatted to “.GCT” format. This can be done manually in *Excel*; details on this file format can be found at: http://www.broadinstitute.org/cancer/software/genepattern/tutorial/gp_fileformats.html. Alternatively, one can use a *Python* script to reformat the data, as detailed in the online tutorial. Go to <http://www.broadinstitute.org/cancer/software/genepattern/> and select “GP @ Broad” to run an analysis on the server at the Broad Institute.
15. Select “Clustering,” then “Hierarchical clustering” in the pop-up window that appears. Under “Step 2” select “Open HierarchicalClustering.”
16. Select the location of your “.GCT” file, and then set “column distance measure” and “row distance measure” both to “Pearson correlation.” For “clustering method” select “Pairwise complete-linkage.” Do not change any other settings. Click “Run.”
17. When the analysis is complete, three files will be generated. Access the drop-down box to one of these files by clicking on the arrow that appears next to it. Select HierarchicalClusteringViewer. When the new dialogue comes up, select “Run.” A clustered heat map of your data will be generated. It is possible to toggle the display between a global array (across all cells) or a relative array (across rows). Export your data as an image file (Fig. 1).

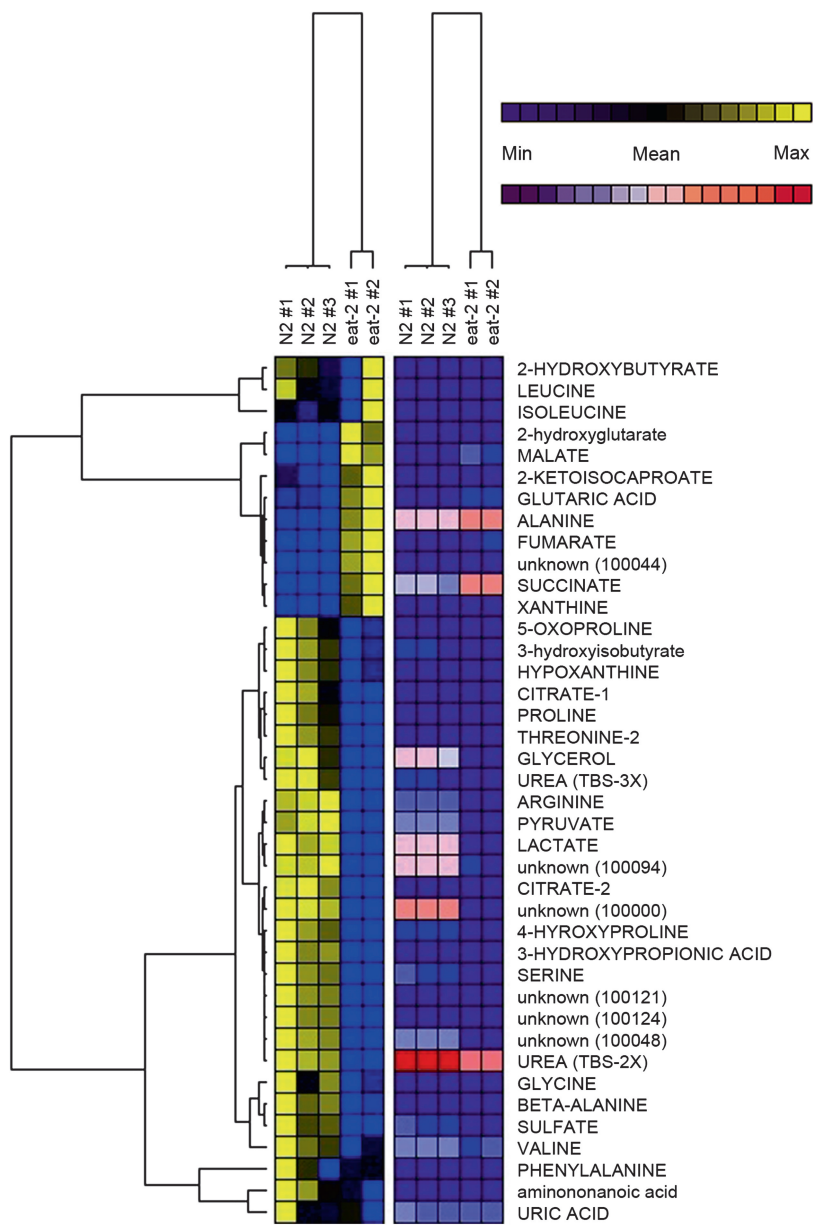


Fig. 1 Hierarchical clustering was used to segregate exometabolome samples from wild-type (N2) animals and *eat-2(ad465)* mutants. Integrated peak areas for each metabolite were normalized to an internal standard and to total protein. Low-abundance metabolites were removed prior to clustering. Heat maps are colored according to (1) individual metabolite variation across the sample set (*blue–yellow*) and (2) global variation among metabolites over the entire exometabolome dataset (*blue–red*)

4 Notes

1. When autoclaving liquids, caps should be loosely fitted to the glassware. Tightening the caps all the way can result in a buildup of pressure inside the bottle and in extreme instances bottle breakage. Solutions can become superheated in the autoclave and should be allowed to cool to room temperature prior to handling, to avoid sudden boiling.
2. To control for exogenous bacterial contamination, 5 mL of LB should be removed from the flask prior to inoculation and transferred to a 15-mL conical tube using sterile techniques. This tube should be taped to the side of the flask and the two incubated together overnight. If the control tube appears cloudy the next day, it indicates a contamination in the LB, and the entire batch should be discarded.
3. All components of the liquid dispenser which will come in contact with the agar solution (rubber tubing, nozzle) must be sterilized by autoclave prior to use. After dispensing all of the solution, the rubber hose should be immediately cleaned by pumping hot water through it. If this is not done, agar will solidify inside the tubing, clogging it and making it difficult to clean.
4. We have previously used 15-mL polystyrene tubes and found these to be susceptible to cracking during centrifugation. Therefore, it is recommended to use polypropylene only, since these are better able to stand high centrifugation speeds.
5. When using plasticware, it is important to be sure that no plasticizers leech out into solution. We have tested this particular brand and part number for leeching and found that it does not interfere with our analyses.
6. If an alternate protein assay is employed, it is critical that the investigator be sure that the reagents are compatible with concentrations of sodium dodecyl sulfate up to 1.25 % w/v.
7. Diethyl ether can potentially decompose over time, forming explosive peroxides. We recommend storing this reagent at 4 °C for up to a year. Expired reagent, or any bottle with white deposits around the cap, should be considered dangerous and disposed of properly.
8. Anhydrous pyridine is hygroscopic and care should be taken to prevent introduction of moisture. Water will interfere with the derivatization reactions.
9. In our experience, large populations of synchronous animals can be obtained by placing 10,000 animals (wild type, arrested L1 larval stage), on a 10 cm/OP50 plate and allowing them to starve out the plate. This will allow the animals enough food to

reach gravid adulthood and to lay eggs before starving. Once the eggs hatch, the larvae should not have enough food available to progress past the first larval stage and will arrest as L1s. Do not allow L1 larvae to remain starved beyond 24 h, otherwise they exit arrest at different rates when finally provided with food.

10. For triplicate experiments, we typically prepare 36 plates of worms and collect and pool adult worms prior to washing (Subheading 3.1, **step 2**). Following washing, we split the 360,000 animals into three separate populations for the 18-h metabolite collection step. For fully independent experiments, we recommend pouring three separate batches of 12 × 10-cm plates and using animals from three independent starting populations of L1 larvae.
11. The purpose of this step is to remove any remaining bacteria clinging to the cuticle of the animals. Exposure to high concentrations of sucrose places the animals under osmotic shock; therefore, these steps should be done as quickly as possible, and at 4 °C. In our hands, the sucrose float plus all subsequent washes should take no more than 15 min. While this is standard procedure in a *C. elegans* laboratory, it should be noted that we have not observed any significant differences in the exometabolome of wild-type animals treated with a sucrose flotation versus untreated animals [16].
12. It is important to aspirate over the cuticle carefully, since the cuticle does not dissolve in SDS, any remaining cuticle may adversely affect the protein analysis (unpublished observation). The GC-MS data generated later will be normalized to crude protein mass, so it is imperative to get an accurate reading.
13. After protein extraction, protein samples can be stored at –80 °C until analysis; however, we have experienced problems reproducing protein estimates when using frozen samples containing SDS. To circumvent this, we advise to reboil any frozen samples prior to analysis.
14. Acetonitrile precipitates enzymes and creates an azeotrope with water to aid in drying.
15. We have noticed that the Eppendorf polypropylene tubes have a tendency to pop open during incubation at 80 °C, possibly leading to contamination. To prevent this, we suggest resting a heating block or heat-resistant tube rack over the tubes to weigh down the lids. Alternatively, boiling locks may be used.
16. The exogenously added internal standards are easily identified, since they should be three of the largest peaks in your GC traces; they will also appear in the blank and standards samples. To aid you in identifying these peaks, the representative masses for each peak are 186.2 (norvaline), 250.1 (phenylpyruvate),

and 239.0 (3,4-dimethylbenzoate). Note that there will also be a large phosphate peak in all samples from the S-Basal buffer; do not confuse this as an internal standard. Phosphate has a representative mass of 383.2. It will be advantageous at this point to start a database which contains a list of ion masses and retention times, along with ID numbers and putative IDs.

17. Some peaks in your GC spectra will be artifacts arising from the derivatization procedure, as opposed to actual metabolites. These peaks can be identified by their presence in a blank sample, and should be noted accordingly as artifacts in your database for future reference. Rather than integrating these peaks, we opt to enter an integrated value of "0" to indicate that that peak was found but not integrated. To distinguish these peaks from actual metabolites, we enter a value of "1" for a metabolite with zero integrated intensity (i.e., the metabolite is not present in a given sample). Some peaks that appear to be artifacts may later turn out to be actual metabolites (e.g., if there is GC column bleed causing high-intensity metabolites to appear in the blank sample), so it is important to keep note of these peaks in case you wish to go back and integrate them later. We recommend, for the sake of time, removing peaks determined to be artifacts from your IRT list so that they are not integrated, but keeping track of them in a separate file. The set of full standards is for comparison and identification purposes, and peaks in this dataset do not need to be integrated properly, since they will not be part of the final analysis.

Acknowledgements

The authors gratefully acknowledge Kevin Hakala and Sue Weintraub of the Institutional Mass Spectrometry Laboratory of the University of Texas Health Science Center at San Antonio for their assistance in the development of GC-MS methods. Financial support was provided by the National Institute on Aging (to R.J.M. and S.L.R.) and the Ellison Medical Foundation (S.L.R.).

References

1. Falk MJ, Zhang Z, Rosenjack JR, Nissim I, Daikhin E, Sedensky MM, Yudkoff M, Morgan PG (2008) Metabolic pathway profiling of mitochondrial respiratory chain mutants in *C. elegans*. *Mol Genet Metab* 93:388–397. doi:10.1016/j.ymgme.2007.11.007
2. Rea SL, Graham BH, Nakamaru-Ogiso E, Kar A, Falk MJ (2010) Bacteria, yeast, worms, and flies: exploiting simple model organisms to investigate human mitochondrial diseases. *Dev Disabil Res Rev* 16:200–218
3. Fontana L, Partridge L, Longo VD (2010) Extending healthy life span from yeast to humans. *Science* 328:321–326. doi:10.1126/science.1172539
4. Yuan J, Horvitz HR (1990) The *Caenorhabditis elegans* genes *ced-3* and *ced-4* act cell

- autonomously to cause programmed cell death. *Dev Biol* 138(1):33–41. doi:10.1016/0012-1606(90)90174-h
5. Liu DW, Thomas JH (1994) Regulation of a periodic motor program in *C. elegans*. *J Neurosci* 14:1953–1962
 6. Gems D, Riddle DL (2000) Defining wild-type life span in *Caenorhabditis elegans*. *J Gerontol A Biol Sci Med Sci* 55(5):B215–B219
 7. Felkai S, Ewbank JJ, Lemieux J, Labbe JC, Brown GG, Hekimi S (1999) CLK-1 controls respiration, behavior and aging in the nematode *Caenorhabditis elegans*. *EMBO J* 18(7):1783–1792. doi:10.1093/emboj/18.7.1783
 8. Lakowski B, Hekimi S (1996) Determination of life-span in *Caenorhabditis elegans* by four Clock genes. *Science* 272(5264):1010–1013. doi:10.1126/science.272.5264.1010
 9. Feng J, Bussiere F, Hekimi S (2001) Mitochondrial electron transport is a key determinant of life span in *Caenorhabditis elegans*. *Dev Cell* 1(5):633–644. doi:10.1016/s1534-5807(01)00071-5
 10. Yang W, Hekimi S (2010) Two modes of mitochondrial dysfunction lead independently to lifespan extension in *Caenorhabditis elegans*. *Aging Cell* 9(3):433–447. doi:10.1111/j.1474-9726.2010.00571.x
 11. Iser WB, Wolkow CA (2007) DAF-2/insulin-like signaling in *C. elegans* modifies effects of dietary restriction and nutrient stress on aging, stress and growth. *PLoS One* 2(11). doi:10.1371/journal.pone.0001240
 12. Butler JA, Ventura N, Johnson TE, Rea SL (2010) Long-lived mitochondrial (Mit) mutants of *Caenorhabditis elegans* utilize a novel metabolism. *FASEB J* 24:4977–4988. doi:10.1096/fj.10-162941
 13. Lakowski B, Hekimi S (1998) The genetics of caloric restriction in *Caenorhabditis elegans*. *Proc Natl Acad Sci U S A* 95:13091–13096. doi:10.1073/pnas.95.22.13091
 14. Hiller K, Hangebrauk J, Jager C, Spura J, Schreiber K, Schomburg D (2009) MetaboliteDetector: comprehensive analysis tool for targeted and nontargeted GC/MS based metabolome analysis. *Anal Chem* 81(9):3429–3439. doi:10.1021/ac802689c
 15. Xia J, Psychogios N, Young N, Wishart DS (2009) MetaboAnalyst: a web server for metabolomic data analysis and interpretation. *Nucleic Acids Res* 37:W652–W660. doi:10.1093/nar/gkp356
 16. Butler JA, Mishur RJ, Bokov AF, Hakala KW, Weintraub ST, Rea SL (2012) Profiling the anaerobic response of *C. elegans* using GC-MS. *PLoS One* 7(9):e46140

Detecting Polymorphisms in Human Longevity Studies: HLA Typing and SNP Genotyping by Amplicon Sequencing

Gilberto Vargas-Alarcón and Carmina Flores-Domínguez

Abstract

Life expectancy has always been associated to several determinants, such as environmental and genetic factors. Studies have related human lifespan as being 25–32 % due to genetic polymorphisms between individuals associated to longevity and aging. Nonetheless, no single gene will convey a phenotype like longevity. Aging is a process that occurs from changes in various levels of the cell, from genes to functions. Longevity is the ability to cope and repair the damage that results from these changes. It has been described as the result of an optimal performance of immune system and as an overexpression of anti-inflammatory sequence variants of immune/inflammatory genes.

Longevity gene candidates can be separated into the following categories: inflammatory and immune-related, stress response elements, mediators of glucose and lipid metabolism, DNA repair components and cellular proliferation, and DNA haplogroups.

Studies have related lifespan with Common Single-Nucleotide Polymorphisms (SNPs); polygenic effects can explain an important part of how genetics influence it. In this chapter we describe how to sequence Class I HLA allele polymorphism, as well as SNP sequencing, two methodologies most frequently used in polymorphism detection.

Key words Polymorphism, Longevity, Lifespan, Aging, Immunogenetics, SNPs, HLA, Sequencing

1 Introduction

Science breakthroughs and improvement of public health have allowed us to have a greater life expectancy. There are an increasing number of centenarians, most importantly, in “good health state” according to their age. Longevity has been described as the result of an optimal performance of immune system and as an overexpression of anti-inflammatory sequence variants of immune/inflammatory genes [1]. Genetic polymorphisms have been associated to longevity and aging, nevertheless, no single gene will convey a phenotype like longevity.

Life expectancy has always been associated to several determinants, such as environmental and genetic factors. Studies have related human lifespan as being 25–32 % due to genetic

polymorphisms between individuals [2, 3] associated to longevity and aging [4]. Aging is a process that occurs from changes in various levels of the cell, from genes to functions, so longevity is the ability to cope and repair the damage that results from these changes [5].

Aging has been a major concern for human beings since the beginning of time. One of the most important breakthroughs for understanding aging was the discovery of the limited lifespan cultured cells have [6]. The main alterations cells suffer in aging are genomic instability, genetic programs, and/or reactive oxygen species [7]. The immune system has also been related to aging, due to chronic inflammatory activity [8], particularly prostaglandins, cytokines, chemokines, angiogenic factors and NF- κ B [9, 10], and the modulation of ubiquitin proteasome pathway [11].

Aging is related with immune deterioration, outcome of genetic information, and environmental factors [12]. From an immunogenetic approach, the association of HLA genes to inflammation and aging is being studied [13]. Survival and longevity could be associated with a selection of alleles that could confer resistance to infectious diseases [14]. Genes that encode inflammation and immune regulation, as well as stress proteins, all related to longevity and aging [15], are located on HLA [16–18]. Particularly, HLA I and II class gene polymorphisms have been associated, hence suggesting the effects of HLA on longevity, and therefore, aging [19, 20] (Table 1).

Longevity gene candidates can be separated into the following categories: inflammatory and immune-related, stress response elements, mediators or glucose and lipid metabolism, DNA repair components and cellular proliferation, and DNA haplogroups [3].

Lifespan has been reported as influenced by Common Single-Nucleotide Polymorphisms (SNPs) [31, 32]. Polygenic effects can explain an important part of how genetics influence lifespan [33]. For example, *TLR4* gene polymorphism has also been associated to aging [34].

Several studies have related polymorphisms to longevity, such as *APOE* [rs429358, rs2075650, and 4s7412 SNPs] [33, 35–37], *CETP*, *IL-6*, *HSPA14* [38], *TP53*, *NFKB1* [39], *FOXO3* [40, 41], *TERC*, and *TERT* [42]. Some of the gene polymorphisms associated with longevity can be consulted on Table 2.

- *APOE* polymorphism is involved in the maintenance of the vascular integrity, and it is decreased in elderly and centenarians [34–37, 42–45].
- *FOXO3A* polymorphism is involved in the control of cell homeostasis, and it is increased in elderly and centenarians [46–48].

Table 1
HLA allele associated with longevity (Modified from Naumova E. [13])

HLA allele	Population	Reference
A1B8Cw7DR3	Irish males	Rea [21]
A13	Italians	Ricci [22]
A9	Chinese	Ma [23]
A*0101-B*5101-	Bulgarians	Naumova [13]
A*0201-B*1081-	Bulgarians	Naumova [13]
B16	Greek	Papasteriades [24]
B7 Cw7	Italians	Ricci [22]
DQ1	Italians	Ricci [22]
DRB1*0101	Japanese	Akisaka [25]
DRB1*07	French men	Ivanova [26]
DRB1*1201	Japanese	Akisaka [25]
DRB1*1401	Japanese	Akisaka [25]
DRB1-1101	Bulgarians	Naumova [13]
DRB1*11	French women	Ivanova [26]
DRB1*11	French	Henon [27]
DRB1*11	Dutch women	Lagaay [28]
DRB1*11	Mexican mestizo women	Soto-Vega [29]
DRB1*13	French	Ivanova [26]
DRB1*15	Sardinians	Lio [30]
DRB1*1601	Bulgarians	Naumova [13]
DQA1*0101, *05	Japanese	Akisaka [25]
DQB1*0503	Japanese	Akisaka [25]

- *CAM K4*, *ATXN1*, and *DCAMKLI* are involved in the modulation of *CREB*, *CAMK4* is also involved in the modulation of *FOXO3A*, and they are also increased in elderly and centenarians [49].

There are other biomarkers related to aging; for instance, the length of leukocyte's telomere is considered a biomarker of human age; particularly SNP's polymorphism of *SIRT1* gene has effects on telomere length [58].

Aging and lifespan have been related to the presence or absence of morbidity; some gene polymorphisms have been associated to

Table 2
Gene polymorphisms associated with longevity

Gene polymorphism	Reference
<i>APOE</i>	Soerensen [42]
rs429358	Schachter [43]
rs20775650	Kervinen [44]
rs769449	Novelli [45]
	Ferrario [46]
<i>FOXO3A</i>	Ferrario [46]
	Wilcox [47]
	Flaschbart [48]
	Anselmi [49]
rs2802292	
rs9486902	
rs12206094	
rs2764264	
rs13217795	
rs7762395	
<i>CAM K4</i>	Ferrario [46]
rs10491334	Malovini [50]
<i>ATXN</i>	Ferrario [46]
rs697739	Malovini [50]
<i>DCAMKLI</i>	Ferrario [46]
Rs9315385	Malovini [50]
<i>CETP (Taq IB)</i>	Soerensen [42]
rs9923854	Wilcox [46]
	Pan [51]
	Kolovou [52]
<i>TOMM 40</i>	Sebastiani [53]
	Deelen [36]
rs2075650	
<i>ACE DD</i>	Zajc Petranović [54]
<i>TP53</i>	Mustafina [39]
rs1042522	

(continued)

Table 2
(continued)

Gene polymorphism	Reference
<i>NFKB1</i>	Mustafina [39]
rs4648110	
<i>IL-6-74 C/G</i>	Soerensen [42]
rs2069827	Bonafe [55]
	Rea [56]
<i>APOC1</i>	Nebel [31]
rs4420638	
<i>OTOL1</i>	Walter [66]
rs1425609	
<i>MINPPI</i>	Newman [67]
rs9664222	
<i>UCP2</i>	
rs6593669	Rose [68]
9p21.3	
rs1333049	Emanuele [69]

fragility syndrome that produces adverse health outcomes on the elderly, such as *MTR*, *CASP8*, *CREBBP*, *KAT2B*, and *BTRC* [59].

How Can Longevity Genes Be Detected?

Among the several techniques employed for identifying genetic polymorphisms, HLA alleles can be detected by automated sequencing. The PCR technique is employed first to amplify all the HLA allele genes using generic primers. These products are sequenced, and the results are compared to a sequence database that holds all known alleles in order to identify them.

SNPs are common associated allelic gene variants, with differences on the function of codified proteins. Because these polymorphisms could mean differences on the bioactivity of the coded protein, it is expected that the association of an allele with a phenotype may vary between populations [59]. Amplification of genomic DNA by the polymerase chain reaction (PCR) has greatly simplified the identification of SNPs by eliminating the need to clone and isolate regions of the genome from multiple individuals [60]. The advance in complex genome typing has urged the need of several computing programs that allows a better analysis of the results, such as PolyPhred which automatically detects the presence of

heterozygous single-nucleotide substitutions by fluorescence-based sequencing of PCR products. Its operations are integrated with the use of the Phred, Phrap, and Consed programs, and together these tools generate a high-throughput system for detecting DNA polymorphisms and mutations by large-scale fluorescence-based sequencing [61]. Some of the SNPs in longevity genes reported have been typified with the described technique [60] or by the TaqMan[®] assay (Applied Biosystems) [62].

2 Materials

2.1 DNA Extraction

1. 10–15 ml blood sample.
2. 15 % EDTA.
3. Cell lysis solution (Promega[®] Wizard Genomic DNA Purification Kit Cat #A1120).
4. Nuclei lysis solution (Promega[®] Wizard Genomic DNA Purification Kit Cat #A1120).
5. RNase.
6. Precipitation solution (Promega[®] Wizard Genomic DNA Purification Kit Cat #A1120).
7. Pure molecular grade isopropanol.
8. 70 % ethanol.
9. DNA rehydration solution (Promega[®] Wizard Genomic DNA Purification Kit Cat #A1120).

2.2 Class I HLA Sequencing

1. Premix Abbott Allele SEQR HLA Sequencing Kit[®].
2. Taq polymerase (Perkin-Elmer[®], Foster City, CA).
3. EXOSAP-IT Abbott Allele SEQR HLA Sequencing Kit[®].
4. MicroAmp optical 96-well plate from Applied Biosystems[®].
5. BigDye terminators (Applied Biosystems[®]).
6. MicroAmp optical adhesive film (Applied Biosystems[®]).
7. TBE.
8. Acetate.
9. Pure ethanol.
10. 80 % cold ethanol.
11. Formamide.
12. Genomics Assign 3.5[®] platform with an IMGT/HLA database.

2.3 PCR Gene Amplification, Sequencing, and SNP Identification [60]

1. Specific PCR primers to amplify a unique region of the genome.
2. 10× PCR buffer: 100 mM Tris-HCl, pH 8.3; 500 mM KCl, and 15 mM MgCl₂.
3. AmpliTaq DNA polymerase (Perkin-Elmer[®], Foster City, CA).
4. dNTPs (4 mM each).
5. Distilled H₂O.
6. Thermocycler.
7. PCR product presequencing kit, exonuclease I (10 U/μL), and shrimp alkaline phosphatase (SAP) (2 U/μL) (Amersham Life Sciences, Cleveland, OH).
8. BigDye terminator sequence ready-reaction kit (Perkin-Elmer[®]).
9. 30 % acrylamide stock: 37.5:1 acrylamide: *N,N'*-methylenebisacrylamide (Bio-Rad[®], Hercules, CA).
10. 377 DNA analyzer (Perkin-Elmer[®]).
11. 4 % denaturing polyacrylamide gel prepared and casted for sequence analysis by the 377 instrument directly according to the manufacturer's instructions (Perkin-Elmer[®]).
12. 95 % ethanol.
13. Loading buffer: 5:1 deionized formamide:50 mM EDTA, pH 8.0.
14. Sequence analysis tools, *see* Notes 2–5.

3 Methods

3.1 DNA Extraction [63]

1. Take a 10–15 ml peripheral blood sample from each individual on a 15 % EDTA sample tube.
2. Centrifuge at 3,000 rpm (1,008 RCF) for 5 min to obtain the white cells layer.
3. Follow the Promega[®] Wizard Genomic DNA Purification Kit Cat#A1120 instructions.
 - (a) Transfer 50 μl from the white cell layer to a 1.5 ml Eppendorf tube and add 150 μl of the lysis solution (Cell Lysis).
 - (b) Mix and lay still for 10 min at room temperature (*see* Note 1) and centrifuge at 3,000 rpm (1,008 RCF) for 10 min.
 - (c) Eliminate the supernatant and maintain the pellet. Wash until the pellet is completely white.
 - (d) Add 50 μl of nuclear lysis solution (Nuclei Lysis) and 1.5 μl of RNase, mix, and incubate at 38 °C for 15 min.

- (e) Precipitate proteins adding 16.5 µl of precipitation solution (Precipitation Solution), mix with the vortex for 20 s, and centrifuge at 2,000 rpm (448 RCF) for 10 min.
- (f) Transfer the supernatant to 1.5 ml Eppendorf tubes, and add 50 µl of pure molecular grade isopropanol at room temperature. Mix by inversion until DNA threads are present.
- (g) Centrifuge at 14,000 rpm (21,952 RCF) for 1 min and discard the supernatant.
- (h) Wash the DNA pellet with 50 µl of 70 % ethanol, centrifuge at 14,000 rpm (21,952 RCF) for 1 min, and discard the supernatant.
- (i) Let dry for 10–15 min and resuspend on 20 µl of rehydrating solution (DNA rehydration).
- (j) Place on water tub at 65°C for 1 h (*see Note 2*).

3.1.1 DNA Integrity Verification

1. Once DNA is extracted, DNA's integrity is verified on a 0.8 % agarose gel tinted dyed with ethidium bromide.
2. DNA quantification is made by spectrophotometry at 260 and 280 nm; ND-1000 (NanoDrop®) is used.
3. Use this formula to calculate its purity (*see Note 3*):

$$[\text{DNA}] = D = 260 \times F \times d$$

where OD260 is 260 nm optical density

F is a constant equal to 0.05 (50 µg of DNA = 1 DO at 260 nm)

d is the dilution factor

4. Store at –20 °C for optimal preservation and further use.

3.2 Class I HLA Sequencing [64]

1. Use Abbott Allele SEQR HLA Sequencing Kit®—Combined Protocol Core + HARP for Class I HLA amplification.
2. Place 20–120 ng/ml of DNA sample at 45 °C for 10 min.
3. Add 16 µl of premix Abbott Allele SEQR HLA Sequencing Kit® + 0.3 Taq polymerase to make the Master Mix.
4. Place the DNA-Master Mix on an Eppendorf tube on a 4 µl of DNA + 16 µ Master Mix.
5. Centrifuge at 500 rpm (28 RCF) for 10 min.
6. Place on the Gene Amp PCR System 9700 of Applied Biosystems® Thermocycler (*see Note 4*) for 4 h:
 - (a) One 95 °C for 10 min cycle.
 - (b) 36 cycles: 96 °C for 20 s, 60 °C for 30 s, 72 °C for 3 min.
 - (c) Let at 4 °C indefinitely

7. Verify the presence of amplification product on a 0.8 % agarose gel.
8. Amplification product is a 1,800 bp for Allele A and 1,200 and 1,500 bp band for Allele B.

3.2.1 PCR Product Purification

1. Add 3 μ l of EXOSAP-IT on each PCR product tube and centrifuge at 80 rpm (1 RCF) for 10 min.
2. Place on Gene Amp PCR System 9700 of Applied Biosystems[®] Thermocycler (*see Note 5*).
 - (a) One cycle at 37 °C for 15 min.
 - (b) 36 cycles at 96 °C for 20 s, 60 °C for 30 s, 72 °C for 3 min.
 - (c) Let at 4 °C indefinitely.

3.2.2 PCR for Allele A and B Sequencing

1. Use a MicroAmpOptical 96-well plate from Applied Biosystems[®] where exons 2, 3, and 4 of HLA B alleles are placed and marked with BigDye terminators (Applied Biosystems[®]), and cover it with MicroAmp optical adhesive film (Applied Biosystems[®]) (*see Note 6*).
2. Place the plate on an aluminum foil so that light does not affect the fluorochromes (*see Note 7*).
3. Place a relation of 1:1 amplified product with TBE.
4. Mix 1:8 μ l of Master Mix + 2 μ l of the sample and centrifuge at 500 rpm (28 RCF) for 10 min.
5. Place on a Gene Amp PCR System 9700 of Applied Biosystems[®] Thermocycler (*see Note 8*).
 - (a) 25 cycles at 96 °C for 20 s, 50 °C for 30 s, 60 °C for 2 min.
 - (b) Leave at 4 °C indefinitely.

3.2.3 Product Purification

1. Mix amplicon + 2 μ l of acetate and centrifuge at 500 rpm for 5 min.
2. Add 25 μ l of pure ethanol and agitate with the vortex.
3. Centrifuge at 200 rpm (4 RCF) for 30 s.
4. Eliminate the supernatant and centrifuge at 80 rpm (1 RCF) for 10 min.
5. Add 5 μ l of 80 % cold ethanol and centrifuge at 2,000 rpm (448 RCF) for 5 min.
6. Eliminate supernatant and centrifuge at 80 rpm for 10 min.
7. Add 15 μ l of formamide and centrifuge at 500 rpm for 10 min.
8. Place on a Gene Amp PCR System 9700 of Applied Biosystems[®] Thermocycler (*see Note 9*).
 - (a) One cycle at 96 °C for 2 min.
 - (b) Leave at 4 °C indefinitely.

3.2.4 Sequencing [65]

1. Take the samples on an ice tray and cover with aluminum foil.
2. Use an ABI 3100 Applied Biosystems[®] sequencer with the recommended manufacturer recommendations with the Abbott Allele SEQR HLA Sequencing Kit—Combined Protocol Core + HARP[®].
3. Program with a DT 3130POP6(BD).mob mobility with a RapidSeq36_POP-6 Default; injection parameters were 1.0 KV for 10 s and a sample pick of 1,800 s as instructed by the manufacturer.
4. Charge the plate with the following names: sample number, low hyphen, analyzed allele, low hyphen, and utilized primer (*see Note 10*).

Example:

For sample 425 to analyze HLA B Allele using primer 2R:

425_B_2R

3.2.5 Sequence Analysis

1. Use Genomics Assign 3.5[®] platform with an IMGT/HLA database for allele B.
2. Open electropherograms for each sample, and observe the alignment of exons 2,3, and 4, as well as the sequence quality.
3. Verify each nucleotide until NM equals 0 as a result.

3.3 SNP Identification

3.3.1 PCR Gene Amplification [60]

1. Amplify the genomic region in a mixture of 1× PCR buffer, 0.001 % gelatin, 0.40.4 mM dNTPs, 0.5 mM of each PCR primer, 0.5 U of AmpliTaq DNA polymerase, and 20 ng of DNA.
2. Combine 5 µL of the PCR product with 1 µL of 10 U/µL exonuclease and 1 µL of 2 U/µL SAP to inactivate unincorporated PCR primers and deoxynucleotide triphosphates.
3. Incubate at 37 °C for 30 min, followed by 90 °C for 15 min to inactivate exonuclease and SAP enzymes.

3.3.2 Sequencing [60]

1. Mix 3.2 µL of the enzyme-treated PCR product with 4 pmol of sequencing primer in 2.8 µL of dH₂O, 2 µL of 400 mM Tris–HCl, pH 9.0; 10 mM MgCl₂; and 2 µL of ready-reaction BigDye terminator mix (*see Note 11*).
2. Place at the Thermocycler at 95 °C for 5 min, 30 cycles of 95 °C for 30 s, 50 °C for 10 s, and 60 °C for 4 min.
3. Add 8 µL of deionized water and 32 µL of 95 % ethanol. Centrifuge at 1,639 rpm (3,000 RCF) for 45 min.
4. Remove ethanol and centrifuge at 792 rpm (700 RCF) for 1 min.
5. Resuspend in 3 µL of loading buffer.

6. Heat the samples for 2 min at 90 °C and electrophorese through a pre-run 4 % denaturing polyacrylamide gel using a 377 DNA analyzer (Perkin Elmer®).

3.3.3 SNP Identification [60]

1. Verify lane tracking and extract data and first-pass sequence analysis using the installed 377 software.
2. Transfer chromatogram files to a workstation and analyze again, now using the base-calling software Phred.
3. Assemble the sequences using Phrap.
4. Execute PolyPhred (*see Note 12*) to identify heterozygous single-nucleotide variants in fluorescence-based sequencing traces [61]. PolyPhred (*see Note 12*) reads normalized peak information obtained by Phred for each position in a sequence (*see Note 13*). It searches for reductions in peaks across the groups assembled by Phrap (*see Note 14*). If a peak drop and second base are detected, PolyPhred calls the site a potential polymorphic site and tags the position with their determined genotypes for viewing with the Consed program (*see Note 15*).
5. Analyze the assembled sequence reads, and mark polymorphic single-nucleotide variants by color-coded tags.

4 Notes

1. Mix by inverting every 5 min.
2. You can also leave it for the whole night at room temperature.
3. Purity criteria evaluated in this formula was $260/280 \text{ nm} \geq 1.6$.
4. PCR-HLA program.
5. EXO-HLA program.
6. It is important to cover the plate to protect it.
7. It is important to place it on ice.
8. SEQ-HLA program.
9. DESNAT program.
10. All wells must be filled because the sequenciator reads four wells simultaneously.
11. Use less of the BigDye terminator mix.
12. PolyPhred is program that compares fluorescence-based sequences across traces obtained from different individuals to identify heterozygous sites for single-nucleotide substitutions. It is composed by three programs: Phred, Phrap, and Consed. For information consult <http://droog.gs.washington.edu/polyphred/>.

13. Phred calls bases and assigns a quality value to each called base. For information consult <http://www.phrap.org/phredphrap-consed.html>.
14. Phrap is a program for assembling shotgun DNA sequence data. It allows use of the entire read and not just the trimmed high-quality part; it constructs the contig sequence as a mosaic of the highest-quality read segments rather than a consensus and provides extensive assembly information to assist in troubleshooting assembly problems. For information consult <http://www.phrap.org/phredphrapconsed.html>.
15. Consed is a tool for viewing, editing, and finishing sequence assemblies created with Phrap. For information consult <http://bozeman.mbt.washington.edu/consed/consed.html>.

References

1. Balistreri CR, Candore G, Accardi G et al (2012) Genetics of longevity. Data from the studies on Sicilian centenarians. *Immun Ageing* 9(1):8
2. Mari D (2011) Role of the IGF/Insulin system in longevity. *Minerva Endocrinol* 36 (3):181–185
3. Naumova E, Ivanova M, Pawelec G (2011) Immunogenetics of aging. *Int J Immunogenet* 38(5):378–381
4. Glotov OS, Baranov VS (2007) Genetic polymorphism and aging. *Adv Gerontol* 20 (2):35–55
5. Rattan SI (2006) Theories of biological aging: genes, proteins, and free radicals. *Free Radic Res* 40(12):1230–1238
6. Hayflick L, Morehead PS (1961) The serial cultivation of human diploid cell strains. *Exp Cell Res* 25:585–621
7. Tollesbol TO (2007) Techniques for analysis of biological aging. *Methods Mol Biol* 371:1–7
8. Bruunsgaard H (2001) Aging and proinflammatory cytokines. *Curr Opin Hematol* 8:131–136
9. Li Q, Whithoff S, Verma IM (2005) Inflammation-associated cancer: NF-kappaB is the lynchpin. *Trends Immunol* 26(6):318–325
10. Ahmad A, Banerjee S, Wang Z et al (2009) Aging and inflammation: etiological culprits of cancer. *Curr Aging Sci* 2(3):174–186
11. Ponnappan S, Ponnappan U (2011) Aging and the immune function: molecular mechanisms to interventions. *Antioxid Redox Signal* 14 (8):1551–1585
12. De Benedectis G (1996) Genes and longevity. *Aging Clin Exp Res* 8:367–369
13. Naumova E, Pawelec G, Ivanova M et al (2007) 14th international HLA and immunogenetics workshop: report on the immunogenetics of aging. *Tissue Antigens* 69(Suppl 1):304–310
14. Candore G, Balistreri C, Listi F et al (2006) Immunogenetics, gender and longevity. *Ann N Y Acad Sci* 1089:516–537
15. Yashin AI, Wu D, Arbeev KG et al (2012) How genes influence life span: the biodemography of human survival. *Rejuvenation Res* 15 (4):374–380
16. Matzinger P, Zamoyska R (1982) A beginner's guide to major histocompatibility complex function. *Nature* 297(5868):628
17. Rabian C (1982) Le complexe majeur d'histocompatibilité et les gènes de la réponse immune chez l'homme. *Arch Fr Pediatr* 39:483–485
18. Klein J, Sato A (2000) The HLA system. *N Engl J Med* 343:702–709
19. Caruso C et al (2000) HLA, aging, and longevity: a critical reappraisal. *Hum Immunol* 61:942–949
20. Caruso C et al (2001) Immunogenetics of longevity. Is major histocompatibility complex polymorphism relevant to the control of human longevity? A review of literature data. *Mech Ageing Dev* 122:445–462
21. Rea IM, Middleton D (1994) Is the phenotypic combination A1B8Cw7DR3 a marker for male longevity? *J Am Geriatr Soc* 42 (9):978–983
22. Ricci G, Colombo C, Ghiazza B et al (1998) Association between longevity and allelic forms of human leukocyte antigens (HLA): population study of aged Italian human subjects. *Arch Immunol Ther Exp (Warsz)* 46(1):31–34

23. Ma YX, Zhu Y, Wang ZS et al (1997) HLA and longevity or aging among Shanghai Chinese. *Mech Ageing Dev* 94(1–3):191–198
24. Papasteriades C, Boki K, Pappa H et al (1997) HLA phenotypes in healthy aged subjects. *Gerontology* 43(3):176–181
25. Akisaka M, Suzuki M (1998) Okinawa longevity study. Molecular genetic analysis of HLA genes in the very old. *Nihon Ronen Igakkai Zasshi* 35(4):294–298
26. Ivanova R, Henon N, Lepage V et al (1998) HLA-DR alleles display sex-dependent effects on survival and discriminate between individual and familial longevity. *Hum Mol Genet* 7(2):187–194
27. Henon N, Busson M, Dehay-Martuchou C et al (1999) Familial versus sporadic longevity and MHC markers. *J Biol Regul Homeost Agents* 13(1):27–31
28. Lagaay AM, D'Amato J, Ligthart GJ et al (1991) Longevity and heredity in humans. Association with the human leucocyte antigen phenotype. *Ann N Y Acad Sci* 621:78–89
29. Soto-Vega E, Richaud-Patin Y, Llorente L (2005) Human leukocyte antigen class I, class II, and tumor necrosis factor- α polymorphisms in a healthy elder Mexican Mestizo population. *Immun Ageing* 2:13
30. Lio D, Balistreri CR, Colonna-Romano G et al (2002) Association between the MHC class I gene HFE polymorphisms and longevity: a study in Sicilian population. *Genes Immun* 3(1):20–24
31. Nebel A, Kleindrop R, Caliebe A et al (2011) A genome-wide association study confirms APOE as the major gene influencing survival in long-lived individuals. *Mech Ageing Dev* 132(6–7):324–330
32. Lunetta KL, D'Agostino RB Sr, Karasik D et al (2007) Genetic correlates of longevity and selected age-related phenotypes: a genome-wide association study in the Framingham Study. *BMC Med Genet* 8(Suppl 1):S13
33. Yashin AI, Wu D, Arbeev KG et al (2012) Polygenic effects of common single-nucleotide polymorphisms on life span: when association meets causality. *Rejuvenation Res* 15(4):381–394
34. Balistreri CR, Colonna-Romano G, Lio D et al (2009) TLR4 polymorphisms and aging: implications for the pathophysiology of age-related diseases. *J Clin Immunol* 29(4):406–415
35. Napolioni V, Gianni P, Carpi FM et al (2011) APOE haplotypes are associated with human longevity in a Central Italy population: evidence for epistasis with HP 1/2 polymorphism. *Clin Chim Acta* 412(19–20):1821–1824
36. Deelen J, Beekman M, Uh HW et al (2011) Genome-wide association study identifies a single major locus contributing to survival into old age; the APOE locus revisited. *Aging Cell* 10(4):686–698
37. Feng J, Xiang L, Wang G et al (2011) Is APOE E3 a favourable factor for the longevity: an association study in Chinese population. *J Genet* 90(2):343–347
38. Soerensen M, Dato S, Tan Q et al (2012) Evidence from case-control and longitudinal studies supports associations of genetic variation of APOE, CETP, and IL6 with human longevity. *Age (Dordr)* 35(2):487–500
39. Mustafina OE, Nasibulin TR, Erdman VV et al (2011) Association analysis of polymorphic loci of TP53 and NFKB1 genes with human age and longevity. *Adv Gerontol* 24(3):397–404
40. Nair AK, Sugunan D, Kumar H et al (2012) Association analysis of common variants in FOXO3 with type 2 diabetes in a South Indian Dravidian population. *Gene* 491(2):182–186
41. Campa D, Hüsing A, Dostal L et al (2011) Genetic variability of the forkhead box O₃ and prostate cancer risk in the European prospective investigation on cancer. *Oncol Rep* 26(4):979–986
42. Soerensen M (2012) Genetic variation and human longevity. *Dan Med J* 59(5):B4454
43. Schachter F, Faure-Delanef L, Guenot F et al (1994) Genetic associations with human longevity at the APOE and ACE loci. *Nat Genet* 6:29–32
44. Kervinen K, Savolainen MJ, Salokannel J et al (1994) Apolipoprotein E and B polymorphisms—longevity factors assessed in nonagenarians. *Atherosclerosis* 105(1):89–95
45. Novelli V, Viviani Anselmi C et al (2008) Lack of replication of genetic associations with human longevity. *Biogerontology* 9(2):85–92
46. Ferrario A, Villa F, Malovini A et al (2012) The application of genetics approaches to the study of exceptional longevity in humans: potential and limitations. *Immun Ageing* 9(1):7
47. Willcox BJ, Donlon TA, He Q et al (2008) FOXO3A genotype is strongly associated with human longevity. *Proc Natl Acad Sci* 105:13987–13992
48. Flachsbarth F, Caliebe A, Kleindrop R et al (2009) Association of FOXO3A variation with human longevity confirmed in German centenarians. *Proc Natl Acad Sci USA* 106(8):2700–2705

49. Anselmi CV, Malovini A, Roncarati R et al (2009) Association of the FOXO3A locus with extreme longevity in a southern Italian centenarian study. *Rejuvenation Res* 12 (2):95–104
50. Malovini A, Illario M, Iaccarino G et al (2011) Association study on long-living individuals from Southern Italy identifies rs10491334 in the CAMKIV gene that regulates survival proteins. *Rejuvenation Res* 14:283–291
51. Pan SL, Wang F, Lu ZP et al (2012) Cholesteryl ester transfer protein TaqIB polymorphism and its association with serum lipid levels and longevity in Chinese Bama Zhuang population. *Lipids Health Dis* 11:26
52. Kolovou G, Stamatielou M, Anagnostopoulou K et al (2010) Cholesteryl ester transfer protein gene polymorphisms and longevity syndrome. *Open Cardiovasc Med J* 4:14–19
53. Sebastiani P, Solovieff N, Dewan AT et al (2012) Genetic signatures of exceptional longevity in humans. *PLoS One* 7(1):e29848
54. Zajc Petranović M, Skarić-Jurić T, Smolej Naranić N et al (2012) Angiotensin-converting enzyme deletion allele is beneficial for the longevity of Europeans. *Age (Dordr)* 34 (3):583–595
55. Bonafè M, Olivieri F, Cavallone L et al (2001) A gender-dependent genetic predisposition to produce high levels of IL-6 is detrimental for longevity. *Eur J Immunol* 31(8):2357–2361
56. Rea IM, Ross OA, Armstrong M et al (2003) Interleukin-6-gene C/G 174 polymorphism in nonagenarian and octogenarian subjects in the BELFAST study. Reciprocal effects on IL-6, soluble IL-6 receptor and for IL-10 in serum and monocyte supernatants. *Mech Ageing Dev* 124(4):555–561
57. Kim S, Bi X, Czarny-Ratajczak M et al (2012) Telomere maintenance genes SIRT1 and XRCC6 impact age-related decline in telomere length but only SIRT1 is associated with human longevity. *Biogerontology* 13 (2):119–131
58. Ho YY, Matteini AM, Beamer B et al (2011) Exploring biologically relevant pathways in fragility. *J Gerontol A Biol Sci Med Sci* 66 (9):975–979
59. Syvänen AC (2001) Accessing genetic variation: genotyping single nucleotide polymorphisms. *Nat Rev Genet* 2(12):930–942
60. Nickerson DA, Kolter N, Taylor SL et al (2001) Sequence-based detection of single nucleotide polymorphisms. In: Starkey MP, Elavarapu R (eds) *Methods in molecular biology*, vol. 175: genomics protocols. Humana Press, Totowa, NJ
61. Nickerson DA, Tobe VO, Taylor SL (1997) PolyPhred: automating the detection and genotyping of single nucleotide substitutions using fluorescence-based resequencing. *Nucleic Acids Res* 25(14):2745–2751
62. Holland PM, Abramson RD, Watson R et al (1991) Detection of specific polymerase chain reaction product by utilizing the 50–30 exonuclease activity of *Thermus aquaticus* DNA polymerase. *Proc Natl Acad Sci USA* 88 (16):7276–7280
63. Promega® Wizard Genomic DNA Purification Kit Cat #A1120 Technical Manual. Consulted on: <http://www.promega.com/~media/files/resources/protocols/technical%20manuals/0/wizard%20genomic%20dna%20purification%20kit%20protocol.pdf?la=en>
64. Allele SEQR HLA Sequencing Kit Combined Protocol Core + HARP (2012) Applied Biosystems® Technical Manual
65. Nagy M, Entz P, Otremba P et al (2007) Haplotype-specific extraction: a universal method to resolve ambiguous genotypes and detect new alleles-demonstrated on HLA-B. *Tissue Antigens* 69(2):176–180
66. Walter S, Atzmon G, Demerath EW et al (2011) A genome-wide association study of aging. *Neurobiol Aging* 32(11):2109e15–2109e28
67. Newman AB, Walter S, Lunetta KL et al (2010) A meta-analysis of four genome-wide association studies of survival to age 90 years or older: the Cohorts for Heart and Aging Research in Genomic Epidemiology Consortium. *J Gerontol A Biol Sci Med Sci* 65 (5):478–487
68. Rose G, Crocco P, De Rango F, Montesanto A, Passarino G (2011) Further support to the uncoupling-to-survive theory: the genetic variation of human UCP genes is associated with longevity. *PLoS One* 6(12):e29650
69. Emanuele E, Fontana JM, Minoretto P, Geroldi D (2010) Preliminary evidence of a genetic association between chromosome 9p21.3 and human longevity. *Rejuvenation Res* 13 (1):23–26

Gel Electrophoresis-Based Proteomics of Senescent Tissues

Steven Carberry and Kay Ohlendieck

Abstract

Cellular aging is a fundamental biological process, and mass spectrometry-based proteomics has been widely used for the global identification of age-related changes in a variety of tissues. The proteomic profiling of senescent skeletal muscles has revealed a variety of alterations in proteins associated with the contractile apparatus, cell signaling, ion homeostasis, metabolism, and the cellular stress response. Here, we outline the two-dimensional gel electrophoretic separation and fluorescent labeling of the urea-soluble protein complement from aged diaphragm muscle. This chapter describes the various experimental steps involved in gel electrophoresis-based proteomics, including protein extraction, isoelectric focusing, slab gel electrophoresis, fluorescence labeling, image analysis, protein digestion, mass spectrometric identification of proteins and immunoblotting.

Key words Aging, Mass spectrometry, Proteomics, Ruthenium tris-bathophenanthroline disulfonate, Sarcopenia, Two-dimensional gel electrophoresis

1 Introduction

Aging is a highly complex and fundamental biological process. Systems biological approaches have been initiated to better understand the multiple causal mechanisms and the pathophysiological hierarchy in degenerative pathways that are involved in cellular senescence [1–3]. In order to determine global changes and adaptations in the protein complement of aged tissues, mass spectrometry-based proteomics represents an ideal large-scale and high-throughput methodology and has been widely employed in the field of biogerontology [4–7]. One of the most striking changes in aging mammals is the loss of skeletal muscle mass and function. In humans, the age-related loss in skeletal muscle mass is usually accompanied by a drastic decline in contractile strength and has been termed sarcopenia of old age [8]. The progressive deterioration of neuromuscular integrity increases the risk of poor balance, frequent falling, and impaired mobility in the elderly [9]. Epidemiological studies of sarcopenia indicate that nearly half the population over 75 years of age suffers from some form of debilitating

muscle degeneration, which may lead in progressive cases to loss of independence [10]. The scale of this common geriatric condition warrants large-scale studies for the identification of novel biomarkers of sarcopenia. The establishment of a comprehensive signature of aging markers is crucial for developing improved diagnostic tests to properly evaluate and classify sarcopenia and the frailty syndrome, as well as for identifying new therapeutic targets to treat age-related motor neuron and skeletal muscle degeneration.

Over the last few years, mass spectrometry-based proteomics has been employed to study normal and diseased skeletal muscles [11–13], including the aging neuromuscular system [14–16]. Most mature skeletal muscles contain a mixture of three main fiber types, i.e. slow oxidative type I fibers, fast oxidative-glycolytic type IIa fibers and fast glycolytic type IIb/IIx fibers, plus a variety of hybrid fibers [17]. Proteomics has been instrumental in the establishment of fast-to-slow muscle fiber type transitions during aging [15], indicating a glycolytic-to-oxidative shift of muscle metabolism in a slower-contracting population of senescent fibers [18–20]. In addition to major alterations in metabolic pathways and the isoform expression pattern of contractile elements, the gel electrophoresis-based proteomic analysis of muscle aging has established a variety of changes in proteins associated with cell signaling, ion homeostasis, and the cellular stress response [14]. Physiological, biochemical, and structural studies have shown that aging of the diaphragm is associated with (a) an increased susceptibility to muscular atrophy, (b) morphological alterations affecting especially the neuromuscular junction region, (c) a slowing in time-to-peak tension, (d) a decrease in the rate of muscle relaxation and (e) a significant depression in the ability to generate maximal isometric tension [21–24]. These changes in the senescent diaphragm suggest that this type of skeletal muscle is an interesting model system for studying proteome-wide changes during aging. We have therefore used here aged mouse diaphragm muscle to describe in detail a widely employed gel electrophoresis-based approach for the analysis of urea-soluble skeletal muscle proteins.

The successful application of two-dimensional gel electrophoresis in combination with advanced mass spectrometry emphasizes the analytical power of the proteomic approach to determine global changes during tissue aging. The flowchart in Fig. 1 summarizes the various steps involved in gel electrophoresis-based proteomics. High-resolution two-dimensional gel electrophoresis, using isoelectric focusing in the first-dimension and slab gel electrophoresis in the second dimension [25], presents an unbiased analytical tool to investigate complex changes in the protein complement of specific tissues [26]. Two-dimensional gel electrophoresis with immobilized pH gradients is one of the most frequently employed protein separation techniques in comparative proteomics [27–29]. Protein detection in gel electrophoresis is often carried

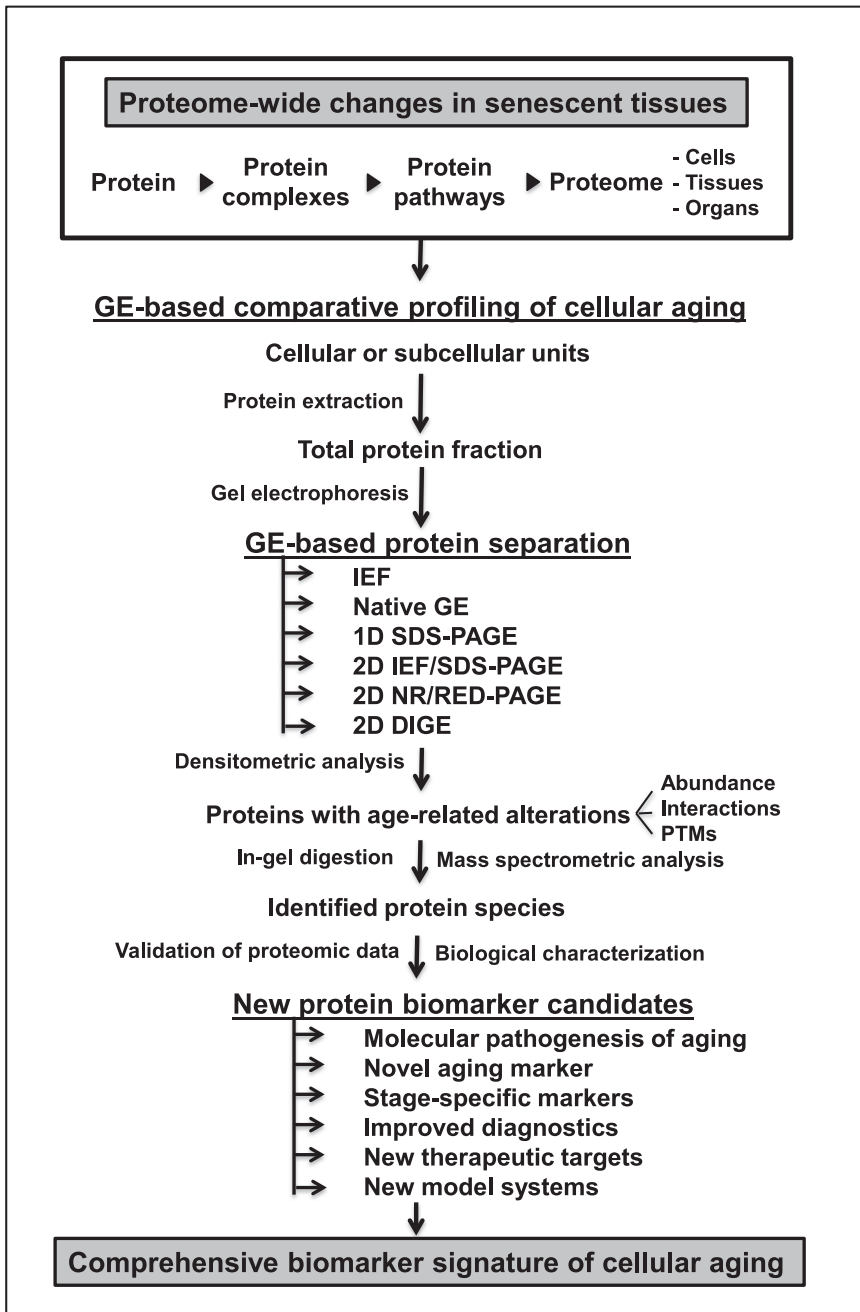


Fig. 1 Overview of gel electrophoresis-based proteomic analysis of aged tissues. Shown is a flow chart summarizing the various steps involved in the proteomic analysis of senescent tissue samples, including protein extraction, various gel electrophoretic methods (*GE* gel electrophoresis, *SDS-PAGE* sodium dodecyl sulfate polyacrylamide gel electrophoresis, *IEF* isoelectric focusing, *NR/RED* non-reducing/reducing, *DIGE* difference in-gel electrophoresis, *PTMs* post-translational modifications), densitometric scanning, mass spectrometric identification of changed proteins and independent verification of proteomic data

out with highly sensitive fluorescent dyes [30]. Besides CyDyes used in fluorescence pre-labeling for difference in-gel electrophoresis [31, 32], a commonly employed fluorescent dye for post-electrophoretic staining is ruthenium tris-bathophenanthroline disulfonate (RuBPs) [33–35]. The advantages of RuBPs lie in its dynamic labeling range, its reliability for the highly reproducible staining of gel electrophoretically separated proteins and the relative ease and low cost associated with its synthesis [33, 35]. This is why RuBPs has been the fluorescent dye of choice in numerous proteomic studies [29], including the field of skeletal muscle proteomics [36–39]. Analytical conditions for protein identification have to be optimized with specific mass spectrometers. Several excellent articles have been published in the *Methods in Molecular Biology* series on the comprehensive description of methodological particulars of modern mass spectrometry [40–43]. Here, we describe in detail the application of gel electrophoresis-based proteomics for studying senescent diaphragm muscle specimens.

2 Materials

2.1 Equipment

Equipment for gel electrophoresis, protein labeling, gel imaging, mass spectrometry and immunoblotting was from the following suppliers:

1. IPG (immobilized pH gradient) DryStrip reswelling tray (Amersham/GE Healthcare).
2. IPGphor IEF unit (Amersham/GE Healthcare).
3. Sample loading cups (Amersham/GE Healthcare).
4. Manifold (Amersham/GE Healthcare).
5. Gel casting box (Amersham/GE Healthcare).
6. Cassette racks (Amersham/GE Healthcare).
7. Ettan DALT*twelve* multiple vertical slab gel electrophoresis apparatus (Amersham/GE Healthcare).
8. Glass plates suitable for fluorescent gel electrophoretic analysis (Amersham/GE Healthcare).
9. Typhoon Trio variable mode imager (Amersham/GE Healthcare).
10. ImageScanner UMax (Amersham/GE Healthcare).
11. Vortex Genie-2 (Scientific Industries).
12. Stuart SSL4 shaker (Lennox Laboratory Supplies).
13. Heto speedvac concentrator (Medical Supply Company).
14. Model 5417R centrifuge (Eppendorf).
15. Agilent 6340 Ion Trap LC mass spectrometer using electrospray ionization (Agilent Technologies).

16. Nanoflow Agilent 1200 series system, equipped with a Zorbax 300SB C18 μ m, 4 mm 40 nl pre-column was employed for the separation of peptides (Agilent Technologies).
17. Mini-gel PROTEAN Tetra Cell system (Bio-Rad).
18. Transblot Cell for electrophoretic transfer of proteins to Immobilon NC-pure nitrocellulose membranes (Bio-Rad).
19. Exposure cassettes (Kodak).

2.2 Reagent Solutions

In order to keep contaminations of protein samples to a minimum, all reagent solutions should be prepared with ultrapure water. Reagent solutions for gel electrophoresis, protein labeling, mass spectrometry and immunoblotting were from the following suppliers:

1. Ruthenium batho-phenanthrolinedisulfonate chelate (RuBPs) (Reagecon Diagnostic Ltd).
2. Ultrapure Protogel acrylamide stock solution (National Diagnostics).
3. Immobilized pH gradient (IPG) strips (Amersham/GE Healthcare).
4. IPG buffer (Amersham/GE Healthcare).
5. Iodoacetamide (Amersham/GE Healthcare).
6. Dithiothreitol (Sigma).
7. Destreak agent (Amersham/GE Healthcare).
8. Laemmli-type buffer system (Bio-Rad).
9. Coomassie Brilliant Blue G250 dye (Bio-Rad).
10. Protein molecular mass markers (Bio-Rad).
11. Sequencing grade-modified trypsin (Promega).
12. Formic acid (Fluka).
13. LC-MS Chromasolv water (Fluka).
14. Nitrocellulose (Pierce).
15. X-ray film (Fisher).
16. Chemiluminescence substrate (Roche).
17. Developer (Sigma).
18. Fixer (Sigma).
19. Protease inhibitors (Roche).
20. Primary antibody to collagen (Abcam).
21. Secondary peroxidase-conjugated antibody (Chemicon International).
22. All other chemicals used were of analytical grade and purchased from Sigma.

2.2.1 Preparation of Crude Tissue Extracts

1. Lysis buffer: 7 M urea, 2 M thiourea, 4 % (w/v) CHAPS, 2 % (w/v) IPG buffer pH 3–10, 2 % (w/v) dithiothreitol. Stock solutions of lysis buffer can be dispensed into 1 ml aliquots and conveniently stored in a freezer at -20°C .
2. Lysis buffer should always be supplemented with protease inhibitors in order to prevent excess proteolytic degradation of proteins. Suitable protease inhibitor cocktails are commercially available (*see Note 1*).

2.2.2 Rehydration of Immobilized pH Gradient Strips

1. Rehydration buffer: Add 12 μl of Destreak reagent and 0.002 % (w/v) Bromophenol Blue to 1 ml of lysis buffer (*see Note 2*).

2.2.3 Second Dimension Gel Electrophoresis

1. Equilibrium buffer: 8 M urea, 30 % (v/v) glycerol, 2 % (w/v) sodium dodecyl sulfate, 50 mM Tris-HCl pH 8.8, 0.002 % (w/v) Bromophenol Blue (*see Note 3*). Aliquots of this solution can be stored at -20°C .
2. Reducing buffer: Add 100 mg dithiothreitol per 10 ml of equilibrium buffer. Make this solution freshly prior to use in gel electrophoresis.
3. Alkylating buffer: Add 250 mg iodoacetamide per 10 ml of equilibrium buffer. Prepare solutions in the dark and immediately before usage in gel electrophoresis.
4. $10\times$ SDS buffer: 25 mM Tris, 192 mM glycine, 0.1 % (w/v) sodium dodecyl sulfate. Store this solution at room temperature.
5. Agarose sealing solution: 1 % (w/v) agarose in $1\times$ SDS buffer and Bromophenol Blue. Heat solution until agarose has properly dissolved. Store the solution at room temperature (*see Note 4*).

2.2.4 Protein Visualization Using Fluorescent Ruthenium Tris-Bathophenanthroline Disulfonate Dye (RuBPs)

1. RuBPs dye (*see Subheading 3.5 for detailed description of ruthenium tris-bathophenanthroline disulfonate synthesis*).
2. Fixation solution: 30 % (v/v) ethanol and 10 % (v/v) acetic acid.
3. Wash solution: 20 % (v/v) ethanol.
4. Destain solution: 40 % (v/v) ethanol and 10 % (v/v) acetic acid.

2.2.5 Protein Visualization Using Coomassie Brilliant Blue

1. Buffer A: 10 % (w/v) ammonium sulfate, 2 % (v/v) phosphoric acid.
2. Buffer B: 5 % (w/v) Coomassie Brilliant Blue G-250 in water.
3. Coomassie staining solution: 2 ml Buffer B plus 80 ml Buffer A and 20 ml methanol.
4. Neutralization buffer: 0.1 M Tris-HCl at pH 6.5.
5. Wash buffer: 25 % (v/v) methanol.
6. Fixation buffer: 20 % (w/v) ammonium sulfate.

2.2.6 In-Gel Digestion of Protein Spots for Mass Spectrometric Identification

1. Trypsin resuspension buffer: 50 mM acetic acid.
2. Trypsination buffer: 20 µg of sequencing grade-modified trypsin in 100 µl resuspension buffer (*see Note 5*). For in-gel digestion, dissolve 10 µl aliquots into 500 µl of 50 mM ammonium bicarbonate.
3. In-gel destaining buffer: 1:1 (v/v) 100 mM ammonium bicarbonate/acetonitrile.
4. Extraction buffer: 1:2 (v/v) formic acid/acetonitrile. Make this solution freshly and use it immediately for peptide extraction.

2.2.7 Electrophoretic Transfer and Immunoblot Analysis

1. Electrophoretic transfer buffer: 25 mM Tris, 192 mM glycine, pH 8.3, 20 % (v/v) methanol.
2. Ponceau staining solution: 0.5 % (w/v) Ponceau S dye in 1 % (v/v) acetic acid (*see Note 6*).
3. Phosphate-buffered saline solution: 0.9 % (w/v) NaCl, 50 mM monobasic sodium phosphate, pH 7.4 (*see Note 7*).
4. Blocking solution: 5 % (w/v) fat-free milk powder in phosphate-buffered saline.
5. Primary antibody solution: 1:5,000 diluted primary antibody in blocking solution (*see Note 8*).
6. Secondary antibody solution: 1:1,000 diluted secondary peroxidase-conjugated antibody in blocking solution (*see Note 9*).

3 Methods

For the highly reproducible separation of urea-soluble proteins, two-dimensional gel electrophoresis presents an ideal method. Since fluorescent staining techniques in combination with mass spectrometric identification approaches are very sensitive, cross-contamination of analytical samples, and keratin-based impurities have to be kept to a minimum. Thus, researchers involved in proteomic studies are advised to wear protective clothing and gloves during all preparative steps. Ideally, gel electrophoretic and analytical solutions should be prepared and stored in laboratory facilities with at least semi-clean analytical status. Electrophoretic separation steps should be carried out under designated fume hoods or in special rooms that lack excess air passage. For proteomic profiling analyses, mass spectrometry should be performed in a separate proteomics facility that is ideally air-conditioned and kept free from potential contaminants. Depending on the protein range of interest, different pH ranges in the first-dimension and concentration gradients in the second dimension slab gel can be combined for optimum two-dimensional gel electrophoretic separation. The total amount

of protein loaded on gels has to be chosen according to the main goal of individual studies. Large amounts of protein can result in excess streaking and cross-contamination of two-dimensional spots, while low concentrations of protein samples may be ineffective for proper labeling of individual protein species. The analysis described here is a previously optimized method for studying skeletal muscle aging using first-dimension isoelectric focusing with pH 3–10 strips and second dimension 12.5 % slab gel electrophoresis with 500 μ g protein per gel.

3.1 Preparation of Crude Skeletal Muscle Extracts

1. Weigh skeletal muscle tissue from differently aged mice. Diaphragm muscle shows a range of age-related changes, including a drastic increase in the extracellular matrix component collagen [38]. Thus, as an illustrative example of a proteomic investigation of senescent tissues, the below outlined protocol focuses on this particular type of skeletal muscle.
2. For the initial break-up of tough contractile fibers and associated cellular structures, transfer freshly dissected muscle specimens of differing age to suitable containers with liquid nitrogen and grind tissue to a fine powder with mortar and pestle (*see Note 10*).
3. Diaphragm muscle powder should be added to lysis buffer at a ratio of 1:10 (w/v).
4. Carefully vortex the solution. The suspension should be incubated on a rocker for 1 h at room temperature, with gentle vortexing every 10 min for 30 s.
5. Centrifuge the solution at $20,000 \times g$ for 20 min at 4 °C. The protein-containing middle layer should be saved. Discard the pellet and uppermost fatty layer.
6. Protein quantification of skeletal muscle extracts should be carried out with a reliable assay kit (*see Note 11*).
7. If samples have to be stored at this stage of the analysis, dispense protein extracts into aliquots of 50 μ l and place them in a freezer at –80 °C.

3.2 In-Gel Rehydration of First- Dimension Gel Strips

1. Add 500 μ g of protein sample to rehydration buffer and bring the solution up to 450 μ l. Pipette this solution into the reservoir slots of the Ettan IPGphor DryStrip reswelling tray.
2. Remove plastic backing from 24 cm-long IPG strips of pH 3–10 by peeling from the (–) end and push the (+) end towards the top of strip holder.
3. Place strips gel side down into rehydration buffer and rehydrate for at least 12 h.

3.3 First-Dimension Isoelectric Focusing

1. Transfer isoelectric focusing strips to manifold gel side up on the Ettan Multiphor II (GE Healthcare). Lift by the (–) end, and place the (+) end of strips towards the (+) end marked on the IPGphor.
2. Cover strips with cover fluid by addition of 108 ml of drystrip cover fluid over entire manifold.
3. Place wicks, wet with deionized water, onto ends of strips.
4. Position the electrodes. Isoelectric focusing is carried out at 20 °C as follows: 4 h at 80 V, 2 h at 100 V, 1.5 h at 500 V, 1.5 h at 1,000 V, 1 h at 2,000 V, 1 h at 4,000 V, 2 h at 6,000 V and a final 2.5 h step at 8,000 V.
5. After completion of the first-dimensional gel separation, IEF strips can be stored at –20 °C.

3.4 Second Dimension Slab Gel Electrophoresis

1. Incubate isoelectric focusing strips in 10 ml dithiothreitol-containing equilibrium buffer while rocking for 15 min.
2. Remove reducing solution and incubate while rocking in 10 ml iodoacetamide-containing equilibrium buffer for 15 min.
3. Remove alkylating solution, wash strips briefly in 1× SDS running buffer and then place isoelectric focusing strips (+) end to left, gel side facing out, onto a 12.5 % resolving slab gel (*see Note 12*).
4. Strips should be pressed against gel when adding warmed overlay sealing solution so as to eliminate air bubbles.
5. Place gels in the Ettan DALT^{twelve} tank and carry out electrophoresis at 0.5 W/gel for 1 h, followed by 1.5 W/gel overnight until Bromophenol Blue dye front runs off.
6. Following slab gel electrophoresis, carefully remove gels from glass plates and mark one corner of two-dimensional gel to track orientation. Strips should remain with slab gels as each contains a unique identification number to allow tracking of samples.

3.5 Preparation of 20 mM RuBPs Dye Stock Solution for Gel Staining

1. Potassium pentachloro aquo ruthenate (0.2 g) is dissolved in 20 ml boiling water and kept under reflux. This process results in a deep red-brown solution.
2. Bathophenanthroline disulfonate (0.9 g) is added to the solution and refluxing continued for 20 min, resulting in a deep green-brown solution.
3. 5 ml of 0.5 M sodium ascorbate is added and refluxing continued for 20 min. This process results in a deep orange-brown solution.
4. RuBPs dye stock solution is then allowed to cool and adjusted to pH 7.0 with sodium hydroxide. Total volume is adjusted to 26 ml dye stock solution (*see Note 13*).

3.6 Protein Visualization Using Fluorescent RuBPs Staining

1. To produce RuBPs staining solution, add 50 μ l RuBPs dye stock solution to 200 ml of 20 % (v/v) ethanol. For this mass spectrometry-compatible method, approximately 200 ml of diluted RuBPs solution is needed per slab gel and staining step.
2. Place gels in clean trays and add fixative solution for a minimum of 30 min. Gently agitate gels during the fixation step. If necessary, gels can be left overnight in fixing solution.
3. Rinse gels three times for 30 min in wash solution with gentle agitation.
4. Stain gels with RuBPs staining solution for 6 h.
5. Rinse gels with deionized water twice for 10 min with gentle agitation.
6. Destaining of gels should be carried out for 16 h.
7. Rinse gels with deionized water twice for 10 min with gentle agitation prior to scanning.

3.7 Image Analysis of Two-Dimensional Protein Spot Pattern in RuBPs-Labeled Gels

1. Scan RuBPs-labeled gels using a suitable variable mode imager, such as the Amersham/GE Healthcare Typhoon Trio apparatus.
2. For image acquisition, scan RuBPs-stained muscle proteins at a wavelength of $\lambda = 532$ nm. Photomultiplier tube PMT-values should be optimized so that the volume of the most abundant protein spot is between 80,000 and 99,000 when scanned at a resolution of 100 μ m (*see Note 14*).
3. Sample images of differently aged muscle proteomes are then evaluated using two-dimensional gel analysis software, such as Progenesis SameSpots analysis software (NonLinear Dynamics, Newcastle upon Tyne, UK; software version 3.2.3), and are normalized against their biological replicates.
4. Two-dimensional gels are aligned to the reference image. *See Fig. 2* for a representative RuBPs-labeled master gel.
5. Following detection of two-dimensional spots, gels are placed into groups (young muscle versus aged muscle images) and analyzed to determine significant changes in the abundance of distinct protein spots.
6. For proteomic profiling, paired Student's *t*-test values are calculated for each protein spot across all two-dimensional gels. An ANOVA score of 0.5 is required for spots to be included in the subsequent detailed evaluation of changes in protein expression patterns. Then principal component analysis (PCA) is verified; changes displaying power of <0.8 are removed from subsequent analysis. All remaining changed protein spots that exhibit a fold change of 1.5 or greater and meet the significance criteria should be visually checked on the aligned gels to ensure feasibility.

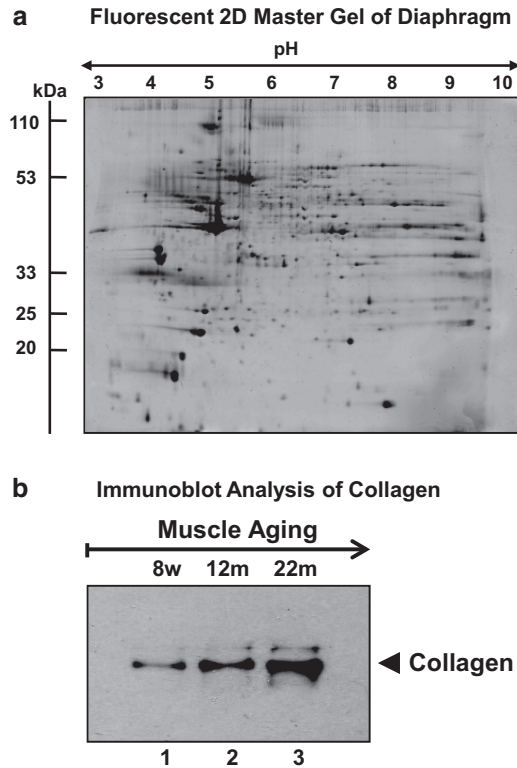


Fig. 2 Gel electrophoretic and immunoblot analysis of aged diaphragm muscle. Shown is a fluorescent RuBPs-labeled master gel of the total urea-soluble protein complement from mouse diaphragm muscle (**a**). The pH values of the first-dimension gel system and molecular mass standards of the second dimension are indicated on the *top* and on the *left* of the panels, respectively. Panel (**b**) illustrates an example of independent verification of proteomic data. The representative immunoblot shows expanded views of protein bands labeled with an antibody to the extracellular matrix protein collagen. *Lanes 1–3* represent 8 week-, 12 month- and 22 month-old mouse diaphragm muscle, respectively. Collagen levels are clearly increased during skeletal muscle aging

3.8 Coomassie Brilliant Blue Staining, Scanning, and Protein Excision from Pick Gels

1. Following gel electrophoretic separation, slab gels are washed in distilled water.
2. Slab gels are carefully transferred to a clean dish containing Coomassie Brilliant Blue staining solution and incubated for 6 h or overnight with gentle agitation.
3. Gels are transferred into neutralization buffer for 3 min.
4. Gels are then incubated in wash buffer for 1 min.
5. Following washing, slab gels are transferred to fixation buffer (*see Note 15*).

6. Coomassie Brilliant Blue-stained preparative slab gels are scanned using a suitable instrument, such as the ImageScanner UMax (Amersham/GE Healthcare). Gel images are then added to the Progenesis software programme to serve as a pick gel and aligned to RuBPs-labeled gel images.
7. Proteins of interest can be picked manually from two-dimensional gels. Protein spots can be conveniently removed and transferred with the help of sterile pipette tips with their ends cut off. Place the tip over the individual protein spot, press firmly down through the gel, take the plug up into the tip and aspirate it into a fresh plastic tube.

3.9 In-Gel Digestion of Protein for Mass Spectrometric Identification

1. Destain gel plugs in 100 mM ammonium bicarbonate/acetonitrile (1:1) until completely destained.
2. Shrink gel plugs with acetonitrile and remove all liquid (*see Note 16*).
3. Add 50 μ l of trypsin buffer and incubate gel plugs for 30 min at 4 °C.
4. Add more buffer to fully cover gel plugs and incubate proteins for a further 90 min at 4 °C (*see Note 17*).
5. Incubate for 4 h or overnight at 37 °C.
6. Add 100 μ l of extraction buffer and incubate proteins for 15 min at 37 °C with shaking.
7. Using gel-loading tips, transfer all supernatant fractions into individual 0.2 ml plastic tubes.
8. Dry down peptides in a standard speedvac concentrator (*see Note 18*).

3.10 Electrospray Ionization-Mass Spectrometric Analysis

1. Reconstitute peptides in 12 μ l of 0.1 % formic acid.
2. Samples should then be briefly vortexed, sonicated for 5 min and briefly centrifuged.
3. To remove any gel particles, centrifuge samples for 20 min in cellulose spin filter tubes at 14,000 $\times g$.
4. Using fresh tips for each sample, pipette samples to individually labeled LC-MS vials.
5. To identify muscle-associated proteins of interest, analyze peptide mixtures on an ion trap LC mass spectrometer by injecting 5 μ l of sample.
6. Although conditions have to be optimized with specific mass spectrometers, using a 10-min gradient of 5–100 % acetonitrile/0.1 % formic acid and a post run of 1 min through a Zorbax 300SB C18 μ m column gives reliable results with muscle proteins.

7. Separation of peptides can for example be achieved with a nanoflow Agilent 1200 series system, equipped with a Zorbax 300SB C18 5 μm , 4 mm 40 nl pre-column and a Zorbax 300SB C18 5 μm , 43 mm \times 75 μm analytical reversed phase column using HPLC-Chip technology.
8. Mobile phases should be (A), 0.1 % formic acid, and (B), 90 % acetonitrile and 0.1 % formic acid. Load samples into the enrichment at a capillary flow rate set to 4 $\mu\text{l}/\text{min}$ with a mix of A and B at a ratio 19:1.
9. Elute tryptic peptides with a linear gradient of 5–70 % solvent B over 6 min, 70–100 % for 1 min and 100 % for 1 min with a constant nano pump flow of 0.6 $\mu\text{l}/\text{min}$. A 1-min post-time of Solvent A should be used to remove sample carryover.
10. Set the capillary voltage to 2,000 V. The flow rate and the temperature of the drying gas should be 4 l/min and 300 $^{\circ}\text{C}$, respectively.
11. In order to identify distinct protein species, utilize database search engines such as Mascot MS/MS Ion search from Matrix Science (London, UK; NCBI database, release 20100212).

3.11 Immunoblot Analysis for Verification of Proteomic Data

1. Run one-dimensional gradient gels using a suitable mini-gel system. Please refer to the manufacturer's instructions for a detailed description of the assembly of individual slab gel apparatuses. To separate proteins with a wide range of molecular masses, 3–10 % resolving gels can be conveniently poured with the help of a gradient maker. For most routine immunoblotting experiments, loading of 10 μg protein per gel lane is sufficient to detect most antigens of interest. Samples should be electrophoresed at a constant voltage of 50 V until the Bromophenol Blue dye front runs off.
2. Prepare the transblot system by cutting nitrocellulose membranes and filter papers to the same or slightly bigger size as the gels to be transferred.
3. For construction of a gel sandwich for wet transfer, assemble the transblot holders in a tray with transfer buffer (*see Note 19*).
4. Soak several filter papers in transfer buffer and layer them on top of an electrophoretic sponge on the anode side in transfer holders without introducing any air bubbles.
5. A sheet of nitrocellulose membrane is carefully floated on transfer buffer until evenly wet and is then submerged on top of the layer of filter papers.
6. Carefully remove the analytical slab gel from its glass plate, rinse it briefly in transfer buffer and place it on top of the nitrocellulose membrane.

7. Soak several sheets of filter paper in transfer buffer and place them on top of the gel.
8. The cathode side of the transfer holder is placed on the assembly and transferred to the electrophoretic transfer unit.
9. Electrophoretic transfer is carried out at 4 °C for 70 min at 100 V.
10. Transfer efficiency is evaluated by staining nitrocellulose sheets in Ponceau solution for 1 min. Sheets are rinsed in distilled water to remove excess pink protein dye.
11. Ponceau staining is removed by soaking nitrocellulose sheets in phosphate-buffered saline for three times, each time for 10 min.
12. Prior to immuno decoration, nitrocellulose membranes are blocked in a milk protein solution for 1 h and then incubated for 3 h or overnight with gentle agitation with primary antibody solution at room temperature.
13. Blots are washed twice with blocking solution for 10 min.
14. Washed blots are incubated for 1 h with secondary peroxidase-conjugated antibody solution at room temperature.
15. Following two washing steps with blocking solution for 10 min and then two rinsing steps with phosphate-buffered saline, antibody-decorated bands are visualized by the enhanced chemiluminescence (ECL) method (*see* **Note 20**).
16. If a commercial ECL kit is used for visualization of immuno-decorated protein bands by enhanced chemiluminescence, all necessary solutions are provided (*see* **Note 21**).
17. Prepare a suitable darkroom for carrying out the chemiluminescence reaction and subsequent development of X-ray film.
18. For nitrocellulose replicas of mini-gels, incubate washed blots for 1 min with sufficient ECL solution, consisting of 50 µl ECL starting solution and 5 ml luminescence substrate for 1 min.
19. Remove blots from substrate solution and transfer between acetate plastic sheets, making sure to remove all air bubbles.
20. In the dark, place X-ray film on top of the blot in its plastic membrane protection in an exposure cassette and incubate this assembly for 1–3 min (**Note 22**).
21. Finally, use commercially available developer and fixer to generate an image of immuno-decorated protein bands.
22. In the case developer concentrate from Sigma is used, dilute 50 ml developer with 200 ml of water.
23. Develop X-ray films until bands are clearly visible.
24. In the case fixer concentrate from Sigma is used, dilute 50 ml fixer with 200 ml of water.

25. Transfer developed X-ray films into fixer solution, followed by washing and drying of films.
26. Dried films with developed bands are now ready for densitometric analysis (**Note 23**).

4 Notes

1. To avoid excess proteolytic degradation of sensitive muscle proteins during the preparation of crude tissue extracts, the usage of one tablet of “Complete Mini” from Roche per 10 ml of buffer can serve as a suitable protease inhibitor cocktail.
2. If the tracking dye interferes with fluorescent signals, omit the usage of Bromophenol Blue in RuBPs-labeled gels.
3. The equilibrium buffer is a stock solution. Dithiothreitol or iodoacetamide must be added prior to use.
4. Agarose sealing solution should be melted prior to use.
5. Aliquot trypsin buffer into 10 μ l portions and store at -20°C for up to 2 weeks.
6. Ready to use Ponceau solution for determining transfer efficiency is commercially available from various companies.
7. Phosphate-buffered saline solution can be prepared from individual chemicals or be conveniently made from commercially available buffer tablets.
8. Suitable dilution rates for preparing primary antibody solutions have to be determined by trial and error. Dilutions between 1:100 and 1:10,000 are routinely used for immunoblotting experiments, depending heavily on antigen concentration, antigen conformation, and antibody specificity.
9. Suitable dilution rates for preparing secondary peroxidase-conjugated antibody solutions have to be determined by trial and error. Dilutions between 1:500 and 1:5,000 are routinely used for immunoblotting experiments, depending mostly on the concentration of the antigen-bound primary antibody and specificity of the secondary antibody for the primary target antibody.
10. Liquid nitrogen is an extremely dangerous material and its potential to cause severe cold burns, pressure-related explosions, or asphyxiation is greatly underestimated. Thus, when handling liquid nitrogen, protective clothing that is inert to capturing liquid spills should be worn. In addition, thick cold-insulated gloves and safety goggles or a sturdy face shield should be used when handling liquid nitrogen.

11. Several protein quantitation kits are commercially available that are especially designed for the accurate determination of protein concentration in samples to be analyzed by high-resolution two-dimensional gel electrophoresis. In our experience, a suitable protein quantification assay system for studying muscle proteins is the 2-D Quant Kit from Amersham/GE Healthcare.
12. It is crucial to ensure no bubbles remain trapped under the IEF strip when laying down first-dimension strips. In order to reduce air bubbles forming between isoelectric focusing strip and slab gel, SDS running buffer can be conveniently used to slide the first-dimension strip smoothly onto second dimension gels.
13. Fluorescent RuBPs dye stock solution can be stored at 4 °C for several months.
14. The initial PMT value should range between 500 and 600. Optimized PMT values guarantee that no two-dimensional protein spot will be saturated on the gel, therefore allowing accurate and quantifiable proteomic analysis.
15. For Coomassie Brilliant Blue G-250 dye labeling, individual staining, neutralization, washing and fixation steps can be repeated several times until gels are sufficiently stained for proper recognition of individual two-dimensional protein spots of interest.
16. Protein samples are now ready for in-gel digestion. Alternatively, they can be stored at −20 °C.
17. Incubating at 4 °C allows the slow and efficient diffusion of trypsin into gel plugs.
18. If necessary, dried-down peptide extracts can be stored at −20 °C.
19. Transfer buffer should ideally be stored and used at 4 °C.
20. Enhanced chemiluminescence can be carried out with commercially available kits and is highly suitable for detecting immunodecorated protein bands.
21. In our laboratory, we routinely use BM Chemiluminescence Blotting Substrate (POD) from Roche, developer and fixer from Sigma, and X-ray film from Fisher, but many other companies supply these essential materials and chemicals for ECL-based detection methods.
22. Suitable length of exposure of X-ray film with ECL-treated immunoblot depends heavily on the intensity of the antibody-decorated protein band and has to be determined by trial and error. In the case of weak immuno-labeling, X-ray exposure may need to be carried out for longer periods of time, such as several hours or overnight.

23. Routine densitometric analyses of developed X-ray films can be performed with a suitable scanner, such as a Molecular Dynamics computing densitometer and Imagequant analysis software.

References

1. Soltow QA, Jones DP, Promislow DE (2010) A network perspective on metabolism and aging. *Integr Comp Biol* 50:844–854
2. Cevenini E, Bellavista E, Tieri P, Castellani G, Lescai F, Francesconi M, Mishto M, Santoro A, Valensin S, Salvioli S, Capri M, Zaikin A, Monti D, de Magalhães JP, Franceschi C (2010) Systems biology and longevity: an emerging approach to identify innovative anti-aging targets and strategies. *Curr Pharm Des* 16:802–813
3. Kirkwood TB (2011) Systems biology of ageing and longevity. *Philos Trans R Soc Lond B Biol Sci* 366:64–70
4. Sharov VS, Schöneich C (2007) Proteomic approach to aging research. *Expert Rev Proteomics* 4:309–321
5. Schiffer E, Mischak H, Zimmerli LU (2009) Proteomics in gerontology: current applications and future aspects—a mini-review. *Gerontology* 55:123–137
6. Siwy J, Vlahou A, Zimmerli LU, Züribig P, Schiffer E (2011) Clinical proteomics: current techniques and potential applications in the elderly. *Maturitas* 68:233–244
7. Silvestri E, Lombardi A, de Lange P, Glinni D, Senese R, Cioffi F, Lanni A, Goglia F, Moreno M (2011) Studies of complex biological systems with applications to molecular medicine: the need to integrate transcriptomic and proteomic approaches. *J Biomed Biotechnol* 2011:810242
8. Faulkner JA, Larkin LM, Claflin DR, Brooks SV (2007) Age-related changes in the structure and function of skeletal muscles. *Clin Exp Pharmacol Physiol* 34:1091–1096
9. Malafarina V, Uriz-Otano F, Iniesta R, Gil-Guerrero L (2012) Sarcopenia in the elderly: diagnosis, physiopathology and treatment. *Maturitas* 71:109–114
10. Berger MJ, Doherty TJ (2010) Sarcopenia: prevalence, mechanisms, and functional consequences. *Interdiscip Top Gerontol* 37:94–114
11. Ohlndieck K (2010) Proteomics of skeletal muscle differentiation, neuromuscular disorders and aging. *Expert Rev Proteomics* 7:283–296
12. Gelfi C, Vasso M, Cerretelli P (2011) Diversity of human skeletal muscle in health and disease: contribution of proteomics. *J Proteomics* 74:774–795
13. Ohlndieck K (2011) Skeletal muscle proteomics: current approaches, technical challenges and emerging techniques. *Skelet Muscle* 1:6
14. Doran P, Donoghue P, O'Connell K, Gannon J, Ohlndieck K (2009) Proteomics of skeletal muscle aging. *Proteomics* 9:989–1003
15. Ohlndieck K (2011) Proteomic profiling of fast-to-slow muscle transitions during aging. *Front Physiol* 2:105
16. Staunton L, O'Connell K, Ohlndieck K (2011) Proteomic profiling of mitochondrial enzymes during skeletal muscle aging. *J Aging Res* 2011:908035
17. Schiaffino S, Reggiani C (2011) Fiber types in mammalian skeletal muscles. *Physiol Rev* 91:1447–1531
18. Gelfi C, Vigano A, Ripamonti M, Pontoglio A, Begum S, Pellegrino MA, Grassi B, Bottinelli R, Wait R, Cerretelli P (2006) The human muscle proteome in aging. *J Proteome Res* 5:1344–1353
19. Doran P, O'Connell K, Gannon J, Kavanagh M, Ohlndieck K (2008) Opposite pathobiochemical fate of pyruvate kinase and adenylate kinase in aged rat skeletal muscle as revealed by proteomic DIGE analysis. *Proteomics* 8:364–377
20. O'Connell K, Ohlndieck K (2009) Proteomic DIGE analysis of the mitochondria-enriched fraction from aged rat skeletal muscle. *Proteomics* 9:5509–5524
21. Caskey CI, Zerhouni EA, Fishman EK, Rahmouni AD (1989) Aging of the diaphragm: a CT study. *Radiology* 171:385–389
22. Zhang YL, Kelsen SG (1990) Effects of aging on diaphragm contractile function in golden hamsters. *Am Rev Respir Dis* 142:1396–1401
23. Criswell DS, Shanely RA, Betters JJ, McKenzie MJ, Sellman JE, Van Gammeren DL, Powers SK (2003) Cumulative effects of aging and mechanical ventilation on in vitro diaphragm function. *Chest* 124:2302–2308
24. Suzuki T, Maruyama A, Sugiura T, Machida S, Miyata H (2009) Age-related changes in two- and three-dimensional morphology of type-identified endplates in the rat diaphragm. *J Physiol Sci* 59:57–62

25. Rabilloud T, Lelong C (2011) Two-dimensional gel electrophoresis in proteomics: a tutorial. *J Proteomics* 74:1829–1841
26. Weiss W, Görg A (2009) High-resolution two-dimensional electrophoresis. *Methods Mol Biol* 564:13–32
27. Friedman DB, Hoving S, Westermeier R (2009) Isoelectric focusing and two-dimensional gel electrophoresis. *Methods Enzymol* 463:515–540
28. Carrette O, Burkhard PR, Sanchez JC, Hochstrasser DF (2006) State-of-the-art two-dimensional gel electrophoresis: a key tool of proteomics research. *Nat Protoc* 1:812–823
29. Rabilloud T, Chevallet M, Luche S, Lelong C (2010) Two-dimensional gel electrophoresis in proteomics: past, present and future. *J Proteomics* 73:2064–2077
30. Gauci VJ, Wright EP, Coorssen JR (2011) Quantitative proteomics: assessing the spectrum of in-gel protein detection methods. *J Chem Biol* 4:3–29
31. Minden JS, Dowd SR, Meyer HE, Stühler K (2009) Difference gel electrophoresis. *Electrophoresis* 30:S156–S161
32. Lewis C, Doran P, Ohlendieck K (2012) Proteomic analysis of dystrophic muscle. *Methods Mol Biol* 798:357–369
33. Rabilloud T, Strub JM, Luche S, van Dorsselaer SA, Lunardi J (2001) A comparison between Sypro Ruby and ruthenium II tris (bathophenanthroline disulfonate) as fluorescent stains for protein detection in gels. *Proteomics* 1:699–704
34. Moebius J, Denker K, Sickmann A (2007) Ruthenium (II) tris-bathophenanthroline disulfonate is well suitable for Tris-Glycine PAGE but not for Bis-Tris gels. *Proteomics* 7:524–527
35. Aude-Garcia C, Collin-Faure V, Luche S, Rabilloud T (2011) Improvements and simplifications in in-gel fluorescent detection of proteins using ruthenium II tris-(bathophenanthroline disulfonate): the poor man's fluorescent detection method. *Proteomics* 11:324–328
36. Gannon J, Staunton L, O'Connell K, Doran P, Ohlendieck K (2008) Phosphoproteomic analysis of aged skeletal muscle. *Int J Mol Med* 22:33–42
37. Staunton L, Jockusch H, Wiegand C, Albrecht T, Ohlendieck K (2011) Identification of secondary effects of hyperexcitability by proteomic profiling of myotonic mouse muscle. *Mol Biosyst* 7:2480–2489
38. Carberry S, Zwyer M, Swandulla D, Ohlendieck K (2012) Proteomics reveals drastic increase of extracellular matrix proteins collagen and dermatopontin in aged mdx diaphragm muscle. *Int J Mol Med* 30:229–234
39. Carberry S, Zwyer M, Swandulla D, Ohlendieck K (2012) Proteomic profiling of age-related changes in the tibialis anterior muscle proteome of the mdx mouse model of dystrophinopathy. *J Biomed Biotechnol* 2012:691641
40. Fröhlich T, Arnold GJ (2009) A newcomer's guide to nano-liquid-chromatography of peptides. *Methods Mol Biol* 564:123–141
41. Gaspari M, Cuda G (2011) Nano LC-MS/MS: a robust setup for proteomic analysis. *Methods Mol Biol* 790:115–126
42. Nikolov M, Schmidt C, Urlaub H (2012) Quantitative mass spectrometry-based proteomics: an overview. *Methods Mol Biol* 893:85–100
43. Zhou W, Petricoin EF 3rd, Longo C (2012) Mass spectrometry-based biomarker discovery. *Methods Mol Biol* 823:251–264

Single-Cell Semiconductor Sequencing

Andrea B. Kohn, Tatiana P. Moroz, Jeffrey P. Barnes, Mandy Netherton,
and Leonid L. Moroz

Abstract

RNA-seq or transcriptome analysis of individual cells and small-cell populations is essential for virtually any biomedical field. It is especially critical for developmental, aging, and cancer biology as well as neuroscience where the enormous heterogeneity of cells present a significant methodological and conceptual challenge. Here we present two methods that allow for fast and cost-efficient transcriptome sequencing from ultra-small amounts of tissue or even from individual cells using semiconductor sequencing technology (Ion Torrent, Life Technologies). The first method is a reduced representation sequencing which maximizes capture of RNAs and preserves transcripts' directionality. The second, a template-switch protocol, is designed for small mammalian neurons. Both protocols, from cell/tissue isolation to final sequence data, take up to 4 days. The efficiency of these protocols has been validated with single hippocampal neurons and various invertebrate tissues including individually identified neurons within a simpler memory-forming circuit of *Aplysia californica* and early (1-, 2-, 4-, 8-cells) embryonic and developmental stages from basal metazoans.

Key words Single-cell RNA-seq, CA1 neurons, Transcriptome, *Aplysia*, Ctenophores, Hippocampus, Ion Torrent, Ion proton

1 Introduction

DNA and RNA sequencing has and will continue to make a profound impact on medicine, clinical, and basic research. It has become indispensable for virtually any biomedical field, providing an unbiased view of the entire molecular machinery within a biological system of interest. The current trends are to adapt high-throughput sequencing technologies to the level of small-cell populations and even individual cells [1–3]. It is especially critical for developmental and aging biology and neuroscience where the enormous heterogeneity of cells present a significant methodological and conceptual challenge [4, 5]. Equally important is to achieve fast and cost-efficient sequencing targeting true real-time genomics where direct physiological measurements from defined cells or cell populations are coupled with genome-wide

sequencing and analysis from the very same cells with feedback for investigators within 3–4 days or even 1 day. The recently introduced semiconductor sequencers (*Ion Torrent* Personal Genome Machine (PGM) and *Ion Torrent* Proton) provide novel opportunities toward coupling transcriptional changes and physiological measurements [6, 7]. These platforms, tested in our laboratory, allow us to perform multiple experiments, even single-cell RNA-seq, at low cost with 3–4 day's turnaround time from cell sampling to sequencing and initial annotation. Here we briefly describe the principle of semiconductor sequencing and provide a practical protocol for both invertebrate and vertebrate preparations.

Beginning with Frederic Sanger's Nobel prize winning classical methodology and followed by the majority of commercial next generation sequencing platforms (such as 454/Roche, Solexa/Illumina, SOLiD and Helicos and Pacific Bioscience), detection schemes have relied upon optical measurements which, although precise, have a number of limitations with regard to sample and data processing, as well as manufacturing, sample preparation cost, and starting amount. In 2011 Life Technologies reported an electrochemical (light-independent) detection scheme integrated with a semiconductor platform; as the proof-of-the-concept for the technology, they resequenced the human genome [7]. The principle of semiconductor sequencing is illustrated in Fig. 1. It is based on the simple, natural chemistry of DNA synthesis where addition of a new base in the growing DNA strand leads to release of hydrogen ions (H^+ , Fig. 1a). As a result, the detector is a modified ultra-small pH sensor (Fig. 1b) on a silicon substrate—it is a semiconductor in which each well lies above an ion-sensitive metallic oxide layer coupled to an electronic sensor that registers miniscule (0.02 pH unit) and transient (with a half-life <1 s) pH changes [7]. The process can be performed in parallel on millions of ultra-small wells within electronic semiconductor chips (Fig. 1c, d). The density of these nano-wells is growing with the accumulated advances of more than 30 years of silicon/computer technologies. Today, there are four currently available sequencing chips with different densities of wells per chip; their sequencing parameters and yield are summarized in Fig. 2. Here, the data reported for the three series of chips (314, 316, and 318) and P1 were obtained in our laboratory at the University of Florida in 2012, while the parameters for novel Ion Proton (IP) chips are provided by Life Technologies.

The overall experimental workflow for the semiconductor sequencing is outlined in Fig. 3. After cell and RNA isolation and construction of sequencing libraries from a target cDNA sample (Figs. 6 and 7), each individual DNA fragment is immobilized on an Ion Sphere Particle and clonally amplified (Fig. 4). The process is automatic with a supplementary OneTouch System (Fig. 4). The resulting beads with amplified (emulsion PCR), individually cloned

Principle and Elements of Semiconductor Sequencing

Simple Natural Chemistry of Sequencing-by-Synthesis with H⁺ release detection

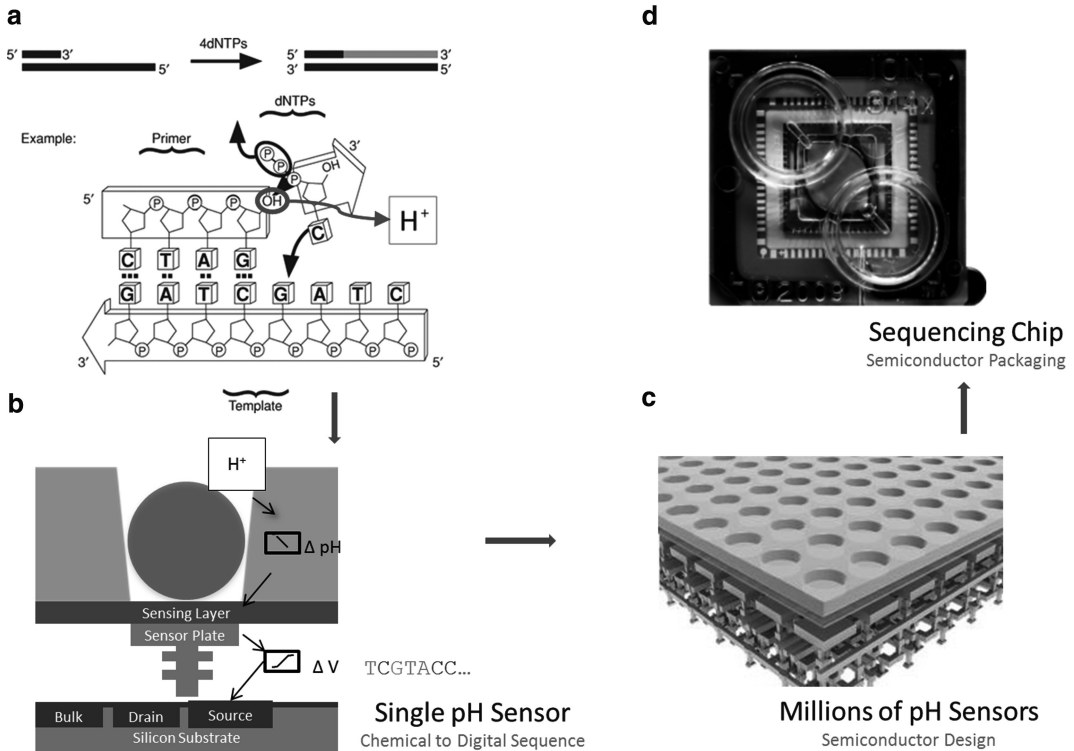
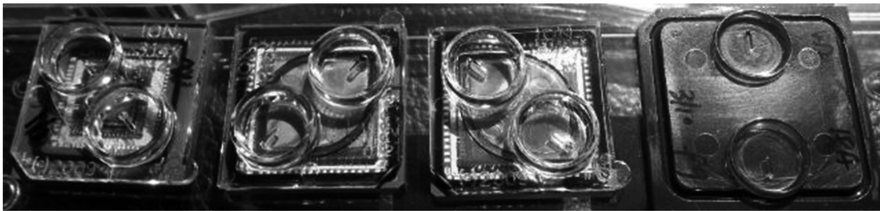


Fig. 1 Principles and elements of semiconductor sequencing. Simpler natural chemistry of sequencing by synthesis is implemented in the Ion Torrent platform. As the second strand of DNA is synthesized, the addition of every new nucleotide leads to a release of H^+ (a) which is detected by a silicon pH sensor (b). Several million pH sensors (c) are arranged within a sequencing chip (d). Cross-sectional view (c) shows the ion-sensitive layer in green with the microwells on the top surface (3 μm) and the transistor stack underneath. The present design reduces the complexity of light detection schemes such as the use of modified and fluorescent bases and optical/laser detection. PGM functions by delivering natural unmodified nucleotides one at a time over the surface of the chip. Because nucleotides are unmodified and detection does not require any additional enzyme/amplification cascades, it also eliminates many sources of error, thereby delivering long accurate reads with highly uniform genome coverage. Modified from ref. 7

DNA fragments are then enriched to eliminate “empty” beads—this process is also performed by a robotic enrichment system (ES) (Fig. 4). Finally, after being loaded on a selected sequencing chip, the beads containing clonal populations of the DNA from an experimental sample are arrayed in wells and incubated serially with pure nucleotides of DNA. Incorporation of a nucleotide is continuously detected by measuring changes in the hydrogen ion concentration during the sequencing process on the PGM machine and simultaneously processed on a server for further analysis and assembly (Fig. 3).

Semiconductor Sequencing Chips



Chip Types ¹	314	316	318	IP1/IP2/IP3*
# Wells per Chip	1,262,528	6,348,216	11,302,473	165 M/660M/1.2B
Volume, μ L	7	30	30	55
# of Reads ¹	295,736	1,592,020	4,580,123	124-496,000,000
Yield/Q20, bases	24.6/ 21.9 Mb	146.7/ 122.5 Mb	600/ 500 Mb	10 / 60 / 480 Gb
Mean Read ¹ , bp	83	92	129	Up to 300
Longest Reads ¹	396	307	386	640
Run Time ¹ , Hrs	2.4	3.1	4.5	~4
Processing, Hrs ¹	0.3	2.0	4.5	Up to 8 hrs
Analysis ² , Hrs	12	18	30	Up to 1 day
Template Molecules	2.5×10^7	5×10^7	5×10^7	2.5×10^7
Cost per Run	\$400	\$500	\$800	\$1,000

Fig. 2 Semiconductor sequencing chips. The table summarizes statistics for various sequencing runs and their assessments for each chip type: 314, 316, 318 Ion Torrent PGM, and Ion Proton (IP1/IP2/IP3). All runs were based on 200 bp chemistry and OneTouch™ template preparation with Torrent Suite server version 2.2. Q20 refers to 99 % accuracy of a base call. ¹Data were obtained in our laboratory at the University of Florida. ²Analysis includes assembly and initial annotation of a given sequencing run using a High Performance Computer Cluster (64 Intel(R) Xeon(R) X7550 2.00GHz CPUs, 512GB of RAM, and 6TB of storage). *All Proton data were provided by Ion Torrent, Life Technologies

The Ion Torrent PGM and Proton are benchtop sequencers that can be put in any individual laboratory and not necessarily a sequencing center or core facility. Figure 5 illustrates the setup in our laboratory. Initial training and practical experience can be obtained within a couple of weeks for most laboratories. As such, the Ion PGM and Proton can facilitate the genome-wide sequencing components for physiological, developmental, cell, and aging biology-focused laboratories in a simple and scalable way.

Here we summarize two protocols that allow fast and cost-efficient transcriptome sequencing from ultra-small amounts of tissues or even from individual cells. We show that as little as 40 pg of total RNA can be used to produce reliable sequencing libraries (we tested it using single mechanosensory neurons from *Aplysia* with 40–50 μ m cell body diameter—see ref. 8). Specifically, we implemented reduced representation sequencing for the current

Experimental Workflow for RNA-seq

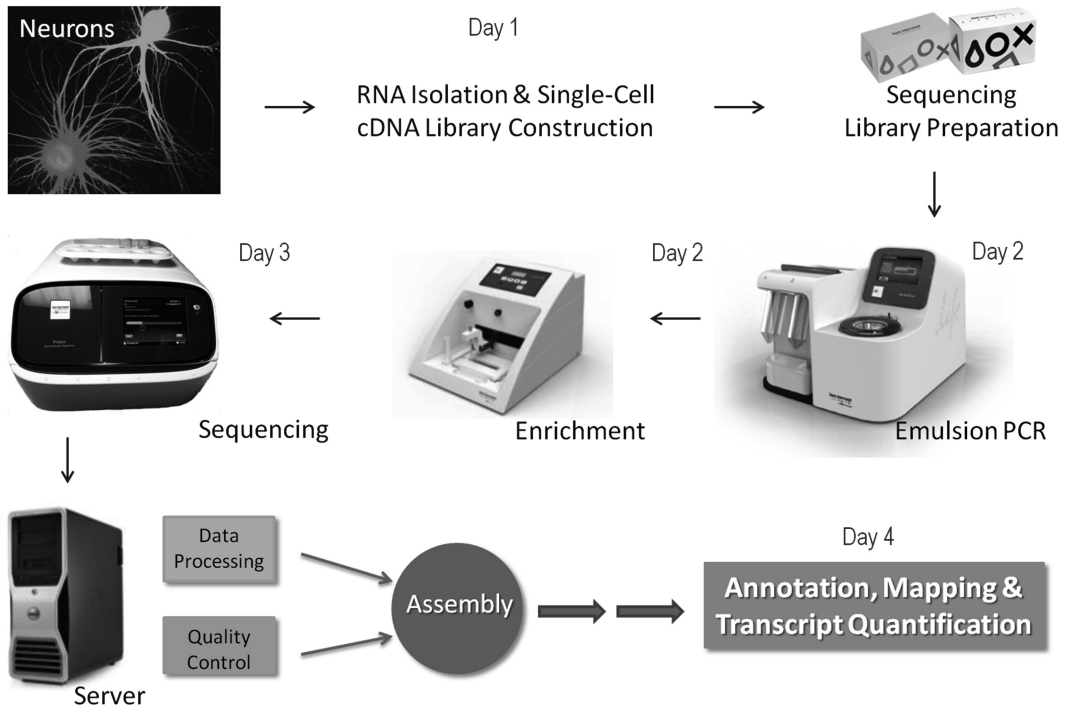


Fig. 3 Experimental workflow for RNA-seq using the Ion Torrent (see details in the text). The equipment set includes OneTouch™ Instrument for templated bead preparation (Subheadings 3.5.1, 3.5.2, and 3.5.3), an Ion OneTouch™ ES robotic system for sample enrichment (Subheadings 3.5.4, 3.5.5, and 3.5.6), Personalized Genome Sequencer™ (Subheading 3.6), and an Ion Torrent server containing Torrent Software Suite for base calling and mapping and web portal access for data review and sharing for sequencing and primary data analysis within hours. Combined, this innovative approach allows us to perform multiple, even single-cell RNA-seq experiments at the lowest possible cost today within 3–4 day's turnaround time: from cell sampling to sequencing and initial annotation

Ion Torrent platform and developed an unbiased method of RNA-seq library construction using commercially available kits to ensure consistency and reproducibility. Second, we implemented a template-switch method, where single cells or neurons are lysed in the buffer for the library construction and then sequenced.

Both protocols, from cell/RNA isolation to the final sequencing data, can be completed within a week. After sequencing libraries are prepared, it takes about 7 h for PGM instrument and about 1 day for Ion Proton to complete the RNA-seq run, including templated bead preparation and sequencing. For example, this combination of library construction and semiconductor sequencing enables us to measure changes in small-cell populations following physiological tests associated with learning and memory formation or as a function of age-related memory loss.

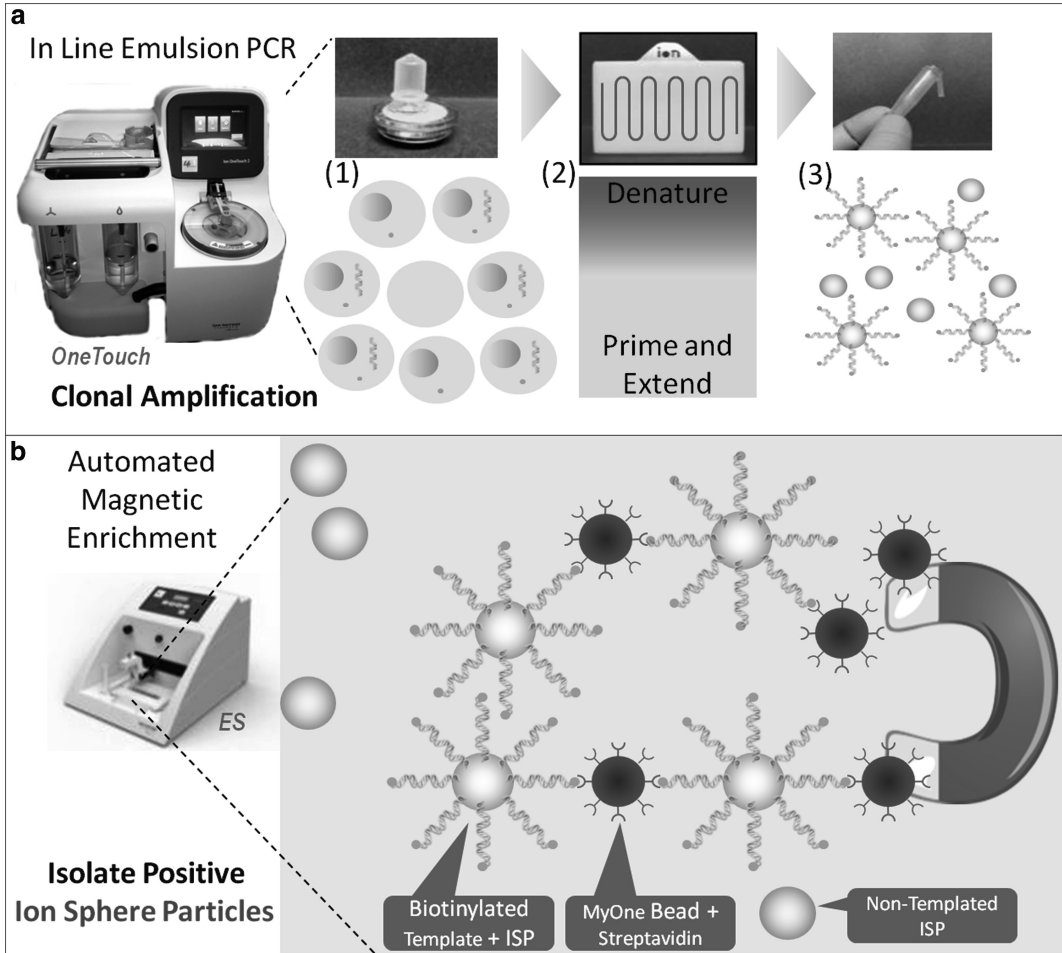


Fig. 4 In-line emulsion PCR technology. The schematic diagram illustrates key steps in the process using OneTouch™ instrumentation. **(a)** The Ion OneTouch™ Instrument has three key technologies that enable automated delivery of templated Ion Sphere™ particles. The first is a reaction filter (A1) that creates millions of microreactors in which clonal amplification occurs. The second is the in-line PCR amplification plate (A2) that enables thermal cycling of the microreactors. The third is the integrated centrifuge (A3), which recovers the templated Ion Sphere™ particles. The green dots represent Biotin that has been incorporated on the primer 5'-end of the template or DNA molecule during the emPCR process. The Biotin is used to isolate only the template-positive ISP by binding to Streptavidin-linked C1 Magnetic Beads (*large red dots*) during the enrichment step on the Ion OneTouch™ ES. **(b)** The Ion OneTouch™ ES uses magnetic bead (*large red dots*) technology to isolate template-positive Ion Sphere™ particles that can be loaded directly onto the Ion semiconductor chip, thus delivering automated, highly reproducible enrichment with every run (Color figure online)

The efficiency of both protocols has been validated using individually identified neurons of *Aplysia californica*, one of the well-recognized models in learning and memory research [9–11] and cell biology of development and aging [4, 9–17]. We also successfully tested the protocol on single hippocampal CA1 neurons and

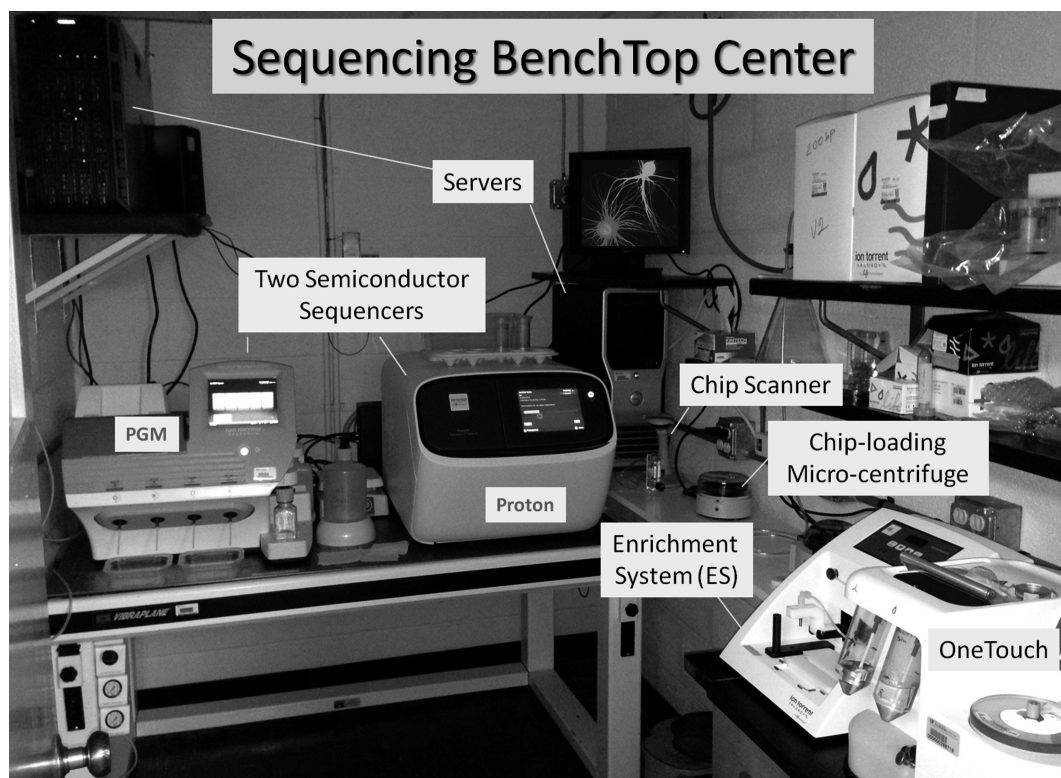


Fig. 5 Sequencing BenchTop Center. The photo shows the arrangement of key instruments required for semiconductor sequencing in an individual laboratory

more than three dozen different invertebrate tissues and cells including early embryonic stages of the ctenophore *Pleurobrachia bachei*. It can also be applied to a broad spectrum of experimental preparations in the biology of aging.

2 Materials

Reagents:

- RNAqueous-MicroTM (Cat # 1931, Ambion, Life Technologies).
- RNAqueousTM (Cat # 1912, Ambion, Life Technologies).
- RiboMinusTM Eukaryote Kit (Cat # A10837-08, Invitrogen, Life Technologies).
- RiboMinusTM Concentration Module (Cat # K1550-05, Invitrogen, Life Technologies).
- Marathon cDNA Amplification Kit (Cat # 634913, Clontech, Takara Bio).

- All enzymes for first and second strand synthesis are inclusive
- 5× First-Strand Buffer:
 - 250 mM Tris-HCl (pH 8.5).
 - 40 mM MgCl₂.
 - 150 mM KCl.
 - 5 mM Dithiothreitol (DTT).
- 20× Second Strand Enzyme Cocktail
 - E. coli* DNA polymerase I (6 U/μL).
 - E. coli* DNA ligase (1.2 U/μL).
 - E. coli* RNaseH (0.25 U/μL).
- SMARTer[®] PCR cDNA Synthesis Kit (Clontech Cat # 634926).
- Alu I and NEB buffer 4 (Cat # R0137S, New England BioLabs).
- Rsa I (Cat # R0167S, New England BioLabs).
- Ligate-IT Rapid Ligation Kit (Cat # 78400, Affymetrix).
- 5× Quick Ligation Reaction Buffer:
 - 132 mM Tris-HCl.
 - 20 mM MgCl₂.
 - 2 mM Dithiothreitol.
 - 2 mM ATP.
 - 15 % Polyethylene glycol (PEG 6000) pH 7.6 at 25 °C.
- AMPure XP Reagent (Cat # A63880, Agencourt, Beckman Coulter, Inc.).
- ArrayControl[™] RNA Spike-in control RNAs (Catalog # 1780, Ambion, Applied Biosystems).
- Advantage[®] UltraPure PCR Deoxynucleotide Mix (10 mM each dNTP) (Clontech cat # 639125).
- Ion Plus Fragment Library Kit (Cat. no. 4471252, Life Technologies).
- Platinum[®] PCR SuperMix High Fidelity (Cat # 12532-016, Invitrogen, Life Technologies)
 - 22 U/ml complexed recombinant Taq DNA polymerase.
 - Pyrococcus species GB-D thermostable polymerase.
 - Platinum[®] Taq Antibody.
 - 66.0 mM Tris-SO₄ (pH 8.9).
 - 19.8 mM (NH₄)₂SO₄.
 - 2.4 mM MgSO₄.
 - 220.0 μM dNTPs stabilizers.

- Advantage[®] 2 Polymerase Mix and the buffer (Cat # 639201, Clontech).
 50× Advantage[®] 2 Polymerase Mix.
 Includes TITANIUM Taq DNA Polymerase and a small amount of proofreading polymerase and TaqStart Antibody (1.1 µg/µl).
 50 % Glycerol.
 15 mM Tris-HCl (pH 8.0) 0.3 mM.
 75 mM KCl 1.5 mM.
 0.05 mM EDTA 1.0 µM.
 10× Advantage[®] 2 PCR Buffer.
 400 mM Tricine-KOH (pH 8.7 at 25 °C).
 150 mM KOAc.
 35 mM Mg(OAc)₂.
 37.5 µg/ml BSA.
 0.05 % Tween 20.
 0.05 % Nonidet-P40.
- Ion PGM[™] 200 Xpress Template Kit (Cat # 4474280 Ion Torrent, Life Technologies).
- Ion OneTouch[™] 200 Template Kit v2 (Cat # 4478316 Ion Torrent, Life Technologies).
- Ion PGM[™] 200 Sequencing Kit (Cat # 4474004, Ion Torrent, Life Technologies).
- Ion 314[™] Chip (Cat # 4462923; 8 pack), 316[™] Chip (Cat # 4466616; 4 pack), 318[™] Chip (Cat # 4466617; 4 pack) (Ion Torrent, Life Technologies).
- Ion Sphere[™] Quality Control Kit (Cat # 4468802, Ion Torrent, Life Technologies).
- Dynabeads[®] MyOne[™] Streptavidin C1 Magnetic Beads (Cat # 65001, Invitrogen, Life Technologies).
- Covaris microTUBE AFA Fiber Screw-Cap 6 × 16 mm (Cat # SKU:520096, Covaris).
- Agilent Bioanalyzer[™] High Sensitivity DNA Kit (Cat # 5067-4626, Agilent Technologies).
- Agilent Bioanalyzer[™] RNA 6000 Pico Kit (Cat # 5067-1513, Agilent Technologies).
- Agilent Bioanalyzer[™] RNA 6000 Nano Kit (Cat # 5067-1511, Agilent Technologies).
- E-Gel[®] SizeSelect[™] 2 % Agarose (Cat # G6610-02, Invitrogen, Life Technologies).
- Primers 0.2 µM scale HPLC purified, IDT, Integrated DNA Technologies, Inc (*see* Table 1 for all primer and adaptor sequences).

Table 1
Adaptors and primers for Ion Torrent libraries

Primer name	Primer sequence
Trsa	5'-CGCAGTCGGTAC (T) ₁₃ -3'
Adaptor A	5'-CCATCTCATCCCTGCGTGTCTCCGACTCAG-3' and 5'-CTGAGTCGGAGACACGCAGG-3'
P1 adaptor	5'-CCACTACGCCTCCGCTTTCCTCTCTATGGGCAG TCGGTGAT-3' and 5'-ATCACCGACTGCCCATAGAGA GGAAAGCGGA-3'
3' SMART CDS Primer IIA	5'-AAGCAGTGGTATCAACGCAGAGTACT(30)N-1N-3'
SMARTer II A Oligonucleotide	5'-AAGCAGTGGTATCAACGCAGAGTACXXXXX-3'
5' PCR Primer IIA	5'-AAGCAGTGGTATCAACGCAGAGT-3'
A PCR Primer	5'-CCATCTCATCCCTGCGTGTCTCCGACTCAG-3'
P1 PCR Primer	5'-CCACTACGCCTCCGCTTTCCTCTCTATG-3'

Gray shading is primers for reduced representation library, and yellow shading is primers for template-switch single cell/neuron library. The same primers are used for the sequencing library PCR amplification

Equipment:

- LoBind tubes 0.5 and 1.5 µL (Cat # 80077-236, 80077-230 Eppendorf, VWR International, LLC).
- DynaMag™-2 magnet (microcentrifuge tube magnet) (Cat # 123-21D, Invitrogen, Life Technologies).
- Covaris M220 Focused-ultrasonicator (Covaris).
- Agilent Bioanalyzer™ 2100 (Cat # G2947CA, Agilent Technologies).
- Agilent TapeStation 220 (Cat # G2965AA, Agilent Technologies).
- Galaxy MiniStar Centrifuge (120 V, 50/60 Hz) (Cat # 93000-196, VWR International).
- sonicating bath (2- to 3-L tank; 80 W, 40 kHz transducer) (Cat # 15-335-20, Fisher).
- Thermolyne Labquake Tube Shaker/Rotator (Cat # 56264-302, VWR International).
- Qubit® 2.0 Fluorometer (Cat # Q32866, Invitrogen, Life Technologies).
- MJ Research Thermo Cycler (Cat # PTC-100, MJ Research).
- E-Gel® iBase™ and E-Gel® Safe Imager™ Combo Kit (Cat # G6465, Invitrogen, Life Technologies).
- Personal Genome Machine (PGM™) Sequencer (Cat # 4462917, Ion Torrent Life Technologies).

- Ion PGM™ OneTouch™ System which is comprised of two modules: the Ion OneTouch™ Instrument and the Ion OneTouch™ ES (enrichment system) (Cat # 4470001, Ion Torrent Life Technologies).
- Torrent Server (Cat # 4462918, Ion Torrent, Life Technologies).

3 Methods

3.1 Sample Preparation

Sample preparation is dependent on species, tissue, and even the type of cell from which RNA will be isolated. The efficiency of the protocols below has been validated using both small numbers (20–200) of cells and even single hippocampal neurons (CA1, CA3, and DG areas in collaboration with the Dr. Thomas Foster and C. Jason Frazier laboratories, University of Florida), various invertebrate tissues including early embryonic (1-, 2-, 4-, 8-, 16-, 32, 64-cells) and later developmental stages from basal metazoans (*Pleurobrachia bachei*), and individually identified neurons within a simpler memory-forming circuit of *Aplysia californica* [11, 14]. Typically animals are anesthetized appropriately followed by removal of tissue such as regions of the central nervous system or ganglia. For example, if identified neurons are to be isolated from the mollusc *Aplysia*, ganglia are dissected, connection tissues are removed, and single cells are isolated as described in [1, 13] (*see Note 1* for tissue/single-cell storage).

For single-cell library construction from small mammalian neurons, RNA is not isolated because the amount of RNA is too low to detect by conventional instruments such as a Bioanalyzer. Single CA1 neurons from mice were placed directly into a buffer for library construction, briefly sonicated (5–15 s) in a sonicating bath, then snap frozen at -80°C . Critical to this process is performance of cell isolations under controllable or sterile conditions. The rig, experimental chamber, microelectrodes, solutions, and anything that comes in contact with the tissue/cells can be potential sources for bacterial, fungal, or human contamination.

3.2 RNA Isolation

Obtaining high-quality RNA is the first and often the most important step in performing many molecular techniques such as high-throughput sequencing. We find the best RNA isolation method is quite often species-dependent and needs to be experimentally determined (*see Note 2* for a comment on RNA isolation kits). We choose the RNA isolation kit or method that has been experimentally tested based on the quality and quantity of RNA for a specific animal, tissue, or even single cell (see additional details about single neuron isolation in ref. 1). RNA quality is analyzed using an Agilent 2100 Bioanalyzer™ on a 6000 Nano LabChip or

the new Agilent TapeStation. For very small quantities, the 6000 Pico LabChip can be used. We may also use the Qubit to determine quantity of RNA for a sample but only if there is a sufficient amount of material. Understanding the properties of a species RNA is important. For example, many molluscs tested have a hidden break in their 28s ribosomal subunit causing the 28s subunit rRNA to migrate with the 18s subunit, thus generating one peak; *see* Fig. 6 for an electropherogram from an *Aplysia* single neuron (*see* **Note 3** on invertebrate rRNA [18]). Once the quality and quantity is satisfactory, this material is used to construct a sequencing library. This can also be a *pause point* and samples should be stored at -80°C .

3.3 Library Construction: Timing 6 h

Quality sequencing such as RNA-seq depends on a good library. We present here two RNA-seq library protocols based on the amount of the planned sequencing output. First, we present a reduced representation RNA-seq library protocol for maximum capture of transcriptional output which requires relatively lower sequence coverage compared to the complementary protocol. This second protocol is designed for small single mammalian neurons which are lysed directly in the buffer for library construction, then sequenced.

The first protocol, Subheading 3.3.1 describes an unbiased method of library construction. Specifically, it is designed for both quantitative and qualitative analysis of mRNA from ultra-small amounts of material and can be applicable for small neuronal populations and even large single neurons. The distinct feature of this protocol is preservation of the direction of transcripts which allows equal identification of both sense and antisense RNA. It was validated for both individual identified *Aplysia* neurons as well as for small clusters of 20–200 CA1, CA3 hippocampal neurons from rat, and 100–200 μm invertebrate embryos (e.g., *Pleurobrachia*).

We can use commercially available kits such as the Marathon[®] cDNA Amplification Kit from Clontech to ensure consistency and reproducibility but suggest cheaper alternatives to these kits. Although we focused on the use of limited amounts of starting material (starting from 20 to 40 pg), our protocol is also applicable to larger quantities of material (up to 1 μg).

Library construction starts with total RNA isolation (*see* Subheading 3.2), then RNA is reverse transcribed to cDNA with an oligo dT primer and a second strand generated (*see* Fig. 6). The double stranded cDNA is fragmented with a combination of restriction enzymes. Sequential ligation of adaptors is used to generate a reduced representation library. Fragmented DNA with ligated adaptors is processed through an emulsion-based clonal amplification (template bead preparation *see* Subheading 3.5 and Fig. 4) and captured onto Ion Sphere Particles (from Ion Torrent) as required for subsequent sequencing steps. DNA-captured beads are placed onto a semiconductor chip for sequencing. Because our

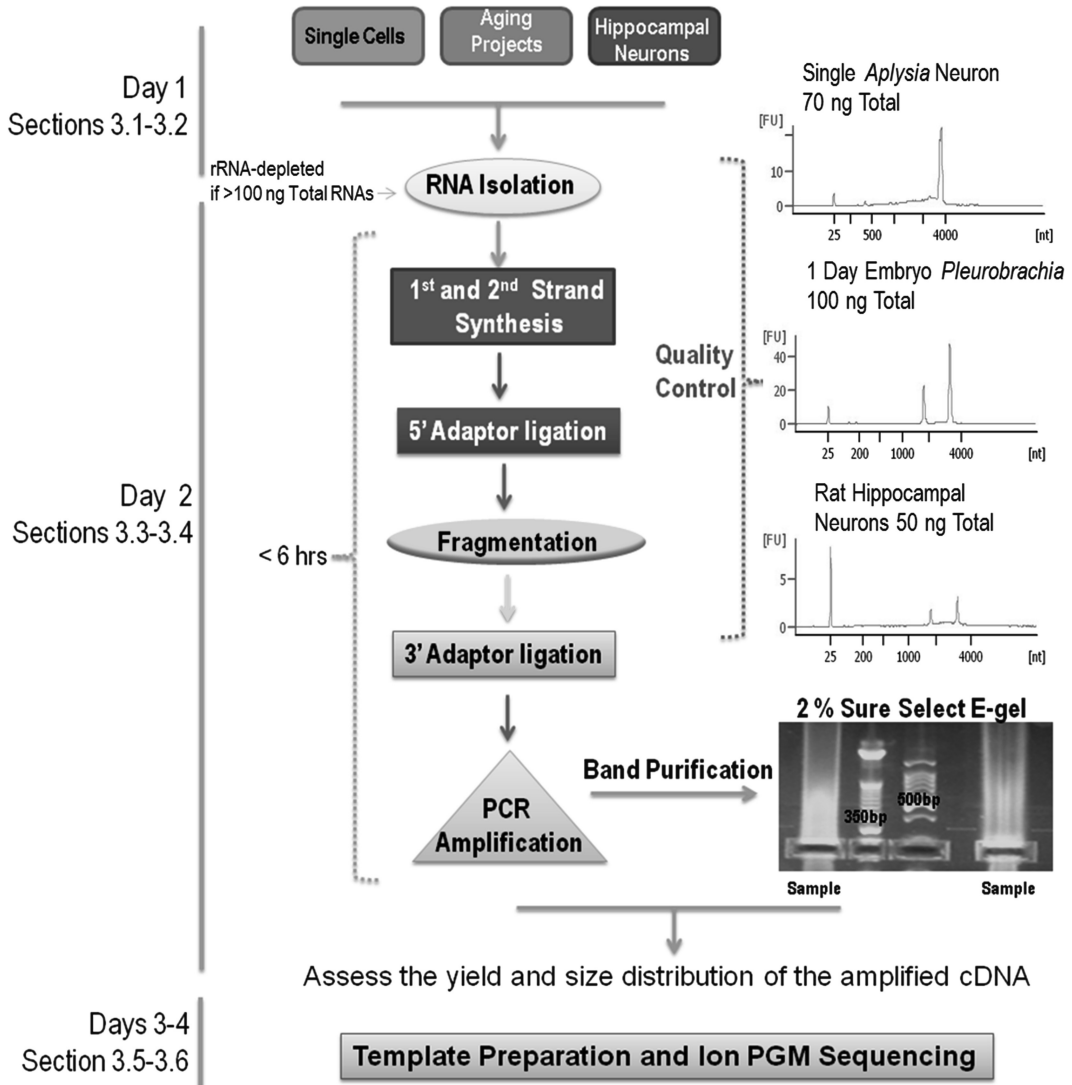


Fig. 6 Preparation of sequencing libraries using a reduced representation protocol. The diagram presents a workflow for library construction and sequencing on Ion PGM. The number of days and corresponding sections are listed in the *far left*. Tested samples (e.g., hippocampal or *Aplysia* neurons or developmental/aging cell populations) are prepared for RNA isolation (see Subheadings 3.1 and 3.2) with quality of the RNA checked by a Bioanalyzer (quality control). The insert electropherograms are illustrative examples of RNA isolated from a single *Aplysia* neuron, 1 day embryos of *Pleurobrachia*, and rat hippocampal neuronal cluster from the CA3 region (ng amount of total RNA is listed for the entire extraction from each corresponding sample). The library construction process is summarized in Subheading 3.3.1 (see text). Illustrative examples of an E-gel for two libraries are shown in the second insert (here two different markers were run between the samples, and the bright bands are labeled with appropriate sizes). The library quality control assessment is summarized in Subheading 3.4 (see text). The template preparation and sequencing is followed as in Subheadings 3.5 and 3.6 (see text)

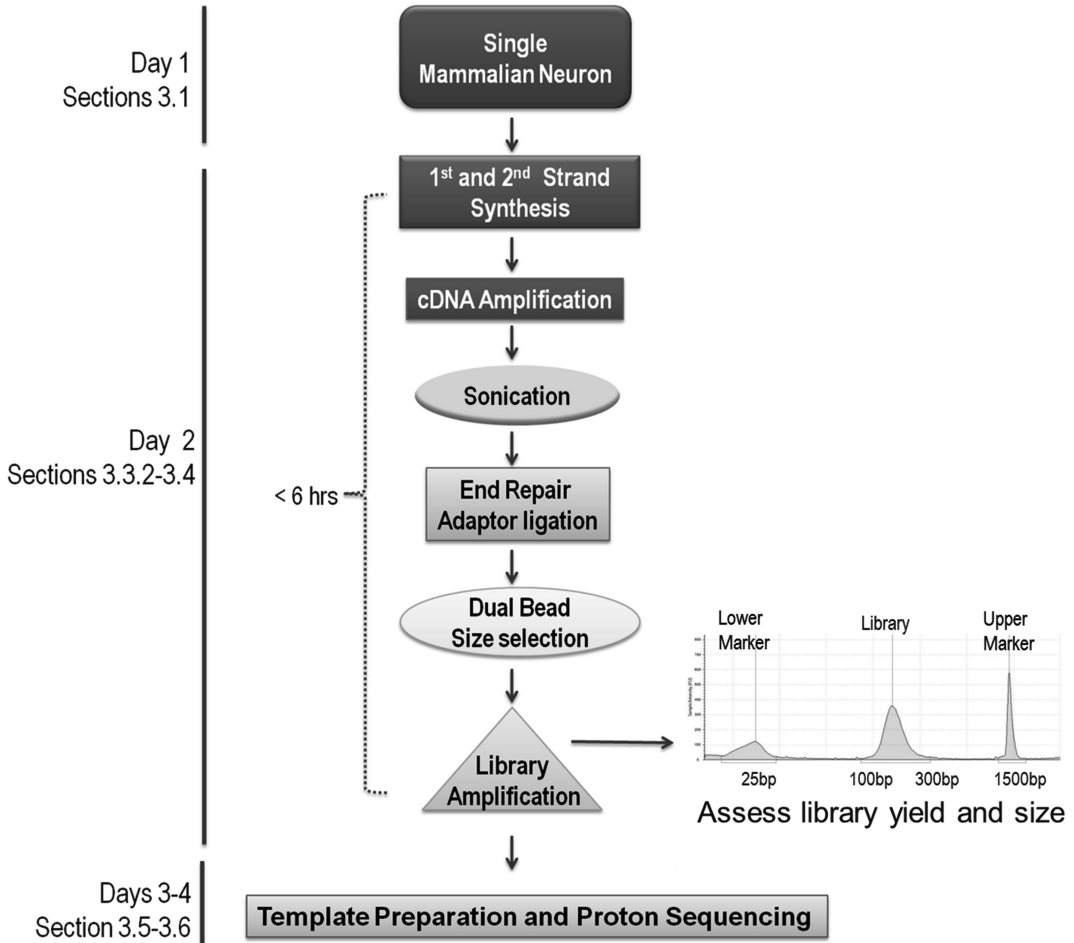


Fig. 7 Preparation of sequencing libraries using template switch from single neurons. The diagram presents a workflow for library construction and sequencing on Ion PGM or Proton. The number of days and corresponding sections are listed in the *far left*. Tested samples are single mouse hippocampal neurons. The library construction process is summarized in Subheading 3.3.2 (see text). Illustrative example of a TapeStation 2200 analysis from a single CA1 neuron is in the left side insert. The library quality control assessment is summarized in Subheading 3.4 (see text). The template preparation and sequencing is followed as in Subheadings 3.5 and 3.6 (see text)

libraries are constructed in a reduced representation process, smaller sequencing coverage is needed to capture a representative transcriptional output (e.g., using 314 or 318 sequencing chips).

The second library construction protocol (Subheading 3.3.2) uses a template-switch method and is designed for single mammalian neurons. Here, freshly isolated neurons are lysed directly in the buffer for library construction (*see* Fig. 7). We take advantage of the unique properties of the Moloney murine leukemia

virus (MMLV) reverse transcriptase for the first and second strand synthesis (*see Note 6*). The MMLV reverse transcriptase supports a template-switch method to synthesize both the first and second strand cDNA from an RNA template using an oligo (dT) primer. This enzyme synthesizes additional nucleotides at the 3' end of the first-strand cDNA, then with a template-switch oligo, the direction is switched and the enzyme makes the complementary second strand (*see Fig. 7*). Commercial kits can be used such as SMARTer[®] PCR cDNA Synthesis Kit (Clontech), or some components of the procedure can be made or combined separately. Once cDNA is constructed, it is amplified, fragmented, ligated with sequencing adaptors, and the final sequencing library amplified. This method is not a reduced representation of the transcriptome and is best paired with either a 318 PGM chip or a new Proton (P1) chip providing greater sequencing yield. This method is also not directional. It should be noted that a similar protocol using the template-switch method for sequencing single cells has been independently suggested [19]. However, Ramskold et al. [19] used the Nextera method of fragmentation and adaptor insertion, called “tagmentation,” that is specialized for human and mouse DNA, then followed with Illumina sequencing which takes weeks to obtain data. Below, we present a protocol that can be used for single-neuron RNA-seq.

3.3.1 Library

Construction Protocol: Reduced Representation

1. (Optional) If there is a sufficient amount of material (i.e., > 100 ng), RiboMinus[™] is employed, and the protocol is followed according to manufacturer's recommendations (*see Note 4*). If not, the total RNA is processed to cDNA.
2. Whenever possible, use a master mix of reagents. For X number of samples, multiply all reagent volumes by $X.5$ so as to accommodate pipetting errors. Use of master mixes will save time, produce fewer errors, and generate more reproducible results.
3. cDNA is generated using the Marathon cDNA Amplification Kit to promote consistency between libraries (Fig. 6) (*see Note 5* for other options and **Note 6**).
4. To begin first-strand synthesis, 5 μ L of total RNA or RiboMinus RNA and 1 μ L of Trsa (sequence in Table 1) cDNA synthesis primer (10 mM) are incubated at 70 °C for 2 min then briefly spun (*see Note 7*). Ribosomal-depleted starting material will ensure no ribosomal “contamination” in the library.

5. The following is added to the sample RNA containing tube:

2.0 μL	5 \times First Stand Buffer
1.0 μL	dNTP Mix (10 mM)
1.0 μL	AMV Reverse Transcriptase (20 U/ μL)
10 μL	Total volume

6. This mixture is triturated gently then incubated at 42 °C for 1 h.
7. (Optional) Eight individual bacterial RNA transcripts ranging in size from 750 to 2,000 bases with a 30-base 3' poly (A) tail (ArrayControl™ RNA Spike-in control RNAs) at different concentrations have been added at the beginning of the library construction for previous sequencing libraries to test the quality of the library (*see* **Note 8**).
8. Reaction is terminated by placing on ice.
9. Second strand synthesis is performed by adding the following to the first-strand tube:

48.4 μL	RNase-free water
16.0 μL	5 \times Second Strand Buffer
1.6 μL	dNTP Mix (10 mM)
4.0 μL	20 \times Second Strand Enzyme Cocktail
80.0 μL	Total volume

10. This mixture is triturated gently then incubated at 16 °C for 2h.

Then 2 μL (6 U) of T4 DNA polymerase is added and incubated at 16 °C for an additional 30 min.

Comment 1: The presented protocol is relatively short compared to other protocols [3, 20–22]. For low amounts of starting material, we recommend cDNA production before fragmentation, because the alternative ribosomal depleted RNA fragmentation methods require much larger quantities of starting material. Efficient removing of ribosomal RNA is not possible when working with very low amounts of RNA such as that from small cells and their compartments.

11. The library is purified with AMPure XP Reagent.
- (i) 1.8 volumes of AMPure XP Reagent (144 μL) is added to the dsDNA tube and set 5 min.
 - (ii) The mixture is placed on the Magnetic Particle Separator for 1 min or until the solution is cleared and the supernatant removed.

- (iii) The mixture is washed two times with freshly prepared 70 % ethanol and allowed to dry for 5 min.
 - (iv) The dsDNA is then eluted with 13 μL of RNase-free water.
12. 5' Adaptor ligation is performed by adding the following to the purified dsDNA (*see* **Notes 9** and **10**):

4.0 μL	5 \times Quick Ligation Reaction Buffer
1.0 μL	Quick T4 DNA Ligase
2.0 μL	Adaptor A (<i>see</i> Table 1)
13.0 μL	dsDNA
20.0 μL	Total volume

13. This mixture is incubated for 10 min at room temperature.
- Comment 2:* The ligation of Adaptor A at this point also allows for reduced representation of the library. Only one fragment per transcript can be ligated with the Adaptor A and later the P1. As a result, such reduced representation libraries allow observation of more distinct transcripts given the same amount of sequencing coverage. Our quantification of 1 transcript per 1 read produces higher coverage of the transcriptome than alternative protocols, when all fragments from a single transcript are ligated with library adaptors for the same amount of sequencing.
14. The ligation mixture is purified with 1.8 volumes of AMPure XP Reagent (36.0 μL) as described above and eluted with 17.0 μL of RNase-free water.
15. The purified A Adaptor-ligated dsDNA is fragmented by digestion with two 4 base blunt-end cutting restriction enzymes by adding:

1.0 μL	AluI (10 U)
1.0 μL	RsaI (10 U)
2.0 μL	NEB buffer 4
17.0 μL	dsDNA
21.0 μL	Total volume

16. Mixture is incubated at 37 °C for 2 h (*see* **Note 11**).
17. The digested mixture is then ligated with the P1 adaptor.

18. 3' Adaptor ligation is performed by adding the following to the purified dsDNA:

6.0 µL	5× Quick Ligation Reaction Buffer
1.0 µL	Quick T4 DNA Ligase
2.0 µL	Adaptor P1 (<i>see</i> Table 1)
21.0 µL	dsDNA
30.0 µL	Total volume

19. This mixture is incubated for 10 min at room temperature.
20. The ligation mixture is purified with 1.8 volumes of AMPure XP Reagent (54 µL) as described above and eluted with 40 µL of Nuclease-free water.
21. PCR amplification is performed on the adaptor-ligated purified dsDNA:

200.0 µL	Platinum® PCR SuperMix High Fidelity (<i>see</i> Note 12)
10.0 µL	PCR Primers mix (10 µM) each (Table 1)
40.0 µL	dsDNA
250.0 µL	Total volume

22. The above mixture is amplified with the following conditions (*see* **Note 13**):
- 95 °C for 30 s 1 cycle
- X cycles: (typical cycles are 16–18 for >100 µg total RNA and 18–23 for single cells)
- 95 °C for 30 s
- 58 °C for 30 s
- 72 °C for 1 min
- Hold 4 °C ∞
23. This is can be a *pause point* and samples can be stored at –20 °C (*see* **Note 14**).

3.3.2 *Single-Neuron
Library Construction
Using a Template-Switch
Method*

Library construction with SMARTer® PCR cDNA Synthesis Kit (Fig. 7) (*see* **Note 15**).

1. Thaw the single cell/neuron in 4.5 µL of 1× First-Strand Buffer (*see* Subheading 3.1).
2. First and second strand synthesis with the template-switch method. Add to the single cell sample.

1 μ L	3' SMART CDS Primer II A (12 μ M) (Table 1)
1 μ L	5 \times First-Strand Buffer
0.25 μ L	DTT (100 mM)
1 μ L	dNTP Mix (10 mM)
1 μ L	SMARTer II A Oligonucleotide (12 μ M) (<i>see</i> Note 16)
0.25 μ L	RNase Inhibitor
1 μ L	SMARTScribe Reverse Transcriptase (100 U)*
10 μ L	Total
*Add the reverse transcriptase just prior to use. Mix well by pipetting and spin the tube briefly in a microcentrifuge	

- Incubate the tubes at 42 °C for 1½ h.
- PCR amplification is performed on the cDNA. Prepare a PCR Master Mix for all reactions. Combine the following reagents in the order shown then add to cDNA:

74 μ L	Deionized H ₂ O
10 μ L	10 \times Advantage 2 PCR Buffer
2 μ L	50 \times dNTP Mix (10 mM)
2 μ L	5' PCR Primer II A (12 μ M) (Table 1)
2 μ L	50 \times Advantage 2 Polymerase Mix
10 μ L	cDNA
100 μ L	Total

- The above mixture is amplified with the following conditions:
95 °C 1 min 1 cycle
X cycles (16–23):
95 °C 15 s
65 °C 30 s
68 °C 3 min
Hold 4 °C ∞ *
- Check amplification on an agarose gel with 10 μ L (*see* **Note 17**).
- Purify the amplified cDNA with 1.8 volumes of AMPure XP Reagent (180 μ L) as described in Subheading 3.3.1, **step 10** and eluted with 50 μ L of Nuclease-free water. Transfer the supernatant containing the eluted DNA to a Covaris

microTUBE AFA Fiber Screw-Cap tube. It is optional to Qubit the sample to obtain a DNA concentration. Run a gel with 5 μL .

8. Covaris shearing: DNA Shearing with M220 Focused-ultrasonicator.
- Sonicate to 200–300 bp depending on the sequencing protocol (300 for PGM and 200 for Proton).
9. End repair and purify the DNA with components from an Ion Plus Fragment Library Kit (*see* **Note 18**). Add 29 μL Nuclease-free water to the fragmented DNA to bring the total volume to 79 μL .

79 μL	Fragmented gDNA
20 μL	5 \times End Repair Buffer
1 μL	End Repair Enzyme
100 μL	Total

10. Incubate the end repair reaction for 20 min at room temperature.
11. Purify the amplified cDNA with 1.8 volumes of AMPure XP Reagent (180 μL) as described in Subheading 3.3.1, **step 10** and eluted with 25 μL of Nuclease-free water.
12. Ligate and nick repair the end repair DNA.
- 25 $^{\circ}\text{C}$ 15 min
- 72 $^{\circ}\text{C}$ 5 min
- Hold 4 $^{\circ}\text{C}$ ∞

25 μL	DNA
10 μL	10 \times Ligase Buffer
2 μL	Adapters*
2 μL	dNTP Mix
51 μL	Nuclease-free water
2 μL	DNA Ligase
8 μL	Nick Repair Polymerase
100 μL	Total
*If barcoded libraries are needed, P1 Adapter and the desired barcode adapters can be substituted	

Place the tube in a thermal cycler and run the following program:

13. Purify the amplified cDNA with 1.8 volumes of AMPure XP Reagent (180 μ L) as described in Subheading 3.3.1, **step 10** and eluted with 40 μ L of Nuclease-free water.
14. PCR amplification is performed on the adaptor-ligated purified dsDNA:

200.0 μ L	Platinum [®] PCR SuperMix High Fidelity (<i>see</i> Note 12)
10.0 μ L	PCR Primers mix (10 μ M) each (Table 1)
40.0 μ L	dsDNA
250.0 μ L	Total volume

15. The above mixture is amplified with the following conditions (*see* **Note 13**):
 - 95 °C for 30 s 1 cycle
 - X cycles: (16–18)
 - 95 °C for 30 s
 - 58 °C for 30 s
 - 72 °C for 1 min
 - Hold 4 °C ∞
16. Purify the amplified cDNA with 1.8 volumes of AMPure XP Reagent (180 μ L) as described in Subheading 3.3.1, **step 10** and eluted with 25 μ L of Nuclease-free water. Proceed to size selection.

This can be a *pause point* and samples can be stored at -20°C (*see* **Note 14**).

3.4 Library Size Selection Quality/ Quantity Assessment: Timing 2 h

There are two criteria for a quality library: the library size and DNA amount. Ideally when a library is visualized on an agarose gel, there will be one very sharp band at the appropriate size. However, there is usually a smear. There are several options to obtain the perfect size. One way is to size select with the AMPure XP or SPRIselect reagent kit (Cat # B23317, Beckman Coulter, Inc.). Here, a double extraction is performed to remove the larger then smaller fragments of dsDNA. The new SPRIselect reagent kit is reported to give a tighter selection but was not demonstrated in our lab. If the bead size selection is not precise enough, we use the E-Gel[®] Size-Select[™] system run with several markers to obtain the appropriate size. With very low amounts of starting RNA, we can adjust the number of cycles and/or increase the volume in the PCR to increase the final amount of product. The size and quantity are optimized by analyzing the collected samples on a Bioanalyzer/

TapeStation and Qubit. However, the disadvantage to the E-Gel[®] system is a larger amount of material lost.

1. The amplified PCR product is visualized on a 2 % agarose gel for adequate concentration.
 - (i) The amplified PCR product is purified with 1.8 volumes of AMPure XP Reagent (450 μ L) as described above and eluted with 20 μ L of Nuclease-free water.
 - (ii) Fractionation to the appropriate size is performed on an E-Gel[®] SizeSelect[™] 2 % Agarose; *see* Fig. 6 (*see* **Note 19**). Size of the band isolation is dependent on the templating and sequencing kits. For 200 bp templating and sequencing kits, the sequencing library cannot be >320 bp.
 - (iii) Band isolations are then run on an Agilent Bioanalyzer[™] High Sensitivity DNA chip to assess size and quantity; *see* Fig. 8a (*see* **Note 20**).
 - (iv) If sample concentration is adequate, the sample is ready for emulsion PCR.
2. In general, 2–3 libraries can be constructed in parallel by one person and, including the quality assignment step, we recommend reserving a separate day for this part of the protocol.

3.5 Template Preparation: Day 2, Timing 5 h Total

3.5.1 Clonal Amplification and Enrichment

Resultant cDNA produced from a library cannot be sequenced directly due to a limited sensitivity of the Ion Torrent sequencing platform. Thus, amplification steps are required using emulsion PCR (emPCR, Fig. 4). Key to the success of this procedure is obtaining one DNA molecule per Ion Sphere[™] particle (single primer-coated bead) in an oil emulsion. During this amplification, each droplet contains a single DNA template attached to an Ion Sphere[™] particle forming a clonal colony; this is the final template (**Note 21**). Using the described number of molecules in Ion Torrent, sample preparations are critical for an optimal sequencing run. The amount of DNA in the library (e.g., in picomoles) can be measured using a typical Bioanalyzer assay step; the number of molecules can be determined by multiplying with Avogadro's number and then performing a unit conversion. For the 200 bp templating and sequencing kits, the optimal concentration is 15.5×10^6 molecules per μ L. An alternative would be qRT-PCR, but this is a more time-consuming step. The final determination of the optimal number of molecules in the sequencing sample has been determined by Ion Torrent; thus performing titration steps might not be necessary.

There are two ways to achieve the template bead preparation: (a) the automated OneTouch[™] system coupled with the enrichment Ion OneTouch[™] ES instrument (Fig. 4) or (b) a manual method to set up clonal amplification and enrichment.

Key Quality Control Steps in Semiconductor Sequencing

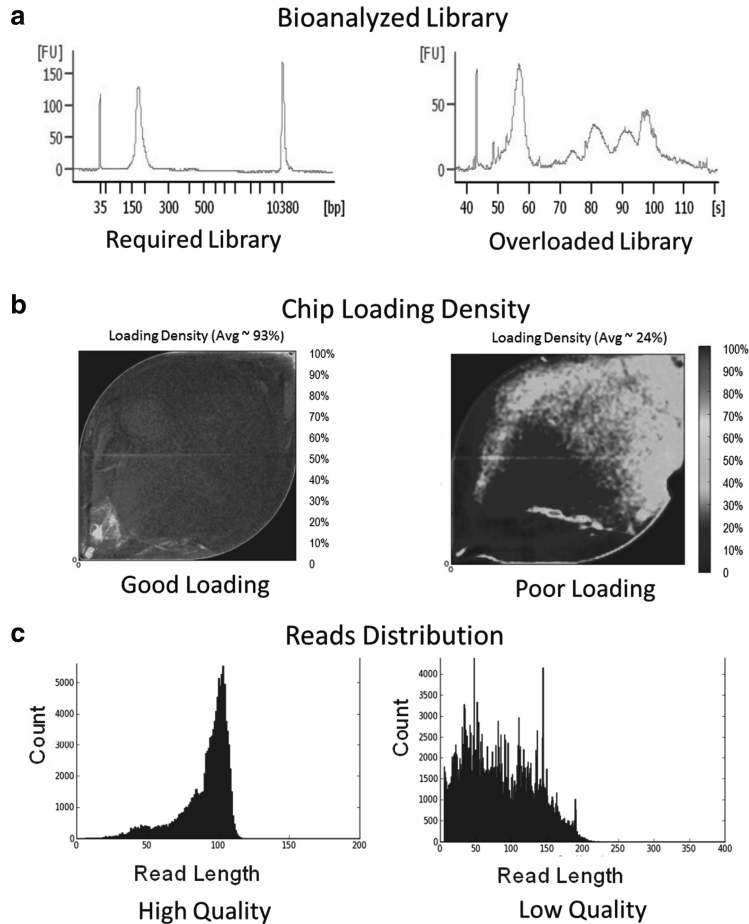


Fig. 8 Quality controls for Ion PGM sequencing. **(a)** Electropherograms of high-quality Bioanalyzer runs of sequencing libraries showing a sharp peak at 200 bp on *left*. The second electropherogram is an example of overloading that will not give accurate concentrations. **(b)** Examples of different loading density on an Ion chip. The higher density, indicated by *red*, gives more sequences. **(c)** Examples of sequencing read distributions from two different Ion Torrent sequencing runs. The plot on *left* shows a higher-quality distribution compared to a low-quality distribution of the sequencing reads in the plot on the *right*. The high-quality plot was from ~30 cells in the CA1 area of the rat hippocampus and the lower-quality plot was from *Aplysia californica* (Color figure online)

Here, we describe the automated OneTouch™ System requiring as little as 5 min of hands-on time and less than 5 h for the total duration of the procedure.

The Ion OneTouch™ Instrument has three key technologies that enable automated delivery of templated Ion Sphere™ particles. First is a reaction filter that creates millions of microreactors in

3.5.2 Preparation of
Template-Positive
Particles (ISPs) on the Ion
OneTouch™ Instrument

which clonal amplification occurs. Second is the in-line PCR amplification plate that enables thermal cycling of the microreactors. Third is the integrated centrifuge, which recovers the templated Ion Sphere™ particles. Combined with the Ion OneTouch™ ES, this is the first automated massively parallel clonal amplification and recovery process that permits minimal hands-on time on the market today.

- 1. OneTouch setup:
 - (i) Install the amplification plate from the kit.
 - (ii) Ion OneTouch™ Oil is installed on the left front port.
 - (iii) Ion OneTouch™ Recovery Solution is installed on the right front port.
 - (iv) 2 Ion OneTouch™ Recovery Tubes and the Ion One Touch™ Recovery Router are installed in the centrifuge.
- 2. Prepare the amplification solution in order listed:

280.0 µL	Nuclease-free water
500.0 µL	Ion OneTouch™ 2× Reagent Mix (<i>see Note 17</i>)
100.0 µL	Ion OneTouch™ Enzyme Mix
100.0 µL	Ion OneTouch 200 Reagent P
20.0 µL	Diluted library (15.5×10^6 molecules per µL)
100.0 µL	Ion OneTouch™ 200 Ion Sphere™ Particles (vortexed for 1 min)
1,000.0 µL	Total volume

- 3. Mix this amplification solution by pipetting up and down, then transfer the entire volume to the Ion OneTouch™ Reaction Tube/filter assembly.
- 4. Gently layer and fill the tube with 1,500 µL Ion OneTouch™ Reaction Oil over the amplification solution.
- 5. Secure an Ion OneTouch™ Reaction Filter to the Reaction Tube.
- 6. Slowly invert the Reaction Filter/Reaction Tube assembly.
- 7. Firmly insert the three prongs of the inverted Reaction Filter into the three ports on the top stage of the Ion OneTouch™ Instrument.
- 8. Run the Ion OneTouch™ Instrument (we typically do two samples a day and run the second sample overnight). This can be a *pause point*.

3.5.3 Ion Sphere™ Particles Recovery

This step removes template-positive ISPs from the OneTouch™ Recovery Solution and prepares them for enrichment.

1. Remove both Recovery Tubes from the centrifuge, then remove all but ~50 µL of Ion OneTouch™ Recovery Solution from each Ion OneTouch™ Recovery Tube (*see Note 22*).
2. Resuspend the template-positive ISPs in the remaining Recovery Solution by pipetting the pellet up and down.
3. Add 1 mL of Ion OneTouch™ Wash Solution to the pooled template-positive ISPs.
4. Centrifuge for 2.5 min at $15,500 \times g$, and then remove all but 100 µL of supernatant, and vortex the pellet for 10 s to completely resuspend.
5. Transfer a 2.0 µL aliquot of the recovered material to a 0.2 mL PCR Tube; then assess the quality using a Qubit® 2.0 Fluorometer.
6. Sample is ready for enrichment.

3.5.4 Enriching the Template-Positive ISPs with the Ion OneTouch™ ES

After clonal amplification, the non-templated ISPs are removed from the templated ISPs. The Ion OneTouch™ ES uses magnetic bead technology to isolate template-positive Ion Sphere™ particles that can be loaded directly onto the Ion semiconductor chip thus delivering automated, highly reproducible enrichment with every run.

1. Prepare fresh Melt-Off Solution daily.

865.0 µL	Nuclease-free water
125.0 µL	1 M NaOH
10.0 µL	10 % Tween 20 in Nuclease-free water
1,000.0 µL	Total volume

2. Add 130.0 µL of MyOne™ Beads Wash Solution and 13.0 µL of Dynabeads MyOne™ Streptavidin C1 magnetic beads to a 1.5 mL LoBind Tube and mix.
3. Place the tube on a magnet such as a DynaMag™-2 magnet for 2 min, then remove and discard the supernatant. Repeat two times.
4. Resuspend MyOne™ Beads in 130.0 µL of MyOne™ Beads Wash Solution.
5. Obtain an 8-well strip from the Ion OneTouch™ kit. Ensure that the square-shaped tab of the 8-well strip is on the left.
6. Transfer the entire volume (100.0 µL) of the sample to Well 1.

7. Add the resuspended MyOne™ Beads (130.0 µL) to Well 2.
8. In Wells 3, 4, and 5 add Ion OneTouch™ Wash Solution.
9. Leave Wells 6 and 8 empty and fill Well 7 with 300.0 µL of fresh melt-off solution.

3.5.5 Prepare the Ion OneTouch™ ES

1. Place a new tip on the Tip Arm.
2. Place a new 0.2 mL PCR Tube in the base of the Tip Loader with cap open.
3. Place the eight-well strip in right side of slot.
4. Run the enrichment.

3.5.6 Remove and Wash the Template-Positive Ion Sphere™ Particles

1. Spin the enriched sample at $15,500 \times g$ for 1.5 min. Check that there is no carryover of the brown MyOne™ Beads in the pellet (*see Note 23*).
2. Remove all but ~10 µL of supernatant without disturbing the pellet, then add 200 µL of Ion OneTouch™ Wash Solution, resuspend, and repeat centrifugation.
3. Remove all but ~10 µL of supernatant without disturbing the pellet and add up to 100 µL of Ion OneTouch™ Wash Solution and resuspend. Sample is ready to sequence.
4. Transfer a 10 µL aliquot of the recovered material to a 0.2 mL PCR Tube; then assess the quality using a Qubit® 2.0 Fluorometer (*see Note 24* for the Ion Sphere™ Quality Control Kit process).

3.6 Sequencing on the Ion Torrent: Timing 4 h (Depending on Chip)

All reagents are from the Ion PGM™200 Sequencing Kit (Cat # 4474004, Ion Torrent, Life Technologies) and Ion 314™ Chip Cat # 4462923 (8 pack), 316™ Chip Cat # 4466616 (4 pack), 318™ Chip Cat # 4466617 (4 pack) Life Technologies. The protocol is basically the same with variation in the volumes of some reagents for the three different chips. We will focus on the 314 chip because this is the chip we have used the most.

1. Clean the Ion Torrent as recommended by following on-screen prompts.
2. Wash all bottles with MilliQ water (or an equivalent 18 MΩ water system) three times.
3. Prepare fresh solutions of 1 M and 100 mM NaOH.
4. Add buffers to Wash 1 and Wash 3 bottles.
5. Prepare Wash 2 solution.
6. Add dNTPs to conical tubes.
7. Initialize the Ion Torrent and follow on-screen prompts.

3.6.1 Sample Preparation

1. Prepare enriched sample (template-positive ISPs) for sequencing.
2. Transfer half of the volume of enriched ISPs to a 200.0 μL PCR Tube.
3. Vortex the Control Ion Sphere™ particles and add 5.0 μL to the sample.
4. Add 100.0 μL of Annealing Buffer, mix by pipetting, and centrifuge for 1.5 min at $15,500 \times g$.
5. Carefully remove the supernatant leaving approximately 3.0 μL in the tube, add 3.0 μL of Sequencing Primer, and pipette up and down thoroughly to disrupt the pellet.
6. PCR:
 - 94 °C for 2 min
 - 37 °C for 2 min

3.6.2 Chip Check and Preparation

1. Place the chip on the PGM™ System grounding plate.
2. Press Experiment on the main menu of the PGM.
3. When prompted, lift the chip clamp and replace the old chip with your new chip, then close the chip clamp.
4. Press Chip Check and look for leaks.
5. Add 50.0 μL of 100 % isopropanol to the loading port of the chip, and then remove excess liquid from the other port. Then repeat twice with 50.0 μL of Annealing Buffer. When pipetting liquid into the chip, keep the pipette tip at a 90° angle to the chip, press the tip firmly into the circular loading port, and apply gentle pressure between the pipette tip and chip.

3.6.3 Load the Chip

1. Remove the template-positive ISPs from the thermal cycler and add 1.0 μL of PGM™ 200 Sequencing Polymerase to a final volume of 7.0 μL , mix, and let set at room temperature for 5 min.
2. Remove residual Annealing Buffer from the chip by tilting the chip at 45 °C, then inserting the pipette tip into the loading port, and removing all liquid.
3. Centrifuge the chip upside-down with tab pointing in for 5 s.
4. Following polymerase incubation, load the entire sample (~7 μL) into the loading port by dialing down the pipette to gently and slowly deposit the ISPs at a rate of ~1 μL per second.
5. Remove any displaced liquid from the other port of the chip.
6. Centrifuge for 30 s.

7. Mix the sample on the chip.
 - (i) Set the pipette volume to 5.0 μL .
 - (ii) Tilt the chip at a 45° angle so that the loading port is the lower port.
 - (iii) Insert the pipette tip into the loading port and slowly pipette the sample in and out three times. Avoid creating small bubbles.
 - (iv) Centrifuge for 30 s with tab pointing out.
 - (v) Repeat step (iii).
 - (vi) Centrifuge for 30 s with tab pointing in.
8. Tilt the chip at a 45° angle and slowly remove as much liquid as possible from the loading port by dialing the pipette. Discard the liquid (*see Note 25*).
9. Spin or tap the chip to remove excess liquid.
10. Perform Run.
11. Upload Run Plan with all information and follow on-screen prompts.
12. Press Next to begin the run.
13. When the run is complete, the touch screen will return to the Main Menu. You can then proceed with another run or perform a cleaning/initializing step if required (*see Note 26*).

3.7 Assessing the Sequencing Run

1. The quality of a run is dependent on many factors:
 - (i) Quality and quantity of the templated library needs to meet specifications. For the 200PGM sequencing kit, we load 15.5×10^6 molecules with as tight as possible distribution between 200 and 320 bp for templating on the OneTouch; *see* Fig. 8a (*see Note 20* for Bioanalyzer suggestions).
 - (ii) Loading of the chip, *see* Fig. 8b. The higher the density, the better (*see Note 25*).
 - (iii) Size distribution should be in an appropriate range for the sequencing kit used and the size of the band isolated from the library; *see* Fig. 8b. It is best to have a tight distribution rather than a wide distribution with a high population of short fragments; *see* Fig. 8c.
 - (iv) Homopolymers are problematic with flow-based sequencing technology. With Torrent Suite Software version 3.2's Variant Caller, sensitivity has increased more than two times, allowing indels to be called accurately within homopolymer regions 2–8 bp in length.

3.7.1 Summary Statistics for a Sequencing Run and Assessment

The number of reads and bases generated are dependent on the chip type, sequencing kit, and server software used in the process (*see* Fig. 2 table). In the last year we have experienced a 100-fold increase in sequence output with the cost remaining the same. The existing four different chips offer substantial flexibility to design different projects from pilot and time-course studies to deep sequencing of selected samples. For example, samples with less confidence can quickly be sequenced on a 314 chip for \$350.00 (*see* **Note 27**). Once data are generated, a decision can be made whether to proceed with greater sequencing coverage as the next step—which can still be performed in less than 2 days. The speed of the described pipeline allows for a plethora of experiments following development, neuroplasticity, or aging steps in a rapid and cost-efficient manner that can be rapidly adjusted for emerging experimental needs.

3.7.2 Bioinformatic Pipeline “Zero-Click”

Although it is not described in the current protocol, we developed and implemented an automated transcriptome analysis pipeline [23] that assembles Ion Torrent output directly from the server without human intervention, following its automatic annotation using NCBI and Swiss-Prot databases. This *fast turnaround-time* pipeline is also integrated with GO ontology, KEGG pathways, and Pfam Domains. Other prediction systems can be incorporated such as secretory/signaling peptide predictions. With the “Zero-click pipeline,” once sequencing begins, the data are removed from the server, automatically processed, and uploaded to our database for viewing with all features accessible.

3.7.3 Update and Future Directions

For all practical purposes, most of the current 314 and 316 series chips optimally target the smRNA, amplicon, and smaller microbial genome sequencing applications. The current 318 chips for semiconductor sequencing are also well suited for deep de novo transcriptome analysis, small genome resequencing, and even enriched methylome sequencing [1]. However, the Ion PGM is not the best choice for sequencing larger genomes (>0.1 Gb) because of its limited throughput. To accommodate the demand for applications requiring higher throughput, such as sequencing of more complex/animal genomes, Life Technologies has released a new sequencer called the Ion Proton [6] that we successfully tested in our laboratory (IP1 chip), collecting about 9–10 Gb of sequencing data for the same applications indicated above, as well as for human exomes. Although it uses the same principle, the second version of the IP2 chip is expected to produce 33 Gb, and the third iteration IP2 chip might produce about 124 Gb of sequencing data (Fig. 2). This throughput will be sufficient to sequence a human-size genome within a day or multiple transcriptomes/exomes using barcoding options. Along with the growth of the sequence output, the length of reads is also improving, with sequencing lengths

of 400 bp currently achievable (Fig. 2) and longer reads of up to 640 bp reported at the latest AGBT-2013 meeting (http://ioncommunity.lifetechnologies.com/community/programs_and_events/agbt2013). Further technology improvements [6] include introduction of the Ion ChefTM as an integrated liquid handling and robotic station, as well as development of alternatives to emulsion PCR (e.g., *Avalanche*TM). Critical to genome sequencing is the paired end and mate-pair library options which are also available. In addition, the upgrade of the Ion server software suite to version 2.2 and now 3.2 greatly improved accuracy compared to the 2.0 version, as has been reported [24].

For practical purposes, a new OneTouch kit was recently released, Ion OneTouchTM 200 Template Kit v2 DL (Cat # 4480285 Ion Torrent, Life Technologies), together with new Ion server software suite version 3.2. The new OneTouchTM 200 Template Kit v2 DL kit helps prevent clogging issues with the OneTouch instrument, and the new software has new user interfaces for planning. Additional resources, descriptions, and demonstrations can be found on the Ion community at <http://ioncommunity.iontorrent.com>. The webpage provides both the latest updates and allows download of novel protocols. The site also includes a discussion page where users can submit problems and discuss potential problems with both other users and consultants.

In summary, the combination of the *Ion PGM* and the *Ion Proton* instruments can make a single laboratory as a task-oriented complementary sequencing center able to sequence transcriptomes, genomes, and methylomes. Considering the enormous heterogeneity of cell populations in nervous systems and the complexity of developmental, neurodegenerative, and aging processes, the current advances in semiconductor sequencing offer novel opportunities for many fields of experimental biology and clinical studies: from whole genome sequencing in personalized medicine down to targeted probing of dynamic genomic and epigenomic organizations of individual cells (see additional details in ref. 1).

4 Notes

1. From our experience with more than 200 different invertebrate species, if RNA cannot be isolated immediately from tissue or even single cells, we prefer placing the tissue in 100 % ethanol rather than Ambion's RNAlater[®] for shipping or storage. We have obtained mixed results with RNAlater[®] based on the quality of the RNA isolated. Tissue and/or single cells can be stored in lysis buffer and frozen at -20°C as long as the cells or tissues are totally lysed before freezing. The kits with a lysis buffer that we find work best for this procedure are Ambion/

Life Technologies, RNAqueous[®] Kits. We use the Ambion RNAqueous-Micro[™] Kit for individual *Aplysia* cells and hippocampal neurons and the regular RNAqueous[®] Kit for larger parts of the rat brain and developmental tissues. We did not note any substantial RNA degradation for up to a month using the described storage.

2. A number of RNA isolation methods and protocols are widely available and can be classified into four general techniques: organic extraction methods, spin basket or column formats, magnetic particle methods, and direct lysis methods. For the organic extraction process, the sample is homogenized in a phenol-containing solution and the sample is then centrifuged. This method cannot be efficiently used for the small amounts of starting material in single cells and is not considered here. The spin bucket or column protocol is best for small samples. Two kits have proven to work best for our samples: Ambion/Life Technologies RNAqueous[™] and the RNAqueous-Micro[™] kits. Qiagen's RNeasy Plus Mini Kit with gDNA Eliminator Spin Columns (Cat # 74134) as well as the QIAshredder (Cat # 79654) tissue shredders are also convenient. The QIAshredder can be used for simple and rapid homogenization of cell and tissue lysates. There is also the mini version of RNeasy Micro Kit (Cat # 74004) for small amounts of tissue, like single cells. We also efficiently used Qiagen kits, especially the columns for removal of the gDNA, and have gotten very good results.

Nevertheless, the kits described above cannot be used effectively with pigmented tissue like retina or chromatophores. For these purposes, we employed NUCLEOSPIN RNA II from Macherey-Nagel (Fisher Cat # NC9581114). Here, we have used the RNAqueous[™] lysis buffer to lyse pigmented tissue then followed the column spin protocol in this kit to get excellent RNA quality and yield.

3. Many invertebrates including gastropod molluscs such as *Aplysia* have rRNA that does not have the same electrophoretic mobility as vertebrate rRNA, in which the intact total RNA has a larger (28s) rRNA band that is twice as intense as the smaller (18s) band when denatured. *Aplysia*'s 28s rRNA has a true break in the middle of the rRNA molecule, which is called the "hidden break," and under non-denaturing conditions, the rRNA molecule is held in one piece by the hydrogen bonding between its secondary structure elements [18]. However when heated, the two halves of the 28s rRNA separate and have similar electrophoretic mobility to the 18s rRNA, thus producing only one peak on the Bioanalyzer. The electrophoretic mobility pattern is species specific, creating many unique patterns (*see* Fig. 6 for several examples).

4. We have successfully employed RiboMinus™ on as little as 20 ng of total RNA starting material.

Ribosomal-depleted starting material will ensure reduced ribosomal “contamination” in the final sequencing library. This is an optional step and is useful to reduce nonspecific capture of rRNAs, which is very common for any existing protocol. Clearly, this step is essential if random primers are to be used.

5. We like the convenience of one kit having all the cDNA synthesis components, as with Clontech’s Marathon cDNA amplification kit. However, cheaper and just as effective alternatives are available. Any of the MMLV reverse transcriptases can be used for first-strand synthesis, *see* **Note 6**. Recently NEB came out with NEBNext® mRNA second strand synthesis module (NEB Cat # E6111) that is compatible with this protocol. These alternatives reduce the library construction costs by a quarter of the price of the Marathon cDNA amplification kit.
6. Currently, we are unable to sequence RNA directly; therefore RNA must be converted to cDNA, then to double stranded DNA (dsDNA) for sequencing library constructions. The starting point of all sequencing comes in a form of RNA amplification for which there are two major strategies. First is the linear amplification of in vitro transcription (IVT) which was widely employed by the microarray industry. The second approach is PCR-based amplification. Both strategies have their advantages and disadvantages. For ultra-small amounts of material such as a single cell, PCR methodology is far more applicable. PCR amplification methods still require generation of cDNA, and several options for reverse transcriptases (RT) are commercially available [avian myeloblastosis virus (AMV) and Moloney murine leukemia virus (MMLV)]. With the more traditional AMV RT, first-strand cDNA is synthesized then the second strand is synthesized with a cocktail of enzymes. Another popular method of cDNA generation is the template-switch method with an MMLV RT such as SMARTScribe™ (Cat # 634925, Clontech). This template-switch method uses the unique properties of the MMLV enzyme to synthesize additional nucleotides at the 3′ end of the cDNA, then uses a template-switch oligo to reverse direction and make the complementary second strand. Fragmentation of sequencing material is critical for all technologies. One can start RNA fragmentation using one of several techniques (heat, NaOH, RNaseIII), followed by ligation of RNA adaptors, then cDNA can be generated and PCR amplified (as in the Illumina, SOLiD, and the new Ion Torrent RNA-seq libraries). This approach does generate directionality to the library, but requires µg quantities of starting material and is not applicable to low amounts of starting material. For single cells, the

template-switch method is attractive and what we use for the second protocol presented here. We use a commercially produced kit for reproducibility, consistency, and quality control, Marathon cDNA Amplification Kit (Cat # 634913, Clontech) which contains an AMV reverse transcriptase and a DNA polymerase I/RNaseH/DNA ligase enzyme cocktail. Once the second strand cDNA is produced, we polish the ends with T4 DNA polymerase, making it suitable for sequential blunt-end library-specific adaptor ligations followed by PCR amplification.

7. We used a shorter than usual oligo dT (13Ts compared to 30Ts) primer in our reverse transcription because we were promoting a more promiscuous priming of the oligo dT in hopes of priming upstream of the terminal oligo dT tail, thus obtaining less of the 3'UTR. This method was efficiently used for our EST collections as described [14]. Also the oligo dT portion of the primer was designed to target invertebrate RNA.
8. These controls allow us to monitor the quality of the library. The directionality was confirmed with the spike-ins (only 0.7 % was sequenced in the antisense direction). Also, their spiked-in copy number showed a linear relation to their specific number of reads [1].
9. The Adaptors A and P1 are made with one primer having a large overhang. This overhang helps prevent adaptors ligating to each other and forming primer/dimers. To produce the adaptors, individual primers are annealed together by mixing equal molar concentrations of each primer, then heating the mixtures at 72 °C for 2 min, 42 °C for 2 min, then 37 °C for 30 min.
10. Sequential addition of adaptors with purification between steps ensures strandedness of the fragments and thus directionality to our libraries. This also promotes reduced representation of the library. Purification between steps does cause loss of material, but insures directionality as well as reduced representation of the overall library (*see Comment 2*). Thus, the same amount of sequencing coverage captures more distinct transcripts from a cell. Second, by preserving strandedness, this approach unbiasedly represents both sense and antisense RNAs expressed in a given cell. Some potential drawbacks of using reduced representation methods (versus methods with random fragmentation of all transcripts) might be a reduced ability to observe certain events such as alternative splicing from the 5' end of very long transcripts. However, in contrast to the current reduced representation method, conventional random fragmentation protocols do require a significantly deeper sequence coverage and inability to separate sense and antisense transcriptional events.

11. The time and combination of restriction enzymes can be varied for the technology used. Both AluI and RsaI are 4 base blunt-end cutters and in theory should cut every 256 bases if the DNA was random. By combining the enzymes, you can obtain smaller fragmentation of the library or vice versa.
12. The number of cycles of PCR amplification is dependent on the amount of starting material. We have started with as little as 40 pg of total RNA. Most times we use between 15 and 22 cycles of PCR amplification.
13. We like LA Taq™ (Cat # RR002M, Clontech) and Advantage® 2 Polymerase Mix (Cat # 639201, Clontech) just as well as Platinum Taq. All are interchangeable and give similar results with slight variations in price.
14. The design of this library is to target the 5' end of a transcript. A complementary 3' targeted library can be constructed in which the timing of the ligation of adaptors and digestion is adjusted. Here, after second strand synthesis the dsDNA is digested with the same enzyme pair as above, then purified with AMPure XP Reagent. Then the 5' adaptor A is ligated. The PCR amplification uses the A primer and a P1 primer extension of the cDNA synthesis primer. This library maintains directionality and quantification. When working with very low amounts of starting material (picograms), this method is preferred because it requires the least amount of manipulation and steps. 15–21 PCR cycles are typically required in stage 21 of library construction. However, in a case of small cells (40–50 µm, such as *Aplysia* sensory neurons and interneurons), we successfully used up to 23 cycles.
15. A cheaper method of library construction is to make your own template-switch oligo and use your preferred MMLV reverse transcriptase such as SuperScript® (Invitrogen/ Life technologies) or SMARTScribe Reverse Transcriptase (Clontech). This will cut the cost of a library by 75 %. However, the SMARTer® PCR cDNA Synthesis Kit (Clontech) is convenient and great for less-experienced people to work with.
16. The SMARTer II A Oligonucleotide can be synthesized by substituting three ribo Guanosine (rG) for the proprietary Xs (Table 1). We did side-by-side comparisons of the commercial and our oligo, and they both produce the same amount of amplified cDNA under the same conditions.
17. The amplification product for the cDNA will appear as a smear on an agarose gel. It is best to check several time points so as to not over amplify. Overcycled cDNA will have large molecular weight fragments.
18. New England BioLabs Inc. recently introduced their line of library construction kits for Ion Torrent, NEBNext® Fast DNA

Library Prep Set for Ion Torrent™ (Cat # E6270S, NEB). We did side-by-side comparisons and got comparable results from the Ion Torrent/Life Technologies and NEB kits.

19. E-Gel® technology is a quick and easy 15 min size separation and recovery system for library construction. However, it is critical to collect more than one sample for the library process. Getting the exact size and concentration of amplified library can be more complicated. We do four different sample extractions for each library around the size of interest on the gel, also making sure to replace the liquid in the wells (each sample should be run on the Bioanalyzer for RNA quality). For 200 bp templating and sequencing kits, we start collecting samples at ~280 bp, then 300 and 320 bp, and finally reverse to 300 bp again. This ensures that we get the best combination of size and concentration for described libraries.
20. Using the Agilent Bioanalyzer™ High Sensitivity DNA Kit can be complicated and time consuming and remains the current and substantial bottleneck (ironically, one almost needs to know the concentration of a sample before it can be run for the assay). We usually obtain the concentration of a sample with Qubit if we have enough material, but for single cells it is not an option. It is also important not to load over 500 pg/μL in each well, since it might clog the Bioanalyzer pins. Recently, the Agilent TapeStation 2200 was introduced and may be complementary to the Bioanalyzer. The TapeStation 2200 allows a laboratory to work with a few samples for faster assays. We have demonstrated that both machines produce comparable results.
21. The Ion OneTouch™ Reagent Mix has been problematic in the past. Small, undissolved particles can cause incomplete injection of the sample into the OneTouch™ machine. We let the reagent tube come to room temperature for 1 h and vortex for at least 1 min several times during that hour.
In principle, the emulsion PCR is one of the most critical steps in the process. At the beginning of the amplification, each droplet should (ideally) contain a single progenitor molecule at the *outset* of the emulsion PCR process (Fig. 4). These are amplified within the droplets, such that the result is that each bead contains many clonal copies of the progenitor molecule. A noticeable disadvantage of this approach is that it is necessary to carefully titrate the library prior to emulsion PCR in order to obtain no more than one library molecule per droplet. In practice, we often chose to make suggested calculations (as in Subheading 3.5.1) for initial screenings and, unfortunately, must tolerate up to 20–50 % of polyclonal reads that can be automatically removed by the Ion Torrent server. At the time of the writing, Life Technology announced that there is a possibility to eliminate the emulsion PCR step in the future,

which will make the entire procedure more robust and straightforward. Finally, for the proposed single-cell RNA-seq, we noted that homopolymers at the scale of 4–5 bases do not represent a problem in the initial mapping and annotation of transcripts. However, they might cause a problem for genotyping of repetitive and homopolymer regions in clinical applications. The expected greater coverage of the Ion Proton should (Fig. 2) also improve the accuracy of sequencing.

22. It is really difficult to visualize the Ion Spheres. So when centrifuging the Ion Spheres, it is always suggested to leave a certain volume in the tube and not disturb the pelleted spheres. For practical purposes, we fill the same size centrifuge tube with the appropriate volume then cap and tape them to shelves in front of the bench for quick eye level comparisons. This simple procedure speeds up the process for all the steps requiring this type of comparison.
23. Calibration of the Ion OneTouch™ ES magnetic enrichment machine is critical to avoid carryover of the brown MyOne™ Beads in the pelleted template-positive particles (ISPs). We found that if this happens it is best to redo the process from the preparation of template-positive particles (ISPs) on the Ion OneTouch™ instrument.
24. The Ion Sphere™ Quality Control Kit is used to perform templated bead quality control using the Qubit fluorometer. The process labels a sample by hybridizing the Ion Sphere™ Particles (ISPs) 200 with two different fluorophores: Alexa Fluor® 488 and Alexa Fluor® 647. The probe labeled Alexa Fluor® 488 anneals to primer B sites, or all of the ISPs present, and the probe labeled Alexa Fluor® 647 anneals to primer A sites, or only the ISPs with extended templates. Then the ratio of the Alexa Fluor® 488 fluorescence (all ISPs present) to the Alexa Fluor® 647 fluorescence (templated ISPs) yields the % templated ISPs. The protocol is a short hybridization of the labeled probes and templated ISPs followed by several washes to remove the excess probes. Unenriched templated ISPs are collected after the emPCR with the Ion OneTouch™ instrument, and enriched templated ISPs are collected after enrichment on the Ion OneTouch™ ES magnetic enrichment machine. An excel format of the Qubit® 2.0 Easy Calculator containing the Calibration Factor (obtained from the ISP lot used) is used to calculate Percent Templated ISPs. Optimal values are between 10 and 30 % for an unenriched templated ISPs and >50 % for an enriched templated ISPs. It can be determined if a sample has been properly templated and/or enriched. We use this on questionable samples.

25. Removing liquid from the chip gives better loading; however, removing all liquid from the 314 chip is very challenging. Even if a small amount of liquid remains, our yields are above company specifications.
26. The Ion Torrent system recommends performing two sequencing runs per instrument initialization. We always sequence two samples consecutively for cost benefits.
27. Cost as of July 2012 for sequencing one sample is the following: 314 chip—\$99.00, 316 chip—\$150.00, and 318 chip—\$499.00. The OneTouch™ and sequencing reagents are the same for all chips, \$125.00 for the OneTouch™ and \$125.00 for sequencing per sample.

Acknowledgements

We would like to thank our collaborators Drs. Thomas Foster, C. Jason Frazier, Scott Harden and Mrs Elena Bobkiva (University of Florida) for the single neuron isolations and help with dissections. We also want to thank Alexander Fodor for help in single-cell library construction. We thank Mr. James Netherton for reading and commenting on the manuscript. We thank Dr. Manfred Lee for his technical advice and guidance with the Ion PGM sequencing process. We also thank Miss Brandi McLaughlin for help with her guidance and updates for semiconductor sequencing technologies and novel chips as well as for providing photos and schematic diagrams for Figs. 1a–c and 5. This work is supported by NIH grants 1R01GM097502, R21RR025699, 5R21DA030118, R01MH097062, McKnight Brain Research Foundation, Florida Biodiversity Institute as well as NSF-0744649, NSF CNS-0821622, and UF Opportunity Fund awards to LLM.

References

1. Moroz LL, Kohn AB (2013) Single-neuron transcriptome and methylome sequencing for epigenomic analysis of aging. In: Trygve O. Tollefsbol (ed.), *Biological Aging: Methods and Protocols*, Methods in Molecular Biology: Methods and Protocols, vol. 1048, DOI 10.1007/978-1-62703-556-9_21, # Springer Science +Business Media, New York 2013
2. Evrony GD, Cai X, Lee E, Hills LB, Elhosary PC, Lehmann HS, Parker JJ, Atabay KD, Gilmore EC, Poduri A, Park PJ, Walsh CA (2012) Single-neuron sequencing analysis of 11 retrotransposition and somatic mutation in the human brain. *Cell* 151:483–496
3. Tang F, Lao K, Surani MA (2011) Development and applications of single-cell transcriptome analysis. *Nat Methods* 8:S6–S11
4. Moroz LL, Kohn AB (2010) Do different neurons age differently? Direct genome-wide analysis of aging in single identified cholinergic neurons. *Front Aging Neurosci* 2:1–18
5. Navin N, Kendall J, Troge J, Andrews P, Rodgers L, McIndoo J, Cook K, Stepansky A, Levy D, Esposito D, Muthuswamy L, Krasnitz A, McCombie WR, Hicks J, Wigler M (2011) Tumour evolution inferred by single-cell sequencing. *Nature* 472:90–94
6. Merriman B, Rothberg JM (2012) Progress in ion torrent semiconductor chip based sequencing. *Electrophoresis* 33:3397–3417
7. Rothberg JM, Hinz W, Rearick TM, Schultz J, Mileski W, Davey M, Leamon JH, Johnson K, Milgrew MJ, Edwards M, Hoon J, Simons JF,

- Marran D, Myers JW, Davidson JF, Branting A, Nobile JR, Puc BP, Light D, Clark TA, Huber M, Branciforte JT, Stoner IB, Cawley SE, Lyons M, Fu Y, Homer N, Sedova M, Miao X, Reed B, Sabina J, Feierstein E, Schorn M, Alanjary M, Dimalanta E, Dressman D, Kasinskas R, Sokolsky T, Fidanza JA, Namsaraev E, McKernan KJ, Williams A, Roth GT, Bustillo J (2011) An integrated semiconductor device enabling non-optical genome sequencing. *Nature* 475:348–352
8. Walters ET, Bodnarova M, Billy AJ, Dulin MF, Diaz-Rios M, Miller MW, Moroz LL (2004) Somatotopic organization and functional properties of mechanosensory neurons expressing sensorin-A mRNA in *Aplysia californica*. *J Comp Neurol* 471:219–240
 9. Kandel ER (1976) Cellular basis of behavior. W.H. Freeman and Company, San Francisco
 10. Kandel ER (2001) The molecular biology of memory storage: a dialogue between genes and synapses. *Science* 294:1030–1038
 11. Moroz LL (2011) *Aplysia*. *Curr Biol* 21: R60–R61
 12. Ha TJ, Kohn AB, Bobkova YV, Moroz LL (2006) Molecular characterization of NMDA-like receptors in *Aplysia* and *Lymnaea*: relevance to memory mechanisms. *Biol Bull* 210:255–270
 13. Lovell P, Moroz LL (2006) The largest growth cones in the animal kingdom and dynamics of neuronal growth in cell culture of *Aplysia*. *Integr Comp Biol* 46:847–870
 14. Moroz LL, Edwards JR, Puthanveetil SV, Kohn AB, Ha T, Heyland A, Knudsen B, Sahni A, Yu F, Liu L, Jezzini S, Lovell P, Ianucculli W, Chen M, Nguyen T, Sheng H, Shaw R, Kalachikov S, Panchin YV, Farmerie W, Russo JJ, Ju J, Kandel ER (2006) Neuronal transcriptome of *Aplysia*: neuronal compartments and circuitry. *Cell* 127:1453–1467
 15. Heyland A, Vue Z, Voolstra CR, Medina M, Moroz LL (2011) Developmental transcriptome of *Aplysia californica*. *J Exp Zool B Mol Dev Evol* 316B:113–134
 16. Moroz LL (2006) Localization of putative nitrergic neurons in peripheral chemosensory areas and the central nervous system of *Aplysia californica*. *J Comp Neurol* 495:10–20
 17. Heyland A, Moroz LL (2006) Signaling mechanisms underlying metamorphic transitions in animals. *Integr Comp Biol* 46:743–759
 18. Karlstedt KA, Paatero GI, Makela JH, Wikgren BJ (1992) A hidden break in the 28.0S rRNA from *Diphyllbothrium dendriticum*. *J Helminthol* 66:193–197
 19. Ramskold D, Luo S, Wang YC, Li R, Deng Q, Faridani OR, Daniels GA, Khrebtsukova I, Loring JF, Laurent LC, Schroth GP, Sandberg R (2012) Full-length mRNA-Seq from single-cell levels of RNA and individual circulating tumor cells. *Nat Biotechnol* 30:777–782
 20. Islam S, Kjallquist U, Moliner A, Zajac P, Fan JB, Lonnerberg P, Linnarsson S (2011) Characterization of the single-cell transcriptional landscape by highly multiplex RNA-seq. *Genome Res* 21:1160–1167
 21. Tang F, Barbacioru C, Nordman E, Li B, Xu N, Bashkirov VI, Lao K, Surani MA (2010) RNA-Seq analysis to capture the transcriptome landscape of a single cell. *Nat Protoc* 5:516–535
 22. Tang F, Barbacioru C, Wang Y, Nordman E, Lee C, Xu N, Wang X, Bodeau J, Tuch BB, Siddiqui A, Lao K, Surani MA (2009) mRNA-Seq whole-transcriptome analysis of a single cell. *Nat Methods* 6:377–382
 23. Girardo DO, Citarella MR, Kohn AB, Moroz LL (2012) Automatic transcriptome analysis and quest for signaling molecules in basal metazoans. In: Society for integrative and comparative biology abstracts, Charleston, 3–7 Jan
 24. Loman NJ, Misra RV, Dallman TJ, Constantinidou C, Gharbia SE, Wain J, Pallen MJ (2012) Performance comparison of benchtop high-throughput sequencing platforms. *Nat Biotechnol* 30:434–439

Application of DNA Microarray Technology to Gerontological Studies

Kiyoshi Masuda, Yuki Kuwano, Kensei Nishida, and Kazuhito Rokutan

Abstract

Gene expression patterns change dramatically in aging and age-related events. The DNA microarray is now recognized as a useful device in molecular biology and widely used to identify the molecular mechanisms of aging and the biological effects of drugs for therapeutic purpose in age-related diseases. Recently, numerous technological advantages have led to the evolution of DNA microarrays and microarray-based techniques, revealing the genomic modification and all transcriptional activity. Here, we show the step-by-step methods currently used in our lab to handling the oligonucleotide microarray and miRNA microarray. Moreover, we introduce the protocols of ribonucleoprotein [RNP] immunoprecipitation followed by microarray analysis (RIP-chip) which reveal the target mRNA of age-related RNA-binding proteins.

Key words DNA microarray, Gerontological study, Aging, miRNA, RNA-binding protein, RIP-chip

1 Introduction

Gene expression patterns change dramatically depending on tissue and age. The specific subsets of proteins expressed at each time point allow cells to carry out the functions needed during development and differentiation. The tissue-specific patterns of gene expression at different developmental stages are potently regulated at the transcriptional level through the action of transcription factors such as FOXO (forkhead box), PPAR (peroxisome proliferator-activated receptor)- γ , p53, C/EBPs (CCAAT/enhancer-binding proteins), and chromatin remodeling factors such as MRG (mortality factor on chromosome 4 (MORF4)-related gene), and HDACs (histone deacetylases) (Table 1) [1–6].

Gene expression patterns are also regulated at the posttranscriptional levels via processes such as pre-mRNA splicing, export to the cytoplasm, turnover, storage, and translation. The key regulators of these posttranscriptional processes are RNA-binding proteins and microRNAs [7–11]. Although little is known about the role of RBPs and microRNAs in aging and age-related events,

Table 1
Gene lists regulating the age-related gene expression at the transcriptional level

Type of gene	Gene symbol	References
Transcriptional factor	FOXO	[4]
	PPAR	[3, 6]
	p53	[1, 2]
	C/EBPs	[3]
Chromatin remodeling factor	MRG	[2]
	HDACs	[2, 5]

many proteins implicated in age-related processes are encoded by mRNAs which are labile and/or subject to translational control by translation and turnover regulatory (TTR) RBPs. Examples of those genes are p16^{INK4}; p21^{CIP1}; p27^{KIP1}; cyclins (D1, E, A, B1, and H); cdk1 (cyclin-dependent kinase 1); amyloid precursor protein (APP); TNF- α ; interleukins (IL) including IL-1, IL-2, IL-3, IL-6, and IL-8; Mn superoxide dismutase (SOD); growth arrest- and DNA damage-inducible (GADD)45; plasminogen activator inhibitor (PAI)-1; COX-2; granulocyte macrophage-colony-stimulating factor (GM-CSF) and M-CSF; p53; bcl-2; Mdm-2; sirtuin 1 (SIRT1); prothymosin alpha (ProT α); c-fos; c-myc; DP-1; VEGF; TGF- β ; and type I insulin-like growth factor receptor (IGF-IR) (Table 2) [12–47]; for reviews, *see* Refs. 48, 49. Thus, high-throughput studies of the age-related gene expression, the expression of regulatory molecules including miRNAs, and the target mRNAs regulated by age-related RBPs may provide important clues to understand senescence, aging process, and age-related diseases [50–57].

The DNA microarray is now recognized as a useful clinical device to make diagnostic, therapeutic, or prognostic decision for patients. Generally, DNA microarrays consist of two categories, such as cDNA microarrays and oligonucleotide microarrays (Table 3). Both DNA microarray formats have individual advantages and disadvantages, such as expenses, probe synthesis, and hybridization process. Oligonucleotide microarrays are printed 20–25 to 70–80 nucleotides long synthesized probes over the solid surfaces. As these probes are derived from the biophysically optimized sequences and spotted with the constant concentration across the array surface, oligonucleotide array can provide reproducible and accurate quantitative results. cDNA microarrays are printed the corrections of 500–2,000 nucleotides long bacterial clones containing inserts on glass slides. Although cDNA arrays

Table 2**List of age-related genes regulated at the posttranscriptional levels**

Type of gene	Gene symbol	References
Cell cycle regulation	p16 ^{INK4}	[12]
	p21 ^{CIP1}	[13, 14]
	Cyclin D1	[16]
	Cyclin E	[17, 18]
	Cyclin A	[21]
	Cyclin B1	[21]
	Cyclin H	[19, 20]
	cdk1	[23]
Amyloid processing	APP	[24]
Immune response	TNF- α	[25–27]
	IL-1 β	[28]
	IL-2	[29, 30]
	IL-3	[31]
	IL-6	[28]
	IL-8	[32]
	COX-2	[36]
Response to oxidative stress	MnSOD	[33]
Blood coagulation	PAI-1	[35]
Cell differentiation	GM-CSF	[37]
	M-CSF	[37]
Apoptosis and Cell proliferation	p53	[38]
	bcl-2	[39]
	Mdm-2	[40]
	SIRT1	[41]
	ProT α	[42]
	GADD45	[34]
Transcriptional factor	c-fos	[22]
	c-myc	[43, 44]
	DP-1	[22]
Growth factor	VEGF	[45]
	TGF- β	[46]
	IGF-IR	[47]

are thought as labor intensive and less preferential for certain application, these long cDNA probes generally provide the results in less cross-hybridization of unrelated sequences. Over the course of just a few years, numerous technological advantages have led to the evolution of DNA microarrays and microarray-based techniques, revealing the genomic modification and all transcriptional activity. Examples are CpG methylation array, ChIP-on-chip, SNP

Table 3
Comparison of the oligonucleotide and cDNA-based microarray systems

	Oligonucleotide microarray	cDNA microarray
Probe size	20–25 or 70–80 nucleotides	500–2,000 nucleotides
Probe synthesis	Chemical synthesis	Bacterial clones
Labor requirement for synthesizing probes	Less	Intensive
Specificity	Intensive	Less to detect individual genes, mutation or SNP
Reproducibility	Intensive	Less
Cost for equipment	Expensive	Low cost

Table 4
Types of DNA array platforms and microarray-based technique to gerontological studies

Microarray-based technique	Purpose	References
CpG methylation array	High-throughput methylation profiling of the human genome	[58]
SNP microarray	Detection polymorphisms within a population	[60, 61]
Comparative Genomic Hybridization (CGH) microarray	Detection of copy number changes	[62]
ChIP-on-chip	Identification the functional elements of DNA-binding proteins, such as transcriptional factor, promoter, enhancer, repressor, in the genome	[59]
Expression array	High-throughput profiling of gene expression	[78]
miRNA array	High-throughput profiling of miRNA expression	[63]
Exon array	High-throughput profiling of alternative splicing pattern	[64]
RIP-Chip	Identification the functional target mRNAs of RNA-binding proteins	[78]

array, comparative genomic hybridization (CGH) microarray, miRNA array, exon array, and ribonucleoprotein [RNP] immunoprecipitation followed by microarray analysis (RIP-chip) [58–64, 78] (Table 4).

In this chapter, we show the protocols that embrace the actual handling of oligonucleotide microarray and miRNA microarray. In addition, we introduce the protocols of RIP-chip which can reveal the target mRNAs of age-related RBPs.

2 Materials

2.1 Oligonucleotide Microarray Hybridization Protocol and Fluorescent Labeling

2.1.1 One-Color Method

1. Quick Amp Labeling Kit, one-color (Agilent Technologies). This kit contains reagents necessary for the synthesis of fluorescent cRNA, including enzymes, buffer, and cyanine 3(Cy3)-CTP. Store at -20°C , and protect from light.
2. RNA Spike-In Kit, one-color (Agilent Technologies). Store at -80°C .
3. RNeasy Mini Kit (Qiagen). Buffer RPE is supplied as a concentrate. Before using for the first time, add 4 volumes of ethanol (96–100 % purity) as indicated on the bottle to obtain a working solution.
4. Gene Expression Hybridization Kit (Agilent Technologies).
5. Gene Expression Wash Buffer 1 and 2 (Agilent Technologies). The addition of 0.005 % Triton X-102 to the Gene Expression Wash Buffer 1 and 2 when the cubitainer of wash buffer is first opened.
6. Hybridization chamber (Agilent Technologies). Hybridization chamber should be washed after the hybridization and cleaned with RNaseZap (Ambion) and 70 % ethanol before the hybridization.

2.1.2 Two-Color Method

1. Quick Amp Labeling Kit, two-color (Agilent Technologies). This kit contains reagents necessary for the synthesis of fluorescent cRNA, including enzymes, buffer, cyanine 3(Cy3)-CTP, and cyanine 5(Cy5)-CTP. Store at -20°C , and protect from light.
2. RNA Spike-In Kit, two-color (Agilent Technologies). Store at -80°C .
3. RNeasy Mini Kit (Qiagen). Buffer RPE is supplied as a concentrate. Before using for the first time, add 4 volumes of ethanol (96–100 % purity) as indicated on the bottle to obtain a working solution.
4. Gene Expression Hybridization Kit (Agilent Technologies).
5. Gene Expression Wash Buffer 1 and 2 (Agilent Technologies). The addition of 0.005 % Triton X-102 to the Gene Expression Wash Buffer 1 and 2 when the cubitainer of wash buffer is first opened.
6. Hybridization chamber (Agilent Technologies). Hybridization chamber should be washed after the hybridization and cleaned with RNaseZap (Ambion) and 70 % ethanol before the hybridization.

**2.2 miRNA
Microarray
Hybridization Protocol
and Fluorescent
Labeling**

1. miRNA Complete Labeling and Hyb Kit (Agilent Technologies). This kit contains reagents necessary for the synthesis of fluorescent miRNA and the hybridization of microarray, including enzymes, buffer, cyanine3(Cy3)-pCp, and hybridization buffer. All reagents are stored at -20°C , but $2\times$ Hi-RPM Hybridization Buffer and $10\times$ GE Blocking Agent are stored at room temperature.
2. MicroRNA Spike-In kit (Agilent Technologies). Store at -20°C .
3. Gene Expression Wash Buffer 1 and 2 (Agilent Technologies). The addition of 0.005 % Triton X-102 to the Gene Expression Wash Buffer 1 and 2 when the cubitainer of wash buffer is first opened.
4. Hybridization chamber (Agilent Technologies). Hybridization chamber should be washed after the hybridization and cleaned with RNaseZap (Ambion) and 70 % ethanol before the hybridization.

**2.3 Ribonucleo-
protein [RNP]
Immunoprecipitation
Followed by
Microarray Analysis
(RIP-Chip)**

1. Protein A-Sepharose beads (Sigma).
2. Buffer A (pH 8.0):
20 mM NaH_2PO_4
150 mM NaCl
3. Antibodies against proteins of interest
4. Polysome lysis buffer (PLB):
100 mM KCl
5 mM MgCl_2
10 mM Hepes, pH 7.0
0.5 % Nonidet P-40
10 μM Dithiothreitol (DTT)
5. NT2 buffer:
50 mM Tris, pH 7.4
150 mM NaCl
1 mM MgCl_2
0.05 % Nonidet P-40

3 Methods

As numerous platforms of DNA microarray are available, any universal protocol or reagent could not be established. Each commercial microarray platform has individual advantages and disadvantages, such as expenses, sensitivity, reproducibility, and customization [65, 66]. Although the methods described below are based on the

protocols established by Agilent Technologies and our laboratory, each experimental stage, such as labeling, hybridization, and wash, is common for every array platform (Fig. 1a).

To obtain the appropriate results, it is important to pay attention to maintain the sufficient RNA quality [67]. To prevent contamination of reagents by nucleases, always wear powder-free laboratory gloves, and use dedicated solutions and pipettors with nuclease-free aerosol-resistant tips. It is also better to clean up the work surfaces and globes using RNaseZap (Ambion). The endogenous RNases in the tissues have to be inactivated by inhibitors or by chemical treatment such as guanidinium thiocyanate. Recently, some commercial kits (e.g., RNeasy kit provided by Qiagen) are explicitly declared their suitability for microarray analysis. After the purification, it should be better to check the RNA quality using Agilent 2100 Bioanalyzer (Agilent Technologies).

Technological equipment employed for data acquisition and statistical analysis of experimental data derived from microarray experiments vary in different laboratories. The important factors for selecting an appropriate microarray platform and experimental designs would include sensitivity, specificity and both inter- and intra-assay reproducibility. In the early days, microarrays designed by different companies appeared to produce different results with the same samples [68, 69]. Several large efforts, such as the Micro-Array Quality Control (MAQC) consortium, have been initiated to create standardized protocols for microarray experiments (from probe annotation to data analysis) [70]. These recognitions of biases and other artifacts by individual labs have developed experimental and computational methods for dealing with systematic variation between laboratories [71–74]. Moreover, to evaluate the performance characteristic of microarray measurement and the data it generated, it should always be validated using an alternative approach, such as conventional reverse transcription (RT)-PCR, quantitative real-time PCR, or others.

3.1 Oligonucleotide Microarray Hybridization Protocol and Fluorescent Labeling

It needs to make the decision whether to use a one-color or two-color approach, when we plan a microarray experiment (Table 5). In one-color approach, a single sample is labeled with a single dye, like cyanine-3 (Cy3) or cyanine-5 (Cy5), and hybridized to each microarray (Fig. 1a). The one-color design facilitates comparisons across microarray and between groups of samples, although it has the inconsistency across assays due to multiple sources of variability, including microarray fabrication and processing. On the other hand, in the two-color approach, two samples (e. g., experimental and control) are labeled with different dye (usually Cy3 and Cy5) and hybridized together on a single microarray (Fig. 1a). In two-color designs, the hybridization of two samples on same microarray allows a direct comparison, minimizing variability due to processing multiple microarrays per assay and increasing accuracy in

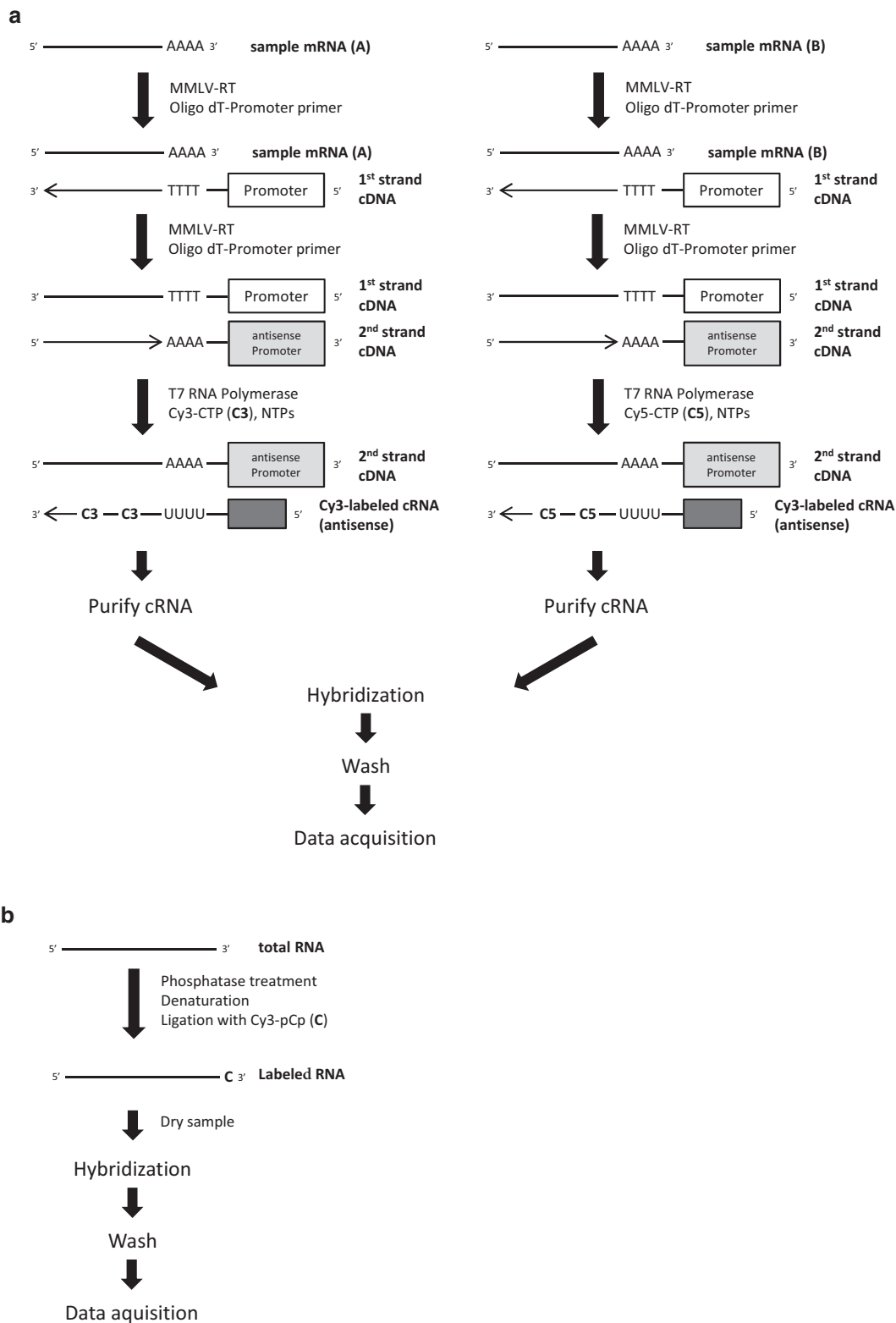


Fig. 1 Schematic procedures of oligonucleotide microarray and miRNA microarray. **(a)** Generation of cRNA for a two-color microarray experiment is shown. When you generate targets for a one-color microarray experiment, only the Cy3-labeled sample is produced and hybridized. **C3** indicated as cyanine3-CTP. **C5** indicated as cyanine5-CTP. **(b)** miRNA microarray; fluorescent labeling. **C** indicated as cyanine 3-pCp

Table 5
Comparison of one-color and two-color methods

	One-color methods	Two-color methods
	Single sample is labeled with a single dye	Two samples are labeled with different dye and hybridized together on a single microarray
Advantage	Comparison across microarrays and between groups of samples Apparent increase in the number of arrays needed Better geared toward estimating raw transcript abundance	Directly comparison between two samples Minimizing variability due to processing multiple microarray Increasing accuracy in determining levels of differential expression between sample pairs
Disadvantage	Inconsistency across arrays	Need to correct the systematic and gene-specific dye bias (dye swap) Need the common reference to compare between multiple samples

determining levels of differential expression between sample pairs. Moreover, two-color designs allow the comparison across multiple samples using complex hybridization schemes including hybridization with common reference samples [75]. Although dye-specific biases can substantially affect results when experiments are performed using two-color designs, these biases can be mitigated by performing dye-reversed replicates, such as dye swaps or fluorophore reversals [75].

3.1.1 Synthesis of Fluorescent Probe

1. Dilute or concentrate total RNA (200–1,000 ng) to 10.3 µl in a 1.5-ml microcentrifuge tube.
2. Add 1.2 µl of T7 promoter primer.
3. Denature the primer and the template by incubating the reaction at 65 °C for 10 min.
4. Place the reactions on ice and incubate for 5 min.
5. Pre-warm the 5× first-strand buffer at 80 °C for 3–4 min to ensure adequate resuspensions of the buffer components. For optimal resuspension, briefly mix on a vortex mixer and spin the tube in microcentrifuge to drive down the contents from the tube walls. Keep at room temperature until needed.
6. Immediately prior to use, mix the following components for cDNA Master Mix in the clean tube by gently pipetting (volume per reaction):
 - 5× first-strand buffer: 4 µl
 - 0.1 M DTT: 2 µl
 - 10 mM dNTP mix: 1 µl (*see Note 1*)

MMLV-RT: 1 µl

RNase Inhibitor: 0.5 µl

7. Add 8.5 µl of cDNA Master Mix to each sample tube and mix by pipetting.
8. Incubate samples at 40 °C for 2 h.
9. Incubate samples at 65 °C for 15 min to inactivate the MMLV-RT.
10. Move samples to ice. Incubate for 5 min.
11. Spin the samples in microcentrifuge to drive down the contents from the tube walls.
12. Pre-warm 50 % PEG solution for 1 min at 40 °C, vortex briefly, and spin briefly.
13. Immediately prior to use, gently mix the following components in a clean tube (volume per reaction):
 - 4× transcription buffer: 20 µl
 - 0.1 M DTT: 6 µl
 - NTP mix: 8 µl (*see Note 1*)
 - 50 % PEG: 6.4 µl
 - RNase inhibitor: 0.5 µl
 - Inorganic pyrophosphatase: 0.6 µl
 - T7 RNA polymerase: 0.8 µl (*see Note 3*)
 - Cyanine 3-CTP or cyanine 5-CTP: 2.4 µl (*see Notes 2 and 3*)
 - Nuclease-free water: 15.3 µl
14. Add 60 µl of Transcription Master Mix to each samples, gently mix by pipetting.
15. Incubate the samples at 40 °C for 2 h (*see Note 2*).

3.1.2 Purification of Fluorescent Probe

1. Add 20 µl of nuclease-free water to the cRNA sample, for total volume of 100 µl.
2. Add 350 µl of Buffer RTL and mix well by pipetting.
3. Add 260 µl of ethanol (96–100 % purity) and mix thoroughly with pipetting. Do not centrifuge, and proceed immediately to **step 4**.
4. Transfer the 700 µl of the cRNA sample to an RNeasy mini column in a 2-ml collection tube. Centrifuge the sample at 4 °C for 30 s at 16,000 × *g*. Discard the flow-through and collection tube.
5. Transfer the RNeasy mini column to a new collection tube and add 500 µl of RPE buffer containing ethanol to the column. Centrifuge the sample at 4 °C for 30 s at 16,000 × *g*. Discard the flow-through, and reuse the collection tube.

6. Add another 500 μl of RPE buffer to the column. Centrifuge the sample at 4 °C for 2 min at $16,000 \times g$. Discard the flow-through and collection tube (*see Note 4*).
7. Transfer the RNeasy mini column to a new 1.5 ml collection tube and centrifuge the sample at 4 °C for 30 s at $16,000 \times g$ to remove any remaining traces of RPE buffer. Discard this collection tube, and transfer to the new 1.5 ml collection tube (*see Note 5*).
8. Add 30 μl of RNase-free water directly onto the RNeasy filter membrane. Incubate for 60 s, then centrifuge for 30 s at $16,000 \times g$ at 4 °C.
9. Maintain the cRNA sample-containing flow-through on ice.
10. Measure fluorescent dye incorporation using nuclease-free water as blank (*see Note 6*).

3.1.3 Hybridization

One-Color Method

1. Add 500 μl of nuclease-free water to the vial containing lyophilized 10 \times Blocking Agent supplied with the Gene Expression Hybridization kit. Mix by gently vortexing and spin the tube in microcentrifuge to drive down the contents from the tube walls (*see Note 7*).
2. Equilibrate water bath to 60 °C.
3. For each microarray, add each of the components in 1.5 ml tube as follow:
 Cy3-labeled, linearly amplified cRNA: 1.65 μg
 10 \times Blocking Agent: 11 μl
 Nuclease-free water: bring volume to 52.8 μl
 25 \times Fragmentation Buffer: 2.2 μl
4. Mix gently on a vortex mixer.
5. Incubate at 60 °C for exactly 30 min to fragment RNA (*see Note 2*).
6. Immediately cool on ice for 1 min.
7. Add 55 μl of 2 \times GE Hybridization Buffer HI-RPM to the microarray formats to stop the fragmentation reaction.
8. Mix well by careful pipetting (*see Note 8*).
9. Spin for 1 min at room temperature at $16,000 \times g$ in microcentrifuge to drive the sample off the walls and lid.
10. Place sample on ice and load onto the array immediately.
11. Load a clean gasket slide into the chamber base with the label facing up and aligned with the rectangular section of the chamber base. Ensure that the gasket slide is flush with the chamber base and is not ajar.

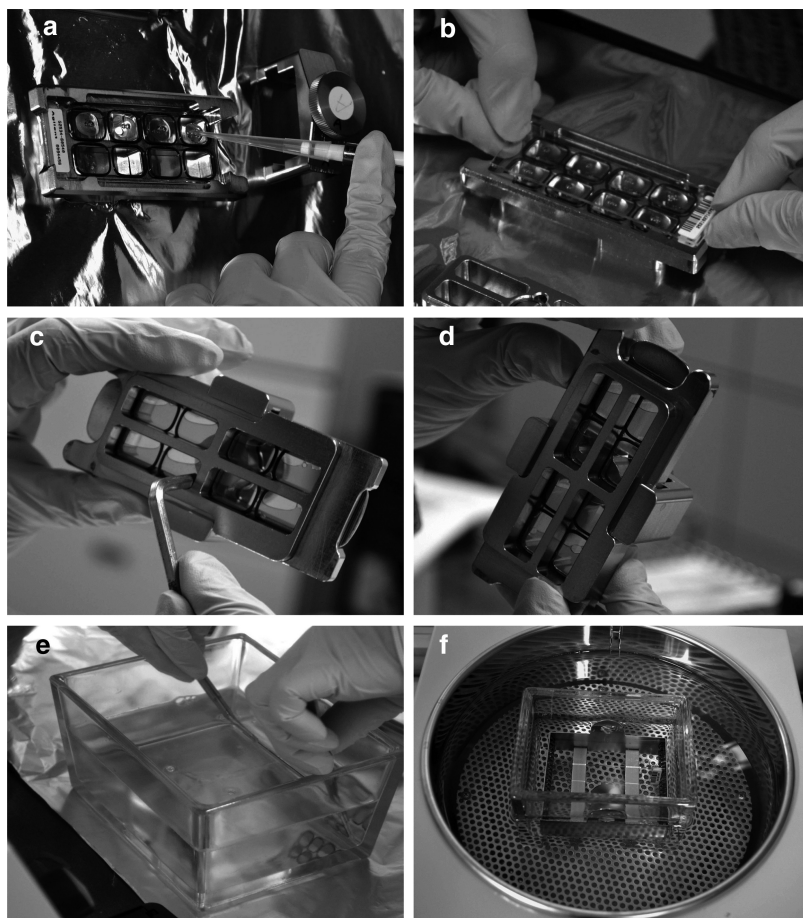


Fig. 2 Handling the array slide on hybridization steps and post-hybridization washes steps. **(a)** Distribute the Cy3-labeled hybridization sample onto the gasket well. **(b)** Slowly place an array slide over the gasket with the active side facing down. **(c)** Vertically rotate the assembled chamber to assess the mobility of the bubbles. **(d)** Tap the assembly to move stationary bubbles. **(e)** Disassembly the array-gasket sandwich in the slide-staining dish filled with Wash buffer 1. Let the gasket slide drop to the bottom of the staining dish. **(f)** Wash the array slide in slide-staining dish with pre-warmed Wash buffer 2. The slide-staining dish is warmed to 37 °C with heating element such as a water bath

12. Slowly dispense the volume of hybridization sample onto the gasket well in a drag and dispense manner (Fig. 2a).
13. Slowly place an array active side down onto the gasket slide, and assemble the chamber (Fig. 2b).
14. Vertically rotate the assembled chamber to wet the gasket and assess the mobility of the bubbles (*see Note 9* and Fig. 2c, d).

15. Place the chamber in the hybridization oven. Set the hybridization rotator to rotate at 10 rpm. Hybridize the probe with the microarray at 65 °C for 17 h.

Two-Color Method

1. Proceed to **steps 1 and 2** described in Subheading 3.1.3.1.
2. For each microarray, add each of the components in 1.5 ml tube as follow:
 Cy3-labeled, linearly amplified cRNA: 0.825 µg
 Cy5-labeled, linearly amplified cRNA: 0.825 µg
 10× Blocking Agent: 11 µl
 Nuclease-free water: bring volume to 52.8 µl
 25× Fragmentation Buffer: 2.2 µl
3. Proceed to **steps 4–15** described in Subheading 3.1.3.1.

3.1.4 Post-Hybridization Washes

1. Pre-warm Wash buffer 2 and wash container #3 at 37 °C the night before washing the array (*see Note 10*).
2. Set a water bath with magnetic stir plate at 37 °C.
3. Completely fill the wash container #1 with Wash buffer 1 at room temperature.
4. Place a slide rack into the wash container #2, and add a magnetic stir bar. Fill the wash container #2 with Wash buffer 1 at room temperature to cover the slide rack. Place this container on a magnetic stir plate.
5. Place the pre-warmed container #3 into the water bath with magnetic stir plate, and add a magnetic stir bar. Completely fill the container #3 with the pre-warmed (37 °C) Wash buffer 2 at 37 °C.
6. Disassembly the hybridization chamber and remove the array-gasket sandwich from the chamber base by grabbing the slide from their ends. Quickly transfer the sandwich to container #1.
7. With the sandwich completely submerged in Wash buffer 1, pry the sandwich open (Fig. 2e).
 - (a) Slip one of the blunt ends of the forceps between the slides.
 - (b) Gently turn the forceps upwards or downwards to separate the slides.
 - (c) Let the gasket slide drop to the bottom of container.
 - (d) Remove the microarray slide and place into slide rack in the container #2 containing Wash buffer 1 at room temperature.
8. Repeat **steps 6** through **7** for additional slides.
9. When all slides are placed into the slide rack in container #2, stir gently for 1 min.

10. Transfer slide rack to container #3 containing Wash buffer 2 at 37 °C. Stir gently for 1 min (Fig. 2f).
11. Slowly remove the slide rack minimizing droplets on the slides.
12. Put the slides in a slide holder.

3.1.5 Data Acquisition and Analysis

1. Scan slides immediately to minimize the impact of environmental oxidants on signal intensities.
2. Extract the microarray scan data using available software packages (e.g., Agilent Feature Extraction [Agilent Technologies]). Gene Spring GX software (Agilent Technologies) is suggested for data acquisition and background subtraction.

3.2 miRNA Microarray Hybridization Protocol, Fluorescent Labeling

MicroRNAs (miRNAs) are a class of short (18–25 nucleotides), noncoding RNAs that have been found existence in animals, plants, and viruses. Microarray-based assays offer an efficient method for measuring the expression profile of large numbers of miRNAs simultaneously. The method described here is a miRNA assay employing direct labeling of total RNA without amplification or size fractionation [76] (Fig. 1b). Moreover, in situ synthesized DNA microarray probes are both sequence and size selective for mature miRNAs [77].

3.2.1 Synthesis of Fluorescent Probe

1. Dilute total RNA sample to 50 ng/μl in nuclease-free water (*see Note 11*).
2. Add 2 μl (100 ng) of the diluted total RNA to a 1.5 ml tube and maintain on ice.
3. Immediately prior to use, gently mix the following components for Calf Intestinal Alkaline Phosphatase (CIP) Master Mix in a clean tube (volume per reaction):
 - 10× CIP buffer: 0.4 μl
 - Nuclease-free water: 1.1 μl
 - CIP: 0.5 μl
4. Add 2 μl of the CIP Master Mix to each sample tube, and mix gently by pipetting.
5. Incubate the reaction at 37 °C for 30 min.
6. Add 2.8 μl of 100 % DMSO to each sample.
7. Incubate the samples at 100 °C for 5–10 min (*see Note 12*).
8. Immediately transfer to ice-water bath (*see Note 13*).
9. Warm the 10× T4 RNA Ligase Buffer at 37 °C and vortex well.
10. Immediately prior to use, gently mix the following components for Ligation Master Mix in a clean tube (volume per reaction):

10× T4 RNA Ligase Buffer: 1.0 µl

Cyanine3-pCp: 3.0 µl (*see Note 2*)

T4 RNA Ligase: 0.5 µl

11. Immediately add 4.5 µl of the Ligation Master Mix to each sample tube and gently mix by pipetting (*see Note 14*).
12. Incubate at 16 °C for 2 h.
13. Completely dry the samples using a vacuum concentrator at room temperature for 2 h (*see Note 15*).

3.2.2 Hybridization

1. Add 125 µl of nuclease-free water to the vial containing lyophilized 10× GE Blocking Agent, and mix gently with vortex.
2. Resuspend the dried sample in 18 µl of nuclease-free water.
3. Add 4.5 µl of the 10× GE Blocking Agent to each sample.
4. Add 22.5 µl of 2× Hi-RPM Hybridization Buffer to each sample, and mix gently with vortex.
5. Incubate at 100 °C for 5 min.
6. Immediately transfer to an ice-water bath for 5 min (*see Note 16*).
7. Load a clean gasket slide into the chamber base with the label facing up and aligned with the rectangular section of the chamber base. Ensure that the gasket slide is flush with the chamber base and is not ajar.
8. Slowly dispense the volume of hybridization sample onto the gasket well in a drag and dispense manner (Fig. 2a).
9. Slowly place an array active side down onto the gasket slide, and assemble the chamber (Fig. 2b).
10. Vertically rotate the assembled chamber to wet the gasket and assess the mobility of the bubbles (*see Note 9* and Fig. 2c, d).
11. Place the chamber in the hybridization oven. Set the hybridization rotator to rotate at 20 rpm. Hybridize the probe with the microarray at 55 °C for 20 h.

3.2.3 Post-Hybridization Washes

1. Pre-warm Wash buffer 2 and wash container #3 at 37 °C the night before washing the array (*see Note 10*).
2. Set a water bath with magnetic stir plate at 37 °C.
3. Completely fill the wash container #1 with Wash buffer 1 at room temperature.
4. Place a slide rack into the wash container #2, and add a magnetic stir bar. Fill the wash container #2 with Wash buffer 1 at room temperature to cover the slide rack. Place this container on a magnetic stir plate.

5. Place the pre-warmed container #3 into the water bath with magnetic stir plate, and add a magnetic stir bar. Completely fill the container #3 with the pre-warmed Wash buffer 2 at 37 °C.
6. Disassembly the hybridization chamber and remove the array-gasket sandwich from the chamber base by grabbing the slide from their ends. Quickly transfer the sandwich to container #1.
7. With the sandwich completely submerged in Wash buffer 1, pry the sandwich open (Fig. 2e).
 - (a) Slip one of the blunt ends of the forceps between the slides.
 - (b) Gently turn the forceps upwards or downwards to separate the slides.
 - (c) Let the gasket slide drop to the bottom of container.
 - (d) Remove the microarray slide and place into slide rack in the container #2 containing Wash buffer 1 at room temperature.
8. Repeat **steps 6** through **7** for additional slides.
9. When all slides are placed into the slide rack in container #2, stir gently for 5 min.
10. Transfer slide rack to container #3 containing Wash buffer 2 at 37 °C. Stir gently for 5 min (Fig. 2f).
11. Slowly remove the slide rack minimizing droplets on the slides.
12. Put the slides in a slide holder.

3.2.4 Data Acquisition and Analysis

1. Scan slides immediately to minimize the impact of environmental oxidants on signal intensities.
2. Extract the microarray scan data using available software packages (e.g., Agilent Feature Extraction [Agilent Technologies]). Gene Spring GX software (Agilent Technologies) is suggested for data acquisition and background subtraction.

3.3 Ribonucleo-protein [RNP] Immunoprecipitation Followed by Microarray Analysis (RIP-Chip)

Many age-related proteins are encoded by mRNAs that are targets of RBPs, including HuR, AUF1, TIA-1, CPEB, CIRP, CUGBP1, CRT and TTP [55, 57]. These RBPs interact to their target mRNAs which are positively or negatively regulate their half-life and translation status. Ribonucleoprotein [RNP] immunoprecipitation followed by microarray analysis (RIP-chip) is often used to identify the stable native target mRNA of TTR-RBPs [78, 79] (Fig. 3).

3.3.1 Preparation of RNP Lysate from Culture Cells

1. Grow cells in appropriate medium and supplements. Typically, cells cultured in 150 cm² dish are needed.
2. Collect cells using scraper, transfer to 1.5 ml tube, and pellet by centrifugation at 4 °C for 3 min at 100 × *g*.

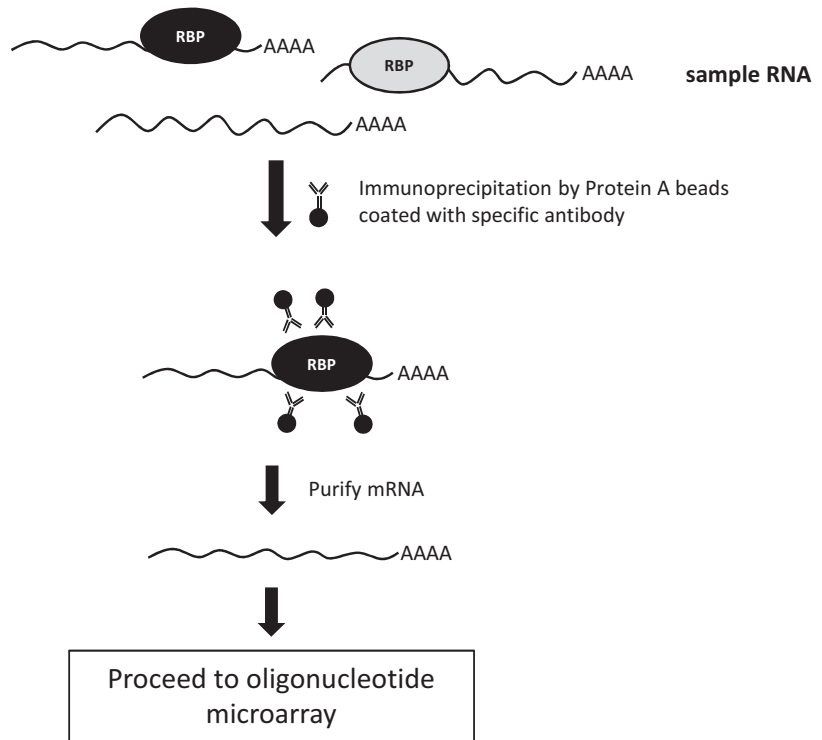


Fig. 3 Schematic procedures of ribonucleoprotein [RNP] immunoprecipitation followed by microarray analysis (RIP-chip)

3. Loosen the cell pellet by gently flicking the bottom of the tube and add an approximately equal pellet volume of ice-cold PLB buffer supplemented with RNase inhibitors and protease inhibitors.
4. Mix cells by pipetting several times, and place on ice for 10 min. Do not mix on a vortex mixer.
5. Centrifuge at 4 °C for 30 min at $10,000 \times g$. Transfer supernatant to new 1.5 ml tube.
6. Preclear the supernatant with 15 μ g of control IgG1 for 30 min at 4 °C. Add 50 μ l protein A beads, and incubate for 30 min at 4 °C with rotation.
7. Centrifuge at 4 °C for 5 min at $5,000 \times g$, and transfer the supernatant to new 1.5 ml tube.

3.3.2 Coating the Protein A Beads with Antibody

1. Before using for the first time, add 4 ml of Buffer A to 1 g lyophilized beads. Incubate for 30 min at room temperature to swell beads.
2. Add 60 μ l of protein A beads to 1 ml of NT2 buffer in a 1.5 ml tube.
3. Centrifuge at 4 °C for 5 min at $5,000 \times g$, and discard the supernatant with pipet.

4. Wash the beads with 1 ml of ice-cold NT2 buffer.
5. Centrifuge at 4 °C for 5 min at $5,000 \times g$, and discard the supernatant with pipet.
6. Again, wash the beads as **steps 4 and 5**.
7. Add 800 μ l of NT2 buffer to the beads. Then, add 30 μ g of antibody or control IgG1 to the indicated beads (*see Note 17*).
8. Incubate overnight on rotator at 4 °C to coat the beads with appreciate antibody

3.3.3 Immunoprecipitation of RNPs

1. Centrifuge at 4 °C for 5 min at $5,000 \times g$, and discard the supernatant with pipet.
2. Wash the beads for three times as **steps 4 and 5** subscribing in Subheading 3.3.2.
3. Mix the following components for IP Mix in the clean tube by gently pipetting (volume per reaction).
NT2 buffer: 800 μ l
0.1 M DTT: 10 μ l
RNase inhibitor (40 U/ μ l): 5 μ l
4. Add 800 μ l of IP Mix to the beads coated with antibody or control IgG1.
5. Add 500–1,000 μ g of RNP lysate, and incubate for 1–2 h on rotator at 4 °C.
6. Centrifuge at 4 °C for 5 min at $5,000 \times g$, and discard the supernatant with pipet.
7. Wash the beads for five times as **steps 4 and 5** subscribing in Subheading 3.3.2.
8. Mix the following components for DNase I Mix in the clean tube by gently pipetting (volume per reaction).
NT2 buffer: 100 μ l
DNase I (2 U/ μ l): 5 μ l
9. Add 100 μ l of DNase I Mix to the beads, and incubate at 37 °C for 15 min.
10. Fill up with 1,000 ml of NT2 buffer.
11. Centrifuge at 4 °C for 5 min at $5,000 \times g$, and discard the supernatant with pipet.
12. Mix the following components for Proteinase K Mix in the clean tube by gently pipetting (volume per reaction).
NT2 buffer: 100 μ l
Proteinase K (10 mg/ml): 5 μ l
10 % SDS: 1 μ l

13. Add 100 μ l of Proteinase K Mix to the beads, and incubate at 55 °C for 30 min with mixing.
14. Add 220 μ l of NT2 buffer and centrifuge at 4 °C for 5 min at 5,000 $\times g$. Then, transfer supernatant to new 1.5 ml tube.
15. Add 300 μ l of acid phenol-CHCl₃, and mix well on a vortex mixer.
16. Incubate at room temperature for 1 min, and centrifuge at 4 °C for 5 min at 16,000 $\times g$.
17. Transfer 250 μ l of the aqueous phase of the sample to clean 1.5 ml tube.
18. Add 25 μ l of 3 M sodium acetate, pH 5.2, and 625 μ l of 100 % ethanol (*see Note 18*).
19. Mix well on a vortex mixer, and incubate overnight at -20 °C.
20. Centrifuge at 4 °C for 20 min at 16,000 $\times g$, and discard the supernatant with pipet.
21. Wash the pellet with 1 ml of 70 % ethanol, and centrifuge at 4 °C for 10 min at 16,000 $\times g$.
22. Discard the supernatant with pipet, and air dry the RNA pellet for 5–10 min.
23. Proceed to “Oligonucleotide Microarray Hybridization Protocol” described in Subheading 3.1.

4 Notes

1. Quick Amp Labeling Kit contains two vials of dNTPs, labeled as “10 mM dNTP mix” and “NTP mix.” Be sure to use the appropriate reagents.
2. Cyanine 3(Cy3)-CTP, cyanine 5(Cy5)-CTP, and cyanine 3-pCp fluorescent dye are highly light sensitive. Minimize exposure of light at every stage of the protocol (i.e., cover the sample with foil when handling and store, close water bath with lids, etc.)
3. Add the cyanine 3(Cy3)-CTP (or cyanine 5(Cy5)-CTP) and enzyme to the mix, immediately prior use.
4. The long centrifugation dries the spin column membrane, ensuring that no ethanol is carried over during RNA elution. After centrifugation, carefully remove the spin column from the collection tube so that the column does not contact the flow-through.
5. It is suggested to perform this step to eliminate any possible carryover of buffer RPE or if residual flow-through remains on the outside of the spin column.

6. We usually quantitate cRNA using NanoDrop ND-100 UV-VIS Spectrophotometer. The yield of cRNA and amount of Cy3-CTP or Cy5-CTP incorporation (pmol Cy3 or Cy5 per μg cRNA) can be calculated using the following formula: The cRNA concentration ($\text{ng}/\mu\text{l}$) = $A_{260} \times 10 \times 40 \mu\text{g}/\text{ml}$; The yield of cRNA (μg) = cRNA concentration ($\text{ng}/\mu\text{l}$) $\times 30 (\mu\text{l})/1,000$; Cy3-CTP or Cy5-CTP concentration ($\text{pmol}/\mu\text{l}$) = $A_{550} \times 10 \times 1,000/150$; Cy3-CTP or Cy5-CTP incorporation ($\text{pmol}/\mu\text{g}$) = Cy3-CTP or Cy5-CTP concentration ($\text{pmol}/\mu\text{l}$) $\times 1,000/\text{cRNA concentration } (\text{ng}/\mu\text{l})$. Using Quick Amp Labeling Kit (Agilent Technologies), more than $1.65 \mu\text{g}$ of cRNA and more than $9 \text{ pmol}/\mu\text{g}$ of Cy3-CTP or Cy5-CTP incorporation can normally be obtained.
7. If the pellet does not go into solution completely, heat the mix for 4–5 min at 37°C .
8. Take care to avoid introducing bubbles. Do not mix on a vortex mixer.
9. Tap the assembly on a hard surface to move stationary bubbles (*see* Fig. 2d).
10. Always use the clean equipment when doing the hybridization and wash steps. Wash the equipment that is used in previous experiments with Milli-Q water.
11. miRNA Complete Labeling and Hyb Kit (Agilent Technologies) generates fluorescently labeled miRNA from 100 ng of total RNA. This method involves the ligation of one cyanine 3-pCp molecule to the 3' end of an RNA molecule.
12. Incubate no less than 5 min and no more than 10 min, or the labeling efficiency of the sample will be affected.
13. Use an ice-water bath and not just crushed ice to ensure that the samples remain properly denatured. When using a thermocycler, transfer the sample to ice-water bath immediately after incubating at 100°C to prevent the RNA from reannealing. Thermocycler do not cool as quickly as is needed.
14. Be sure to use the Ligation Master Mix within 15 min of mixing all the components. Failure to do may affect the labeling efficiency.
15. The sample must be completely dried after labeling to remove residual DMSO. Residual DMSO will adversely affect the hybridization results.
16. Do not leave samples in the ice-water bath for more than 15 min, as longer incubations may adversely affect the hybridization results.
17. The amount of the antibody required for IP will depend on the protein. The optimal amount of the antibody needed should be

determined by doing IP with this protocol with 1, 5, 10 and 30 µg of antibody. Usually, we use 10 µg of antibody for protein like HuR, and 30 µg for proteins like TIA-1, TIAR.

18. We usually use the nucleic acid coprecipitant, such as Glyco-Blue Coprecipitant (Ambion) and Dr. GenTLE Precipitation Carrier (Takara), to increase the size and visibility of pellet. Be sure that the coprecipitant you use does not interfere with molecular biology procedures including reverse transcription or fluorescent labeling of cRNA.

Acknowledgments

The protocols above are based on the protocols establishes in Agilent Technologies (oligonucleotide microarray, and miRNA microarray) and the Laboratory of Molecular Biology and Immunology, National institute on Aging-Intramural Research Program, National Institutes of Health, Baltimore, MD (ribonucleoprotein immunoprecipitation followed by microarray analysis). We would like to thank Myriam Gorospe (NIA/NIH) for important technical assistance. The part of this work was supported by Grants-in-Aid for Scientific Research (C) number 24590943.

References

1. Matheu A, Maraver A, Serrano M (2008) The Arf/p53 pathway in cancer and aging. *Cancer Res* 68:6031–6034
2. Garcia SN, Pereira-Smith O (2008) MRGing chromatin dynamics and cellular senescence. *Cell Biochem Biophys* 50:133–141
3. Kirkland JL, Tchkonina T, Pirtskhalava T et al (2002) Adipogenesis and aging: does aging make fat go MAD? *Exp Gerontol* 37:757–767
4. Salih DA, Brunet A (2008) FoxO transcription factors in the maintenance of cellular homeostasis during aging. *Curr Opin Cell Biol* 20:126–136
5. Sedivy JM, Banumathy G, Adams PD (2008) Aging by epigenetics—a consequence of chromatin damage? *Exp Cell Res* 314:1909–1917
6. Zhang R, Zheng F (2008) PPAR- γ and aging: one link through klotho? *Kidney Int* 74:702–704
7. Fabian MR, Sonenberg N, Filipowicz W (2010) Regulation of mRNA translation and stability by microRNAs. *Annu Rev Biochem* 79:351–379
8. Keene JD (2007) RNA regulons: coordination of post-transcriptional events. *Nat Rev Genet* 8:533–543
9. Mitchell P, Tollervey D (2000) mRNA stability in eukaryotes. *Curr Opin Genet Dev* 10:193–198
10. Moore MJ (2005) From birth to death: the complex lives of eukaryotic mRNAs. *Science* 309:1514–1518
11. Orphanides G, Reinberg D (2002) A unified theory of gene expression. *Cell* 108:439–451
12. Wang W, Martindale JL, Yang X et al (2005) Increased stability of the p16 mRNA with replicative senescence. *EMBO Rep* 6:158–164
13. Lafarga V, Cuadrado A, Lopez de Silanes I et al (2009) p38 Mitogen-activated protein kinase- and HuR-dependent stabilization of p21(Cip1) mRNA mediates the G(1)/S checkpoint. *Mol Cell Biol* 29:4341–4351
14. Wang W, Furneaux H, Cheng H et al (2000) HuR regulates p21 mRNA stabilization by UV light. *Mol Cell Biol* 20:760–769
15. Kullmann M, Gopfert U, Siewe B et al (2002) ELAV/Hu proteins inhibit p27 translation via an IRES element in the p27 5'UTR. *Genes Dev* 16:3087–3099
16. Lal A, Mazan-Mamczarz K, Kawai T et al (2004) Concurrent versus individual binding of HuR and AUF1 to common labile target mRNAs. *EMBO J* 23:3092–3102

17. Guo X, Hartley RS (2006) HuR contributes to cyclin E1 deregulation in MCF-7 breast cancer cells. *Cancer Res* 66:7948–7956
18. Guo X, Wu Y, Hartley RS (2010) Cold-inducible RNA-binding protein contributes to human antigen R and cyclin E1 deregulation in breast cancer. *Mol Carcinog* 49:130–140
19. Kim HH, Yang X, Kuwano Y et al (2008) Modification at HuR(S242) alters HuR localization and proliferative influence. *Cell Cycle* 7:3371–3377
20. Kim HH, Abdelmohsen K, Lal A et al (2008) Nuclear HuR accumulation through phosphorylation by Cdk1. *Genes Dev* 22:1804–1815
21. Wang W, Caldwell MC, Lin S et al (2000) HuR regulates cyclin A and cyclin B1 mRNA stability during cell proliferation. *EMBO J* 19:2340–2350
22. Wang W, Yang X, Cristofalo VJ et al (2001) Loss of HuR is linked to reduced expression of proliferative genes during replicative senescence. *Mol Cell Biol* 21:5889–5898
23. Kakuguchi W, Kitamura T, Kuroshima T et al (2010) HuR Knockdown Changes the Oncogenic Potential of Oral Cancer Cells. *Mol Cancer Res* 8:520–528
24. Lee EK, Kim HH, Kuwano Y et al (2010) hnRNP C promotes APP translation by competing with FMRP for APP mRNA recruitment to P bodies. *Nat Struct Mol Biol* 17:732–739
25. Dean JL, Wait R, Mahtani KR et al (2001) The 3' untranslated region of tumor necrosis factor alpha mRNA is a target of the mRNA-stabilizing factor HuR. *Mol Cell Biol* 21:721–730
26. Sun L, Stoecklin G, Van Way S et al (2007) Tristetraprolin (TTP)-14-3-3 complex formation protects TTP from dephosphorylation by protein phosphatase 2a and stabilizes tumor necrosis factor-alpha mRNA. *J Biol Chem* 282:3766–3777
27. Piecyk M, Wax S, Beck AR et al (2000) TIA-1 is a translational silencer that selectively regulates the expression of TNF-alpha. *EMBO J* 19:4154–4163
28. Lu JY, Sadri N, Schneider RJ (2006) Endotoxic shock in AUF1 knockout mice mediated by failure to degrade proinflammatory cytokine mRNAs. *Genes Dev* 20:3174–3184
29. Shim J, Lim H, R Yates J et al (2002) Nuclear export of NF90 is required for interleukin-2 mRNA stabilization. *Mol Cell* 10:1331–1344
30. Hau HH, Walsh RJ, Ogilvie RL et al (2007) Tristetraprolin recruits functional mRNA decay complexes to ARE sequences. *J Cell Biochem* 100:1477–1492
31. Ming XF, Kaiser M, Moroni C (1998) c-jun N-terminal kinase is involved in AUUUA-mediated interleukin-3 mRNA turnover in mast cells. *EMBO J* 17:6039–6048
32. Palanisamy V, Park NJ, Wang J et al (2008) AUF1 and HuR proteins stabilize interleukin-8 mRNA in human saliva. *J Dent Res* 87:772–776
33. Knirsch L, Clerch LB (2000) A region in the 3' UTR of MnSOD RNA enhances translation of a heterologous RNA. *Biochem Biophys Res Commun* 272:164–168
34. Lal A, Abdelmohsen K, Pullmann R et al (2006) Posttranscriptional derepression of GADD45alpha by genotoxic stress. *Mol Cell* 22:117–128
35. Doller A, Gauer S, Sobkowiak E et al (2009) Angiotensin II induces renal plasminogen activator inhibitor-1 and cyclooxygenase-2 expression post-transcriptionally via activation of the mRNA-stabilizing factor human-antigen R. *Am J Pathol* 174:1252–1263
36. Dixon DA, Balch GC, Kedersha N et al (2003) Regulation of cyclooxygenase-2 expression by the translational silencer TIA-1. *J Exp Med* 198:475–481
37. Buzby JS, Lee SM, Van Winkle P et al (1996) Increased granulocyte-macrophage colony-stimulating factor mRNA instability in cord versus adult mononuclear cells is translation-dependent and associated with increased levels of A + U-rich element binding factor. *Blood* 88:2889–2897
38. Mazan-Mamczarz K, Galban S, Lopez de Silanes I et al (2003) RNA-binding protein HuR enhances p53 translation in response to ultraviolet light irradiation. *Proc Natl Acad Sci USA* 100:8354–8359
39. Abdelmohsen K, Lal A, Kim HH et al (2007) Posttranscriptional orchestration of an anti-apoptotic program by HuR. *Cell Cycle* 6:1288–1292
40. Ghosh M, Aguila HL, Michaud J et al (2009) Essential role of the RNA-binding protein HuR in progenitor cell survival in mice. *J Clin Invest* 119:3530–3543
41. Abdelmohsen K, Pullmann R Jr, Lal A et al (2007) Phosphorylation of HuR by Chk2 regulates SIRT1 expression. *Mol Cell* 25:543–557
42. Lal A, Kawai T, Yang X et al (2005) Antiapoptotic function of RNA-binding protein HuR effected through prothymosin alpha. *EMBO J* 24:1852–1862
43. Lafon I, Carballes F, Brewer G et al (1998) Developmental expression of AUF1 and HuR,

- two c-myc mRNA binding proteins. *Oncogene* 16:3413–3421
44. Kim HH, Kuwano Y, Srikantan S et al (2009) HuR recruits let-7/RISC to repress c-Myc expression. *Genes Dev* 23:1743–1748
45. Levy NS, Chung S, Furneaux H et al (1998) Hypoxic stabilization of vascular endothelial growth factor mRNA by the RNA-binding protein HuR. *J Biol Chem* 273:6417–6423
46. Nabors LB, Gillespie GY, Harkins L et al (2001) HuR, a RNA stability factor, is expressed in malignant brain tumors and binds to adenine- and uridine-rich elements within the 3' untranslated regions of cytokine and angiogenic factor mRNAs. *Cancer Res* 61:2154–2161
47. Meng Z, King PH, Nabors LB et al (2005) The ELAV RNA-stability factor HuR binds the 5'-untranslated region of the human IGF-IR transcript and differentially represses cap-dependent and IRES-mediated translation. *Nucleic Acids Res* 33:2962–2979
48. Abdelmohsen K, Kuwano Y, Kim HH et al (2008) Posttranscriptional gene regulation by RNA-binding proteins during oxidative stress: implications for cellular senescence. *Biol Chem* 389:243–255
49. Abdelmohsen K, Gorospe M (2010) Posttranscriptional regulation of cancer traits by HuR. *Wiley Interdiscip Rev RNA* 1:214–229
50. Ida H, Boylan SA, Weigel AL et al (2003) Age-related changes in the transcriptional profile of mouse RPE/choroid. *Physiol Genomics* 15:258–262
51. Blalock EM, Chen KC, Stromberg AJ et al (2005) Harnessing the power of gene microarrays for the study of brain aging and Alzheimer's disease: statistical reliability and functional correlation. *Ageing Res Rev* 4:481–512
52. Hamatani T, Falco G, Carter MG et al (2004) Age-associated alteration of gene expression patterns in mouse oocytes. *Hum Mol Genet* 13:2263–2278
53. Park SK, Prolla TA (2005) Gene expression profiling studies of aging in cardiac and skeletal muscles. *Cardiovasc Res* 66:205–212
54. Park SK, Kim K, Page GP et al (2009) Gene expression profiling of aging in multiple mouse strains: identification of aging biomarkers and impact of dietary antioxidants. *Aging Cell* 8:484–495
55. Masuda K, Kuwano Y, Nishida K et al (2012) General RBP expression in human tissues as a function of age. *Ageing Res Rev* 11:423–431
56. Abdelmohsen K, Srikantan S, Kang MJ et al (2012) Regulation of senescence by microRNA biogenesis factors. *Ageing Res Rev* 11:491–500
57. Wang W (2012) Regulatory RNA-binding proteins in senescence. *Ageing Res Rev* 11:485–490
58. Christensen BC, Houseman EA, Marsit CJ et al (2009) Aging and Environmental Exposures Alter Tissue-Specific DNA Methylation Dependent upon CpG Island Context. *PLoS Genet* 5:e1000602
59. Oberdoerffer P, Michan S, McVay M et al (2008) SIRT1 Redistribution on chromatin promotes genomic stability but alters gene expression during aging. *Cell* 135:907–918
60. Fan JB, Chen X, Halushka MK et al (2000) Parallel genotyping of human SNPs using generic high-density oligonucleotide tag arrays. *Genome Res* 10:853–860
61. Favis R, Day JP, Gerry NP et al (2000) Universal DNA array detection of small insertions and deletions in BRCA1 and BRCA2. *Nat Biotechnol* 18:561–564
62. Begus-Nahrmann Y, Lechel A, Obenaus AC et al (2009) p53 deletion impairs clearance of chromosomal-unstable stem cells in aging telomere-dysfunctional mice. *Nat Genet* 41:1138–1143
63. Liang R, Bates DJ, Wang E (2009) Epigenetic control of MicroRNA expression and aging. *Curr Genomics* 10:184–193
64. Chen P, Lepikhova T, Hu Y et al (2011) Comprehensive exon array data processing method for quantitative analysis of alternative spliced variants. *Nucleic Acids Res* 39:e123
65. Hardiman G (2004) Microarray platforms—comparisons and contrasts. *Pharmacogenomics* 5:487–502
66. Barnes M, Freudenberger J, Thompson S et al (2005) Experimental comparison and cross-validation of the Affymetrix and Illumina gene expression analysis platforms. *Nucleic Acids Res* 33:5914–5923
67. Vomelova I, Vanickova Z, Sedo A (2009) Methods of RNA purification. All ways (should) lead to Rome. *Folia Biol (Praha)* 55:243–251
68. Li J, Pankratz M, Johnson JA (2002) Differential gene expression patterns revealed by oligonucleotide versus long cDNA arrays. *Toxicol Sci* 69:383–390
69. Tan PK, Downey TJ, Spitznagel EL Jr et al (2003) Evaluation of gene expression measurements from commercial microarray platforms. *Nucleic Acids Res* 31:5676–5684
70. Shi L, Reid LH, Jones WD et al (2006) The MicroArray quality control (MAQC) project shows inter- and intraplatform reproducibility

- of gene expression measurements. *Nat Biotechnol* 24:1151–1161
71. Reimers M (2010) Making informed choices about microarray data analysis. *PLoS Comput Biol* 6:e1000786
 72. Fan X, Lobenhofer EK, Chen M et al (2010) Consistency of predictive signature genes and classifiers generated using different microarray platforms. *Pharmacogenomics J* 10:247–257
 73. Luo J, Schumacher M, Scherer A et al (2010) A comparison of batch effect removal methods for enhancement of prediction performance using MAQC-II microarray gene expression data. *Pharmacogenomics J* 10:278–291
 74. Shi L, Campbell G, Jones WD et al (2010) The MicroArray quality control (MAQC)-II study of common practices for the development and validation of microarray-based predictive models. *Nat Biotechnol* 28:827–838
 75. Churchill GA (2002) Fundamentals of experimental design for cDNA microarrays. *Nat Genet* 32(Suppl):490–495
 76. Wang H, Ach RA, Curry B (2007) Direct and sensitive miRNA profiling from low-input total RNA. *RNA* 13:151–159
 77. Hughes TR, Mao M, Jones AR et al (2001) Expression profiling using microarrays fabricated by an ink-jet oligonucleotide synthesizer. *Nat Biotechnol* 19:342–347
 78. Masuda K, Abdelmohsen K, Kim MM et al (2011) Global dissociation of HuR-mRNA complexes promotes cell survival after ionizing radiation. *EMBO J* 30:1040–1053
 79. Mukherjee N, Corcoran DL, Nusbaum JD et al (2011) Integrative regulatory mapping indicates that the RNA-binding protein HuR couples pre-mRNA processing and mRNA stability. *Mol Cell* 43:327–339

Epigenetic Biomarker to Determine Replicative Senescence of Cultured Cells

Carmen M. Koch and Wolfgang Wagner

Abstract

Somatic cells change continuously during culture expansion—long-term culture evokes increasing cell size, declining differentiation potential, and ultimate cell cycle arrest upon senescence. These changes are of particular relevance for cellular therapy which necessitates standardized products and reliable quality control. Recently, replicative senescence has been shown to be associated with highly reproducible epigenetic modifications. Here, we describe a simple method to track the state of senescence in mesenchymal stromal cells (MSCs) or fibroblasts by monitoring continuous DNA methylation (DNAm) changes at specific sites in the genome. Six CpG sites have been identified which reveal either linear hypermethylation or hypomethylation with respect to the number of cumulative population doublings (cPDs). Conversely, the DNAm level at these CpG sites can be analyzed—for example, by pyrosequencing of bisulfite-converted DNA—and then used for linear regression models to predict cPDs. Our method provides an epigenetic biomarker to determine the state of senescence in cell preparations.

Key words Replicative senescence, Epigenetics, Epigenetic senescence signature, DNA methylation, Mesenchymal stromal cells, Fibroblasts

1 Introduction

In vitro, cells can be expanded to relatively large cell numbers. They undergo numerous population doublings before entering a senescent state—unless they have been transformed into immortalized cells. In the course of culture expansion, cells acquire continuous phenotypic and functional changes, such as cell enlargement and loss of differentiation potential [1]. The phenomenon of replicative senescence has already been described 50 years ago by Leonard Hayflick [2]. A common hypothesis favors the view that replicative senescence is necessary to prevent malignant transformation in vivo [3], but the underlying molecular mechanisms are still not fully understood.

It is widely accepted that culture expansion results in cellular defects as consequence of cellular stresses such as irradiation, extensive proliferation, and oxidative stress. Among other consequences, this entails upregulation of tumor suppressor genes—such as CDKN1A (p21), CDKN2A (p16), or TP53 (p53)—resulting in sustained cell cycle arrest [4]. Telomere attrition has also been shown to play a major role in replicative senescence: telomere length declines with each cell division cycle until a critical length is reached, and it has been shown that few truncated telomeres are sufficient to trigger senescence [4]. Yet, even expression of telomerase and telomere extension cannot always prevent replicative senescence indicating that telomere erosion is not the only cause of replicative senescence [5]. More recently, we have demonstrated that replicative senescence is associated with DNA methylation (DNAm) changes at specific sites in the genome—particularly in developmental genes [6–10]. This observation supports the notion that replicative senescence resembles a highly organized epigenetically controlled process.

Analysis of replicative senescence is of particular relevance for cellular therapy. Therapeutic products require a highly standardized manufacturing process and reliable quality control. However, tracking of replicative senescence in cultured cells is not trivial [11–13]. One approach is analysis of the percentage of highly proliferative cells which are capable of forming fibroblastoid colony-forming units (CFU-Fs). The proportion of CFU-F-forming cells declines continuously over subsequent passages and can therefore be used as surrogate for the remaining cPDs until replicative senescence [14]. However, such functional assays require labor-intensive cell culture methods and can only be used for prospective analysis—therefore a molecular marker might be advantageous. Telomere length has been shown to decline during cellular aging, but due to large interindividual and cell type-specific differences, the assessment of telomere length is usually not applied to monitor replicative senescence. Cells at higher passages accumulate senescence-associated β -galactosidase (SA- β -gal), which can be detected by histochemical staining methods of metabolic products [15]. A fluorescence-based adaptation of this method was described by Debacq-Chainiaux and coworkers, in which the increase of SA- β -gal is detected by flow cytometry [16]. However, this method is limited with respect to providing a quantitative measure of the progress towards the state of replicative senescence. It has also been shown that long-term culture is associated with specific gene expression changes, such as upregulation of CDKN1A, CDKN2A, or TP53 and many more—these changes can be measured relatively easily but the method usually requires a reference of early passage and it is influenced by cell culture procedures [12, 17].

As an alternative to these approaches, we investigated if the aforementioned epigenetic modifications can be used to monitor

replicative senescence [8]. We combined all publically available DNAm data from healthy donors which had been generated with the Infinium HumanMethylation27 BeadChip. This platform facilitates simultaneous DNAm analysis of more than 27,000 CpG sites at single base resolution. Subsequently, we filtered for those CpG sites which reveal a linear increase in DNAm level over subsequent passages, days in culture, or cumulative population doublings (cPDs). Six specific CpG sites were identified by Pavlidis Template Matching (PTM) which fulfilled these parameters [18]. Analysis of DNAm at these CpG sites can conversely be used to predict the state of replicative senescence from various cultured cell preparations. This signature has been validated in mesenchymal stromal cells (MSCs) derived from bone marrow and adipose tissue as well as in dermal fibroblasts. Furthermore, the method was applicable for cells which were propagated in different culture media (supplemented with either fetal calf serum or human platelet lysate) or at different seeding densities [8].

It is tempting to speculate that these DNAm changes are also related to aging of the organism. In fact, comparison of young and elderly donors revealed many age-associated DNAm changes, and overall there is a significant association with long-term culture-associated DNAm changes [6, 9, 19, 20]. However, this association is not observed at most differentially methylated CpG sites and the epigenetic senescence signature described here has been generated regardless of donor age. Interestingly, neither irradiation-induced senescence nor immortalization with hTERT/SV40TAg prevented these long-term culture-associated epigenetic modifications [10]. However, when we reprogrammed MSC into iPSC, the DNAm changes appear to be reset to a state of noncultured cells [10, 21]. Therefore, these epigenetic modifications do not seem to resemble a cell culture artifact—they rather seem to be associated with a tightly regulated epigenetic process which seems to be reversed during rejuvenation into pluripotent cells.

In the following sections, we provide a step-by-step guidance for the use of this epigenetic senescence signature.

2 Material

2.1 *Biological Material*

The method we describe is applicable for different cell types—particularly for mesenchymal stromal cells (MSCs) and fibroblasts. All our cell preparations were isolated after written consent according to the guidelines of the local ethics committees. Bone marrow derived MSCs (BM-MSCs) were isolated from bone marrow aspirates (iliac crest; IC) of healthy donors for allogeneic transplantation (Ethics statement #348/2004, Heidelberg, Germany), from caput femoris (CF) after hip fracture, or from tibia plateau (TP;

#EK128/09, Aachen, Germany, and #076/2007, Heidelberg). Adipose tissue-derived MSCs (AT-MSCs) were isolated from lipoaspirates of healthy adult donors (#EK163/07, Aachen). Dermal fibroblasts (D-Fib) were isolated from patients undergoing plastic surgery (#EK173/07, Aachen). The following sections exemplarily describe culture expansion of BM-MSC in medium supplemented with 10 % human platelet lysate (hPL) [22] (*see Note 1*).

2.2 Human Platelet Lysate

Human platelet lysate (hPL) is generated by two cycles of freezing and thawing of thrombocyte concentrate units from healthy donors (provided by the blood bank, University Hospital, Aachen) as described before [23] (*see Notes 2 and 3*).

2.3 Culture Medium and Passaging

1. 500 mL laboratory bottle (Duran, Wertheim, Germany).
2. 500 mL rapid-Filtermax, vacuum filtration unit (TPP, Trasadingen, Switzerland).
3. 2 U/mL heparin (Ratiopharm, Ulm, Germany).
4. Dulbecco's Modified Eagles Medium-Low Glucose (DMEM-LG; PAA, Pasching, Austria).
5. 2 mM L-glutamine (Sigma-Aldrich, München, Germany).
6. 100 U/mL penicillin/streptomycin (pen/strep; Gibco, Invitrogen, Carlsbad, USA).
7. 0.25 % Trypsin-EDTA solution (1×) (Gibco).
8. 1× phosphate-buffered saline (PBS) (PAA).
9. Tissue culture flasks 75 cm² (Nunc Thermo Fisher Scientific, Langenselbold, Germany).
10. Hemocytometer (Neubauer counting chamber, Brand, Wertheim, Germany).
11. 0.4 % Trypan Blue solution (Sigma).
12. 15 and 50 mL Falcon tubes (BD).

2.4 DNA Preparation

1. QIAamp DNA Blood Midi Kit (Qiagen, Hilden Germany) (*see Note 4*).
2. 15 mL Falcon tubes (BD).
3. 0.5 mL Safelock tubes (Sarstedt, Nümbrecht, Germany).
4. Nuclease-free water (Qiagen).
5. Water bath (70 °C).

2.5 DNAm Analysis at Specific CpG Sites

This model is based on the DNAm at six specific CpG sites. Various methods can be used for detection of the methylation level. These CpG sites can easily be selected from DNAm profiles obtained using the Infinium HumanMethylation27 BeadChip [24] (*see Note 5*).

Table 1
Pyrosequencing primers for the six relevant CpG sites

Gene	Forward primer (5'→3')	Reverse primer (5'→3')	Sequencing primer (5'→3')
<i>GRM7</i>	TTGGGATTATTGTTGATTT	CCCCTACTACCTAC TAAAAATA	TACCTACTAAAA ATACTCCT
<i>CASR</i>	TGTAATAGGTATTTG GTTGTAGT	CCCAAACCTCTTACT CATTCTA	TTGGTTGTAGT TAGGAA
<i>PRAMEF2</i>	TTTGAGGGTATTT AGAAGAGAT	TCCCTAACTAACTAAC TACTAATC	TAGAATTTTGT AAAGTGAG
<i>SELP</i>	AGAAGGTAGAAAATT AGTAGAGTT	CAACATAAAACTCCA TAACTA	AGGTAAAGGTT TAGAAAG
<i>CASP14</i>	TTGGAGATTTAG TGAGATAATA	AACAAAACAAATAAC CCATATA	TATTTTTTTTGA GATGGT
<i>KRTAP13-3</i>	GAGATTTGTTGGAGGTTTAA	CCCAATAAAAAA CAACTCC	ATTTTTTGTTT GATTATGTA

Gene symbols of genes are listed which are associated with the relevant CpG site

We expect that it is alternatively possible to determine the DNAm level by MassARRAY assay [25]. In the following sections we will particularly focus on the specific analysis of bisulfite-converted DNA via pyrosequencing.

1. 600 ng of purified genomic DNA (*see* Subheading 2.4).
2. EpiTect Bisulfite Kit (Qiagen, Hilden, Germany).
3. Q24 Instrument or PyroMark ID Instrument (Qiagen).
4. Pyrosequencing primers are depicted in Table 1 (for sequence information of the relevant CpG sites *see* Table 2).

3 Methods

3.1 Long-Term Culture of Mesenchymal Stromal Cells (See Note 6)

1. Add L-glutamine, penicillin/streptomycin, heparin, and human platelet lysate (10 %) to the DMEM-LG medium to a final volume of 500 mL.
2. Sterile filter medium and store at 4 °C up to 2 weeks.
3. Seed BM-MSC after isolation at a density of 5,000 cells/cm² into culture flasks (*see* Notes 7 and 8).
4. Upon 80 % confluence remove medium and wash cells with PBS twice.
5. Add 1 mL of trypsin–EDTA solution and incubate at 37 °C for 1 min.

Table 2

Depiction of ID numbers, gene names, and sequences of the six relevant CpG sites of the epigenetic senescence signature

CpG site	ID	Associated gene	Sequence surrounding relevant CpG site
1	cg02332525	<i>GRM7</i>	GTGCTGGAGGTGCTCCTGTG CG CGCTGGCGGC GGCGGCGCGC
2	cg17453778	<i>CASR</i>	TGGCTGCAGCCAGGAAGGAC CG CACGCCCTTT CGCGCAGGAG
3	cg03891191	<i>PRAMEF2</i>	AGAAGGTGGTGACTTACCAG CG CTGGACTCA CTTTCAGAGT
4	cg01459453	<i>SELP</i>	ACATAAAACTCCATGGCTAT CG CTGTTCTCTCA CTTTCTGAAC
5	cg01999333	<i>CASP14</i>	CTCTTCTACCTAGGAGATGAC CG GGCTGGGGA AGCCATCTCAA
6	cg16431978	<i>KRTAP13-3</i>	TGACTATGCATGTTGGGTCT CG GGGTTTTG GATCCAATAGCT

The relevant CpG site is indicated in bold

6. After cell detachment, stop trypsinization by application of 5 mL culture medium.
7. Transfer solution into 15 mL Falcon tube and centrifuge at $350 \times g$ for 7 min.
8. Discard supernatant and resuspend pellet in 1 mL culture medium.
9. Count cells in a Neubauer counting chamber after application of Trypan Blue dye for exclusion of dead cells (*see* **Note 9**).
10. Reseed cells at a density of 5,000 cells/cm².
11. Document cell count for calculation of cumulative population doublings (*see* Subheading 3.2).

3.2 Calculation of Real Cumulative Population Doublings

Calculate cumulative population doublings from the first passage until the destined number of passages by employing the following formula: $CPD = \sum_{i=1 \dots n} \log_2(h_i/s_i)$; where n is the total number of passages, s_i is the number of cells seeded at passage i , and h_i is the number of cells harvested in passage i [26] (*see* **Notes 10** and **11**) (Fig. 1).

3.3 DNA Preparation and Bisulfite Conversion

1. Isolate genomic DNA with the QIAamp DNA Blood Midi Kit following the manufacturer's instructions.
2. Elute DNA in 300 μ L nuclease-free water or in the provided elution buffer for long-term storage.

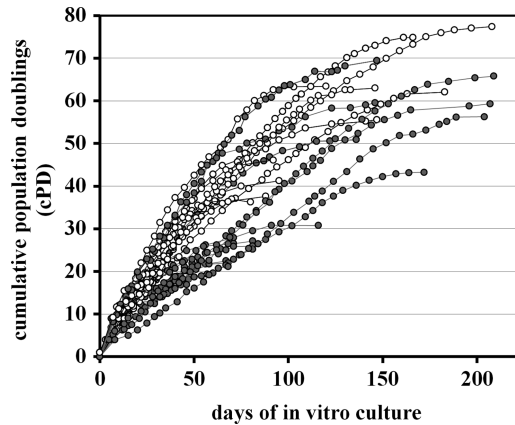


Fig. 1 Long-term growth curves of culture-expanded cells. Human dermal fibroblasts (D-Fib) and mesenchymal stromal cells from bone marrow (BM-MSCs) and adipose tissue (AT-MSCs) were expanded in vitro (*gray symbols*: samples which were analyzed by Illumina BeadChip; *open symbols*: samples analyzed by pyrosequencing). Long-term growth curves are based on the documentation of culture time and calculation of cumulative population doublings as indicated in the text

3. Assess concentration and quality via photometric measurement and agarose gel electrophoresis.
4. Conduct bisulfite conversion of 600 ng purified genomic DNA using the EpiTect Bisulfite Kit according to the manufacturer's instructions. In brief, this treatment is based on the following principle: addition of sodium bisulfite converts unmethylated cytosine residues into uracil, while leaving the methylated cytosines unchanged. A special buffer prevents fragmentation of DNA by controlling the pH condition necessary for cytosine conversion. The optimized thermal cycling program ensures high cytosine conversion rates (over 99 %) and the on-column procedure allows subsequent elution of purified DNA, which can subsequently be analyzed by pyrosequencing.

3.4 DNA Methylation Analysis of the Six Specific CpG Sites

Analysis of DNAm at six specific CpG sites is the prerequisite for use of the epigenetic senescence signature. These sites were selected to correlate with the number of cPDs (Fig. 2). If DNAm profiles based on the Illumina HumanMethylation27k Chip are available, these can be directly extracted by the IDs (Table 2). Alternatively, DNAm at the relevant sites can be determined by pyrosequencing (*see* Subheading 2.5; *see* **Note 12**):

1. Pyrosequencing of bisulfite-converted DNA from cell preparations of known passage and with consecutive cPD calculations can be performed using, for example, the Q24 Instrument or the PyroMark ID Instrument (Qiagen) according to the manufacturer's instructions.

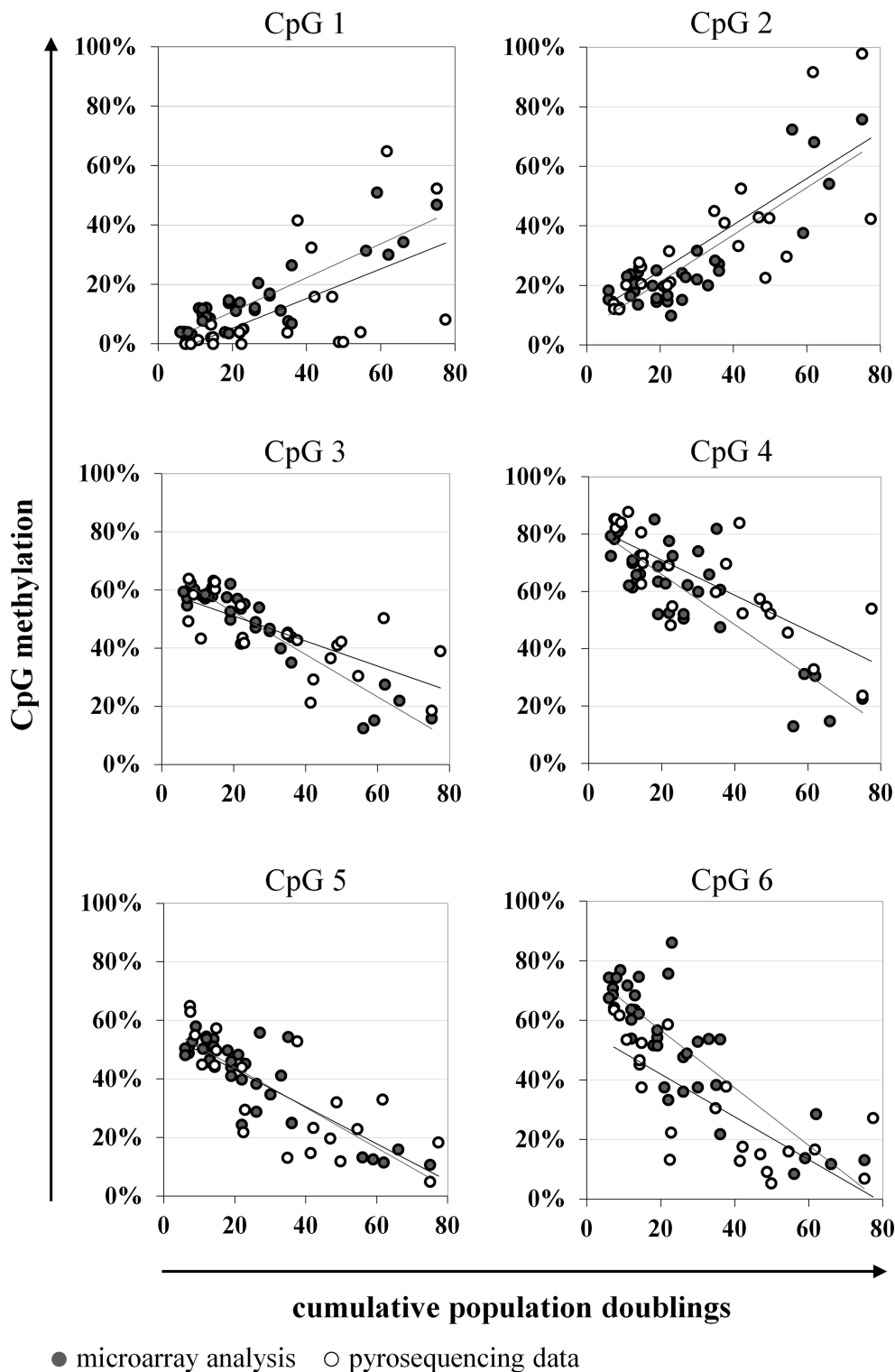


Fig. 2 Cumulative population doublings (cPDs) are reflected by the DNA methylation level of specific CpG sites. The DNA methylation levels of six specific CpG sites are plotted against the corresponding cPDs. These data were either analyzed by Illumina BeadChip technology (*gray symbols and gray regression lines*) or by pyrosequencing of the six CpG sites (*open symbols and black regression lines*)

Monitoring of Cellular Senescence by DNA-Methylation at Specific CpG sites

Carmen M. Koch, Sylvia Joussen, Anne Schellenberg, Qiong Lin, Martin Zenke, Wolfgang Wagner

Instruction for Web Tool:

1. Prerequisite for this tool is the detection of the methylation levels of CpG sites highlighted in red, e.g. by pyrosequencing or Illumina Human Methylation BeadChip.
2. Enter methylation levels into the corresponding fields below (such as beta values, ranging from 0 to 100%).
3. Press the "Calculate" button and retrieve the predicted condition of the cell preparation.

	Gene	Sequence	Methylation level %
CpG1	GRM7	GTGCTGGAGGTGCTCCTGTGCGCGCTGGCGGCGGCGCGGC	<input type="text" value="4"/>
CpG2	CASR	TGGCTGCAGCCAGGAAGGACCGCACGCCCTTCGCGCAGGAG	<input type="text" value="30"/>
CpG3	PRAMEF2	AGAAGGTGGTGACTTACCAGCGCTGGACTCACTTTCAGAGT	<input type="text" value="30"/>
CpG4	SELP	ACATAAACTCCATGGCTATCGCTGTTCTCACTTCTGAAC	<input type="text" value="46"/>
CpG5	CASP14	CTCTTCTACCTAGGAGATGACGGGCTGGGGAAGCCATCTCAA	<input type="text" value="23"/>
CpG6	KRTAP13-3	TGACTATGCATGTTGGGTCTCGGGTTTTGGATCCAATAGCT	<input type="text" value="16"/>

predicted passage: 19

predicted cumulative population doublings: 40

predicted time in culture: 109

Fig. 3 Screenshot of the webpage for the epigenetic senescence signature. The webtool simplifies the prediction of cPDs, passages, and days in culture of a given cell preparation (<http://www.molcell.rwth-aachen.de/dms/>). After typing in the corresponding methylation value of the six specific CpG sites (see Subheading 3.5) and pressing the *Calculate* button, the results are provided

2. Primers used for pyrosequencing are summarized in Table 1 (see Subheading 2.5).

3.5 Analysis of the Epigenetic Senescence Signature with an Online Webtool

For each CpG site the DNAm values are inserted into the corresponding linear regression models (Fig. 2). These equations are described in our previous work [8]. Thereby, predictions for cPDs are generated for each individual CpG site and the mean of these is subsequently calculated for the final value. To simplify the calculation we designed a webtool, where the DNAm values can be easily integrated. This tool is accessible under: <http://www.molcell.rwth-aachen.de/dms/> (Fig. 3).

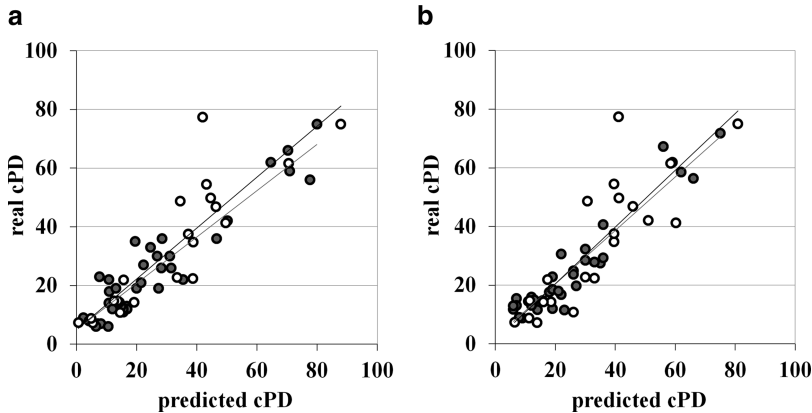


Fig. 4 Prediction of cPDs by either linear regression analysis or multivariate analysis. Single linear regression models on the basis of DNA methylation at six specific CpG sites are applied to calculate cPDs (a). Similar results are received after application of the multivariate model for cPD calculation (b). Beta-values were either measured by Illumina BeadChip technology (gray symbols and gray regression lines) or by pyrosequencing (open symbols and black regression lines)

1. Type in the corresponding beta-values of the 6 CpG sites and press *Calculate* for the predictions (see **Note 13**).
2. Compare results with the calculated real cPDs of the cell preparations (see Subheading 3.2; Fig. 4a).

3.6 Analysis of the Epigenetic Senescence Signature with a Multivariate Model

Alternatively, we have generated a multivariate model which combines the six linear regressions into one equation. Instead of averaging the six independent regression analyses, this single equation method might be easier to use:

$$\text{Predicted cPD} = 45.89 + (23.63 \times \text{cg02332525}) + (31.61 \times \text{cg17453778}) + (-53.70 \times \text{cg03891191}) + (14.86 \times \text{cg01459453}) + (-23.94 \times \text{cg01999333}) + (-10.34 \times \text{cg16431978})$$

The corresponding beta-values for the six CpG sites have to be inserted. This method generates very similar results as the above mentioned method (Fig. 4b).

4 Notes

1. Generation and validation of the epigenetic senescence signature have been performed with bone marrow MSC, adipose tissue-derived MSC, and dermal fibroblasts. For additional validation we used publically available DNA methylation datasets from freshly isolated primary cells (dermal, epidermal, ovarian, and cervical cells as well as blood-derived cells), which were predicted to be close to noncultured cells. Furthermore,

we analyzed public data from several transformed cancer cell lines of different tissues, and these cells were predicted to have a long history of culture expansion [8]. Therefore, the method is probably also applicable for various other cell types although the regression models may have to be adapted. So far, we have not specifically tested applicability for epithelial cells.

2. Thrombocyte units can be used after their date of expiry for clinical application.
3. The donor age of hPL is also relevant. MSCs proliferate faster in culture medium supplemented with hPL from younger donors. Furthermore, the percentage of SA- β -gal-expressing cells is lower than using hPL from elderly donors [27].
4. Alternatively various other commercial kits for DNA isolation can be used.
5. It is also possible to use the Infinium HumanMethylation450 BeadChip [28]. However, this platform does not include the CpG site associated with PRAMEF2. Either this CpG site is then excluded from analysis—which might impair the result—or it is measured by alternative procedures (e.g., pyrosequencing).
6. The epigenetic senescence signature was generated and validated using cells which were harvested during culture expansion under conventional culture conditions. Recently, we have demonstrated that irradiation-induced premature senescence did not affect these DNAm changes [10]. However, we did not test other senescence stimuli such as reactive oxygen species (ROS) or oncogenic RAS expression—it is conceivable that such treatments for premature senescence also have impact on the epigenetic senescence signature.
7. Application of different media and seeding densities is feasible as the epigenetic senescence signature was originally identified in very different cell preparations—yet it may be advantageous to adapt the equations to specific culture conditions if larger datasets are available.
8. Theoretically, seeding density can affect the heterogeneity of replicative senescence within the cell preparations [26]. While this effect cannot be ruled out, we recommend using the same seeding density throughout culture expansion.
9. Alternatively various other methods can be used for cell counting (e.g., by CASY cell counter, Roche Diagnostics, Mannheim, Germany).
10. cPDs can also be estimated without long-term growth curves. However, to validate the accuracy of the method for the corresponding cell preparations, it is necessary to generate these data to determine real cPDs.

11. Estimation of the initial cPDs after the first cell seeding can be performed by a fibroblastoid colony-forming unit (CFU-F) assay in limiting dilutions [14].
12. This technology may not be available in many laboratories: these measurements can be provided by core facilities or commercial service providers. DNA is relatively stable and can easily be shipped. You can contact us for advice.
13. DNAm levels are usually provided as beta-value, ranging from 0 (non-methylated) to 1 (100 % methylation).

Acknowledgments

We thank Anne Schellenberg for critical reading of the manuscript and Qiong Lin for contribution of the multivariate model. RWTH Aachen Medical School has applied for a patent application for the above mentioned method. This work was supported by the excellence initiative of the German federal and state governments within the START Program of the Faculty of Medicine, RWTH Aachen (W.W.), by the Stem Cell Network North Rhine Westphalia (W.W.) and by the Else-Kröner Fresenius Stiftung (W.W. and C.K.).

References

1. Wagner W, Horn P, Castoldi M et al (2008) Replicative senescence of mesenchymal stem cells—a continuous and organized process. *PLoS One* 5:e2213
2. Hayflick L (1965) The limited in vitro lifetime of human diploid cell strains. *Exp Cell Res* 37:614–636
3. Kang TW, Yevsa T, Woller N et al (2011) Senescence surveillance of pre-malignant hepatocytes limits liver cancer development. *Nature* 479:547–551
4. Campisi J, d'Adda di FF (2007) Cellular senescence: when bad things happen to good cells. *Nat Rev Mol Cell Biol* 8:729–740
5. Kiyono T, Foster SA, Koop JJ, McDougall JK, Galloway DA, Klingelutz AJ (1998) Both Rb/p16INK4a inactivation and telomerase activity are required to immortalize human epithelial cells. *Nature* 396:84–88
6. Bork S, Pfister S, Witt H et al (2010) DNA methylation pattern changes upon long-term culture and aging of human mesenchymal stromal cells. *Aging Cell* 9:54–63
7. Schellenberg A, Lin Q, Schueler H et al (2011) Replicative senescence of mesenchymal stem cells causes DNA-methylation changes which correlate with repressive histone marks. *Aging (Albany NY)* 3:873–888
8. Koch CM, Joussen S, Schellenberg A, Lin Q, Zenke M, Wagner W (2012) Monitoring of cellular senescence by DNA-methylation at specific CpG sites. *Aging Cell* 11:366–369
9. Koch C, Suschek CV, Lin Q et al (2011) Specific age-associated DNA methylation changes in human dermal fibroblasts. *PLoS One* 6:e16679
10. Koch C, Reck K, Shao K et al (2012) Pluripotent stem cells escape from senescence-associated DNA methylation changes. *Genome Res* 23(2):248–259
11. Roobrouck VD, Ulloa-Montoya F, Verfaillie CM (2008) Self-renewal and differentiation capacity of young and aged stem cells. *Exp Cell Res* 314:1937–1944
12. Wagner W, Bork S, Lepperdinger G et al (2010) How to track cellular aging of mesenchymal stromal cells. *Aging (Albany NY)* 2:224–230
13. Wagner W, Ho AD, Zenke M (2010) Different facets of aging in human mesenchymal stem cells. *Tissue Eng Part B Rev* 16:445–453
14. Schellenberg A, Stiehl T, Horn P et al (2012) Population dynamics of mesenchymal stromal cells during culture expansion. *Cytherapy* 14:401–411

15. Dimri GP, Lee X, Basile G et al (1995) A biomarker that identifies senescent human cells in culture and in aging skin in vivo. *Proc Natl Acad Sci USA* 92:9363–9367
16. Debacq-Chainiaux F, Erusalimsky JD, Campisi J, Toussaint O (2009) Protocols to detect senescence-associated beta-galactosidase (SA-beta-gal) activity, a biomarker of senescent cells in culture and in vivo. *Nat Protoc* 4:1798–1806
17. Schallmoser K, Bartmann C, Rohde E et al (2010) Replicative senescence-associated gene expression changes in mesenchymal stromal cells are similar under different culture conditions. *Haematologica* 95:867–874
18. Pavlidis P, Noble WS (2001) Analysis of strain and regional variation in gene expression in mouse brain. *Genome Biol* 2:42
19. Bocklandt S, Lin W, Sehl ME et al (2011) Epigenetic predictor of age. *PLoS One* 6: e14821
20. Koch CM, Wagner W (2011) Epigenetic-aging-signature to determine age in different tissues. *Aging (Albany NY)* 3:1018–1027
21. Shao K, Koch CM, Gupta MK et al (2013) Induced pluripotent mesenchymal stromal cell clones retain donor-derived differences in DNA methylation profiles. *Mol Ther* 21 (1):240–250
22. Schallmoser K, Bartmann C, Rohde E et al (2007) Human platelet lysate can replace fetal bovine serum for clinical-scale expansion of functional mesenchymal stromal cells. *Transfusion* 47:1436–1446
23. Horn P, Bokermann G, Cholewa D et al (2010) Comparison of individual platelet lysates for isolation of human mesenchymal stromal cells. *Cytotherapy* 12:888–898
24. Bibikova M, Le J, Barnes R et al (2009) Genome-wide DNA methylation profiling using Infinium assay. *Epigenomics* 1:177–200
25. Ehrich M, Nelson MR, Stanssens P et al (2005) Quantitative high-throughput analysis of DNA methylation patterns by base-specific cleavage and mass spectrometry. *Proc Natl Acad Sci USA* 102:15785–15790
26. Cholewa D, Stiehl T, Schellenberg A et al (2011) Expansion of adipose mesenchymal stromal cells is affected by human platelet lysate and plating density. *Cell Transplant* 20:1409–1922
27. Lohmann M, Walenda G, Hemeda H et al (2012) Donor Age of human platelet lysate affects proliferation and differentiation of mesenchymal stem cells. *PLoS One* 7:e37839
28. Bibikova M, Barnes B, Tsan C et al (2011) High density DNA methylation array with single CpG site resolution. *Genomics* 98:288–295

Single-Neuron Transcriptome and Methylome Sequencing for Epigenomic Analysis of Aging

Leonid L. Moroz and Andrea B. Kohn

Abstract

Enormous heterogeneity in transcription and signaling is the feature that slows down progress in our understanding of the mechanisms of normal aging and age-related diseases. This is critical for neurobiology of aging where the enormous diversity of neuronal populations presents a significant challenge in experimental design. Here, we introduce *Aplysia* as a model for genomic analysis of aging at the single-cell level and provide protocols for integrated transcriptome and methylome profiling of individually identified neurons during the aging process. These single-cell RNA-seq and DNA methylation assays (methyl-capture/methyl enrichment) are compatible with all major next generation sequencing platforms (we used Roche/454 and SOLiD/Life Technologies as illustrative examples) and can be used to integrate an epigenetic signature with transcriptional output. The described sequencing library construction protocol provides both quantitative and directional information from transcriptional profiling of individual cells. Our results also confirm that different copies of DNA in polyploid *Aplysia* neurons behave similarly with respect to their DNA methylation.

Key words Single-cell RNA-seq, DNA methylation, Transcriptome, *Aplysia*, Epigenomics, Epigenetics, Aging, Memory, Next generation sequencing

1 Introduction

Enormous and highly dynamic cell heterogeneity in transcription and signaling is the feature that slows down progress in our understanding of the mechanisms of normal aging and age-related diseases. This is particularly important in neuroscience and neurobiology of aging where the enormous diversity of neuronal populations present a significant challenge in experimental designs. Thus, it is highly desirable to *directly measure molecular signatures and identify mechanisms of aging in neural circuits at single-cell resolution*. Although it is technically difficult, if not impossible, from mammalian preparations, such single-cell resolution is achievable using some invertebrate model organisms.

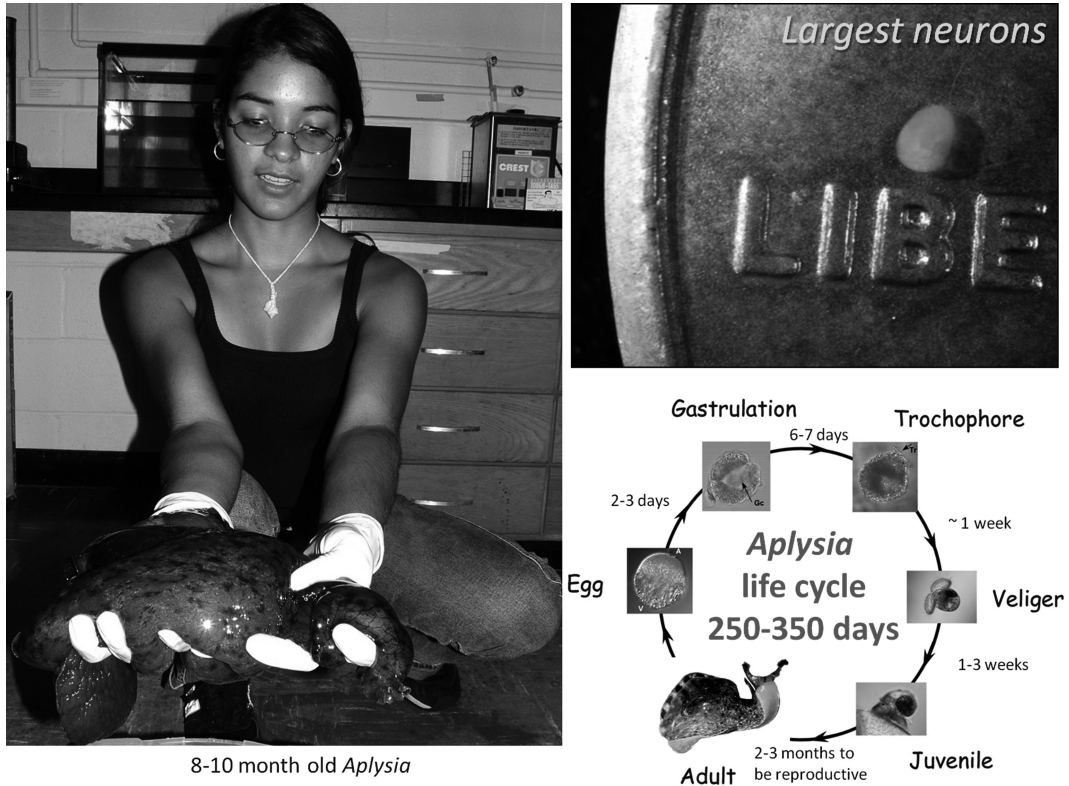


Fig. 1 *Aplysia* is an emerging model for cell biology and epigenomics of aging. The life expectancy of *Aplysia* is approximately a year, and the animal can grow very rapidly from a small microscopic swimming larva, less than 0.5 mm in diameter to up to a 1–3 kg mature adult comparable in its size with a rabbit. Yet, the *Aplysia* central nervous system consists of only 10,000 neurons of different coloration. Some of these neurons are the largest in the animal kingdom [57] and are visible to the naked eye. As a result of their surface location and unique morphological and functional properties, these neurons can be reliably identified and mechanically isolated for microchemical and genomic analysis. The isolated cell on a penny is one of the large cholinergic motoneurons (modified from [24, 59, 60])

In this chapter, we will first introduce a model for genomic analysis at the single-cell level—the marine mollusk, *Aplysia californica* (Fig. 1). Second, using individual identified neurons of *Aplysia* as illustrated examples, we will provide protocols for single-cell transcriptome (RNA-seq) and methylome profiling. Importantly, recent single-cell microarray and RNA-seq studies demonstrated that different neurons indeed age differently [1], Fig. 2. The discovered cell-type specificity in expression of more than several thousand genes suggests that a preexisting epigenetic landscape might significantly determine *how neurons would age*. In other words, conceptually both aging and/or memory formation at the single-cell level can be viewed as a Waddington landscape diagram (Fig. 2d).

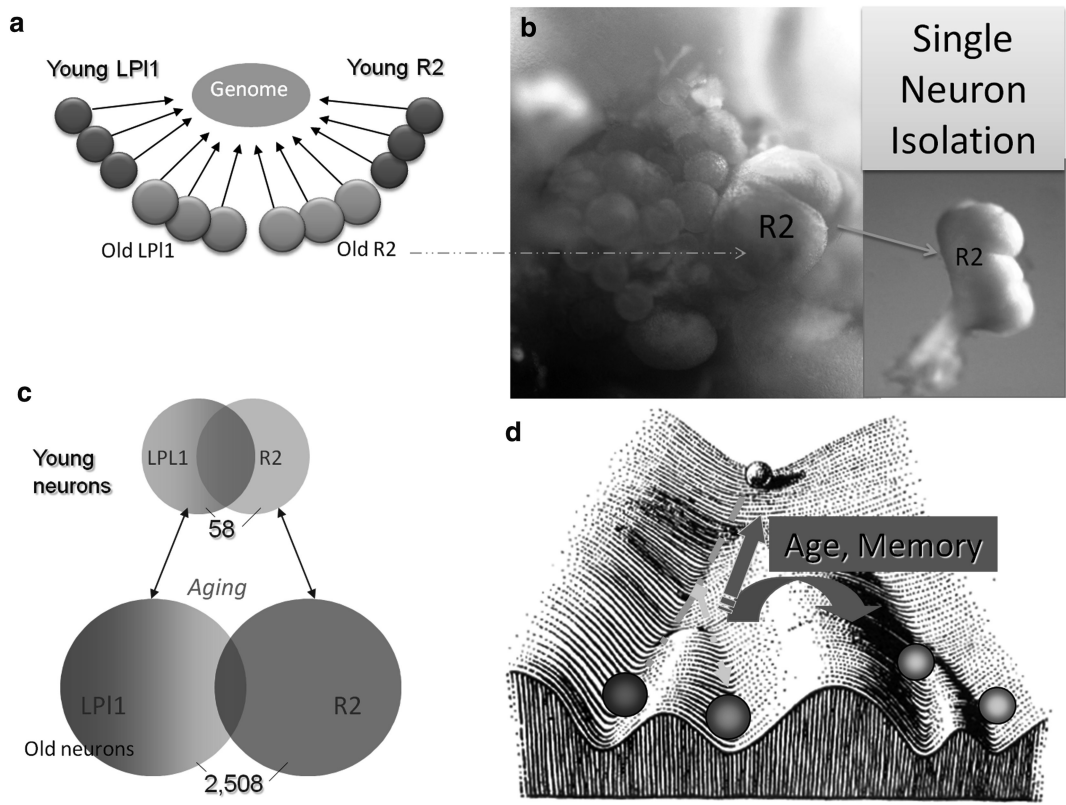


Fig. 2 Different neurons age differently. Comparison of age-related changes in gene expression between two identified cholinergic neurons LPI1 and R2 (modified from [1]). (a) The schematic representation of the reference design microarray experiments to compare two different cell types R2 and LPI1 during the aging process in *Aplysia*. In these microarray tests, individual neurons were compared to the same reference CNS sample. The individual circles represent single neurons (LPI1—blue tones; R2—orange tones) from young or old animals. (b) Photograph of the freshly dissected right abdominal semi-ganglion with the position of R2 and R14 neurons marked (connective tissues from the ganglionic surface were removed and the natural coloration of cell somata were preserved). This R2 cell is the largest neuron ever photographed reaching 1.1 mm in diameter. When this cell was isolated (insert) and fixed in 100 % ethanol it lost its pigmentation. 1.9 μ g of total RNA was obtained from this neuron. (c) We found that only 58 neuronal transcripts (~ 0.1 %) are differentially expressed when LPI1 and R2 neurons are compared from young animals. In contrast, when the same cells were directly compared from old animals, we identified 2,508 differentially expressed transcripts (~ 4.5 %). This suggests that identified cholinergic motoneurons are more similar to each other in younger animals than the same neuronal types in older animals. (d) The landscape diagram is modified from Waddington, C. H., 1956 (Principles of Embryology, op. cit., p. 412; [61]). Following Waddington’s visual schematics, the ball represents a neuronal fate. The valleys are the different fates a given neuron might roll into. At the beginning of its journey, development is plastic, and a cell can have many fates. However, as development and aging or memory proceeds, certain molecular events occur randomly and this can lead to different underlying molecular phenotypes and decisions that cannot be reversed

We are only beginning to realize that at the very core of many neuronal integrative mechanisms is the evolutionarily conserved process of DNA methylation/demethylation [2–9]—i.e., the

covalent modification of cytosine in animal genomes to form a fifth base (5-methylcytosine; (5mC)) or undoing this modification via a sixth base [10, 11] (5-hydroxymethyl cytosine; (5hmC)). Although the levels of 5hmC/5mC have recently been shown to change in the hippocampus with normal aging [12, 13], neither the mechanisms nor cell specificity is known.

It was proposed that age-associated decay of synaptic functions is due to selective, sometimes neuron-specific, downregulation of genes controlling polarized transport of protein-RNA cargos to distant synapses and DNA methylation [1]. Testing these hypotheses at the single-cell level should facilitate identification of molecular markers of aging in general and mechanisms of age sensitivity for certain neuronal classes in particular. The implementation of single-cell epigenomic protocols combined with RNA-seq profiling will also advance our understanding of the logic of gene regulation during normal physiological functions such as loss associative forms of memory. Further progress is also needed in generating efficient model systems to bring together all levels of information, from *genome* to *cell* to *circuit* to *behavior*.

2 *Aplysia* as the Emerging Model for Single-Cell Genomics of Aging

Biology has often advanced by making use of relatively simple model systems. Arguably, *Aplysia* and its simple memory-forming circuit [14–23] is one of only a few currently available model systems [17, 19, 24] that will efficiently advance single-cell studies and encourage new directions in the biology of aging. To stress this point, single-neuron methylation profiling in mammals is currently impossible due to the very small amount of DNA (5–6 pg) and the fact that any required amplification leads to loss of methylation signatures. Thus, a mouse model (e.g., the well-recognized trisynaptic circuit of the hippocampus) of aging *cannot* be used for combined single-cell methylome/RNA-seq profiling. Even reproducible single-cell RNA-seq has not been achieved for any functionally characterized mammalian neuron and initial attempts revealed unprecedented molecular heterogeneity within apparently similar neuronal populations [13, 25, 26]. In contrast, an *Aplysia* neuron yields up to 260 ng of DNA, allowing us to perform single-neuron methylome profiling efficiently (the current limitation is 1 ng of starting material or ~200 mammalian neurons) together with gene expression profiling (RNA-seq) *from the very same cell*, and follows aging at the level of single identified neurons over the entire life span. As such, the *Aplysia* model offers unprecedented advantages to address fundamental questions in aging research.

2.1 The Phenomenology of Aging

Dynamics in *Aplysia* has been studied in sufficient detail (Fig. 1) both in nature and under controlled aquaculture environments [27, 28]. Sexual maturity is generally completed within 2–3 months (~40 % of their life spans) when animals start copulative and egg-laying behaviors (usually in 80–200 g animals). It is easy to culture *Aplysia* and inbred lines can be developed (e.g., in NIH-supported *Aplysia* facilities) (Miami, <http://aplysia.miami.edu/>).

Life expectancy for *Aplysia* is about 150–350 days. *Aplysia* grow linearly without approaching a limiting size (sometimes reaching more than 1–2 kg); thus, the existence of senescence indicates that aging is not a by-product of the cessation of growth [29]. Mean lifespan of animals fed ad libitum was approximately 228 day. In contrast, animals fed standard but limited rations lived much longer (an average of 375 day) and showed a lower initial mortality rate, suggesting that caloric restriction on a single-species diet prolongs lifespan in *Aplysia* [27]. Importantly, animals reared at 13 °C or 15 °C grew as much as four times as large, lived twice as long, matured later, and spawned longer than did animals reared at 18 °C or 21 °C. Aging rate was highest for animals reared at 21 °C—as expected for the accelerated lifecycle at higher temperatures [28].

2.2 Functionally Identified Neural Circuits and Accessible Neurons in Aplysia

Neural circuits controlling both stereotyped and learned behaviors have been identified in the CNS of *Aplysia* [22, 23], providing a solid background to understand cellular bases of behavior at the level of a small number of individually identified neurons. The most significant progress has been made in characterizing memory-forming networks, performed in the laboratory of Eric Kandel, his collaborators, and many other groups [14–23]. The cumulative data obtained during more than 40 years of behavioral, neuronal, and molecular analysis of a network involved in defensive reactions has yielded what is now one of the best understood experimental systems for cellular studies of simple forms of learning and memory [19]. Surprisingly, a large number of critical phenomena associated with long-term synaptic plasticity and memory can be reproduced in a simpler system consisting of only 2–3 neuronal subtypes. This simplest memory-forming network (i.e., a glutamatergic sensory cell, a cholinergic motor neuron, and a serotonergic or FMRFamide-containing interneuron) can also be reconstructed in cell culture. Importantly, this network can be even further reduced to two cells where the action of the facilitatory serotonergic interneurons can be substituted by local application of serotonin (5-HT) [19] or nitric oxide (NO) [30], the neurotransmitters that induce long-term facilitation. Signal transduction pathways underlying 5-HT-induced learning mechanisms are well described [17, 19, 31, 32] and mediated by canonical cAMP/PKA/MAPK/CREB pathways, whereas NO signaling is partially coupled with cGMP pathways [30, 33]. Both of these facilitatory transmitters and aging result

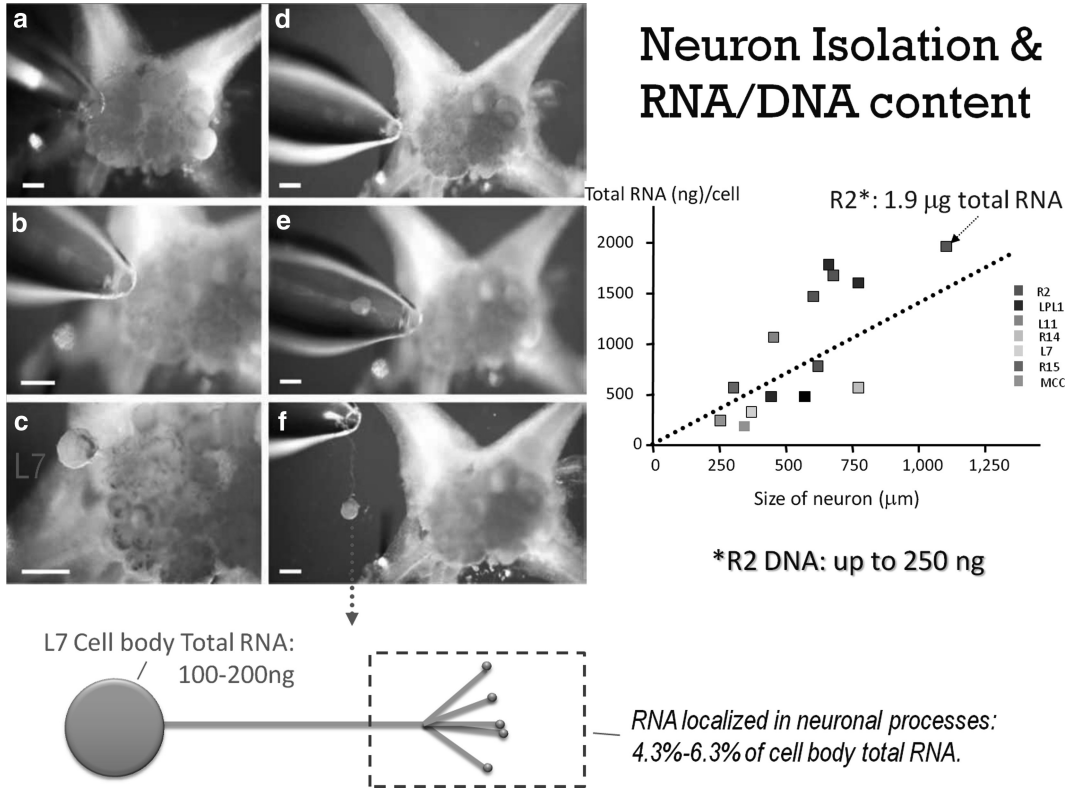


Fig. 3 Isolation of single identified neurons and their RNA/DNA content. (a) Panel of a series of photographs showing the isolation of the L7 neuron with a glass suction pipette (modified from [41]). Below is a schematic depiction of a single neuron and its neurites; the diagram shows the amounts of RNA isolated from neuronal somata and axodendritic processes. (b) The amount of RNA isolated from a single *Aplysia* neuron is directly proportional to the volume of that cell. The gigantic R2 neuron yielded 1.9 μg of total RNA and 250 ng of gDNA

in large-scale changes in gene expression, synaptic reconfiguration, and long-term plasticity within individual neurons and are paralleled from flies to humans and rodents [19].

From a methodological point of view, the most remarkable feature of *Aplysia* is the presence of large, easily identified neurons [22–24]. As we recently measured, these neurons yield from 30 ng to 1.9 μg of total RNA per single neuron [1, 24]. They can also provide from 3 to 250 ng of gDNA depending upon cell size [24]. The accessibility and size of *Aplysia* neurons (ranging from 30 to 1,100 μm) are ideal for development and integration of genomic/epigenomic profiling at a single-cell level. Both single cells and their giant nuclei can be isolated within minutes, making single-cell genomic profiling (RNA-Seq/ChIP-Seq) entirely feasible [1, 34] (Fig. 3). It was also shown that <1 % of the cytoplasm from a single cell is needed to directly characterize and quantify hundreds of intracellular metabolites, signal molecules, and various peptides using capillary electrophoresis and mass spectrometry [35–39].

These posttranscriptional and posttranslational assay protocols are well established and can complement the genomic and epigenetic profiling from the same cells outlined below.

In summary, changes in transcription and DNA methylation with aging have been shown to occur in rodent hippocampus [40], yet mouse and rat models of aging *cannot* be used for integrated single-cell RNA-seq/methylome profiling because the minute amount of DNA (1–2 pg/cell) requires amplification for sequencing, which in turn erases epigenetic and methylation signatures. At present, this type of single-cell experiment is only possible using *Aplysia*, and the protocols for single-cell RNA-seq and DNA methylation profiling are presented in the following sections.

3 Materials

Reagents

- QIAamp[®] DNA Micro genomic DNA isolation kit (Cat # 56304, Qiagen).
- RNAqueous-Micro[™] (Cat # 1931, Ambion/Life Technologies).
- ArrayControl[™] RNA Spike-in control RNAs (Cat #1780, Ambion/Life Technologies).
- High-Capacity cDNA Archive Kit (Cat # 4322171, Applied Biosystems/Life Technologies).
- TaqMan[®] Universal PCR Master Mix (Cat # 4304437, Applied Biosystems/Life Technologies).
- SYBR Green PCR Master Mix (Cat # 4309155, Applied Biosystems/Life Technologies).
- MEGAscript[®] T7 Kit (Cat # 1333, Ambion/Life technologies).
- Quick Ligation[™] Kit (Cat# M2200S, New England BioLabs).
 - 10× Quick Ligation Reaction Buffer:
 - 132 mM Tris-HCl.
 - 20 mM MgCl₂.
 - 2 mM dithiothreitol.
 - 2 mM ATP.
 - 15 % polyethylene glycol (PEG 6000) pH 7.6 at 25 °C.
- AMPure XP Reagent (Cat # A63880, Agencourt, Beckman Coulter, Inc.).
- LA Taq[™] (Cat # RR002M, Clontech) all buffers included.

Table 1
Adaptors and primers for 454 and SOLiD libraries

Primer name	Primer sequence
Trsa	5'-CGCAGTCGGTAC (T) ₁₃ -3'
454 libraries	
A adaptor	5'-GCCTCCCTCGCGCCATCAG-3' and 5'-CCTGATGGCGCGAGGG-3'
B adaptor	5'-GCCTTGCCAGCCCCTCAG-3' and 5'-CTGAGCGGGCTGGCA-3'
A PCR	5'-GCCTCCCTCGCGCCATCAG-3'
B PCR	5'-GCCTTGCCAGCCCCTCAG-3'
SOLiD libraries	
P1 adaptor	5'-CCACTACGCCTCCGCTTTCCTCTCTATGGGCAGTCGGTGAT-3' and 5'-ATCACCGACTGCCCATAGAGAGGAAAGCGGAGGCGTAGTGGTT-3'
P2 adaptor	5'-AGAGAATGAGGAACCCGGGGCAGTT-3' and 5'-CTGCCCCGGGTTCCTCATTCTCT-3'
P1 PCR	5'-CCACTACGCCTCCGCTTTCCTCTCTATG-3'
P2 PCR	5'-CTGCCCCGGGTTCCTCATTCT-3'

- MethylMiner™ (Cat # ME10025, Invitrogen/Life Technologies).
 - Components of the kit include all buffers plus. Dynabeads® M-280 Streptavidin. MBD-Biotin Protein.
- End-It™ DNA End-Repair Kit (Cat# ER0720, Epicentre).
- E-Gel® SizeSelect™ 2 % Agarose (Cat # G6610-02, Invitrogen/Life Technologies).
- Agilent Bioanalyzer™ High Sensitivity DNA Kit (Cat #5067-4626, Agilent Technologies).
- Agilent Bioanalyzer™ RNA 6000 Pico Kit (Cat #5067-1513, Agilent Technologies).
- Primers: 0.2 µM scale HPLC purified, IDT, Integrated DNA Technologies, Inc. (*see* Table 1 for sequences).

Equipment

- Agilent Bioanalyzer™ 2100 (Cat # G2947CA, Agilent Technologies).
- DynaMag™-2 magnet (microcentrifuge tube magnet) (Cat # 123-21D, Invitrogen, Life Technologies).
- Covaris S220 Focused-ultrasonicator.
- ABI 7700 Sequence Detection System (Applied Biosystems/Life Technologies).

- Qubit® 2.0 Fluorometer (Cat # Q32866, Invitrogen/Life Technologies).
- MJ Research Thermo Cycler (Cat # PTC-100, MJ Research).
- E-Gel® iBase™ and E-Gel® Safe Imager™ Combo Kit (Cat # G6465, Invitrogen/Life Technologies).

4 Methods

4.1 Single-Neuron Identification and Isolation

Aplysia californica has the largest neurons in the animal kingdom with the cholinergic motoneuron R2 measuring up to 1.1 mm in diameter (*see* refs. 24, 41 and Fig 2b). Many of the neurons in the central nervous system of *Aplysia* are identified on the basis of distinct function and phenotype [22, 23] and can be easily mechanically isolated. In many cases, the same neuron can be visually identified from animal to animal. If visual identification is not possible, as in the L7 neuron, electrophysiological testing was performed for identification [34, 41]. The illustrated examples of the isolation of two identified neurons are shown in Figs. 2b and 3a using a glass micropipette [41]. In both cases, the ganglia can be pretreated with protease treatment to soften and remove the connective tissues and expose neurons of interest. If visual identification is possible, the easiest and most efficient way to isolate neurons is to place the ganglia in cold (4–10 °C) ethanol for a few minutes. This treatment quickly fixes the ganglia and prevents neuronal injury during the isolation without affecting RNA quality and integrity. Next, a pair of glass microelectrodes (like those used for conventional microelectrode recordings) can be used to mechanically remove individual neurons (Fig. 2b). The procedure takes from 1 to 10–15 min to isolate a neuron of interest (it is a matter of practice and skill).

An alternative and complementary method is to isolate living neurons using the same protocols as for cell culture [41] (*see* detailed description in Lovell and Moroz, 2006); this procedure is illustrated in Fig. 3a. The later procedure can be applied to neurons that require electrophysiological identification and characterization. We have obtained comparable yields of RNA using either of these procedures.

Importantly, as we indicated earlier, it is possible to isolate individual neuronal processes, axons, and even growth cones for transcriptome profiling of extrasomatic RNA. To facilitate the visualization, neuronal processes can be electroporated using fluorescent dyes as described elsewhere [42].

4.2 Single-Neuron RNA Extraction

Once single neurons and/or cell compartments are isolated, total RNA is extracted (*see* Fig. 3a, b). We choose the RNA isolation kit or method that has been experimentally proven best based on the

quality and quantity of RNA for a specific animal, tissue, or even single cell [43] (see below for more details and notes). For single neurons, the RNAqueous-Micro™ Kit produces excellent and reproducible quality RNA. RNA quality is analyzed using an Agilent 2100 Bioanalyzer™ on a 6000 Nano LabChip. For very small quantities the 6000 Pico LabChip can be used. From the cell body of a single L7 neuron, we extracted up to 100–200 ng of RNA (see Fig. 3), and from the processes of sensory neurons in cell culture, we extracted 20–40 pg of total RNA that was used to generate sequencing libraries for the Roche/454 platform.

We show that the total RNA quantity from each neuron is linear in relation to its cell volume ($R^2 = 0.9052$, see also Fig. 3). Therefore, the concentration of RNA molecules is constant regardless of cell size in these neurons. From the single R2 neuron shown in Fig. 2b, 1.9 µg of total RNA was extracted (see Note 1). Up to 250 ng of genomic DNA was extracted from the same identified neuron, R2, which is the largest known neuron in the animal kingdom. However, the procedure was successfully tested for the entire spectrum of neuronal cell diameters from 30 to 300 µm in *Aplysia*, squid (*Loligo*) axoplasm, and for clusters of 20–100 hippocampal neurons from CA1 and CA3 regions of rat brain. Thus, the presented method is not limited to neurons isolated from *Aplysia*, and our protocol can also be easily adapted to samples with larger amounts of material.

4.3 Single-Cell RNA-Seq Library for 454 Pyrosequencing

All commercially available RNA-seq library kits from Illumina, SOLiD, and the new Ion Torrent PGM sequencers require large amounts of starting material (>1.0 µg) and are not feasible for single cells. The general strategy for all these kits starts with rRNA depleted or total mRNA isolated; the resultant RNA is fragmented either chemically or by heat and then ligated with RNA primers specific to a chosen sequencing technology, followed by reverse transcription to generate cDNA by either template switch reverse transcriptase or the traditional first- and second-strand cocktail of enzymes. The resultant dsDNA is amplified, purified, and sequenced.

Recently, two single-cell approaches to RNA-Seq were published—Tang and colleagues [44, 45] and Linnarsson and colleagues [46]. Both protocols demonstrate single-cell sequencing capabilities. Both protocols also start with capture of single cells and direct processing to reverse transcription with no subsequent RNA isolation, and we have used this method with success. However, after this point the two protocols deviate radically, with the Tang protocol becoming a 100-step process over 6 days time that has only been applied to 30 atypical large early embryonic cells (10–100 times larger than most somatic cells) with no internal controls. The Linnarsson protocol uses a template switch method of generating cDNA and validates their method with spiked-in controls.

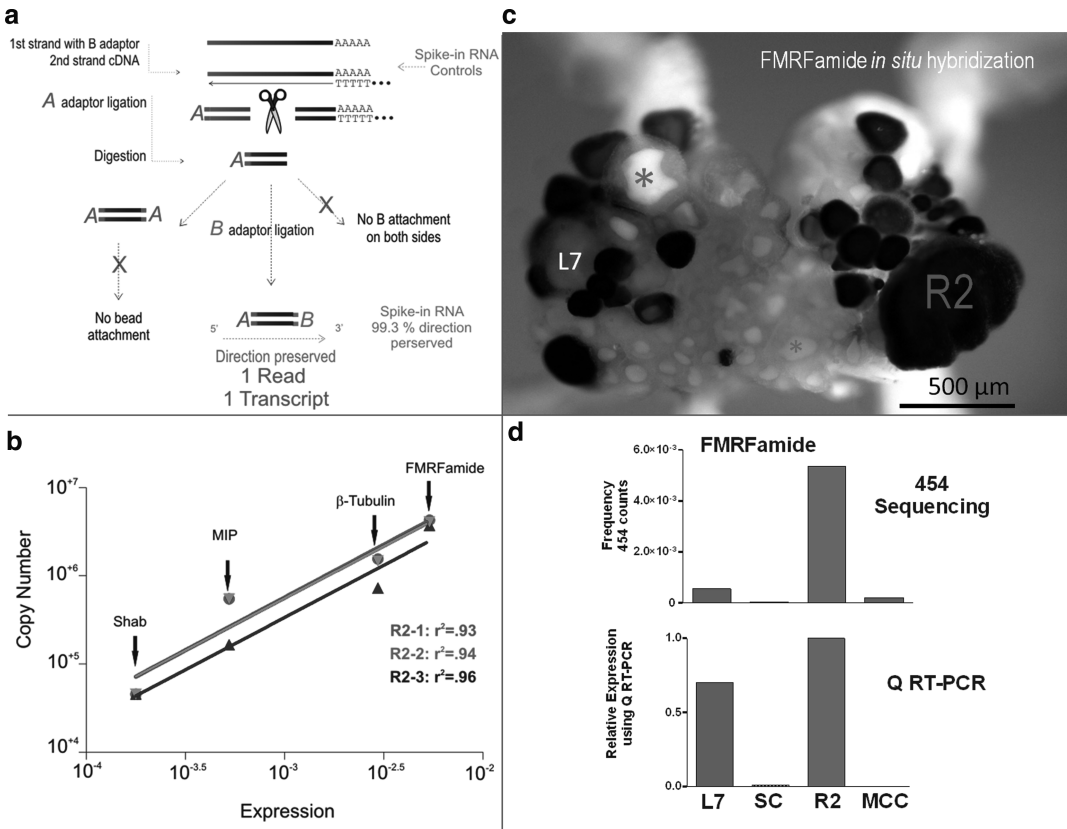


Fig. 4 Single-cell RNA-seq and its validation. **(a)** The diagram presents the workflow of the RNA-seq protocol outlined in the text. Single *Aplysia* neurons were isolated, RNA extracted, and 454 sequencing libraries constructed. **(b)** Absolute RT-PCR was used to generate the intracellular copy numbers for four transcripts of interest. This copy number showed a linear correlation to transcript abundance (expression) in the sequence data set. **(c)** In situ hybridization [42] was performed on one of the neuron-specific and quite abundant transcripts (the neuropeptide FMRFamide) in the R2 neuron. The photo had been captured in 100 % ethanol. Note, the white nuclei (blue asterisks) can be seen in many neurons. **(d)** Quantitative RT-PCR of transcripts of interest (FMRFamide) displayed a correlation between the digital profile in the different single cells and their corresponding quantitative RT-PCR expression. Expression profiles for both the frequency of sequencing reads and the QRT-PCR displayed similar patterns. However, caution should be taken for interpretation of the RNA data, since abundant transcripts known to be selectively transported to synaptic terminals and located on neuronal somata can also be captured by RNA-seq (e.g., in contrast to R2, L7 does not express FMRFamide). Thus, to test cell specificity of expression, a complementary in situ hybridization should be performed **(c)**

Here, we used an unbiased method of library construction for transcriptional profiling that is both quantitative and qualitative, preserves the direction of transcripts, and is applicable for single neurons (see Fig. 4a). All materials and methods for this type of RNA-seq library construction have been described [43]. The only current modification to the protocol is the primers and adaptors that are specific for 454 sequencing technology (see Table 1).

All together for these single-cell 454 specific libraries, we used one cholinergic R2 neuron, one L7 motor neuron, three serotonergic MCC neurons, and a cluster of approximately 200 sensory neurons to validate our method's applicability.

Briefly, library construction starts with total RNA reverse transcribed to cDNA with an oligo-dT primer, and then a second strand is generated (*see* Fig. 4a). The double-stranded cDNA is fragmented with a restriction enzyme, and then 454-specific adaptors are sequentially ligated onto the double-stranded cDNA fragments, which are finally amplified. Fragmented DNA with ligated adaptors is processed through an emulsion-based clonal amplification (emPCR) then captured onto beads as required for subsequent sequencing steps. DNA-captured beads are placed on a PicoTiter-Plate device for pyrosequencing using the 454 GS-FLX platform. We validated both the quantitative aspect with absolute RT-PCR with spiked-in controls and directionality of sequencing (*see* Subheading 4.1, 4.2, 4.4 and Fig. 4b–d).

4.4 Validation of Single-Cell RNA-Seq

RNA-seq, also called “Whole Transcriptome Shotgun Sequencing,” can, by sheer brute force of high sampling, detect RNAs from very low abundance classes (or a rare subpopulation of cells contributing to the sample) and do it unambiguously. Fundamental to all RNA-seq experiments is a validation of quality, quantification, and directionality of the transcription output for a given sample/single cell to substantiate the protocols. Validation of our single-cell RNA-seq has been performed with two types of controls: external (six *spiked-in* RNAs of known concentration) and internal (absolute copy number of four cloned and characterized transcripts). We also performed a correlation of sequenced digital output across different cell types with the results of quantitative RT-PCR. Then we used *in situ* hybridization to confirm cell-specific expression profiling, relative abundance, and expression of predicted antisense transcripts.

4.4.1 Spike-in RNA Controls (External Control)

For the external controls, sequencing was performed with six non-animal oligonucleotides (ArrayControl™ RNA Spike-in control RNAs) spiked-in at various concentrations to the RNA of a single L7 motoneuron at the beginning of the library construction. As a result, we demonstrated a linear correlation between the quantities of each spiked-in sequence added at the beginning of the protocol and the number of reads generated from RNA-seq data (*see* Table 2). Frequency (or “expression level”) is the number of reads divided by the total number of reads in a specific library.

4.4.2 Protocol for Absolute Real-Time PCR (Copy Number Determination)

An internal copy number for four specific transcripts (*see* Table 3) was generated using absolute quantification with the TaqMan® custom gene expression assay from three different individual R2 neurons. The specific transcripts were chosen based on their

Table 2
External controls: *Spike-in* controls starting copy numbers and resulting read frequencies

Spike number	Starting copy number	Reads	Frequency (468,723 total)
Spike_1	2.50E ⁺⁰⁸	5,268	1.13E ⁻⁰²
Spike_2	2.50E ⁺⁰⁷	3,830	8.12E ⁻⁰³
Spike_3	1.87E ⁺⁰⁶	218	4.65E ⁻⁰⁴
Spike_4	1.67E ⁺⁰⁶	109	2.33E ⁻⁰⁴
Spike_5	1.83E ⁺⁰⁴	15	3.20E ⁻⁰⁵
Spike_6	1.27E ⁺⁰²	1	2.13E ⁻⁰⁶

Table 3
Primer and probe sequences for absolute and quantitative real-time PCR

Transcript	Accession number	Forward primer	Reverse primer	Probe
Custom TaqMan				
<i>FMRFamide</i> 0045477209 Custom TaqMan	P08020	5'-GATGACGATG TGCAGGATC TGA-3'	5'-CCCAAACCTCA TGAACCGTTTA TTTAC-3'	5'-FAM-ACCATCAC CAATATCC-3'
<i>b-Tubulin</i> 0045477646 Custom TaqMan	AAP13560	5'-TGGATGTCG TCAGGAAAG AGTCT -3'	5'-CCACCCAAGG AGTGTGTCAA TT-3'	5'-FAM-CCTGCA GACAATCACA-3'
<i>MIP</i> 185429001 Custom TaqMan	AF454399.1	5'-GCTATGGCTC CGAAGTTT TTCG-3'	5'-CTTGTGTCCAGA GCCAATTG TTC-3'	5'-FAM-TCCCACGA GTAATTCT-3'
<i>Shab</i> 0016112793 Custom TaqMan	S68356	5'-GGGCTCGCT CATCAGCAT-3'	5'-CCCCTTGGT GGTGATGGT-3'	5' FAM-CCTGTCGA TCATCCCC-3'

abundances in a single R2 neuron. The intracellular copy numbers for four transcripts of interest also showed a linear correlation to their abundance (expression) in the sequence data set (*see* Fig. 4b). Protocol for Absolute RT-PCR is the following (*see* **Note 3**):

1. Single cells R2, L7, MCC, and sensory cluster had their size measured and were then isolated.
2. Total RNA was extracted from these single cells using RNAqueous-Micro™ as described in Subheading 4.2.

3. cDNA synthesis was produced with random hexamers using the High-Capacity cDNA Archive Kit.
4. Primers and probes were tested for 100 % efficiency by ABI and came premixed in a 20× solution (*see* Table 3 for sequences).
5. Two-Step RT-PCR was performed where the RT and PCR were done separately. The PCR was performed using TaqMan[®] Universal PCR Master Mix on an ABI 7700 Sequence Detection System.
6. The linear dynamic range of the input RNA (cDNA) from 1 ng to 10 pg was determined. All samples and standards were performed in quadruples.
7. The PCR conditions were the manufacture's recommendations which were:
 One cycle at 95 °C for 10 min.
 Followed by 40 cycles.
 95°C for 15 s.
 60 °C for 1 min.
8. The negative control was a cell proven by in situ hybridization to not contain the tested sequence.
9. The standard curve was generated in the following way:
 - (a) A plasmid that contained the sequence of interest was transcribed with MEGAscript[®] T7 Kit to generate cRNA.
 - (b) The concentration of the cRNA was measured with a 2100 Bioanalyzer (Agilent Technologies).
 - (c) A known amount of cRNA was added for cDNA synthesis using the same protocol as the samples.
 - (d) Once the cDNA was produced, dilutions were made to generate 30–300,000 copy numbers based on the starting cRNA concentration.
 - (e) Sample copy number was calculated from the standard curve and standard deviation generated.
 - (f) Expression is the number of reads for the gene of interest divided by the total number of reads for that specific sequencing dataset.
 - (g) R^2 were generated for three individual R2 neurons Fig. 4b.

4.4.3 Localization by In Situ Hybridization for RNA-Seq Validation

In situ hybridization (ISH) is a well-established method that uses a labeled complementary RNA (cRNA) strand (i.e., probe) to localize a specific RNA sequence at single-neuron resolution. Thus, we used in situ hybridization to further confirm neuron-specific expression profiling of more than 50 selected genes selected from corresponding digital RNA-seq profiles (*see* **Note 2**). Finally, observed directionality of the specific genes of interest is shown to

be neuron specific and differential (confirmed by in situ hybridization, see examples of the multicolor in situ hybridization protocols used in [42]). Numerous expression patterns of selected mRNA transcripts have been mapped to individual cells in the central nervous system (CNS) of *Aplysia* as we reported elsewhere [34, 42]. The relative abundance of select transcripts perfectly correlates with their digital expression profiles (see Fig. 4b–d).

4.4.4 Protocol for Quantitative RT-PCR for Identified Neurons

For genes of interest, a correlation between their calculated digital expression profiles in the identified cells with their expression levels using quantitative RT-PCR (QRT-PCR) must be performed to confirm the efficiency of single-cell RNA-seq. For example, expression of the transcript encoding FMRFamide, an R2-specific neuropeptide marker, was confirmed by absolute RT-PCR (Fig. 4d), in situ hybridization (Fig. 4c), and number of sequence reads.

The key steps for the QRT-PCR follow (see **Note 3** as well as [47]):

1. Single-neuron isolation and RNA extraction are described in Subheadings 3.1 and 3.2
2. cDNA is generated as described in the Subheading 4.3.
3. Sequences of the transcript of interest can be loaded into Primer Express[®] software (Applied Biosystems) to design specific primers (amplicon lengths are between 75 and 125 bp).
4. Two-step RT-PCR does the RT and PCR separately with the SYBR Green PCR Master Mix on an ABI 7700 Sequence Detection System (following the same PCR setup as in Subheading 4.4.2).
5. The linear dynamic range of the input RNA (cDNA) is 10 pg–1 ng.
6. All primer sets are tested for optimal dissociation curves with amplification efficiencies between 85 and 100 % (all primer sets not meeting the standards should be redesigned).
7. We usually normalized all runs to *Aplysia* 18s RNA as an endogenous control.
8. The relative standard curve method was employed for analysis and an expression ratio calculated for each sample pair.
9. Ideally all data should be performed in technical triplicate and from at least two biological replicates.

4.4.5 Sense and Antisense Digital Profiling

The library construction protocol presented here preserves directionality and allows us to measure sense and antisense by digital profiling, while the external spiked-in controls allow us to monitor the quality of the library. We also confirmed the directionality with the spike-ins and only 0.7 % were sequenced in the antisense direction.

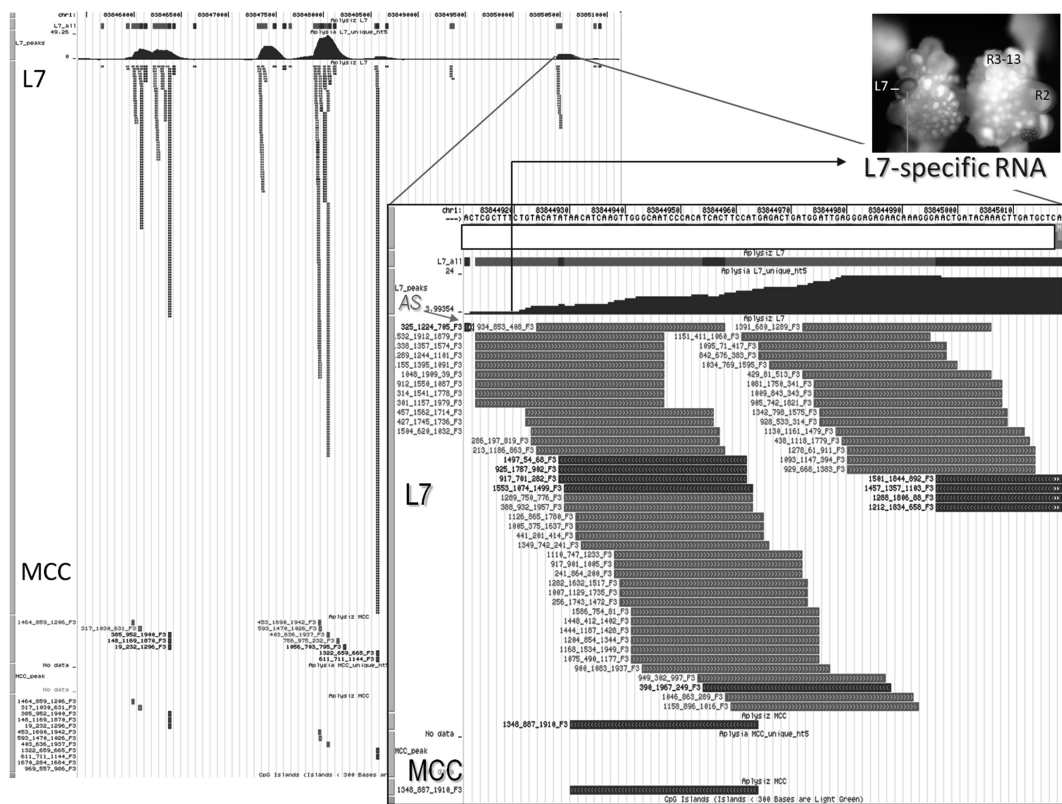


Fig. 5 Neuron-specific expression of sense and antisense transcripts in identified neurons. The library construction protocol reported here preserves directionality and allows quantification of sense (red) and antisense (blue) as revealed by RNA-seq for two identified neurons: the gill motoneuron L7 and feeding interneuron MCC. Differential expression is demonstrated by the abundance of reads for L7-specific secretory peptide (confirmed by in situ hybridization for the same transcript in L7, see *insert*) compared to the interneuron MCC which does not express this gene. Remarkable transcriptional complexity is evident even from a small region of the genome shown here

In contrast, when 317 known *Aplysia* full-length cDNAs (see **Note 4**) were mapped to all the single-neuron transcriptomes, 94.12 % were in the sense orientation and 5.88 % were antisense. These antisense reads were not randomly distributed and were only present for approximately 44 % of the full-length *Aplysia* cDNAs examined. Antisense reads aligned to specific genome regions on the cDNA in one neuron were absent from others. While antisense reads matching specific cDNAs appeared independently in samples derived from different neuronal types and aligned to the same sections along the cDNAs, the percent of antisense was also variable between cells. For example, Fig. 5 demonstrates differential expression and complex patterns of abundance and directionality of specific transcripts between two neurons: the peptidergic motoneuron L7 vs. serotonergic interneuron MCC (the red-colored reads are antisense and the blue-colored reads are sense).

4.5 Single-Cell Enriched Methylated Genomic DNA Library (MethylMiner™)

4.5.1 Introduction to DNA Methylation Protocols

Determining the epigenetic signature of a single cell is an enormous challenge. It would be reasonable to assume that every neuron, because of its unique properties and wiring, might have its own unique transcriptome as well as methylome. *Aplysia*'s large neurons are fully accessible for direct DNA methylation profiling at the entire genomic scale (single-neuron methylome, *see* **Note 5**). In general, it is possible to use the same set of neurons as described for RNA-seq experiments. Specifically, we outline here an enrichment method of 5-methylcytosine (5-mC). It is a more practical first step for methylation profiling, in contrast to bisulfite sequencing, because of the limited amount of genomic DNA even from large *Aplysia* neurons (5–250 ng). The bisulfite sequencing technique relies on the conversion of every unmethylated cytosine residue to uracil, which is then sequenced and recognized as a thymine. If conversion is incomplete the result is false positive calls for methylation sites. A major challenge in bisulfite sequencing is the degradation of DNA that takes place at the same time as the conversion. The conditions necessary for complete conversion, such as long incubation times, elevated temperature, and high bisulfite concentration, can lead to the degradation of ~90 % of the sample DNA. Since the starting amount of genomic DNA in single cells is limited, the extensive degradation associated with bisulfite sequencing can be problematic. A final concern with bisulfite sequencing is that the treatment greatly reduces the level of complexity in the sample to mostly three bases making molecular manipulations more difficult.

Here we present an enrichment capture technique for methylated (5-mC) DNA using the MethylMiner™ approach followed by high-throughput sequencing which is adapted to single neurons (*see* Fig. 6 and **Note 6**).

The most important advantage to the MethylMiner™ enrichment is that, unlike bisulfite treatment, there are no harsh denaturing conditions causing severe degradation and loss of DNA. Genomic DNA is isolated from single cells then fragmented to 150 bp. Methylated DNA is enriched from fragmented genomic DNA via binding to the methyl-CpG binding domain of human MBD2 protein, which is coupled to paramagnetic Dynabeads® M-280 Streptavidin via a biotin linker from the MethylMiner™ kit. It should be noted that *Aplysia* has the MBD protein (Acc# ADM34183.1) which shares 98 % identity with the binding domain of the human MBD2 used in this kit (*see* Fig. 6). The enriched gDNA is eluted with one high-salt elution step. Resultant gDNA is ligated with the appropriate P1 and P2 SOLiD adaptors and amplified. The products were sequenced directly using SOLiD technology (*see* **Note 7**).

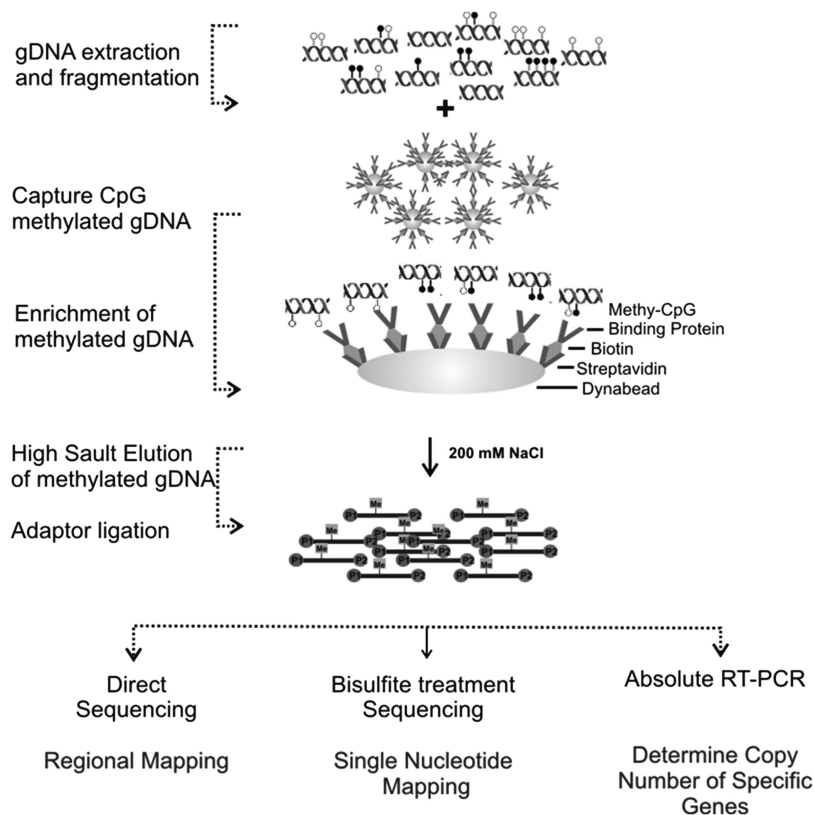


Fig. 6 Single-cell Enriched Methylated Genomic DNA Library constructed using the MethylMiner™ approach. The diagram presents the workflow of the reported MethylMiner™ enriched sequencing library protocol. Genomic DNA is first isolated from single neurons, then fragmented to 150 bp. Methylated DNA is enriched from fragmented genomic DNA via binding to the methyl-CpG binding domain of human MBD2 protein, which is coupled to paramagnetic Dynabeads® M-280 Streptavidin via a biotin linker from the MethylMiner™ kit. The enriched gDNA is eluted with one high-salt elution step. Resultant gDNA is ligated with the appropriate P1 and P2 SOLiD adaptors and amplified. At this point this product can be directly sequenced for regional mapping, bisulfite sequenced for single-nucleotide resolution or used for absolute RT-PCR for copy number determination of genes of interest

4.5.2 Library Construction

1. Genomic DNA was isolated from single cells using a QIAamp® DNA Micro genomic DNA isolation kit (*see Note 8*).
2. Isolated genomic DNA was fragmented to 150 bp with a Covaris S220 Focused-ultrasonicator (*see Note 9*).
3. End repair of fragmented gDNA.

34.0 µL	DNA to end repair
5.0 µL	10× end-repair buffer
5.0 µL	dNTP mix
5.0 µL	ATP
1.0 µL	End-repair enzyme mix
50.0 µL	Total volume

4. Mixture is incubated 20 min at room temperature.
5. The mixture is purified with 1.8 volumes of AMPure XP Reagent (90.0 μ L) as described above and eluted with 35 μ L of nuclease-free water. This fragmented DNA is the template for the methylation enrichment.
6. Methylated DNA was enriched following manufacturer's directions (MethylMiner™).
 - (a) Initial bead wash of the Dynabeads® M-280 Streptavidin.
 - (i) 10.0 μ L of beads were added to the DNA for a final volume of 100.0 μ L
 - (ii) Tubes were placed on a magnetic rack for 1 min to concentrate the beads, and then the liquid was discarded.
 - (iii) An equal volume of 100.0 μ L of 1 \times bind/wash buffer was added to the beads, the beads were resuspended by pipetting, and then the above step was repeated.
 - (b) The Dynabeads® M-280 Streptavidin capture with the MBD-Biotin Protein.
 - (i) Add 7.0 μ L of MBD-Biotin Protein to 100.0 μ L of 1 \times bind/wash buffer.
 - (ii) Transfer the diluted MBD-Biotin Protein to the tube of resuspended beads and mix on a rotating mixer at room temperature for 1 h.
 - (iii) Wash the coupled MBD-beads as in steps (b) (ii)
 - (c) Methylated DNA capture on MBD-beads.
 - (i) Transfer the DNA/buffer mixture to the tube containing the MBD-beads and mix overnight at 4 °C.
 - (d) Removal of non-captured DNA from the Beads.
 - (i) Place the tube on the magnetic rack for 1 min then remove the supernatant.
 - (ii) Wash the beads with 200.0 μ L of 1 \times bind/wash buffer (*see Note 10*).
 - (iii) Mix the beads on a rotating mixer for 3 min.
 - (iv) Place the tube on the magnetic rack for 1 min then remove the supernatant (*see Note 11*).
 - (e) Elution of the captured methylated DNA.
 - (i) The enriched methylated DNA is eluted in 200.0 μ L of the high-salt elution buffer (2,000 mM NaCl) provided in the kit (*see Note 12*).
 - (ii) Beads are incubated on a rotating mixer for 3 min.
 - (iii) Place the tube on the magnetic rack for 1 min then remove the supernatant.

(iv) **Steps 6** (e) (i–iii) are repeated and supernatant combined with first elution.

(v) The enriched methylated DNA from the two high-salt elutions is ethanol precipitated.

7. Sequencing adaptor ligation.

(f) Resultant gDNA is ligated with P1 and P2 SOLiD adaptors and amplified.

10.0 μL	10 \times Quick Ligation Reaction Buffer
5.0 μL	Quick T4 DNA Ligase
10.0 μL	Adaptors P1/P2 (mix 10 μM each) (<i>see</i> Table 1)
75.0 μL	dsDNA
100.0 μL	Total volume

(g) This mixture is incubated for 10 min at room temperature.

(h) The ligation mixture is purified with 1.8 volumes of AMPure XP Reagent (38 μL) as described above and eluted with 35.0 μL of nuclease-free water.

8. PCR amplification is performed on the adaptor-ligated purified dsDNA with LA Taq™.

5.0 μL	10 \times LA PCR Buffer II (Mg^{2+} plus)
8.0 μL	dNTP Mix (2.5 mM each)
2.0 μL	Primers mix A and B (10 μM each)
35.0 μL	Ligated dsDNA
0.5 μL	Takara LA Taq™ DNA Polymerase (5 U/ μL)
50.0 μL	Total volume

9. The above mixture was amplified with the following conditions for eight cycles:

95 °C for 30 s.

8 cycles:

95 °C for 30 s.

58 °C for 30 s.

72 °C for 1 min.

10 °C hold.

10. The amplified PCR product is visualized on a 2 % agarose gel to check for adequate concentration.

11. The amplified PCR product is purified with 1.8 volumes of AMPure XP Reagent (90.0 μL) as described above and eluted with 20.0 μL of TE.

- 12. The appropriate size fractionation is performed on an E-Gel® SizeSelect™ 2 % Agarose.
- 13. Samples were sequenced by SOLiD technology.

5 Data Analysis

As for *Aplysia* neurons, initial annotation of the presented data can be viewed using the *Aplysia* genome browser which outlines ongoing collaborative efforts in the analysis of this newly sequenced genome. The *Aplysia* genome consortium was formed in 2004 (<http://www.genome.gov/Pages/Research/Sequencing/SeqProposals/AplysiaSeq.pdf>), and the *Aplysia* genome sequencing was performed as a collaborative effort between the Broad Institute, Columbia University (E.R. Kandel and J. Ju’s laboratories), and our lab at the University of Florida. The initial *Aplysia* draft (Sanger) genome is located on the UCSC browser <http://genome.ucsc.edu/>. We created a mirror of the UCSC browser with an updated assembly (<http://128.227.123.35:8889/cgi-bin/hgGateway>), and ongoing sequence data is added as tracks to the browser. For example, one can now view the methylation and expression status at the same time for a given gene of interest (Fig. 7). Globally, quantification of methylation reads can be handled in a manner similar to RNA-seq.

Even a single test with these reported protocols will generate a massive data set and require substantial bioinformatics efforts for efficient integration and interpretation of both RNA-seq and methylome results (which certainly should be a subject for separate publications under overall concepts and scope of the ongoing ENCODE projects <http://www.nature.com/encode/?gclid=CMmLjtWlq7MCFQvznAodKEEAiQ#/thread>). Although space restriction prevents

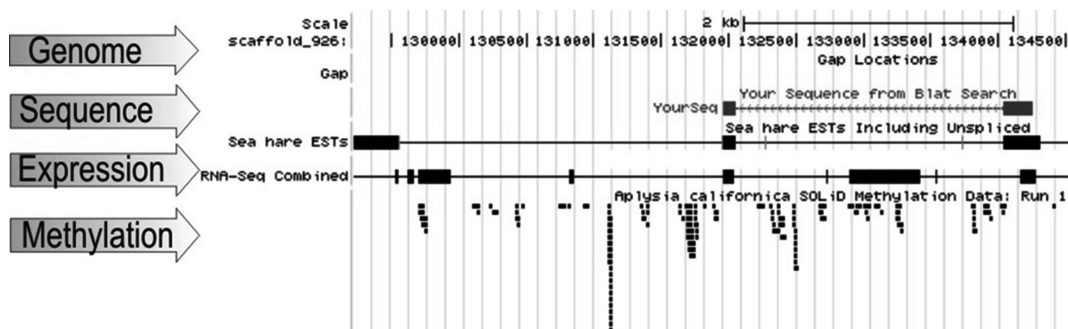


Fig. 7 Data analysis of both expression and methylation profiling. RNA-seq and methylation sequence data are loaded as tracks on the UCSC browser <http://genome.ucsc.edu/>. For a specific gene, the correlation between expression and methylation can be viewed

a detailed presentation and computational data analysis, careful selection of cells and design of time-course series is required for integration of transcriptional data, chromatin states, and reconstruction of gene regulatory circuits (*see* **Note 13**).

6 Future Directions

To the best of our knowledge, nobody has yet been able to achieve integrated transcriptome/methylome profiling from any single cell or identified neuron. Nobody was able to follow up the entire dynamics of aging at the level of any functionally characterized neuron. Technically, it is very difficult using mammalian neurons [44, 46, 48], but now it is entirely possible using selected invertebrate models such *Aplysia* [24, 34, 49]. Although the presented protocols have been successfully validated, one of the major bottlenecks has been the prohibitive cost of sequencing required for multiple time points and biological replications. However, advances in next generation sequencing make these types of experiments achievable even within the logistics of individual laboratories. Indeed, in addition to the more conventional *Illumina* approach with HiSeq2500, it is now possible to employ novel state-of-the-art sequencing platforms such as a cost-efficient semiconductor sequencer (*Ion Torrent Proton*) that can be fully adapted to single-neuron RNA-seq applications and DNA methylation profiling. This innovative approach allows one to perform multiple single-neuron RNA-seq experiments at the lowest possible cost today (<\$100 cell) with just under 2–3 days turnaround time, from cell sampling to sequencing and initial annotation. Ideally, experimental design can also target both transcriptome and methylome profiling from the same single neuron—which is currently technically possible using *Aplysia* preparations.

It also should be noted that emerging single-molecule real-time sequencing (*Pacific Biosciences*) will allow one to map distribution of 5mC and 5hmC *at single-nucleotide resolution*. Currently, the platform is relatively expensive for the entire genome-scale coverage. However, it can be a complementary approach to target DNA methylation of specific genes and their regulatory regions.

7 Conclusion

It is recognized that at least several thousand genes dynamically and persistently change their expression in virtually any neuron in memory-forming circuits to maintain long-term plasticity or compensatory changes in aging. However, the enormous heterogeneity of neurons and unprecedented complexity of their connectivity

currently prevent reliable identification of individual neurons in mammalian circuits. Due to the very small sizes of mammalian neurons (10–40 μm in diameter), the equally considerable challenge is an ability to perform efficient single-cell transcriptome or epigenomic profiling. Although such an analysis is technically difficult, if not impossible, in vertebrate preparations, it can be successfully completed today using the simpler nervous systems of invertebrates such as *Aplysia*, where most of the neurons and synaptic connections in the circuits mediating major forms of learning have been identified. Just as important as the technical advantages offered by the neuroanatomy of *Aplysia* is the extensive background information available on the behaviors mediated by its well-studied neurons. Thus, we are confident that *Aplysia* offers a powerful experimental model to study cell and epigenomic biology of aging at a level that is difficult to achieve elsewhere.

However, the presented approach is not constrained by low input RNA abundance and can be applied to other cells and smaller cell populations such as 20–100 hippocampal neurons, axoplasm from *Loligo*, and embryonic cells, as proven in our experiments. Thus, since the protocol we presented is not limited in its applications to *Aplysia* neurons, we further advocate this model as an efficient preparation to couple a truly integrative analysis of genomic functions with real-time physiological measurements from the very same neurons as they learn and remember, age, or respond to induced injury.

Here, we also would like to comment on the constantly growing concerns about the so-called translational value of *Aplysia* research or research on related invertebrate species. This is also a common critical point from major funding agencies who tend to disfavor most invertebrate models (save *Drosophila* and *C. elegans*) vs. mammalian work. The major complaint to the comparative/invertebrate models research community is that their translational value to vertebrates and in particular to humans might not be justified. This view is detrimental for basic research and overlooks the fact that separation between deuterostome (including vertebrates) and protostome (including molluscs) lineages occurred within a relatively short evolutionary interval, possibly less than 50–100 million years between each other in the later Ediacaran period (it is ended 542 million years ago), while fishes (vertebrates) and human lineages are divided by at least 450–500 million years of independent evolution started during (or after) the “Cambrian explosion” [50, 51]. As a result, the major molecular and genomic blocks underlying bilaterian organization and epigenetic regulation are remarkably similar and highly conservative despite the large evolutionary distances. In fact, even prebilaterian animals, such as the sea starlet anemone *Nematostella* or the placozoan *Trichoplax*, have greater chromosome synteny with humans than flies and nematodes with humans [52, 53]. Ironically, *Drosophila* and *C. elegans* lost a significant part of DNA methylation machinery due

to the rapid evolution in these lineages and short life cycles, whereas *Aplysia* generally preserved this machinery from a common animal ancestor [1, 34, 43, 54]. Moreover, *Aplysia* shares more common genes with humans (including those involved in neurological disorders) than both flies and nematodes [34].

In summary, the current volume is dedicated to methods in biology of aging that are not restricted to vertebrates and humans. Thus, *Aplysia* has been specifically chosen to address questions in neurobiology of aging that currently are technically difficult, if not impossible, to address in humans. For example, it is impossible to work on identified neurons in humans, and there are no reliable protocols for isolation of both DNA and RNA from the very same neuron from intact vertebrate/human brains immediately after physiological tests. Yet, the same procedures are very straightforward in *Aplysia*. Considering that the basic DNA composition and the presence of 5-mC and 5-hmC in *Aplysia* are comparable to what we know in vertebrates [55], the same basic chemistry should work on mammalian models as well. In fact, previous and existing molecular information [19, 56] indicate significant conservation of both signaling and epigenetic mechanisms between *Aplysia* and vertebrates.

8 Notes

1. With *Aplysia*'s large neurons, it is possible to isolate both RNA and DNA from the same cell with the AllPrep DNA/RNA/Protein Mini Kit from Qiagen. However, when using an all-in-one kit, the yield is usually sacrificed.
2. Digital profiling or RNA-seq refers to quantification of sequencing reads. Frequency or expression is calculated by dividing the number of reads of a specific transcript by the total number of reads in a specific library.
3. The RT-PCR protocol followed manufactures' recommendations and is applicable to most RT-PCR machines.
4. *Aplysia californica* full-length cDNAs are all NCBI reported clones and sequences as well as an additional set of unreleased cDNAs cloned in our lab.
5. The large *Aplysia* neurons can go through up to 16 rounds of duplication generating 50–250 ng of gDNA and over 1 µg of RNA. The polyploidy might be viewed like a “photocopy” or “nature PCR machine” multiplying the entire genome complement and thus generating substantial amounts of genomic DNA from a single neuron. The functional significance of neuronal polyploidy is not clear in *Aplysia*. It was determined by histochemical measures that the amount of gDNA in large neurons of *Aplysia* correlates to the number of genomic

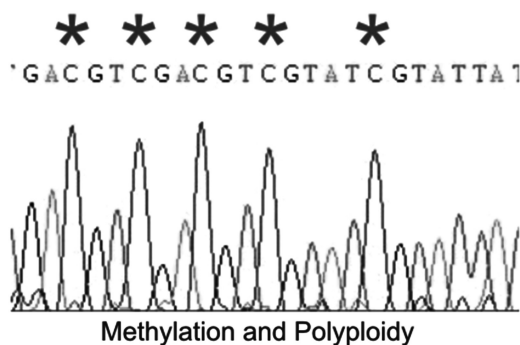


Fig. 8 Methylation in polyploid neurons occurs in all DNA copies. In this illustrated example, after bisulfite sequencing, bands from the amplified PCR reactions were sequenced for DNMT1 gene. The starred cytosines in the sample chromatogram show no background from other nucleotides, thus indicating all the genome copies in *Aplysia* polyploid neurons are equally methylated. If some of the cytosines were not methylated, there would be multiple peaks in the chromatogram indicating a mixed population. However, this is not the case here because there are no background peaks in any of the cytosines marked

duplication and can reach 100,000 genome copies per cell [57]. Although the physiological changes that accompany a polyploidy state are poorly understood, there are several potential advantages to polyploidy. Increase in cell size due to polyploidy might provide a metabolic benefit to support extensive branching of axodendritic processes innervating very large areas. A gene copy redundancy might, in principle, protect polyploid cells from deleterious mutations. However, it is important to know whether all genomic copies in the same *Aplysia* neuron are equally methylated.

To address these questions we looked at the epigenetic mark of 5-mC DNA methylation. Will all copies of the same genome carry the same epigenetic mark of 5-mC DNA methylation? We investigated selected genes involved in synaptic function. An example of the methylation status of DNMT in polyploid neurons is shown in Fig. 8. Here bisulfite sequencing of a band from a PCR product was performed. *The starred cytosines in the sample chromatogram show no background from other nucleotides, thus indicating all the copies of the genome in polyploid neurons are equally methylated.* If some of the cytosines were not methylated, there would be multiple peaks in the chromatogram indicating a mixed population, but this is not the case here because there are no background peaks in any of the cytosines marked. Therefore, we conclude that in *Aplysia* all the copies of the genome in polyploid neurons have the same methylation status.

6. We also think that novel commercial kits exploring similar approaches (e.g., EpiXplore from Clontech) can be adapted

for integrated RNA-seq/methylome profiling. However, their applicability for small amounts of starting material needs to be validated separately.

7. A potential limitation with a simple MethylMiner™ enrichment is the lack of single-nucleotide resolution. In principle, bisulfite sequencing can be conducted after MethylMiner™ enrichment. Nevertheless bisulfite sequencing may require more material (*see* Fig. 6) and additional control experiments need to be performed regarding compatibility between MethylMiner enrichment and bisulfite treatment. For example, it is true that bisulfite conversion can degrade DNA, but magnetic bead capture of methylated DNA might also lead to some aspecific binding. Thus, a combination of protocols with amplification after capture of methylated DNA and following bisulfite treatment can be tested for further single-nucleotide resolution applications. Here, a complementary methyl-sensitive PCR validation for selected genome regions would also be useful.
8. We like the QIAamp® DNA Micro genomic DNA isolation kit because there is a very low void volume for the columns, thus allowing for low volumes (15–20 µL) to elute samples compared to 100–200 µL for most other kits.
9. Other sonicators besides a Covaris such as a Bioruptor® can be used to fragment gDNA.
10. This step removes residual non-captured DNA.
11. This saved liquid is a non-captured DNA wash fraction.
12. We chose to do one high-salt elution to capture all methylated DNA in one fraction. Another option is a multi-fraction elution with a stepwise NaCl gradient that separates distinct populations based on the number of methylation sites per molecule.
13. It is important to remember that separate examination of gene expression arrays from DNA methylation profiles can lead to erroneous and misleading conclusions. The interpretation of the data can also be biased depending on whether you approach this integration from the gene expression perspective or you do the methylation first and then search for its relevance to gene expression. The most typical questions are: Does a specific change in methylation have an impact on gene expression? Likewise can a change in gene expression be due to alterations in DNA methylation? To address these questions, a carefully selected series of experiments with multiple time points should be designed to follow the time course of dynamic genomic organization. Ideally, these should be complemented by capture of nascent RNAs at given time intervals. Similarly, tools of reverse genetics (e.g., RNAi or injections of relevant molecular constructs) should also be applied. Currently, none of these integrative studies have been performed at the level of single identified neurons. However, the implementation of

presented and relevant single-cell protocols on relatively simpler models with functionally characterized neurons would be critical for progress in the field.

Finally, epigenetic modifications in neurons can be both stable and dynamic as a result of programmable changes during development, hormonal or transmitter stimulation, and activity-dependent processes that highly transient in nature [58]. To specifically identify an age-related event in senescent neurons, all of these factors have to be considered together with some environmental challenges or manipulations to show that the epigenetic landscape can change over time given gene-environment interactions. It is achievable using accessible *Aplysia* neurons but, because of enormous heterogeneity and lack of identified neurons, similar tests are extremely challenging using neural circuits in the mammalian brain. Combined, these remarks emphasize the critical importance of *Aplysia* and related species as novel and powerful models in the biology of aging and fundamental neuroscience. We would like to stress this vision and contrast it to growing concerns about the translational value of *Aplysia* that favors short-term applied research over long-term basic research about the integrative genomic biology of aging, circuit organization, and memory in particular.

Acknowledgements

We thank Mr. James Netherton for reading and commenting on the manuscript. We would like to thank Dr. Clarence Lee for help with the MethylMiner libraries. We also thank Dr. Manfred Lee for his technical advice and guidance with the Ion PGM sequencing process as well as anonymous reviewers for their critical comments and suggestions. We also thank Dr. Thomas Ha, Dr. Sami Jezzini, and Mrs. Yelena Bobkova for help with tissue preparations and RNA/DNA quality assays. This work is supported by NIH grants 1R01GM097502, R21RR025699, 5R21DA030118, R01MH097062, McKnight Brain Research Foundation, as well as NSF-0744649, NSF CNS-0821622, and UF Opportunity Fund awards to LLM.

References

1. Moroz LL, Kohn AB (2010) Do different neurons age differently? Direct genome-wide analysis of aging in single identified cholinergic neurons. *Front Aging Neurosci* 2:1–18
2. Day JJ, Sweatt JD (2011) Epigenetic modifications in neurons are essential for formation and storage of behavioral memory. *Neuropsychopharmacology* 36:357–358
3. Day JJ, Sweatt JD (2010) DNA methylation and memory formation. *Nat Neurosci* 13:1319–1323
4. Penner MR, Roth TL, Barnes CA, Sweatt JD (2010) An epigenetic hypothesis of aging-related cognitive dysfunction. *Front Aging Neurosci* 2:9
5. Miller CA, Gavin CF, White JA, Parrish RR, Honasoge A, Yancey CR, Rivera IM, Rubio MD,

- Rumbaugh G, Sweatt JD (2010) Cortical DNA methylation maintains remote memory. *Nat Neurosci* 13:664–666
6. Sweatt JD (2010) Neuroscience. Epigenetics and cognitive aging. *Science* 328:701–702
7. Feng J, Zhou Y, Campbell SL, Le T, Li E, Sweatt JD, Silva AJ, Fan G (2010) Dnmt1 and Dnmt3a maintain DNA methylation and regulate synaptic function in adult forebrain neurons. *Nat Neurosci* 13:423–430
8. Miller CA, Sweatt JD (2007) Covalent modification of DNA regulates memory formation. *Neuron* 53:857–869
9. Levenson JM, Roth TL, Lubin FD, Miller CA, Huang IC, Desai P, Malone LM, Sweatt JD (2006) Evidence that DNA (cytosine-5) methyltransferase regulates synaptic plasticity in the hippocampus. *J Biol Chem* 281:15763–15773
10. Tahiliani M, Koh KP, Shen Y, Pastor WA, Bandukwala H, Brudno Y, Agarwal S, Iyer LM, Liu DR, Aravind L, Rao A (2009) Conversion of 5-methylcytosine to 5-hydroxymethylcytosine in mammalian DNA by MLL partner TET1. *Science* 324:930–935
11. Kriaucionis S, Heintz N (2009) The nuclear DNA base 5-hydroxymethylcytosine is present in Purkinje neurons and the brain. *Science* 324:929–930
12. Szulwach KE, Li X, Li Y, Song CX, Wu H, Dai Q, Irier H, Upadhyay AK, Gearing M, Levey AI, Vasanthakumar A, Godley LA, Chang Q, Cheng X, He C, Jin P (2011) 5-hmC-mediated epigenetic dynamics during postnatal neurodevelopment and aging. *Nat Neurosci* 14:1607–1616
13. Wiers CE (2012) Methylation and the human brain: towards a new discipline of imaging epigenetics. *Eur Arch Psychiatry Clin Neurosci* 262(3):271–273
14. Byrne JH (1987) Cellular analysis of associative learning. *Physiol Rev* 67:329–339
15. Carew TJ, Walters ET, Kandel ER (1981) Classical conditioning in a simple withdrawal reflex in *Aplysia californica*. *J Neurosci* 1:1426–1437
16. Carew TJ, Walters ET, Kandel ER (1981) Associative learning in *Aplysia*: cellular correlates supporting a conditioned fear hypothesis. *Science* 211:501–504
17. Hawkins RD, Kandel ER, Bailey CH (2006) Molecular mechanisms of memory storage in *Aplysia*. *Biol Bull* 210:174–191
18. Hawkins RD, Schacher S (1989) Identified facilitator neurons L29 and L28 are excited by cutaneous stimuli used in dishabituation, sensitization, and classical conditioning of *Aplysia*. *J Neurosci* 9:4236–4245
19. Kandel ER (2001) The molecular biology of memory storage: a dialogue between genes and synapses. *Science* 294:1030–1038
20. Marinesco S, Kolkman KE, Carew TJ (2004) Serotonergic modulation in *Aplysia*. I. Distributed serotonergic network persistently activated by sensitizing stimuli. *J Neurophysiol* 92:2468–2486
21. Marinesco S, Wickremasinghe N, Carew TJ (2006) Regulation of behavioral and synaptic plasticity by serotonin release within local modulatory fields in the CNS of *Aplysia*. *J Neurosci* 26:12682–12693
22. Kandel ER (1976) Cellular basis of behavior. W.H. Freeman and Company, San Francisco
23. Kandel ER (1979) Behavioral biology of aplysia. W.H. Freeman and Company, San Francisco
24. Moroz LL (2011) Aplysia. *Curr Biol* 21:R60–R61
25. Iwamoto K, Bundo M, Ueda J, Oldham MC, Ukai W, Hashimoto E, Saito T, Geschwind DH, Kato T (2011) Neurons show distinctive DNA methylation profile and higher interindividual variations compared with non-neurons. *Genome Res* 21:688–696
26. Iwamoto K, Ueda J, Bundo M, Kojima T, Kato T (2011) Survey of the effect of genetic variations on gene expression in human prefrontal cortex and its application to genetics of psychiatric disorders. *Neurosci Res* 70:238–242
27. Gerdes R, Fieber LA (2006) Life history and aging of captive-reared California sea hares (*Aplysia californica*). *J Am Assoc Lab Anim Sci* 45:40–47
28. Stommes D, Fieber LA, Beno C, Gerdes R, Capo TR (2005) Temperature effects on growth, maturation, and lifespan of the California sea hare (*Aplysia californica*). *Contemp Top Lab Anim Sci* 44:31–35
29. Hirsch HR, Peretz B (1984) Survival and aging of a small laboratory population of a marine mollusc, *Aplysia californica*. *Mech Ageing Dev* 27:43–62
30. Antonov I, Ha T, Antonova I, Moroz LL, Hawkins RD (2007) Role of nitric oxide in classical conditioning of siphon withdrawal in *Aplysia*. *J Neurosci* 27:10993–11002
31. Rajasethupathy P, Fiumara F, Sheridan R, Betel D, Puthanveetil SV, Russo JJ, Sander C, Tuschl T, Kandel E (2009) Characterization of small RNAs in *Aplysia* reveals a role for miR-124 in constraining synaptic plasticity through CREB. *Neuron* 63:803–817
32. Bailey CH, Kandel ER (2008) Synaptic remodeling, synaptic growth and the storage of long-term memory in *Aplysia*. *Prog Brain Res* 169:179–198

33. Moroz LL, Kohn AB (2011) Parallel evolution of nitric oxide signaling: diversity of synthesis and memory pathways. *Front Biosci* 16:2008–2051
34. Moroz LL, Edwards JR, Puthanveetil SV, Kohn AB, Ha T, Heyland A, Knudsen B, Sahni A, Yu F, Liu L, Jezzini S, Lovell P, Iannuccilli W, Chen M, Nguyen T, Sheng H, Shaw R, Kalachikov S, Panchin YV, Farmerie W, Russo JJ, Ju J, Kandel ER (2006) Neuronal transcriptome of *Aplysia*: Neuronal compartments and circuitry. *Cell* 127:1453–1467
35. Moroz LL, Dahlgren RL, Boudko D, Sweedler JV, Lovell P (2005) Direct single cell determination of nitric oxide synthase related metabolites in identified nitrergic neurons. *J Inorg Biochem* 99:929–939
36. Moroz LL, Gillette R, Sweedler JV (1999) Single-cell analyses of nitrergic neurons in simple nervous systems. *J Exp Biol* 202(Pt 4): 333–341
37. Li L, Garden RW, Sweedler JV (2000) Single-cell MALDI: a new tool for direct peptide profiling. *Trends Biotechnol* 18:151–160
38. Li L, Sweedler JV (2008) Peptides in the brain: mass spectrometry based measurement approaches and challenges. *Annu Rev Anal Chem* 1:451–493
39. Fuller RR, Moroz LL, Gillette R, Sweedler JV (1998) Single neuron analysis by capillary electrophoresis with fluorescence spectroscopy. *Neuron* 20:173–181
40. Liu L, van Groen T, Kadish I, Tollefsbol TO (2009) DNA methylation impacts on learning and memory in aging. *Neurobiol Aging* 30:549–560
41. Lovell P, Moroz LL (2006) The largest growth cones in the animal kingdom and dynamics of neuronal growth in cell culture of *Aplysia*. *Integr Comp Biol* 46:847–870
42. Jezzini SH, Bodnarova M, Moroz LL (2005) Two-color in situ hybridization in the CNS of *Aplysia californica*. *J Neurosci Methods* 149:15–25
43. Walters ET, Moroz LL (2009) Molluscan memory of injury: evolutionary insights into chronic pain and neurological disorders. *Brain Behav Evol* 74:206–218
44. Tang F, Barbacioru C, Nordman E, Li B, Xu N, Bashkirov VI, Lao K, Surani MA (2010) RNA-Seq analysis to capture the transcriptome landscape of a single cell. *Nat Protoc* 5:516–535
45. Tang F, Barbacioru C, Wang Y, Nordman E, Lee C, Xu N, Wang X, Bodeau J, Tuch BB, Siddiqui A, Lao K, Surani MA (2009) mRNA-Seq whole-transcriptome analysis of a single cell. *Nat Methods* 6(5):377–382
46. Islam S, Kjallquist U, Moliner A, Zajac P, Fan JB, Lonnerberg P, Linnarsson S (2011) Characterization of the single-cell transcriptional landscape by highly multiplex RNA-seq. *Genome Res* 21:1160–1167
47. Moroz LL, Kohn AB (2010) Do different neurons age differently? Direct genome-wide analysis of aging in single identified cholinergic neurons. *Front Aging Neurosci* 2:6. doi:10.3389/neuro.24.006.2010
48. Evrony GD, Cai X, Lee E, Hills LB, Elhosary PC, Lehmann HS, Parker JJ, Atabay KD, Gilmore EC, Poduri A, Park PJ, Walsh CA (2012) Single-neuron sequencing analysis of 11 retrotransposition and somatic mutation in the human brain. *Cell* 151:483–496
49. Kohn AB, Moroz TP, Barnes JP, Netherton M, Moroz LL (2013) Single-cell semiconductor sequencing. Trygve O, Tollefsbol (eds.). *Biological Aging: Methods and Protocols*, Methods in Mol Biol: Methods and Protocols, vol. 1048, doi:10.1007/978-1-62703-556-9_18, # Springer, New York, This volume
50. Nielsen C (2012) *Animal Evolution: Interrelationships of the living phyla*. Oxford University Press, Oxford
51. Valentine JW (2004) *On the origin of phyla*. The University of Chicago Press, Chicago
52. Srivastava M, Begovic E, Chapman J, Putnam NH, Hellsten U, Kawashima T, Kuo A, Mitros T, Salamov A, Carpenter ML, Signorovitch AY, Moreno MA, Kamm K, Grimwood J, Schmutz J, Shapiro H, Grigoriev IV, Buss LW, Schierwater B, Dellaporta SL, Rokhsar DS (2008) The Trichoplax genome and the nature of placozoans. *Nature* 454:955–960
53. Srivastava M, Simakov O, Chapman J, Fahey B, Gauthier ME, Mitros T, Richards GS, Conaco C, Dacre M, Hellsten U, Larroux C, Putnam NH, Stanke M, Adamska M, Darling A, Degnan SM, Oakley TH, Plachetzki DC, Zhai Y, Adamski M, Calcino A, Cummins SF, Goodstein DM, Harris C, Jackson DJ, Leys SP, Shu S, Woodcroft BJ, Vervoort M, Kosik KS, Manning G, Degnan BM, Rokhsar DS (2010) The Amphimedon queenslandica genome and the evolution of animal complexity. *Nature* 466:720–726
54. Zhang Y, Brown MR, Hyland C, Chen Y, Kronengold J, Fleming MR, Kohn AB, Moroz LL, Kaczmarek LK (2012) Regulation of neuronal excitability by interaction of fragile X mental retardation protein with slack potassium channels. *J Neurosci* 32:15318–15327
55. Moroz LL, Citarella M, Kohn AB (2012) Genome-wide analysis of plasticity-induced active DNA demethylation in memory-forming circuits: Insights from the *Aplysia* genome.

- Society for Neuroscience Meeting, Abstracts, New Orleans, 294.208/CCC233
56. Guan Z, Giustetto M, Lomvardas S, Kim JH, Miniaci MC, Schwartz JH, Thanos D, Kandel ER (2002) Integration of long-term-memory-related synaptic plasticity involves bidirectional regulation of gene expression and chromatin structure. *Cell* 111:483–493
57. Lasek RJ, Dower WJ (1971) *Aplysia californica*: analysis of nuclear DNA in individual nuclei of giant neurons. *Science* 172:278–280
58. Guo JU, Ma DK, Mo H, Ball MP, Jang MH, Bonaguidi MA, Balazer JA, Eaves HL, Xie B, Ford E, Zhang K, Ming GL, Gao Y, Song H (2011) Neuronal activity modifies the DNA methylation landscape in the adult brain. *Nat Neurosci* 14:1345–1351
59. Heyland A, Moroz LL (2006) Signaling mechanisms underlying metamorphic transitions in animals. *Integr Comp Biol* 46:743–759
60. Heyland A, Vue Z, Voolstra CR, Medina M, Moroz LL (2011) Developmental transcriptome of *Aplysia californica*. *J Exp Zool B Mol Dev Evol* 316B:113–134
61. Waddington CH (1956) Principles of Embryology. Allen & Unwin, New York

INDEX

A

- Adeno-associated virus (AAV)..... 161–179
- Age-related RNA binding proteins 285
- Aging
 - biomarkers 3–4, 21–25, 27, 145, 146
 - fibroblasts 5–8
 - phenotypic changes..... 31
 - in vitro* 3–4, 7, 8
- Antioxidant gene therapy 161
- Aplysia*..... 250, 252, 257–259, 269, 277, 280, 324–329, 331–333, 337–339, 343–347, 349

B

- Bone regeneration 181
- Bud scar 56, 57

C

- Caenorhabditis elegans* 65, 195–212
- Calorie restriction mimetics..... 95–105, 152
- Catalase
 - gene..... 162, 168
 - mitochondria-targeted (MCAT) 161–170, 176
- Cell culture
 - senescence 1–8, 309–320
 - subculturing 3, 6
- Cell cycle arrest 36, 127, 135, 136, 310
- Cell sorting 31–45, 56, 137
- Cellular senescence..... 1, 2, 4, 8, 11, 23, 27, 37, 40, 110, 127–132, 135–143, 148, 229
- Comet assay 137–138, 140–141

D

- Deconvolution software 201
- Digital analysis..... 14–16
- DNA
 - damage 3, 21–22, 24–25, 27, 35, 36, 39, 40, 43, 44, 127, 148, 286
 - methylation..... 310, 315–318, 325, 326, 329, 339–342, 344, 345, 347, 348
 - microarray 285–305
- Drosophila melanogaster*..... 65, 77–90, 100

Drugs

- anti-aging..... 145, 156–158
- gene therapy 161–179
- pharmacological 145–158

E

- Embryonic 11, 112, 115–118, 156, 253, 257, 332, 345
- Epigenetics 110, 309–320, 324, 329, 339, 345–347, 349
- Epigenetic senescence signature..... 311, 314, 315, 317–319, 339
- Epigenomics 276, 322–349
- Exometabolome mapping 195–212

F

- Flow cytometry 27, 34–36, 43, 45, 131, 140, 310
- Fluorescence labeling 289–300, 305
- Forward genetics 65
- Free radical 79

G

- β -Galactosidase, senescence-associated 3, 4, 11–17, 21–23, 32, 37, 131, 136, 148
- Gene delivery vehicle 162

H

- Hippocampus 269, 326, 329
- H₂O₂ 136, 137, 139, 141–143, 161, 165, 171, 177

I

- Imaging
 - analysis 11–17, 167, 188, 190–192, 238–239
 - bioluminescence 181–192
- Immunoblotting 101, 104, 232, 233, 241, 243
- Immunogenetics 216
- Ion
 - proton 248, 250, 251, 260, 275, 276, 282, 344
 - torrent 26, 248–251, 255–258, 269, 272–276, 278, 281–283, 332, 344

L

Life-span
 chronological 50
 long-lived 65, 66, 70–73, 79, 196
 replicative 5, 26, 49–62
Locomotor activity 80, 82, 87–88, 90, 147, 151
Longevity 20, 25, 27, 49, 66, 79,
 95, 96, 98–100, 109, 156, 215–226
Luciferase reporter gene 182

M

Magnetic sorting 51, 55–57
Mammalian target of rapamycin (mTOR) 96,
 98–100
Mass spectrometry 196, 204, 229, 230,
 232, 233, 235, 238, 328
MCAT. *See* Catalase, mitochondria-targeted (MCAT)
Memory 154, 251, 252, 257, 324–327, 344, 349
Mesenchymal stromal cells (MSCs) 181, 183,
 185, 187, 311–315, 319
Metabolomics 195–212
Mice
 muscle contractility 161
 running performance 161
Microarray-based techniques 287, 288
Micromanipulation 50, 54, 116, 117, 122
Micro RNA (mi RNAs) 286, 288, 290,
 292, 298–300, 304
Mitochondrial function 25, 40,
 96, 97, 100
MSCs. *See* Mesenchymal stromal cells (MSCs)
mTOR. *See* Mammalian target of rapamycin (mTOR)
Muscle 103–104, 164–168, 171–175, 236
Mutagenesis 66–70, 73, 78
Mutation 1, 65–74, 78, 100, 127,
 148, 156, 162, 220, 288, 347

N

Neuron 230, 256–261, 264, 323–349
Next generation sequencing 248, 344
Nuclear reprogramming 109

O

Oc. *See* Osteocalcin (Oc)
Oncogene-induced senescence 24, 127–130, 136
Oocyte 110, 112–115, 117–124
Osteocalcin (Oc) 182–185, 188–190
Outcross 72, 74
Oxidative stress 20, 21, 24, 25, 27, 36,
 38, 79, 86, 90, 97, 135–143, 148, 161, 287, 310

P

p16 24, 27, 35, 128, 130–132,
 136, 138, 142, 286, 287, 310
p53 24, 32, 105, 128, 131, 136, 138,
 142, 285–287, 310
PD. *See* Population doubling (PD)
Polymorphism 215–226, 288
Population doubling (PD) 4, 5, 8, 12, 17,
 20–22, 26, 32, 35, 39, 309, 311, 314–316
Proteomics 195, 229–245

R

Rapamycin 95, 96, 98–101, 104–105
RAS 127–132, 319
Real-time bioluminescence 181–192
Reproduction 79, 80, 86–87, 90, 147, 196
Resveratrol 60, 62, 98, 100–102
RIP-chip 288, 290, 300–303
RNA binding protein 285, 288
Ruthenium tris-bathophenanthroline disulfonate
 (RuBPs) 232–234, 237–240, 243, 244

S

SAHF. *See* Senescence-associated heterochromatin foci
 (SAHF)
Sarcopenia 149
SCNT. *See* Somatic-cell nuclear transfer (SCNT)
Screen 70–71
 phenotype 147
Senescence-associated heterochromatin foci (SAHF) 3,
 4, 27, 130, 131, 136, 141–142, 148
Single cell RNA-seq 248, 251, 282,
 326, 329, 332–338
SIRT1 25, 27, 96–101, 104, 217, 287
Sirtuin activating compounds (STACs) 96–98
Somatic-cell nuclear transfer (SCNT) 109–124
STACs. *See* Sirtuin activating compounds (STACs)
Starvation 79, 86
Stress
 induced premature senescence 27
 oxidative 21, 24, 79, 86, 135–143, 148

T

Targeted expression 161
Telomere length analysis 138, 141
Tissue engineering 181
Transcriptome 250, 261, 263, 275,
 276, 323–349
Treadmill 162, 168, 175–176, 179
Two-dimensional gel electrophoresis 230, 235, 244

